Vol.II

Proceedings of a Symposium, Bucharest, 17-21 May 1965

non-destructive testing in nuclear technology

INTERNATIONAL ATOMIC ENERGY AGENCY, VIENNA, 1965

NON-DESTRUCTIVE TESTING IN NUCLEAR TECHNOLOGY

VOL. II

The following States are Members of the International Atomic Energy Agency:

AFGHANISTAN
ALBANIA
ALGERIA
ARGENTINA
AUSTRALIA
AUSTRIA
BELGIUM
BOLIVIA
BRAZIL
BULGARIA
BURMA
BYELORUSSIAN SOVIET SOCIALIST REPUBLIC
CAMBODIA
CAMEROON
CANADA
CEYLON
CHILE
CHINA
COLOMBIA
CONGO, DEMOCRATIC REPUBLIC OF
COSTA RICA
CUBA
CYPRUS
CZECHOSLOVAK SOCIALIST REPUBLIC
DENMARK
DOMINICAN REPUBLIC
ECUADOR
EL SALVADOR
ETHIOPIA
FINLAND
FRANCE
FEDERAL REPUBLIC OF GERMANY
GABON
GHANA
GREECE
GUATEMALA
HAITI
HOLY SEE
HONDURAS
HUNGARY
ICELAND
INDIA
INDONESIA
IRAN
IRAQ
ISRAEL
ITALY
IVORY COAST
JAPAN
KENYA
REPUBLIC OF KOREA
KUWAIT
LEBANON
LIBERIA
LIBYA
LUXEMBOURG
MADAGASCAR
MALI
MEXICO
MONACO
MOROCCO
NETHERLANDS
NEW ZEALAND
NICARAGUA
NIGERIA
NORWAY
PAKISTAN
PARAGUAY
PERU
PHILIPPINES
POLAND
PORTUGAL
ROMANIA
SAUDI ARABIA
SENEGAL
SOUTH AFRICA
SPAIN
SUDAN
SWEDEN
SWITZERLAND
SYRIA
THAILAND
TUNISIA
TURKEY
UKRAINIAN SOVIET SOCIALIST REPUBLIC
UNION OF SOVIET SOCIALIST REPUBLICS
UNITED ARAB REPUBLIC
UNITED KINGDOM OF GREAT BRITAIN AND NORTHERN IRELAND
UNITED STATES OF AMERICA
URUGUAY
VENEZUELA
VIET-NAM
YUGOSLAVIA

The Agency's Statute was approved on 23 October 1956 by the Conference on the Statute of the IAEA held at United Nations Headquarters, New York; it entered into force on 29 July 1957. The Headquarters of the Agency are situated in Vienna. Its principal objective is "to accelerate and enlarge the contribution of atomic energy to peace, health and prosperity throughout the world".

Printed by the IAEA in Austria
October 1965

PROCEEDINGS SERIES

NON-DESTRUCTIVE TESTING IN NUCLEAR TECHNOLOGY

PROCEEDINGS OF A SYMPOSIUM ON
NON-DESTRUCTIVE TESTING IN NUCLEAR TECHNOLOGY
HELD BY THE
INTERNATIONAL ATOMIC ENERGY AGENCY
IN BUCHAREST, 17-21 MAY 1965

In two volumes

VOL.II

INTERNATIONAL ATOMIC ENERGY AGENCY
VIENNA, 1965

Symposium on Non-Destructive Testing in Nuclear Technology, Bucharest, 17 - 21 May 1965.
Proceedings ... held by the International Atomic Energy Agency ... Vienna, the Agency, 1965.
2 vols. (IAEA Proceedings series)

620.179.1(063)"1965"
(063)620.179.1"1965"
621.039:620.179.1

NON-DESTRUCTIVE TESTING IN NUCLEAR TECHNOLOGY,
IAEA, VIENNA, 1965
STI/PUB/105

FOREWORD

The Symposium on Non-Destructive Testing in Nuclear Technology was convened by the International Atomic Energy Agency and held, at the invitation of the Romanian People's Republic, in Bucharest from 17 to 21 May 1965.

This was the first large IAEA symposium on this topic and was arranged with the help of the Romanian Institute of Atomic Physics. Over 100 participants from 20 countries and two international organizations presented 46 papers.

The development of non-destructive testing techniques has increased considerably in recent years, particularly in the nuclear field. Non-destructive testing methods such as ultrasonic and radiographic testing are proving increasingly useful for ensuring that reactor materials and components will stand up to prolonged and rigorous use. Such methods are used to test for flaws, to check dimensions such as tube-wall thickness, and to determine the location and distribution of uranium fuel in a fuel element.

Speakers stressed that these methods were invaluable for providing extensive and detailed data on the physical structure and condition of materials and the effects of fabrication processes. Among aspects of non-destructive testing that were discussed were the use of automation; assistance at the design stage for attaining higher strength-to-weight ratios; the testing of welds in reactor containment vessels; and the testing of sintered materials.

The important information presented at the Symposium and the extensive discussions among scientists demonstrated the desire to accelerate solutions to various problems connected with non-destructive testing techniques.

The IAEA wishes to express gratitude to the Romanian Government and the Romanian Institute of Atomic Physics for their generous hospitality and co-operation.

EDITORIAL NOTE

The papers and discussions incorporated in the proceedings published by the International Atomic Energy Agency are edited by the Agency's editorial staff to the extent considered necessary for the reader's assistance. The views expressed and the general style adopted remain, however, the responsibility of the named authors or participants.

For the sake of speed of publication the present Proceedings have been printed by composition typing and photo-offset lithography. Within the limitations imposed by this method, every effort has been made to maintain a high editorial standard; in particular, the units and symbols employed are to the fullest practicable extent those standardized or recommended by the competent international scientific bodies.

The affiliations of authors are those given at the time of nomination.

The use in these Proceedings of particular designations of countries or territories does not imply any judgement by the Agency as to the legal status of such countries or territories, of their authorities and institutions or of the delimitation of their boundaries.

The mention of specific companies or of their products or brand-names does not imply any endorsement or recommendation on the part of the International Atomic Energy Agency.

CONTENTS OF VOL. II

SESSION V

SESSION VI

SESSION VII

SESSION VIII

SESSION IX

SESSION V

CONTRÔLE DES TRAITEMENTS THERMIQUES D'ALLIAGES D'URANIUM PAR ULTRASONS

MARIE-THÉRÈSE DESTRIBATS, C. CHERPENTIER, F. PAPEZIK
ET M. PIGEON
CENTRE D'ÉTUDES NUCLÉAIRES DE SACLAY, FRANCE

Abstract — Résumé — Аннотация — Resumen

ULTRASONIC INSPECTION FOLLOWING HEAT TREATMENT OF URANIUM ALLOYS. To improve the behaviour of low uranium alloys in reactors it is often necessary to reduce grain size by heat treatment. It has proved essential to provide for inspection of the whole element and the entire output in order to discover the exact quality of the fuel used. This inspection cannot be made by micrography because of the time required and the fact that the data obtained are incomplete.

The inspection system adopted is based on the principle of absorption of ultrasonic waves by materials. This absorption depends on the structure of the medium. If λ is small in relation to grain size G, absorption is low; whereas if G is of the order of $\lambda/2$, absorption is very high.

The tests were made first in air, using the multiple-echo system, then by measuring the height of the first echo, and finally by transmission in water, the height of the transmitted echo being compared with that of the initial signal.

In industrial use, the amplitude of the echo transmitted by the material is compared with the echo obtained from a standard of the same characteristics and shape. Inspection takes place in a special machine in which the materials are rotated by rollers and adjustable transducers move over the element.

The helicoidal scanning is carried out with a pitch of less than 5 mm. The ultrasonic generator includes a control system ensuring a constant reference echo.

The paper quotes a series of records showing the results obtained with various alloys and in particular the faults observed in elements treated by induction upon linear displacement. The arrangement can detect faulty treatment zones of less than 1 cm².

The system is at present used to inspect all low alloy uranium fuels of the G2,EL3, EDF1, EDF2 and INCA reactors, i.e. rods and tubes with diameters between 20 and 95 mm.

CONTRÔLE DES TRAITEMENTS THERMIQUES D'ALLIAGE D'URANIUM PAR ULTRASONS. Afin d'obtenir une meilleure tenue des alliages d'uranium faiblement alliés dans les réacteurs, un affinage du grain par traitements thermiques est souvent nécessaire. Il s'est avéré indispensable de pouvoir effectuer un contrôle sur l'ensemble de l'élément et la totalité d'une production afin de connaître exactement la qualité du combustible utilisé. Ce contrôle ne pouvait être envisagé par micrographie en raison de la durée trop longue des opérations et de leurs résultats partiels.

Le contrôle auquel les auteurs ont procédé est basé sur le principe de l'absorption des ultrasons par les matériaux. L'absorption est fonction de la structure du milieu. Si λ est petit par rapport à la taille du grain G, elle est faible; si G est de l'ordre de $\lambda/2$, elle est très grande.

Les tout premiers essais ont été faits dans l'air, par échos multiples, puis en mesurant la hauteur du premier écho, ensuite par transmission dans l'eau, en comparant la hauteur de l'écho transmis à celle de l'écho initial.

Dans le contrôle industriel, on compare l'amplitude de l'écho transmis par le matériau à l'écho obtenu avec un étalon bien traité de même nuance et de même forme géométrique. L'examen se fait dans une machine spéciale; les matériaux sont entraînés en rotation par des galets et les traducteurs orientables se déplacent le long de l'élément. L'exploration hélicoïdale s'effectue avec un pas inférieur à 5 mm. Le générateur d'ultrasons comporte un système de régulation qui maintient l'écho de référence constant.

On montrera une série d'enregistrements obtenus sur divers alliages, en particulier des défauts observés sur les éléments traités par induction au défilé. Des zones mal traitées inférieures à 1 cm² sont détectées.

Actuellement, on contrôle ainsi tous les combustibles en uranium faiblement alliés des divers réacteurs G2, EL3, EDF1, EDF2 et INCA, c'est-à-dire des barres et tubes de diamètre compris entre 20 et 95 mm.

КОНТРОЛЬ ТЕРМИЧЕСКОЙ ОБРАБОТКИ УРАНОВЫХ СПЛАВОВ С ПОМОЩЬЮ УЛЬТРАЗВУКА. Чтобы добиться лучшего режима работы реакторов, в которых используются слегка легированные сплавы урана, часто возникает необходимость измельчать зерна термической обработкой. При этом оказалось необходимым осуществлять контроль за всеми элементами и за всем производством, чтобы точно знать качество использованного топлива. Этот контроль невозможно осуществлять через микрографию, так как он занимает много времени и не дает полных результатов.

Контроль,принятый в ядерном центре, основан на принципе поглощения ультразвуков материалами.

Данное поглощение связано со структурой среды. Если значение λ мало по сравнению с величиной зерна G, то поглощение слабое, а если G составляет порядка $\lambda/2$, то поглощение очень сильное.

Все первые опыты проводили в воздухе на основе анализа многократных эхо и затем измеряли высоты первого эха. Далее измерение проводили в воде. При этом сравнивали высоты пропущенного и первоначального эха.

При промышленном контроле сравнивается амплитуда эха, пропущенного через материал, с эхом, полученным на хорошо обработанном эталоне того же типа и той же геометрической формы. Испытание проводили в специальной установке, когда материалы запускали в ротацию с помощью роликов, а направляемые преобразователи перемещали вдоль элемента.

Винтовое скеннирование осуществляли при шаге менее 5 мм. В ультразвуковом генераторе имеется система регулирования,которая поддерживает контрольное эхо.

Приводится серия записей по различным сплавам, и в частности говорится о дефектах, наблюдаемых у элементов, которые были обработаны индукцией во время прохождения. Обнаруживаются плохо обработанные участки размером менее 1 см^2.

В настоящее время подобным образом осуществляется контроль за всеми типами топлива в виде слегка легированных урановых сплавов, применяемых в реакторах G2 EL3, EF1 EdF2 и INCA, иными словами, контролируются все стержни и трубки с диаметром между 20 и 95 мм.

CONTROL ULTRASONICO DE LOS TRATAMIENTOS TERMICOS DE ALEACIONES DE URANIO. Con el fin de aumentar en los reactores la estabilidad de las aleaciones con bajo contenido de uranio resulta a menudo necessario afinar el grano mediente tratamientos térmicos. Para conocer la calidad del combustible utilizado se considera indispensable controlar el conjunto del elemento y la totalidad de la producción. Este control no puede realizarse por micrografía debido al tiempo prolongado que ésta requiere y a sus resultados de carácter parcial.

El método de control adoptado se basa en el principio de la absorción de ondas ultrasónicas por los distintos materiales. Dicha absorción es función de la estructura del medio. Si λ es pequeña en comparación col el tamaño del grano G, la absorción resultará débil mientras que si G es del orden de $\lambda/2$, la absorción será muy considerable.

Los primeros ensayos se efectuaron en aire, utilizando ecos múltiples y midiendo la altura del primer eco; los siguientes se realizaron por transmisión en agua, comparando la altura del eco transmitido con la del inicial.

En el control industrial, se compara la amplitud del eco transmitido por el material con la del obtenido usando una probeta patrón sometida al tratamiento correcto, de la misma composición y de igual forma geométrica. La inspección se realiza en una máquina especial; los materiales se hacen girar mediante roldanas y los transductores orientables se desplazan a lo largo del elemento.

La exploración helicoidal se lleva a cabo con un paso inferior a 5 mm. El generador de ondas ultrasónicas comprende un sistema de regulación que mantiene constante la intensidad del eco de referencia.

Se presenta una serie de registros obtenidos con diversas aleaciones y, en particular, defectos observados en elementos tratados por inducción durante el avance lineal. Se detectan zonas de tratamiento deficiente, de área inferior a 1 cm^2.

En la actualidad se controlan de esta manera todos los combustibles aleados de bajo contenido de uranio destinados a los reactors G2, EL3, EDF1, EDF2 e INCA, es decir, barras y tubos con diámetros comprendidos entre 20 y 95 mm.

1. INTRODUCTION

Il est souvent indispensable de procéder à des traitements thermiques pour obtenir un affinage du grain et une meilleure stabilité dimensionnelle des alliages d'uranium faiblement allié utilisés dans les réacteurs nucléaires.

Ces traitements thermiques sont effectués

- soit par trempe directe,
- soit par trempe étagée.

suivant la nature de l'alliage. Dans certains cas le traitement est fait dans une machine semi-automatique, dans laquelle chaque barreau est traité individuellement; ce procédé porte le nom de trempe au défilé [1].

Ce procédé, malgré ses avantages certains, présente le risque d'une trempe irrégulière provenant d'un déréglage de la machine. Il est donc apparu nécessaire de procéder, sur les barreaux traités de la sorte, à un contrôle général de chacun des barreaux, contrôle suffisamment rapide et simple pour être applicable à l'ensemble d'une production et permettre de connaître exactement la qualité du combustible utilisé. En outre, en procédant à ce contrôle immédiatement après la trempe, il est possible de suivre de près la qualité de la fabrication et d'y apporter rapidement les corrections nécessaires.

Lorsque la trempe se fait suivant un autre procédé que le procédé au défilé, l'intérêt d'une méthode de contrôle rapide persiste, surtout si la trempe au bain de sels est faite barreau par barreau. L'examen micrographique deviendrait alors rapidement inapplicable en raison du grand nombre d'échantillons; les renseignements que l'on pourrait en tirer ne seraient d'ailleurs que partiels.

Nous nous sommes donc orientés, pour vérifier l'homogénéité de la structure du combustible, vers le contrôle par ultrasons, qui seul peut permettre de contrôler, dans un délai acceptable, la totalité d'un production.

Le principe du contrôle par ultrasons que nous avons utilisé est simple: une onde ultrasonore traversant un milieu polycristallin subit une absorption qui est fonction de la taille des grains du matériau et de la longueur d'onde utilisée. L'absorption est importante pour des longueurs d'onde de l'ordre de deux à trois fois le diamètre des grains. Elle est faible quand ce dernier est petit par rapport à la longueur d'onde [2].

Les tout premiers essais ont commencé en juin 1960; dès novembre 1961 le contrôle suivant le principe indiqué ci-dessus était pratiqué à l'échelle industrielle pour le combustible du réacteur G2 (graphite-gaz). Ce combustible était un alliage d'uranium faiblement allié, le sicral F_1, obtenu par fusion sous vide et traité en bain de sels ou trempé au défilé. Ses teneurs en éléments d'addition étaient les suivantes, en % en poids:

Fe : 0,02 à 0,04,
Cr : 0,005 à 0,015,
Si : 0,005 à 0,015,
Al : 0,05 à 0,09.

Les barreaux avaient les dimensions suivantes:
diamètre : 30 mm,
longueur: 300 mm.

2. DIVERSES TECHNIQUES ÉTUDIÉES

Lorsque nous avons commencé nos essais en juin 1960, ce mode de contrôle n'avait pas encore été utilisé à notre connaissance à l'échelle industrielle. Comme références bibliographiques nous ne connaissions que les travaux de Grossman.

Nous avons donc dû, au début, procéder à de nombreux essais afin de définir une technique convenable et facilement transposable à l'échelle industrielle; ces premiers essais ont eu lieu sur du laiton, puis sur des pastilles d'uranium.

Le générateur d'ultrasons employé pour ces premiers essais était un appareil courant du commerce: le «Metalloradar type RV» de la Société Réalisations ultrasoniques, Meaux (S.-et-M.), France. Cet appareil permet de travailler aux fréquences de 0,5, 1, 2, 3, 5 et 10 MHz avec des puissances, sensibilités et temps d'impulsion variables. Les palpeurs en titanate de baryum sont excités par des impulsions de 0,5 μs de durée totale.

Les premiers essais ont été faits successivement dans l'air, puis dans l'eau, par échos multiples, par réflexions multiples et enfin par mesure de la hauteur du premier écho, à toutes les fréquences disponibles dans l'appareil. Pour les essais dans l'air, le traducteur était placé en contact avec la pièce, le couplage se faisant par un film d'huile. Par contre lors des essais dans l'eau, le traducteur avait une position fixe par rapport à la pièce, le ou les traducteurs et la pièce étant immergés.

2.1. Essais par échos multiples

Un train d'ondes ultrasonores est envoyé sur l'échantillon à examiner; sa propagation est fonction de la structure de celui-ci. Le nombre des réflexions successives de ce train d'ondes est caractéristique de la taille des grains pour une fréquence donnée, et de l'homogénéité du matériau examiné.

Il s'agit donc essentiellement de chiffrer le nombre de réflexions apparaissant sur l'écran du tube cathodique. On observe d'autant moins d'échos que la structure est plus grossière.

2.2. Essais par réflexions multiples

La méthode par réflexions multiples est dérivée de la précédente. Elle consiste à examiner la totalité des échos observables sur l'écran, c'est-à-dire le décrément. On compare alors la distance entre le dernier écho d'amplitude non nulle et l'écho initial des divers échantillons. Plus la longueur de réflexion est grande et plus le grain est fin.

A noter que, dans ces deux méthodes, les résultats peuvent être complètement faussés par la présence de cavités dans les échantillons examinés; c'est ainsi qu'un échantillon à structure grossière peut paraître fin, les échos obtenus étant dus aux défauts.

2.3. Essais par mesure de la hauteur du premier écho

Le principe de cette méthode est le même que celui de la méthode par échos multiples, mais on mesure cette fois la hauteur du premier écho.

L'échantillon qui absorbe le moins d'énergie a le grain le plus fin.

Les signaux sont examinés sur l'écran d'un oscilloscope afin d'avoir une amplification linéaire. A noter que l'écho dont on mesure la hauteur est le premier lorsqu'on procède dans l'air et le second lorsqu'on procède dans l'eau, le premier écho correspondant alors à la face d'entrée.

2.4. Essais par transmission

Dans cette méthode on installe de part et d'autre du matériau à examiner deux traducteurs; l'un de ces traducteurs transmet l'énergie ultrasonore au matériau, l'autre fonctionne comme récepteur. On mesure la hauteur du premier écho de la deuxième face. L'énergie transmise est d'autant plus grande que le matériau a une structure plus fine et homogène. Comme précédemment, les mesures sont faites sur l'écran d'un oscilloscope.

Les essais effectués par transmission dans l'eau sont de loin les plus reproductibles, et les seuls enregistrables.

3. PREMIERS RÉSULTATS OBTENUS

Après avoir décrit rapidement les principes des méthodes utilisées, nous décrirons ci-après les résultats obtenus en laboratoire avec différents matériaux.

3.1. Résultats obtenus sur le laiton

Nous avons utilisé de petits cylindres en laiton de $80 \pm 0{,}5$ mm de longueur et de 35 mm de diamètre. Les échantillons dont nous disposions avaient subi divers traitements thermiques; leur structure était homogène et les diamètres des grains variaient entre 0,025 et 0,140 mm.

Les mesures effectuées par les différentes méthodes que nous venons d'indiquer ont montré que la transmission de l'énergie ultrasonore devient quasiment constante dès que le rapport de la longueur d'onde utilisée à la taille du grain est de l'ordre de 50. Par contre la transmission est très variable dès que ce même rapport est inférieur à 1/10 (fig. 1).

3.2. Résultats obtenus sur des pastilles en sicral F_1

Nous avons eu de grosses difficultés à nous procurer des échantillons de structure homogène et possédant des grains de tailles différentes. Nous avons pu néanmoins disposer de cinq pastilles de 30 mm de diamètre et de 19 mm d'épaisseur ayant des grains de diamètres variant entre 0,125 et 0,450 mm.

Les essais effectués suivant les différentes méthodes donnent des résultats similaires (fig. 2). On remarquera que la meilleure sensibilité est obtenue pour une fréquence de 3 MHz, le rapport de la longueur d'onde au diamètre du grain variant entre 2 et 10. Par contre la sensibilité est très mauvaise pour la fréquence de 1 MHz, le rapport de la longueur d'onde au diamètre du grain étant alors compris entre 3 et 8 (fig. 3).

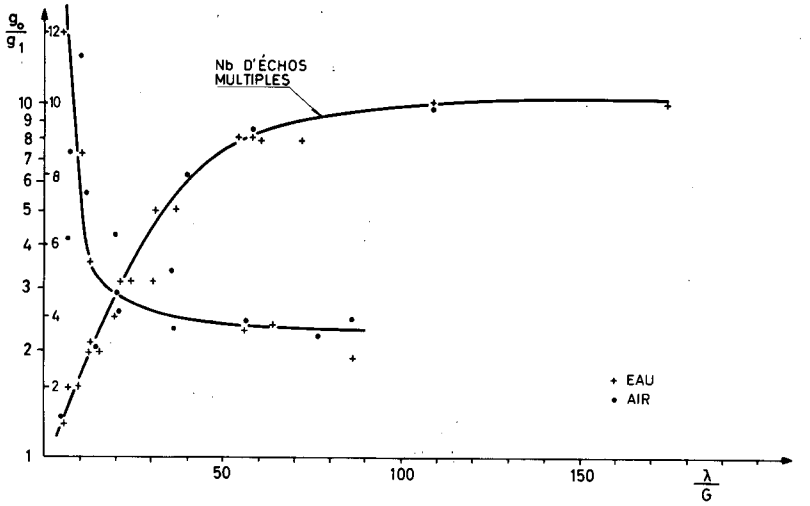

Figure 1

Laiton - Absorption suivant les diverses méthodes utilisées en fonction de λ/G.

λ = longueur d'onde utilisée,
G = taille moyenne du grain,
g_0 = amplitude de l'écho initial,
g_1 = amplitude de l'écho traversant l'échantillon.

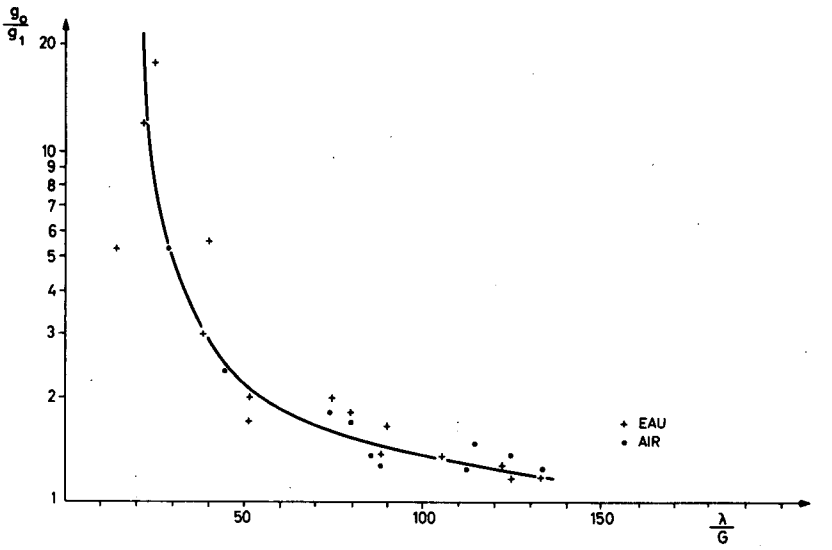

Figure 2

Sicral F_1 - Absorption ultrasonore en fonction de λ/G.

λ = longueur d'onde utilisée,
G = taille moyenne du grain,
g_0 = amplitude de l'écho initial,
g_1 = amplitude de l'écho traversant l'échantillon.

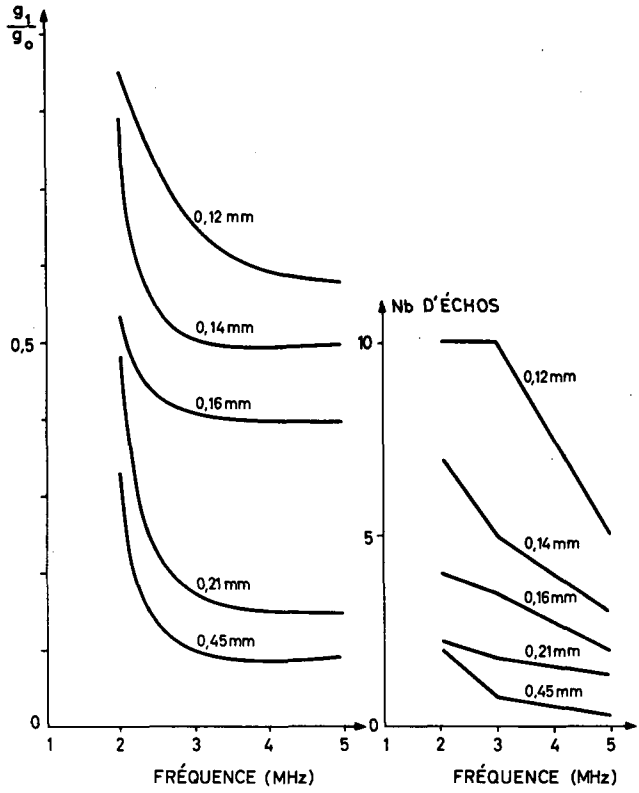

Figure 3

Sicral F_1 - Absorption ultrasonore de divers échantillons utilisés, en fonction de la fréquence.

3. 3. Choix d'une méthode de contrôle industriel

Ces essais à l'échelle du laboratoire ont permis de déterminer une méthode de contrôle industriel, dite par transmission et immersion totale. Cette méthode présente en effet, par rapport aux autres méthodes envisagées, l'avantage d'être reproductible et facilement mécanisable. Le contrôle industriel se fait par comparaison des résultats de mesure avec ceux d'un étalon semblable au matériau utilisé, et sur lequel le contrôle a également été fait par micrographies. Chaque fois que cela est possible, on réalise un étalon présentant une variation lente de la taille du grain sur toute sa longueur, afin de pouvoir apprécier par comparaison la dimension du grain de l'élément examiné (fig. 4).

4. MATÉRIEL DE CONTRÔLE UTILISÉ

Un certain nombre de problèmes d'ordre technique ont dû être résolus:

- réalisation d'un générateur d'ultrasons d'une grande stabilité;

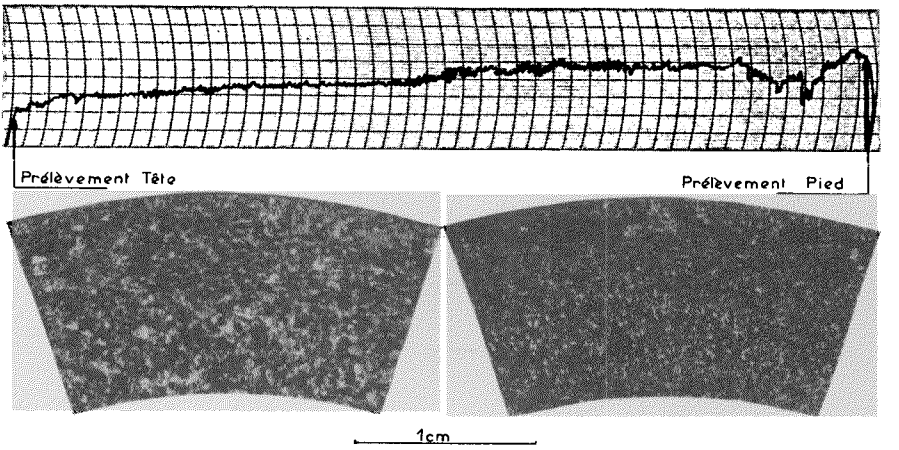

Figure 4

Etalon de sicral F_1 (diamètre: 66 x 83 mm; fréquence: 3 MHz) présentant une variation lente de la taille du grain.

- détermination d'un système d'enregistrement d'amplitude d'échos;
- réalisation d'une cuve satisfaisant aux conditions suivantes:
- possibilité d'examen en rotation de tubes ou de barres de diamètres compris entre 30 et 160 mm et de longueurs comprises entre 200 et 1500 mm;
- maintien des traducteurs animés d'un mouvement de translation en position fixe par rapport au matériau examiné.

4.1. Banc d'examen de contrôle

4.1.1. Caractéristiques mécaniques

La cuve a été construite en tôle d'acier inoxydable soudée de 1 mm d'épaisseur. Elle repose sur un socle formé de deux profilés U soudés donnant une grande rigidité à l'ensemble (fig. 5 - 5 bis). Entre la cuve et le socle sont placés un joint d'étanchéité en néoprène serré par vis et une couche de résine résistant aux détergents et produits chlorés. Les faces latérales de la cuve sont maintenues par une armature en profilé carré soudé avec interposition de tampons en caoutchouc. Sur le socle a été rapportée une table en acier inoxydable sur laquelle vient se fixer la queue d'aronde supportant les mécanismes d'entraînement des barres.

L'entraînement des barres en rotation est assuré par quatre blocs galets dont la position est réglable et qui se déplacent sur un arbre cannelé. Le chariot porte-traducteurs est entraîné en translation par une vis à billes associée à un joint de Holdam procurant un mouvement exempt de vibrations. Trois supports de traducteurs à position et orientation réglables permettent des réglages fins et reproductibles. Toutes les pièces immergées sont en acier inoxydable ou en bronze.

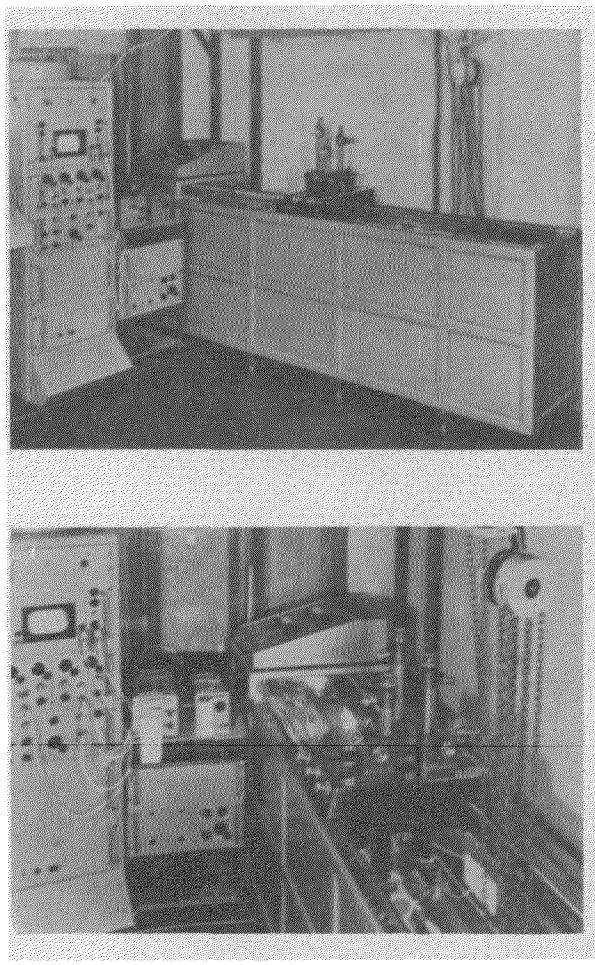

Figure 5

Vue d'ensemble de l'installation de contrôle au laboratoire.

4.1.2. Caractéristiques électriques

Les mouvements de rotation et de translation sont obtenus par des moteurs à courant continu de type shunt. Les vitesses de translation sont comprises entre 200 mm/min et 2,2 m/min. Celles de rotation sont comprises entre 4 et 40 m/min. Ces vitesses sont directement lues en m/min sur les cadrans de contrôle.

Les différentes commandes, de translation, de rotation, de l'éclairage, de la pompe, ainsi que l'affichage des vitesses sont réunis sur un pupitre de commande.

Une pompe à fort débit permet la vidange de la cuve et la récupération par filtre des déchets composés principalement d'uranium et de graphite sous forme de particules en suspension dans l'eau.

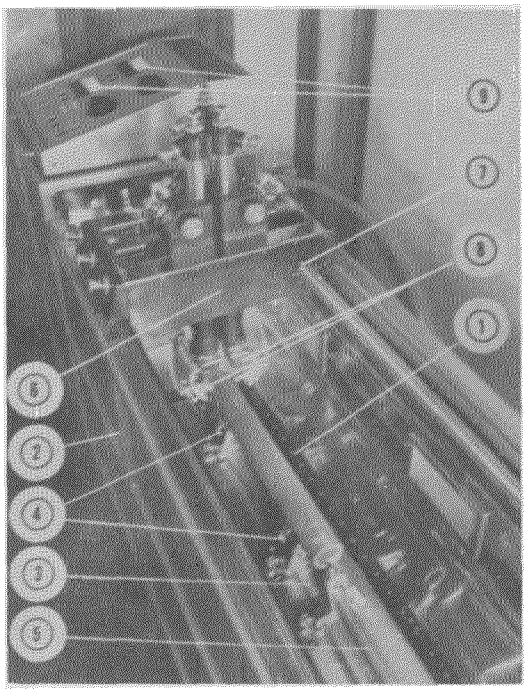

1_ Joint d'étanchéité
2_ Armature
3_ Queue d'aronde
4_ Mécanismes d'entraînement en rotation
5_ Arbre cannelé
6_ Chariot porte-transducteurs
7_ Vis à bille
8_ Supports de transducteurs
9_ Cadrans de contrôle

Figure 5 bis

Cuve de contrôle (détail).

4. 2. Equipement électronique

4.2.1. Générateur d'ultrasons

L'ensemble électronique a été modifié spécialement pour le contrôle des traitements thermiques. Il est composé d'un émetteur-récepteur de type classique («Metalloradar R6») ayant une alimentation stabilisée et deux sélecteurs d'échos avec possibilité d'enregistrement.

L'originalité de l'ensemble réside dans le système de régulation automatique d'amplitude des échos, nécessaire pour un contrôle en série où la constance de l'étalonnage est indispensable. Le système régulateur d'amplitude agit sur le gain de l'amplificateur-récepteur en fonction de l'information donnée par un jeu de traducteurs identiques aux traducteurs de mesure. Toute cause, qu'elle soit électronique ou physique (température, instabilité de l'électronique), entraîne une variation d'amplitude de l'écho de référence. Cette variation est corrigée par la régulation (modification automatique du gain); l'amplitude de l'écho de référence demeure constante. Il est ainsi toujours possible de comparer les échantillons aux étalons.

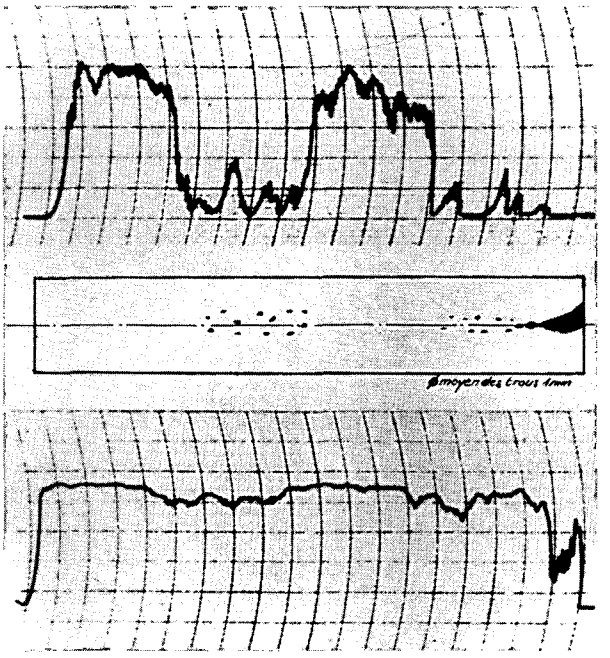

Figure 6

Elimination des cavités importantes (modification de la sensibilité).

4.2.2. Enregistreur

Une difficulté notable se présente pour l'enregistrement et le contrôle automatique des éléments. Elle résulte du fait qu'un élément présentant des cavités, retassures, etc. non gênantes pour la bonne marche du réacteur a l'apparence d'un élément mal traité. On peut évidemment lever l'ambiguïté en procédant à un second traitement ou en faisant une gammagraphie.

Il n'en demeure pas moins que cette difficulté interdit, dans les conditions actuelles, d'envisager un système de tri automatique. Seul est possible un enregistrement sur papier, il permet de connaître la qualité du barreau sur toute la longueur; le diagramme accompagne ensuite la fiche signalétique du barreau.

On procède à l'enregistrement de la manière suivante: par l'intermédiaire d'un sélecteur, l'écho choisi est enregistré après mise en forme et amplification sur un enregistreur à plume. L'amplificateur a un gain, un seuil et un temps de réponse variables. La variation du temps de réponse ou de la sensibilité permet en particulier de minimiser les effets dus à la flèche et aux faibles aspérités et cavités (fig. 6). Ce mode d'enregistrement a été retenu en raison de son faible coût d'exploitation et de sa robustesse.

5. RÉSULTATS

La méthode que nous venons d'examiner est actuellement appliquée pour le contrôle de tous les éléments en uranium faiblement allié, quelles que soient leurs dimensions. Pour les barres pleines on procède à un examen diamétral, le faisceau d'ultrasons étant perpendiculaire à l'axe de la barre. Pour les éléments annulaires l'examen se fait suivant une corde, le faisceau étant tangent à la surface interne. Dans tous les cas le pas d'examen est inférieur à 5 mm.

5.1. Fréquences d'examen utilisées

Les fréquences d'examen sont variables selon les alliages:

Matériau	Fréquence	Taille moyenne du grain
U non allié	2 MHz	0,5 mm
sicral F_1	3 MHz	0,3 mm
sicral F_2	3 MHz	0,2 mm
(Fe 0,03; Al 0,08; Cr 0,02; Si 0,035)		
U Si Fe (Si 0,1; Fe 0,03)	3 MHz	0,25 mm
U Cr (Cr 0,1)	5 MHz	0,1 mm

5.2. Différents défauts observés

En décembre 1961, plus de 4000 barreaux du type G2 en sicral F_1 ont été examinés en laboratoire avant que les usines de production soient équipées pour effectuer ce contrôle.

Les réglages utilisés étaient tels que l'on avait une réponse nulle de l'enregistreur pour une barre brute de fusion et une hauteur d'enregistrement de 30 mm pour un élément bien traité (fig. 7).

Des défauts de différentes natures ont été observés au cours de ces examens:

- un abaissement brutal de l'amplitude de l'enregistrement dans une zone du tube, dû au fait que celle-ci n'a pas été traitée par suite d'un manque d'eau ou d'un glissement dans l'inducteur (fig. 8);
- une variation très nette de l'absorption de l'énergie ultrasonore sur une extrémité ou sur la totalité du barreau, résultant d'une durée de transfert du bain de sels à la trempe trop longue (fig. 9);
- la formation d'une couronne de gros grains qui augmente l'absorption ultrasonore et qui a son origine dans une insuffisance du chauffage des extrémités (fig. 10);

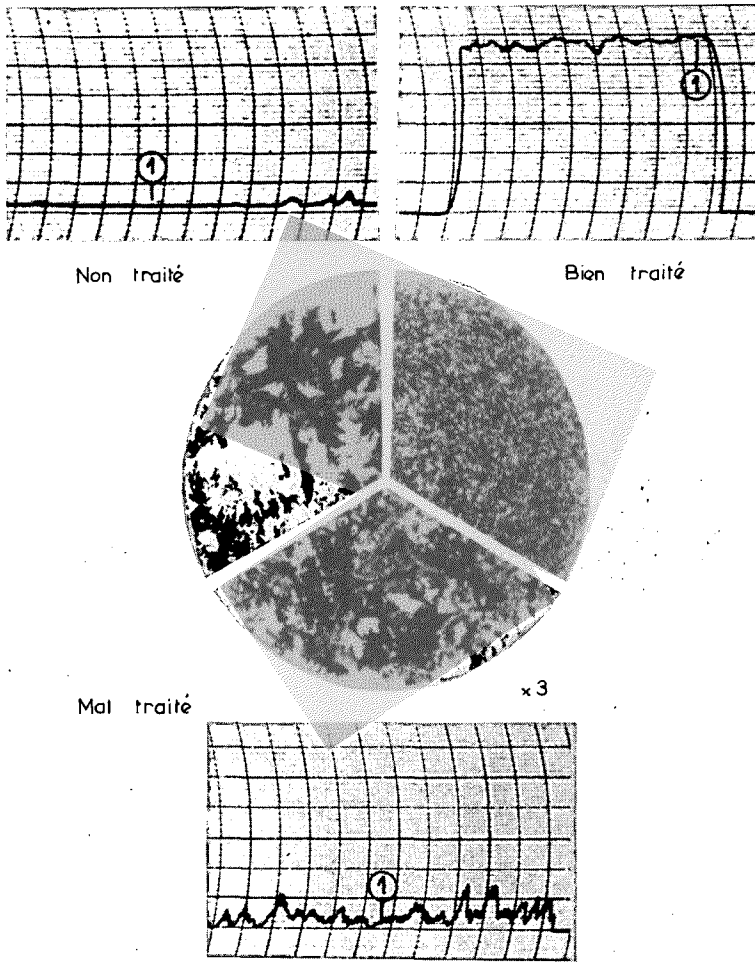

Figure 7

Barreau de sicral F_1 (diamètre: 30 mm; fréquence: 3 MHz)
non traité - bien traité - mal traité.

- tous les contrôles étant faits sur des barres brutes de fusion, il peut se former à la surface de l'élément, s'il est poreux et mal mouillé, un nuage de bulles qui modifie la transmission ultrasonore (fig. 11);
- la réponse ultrasonore peut également être perturbée, même si l'élément est bien traité, lorsque ce dernier présente de nombreuses microporosités (fig. 12).

5. 3. Mise au point d'une machine de trempe au défilé

Le contrôle ultrasonore suivant la méthode décrite plus haut a servi à la mise au point d'une machine semi-automatique de trempe au défilé pour

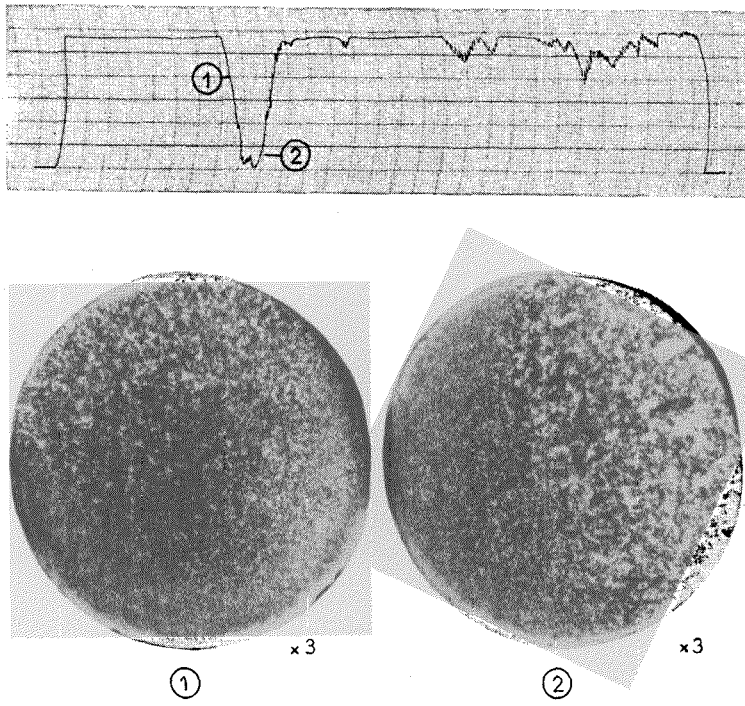

Figure 8

Barreau de sicral F_1 (diamètre: 30 mm; fréquence: 3 MHz)
Traitement au défilé - incident de trempe.

des éléments annulaires de 20 à 35 kg et de diamètres intérieur et extérieur de 54 et 70 mm, 66 et 83 mm, 70 et 95 mm respectivement.

Diverses améliorations ont pu être apportées rapidement, notamment sur les points suivants, qui permettent de corriger des déficiences de la machine qui auraient été difficilement repérables par les seuls examens micrographiques:

- il est apparu dans certains cas que des tubes entiers ou une partie des tubes n'avaient pas été portés à une température suffisante pour atteindre le point de transformation β (fig. 13a); l'enregistrement ultrasonore donnait alors une réponse nulle sur la totalité ou sur une partie du tube.
- de la même manière une insuffisance de la trempe provenant d'un mauvais réglage du collier douche est facilement observable.
- des réponses nulles sur les enregistrements peuvent traduire des frottements anormaux de glissement ou des accrochages résultant d'un mauvais centrage du tube (fig. 13b).
- l'hétérogénéité de la taille des grains le long d'une génératrice (fig. 14) entraîne des oscillations anormales sur l'enregistrement; celles-ci peuvent également être dues à un excentrement du tube.

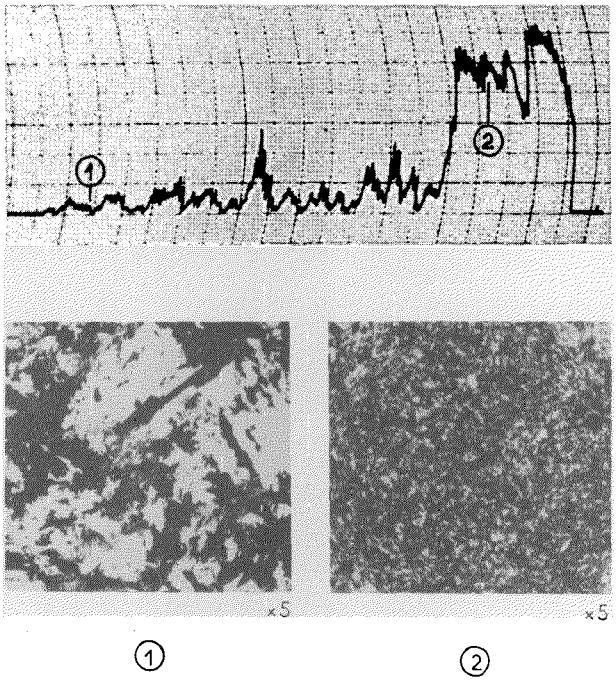

Figure 9

Barreau de sicral F_1 (diamètre: 30 mm; fréquence: 3 MHz)
Traitement en bain de sels - incident de trempe.

5. 4. Conclusion

Nous étions placés en 1960 devant la nécessité de mettre au point un contrôle rapide portant sur la totalité de l'élément combustible. Seule une méthode par ultrasons pouvait permettre d'atteindre ce résultat.

Nous avons donc été amenés à mettre au point dans le courant du second semestre de 1961 un appareillage approprié avec lequel nous avons obtenu une bonne concordance avec les examens micrographiques.

Depuis 1962, les usines de productions d'éléments se sont équipées avec ce matériel. Une de ces usines dispose actuellement d'une machine semi-automatique de contrôle dérivée de la machine que nous avons mise au point. Les manipulations de mise en place des éléments sous le faisceau ultrasonore se trouvent simplifiées, la cadence de contrôle augmentée et la main d'œuvre réduite.

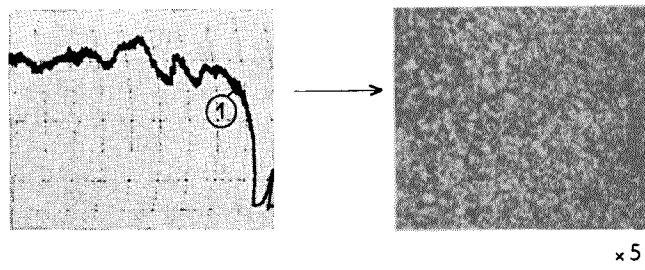

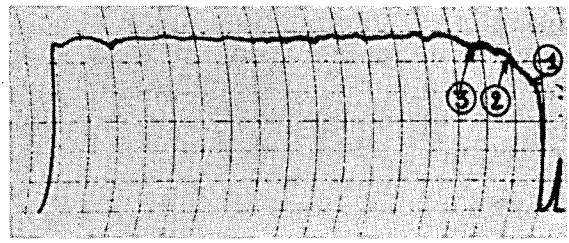

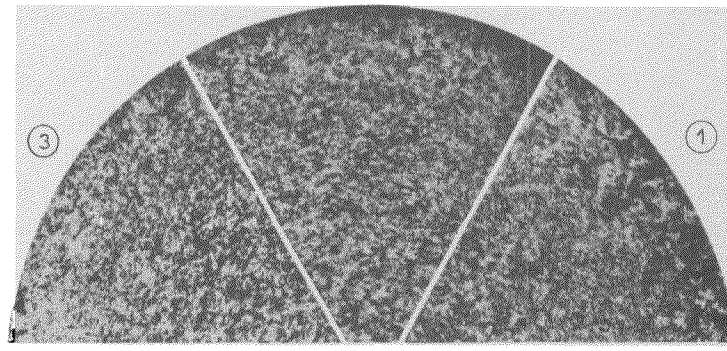

Figure 10

Barreau de sicral F_1 (diamètre: 30 mm; fréquence: 3 MHz)
Défauts d'extrémité.

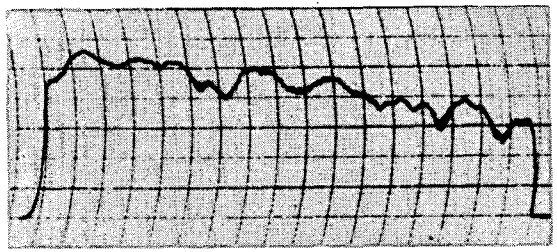

Avant mouillage

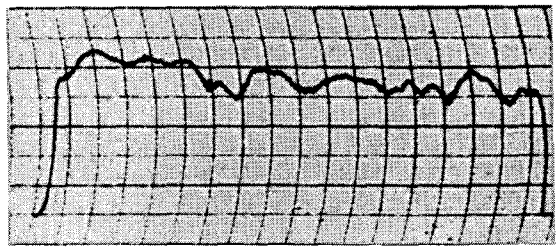

Après mouillage d'une minute

Figure 11

Barreau de sicral F_1 (diamètre: 30 mm; fréquence: 3 MHz)
Influence de l'état de surface.

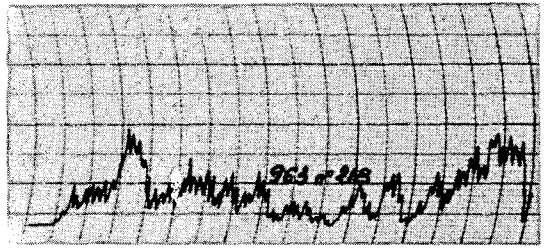

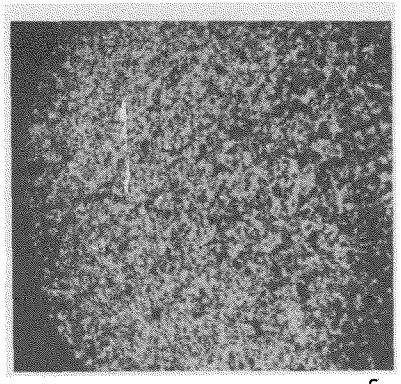

×5

Figure 12

Barreau de sicral F_1 (diamètre: 30 mm; fréquence: 3 MHz)
Influence des porosités.

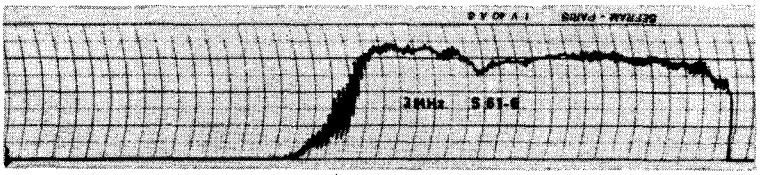

a) Chauffage insuffisant

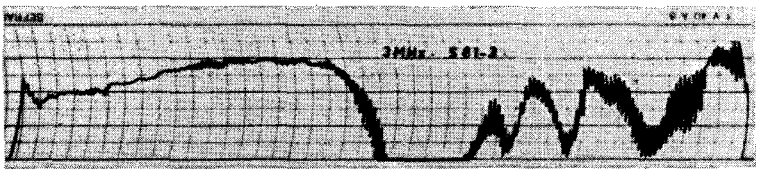

b) Mauvaise alimentation en eau

Figure 13

Tube de sicral F_1 (diamètre: 66 × 83 mm; fréquence: 3 MHz).
a) chauffage insuffisant; b) mauvaise alimentation en eau.

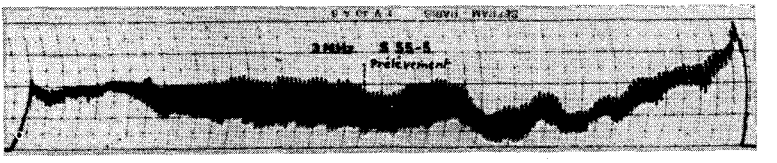

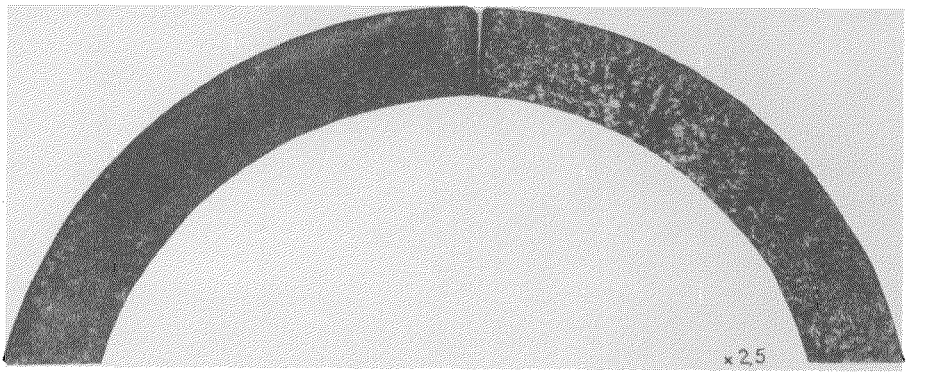

Figure 14

Tube de sicral F_1 (diamètre: 66 × 83 mm; fréquence: 3 MHz).
Hétérogénéité de la taille du grain le long d'une génératrice.

BIBLIOGRAPHIE

AUBERT, H., DESTRIBATS, M.-T., et LANIESSE, J., Contrôle ultrasonore et macrographique d'éléments annulaires 66 x 83 ou sicral F_1 fabriqué par la CERCA, DMT RMA 64-11 (27 mars 1964).

RÉFÉRENCES

[1] LANIESSE, J. et AUBERT, H., Alliages d'uranium à faible teneur pour éléments combustibles, CEA R 25-84 (1964) Ea.

[2] MASON, W. P. and McSKIMIN, H.J., Energy Losses of Sound Waves in Metals due to Scattering, J. appl. Phys. 19 (1948) 940-6.

DISCUSSION

V. V. GORSKY: Could you draw the ultrasonic diagrams for inspection of solid and tubular cores?

M.-T. DESTRIBATS:

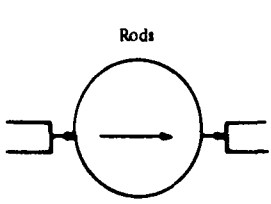

Diametral inspection

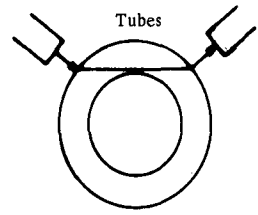

Inspection along a core

V. V. GORSKY: Did you use different ultrasonic frequencies for detecting defects and for core structure measurements?

M.-T. DESTRIBATS: Only one frequency was used. Gamma radiography was used for detecting defects such as cracks and porosity.

R. SHARPE: Have you considered presenting the ultrasonic information on a two-dimensional recorder? We have tried this and found that it can give a considerable amount of detailed information about the grain structure in uranium.

M.-T. DESTRIBATS: No, we have not been able to try this, as we have no two-dimensional recorder.

ULTRASONIC TESTING OF METALLIC URANIUM

Y. NAKAMURA AND Y. TATEISHI
TOKAI REFINERY, ATOMIC FUEL CORPORATION,
JAPAN

(Presented by T. AOKI)

Abstract — Résumé — Аннотация — Resumen

ULTRASONIC TESTING OF METALLIC URANIUM. The development of ultrasonic testing and the results of routine inspection on cast billets and rolled rods for JRR-3 fuel-elements are described. The reactor is a domestic made, heavy-water-moderated and cooled, research reactor of 10 MW capacity, with aluminium-clad metallic uranium fuel-elements.

Cast billets of 3-in diam. were rolled to rods of 1-in diam. Ultrasonic testing was applied for detecting internal voids and cracks and for evaluating random orientation and grain size after heat treatment. The ultrasonic testing of uranium was very difficult because of its high acoustic impedance, and the high sensitivity of the transducers and special beam mask were necessary for the water-immersed transmission method. A set of brass billets with artificial defects was used as the standard. During the development of these standards, several kinds of Cu-Zn alloy were examined for their acoustic properties.

Any internal defects greater than 2 mm and 0.5 mm equivalent diameter were rejected in the case of billets and rolled rods respectively. Two billets which included typical voids were rolled to size, and ultrasonic testing and radiography with Betatron were carried out at several stages to find the behaviour of the voids during fabrication.

The attenuation of ultrasonic waves is affected by the grain size, and is particularly large if the ultrasonic wave-length is comparable to the grain size. This was used for the detection of unsatisfactory heat treatment. The ultrasonic wave-speed is different in the parallel and perpendicular rolling directions in as-rolled state. This difference decreased as the temperature of heat treatment is increased; however, a small difference was observed in a beta-quenched specimen, and real acoustic isotropy was obtained by gamma-quenching.

ESSAI PAR ULTRASONS DE L'URANIUM MÉTALLIQUE. Les auteurs décrivent la mise au point d'une méthode d'essai par ultrasons et donnent les résultats du contrôle routinier de billettes moulées fondues et de barreaux laminés pour les éléments combustibles du réacteur JRR-3. Il s'agit d'un réacteur de recherche japonais, d'une puissance de 10 MW, ralenti et refroidi à l'eau lourde, qui utilise des éléments combustibles en uranium métallique sous gaine d'aluminium.

Des billettes moulées de 76 mm de diamètre sont transformées par laminage en barreaux de 25 mm de diamètre. On procède à des essais par ultrasons pour détecter les vides et les fissures internes ainsi que pour évaluer l'orientation aléatoire et la dimension des grains après traitement thermique. L'inspection par ultrasons de l'uranium est très difficile à cause de l'impédance acoustique élevée de ce métal; des traducteurs extrêmement sensibles et un masque spécial du faisceau sont nécessaires pour la méthode de transmission en immersion dans l'eau. On utilise comme étalon un jeu de billettes en loiton avec des défauts artificiels. Au cours de la mise au point de ces étalons, on a étudié les propriétés acoustiques de plusieurs alliages cuivre-zinc.

On a rejeté toutes les billettes et tous les barreaux présentant des défauts internes de plus de 2 mm et 0,5 mm de diamètre, respectivement. Deux billettes qui présentaient des vides caractéristiques ont été laminées normalement; on les a contrôlées, à divers stades des opérations, par ultrasons et par radiographie à l'aide d'un bêtatron, pour déterminer le comportement des vides.

L'atténuation des ondes ultrasonores dépend de la dimension des grains; elle est particulièrement accusée si la longueur d'onde des ultrasons est comparable à la dimension du grain. Cette particularité est utilisée pour déterminer si le traitement thermique n'était pas défectueux. La vitesse de l'onde ultrasonore est différente, après laminage, suivant qu'il s'agit de la direction parallèle ou de la direction perpendiculaire au laminage. Cette différence diminue lorsque la température du traitement thermique augmente; toutefois, on a observé

une légère différence dans un spécimen ayant subi une trempe aux rayons bêta; on a obtenu une isotropie acoustique parfaite par la trempe aux rayons gamma.

ПРОВЕРКА МЕТАЛЛИЧЕСКОГО УРАНА С ПОМОЩЬЮ УЛЬТРАЗВУКА. Описываются разработка метода проверки с помощью ультразвука и результаты обычной проверки литых заготовок и катаных стержней для топливных элементов реактора JRR-3. Этот исследовательский реактор установленной мощностью 10 мгвт является реактором отечественного производства. В качестве замедлителя и теплоносителя в нем используется тяжелая вода, а в качестве топлива—металлический уран в алюминиевой оболочке.

Литые заготовки диаметром 3 дюйма были прокатаны в стержни диаметром 1 дюйм. Для обнаружения внутренних пустот и трещин и для оценки беспорядочной ориентировки и размеров зерен после термообработки применили ультразвук. Контроль урана с помощью ультразвука является очень трудным делом, так как уран имеет большое акустическое сопротивление, и метод проверки прохождения звука в погруженном в воду состоянии потребовал очень чувствительных датчиков и специальной защиты от пучка. В качестве стандарта использовали набор бронзовых заготовок с искусственными дефектами. В ходе разработки этих стандартов были исследованы акустические свойства нескольких видов сплава Cu—Zn.

Все заготовки и катаные стержни с внутренними дефектами, эквивалентный диаметр которых превышал 2 мм и 0,5 мм соответственно, были забракованы. Две заготовки, содержащие типичные пустоты, были прокатаны до требуемого размера, и на нескольких стадиях их испытали с помощью ультразвука и радиографии с помощью бетатрона, чтобы выявить поведение пустот в процессе изготовления стержней.

На ослабление ультразвуковых волн оказывает влияние размер зерен, и оно особенно велико в том случае, если длина ультразвуковой волны сравнима с размером зерен. Это было использовано для обнаружения неудовлетворительной термообработки. В прокатанном состоянии скорость ультразвуковой волны неодинакова при прокатке в параллельном и перпендикулярном направлениях. Эта разница уменьшается при повышении температуры термообработки, однако была отмечена небольшая разница в образце, прошедшем бета-закалку, а при гамма-закалке была получена действительная акустическая изотропия.

ENSAYO ULTRASONICO DEL URANIO METALICO. Se describe el perfeccionamiento del método ultrasónico de ensayo y los resultados de la inspección corriente del metal en lingotes colados y de las varillas laminadas que se destinan a los elementos combustibles del reactor japonés de investigación Nº 3 (JRR-3). Este reactor de investigación de 10 MW construido en el Japón, es moderado y refrigerado por agua pesada, y sus elementos combustibles consisten en uranio metálico revestido de aluminio.

Con el laminado se reduce a 1 pulg el diámetro de los lingotes colados, que asciende inicialmente de 3 pulg. El ensayo ultrasónico se aplica para localizar los huecos internos y las grietas, y para evaluar la orientación aleatoria y el tamaño del grano tras el tratamiento térmico. El ensayo ultrasónico del uranio es muy difícil a causa de su alta impedancia acústica; por ello, para aplicar el método de inmersión en agua, es preciso utilizar transductores de alta sensibilidad y un diafragma especial para limitar el haz. Como patrón se ha empleado una serie de lingotes de latón con defectos introducidos deliberadamente. Durante la preparación de los patrones, se estudiaron las propiedades acústicas de varias clases de aleaciones de cobre y cinc.

Se rechazaron los lingotes y varillas laminadas que tenían defectos internos de un diámetro equivalente a más de 2 mm y 0,5 mm respectivamente. Dos de los primeros, con fallas típicas, se laminaron al tamaño adecuado y se sometieron en diversas fases al ensayo ultrasónico y radiográfico con Betatrón para observar la evolución de los defectos durante el proceso de fabricación.

El tamaño de grano influye en la atenuación de las ondas ultrasónicas, que resulta particularmente intensa si la longitud de onda es comparable al tamaño del grano. Esta propiedad se aprovecha para detectar un tratamiento térmico defectuoso. En el metal laminado, la onda ultrasónica se propaga con diferente velocidad según sea paralela o perpendicular a la dirección del laminado. Esa diferencia disminuye a medida que aumenta la temperatura del tratamiento térmico; no obstante, se observa una pequeña diferencia en las muestras enfriadas en fase beta, y se consigue una auténtica isotropía acústica por enfriamiento en fase gamma.

INTRODUCTION

Japan Research Reactor-3 (JRR-3) is a heavy-water-moderated and -cooled research reactor of 10 MW capacity, with aluminium-clad metallic

uranium fuel elements. Since the reactor was the first domestic reactor in Japan, it was necessary to develop fuel fabrication techniques as well as non-destructive testing in order to get satisfactory fuel elements.

The Atomic Fuel Corporation, one of the government establishments, supplied cast billets to private companies for rolling, and inspected their products on behalf of JAERI where the reactor is installed.

Owing to the limits in the rolling mills, the size of the billets was relatively small, namely 68 mm and 63 mm in diameter and 730 mm long and there were some difficulties in the casting operation. A suitable inspection technique was required for the quality control in the metal-production plant.

Ultrasonic testing was applied for the detection of internal voids and cracks in the routine production of cast billets. This technique was also applied to the inspection of rolled rods and for the evaluation of random crystal orientation and grain size after the heat treatment.

INSPECTION OF CAST BILLETS

General

As metallic uranium has a large volume change and a small latent heat during solidification, high solubilities of gas in liquid state, and high density, it is very apt to include casting defects such as shrinkage cavity and porosity. It was very important to reject unsound billets, as the total reduction during fabrication was small because of the small size of billets. Uranium is one of the most difficult metals for ultrasonic testing because of its high density, low elastic modulus, large grain size and resultant high acoustic impedance as shown in Table I.

A high-sensitive lithium sulphate transducer and a foamed polystyrene beam mask was necessary to obtain good resolution of internal defects, though the mask reduced the sonic energy as shown in Table II.

Testing method

Test results of the water-immersion transmission method were recorded through an alarm circuit and a electro-discharge recorder to get a defects pattern. The rotation of the specimen was recorded in a horizontal direction and the received sonic energy, greater than pre-set attenuation level, resulted in a solid plotted line. A block diagram of the equipment system is shown in Fig. 1 and a typical result is shown in Fig. 2.

Routine inspection was conducted according to the following conditions:

(1) Cast billet (63 mm diam. or 68 mm diam., machined surface),

Test method	: water-immersion transmission method,
Scanning	: rotating specimen at 20 rpm longitudinally, moving transducer system at 120 mm/min,
Overlap area	: 60%,
Transducer	: quartz-crystal emitter lithium sulphate receiver,

TABLE I

PROPERTIES OF SEVERAL METALS AND ALLOY

	Aluminium	70/30 brass	Lead	Uranium
Density (g/cm^3)	2.69	8.5	11.3	19
Sonic speed (cm/s)	6.35×10^5	4.64×10^5	2.26×10^5	3.43×10^5
Attenuation (db/cm) at 2.25 Mc	0.02	2.0	-	2.0
Acoustic impedance	1.71×10^6	3.96×10^6	2.25×10^6	6.52×10^6
Ejection fraction of sonic energy from water (%)	28	13	20	10

TABLE II

SONIC SENSITIVITY OF THE TESTING SYSTEM

Transmitter	Receiver	Mask	Sensitivity difference (db)
Quartz crystal	Quartz crystal	Without	0
Quartz crystal	Quartz crystal	With	-3 – -5
Quartz crystal	Lithium sulphate	Without	+18 – +20
Quartz crystal	Lithium sulphate	With	+13 – +15

Beam mask : foamed polystyrene with a window of 5 mm × 15 mm,
Test frequency : 2.25 megacycles
Pre-set attenuation level : 20 and 25 db below the maximum received energy along the whole specimen.

(2) Cast rod (25 mm diam., machined surface)
Same as above, but the evaluation was done at the pre-set attenuation level of 15 and 20 db.

(3) Wrought rod (25 mm diam., machined surface rolled rod or extruded rod)
Test frequency : 5 megacycles
Pre-set attenuation level : 3 and 5 db; other conditions were same as (1).

Testing was done at two pre-set attenuation levels as described above, and careful observation of the two defect patterns gave information about the defects as shown in Fig. 3.

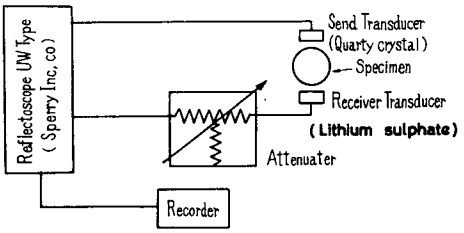

Fig. 1

Block diagram of the testing system

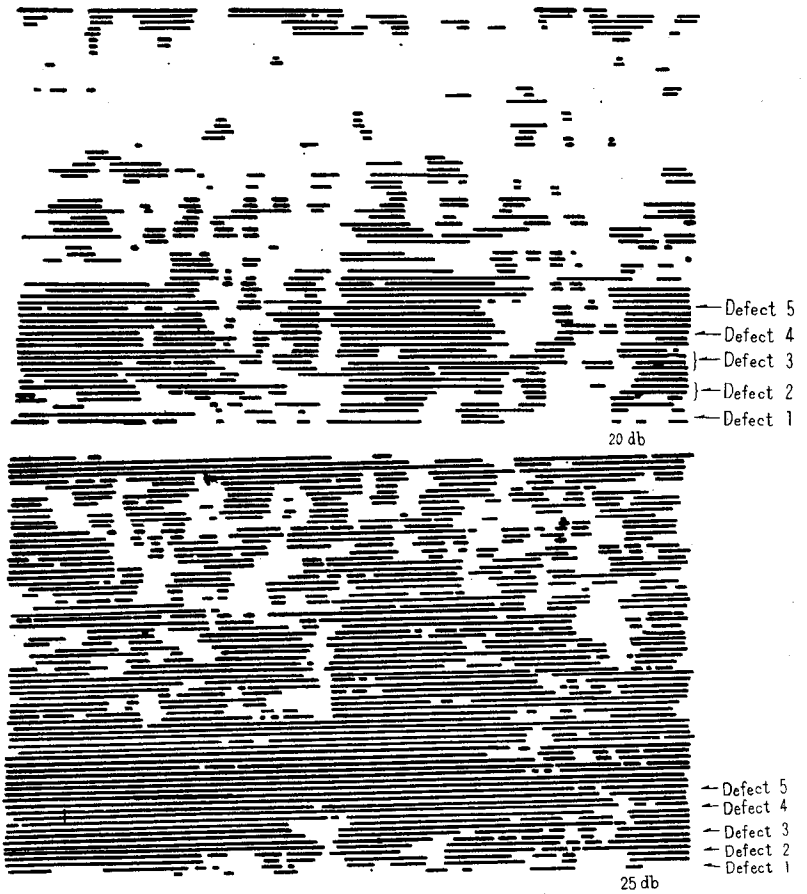

Fig. 2

A typical result of ultrasonic testing on a cast billet

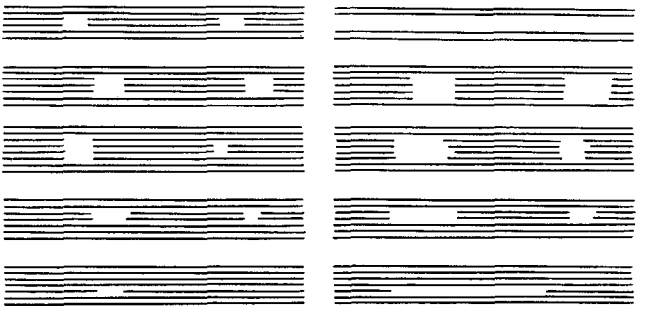

Fig. 3

Explanatory diagrams of the evaluation of test results by the two-level pre-set attenuation method

Test results in routine work

Hundreds of cast billets were inspected, and the results were used to improve casting conditions. The formation of internal defects in cast billets is affected by casting temperatures, mould temperature, spout size in the crucible and distributor, vacuum level and so on, but most defects were found in the area about 200 mm above the bottom and the 200 mm below the top.

Detectable sizes of the internal defects by this method are shown in Table III.

The behaviour of the internal voids was traced by ultrasonic testing, γ-ray radiography and X-ray radiography by betatron at several rolling stages. Specifications on the permissible size of internal defects in the cast billets were decided from this experiment. Figure 4 shows the correlations between the evaluation by ultrasonic testing (A = good, B = medium, C = poor) and the apparent density of the billet calculated from the dimensions and its weight.

Small uranium slugs (25 mm diam. × 200 mm) for a subcritical exponential experiment were machined from cast bar (27 mm diam × 900 mm). Three ways of fabrication were compared from the standpoint of economy and product qualities. The product qualities were specified by their apparent density and surface conditions. Surface defects indices, according to their sizes, were totalled for each slug. In group A, cast bars, 900 mm long, were surface-machined and sectioned into four parts, and a slug was machined from each part and then inspected. Some slugs were rejected according to the specifications. In group B, cast bars were inspected by ultrasonic testing after surface machining and slugs were machined from sound parts. Consequently, sometimes less than four slugs were obtained from one cast bar. Finished slugs were re-inspected. In group C, cast billets of 3 in diam. were rolled to size, and the slugs were machined from a rolled rod and then inspected. The inspection results are shown in Fig. 5.

TABLE III

DETECTABLE SIZES OF THE INTERNAL DEFECTS

	Mask size (mm)	Pre-set level (db)	Detectable defect	
			Single defect (mm diam.)	Group defect (mm diam.)
Cast billet	5×15	20, 25	2.0	0.8
Cast bar	5×15	15, 20	2.0	0.8
Cast and heat-treated bar	5×15	5, 7	1.5	0.3
Rolled rod (diam.)	4.0	3, 5	0.3	0.1

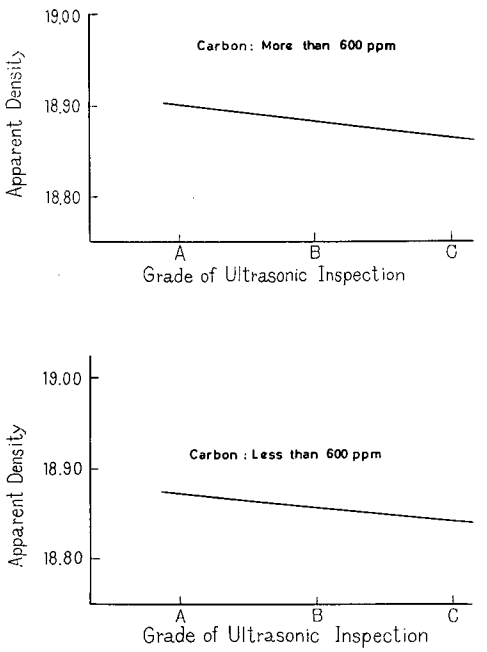

Fig. 4

Comparison of ultrasonic testing versus apparent density of billet

In this particular case the specifications for the product were not so severe, and final fabrication was conducted according to A, but B might be preferable if the specifications were much more severe.

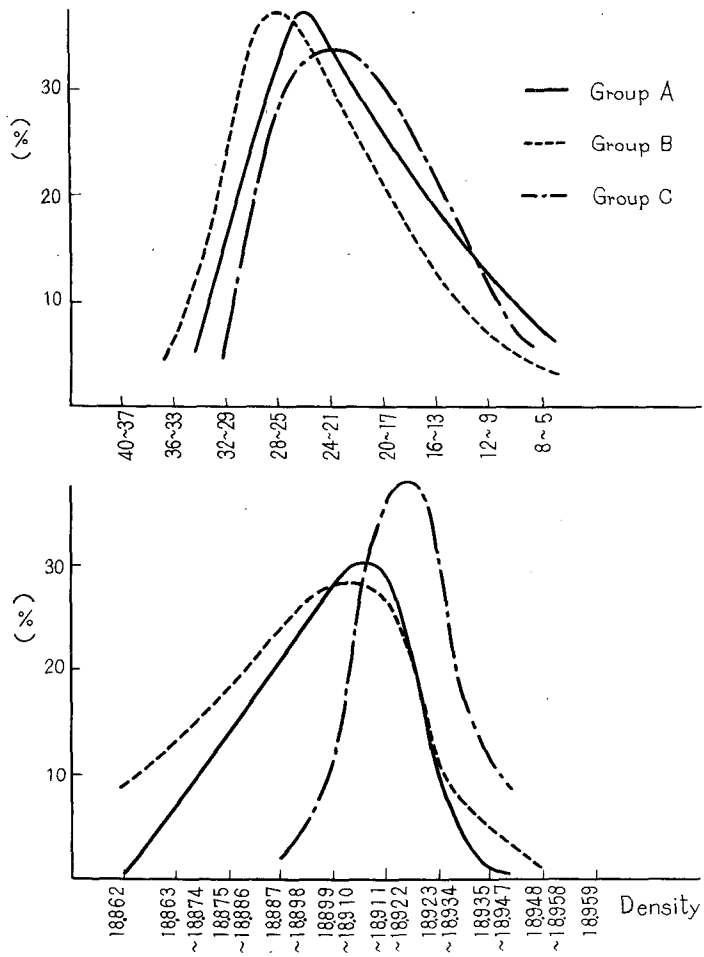

Fig.5

Inspection results of uranium slugs

Preparation of the test standard

A test standard which contains some artificial or pre-determined defects is desirable in routine ultrasonic testing. However, the machining of uranium to reach such a standard was very difficult. Attempts were made to get a model or stand-in instead of uranium. As shown in Figs. 6 and 7, 70/30 brass was found to be similar acoustically to uranium.

Four sections of this material, in whose interface several artificial defects were machined, were put together with thin films of soft solder as shown in Fig. 8. The acoustic resistance through this film was 2-3 db.

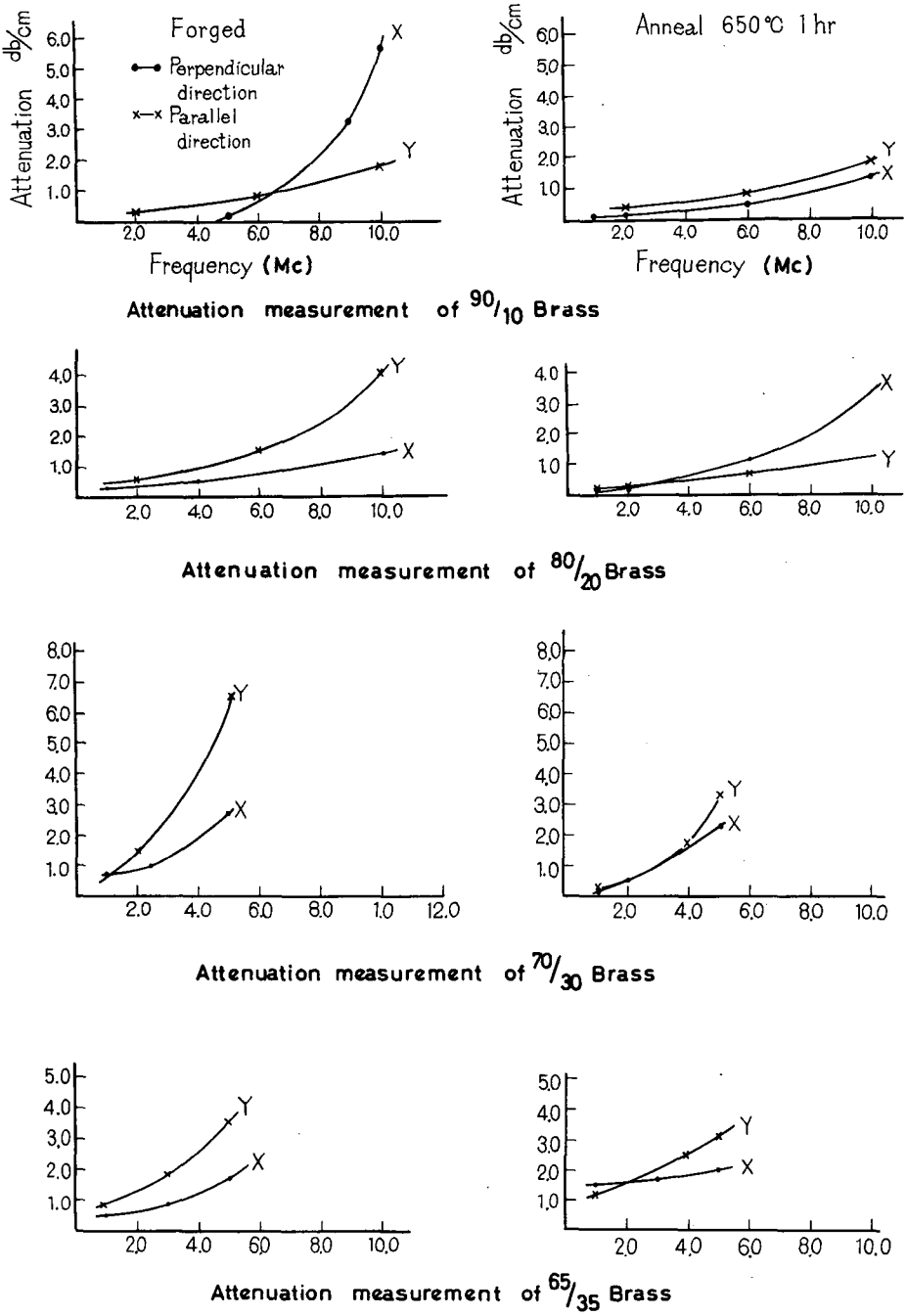

Fig. 6

Acoustic properties of copper-zinc alloys

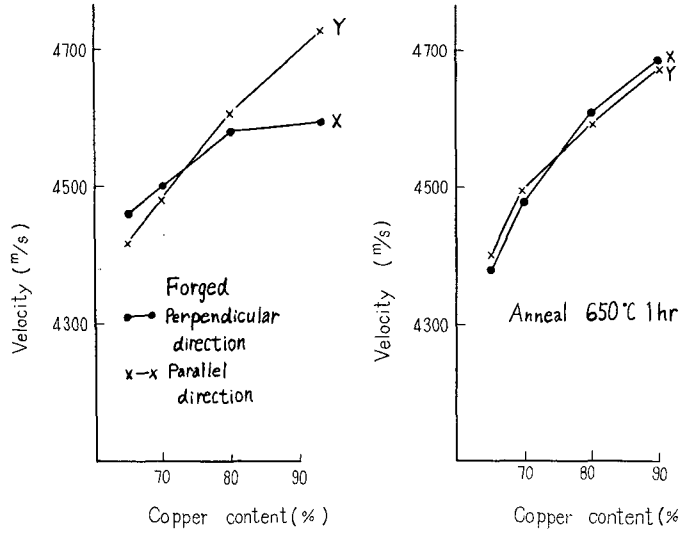

Fig. 7

Acoustic properties of copper-zinc alloy

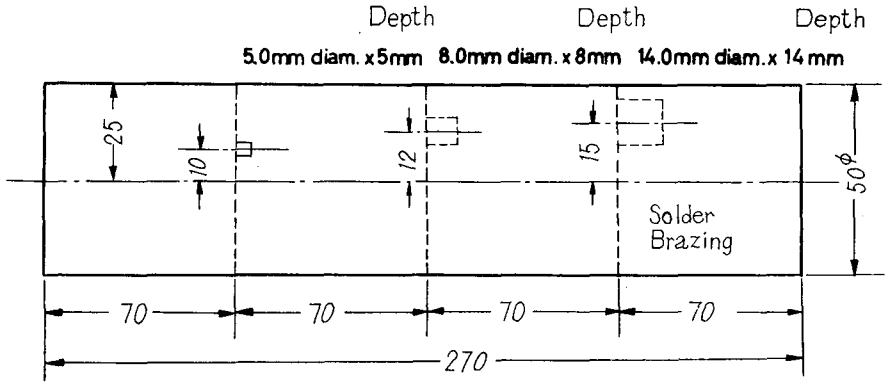

Fig. 8

Test standard block

EXAMINATION OF ISOTROPY IN URANIUM BY ULTRASONIC TESTING

A random crystal orientation is required to avoid preferential irradiation growth, and this state is obtained by heat treatment after rolling. A 20× 20× 20-mm specimen was sectioned from alpha-rolled rod. Sonic speed was measured in the parallel and perpendicular directions against rolling direction by an ultrasonic thickness meter. Grain-orientation measurement by X-ray and metallography were conducted on the specimen. The specimen was heated for half-an-hour at various temperatures step by step and afterwards quenched in water and measured by ultrasonic testing, X-ray and

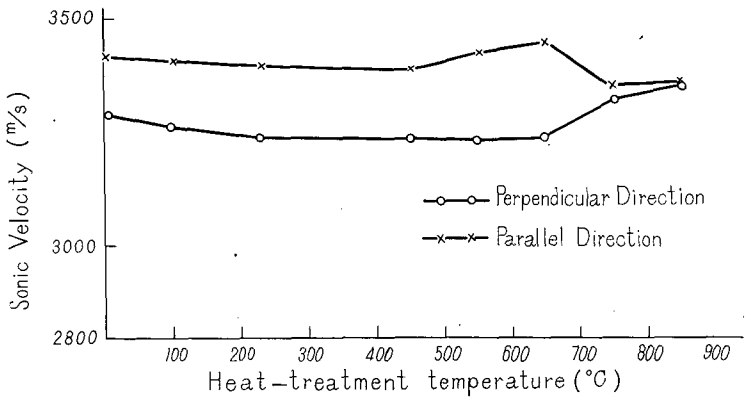

Fig. 9

Acoustic properties of the heat-treated specimen

microscopy. The results are shown in Figs. 9 and 10. As shown in these Figures, the acoustic isotropy is obtained by heat treatment at 750°C, and it has a good correspondence in X-ray analysis, but no difference was observed by metallography on the surfaces of the two directions in the specimen that was heat-treated at temperatures higher than 450°C. This testing was used for evaluating the heat-treatment quality.

EXAMINATION OF URANIUM GRAIN-SIZE BY ULTRASONIC TESTING

Several uranium specimens of different grain size were tested ultrasonically with various frequencies. The results are shown in Fig. 11. The sonic attenuation becomes remarkable at the frequency where the wavelength inside the specimen is close to its grain size.

This phenomenon was used for detecting faulty heat treatment of the rods. It was rather easy to detect the part of a rod which had a small grain size ($\sim 50\ \mu m$), or a very large one (larger than 500 μm), but the determination of grain size within this range failed because of the local heterogenity of grain size, or their non-uniform grain forms as shown in Table IV.

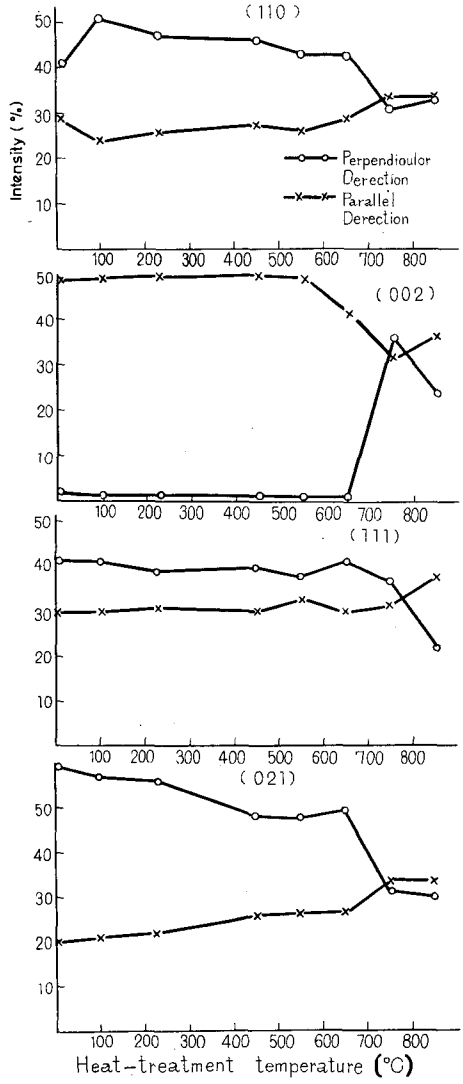

Fig. 10

X-ray analysis of the specimen

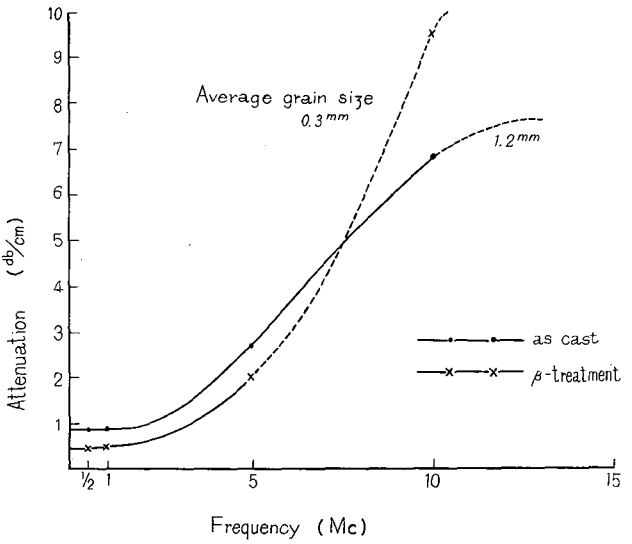

Fig. 11

Attentuation of ultrasonic wave in specimens of different grain size

TABLE IV

ATTENUATION OF ULTRASONIC WAVE IN SPECIMENS OF DIFFERENT GRAIN SIZE

Temperature (°C)	Holding time (min)	Attenuation (db)	Grain size (μm)
700	10	12	180
716	10	8	270
730	10	6.5	180
730	5	7.0	230
735	10	6.0	190
735	5	12.5	190
740	10	7.5	170
740	10	7.0	170
800	10	24.0	190

ULTRASONIC WATER-GAP MEASUREMENTS IN MTR FUEL ELEMENTS

R. DEKNOCK
METALLURGY DEPARTMENT, S. C. K. /C. E. N.,
MOL, BELGIUM

(Presented by P. de MEESTER)

Abstract — Résumé — Аннотация — Resumen

ULTRASONIC WATER-GAP MEASUREMENTS IN MTR FUEL ELEMENTS. The high thermal fluxes, which are usual in the latest materials testing reactors, impose suitable paths for uniform heat transfer and a reliable heat removal avoiding bulk-vapour formation. Furthermore, to control the over-all swelling and reactor fuel behaviour, water-gap measurements will also be performed in post-irradiation experiments on spent fuel elements. For that purpose, a probe for measuring the 3-mm water-gap of the BR-2 fuel element over a 1-m length, based on the principle of ultrasonics, has been developed. In the case of post-irradiation experiments, the measuring probe should operate in a fuel element by being immersed in a water pool at a depth of at least 6 m. The probe can withstand prolonged immersion in water and is not affected by normal gamma-irradiation doses.

Although operating on the usual pulse-reflection method, the system allows emitted and reflected pulses to be separated by a 10-MHz ferro-electric crystal with high inherent energy dissipation.

Oscilloscope read-out can be used, whereby the time is displayed on the horizontal axis, the scanning speed being adjusted to bear a direct relation to the velocity of wave propagation, i.e. the gap distance.

This type of read-out is satisfactory where the number of measurements is restricted, but chart recorder read-out is obviously desirable. In this case, emitted and reflected pulses are shaped and fed to a time-voltage converter using transistor logic techniques. The instrument allows continuous adjustment of output zero for any arbitrary gap distance between 2 and 4 mm thereby permitting zero-centre recording. Furthermore, any desired 100-μm gap distance variation can give a stable 1-V output voltage to a recorder. An accuracy of 5-μm gap-distance variation is easily obtained. Several fuel elements have been measured. The results and reproducibility were very satisfactory.

MESURE PAR ULTRASONS DES ESPACES INTERCALAIRES DANS LES ÉLEMENTS COMBUSTIBLES DES RÉACTEURS D'ESSAI DE MATÉRIAUX. Etant donné que dans les plus récents réacteurs d'essai de matériaux les flux thermiques sont généralement élevés, il est indispensable de prévoir un transfert de chaleur uniforme et un refroidissement régulier empêchant toute formation massive de vapeur. En outre, pour déterminer le gonflement et le comportement général du combustible dans le réacteur, il faudra mesurer les espaces intercalaires dans les éléments combustibles au cours de contrôles après irradiation. A cette fin, on a mis au point une sonde fondée sur le principe des ultrasons, qui permet de mesurer les espaces intercalaires de 3 mm sur 1 m de long dans les éléments combustibles du réacteur BR-2. Lorsqu'on procède à des expériences après irradiation, la sonde doit pouvoir fonctionner dans un élément combustible immergé dans un réservoir d'eau à une profondeur de 6 m au minimum. La sonde peut résister à une immersion prolongée dans l'eau et n'est pas endommagée par une irradiation gamma à des doses normales.

Bien que le système soit fondé sur la méthode classique de la réflexion des impulsions, il permet de séparer les impulsions émises des impulsions réfléchies au moyen d'un cristal ferroélectrique de 10 MHz à pouvoir élevé de dispersion de l'énergie.

Les résultats des mesures peuvent être lus directement sur un oscilloscope: le temps est indiqué sur l'axe horizontal et la vitesse d'exploration est réglée de manière à se trouver en relation directe avec la vitesse de propagation de l'onde, c'est-à-dire avec la distance intercalaire.

Ce mode de lecture est satisfaisant lorsqu'on procède à un nombre limité de mesures, mais il est évidemment préférable d'enregistrer les résultats sur un graphique. Dans ce cas, les impulsions incidentes et les impulsions réfléchies sont transmises à un convertisseur temps-tension au moyen d'un circuit logique transistorisé. Cet appareil permet un ajustement continu du zéro de sortie pour toute distance intercalaire

choisie arbitrairement entre 2 et 4 mm, grâce à quoi on peut obtenir un enregistrement autour d'un axe zéro. En outre, toute variation de 100 μm de la distance intercalaire fournit à un enregistreur une tension stable de sortie de 1 V. Il est facile de mesurer les variations des distances intercalaires avec une précision de 5 μm. Les mesures ont été faites pour plusieurs éléments combustibles. Les résultats et la reproductibilité sont très satisfaisants.

ИЗМЕРЕНИЯ ВОДЯНОГО ЗАЗОРА В ТЕПЛОВЫДЕЛЯЮЩИХ ЭЛЕМЕНТАХ ДЛЯ МАТЕРИАЛОВЕДЧЕСКОГО РЕАКТОРА С ПОМОЩЬЮ УЛЬТРАЗВУКА. Сильные потоки тепловых нейтронов, которые обычно возникают в новейших реакторах для испытания материалов, являются подходящим средством равномерной теплопередачи и надежного отвода тепла, с помощью которого можно избежать образования пара в больших объемах.

Кроме того, в целях контроля над общим распуханием и поведением реакторного топлива измеряют водяной зазор при экспериментах после облучения с отработанными тепловыделяющими элементами.

С этой целью был разработан зонд для измерения 3-мм водяного зазора тепловыделяющего элемента испытательного реактора BR-2 длиной более 1 м, в основу которого положен принцип ультразвука. При экспериментах после облучения измерительный зонд должен действовать в тепловыделяющем элементе, погруженном в бассейн на глубину не менее 6 м. Зонд может выдержать погружение в воду продолжительный период времени, и он не подвергается воздействию обычных доз гамма-облучения.

Хотя система действует на основе обычного метода отражения импульсов, она позволяет разделять испускаемые и отраженные импульсы с помощью 10 Мгц ферроэлектрического кристалла, которому свойственно большое рассеяние энергии.

Можно использовать запись показаний осциллоскопа, в котором время регистрируется на горизонтальной оси, скорость сканнирования подбирается в соответствии со скоростью распространения волны, т.е. с величиной зазора.

Такая запись показаний является удовлетворительной в отношении ограниченного числа измерений, однако явно целесообразно иметь запись показаний самописца. В этом случае испускаемые и отраженные импульсы формируются и подаются в преобразователь время-напряжение с помощью логической схемы с использованием транзистора. С помощью этого прибора можно непрерывно подбирать нулевое значение выхода для любой произвольной величины зазора между 2 и 4 мм, что позволяет использовать нулевой метод записи. Кроме того, путем любого желательного изменения величины зазора на 100 мк можно получить устойчивое выходное напряжение 1 вольт для регистратора. Можно легко контролировать изменение величины зазора с точностью до 5 мк.

Измерено несколько тепловыделяющих элементов. Результаты и воспроизводимость являются весьма удовлетворительными.

MEDICION ULTRASONICA DE LA CAPA DE AGUA EN ELEMENTOS COMBUSTIBLES PARA REACTORES DE ENSAYO DE MATERIALES. Los elevados flujos térmicos que suelen alcanzarse en los recientes reactores de ensayo de materiales, exigen recorridos adecuados para lograr una transmisión uniforme de calor y una disipación segura del mismo, evitando así la formación de vapor en la masa.

Además, a fin de controlar el hinchamiento y el comportamiento del combustible en el reactor, también debe medirse la capa de agua en experimentos realizados después de la irradiación, con elementos combustibles agotados.

A tal efecto se ha diseñado una sonda ultrasónica destinada a medir, en una longitud de 1 m el espesor de 3 mm de agua correspondiente al elemento combustible BR-2. En el caso de los experimentos posteriores a la irradiación, es necesario trabajar con el elemento combustible sumergido en un tanque de agua, a profundidad no menor de 6 m. La sonda puede resistir una prolongada inmersión en agua, y no le afectan las dosis normales de radiación gamma.

Aunque proyectado conforme al método usual de reflexión de impulsos, el sistema permite separar pulsos emitidos y reflejados, usando un cristal ferro-eléctrico de 10 MHz, con elevada disipación inherente de energía.

Puede usarse un osciloscopio para la lectura, en cuyo caso el tiempo se representa en el eje horizontal, regulándose la velocidad de barrido de manera que sea directamente proporcional a la velocidad de propagación de la onda, es decir, al espesor de la capa de agua.

Este tipo de representación da resultados satisfactorios cuando setrata de un número limitado de mediciones, pero sin duda resulta más conveniente el registro gráfico. En este caso, se da a los impulsos emitidos y reflejados la forma deseada y se les inyecta en un convertidor tiempo-tensión con circuitos lógicos transistorizados. El instrumento permite un ajuste continuo del cero para cualquier espesor arbitrario de la capa

de agua entre 2 y 4 mm, con lo cual posibilita un registro con el cero en el centro de la escala. Además, cualquier intervalo deseado de 100 μm puede dar una tensión estable de 1 V a la salida para accionar un registrador. Se puede medir fácilmente cualquier variación en el espesor del agua con una precisión de 5 μm. Se han medido con este método varios elementos combustibles, y los resultados y la reproducibilidad fueron muy satisfactorios.

INTRODUCTION

The high thermal fluxes, which are usual in the latest materials testing reactors, impose suitable paths for uniform heat transfer and a reliable heat removal avoiding bulk vapour formation. The heat output of a BR-2 element, consisting of six co-axial cylindrical fuel tubes, 970 mm long, is evacuated by a pressurized water-flow through a gap of about 3 mm between the cylinders. A slight bowing or eccentricity of the cylinders may reduce this gap. Therefore, the radial distances between the successive fuel tubes of a BR-2 element are subjected to a severe inspection technique. Furthermore, to control the over-all swelling and reactor-fuel behaviour, water-gap measurements will also be done in post-irradiation experiments on spent fuel elements. In the latter case, the measuring probe should operate in a fuel element immersed in a water pool at a depth of at least 6 m.

A survey of several gauging systems for water-gap measurement has been given elsewhere [1]. Of the different devices discussed, the ultrasonic one seems the most reliable, especially for post-irradiation measurements.

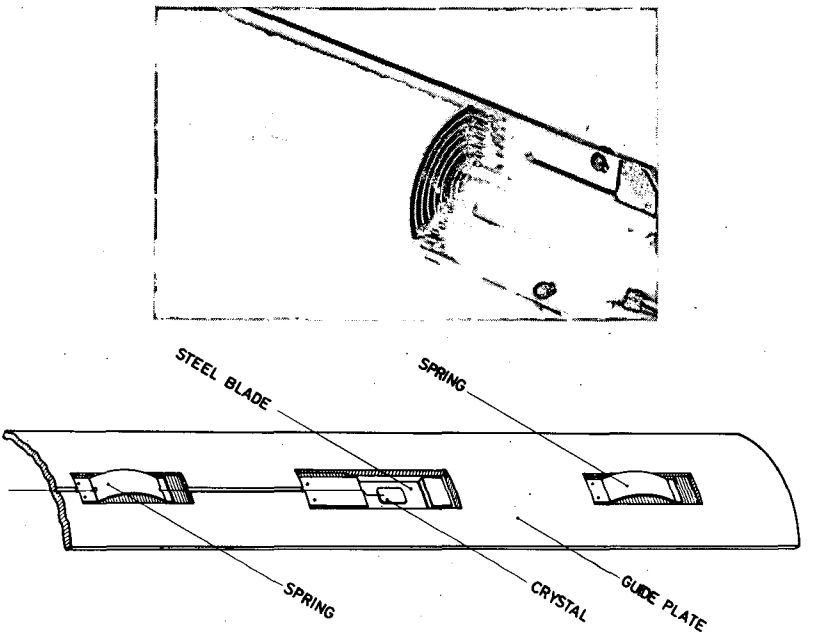

Fig. 1a and 1b

The probe assembly

PRINCIPLE OF MEASUREMENT

One of the more common ultrasonic techniques, which is readily adaptable to the inspection of the radial distance between two successive tubes of a BR-2 fuel element, is the pulse-echo method. The probe consists of a piezo-electric plate mounted on a long steel blade acting as the insertion handle and pressed against one of the cylinder walls by springs (Fig. 1).

The plate is energized by the discharge of a capacitor and controlled by firing a silicon controlled rectifier. The resulting ultrasonic energy is directed to the other cylinder wall and the reflected energy received by the plate is re-converted into an electric signal. The significant parameter for distance measurements is the time interval during transmission and reception of the acoustic energy. As the speed of propagation of the wave through the medium involved is constant and accurately known, the time interval is directly proportional to the gap.

Oscilloscope read-out can be used, whereby the time is displayed on the X-axis, the scanning speed being adjusted to bear a direct relation to the velocity of wave propagation, i.e. the gap distance. The emitted and reflected pulses are presented to the Y-plates of the cathode-ray tube. This type of read-out is satisfactory in a restricted number of measurements, but chart recorder read-out is obviously desirable. In this case emitted and reflected pulses are shaped and fed to a time-voltage convertor.

REQUIREMENTS FOR THE PROBE AND THE INSTRUMENTATION

Each piezo-electric material is particularly efficient for the conversion of electrical energy into mechanical energy, and is further efficient for the reverse transformation. For given energizing, transmitting and reflecting conditions, the output received from crystals of one material relative to another is given by the loop gain. The loop gain determines the inherent sensitivity of the crystal and also indicates the damping, which may be tolerated before the over-all sensitivity becomes too low. In the practical case of a 3-mm gap, reduced by the probe thickness, the choice of a piezo-electric material relative to this loop gain is not critical, since the inverse square reduction of the intensity versus the distance may be neglected. Furthermore, the acoustical impedance of the water medium (1.5×10^6 kg/m^2 s) and the aluminium wall reflector (17×10^6 kg/m^2 s) are sufficiently different to ensure enough reflection.

If a plate of piezo-electric material is shock-excited, the pulses of mechanical energy leaving the slab consist of a damped wave-train at the natural frequency of the slab. To separate the electric pulses from the closely-spaced transmitting and reflecting mechanical wave-trains, the ringing time must be short, so that the crystal is quiescent when it receives the reflected echo. The ringing time is reduced by increasing the damping of the probe crystal. A greater damping widens the bandwidth. This improves the response of the crystal to pulses having a fast rise-time. The position of the pulse is therefore accurately defined. Since external loading of the crystal is almost impossible, a crystal with a large capacity for dissipating the vibrational energy is required. This requirement excludes the use of quartz,

since the energy dissipation per cycle is very small. The ferro-electric ceramics have a much larger energy dissipation than quartz.

The energizing pulse circuit should have a very low output-impedance so as to feed a long (at least 10 m) low-impedance coaxial cable. Also, this low output impedance should carry out an electrical damping of the transmitted pulse; this also assists in shortening the pulse length.

In the case of irradiated material the ferro-electric material should not be affected by the radiation of spent fuel during post-irradiation measurements, and it must withstand prolonged immersion in water without deterioration of its properties.

DESIGN OF PROBE AND INSTRUMENTATION

A plate of lead zirconate, P. 1. 60 ferro-electric ceramic*, is a suitable material for use in the combined transmitter-receiver probe. Some of its properties are given in Table I.

TABLE I

PROPERTIES OF THE P. 1. 60 FERRO-ELECTRIC CERAMIC

Density	7. 25 g/cm^3
Dielectric constant K	1200
Curie temperature (Maximum operating temperature)	325°C
Young's modulus	6. 2×10^{10} N/cm^2
Poisson's coefficient	0. 3
Velocity of sound	3. 3× 10^3 m/s
Acoustic impedance	23. 9×10^6 kg/m^2· s
Input impedance/m^2 radiation surface	4 2×10^5 Ω MHz
Inherent damping (theoretical)	2% dissipation per cycle.

The ceramic is not affected by normal irradiation [2] and it withstands prolonged immersion in water without complete encapsulation of the crystal.

A section of the probe assembly is shown in Fig. 2. The crystal has a thickness of 0. 195 mm corresponding to a natural resonance frequency of 10 MHz. It is cemented to a thin base of brass which serves as the earth electrode. The other electrode at the radiation face of the crystal is a rectangular (8×2 mm^2) nickel foil of 10 μm thickness. Base and crystal are

* Manufactured by "Quartz et Silice", Paris.

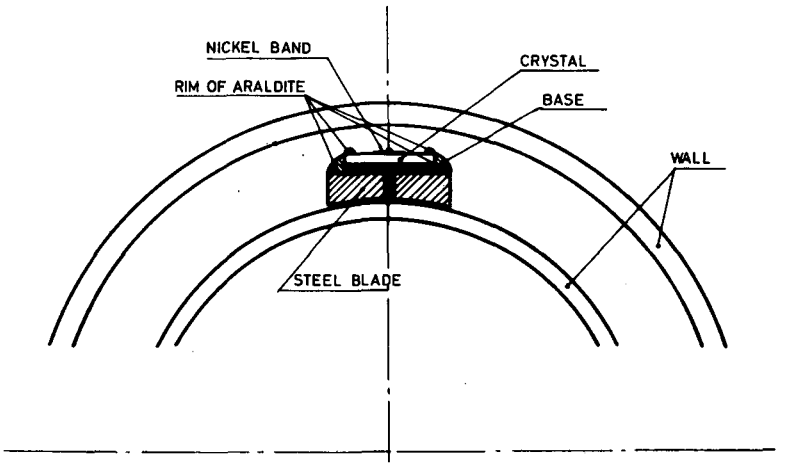

Fig. 2

Section of the crystal mounting

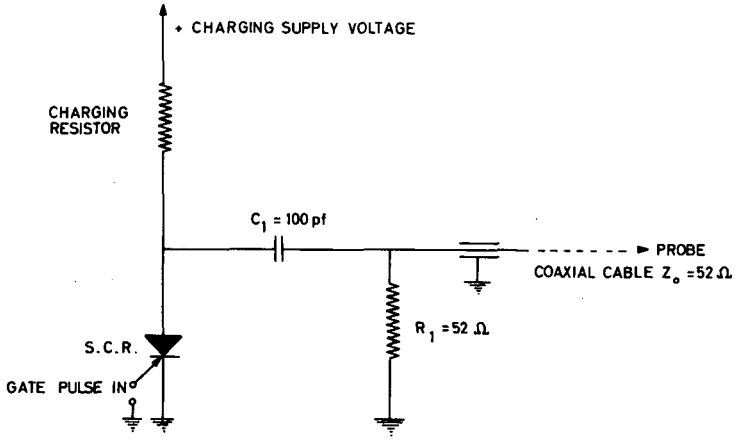

Fig. 3

Basic pulse circuit

mounted on a curved steel blade. A rim of Araldite is provided around the edge of the crystal and the base. Two nipples of Araldite on the crystal shield it against eventual wear during insertion of the probe in the fuel element. The total thickness is approximately 1.15 mm so that the initial gap of 3 mm is reduced to 1.85 mm. Since the velocity of sound in water in 1.49×10^3 m/s the maximum time between the transmitted and reflected pulse should be approximately 2.4 μs.

The energy supplied to the crystal is obtained from the discharge of the capacitor C_1 (Fig. 3). The discharge is initiated by the firing of a silicon controlled rectifier. (S. C. R.) The pulses required to open the gate of the

S. C. R. are obtained from an asymmetrical cathode-coupled multivibrator generating square waves at a repetition frequency of 100 kHz. This pulse-repetition rate is high enough to give sufficient discrimination between different gap distances when a chart recorder read-out is used. An emitter-follower stage provides the current necessary to drive the gate of the S. C. R.

The mechanical energy generated by the crystal is dependent on the electrical energy supplied to it, i. e. on the capacitance of C_1 and on the charging potential of C_1. To obtain short transmission pulses, the time constant of the discharge circuit is low ($R_1 = 52\ \Omega$ and $C_1 = 100$ pF (Fig. 3). A charging voltage of 300 V is used. Electrical damping of the transmitted pulse is performed by R_1. The pulses of mechanical energy from the crystal transducer then consist of a damped wave-train at the natural frequency of the transducer, say 10 MHz at a repetition rate of 100 kHZ. The ultrasonic energy reflected from the wall to the probe is converted into electrical voltage pulses having a wave-form similar to the exciting wave-form. These signals are presented directly to the Y-plates of an oscilloscope whose time base is triggered by the starting pulse, the scanning speed being adjusted so as to have a direct relation with the gap distance. As a chart recorder read-out is desired the signal is amplified, shaped and presented to a time-voltage convertor. Figure 4 gives a block diagram of the apparatus.

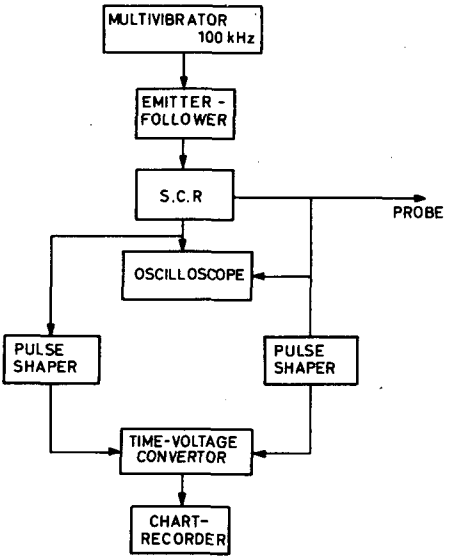

Fig. 4

Block diagram of the apparatus

Since the exciting pulse is negative, and the acoustic impedance of the aluminium wall is higher than that of the water medium, there is no phase reversal, and the reflected wave-form starts with a negative-going half-cycle (Fig. 5). The amplitude of this first half-cycle is very small in relation to the maximum amplitude, and its position is not well defined. A greater damping would enable a better definition of the wave starting-point.

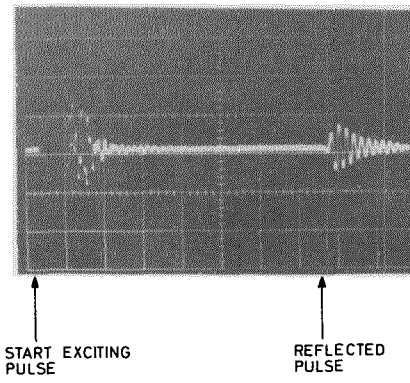

Fig. 5

Driver and reflected wave-forms

Therefore, in the practical case the first position half-cycle is taken into account.

PERFORMANCE OF THE PROBE

As the speed of the wave propagation through the medium is constant, the time interval is directly proportional to the gap distance, and the calibration curve by oscilloscope read-out over the range of 2.4 to 3.4 mm is evidently linear. The discrimination between different gap distances depends largely on the horizontal scanning speed of the oscilloscope. Speeds up to 100 mm/μs are easily available and a 5-μm gap-distance variation is therefore still noticeable.

Theoretical inaccuracy of the gap distance measurement is only due to temperature variations in the water medium. Measurements of the temperature dependence of the propagation velocity of sound in water have been made. The apparent distance variation seems to be 5 μm/°C. Errors can also result from non-linearity in scanning speed of the oscilloscope. However, this is not inherent to the measurement principle.

CONCLUSIONS

Preliminary measurements with the actual device are quite satisfactory. The probe, however, requires further development. A thinner crystal with a higher natural frequency results in a shorter length of the transmitting pulse. As a consequence, the pulse-repetition frequency could be raised to obtain a greater oscilloscope or chart-recorder discrimination between several gap-distances. Also a reduced length of the transmitting pulse allows a greater external damping (e. g. by using a lead mounting base), because the total probe thickness can be increased. On the other hand, a thinner crystal is not conducive to facilitating the assembling of the probe. Finally, inaccuracy of the measurement by temperature gradient along the

fuel element could be obviated by a temperature-sensing element with low heat capacity placed close to the crystal.

ACKNOWLEDGEMENTS

The contributions from colleagues in the Non-Destructive Testing group are gratefully acknowledged. Thanks are due in particular to G. Verstappen. I also wish to thank J.-J. Huet, M. Brabers and P. de Meester for their encouragement.

REFERENCES

[1] de MEESTER, P., DEKNOCK, R. and VERSTAPPEN, "A Survey of Devices to Measure Fuel Element Coolant Channels", to be published in Materials Evaluation.

[2] LUMB, R. F., "Ultrasonic Wall Thickness Measurement on a Highly Active Process Vessel", Brit. J. NDT. 6, 2 (1964).

DISCUSSION

D. BALLARD: Your illustrations only show one probe size. Do you not have to use a larger number of probes of various sizes to match the various curvatures of the cylindrical shells?

P. de MEESTER: The crystal size itself is the same for the different shells, but complete probes exist for each intertube. Actually, the complete apparatus developed is a complex scanning device consisting of 13 different probes, three for each larger intertube and two for the smaller ones. Using a switching disc it is thus possible to measure the complete fuel element in three scans, at 120° to each other.

R. H. McKANE: What is "Araldite", mentioned in Fig. 2, and is it important?

P. de MEESTER: Araldite is a plastic material, an epoxy resin, which is used as an encircling material for the crystal. With an appropriate catalyst it can be cured at room temperature. Araldite is commonly used in ultrasonic transducer techniques as a constituent of backing materials which contain metal powders. It is certainly important for the manufacture of the probe.

P. KNUDSEN: Did you make measurements on irradiated fuel elements? And what was the total gamma dose to which your probes were exposed?

P. de MEESTER: We have not yet performed measurements on irradiated BR-2 fuel elements, though some preliminary tests have been performed under gamma irradiation conditions. The gamma irradiation facility of BR-2 (G. I. F.) was used with spent fuel elements and probes were exposed to about 10^7 rad.

J. DORY: At the repetition frequency of 100 kHz were you not bothered by interference between the echoes from successive emissions?

P. de MEESTER: We have had no trouble with such interference because of the strong attenuation of the secondary echoes returning from the opposite wall. The emission itself only lasts for a few oscillations.

J. DORY: What is the duration of the acoustic pulse employed?

P. de MEESTER: About 0.7 μs.

W. FRANCIS: Have you attempted to use this equipment for measuring deflection and vibration of plates under flowing conditions? I am thinking of hydraulic testing, simulating in-pile conditions.

P. de MEESTER: No, our programme only covers pre-irradiation and post-irradiation measurements under static conditions. The technique you mention is very interesting, and I think it should be tried. However, the discontinuity in water flow, caused by the probe, may present a difficulty in this experiment.

NON-DESTRUCTIVE TESTING OF REACTOR-FUEL, TARGET, AND CONTROL ELEMENTS

R. H. McKANE AND D. L. HONKONEN
ENGINEERING ASSISTANCE SECTION, SAVANNAH RIVER PLANT,
E. I. du PONT DE NEMOURS AND COMPANY, AIKEN, S. C.,
UNITED STATES OF AMERICA

Abstract — Résumé — Аннотация — Resumen

NON-DESTRUCTIVE TESTING OF REACTOR-FUEL, TARGET, AND CONTROL ELEMENTS. At the Savannah River Plant (a production facility of the United States Atomic Energy Commission), fuel, target, and control elements are non-destructively tested before and after irradiation in reactors. Design and performance of unique instruments - used for measuring physical soundness, nuclear properties, and dimensions - are described.

A nickel thickness gauge, utilizing the Hall effect in a magnetic field, is used to measure the thickness of nickel layers on uncanned uranium cores. A similar instrument is used after cores have been diffusion-bonded to aluminium cladding to determine that each core has a layer of residual nickel, and that the end cap is sufficiently thick.

Ultrasonic instruments are used (1) to measure uranium grain size to determine whether the cores were properly heat-treated, and (2) to detect unbonded areas between cladding and core.

The Nuclear Test Gauge (NTG), a small subcritical assembly of U^{235}-Al alloy slugs in an H_2O-moderated lattice, is used to determine the fuel (U^{235}) or absorber (Li^6) content of reactor elements. These determinations, made from changes in neutron multiplication, have a 1-sigma precision of about ± 0.5% for fuel elements containing up to 250 g U^{235}/30.5 cm (1 ft), and about ± 1% for target and control elements containing up to 4 g Li^6/30.5 cm (1 ft).

Compared to the more commonly used large critical test pile, the NTG costs about 1/20 as much; measures fuel or absorber content in about one minute vs. ten minutes; and measures the axial distribution of fuel or absorber which the test pile cannot do.

Irradiated fuel elements are measured under water with (1) differential transformers that can measure diameter and length to an accuracy of ± 0.05 cm (0.002 in), and (2) simple mechanical linkages with dial indicators above water that can measure inside diameter and warp. By keeping the elements submerged in water, personnel are shielded from radiation, and the elements do not undergo the dimensional changes that would occur from self-heating in air.

ESSAIS NON DESTRUCTIFS DES ÉLÉMENTS COMBUSTIBLES DE LA CIBLE ET DES ÉLÉMENTS DE COMMANDE. A la centrale de Savannah River (exploitée pour le compte de la Commission de l'énergie atomique des Etats-Unis), le combustible, la cible et les éléments de commande sont soumis à des essais non destructifs avant et après irradiation en pile. Les auteurs décrivent les caractéristiques et les performances d'instruments inédits, utilisés pour mesurer la qualité, les propriétés nucléaires et les dimensions.

Une jauge d'épaisseur du nickel, fondée sur l'effet Hall dans un champ magnétique, sert à mesurer l'épaisseur de couches de nickel sur des éléments combustibles en uranium sans gainage. Après liaison par diffusion de l'uranium à sa gaine d'aluminium, on a recours à un instrument similaire pour vérifier que chaque élément est revêtu d'une couche de nickel résiduel et que le bouchon de fermeture est suffisamment épais.

Des instruments utilisant les ultrasons servent: a) à mesurer la dimension des grains d'uranium, en vue de déterminer si les éléments combustibles ont subi un traitement thermique approprié; b) à déceler les zones de liaison imparfaite entre la gaine et l'uranium.

La jauge d'essai des propriétés nucléaires, qui est un petit assemblage sous-critique de barreaux en alliage ^{235}U-Al dans un réseau ralenti à l'eau légère, est utilisée pour déterminer la teneur des éléments en combustible (^{235}U) ou en absorbeur (^{6}Li). Ces déterminations, faites à partir des variations de la multiplication des neutrons, ont une précision 1-sigma d'environ ± 0,5% pour les éléments combustibles contenant

jusqu'à 250 g de ^{235}U par 30,5 cm et d'environ ± 1% pour la cible et les éléments de commande contenant jusqu'à 4 g de ^{6}Li par 30,5 cm.

Par rapport à la grande pile d'essais critiques plus généralement utilisée, la jauge décrite présente les avantages suivants: elle coûte environ 20 fois moins cher; elle permet de mesurer la teneur en combustible ou en absorbeur en 1 min environ, contre 10 min pour la pile; elle mesure la distribution axiale du combustible ou de l'absorbeur, ce que la pile ne peut pas faire.

On mesure, en immersion, les éléments combustibles irradiés avec: a) des transformateurs différentiels qui peuvent mesurer le diamètre et la longueur avec une précision de ± 0,05 cm; b) de simples raccords mécaniques, avec des indicateurs au-dessus de la surface de l'eau, qui peuvent mesurer le diamètre intérieur et la déformation. En maintenant les éléments immergés dans l'eau, on met le personnel à l'abri des rayonnements et les éléments ne subissent pas les variations dimensionnelles que créerait l'auto-échauffement dans l'air.

НЕДЕСТРУКТИВНОЕ ИСПЫТАНИЕ ЯДЕРНОГО ТОПЛИВА, МИШЕНИ И УПРАВЛЯЮЩИХ СТЕРЖНЕЙ. На заводе Саванна-Ривер (предприятие Комиссии по атомной энергии США) топливо, мишень и управляющие стержни испытываются без разрушения до и после облучения в реакторах. Описываются конструкции и эксплуатационные качества уникальных приборов, которые используются для измерения физической надежности, ядерных свойств и размеров.

Для измерения толщины слоев никеля на урановых сердечниках без оболочки используют измеритель толщины никелирования, действующий на основе эффекта Холла в магнитном поле. Аналогичный прибор применяют после диффузионного сцепления стержней с алюминиевой оболочкой с целью установить наличие слоя остаточного никеля на каждом сердечнике, а также толщину нижнего наконечника.

Ультразвуковые приборы используют для измерения размера урановых зерен, чтобы определить, подвергнуты ли сердечники достаточной термообработке, а также для обнаружения участков, не имеющих сцепления между оболочкой и сердечником.

Прибор для быстрого измерения реактивности топливных элементов, представляющий собой небольшую подкритическую сборку стержней из сплава уран-235-алюминий в решетке с водным замедлителем, используют для определения топливного (уран-235) или абсорбционного (литий-6) содержания реакторных элементов. Эти определения, сделанные на основе изменений в размножении нейтронов, имеют 1-сигма точности, которая составляет приблизительно ± 0,5% для тепловыделяющих элементов, содержащих до 250г урана-235 на 1 фут (30,5см), и приблизительно ±1% для мишени и управляющих стержней, содержащих до 4г лития-6 на 1фут (30,5см).

По сравнению с обычно используемым крупным критическим испытательным реактором прибор для быстрого измерения реактивности топливных элементов имеет следующие преимущества: стоит приблизительно в 20 раз дешевле; измеряет содержание топлива или поглотителя в течение приблизительно одной минуты вместо 10 минут; измеряет осевое распределение топлива или поглотителя, чего нельзя сделать с помощью испытательного реактора.

Облученные тепловыделяющие элементы измеряются под водой с помощью дифференциальных трансформаторов, способных измерять диаметр и длину с точностью ± 0,05 см (0,002 дюйма), а также с помощью простого механического сцепления с установленными над водой индикаторами со шкалой, способными измерять внутренний диаметр и искривление. За счет того, что элементы остаются погруженными в воду, персонал защищен от радиации, а размеры элементов не подвергаются изменениям, которые произошли бы при самонагревании на воздухе.

ENSAYO NO DESTRUCTIVO DE COMBUSTIBLES, BLANCOS Y ELEMENTOS DE CONTROL PARA REACTORES. En la planta de Savannah River (establecimiento industrial perteneciente a la Comisión de Energía Atómica de los Estados Unidos) los combustibles, blancos y elementos de control se someten a ensayos no destructivos, antes y después de su irradiación en reactores. Se describen en la presente memoria el diseño y rendimiento de algunos aparatos de características especiales, empleados para medir la integridad física, las propiedades nucleares y las dimensiones de dichos elementos.

Para medir el espesor de las capas de níquel aplicadas a barras de uranio, se usa un calibrador basado en el efecto Hall en campos magnéticos. Un instrumento similar se utiliza después que las barras poseen un revestimiento de aluminio aplicado por difusión, a fin de determinar que cada barra cuenta con una capa de níquel residual y que el casquete extremo tiene espesor suficiente.

Se utilizan instrumentos ultrasónicos: a) para medir el tamaño de grano del uranio y determinar si las barras han recibido el tratamiento térmico adecuado; b) para detectar zonas en que el revestimiento no está unido a la barra.

El Nuclear Test Gage (NTG) constituye un pequeño montaje subcrítico de barras de aleación ^{235}U-Al en un reticulado moderado por H_2O; se utiliza para determinar el contenido de combustible (^{235}U) o de absorbente (^{6}Li) en los elementos de reactor. Estas determinaciones, basadas en la variación de la multiplicación neutrónica, permiten alcanzar una precisión de aproximadamente ± 0,5% (1 σ) para elementos combustibles que contienen como máximo 250 g de ^{235}U por cada 30,5 cm (1 pie) de longitud; la precisión es de ± 1% para blancos y elementos de control que contienen como máximo 4 g de ^{6}Li por cada 30,5 cm (1 pie) de longitud.

Comparado con el montaje crítico de gran tamaño corrientemente usado para ensayos, el NTG presenta las siguientes ventajas: su costo es alrededor de la vigésima parte; permite medir el contenido de combustible absorbente en 1 min, mientras se requieren 10 min con el montaje crítico; y permite medir la distribución axial del combustible o absorbente, lo que escapa a las posibilidades del montaje crítico.

Los elementos combustibles irradiados se miden bajo agua, empleando: a) transformadores diferenciales capaces de medir diámetros y longitudes con precisión del orden de ± 0,05 mm (0,002 pulg); b) conexiones mecánicas sencillas, con cuadrantes indicadores sobre el nivel del agua, que permiten medir diámetros internos y alabeo. Manteniendo los elementos sumergidos en agua, se protege al personal contra la radiación y se evitan los cambios dimensionales que se producirían debido al autocalentamiento en el aire.

1. INTRODUCTION

Fuel, target, and control elements used in production reactors at the Savannah River Plant are non-destructively tested before irradiation to avoid failures in the reactors and to assure proper nuclear properties. Fuel elements are measured after irradiation to assess the effects of element-manufacturing and reactor-operation variables on dimensional stability during irradiation.

2. PRE-IRRADIATION TESTING

The general design of metallic uranium fuel elements tested by the equipment to be discussed is shown in Fig. 1. The tubular core is plated with nickel, then the aluminium cladding is bonded to the core by the application of heat and pressure, forming U-Ni intermetallic compounds on one side of the nickel layer and Al-Ni compounds on the other. The nickel-plating and bonding processes must be controlled so that a discrete layer of nickel remains between core and cladding. In addition to being tested for the presence of nickel and continuity of bonding, the elements are reactivity-tested before charging to the reactors.

Uranium-aluminium alloy fuel tubes and lithium-aluminium alloy target and control rods are also reactivity-tested before charging to the reactors. A fuel tube is a 16-ft-long, 3-in-diameter U^{235}-Al tube clad with aluminium. A target or control rod is either a continuous core clad with aluminium or a column of short sections of rod individually clad and contained in an aluminium tube.

2.1. Nickel gauge

Since the uranium core, aluminium cladding, and intermetallic compounds of U-Ni and Al-Ni are non-magnetic compared to metallic nickel,

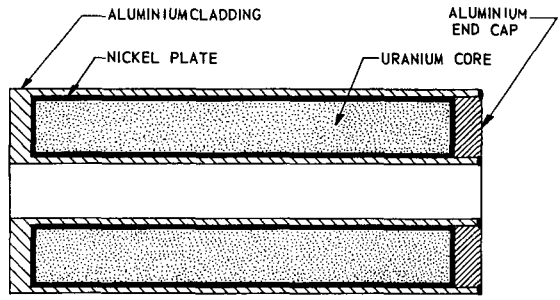

Fig. 1

Uranium fuel element

the nickel plate thickness can be measured using the Hall effect. The Hall effect device,[1] a small, flat crystal of indium arsenide, is mounted on a small permanent magnet (Fig. 2). With a constant "control" current through the crystal, a Hall voltage is generated proportional to the magnetic field strength in the crystal, which in these applications is a function of the thickness and proximity of the nickel layer.

The inner and outer surfaces of the plated cores are scanned simultaneously with test equipment arranged as shown in Fig. 3. A Hall device and magnet are mounted in each probe, along with a temperature-sensitive resistor[2] to compensate for changes in crystal characteristics caused by temperature changes. To minimize variations in probe-to-core spacing, the contact faces of the probes are machined to the contour of the surfaces being examined and the probes are spring-loaded to maintain contact with the surfaces.

The accuracy and reproducibility of the gauge were determined by sectioning the cores through gauged areas and measuring the nickel-plate thickness microscopically. Results obtained are shown in Table I.

2. 2. Nickel detector

This instrument is similar to the nickel gauge but is used on clad elements to determine if metallic nickel remains after the bonding process. It will detect a layer as thin as 0.05 mil under a 40-mil-thick aluminium cladding. It is used on a "Go, No-Go" basis; no attempt is made to measure the thickness of the residual layer.

2. 3. End-cladding thickness gauge

The cladding thickness on the element ends is determined by finding the intersection of the nickel plate on the outer cylindrical and flat end surfaces of the core by means of a small, pointed magnet mounted on a pivoted shaft (Fig. 4). As this magnet seeks the relatively thick nickel plate at the inter-

[1] "Hall-Pak", F. W. Bell, Inc., Columbus, Ohio.

[2] "Sensitor", Texas Instruments, Inc., Dallas, Texas.

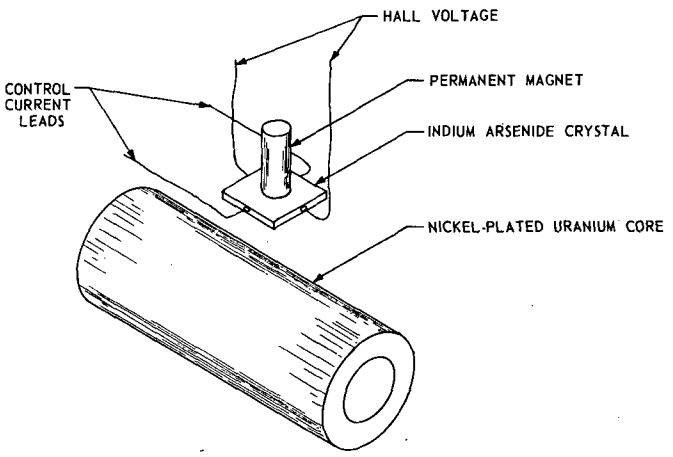

Fig. 2

Nickel thickness gauge

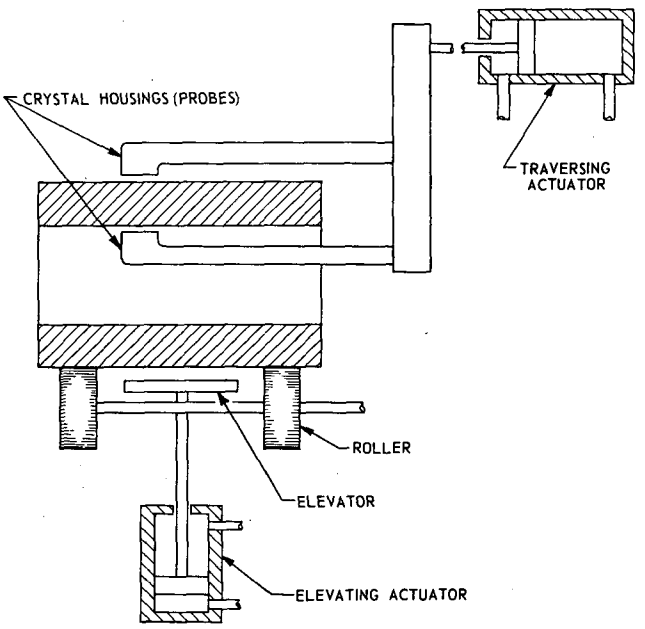

Fig. 3

Fuel-element test arrangement

section, another magnet mounted on the opposite end sweeps across a Hall effect crystal, resulting in a voltage which is an indication of magnet position (end thickness). The instrument is calibrated by using elements with known cap thicknesses. The element is positioned against the end stop, and

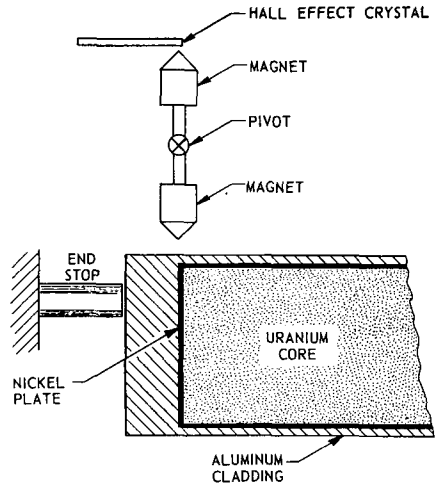

Fig. 4

End-cap thickness gauge

the output meter is adjusted to indicate end-cladding thickness directly in mils. By the destructive examination of a series of elements, the accuracy of the gauge was determined to be about ±8.0 mil* when gauging a cap nominally 150 mil thick.

2.4. Grain-size tester

Before cladding is applied, the grain size of the uranium cores is determined by measuring the attenuation of ultrasound transmitted through the core, using a test arrangement as shown in Fig. 3. In this application the test is performed underwater to couple acoustically the probes to the core; therefore, the probes need not be in contact with the core. This through-transmission method avoids the rigorous spacing and directional problems of refraction techniques.

A $\frac{1}{2}$-in-diam. lead zirconate-titanate crystal continuously generates a signal of 2000 pulses/s of 5.0-Mc sound which is received by a similar crystal after passing through the core wall. The received signal is amplified, detected, and integrated to produce a direct-current signal inversely proportional to the average size of grains traversed.

The probes traverse longitudinally 1/4 in for each revolution of the core, to that there is a continuous scan of overlapping spiral increments. The time-constant of the integrating circuit is adjusted so that the core is rejected if, during any one-third revolution of the core, the average grain size is found to be outside preset limits. A separate circuit accumulates signals to indicate the average grain size for the entire core.

The electronic circuits are composed completely of solid-state components: 9 transistors, 17 diodes, and 2 magnetic amplifiers. The pulse de-modulator

---

* 1 mil = 0.001 in

circuit, made up of a "Unitunnel" diode[3] and a resistor, is particularly simple and reliable and has inherent temperature compensation.

2.5. Non-bond detector

Aluminium cladding is required to protect the core from corrosion by the coolant. Interfaces resist heat transfer and must be minimized by a sound metallurgical bond between core and cladding.

Unbonded areas are detected by measuring the attenuation of ultrasound. As in the grain-size tester, a through-transmission, hydraulically coupled test arrangement is used (Fig. 3), but in this case the probes are contoured and spring-loaded to maintain contact with the element surfaces because the nickel-detector crystals are mounted in the same probes and the two tests are made simultaneously.

The lead zirconate-titanate crystals emit and receive pulses of 1-Mc sound. The crystals are coupled to the water by epoxy resin windows 0.20 in in diam. The test pulses, 30μs in duration, are emitted 4000 times per second while the probes are translated 0.10 in per revolution as the element rotates at 960 rpm. At a frequency of 1 Mc, variations in uranium grain size have no appreciable effect on sound transmission but mechanical gaps do. The receiver crystal output, 900 mV for a bonded element, is fed to a low-level pulse discriminator which is linear over the range from 100 to 1000 mV. The crystal output signal is reduced anywhere from 5% to nearly 100% by non-bonds, depending on their type and area. For each sound pulse that is below a preset level, the discriminator generates an electrical pulse. These pulses are totalled by an electronic counter. A recorder output is available to "map" unbonded areas if required for special tests.

Since the water-bath temperature varies enough to affect the strength of the transmitting crystal signal, an automatic calibration circuit is provided. When the probes are retracted, a preset percentage of the receiving crystal signal is switched to a servo amplifier that drives a motorized potentiometer to adjust the discriminator to the proper trigger level.

2.6. Nuclear test gauge (NTG) [1]

Before fuel, target and control elements are charged to the reactors, they are tested for reactivity in the NTG (Fig. 5), a light-water-moderated subcritical pile of small critical mass (approximately 4 kg U^{235}). The central lattice tank contains a hexagonal array of 39-in-long tubes, 83 of which contain two U^{235}-Al slugs (1-in diam. × 12-in long) at the centre with plastic plugs at each end. The tubes extend through the lattice tank for easy access to the fuel slugs. The tank is surrounded by a 2-ft-thick concrete wall, containing an access hole at each end of the lattice. For radiation shielding, these access holes contain removable water-filled shielding tanks in front of which are placed lead-filled loading doors. The 4-in-diam. test hole at the centre of the lattice contains the samples being tested. Adapters are used as required to test various elements.

---

[3] Hoffman Electronics Corporation, El Monte, California.

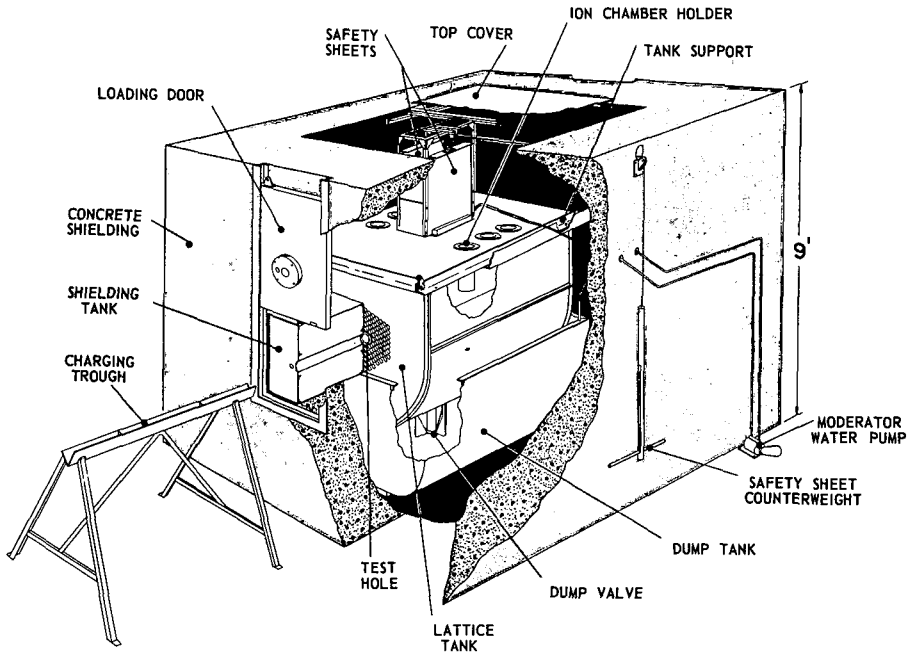

Fig. 5

Nuclear test gauge

TABLE I

ACCURACY OF NICKEL GAUGE MEASUREMENTS

Core number	Plating time (min)	Average plate thickness (mil [a])		
		Nickel gauge	Microscope	Difference
1	6	0.20	0.20	0.00
2	10	0.44	0.40	0.04
3	15	0.52	0.50	0.02
4	20	0.67	0.69	0.02
5	25	0.98	0.94	0.04
6	30	1.10	1.08	0.02

[a] 1 mil = 0.001 in.

A 5-Ci Ra-Be source, centred in one of the tubes, emits 7×10^7 n/s. between about 20 and 100.

The testing sensitivity can also be increased (with no corresponding increase in testing time) by increasing the neutron source strength, S, and decreasing the critical mass of the assembly, m_c. Both of these parameters were given primary consideration in the design; i.e., $S = 7 \times 10^7$ n/s and m_c is slightly in excess of 4.0 kg U^{235}.

2.6.4. Testing procedures

An element is tested by measuring the asymptotic chamber current produced when the element is centred in the test hole. This current is compared with the current produced by a standard having approximately the same dimensions as the test element. Elements more than 2 ft long are tested at different positions along their length to detect composition variations.

Inserting a fuel element into the NTG increases M; inserting a target or control element decreases M. The resulting decrease in testing sensitivity for target or control elements is avoided by inserting in the test hole a fuel tube containing U^{235} as an adapter, and testing the target or control element inside this adapter. One adapter was modified to permit measurements of individual 10-in-long Li-Al slugs inside control rods. This adapter contains two cadmium tubes positioned inside the fuel tube to leave a 10-in gap at the centre.

2.6.5. Testing characteristics

A wide variety of elements has been successfully tested in the NTG. The characteristics of the NTG for some of these tests are shown in Table II. During the tests of natural uranium slugs and high-purity materials, the testing time was lengthened to increase the precision.

3. POST-IRRADIATION EXAMINATION

Selected irradiated fuel elements are visually examined and measured under 10 ft of water in gauging stations to compare their physical condition before and after irradiation. Volume change is measured by weighing the elements in air and water before irradiation and in water afterwards.

3.1. Outside-diameter measurement

The fuel element is placed on a tubular stage having the nominal OD and ID dimensions. This stage, which is also a gauging standard, is mounted on a column of three hydraulic cylinders (Fig. 6) which are actuated in succession to measure, in turn, the outside diameter of the standard and that of the element at its centre and 1 in from each end. The measurements are made by two sets of probes mounted on diametrically opposed, hydraulically actuated differential transformers, 90° apart. The probes are retracted during any movement of the element to prevent mechanical damage to the

TABLE II

NTG TESTING TIME AND PRECISION

	Composition	NTG multiplication before and after insertion of element	Precision (1 σ)	Average time per reading (min)
U^{235}-Al fuel tubes	10 g U^{235}/ft	10; 12	0.04 g U^{235}/ft	0.9
	25 g U^{235}/ft	10; 18	0.11 g U^{235}/ft	0.8
	100 g U^{235}/ft	10; 60	0.11 g U^{235}/ft	1.4
	200 g U^{235}/ft	7; 20	0.4 g U^{235}/ft	-
Li-Al control rods	0.6 g Li^6/ft	22; 17	0.005 g Li^6/ft	0.5
	2.5 g Li^6/ft	22; 16	0.062 g Li^6/ft	0.5
Natural uranium elements	0.71 wt. % U^{235}	92; 56	0.00034 wt. % U^{235}	3.5
Small samples of high-purity materials	$v\Sigma_a$ = 0.03 to 0.22 cm^2	150; 150	0.007 cm^2	3.6

element and to minimize build-up of oxide on the probes. Electrical signals from the transformers are fed to a balancing transformer connected to a mechanical counter which displays, on the operating console, the difference between the diameter of the element and that of the standard. Periodic checks with dummy elements indicate an accuracy of about ±3 mil.
These neutrons are multiplied by the lattice fuel and by any fuel which may be in the test hole. At a neutron multiplication, M, of 100 (an effective multiplication constant, K, of 0.990), the maximum thermal neutron flux in the test hole is 5×10^6 n/cm^2 s.

Six ionization chambers, three on each side of the fuel lattice, convert this neutron flux into an electric current of the order of 10^{-8} A per chamber. Four chambers are connected in parallel and feed either a strip-chart recorder or automatic print-out equipment. Each of the other two chambers is connected to a separate safety circuit.

2.6.1. Nuclear safety

At a preset M of less than 200, each of the safety circuits independently activates two fail-safe shutdown devices. The primary shutdown device is a pair of Boral (a dispersion of boron carbide in aluminium) safety sheets, either of which would stop a reactivity excursion within 0.5 s. Each safety sheet is held above the lattice by an electromagnet and when released falls

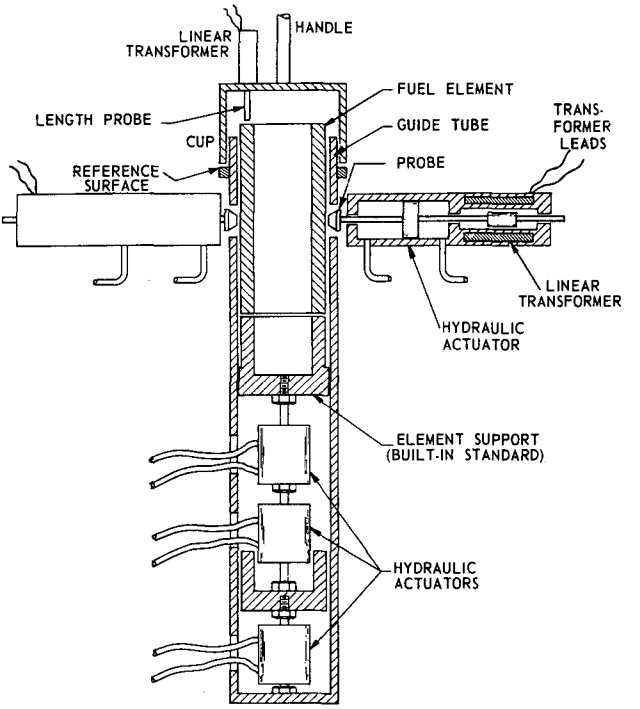

Fig. 6

Outside-diameter and length gauges

by gravity into the lattice. The other shutdown device is an air-operated dump valve which opens an 8-in-diam. hole at the bottom of the lattice tank. The water drops to the lattice midplane 5 s after the preset multiplication is reached.

The NTG lattice contains 166 fuel slugs for testing fuel tubes containing up to 150 g U^{235}/ft and 154 fuel slugs for testing tubes containing up to 250 g U^{235}/ft. The shutdown devices might not react fast enough to prevent a serious nuclear accident if a fuel tube containing as much as 200 g U^{235}/ft or more were rapidly inserted into the 166-slug lattice. To avoid such a nuclear accident, each fuel tube is always mechanically driven into the test hole at a safe speed. Moreover, the drive motor is de-energized when the multiplication reaches a preset level less than 200.

2.6.2. Radiation control

No radiation from the NTG is detected outside the concrete shielding except for a 100 mrem gamma-plus-neutron beam from both ends of the test hole. Since there is virtually no shielding (other than the self-shield of the lattice tank) at the top of the NTG, the gamma-plus-neutron activity at the centre of the top cover is 150 mrem.

Fuel tubes have a maximum gamma activity of 600 mr at 3 in immediately after discharge from the NTG. In 20 min this activity has decayed to 20 mr at 3 in.

2.6.3. Operating characteristics [2]

After a change in neutron multiplication, the neutron flux asymptotically approaches an equilibrium value, which is reached in about 1 min for $M = 100$. For greater values of M, the time required to reach equilibrium increases exponentially. However, testing sensitivity (i.e., the change in neutron flux for a given change in the U^{235} content of a test piece) increases directly as M^2. A reasonable compromise can be obtained by using an M

3.2. Inside-diameter measurement

The inside diameter is measured with a manually operated gauge (Fig. 7) that is lowered into the bore of the element while it is in the gauging station (Fig. 6). At the lower end of the actuating rod, a conical tip forces three spring-loaded probes against the surface of the element. The vertical position of the actuator rod is measured by a dial indicator above water and shows, within ±2 mil, the difference between the inside diameter of the element and that of the standard. The lifting and actuating handles are arranged to retract the probes before the gauge is moved, to avoid damage to probes and element.

3.3. Length measurement

Length is measured by a differential transformer in a cup-shaped mounting, manually placed over the element in the gauging station (Fig. 6). The cup lip rests on a reference surface on the guide tube. After calibration with a dummy element, the transformer system displays, on the console-mounted counter, the difference in length between the dummy and the irradiated elements within ±2 mil.

3.4. Warp measurement

Warp can be measured by a pantograph arrangement in which a dial indicator mounted on an arm above water follows the movement of a similar arm underwater (Fig. 8). As the element - supported between two conical live centres - is rotated, the roller-tipped lower arm follows any diametral deviation of the middle of the element. Accuracy is about ±3 mil. For ribbed elements, the lower arm is lifted over the ribs by a cam and follower on the rotating shaft.

ACKNOWLEDGEMENT

The information contained in this article was developed during the course of work under Contract AT(07-2)-1 with the United States Atomic Energy Commission.

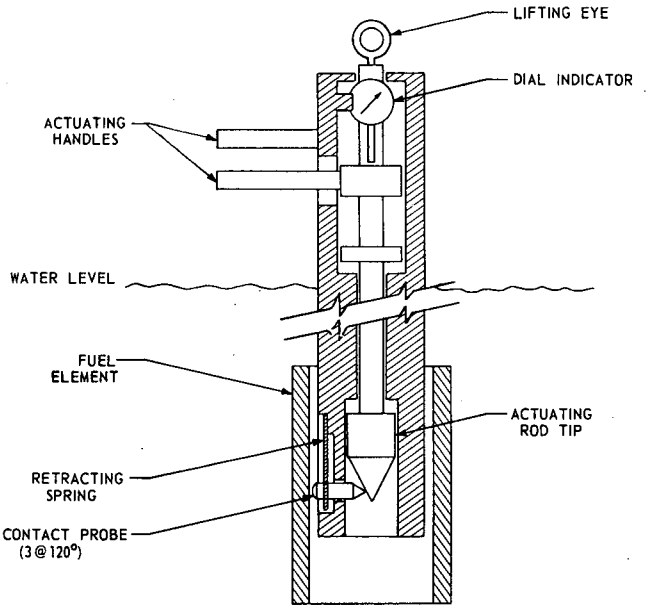

Fig. 7

Inside-diameter gauge

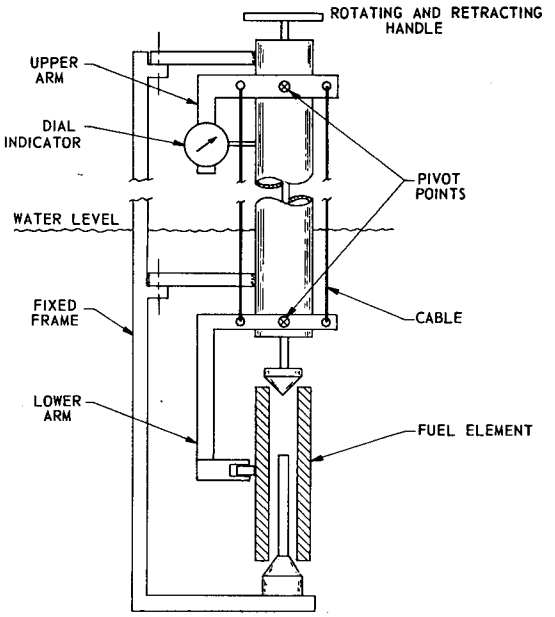

Fig. 8

Warp gauge

REFERENCES

[1] PARKINSON, T. F. et al., USAEC R&D Report DP-147 (1956).
[2] AXTMANN, R. C., DESSAUER, G. and PARKINSON, T. F., USAEC R&D Report DP-48 (1955).

DISCUSSION

R. NEIDER: What advantage does the Hall device have for measuring the Ni thickness over an eddy-current probe or a beta back-scattering device?

R. H. McKANE: Simplicity of the electronic circuitry.

R. NEIDER: What accuracy is obtained in measurement of Ni layers with the Hall device?

R. H. McKANE: From examination of metallurgically prepared specimens, we believe the nickel detector will respond to nickel plate as thin as 0.00005 in. On the same basis, the accuracy of the nickel gauge appears to be ±0.00005 in.

R. S. SHARPE: Are you satisfied that your ultrasonic non-bond tester locates all areas that are significant for reactor service? Are you not concerned that very narrow gaps between fuel and cladding are not detected by your ultrasonic method?

R. H. McKANE: This non-bond detector responds only to gross defects. There is a great need for a better test. I had hoped to learn of one at this symposium.

P. de MEESTER: Are the non-bond areas which were not detected really non-bonds, or poor or pseudo-bonds?

R. H. McKANE: Stud weld tests and metallographic examinations indicate that the areas were actually not bonded.

P. de MEESTER: Could you tell us what heat fluxes per unit area are involved with these elements? You reported that several elements with non-bond areas were irradiated. What size were these areas? We are working with high-flux fuel elements under heat-flux conditions of 400 to 600 W/cm^2 and we impose a maximum non-bond tolerance of a few square millimetres; these figures, however, are based on calculations and no experience supports this specification.

R. H. McKANE: I am afraid your specific question, like the general question what degree of non-bonding is acceptable, is outside the scope of my presentation.

I. PURICA: You mentioned reactivity tests in the NTG sub-critical assembly. Are these tests only for the purpose of assessing the reactivity that the different rods can introduce into a reactor, i.e. the total quantity of fuel, or is the purpose to assess the distribution of uranium along the rod?

R. H. McKANE: Normally, successive 2-ft-long sections of elements are tested. This is one of the advantages of the NTG.

I. PURICA: If I understood correctly, you use a standard for each concentration of uranium. Does the precision given in Table II of your paper refer to a value relative to the standard or to an absolute value in grams of U^{235}?

R. H. McKANE: The precision refers to an absolute value.

A.D. McEACHERN: We have used an identical non-bond test for our NRU fuel elements, and we found extensive areas of indicated bond on unplated elements where destructive examination showed very little bond. The most troublesome areas were those where the uranium cores oxidized heavily before cladding so that there was a heavy layer of uranium oxide between the cladding and the core. We were not able to explain this, but perhaps somebody else can.

Our experience with these unplated areas was bad, and we later switched to nickel-plated elements, which were normally completely bonded. We do not consider the ultrasonic bond test to be capable of protecting the reactor from a poor production process. It has, however, been very useful for control of the production process. We have also always used statistical quality control based on the destructive stud-weld bond test.

R.H. McKANE: The Savannah River Plant also used statistical sampling and destructive metallographic examination for production quality control. As I indicated, the ultrasonic test will find only relatively gross production errors.

D.C. WORLTON: Hanford applies a bond test utilizing a pulse-echo technique, which we believe gives a somewhat better performance than the through transmission method.

R.H. McKANE: Savannah River Plant would be very interested in receiving data obtained from testing elements clad with steam-autoclaved cans.

R.S. SHARPE: Do the infra-red methods now being developed show promise of providing us with a more sensitive technique for non-bond inspection?

R.H. McKANE: I hope so. The method appears to measure directly the variable (heat transfer) in which we are interested. I had hoped that there would be papers on the subject at this symposium.

DOSAGE DU PLUTONIUM PAR DILUTION ISOTOPIQUE A DOUBLE TRACEUR: APPLICATION A LA MESURE DES TAUX DE COMBUSTION

J. CHENOUARD ET MONIQUE LUCAS
CENTRE D'ÉTUDES NUCLÉAIRES DE SACLAY, FRANCE

Abstract — Résumé — Аннотация — Resumen

DETERMINATION OF PLUTONIUM BY DOUBLE-TRACER ISOTOPIC DILUTION: APPLICATION TO BURN-UP MEASUREMENTS. The plutonium content of irradiated fuels can be determined by isotopic dilution using a solution containing both uranium-233 and plutonium-242. The paper describes the measurement method, its calibration, the solution preparation techniques, and analysis by mass spectrometry.

The chemical treatment involves a valence cycle which should give homogeneous distribution of the isotopes in the tracer-sample mixtures and a suitable U/Pu separation. The presence of excess uranium greatly changes the plutonium redox kinetics. Improvements in operating technique have enabled us to make the valence cycle effective, thereby improving the U/Pu separation. The stability of the thermo-ionic emission of Pu in relation to the amount of residual uranium is thus improved, resulting in more accurate analyses.

Isotopic contamination is eliminated to the maximum extent. The tracer is calibrated using a standard solution prepared from weighed quantities of plutonium and uranium of known chemical purity.

The use of an electronic computer shortens the calculations and simplifies the checking of results.

The uranium-235 burn-up in the fuel is measured by isotopic analysis of the metal converted into uranium hexafluoride. The plutonium content is determined with an accuracy of 2%. The U^{235} depletion is measured to within $\pm 5 \times 10^{-4}$.

DOSAGE DU PLUTONIUM PAR DILUTION ISOTOPIQUE A DOUBLE TRACEUR : APPLICATION A LA MESURE DES TAUX DE COMBUSTION. La teneur en plutonium d'un combustible irradié peut être déterminée par dilution isotopique à l'aide d'une solution contenant à la fois de l'uranium-233 et du plutonium-242. La méthode de mesure, son étalonnage, les techniques de préparation des solutions et l'analyse par spectrométrie de masse sont décrits.

Le traitement chimique comporte un cycle de valence qui doit permettre d'obtenir une répartition homogène des isotopes dans les mélanges traceur-échantillon et une séparation U/Pu convenable. La présence d'un excès d'uranium modifie profondément la cinétique d'oxydo-réduction du plutonium. Une amélioration de la technique opératoire a permis de rendre efficace le cycle de valence et d'améliorer de ce fait la séparation U/Pu; la stabilité de l'émission thermoionique du Pu, liée à la quantité d'uranium résiduel a été en conséquence améliorée, conduisant à des analyses plus précises.

Les contaminations isotopiques ont été éliminées au maximum. L'étalonnage du traceur se fait à l'aide d'une solution étalon préparée par pesée de plutonium et d'uranium de pureté chimique connue.

L'utilisation d'une calculatrice électronique permet d'abréger les calculs et de simplifier la vérification des résultats.

La consommation de l'uranium-235 du combustible est mesurée par l'analyse isotopique du métal converti en hexafluorure d'uranium. La teneur en plutonium est déterminée avec une précision de 2%. L'appauvrissement en ^{235}U est mesuré à $\pm 5.10^{-4}$.

ОПРЕДЕЛЕНИЕ ПЛУТОНИЯ МЕТОДОМ ИЗОТОПНОГО РАЗБАВЛЕНИЯ С ДВОЙНЫМ ИНДИКАТОРОМ ПРИ ИЗМЕРЕНИИ ГЛУБИНЫ ВЫГОРАНИЯ. Содержание плутония в облученном топливе можно установить методом изотопного разбавления с помощью раствора, который одновременно содержит уран-233 и плутоний-242. Приводится описание метода измерения, его калибрования, техники изготовления растворов и анализа с помощью масс-спектрометрии.

Химическая обработка включает цикл валентности, который позволяет получить гомогенное распределение изотопов в смесях индикатора и образца, а также соответствующее разделение уран/плутоний. Наличие излишка урана сильно изменяет кинетику окислительно-

восстановительного процесса плутония. Усовершенствование применяемого метода позволило сделать цикл валентности эффективным и в связи с этим улучшить разделение уран/плутоний; устойчивость термоионного излучения плутония, связанная с количеством остаточного урана, оказалась вследствие этого лучшей и дала возможность проводить более точные анализы.

Изотопическое загрязнение было сведено к минимуму. Калибрование индикатора производилось с помощью эталонного раствора, изготовленного по методу взвешивания плутония и урана известной химической чистоты.

Применение электронной вычислительной машины позволило сократить расчеты и упростить проверку результатов.

Выгорание урана-235 в топливе измеряется с помощью изотопического анализа металла, преобразованного, в шестифтористый уран. Содержание плутония определяется с точностью до 2%. Обеднение в уране-235 измеряется до $\pm 5 \cdot 10^{-4}$.

DETERMINACION DE GRADOS DE COMBUSTION POR VALORACION DE PLUTONIO MEDIANTE DILUCION ISOTOPICA CON DOBLE INDICADOR. La concentración de plutonio en un combustible irradiado puede medirse por dilución isotópica con ayuda de una solución que contenga simultáneamente ^{233}U y ^{242}Pu. Se describen en la presente memoria el método de medición, la calibración, las técnicas de preparación de las soluciones y el análisis mediante espectrometría de masas.

El tratamiento químico incluye un ciclo de valencia destinado a asegurar una distribución homogénea de los isótopos en las mezclas indicador-muestra y una separación adecuada de U/Pu. La presencia de un exceso de uranio modifica profundamente la cinética de la oxidorreducción del plutonio. Un perfeccionamiento de la técnica operativa ha permitido tornar eficiente el ciclo de valencia y mejorar con ello la separación de U/Pu; por consiguiente se ha aumentado la estabilidad de la emisión termiónica del Pu, vinculada a la cantidad de uranio residual, y ello ha conducido a análisis de mayor precisión.

Las contaminaciones isotópicas se han aminorado considerablemente. El indicador se calibra por medio de una solución patrón preparada por gravimetría de Pu y U de pureza química conocida.

El empleo de una calculadora electrónica permite abreviar los cálculos y simplificar la verificación de los resultados.

El consumo de ^{235}U del combustible se mide por análisis isotópico del metal transformado en hexafluoruro de uranio. El contenido de Pu se determina con una precisión del 2%, mientras que el empobrecimiento en ^{235}U se mide con una precisión de $\pm 5 \cdot 10^{-4}$.

1. INTRODUCTION

La détermination précise du plutonium dans un combustible nucléaire peut être effectuée par dilution isotopique.

Cette méthode présente de l'intérêt par sa sélectivité et sa grande sensibilité. Si le combustible est homogène, quelques milligrammes seulement d'échantillon sont nécessaires pour mesurer des teneurs en plutonium de l'ordre de 0, 01 à 0, 5%.

Elle peut servir de référence pour des essais non destructifs pratiqués sur les combustibles nucléaires, notamment la mesure des sections efficaces d'échantillons fissiles par oscillation [1, 2].

2. DOSAGE DU PLUTONIUM PAR DILUTION ISOTOPIQUE

2.1. Principe de la dilution isotopique

Pour doser dans un échantillon un élément possédant plusieurs isotopes, on utilise un «traceur», c'est-à-dire un composé où l'élément à doser est présent en quantité connue, dans le même état chimique que dans l'échantillon;

la composition isotopique de l'élément contenu dans le traceur est choisie très différente de celle de l'élément présent dans l'échantillon.

La méthode consiste à mélanger, en proportions connues, l'échantillon et le traceur. Après homogénéisation de la répartition des isotopes, la composition isotopique du mélange dépendra:

a) des quantités d'élément respectivement présentes dans l'échantillon et le traceur;
b) des proportions dans lesquelles le mélange a été effectué;
c) des compositions isotopiques de l'élément dans le traceur et l'échantillon.

La composition isotopique du mélange sera intermédiaire entre celle de l'échantillon et celle du traceur.

Il est fondamental en dilution isotopique d'obtenir une répartition physicochimique homogène des divers isotopes, quelle que soit leur origine: échantillon ou traceur. Cette condition est réalisée par un traitement chimique convenable; si celui-ci n'apporte pas de fractionnement isotopique, il n'est pas indispensable de récupérer intégralement les masses initiales mises en oeuvre, ni de rechercher la pureté absolue de l'élément à doser, ce qui est l'un des intérêts de la méthode.

La masse de l'élément présent dans l'échantillon est aisément calculable. Si P_M, P_T et P_E sont les concentrations isotopiques pondérales* d'un des isotopes de l'élément, respectivement dans le mélange, le traceur et l'échantillon, et si m_T et m_E sont les masses de l'élément dans le traceur et l'échantillon, la loi des mélanges permet d'écrire

$$P_M(m_E + m_T) = P_T m_T + P_E m_E ,$$

d'où

$$m_E = m_T \frac{P_T - P_M}{P_M - P_E} . \qquad (1)$$

m_T est connu; P_M, P_T et P_E sont déterminés par spectrométrie de masse.

Dans le cas où l'échantillon est disponible sous forme de solution, si C_T et C_E sont les concentrations chimiques de l'élément exprimées en masse

---

* Les rapports isotopiques sont mesurés par spectrométrie de masse, c'est-à-dire que pour l'isotope k d'un élément à n isotopes, on mesure des courants d'ions d'intensité I_k proportionnelle au nombre d'atomes de l'isotope k présent dans l'échantillon.

Par définition: la concentration isotopique atomique de l'isotope k est

$$A_k = I_k / \sum_{k=1}^{k=n} I_k .$$

La concentration isotopique en poids exprimée en rapport de masse est

$$P_k = M_k I_k / \sum_{k=1}^{k=n} M_k I_k ,$$

M_k étant la masse atomique de l'isotope k.

par unité de volume, V_T^* et V_E les volumes mélangés de traceur et de solution échantillon

$$C_E = C_T \frac{V_T}{V_E} \frac{P_T - P_M}{P_M - P_E} . \qquad (2)$$

2. 2. Dilution isotopique avec un traceur double [3]

Si l'on désire seulement déterminer le rapport des masses de deux éléments en solution (exemple : U/Pu) on peut utiliser un traceur double contenant les deux éléments correspondants. La dilution isotopique a lieu simultanément pour U et pour Pu au moment où l'on mélange la masse unique du traceur double à l'échantillon. Les compositions isotopiques des deux éléments seront modifiées par le mélange, mais de façon telle que la relation existant entre le rapport des masses des éléments dans l'échantillon et la composition isotopique des éléments dans le mélange sera indépendante des masses mélangées, ce qui permet d'éviter la mesure précise des quantités d'indicateur et d'échantillon que l'on utilise.

Le traceur double employé pour déterminer le rapport U/Pu contient : de l'uranium-233, isotope n'existant pas dans l'uranium naturel, qui est obtenu par irradiation neutronique du thorium-232; du plutonium-242 préparé par irradiation prolongée (plusieurs années) de plutonium-239 dans un réacteur à haut flux. Chaque essai nécessite 0, 2 μg de ^{242}Pu; 1 mg de ^{242}Pu est une quantité suffisante pour 5 000 déterminations.

Dans ces conditions, on calcule le rapport U/Pu de l'échantillon au moyen de la formule suivante, dans laquelle les rapports isotopiques sont exprimés en atomes:

$$\left(\frac{^{238}U}{^{239}Pu}\right)_E = \left(\frac{^{233}U}{^{242}Pu}\right)_T \frac{\left(\frac{^{238}U}{^{233}U}\right)_M - \left(\frac{^{238}U}{^{233}U}\right)_T}{\left(\frac{^{239}Pu}{^{242}Pu}\right)_M - \left(\frac{^{239}Pu}{^{242}Pu}\right)_T} . \qquad (3)$$

2. 3. Etalonnage du traceur double

Le rapport (^{233}U/^{242}Pu) doit être connu avec précision ; il ne peut être mesuré directement par pesée des éléments car on dispose en général de trop faibles quantités de ^{233}U et de ^{242}Pu et leur pureté chimique n'est pas connue.

La détermination précise de ce rapport est obtenue par dilution isotopique à l'aide d'une solution synthétique dite «étalon» préparée par pesée d'uranium naturel et de plutonium de pureté chimique connue.

De la relation (3) on tire la valeur de ce rapport :

$$\left(\frac{^{233}U}{^{242}Pu}\right)_T = \left(\frac{^{238}U}{^{239}Pu}\right)_{Etalon} \frac{\left(\frac{^{239}Pu}{^{242}Pu}\right)_M - \left(\frac{^{239}Pu}{^{242}Pu}\right)_T}{\left(\frac{^{238}U}{^{233}U}\right)_M - \left(\frac{^{238}U}{^{233}U}\right)_T} . \qquad (4)$$

Le rapport du nombre d'atomes d'uranium-238 au nombre d'atomes de plutonium-239 contenus dans l'étalon est calculé à partir des concentrations pondérales [U] et [Pu] à l'aide de la relation

$$\left(\frac{^{238}U}{^{239}Pu}\right)_{Etalon} = \frac{[U]}{[Pu]} \cdot \frac{239 + 240\left(\frac{240}{239}\right)_E}{238 + 235\left(\frac{235}{238}\right)_E}, \qquad (5)$$

dans laquelle les nombres hors parenthèses sont exprimés en unités de masse.

Le rapport ($^{233}U/^{242}Pu$) et les rapports isotopiques relatifs au traceur étant mesurés lors de l'étalonnage, il résulte que la détermination du rapport U/Pu d'un échantillon inconnu d'après la relation (3) se ramène à la mesure de deux rapports isotopiques dans le mélange échantillon-traceur.

3. APPLICATION DE LA MÉTHODE AUX COMBUSTIBLES NUCLÉAIRES

3.1. Traitement chimique [4, 5, 6, 7]

Le plutonium se trouvant à l'état très dilué dans les combustibles nucléaires, les rapports U/Pu fréquemment rencontrés varient entre 200 et 10 000.

La mise en solution par l'acide nitrique concentré a lieu en boîte à gants ou en boîte à pinces, avec protection de plomb si l'échantillon contient des produits de fission.

A partir de telles solutions, on détermine le rapport U/Pu par dilution isotopique, ainsi que la composition isotopique du plutonium présent et éventuellement celle de l'uranium.

L'analyse isotopique du plutonium par spectrométrie de masse ne peut être pratiquée avec les appareils de type courant sans une séparation chimique préalable de l'uranium. Une séparation U/Pu totale n'est pas indispensable, mais la quantité d'uranium résiduel doit être suffisamment faible (rapport U/Pu de l'ordre de 25) pour qu'on obtienne une émission thermoionique du Pu stable et pour permettre la séparation correcte des masses 239 (Pu) et 238 (U).

Le rôle du traitement chimique est très important, car outre une séparation uranium-plutonium convenable, son but est d'obtenir une répartition homogène des isotopes dans les mélanges traceur-échantillon.

La méthode mise au point à cette fin utilise les résines échangeuses d'ions; sur résine anion, les complexes nitriques de Pu^{IV} sont fixés sélectivement et peuvent ainsi être séparés de l'uranium et des produits de fission; une réduction ultérieure du plutonium à la valence III par le chlorhydrate d'hydroxylamine permet d'éluer le plutonium de la résine.

Cette technique, dont le schéma fait l'objet du tableau I, présente deux phases principales:

a) Le cycle de valence destiné à amener la totalité du Pu à la valence IV, afin de permettre sa fixation ultérieure sur résine. Le Pu pouvant exister en solution à des valences supérieures à IV, on pratique d'abord une réduction de tous les ions Pu à la valence III par le chlor-

TABLEAU I

SCHÉMA DU TRAITEMENT CHIMIQUE

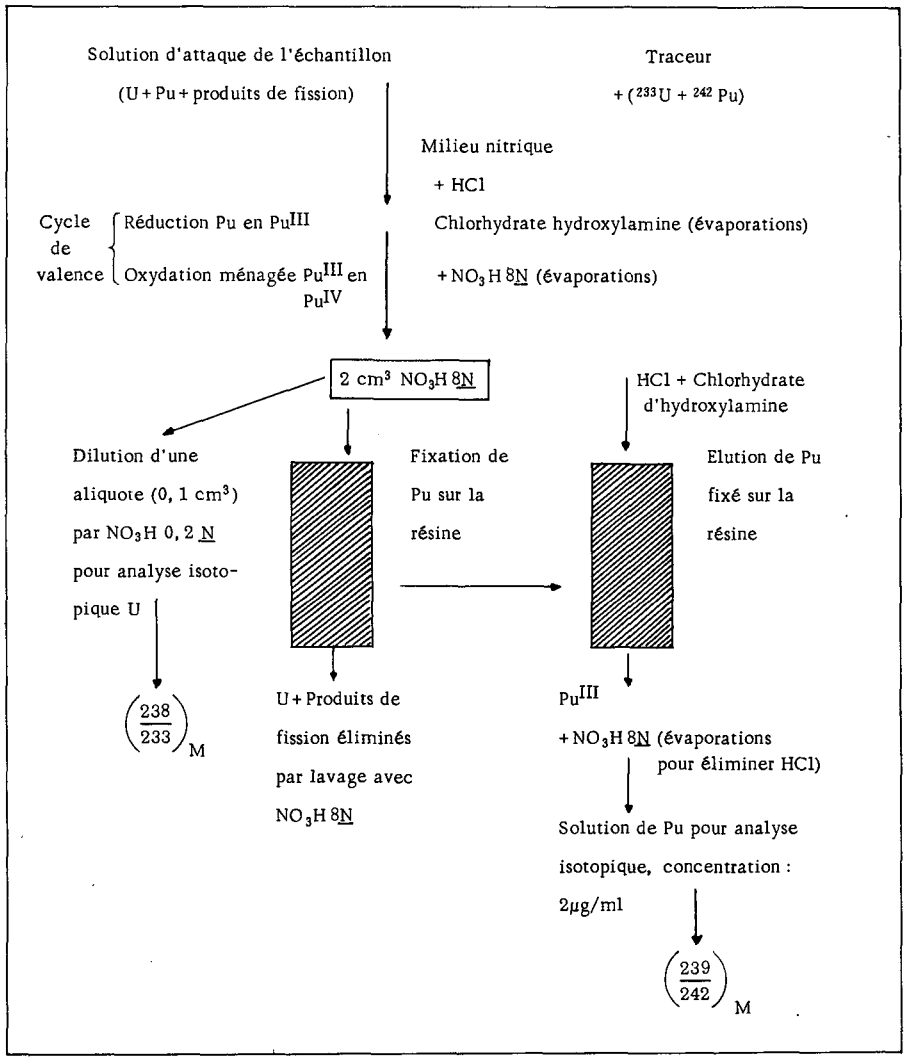

hydrate d'hydroxylamine, puis une réoxydation ménagée à la valence IV par l'acide nitrique; ce cycle doit assurer l'homogénéisation isotopique.

b) Le passage sur résine anion comprenant
   - la fixation du Pu^{IV},
   - le lavage servant à éliminer U et les produits de fission,
   - l'élution du Pu, sous forme de Pu^{III}, au moyen d'une solution réductrice.

Les quantités de plutonium utilisées pour cette séparation chimique sont de l'ordre de $2 \cdot 10^{-6}$ g par essai, ce qui correspond à des quantités initiales de combustible variant de 0, 5 à 20 mg selon la valeur du rapport U/Pu.

3. 2. Mesure des rapports isotopiques par spectrométrie de masse [8]

Les rapports isotopiques sont mesurés à l'aide d'un spectromètre de masse destiné à l'analyse des solides (MS_5 de Associated Electrical Industries, Grande-Bretagne).

Cet appareil est équipé d'une source à thermoionisation constituée de deux parties distinctes :

- la source d'ions proprements dite,
- le pied de source où sont disposés trois filaments ; deux d'entre eux sont utilisés indifféremment pour déposer l'échantillon et sont placés de part et d'autre du filament central où s'effectue l'ionisation. Ce pied de source, aisément amovible, est changé à chaque analyse. Le filament central ionisant en rhénium est chauffé à 2 500°C environ. La température des filaments latéraux où s'effectue l'évaporation varie selon la nature du produit à analyser ; cette technique à filaments multiples permet d'accroître l'efficacité de l'ionisation en élevant la température sans évaporer trop rapidement l'échantillon. La quantité de plutonium déposée sur le filament latéral en rhénium est de l'ordre de $2 \cdot 10^{-8}$ g.

Les dépôts d'uranium ($2 \cdot 10^{-7}$ g) sont effectués sur filaments de tantale ; l'utilisation de tels filaments a permis d'améliorer la sensibilité et la stabilité de l'émission thermoionique. Un appareil a été spécialement étudié pour obtenir des dépôts de très faibles quantités d'échantillon, qui soient reproductibles. Des comptages α sont d'ailleurs effectués sur les filaments pour contrôler la quantité de plutonium qui s'y trouve déposée.

La détection des courants d'ions est faite au moyen d'un multiplicateur d'électrons. Après amplifications, les intensités des courants d'ions relatifs à chaque masse sont enregistrées sur papier. Avec un multiplicateur possédant un gain de 5 000, on obtient aisément des courants stables d'intensités comprises entre 10^{-12} (pic principal) et 10^{-16} A.

La tension d'accélération des ions restant constante, le balayage du spectre par masses croissantes et décroissantes est obtenu par variation du champ magnétique.

Les mesures sont faites sur une série de dix enregistrements successifs du spectre considéré ; les moyennes des hauteurs de pics relatifs à un isotope sont utilisées pour le calcul.

Une calculatrice électronique (IBM 7094) effectue très rapidement un calcul d'erreur statistique pour chaque isotope, à partir des écarts entre les valeurs individuelles des hauteurs de pics et la valeur moyenne. Il lui est demandé, de plus, de donner les valeurs individuelles présentant des écarts supérieurs à une valeur donnée; cette valeur est fonction de la précision relative recherchée. Ceci permet d'attirer l'attention sur une valeur individuelle aberrante et d'en déceler rapidement l'origine : erreur de lecture des hauteurs de pics ou instabilité de l'appareil.

4. DISCUSSION DE LA MÉTHODE

4.1. Sélectivité

Le dosage du plutonium par dilution isotopique n'est pas sensible aux interférences d'ions étrangers, sauf s'il s'agit d'éléments possédant des isotopes de même masse : américium-241; ou de masse très voisine : uranium-238. Le traitement chimique décrit précédemment élimine totalement ^{241}Am et la majeure partie de ^{238}U ; la quantité d'uranium résiduel peut, de plus, être diminuée par un préchauffage de la source d'ions dans le spectromètre, la température de vaporisation de l'uranium étant plus basse que celle du plutonium.

4.2. Précision

Une étude détaillée des diverses causes d'erreur est nécessaire pour évaluer la précision de la méthode. Il faut distinguer en effet les erreurs statistiques inhérentes à la dilution isotopique, les erreurs de nature chimique et les erreurs instrumentales introduites par la spectrométrie de masse.

4.2.1. Erreurs statistiques

En différenciant l'équation générale (1)

$$\frac{dm_E}{m_E} = \frac{dm_T}{m_T} + d\frac{(P_T - P_M)}{P_T - P_M} + d\frac{(P_M - P_E)}{P_M - P_E},$$

nous voyons que nous obtenons une précision d'autant meilleure que $P_T - P_M$ et $P_M - P_E$ sont plus grands, c'est-à-dire lorsque P_T est très différent de P_E. Cette condition est réalisée puisque le traceur est constitué d'isotopes de Pu et d'U n'existant pas dans l'échantillon. D'autre part l'utilisation du traceur double, évitant la mesure précise des quantités d'échantillon et de traceur mélangées, élimine les erreurs pouvant résulter d'une telle détermination.

Un choix judicieux de ces quantités permet d'ailleurs de réduire au maximum l'erreur sur m_E.

4.2.2. Erreurs chimiques

Le traitement chimique ne doit pas introduire d'erreurs systématiques. Il faut s'assurer notamment :

- que l'attaque de l'échantillon est complète et conduit à une solution homogène,
- que le mélange échantillon-traceur est parfaitement réalisé,
- que le traitement chimique n'apporte pas de fractionnement isotopique.

Une étude particulière du cycle de valence a mis en évidence le rôle de l'uranium sur la cinétique d'oxydo-réduction du plutonium ; la technique opératoire a été améliorée en vue d'obtenir dans le même état de valence les isotopes du plutonium provenant de l'échantillon et du traceur.

Nous avons vérifié, d'autre part, que la composition isotopique d'une solution de plutonium n'était pas modifiée par les opérations chimiques utilisées: cycle de valence - passage sur résine échangeuse d'ions.

La précision de la méthode dépend aussi de la pureté de l'uranium et du plutonium utilisés pour préparer la solution «étalon» servant à étalonner le traceur. L'analyse spectrographique préalable des impuretés contenues dans ces métaux a permis d'admettre une pureté d'environ 99, 95%. Les pesées ont fait l'objet de précautions particulières, celle du plutonium étant effectuée en atmosphère inerte.

Précision relative : $2 \cdot 10^{-3}$ pour la pesée du plutonium,
$3 \cdot 10^{-4}$ pour la pesée de l'uranium.

4. 2. 3. Erreurs instrumentales

Les effets de mémoire sont très rares dans les spectromètres à source thermoionique. Les phénomènes de discrimination de masse peuvent être évités en étalonnant le traceur par dilution isotopique ; la solution de référence étant choisie de composition isotopique voisine de celle de la solution à étudier.

Les courants d'ions parasites : fond continu d'hydrocarbures, impuretés contenues dans les filaments etc. sont considérablement réduits par un préchauffage des filaments. L'emploi d'un multiplicateur d'électrons introduit toutefois une correction de bruit statistique qui peut être cause d'une légère erreur (2‰ environ).

En résumé, avec les spectromètres de masse de ce type, nous obtenons une précision relative de 0, 5 à 1% sur la mesure d'un rapport isotopique. L'expérience montre qu'en analyses de routine, la détermination de la teneur en plutonium d'un combustible, qui résulte d'un ensemble de mesures, est connue avec une précision de 2%.

4. 3. Sensibilité

La grande sensibilité de la méthode permet d'opérer sur quelques milligrammes seulement de combustible, donc de travailler avec un niveau d'activité γ faible qui n'impose pas de protection de plomb. Le traitement chimique des solutions et la préparation des dépôts sont effectués en boîte à gants. La fixation du pied de source dans le spectromètre se fait dans une petite boîte à gants qui équipe la partie supérieure de l'appareil.

4. 4. Reproductibilité

Lors d'analyses de série, la manipulation en boîte à gants de nombreuses solutions très diluées, mais de composition isotopique différente, risque d'amener rapidement des contaminations isotopiques qui nuisent à la reproductibilité des résultats.

La nature de ces pollutions peut être variée : origine atmosphérique, contaminations dues aux réactifs ou à des manipulations défectueuses. Nous nous sommes efforcés d'y remédier par un mode opératoire rationnel et l'emploi d'un matériel spécialement étudié.

Les évaporations sont effectuées de façon à éviter la présence de vapeurs saturantes à l'intérieur des boîtes à gants. Le matériel qui ne peut être renouvelé à chaque opération est soigneusement nettoyé à chaque changement d'échantillons.

5. RÉSULTATS

5.1. Etalonnage du traceur

Nous avons, à titre indicatif, groupé dans le tableau II les résultats des diverses déterminations entreprises pour étalonner le traceur.

TABLEAU II

QUANTITÉ PRÉSENTE DANS LA SOLUTION (ATOMES %)

a) Solution étalon

Composition chimique { Uranium 186,8 ± 0,05 g/l ; Plutonium 102 ± 0,2 mg/l }

Isotope	^{239}Pu	^{240}Pu	^{241}Pu	^{242}Pu
Quantité présente dans la solution	97,19 ± 0,05	2,68 ± 0,02	0,13 ± 0,005	-
Isotope	^{234}U	^{235}U	^{238}U	
Quantité présente dans la solution	0,0055 ± 0,0001	0,720 ± 0,005	99,28 ± 0,01	

b) Traceur

Composition chimique approximative { Uranium ≃ 5 g/l ; Plutonium ≃ 1 mg/l }

Isotope	^{239}Pu	^{240}Pu	^{241}Pu	^{242}Pu
Quantité présente dans la solution	1,31 ± 0,01	6,55 ± 0,06	4,03 ± 0,04	88,1 ± 0,1
Isotope	^{233}U	^{234}U	^{235}U	^{238}U
Quantité présenté dans la solution	99,54 ± 0,01	0,420 ± 0,005	-	0,04 ± 0,005

Les analyses isotopiques des mélanges effectués à partir de 0, 2 ml de traceur et de 0, 02 ml de solution étalon ont donné les valeurs figurant au tableau III; le rapport R a été calculé à partir des relations (4) et (5).

TABLEAU III

ANALYSE ISOTOPIQUE DES MÉLANGES

	$(^{238}U/^{233}U)_M$	$(^{239}Pu/^{242}Pu)_M$	$R=(^{233}U/^{242}Pu)_T$
I	$3,54_5 \pm 0,02$	$9,61 \pm 0,09$	5080
II	$3,55 \pm 0,02$	$9,61 \pm 0,09$	5073
		$9,61_5 \pm 0,09$	5076
III	$3,52_5 \pm 0,02$	$9,54_5 \pm 0,09$	5074
IV	$3,38 \pm 0,02$	$9,22 \pm 0,09$	5112
		$9,08 \pm 0,09$	5035
		$9,11 \pm 0,09$	5050

Valeur moyenne de R : $\bar{x} = 5072$

Le calcul statistique montre que, pour une probabilité de 95%, la valeur moyenne vraie est comprise entre les limites $\bar{x} \pm 25$, ce qui donne une précision relative de 0, 5%.

5. 2. Echanges analytiques entre le CEA et l'UKAEA

Quatre échantillons de solutions obtenues à partir d'alliage uranium-plutonium ont été analysés simultanément à Windscale (UKAEA) et à Saclay (CEA) par la méthode de dilution isotopique. Le tableau IV donne, pour chaque échantillon, les résultats de chacune des mesures indépendantes du rapport Pu/U, la moyenne de ces mesures et l'écart relatif entre les moyennes de l'UKAEA et du CEA.

On peut noter de part et d'autre la faible dispersion (1% au maximum) des mesures indépendantes sur un même échantillon et surtout l'excellent accord entre les résultats des deux laboratoires.

6. CONCLUSION

La méthode décrite procure les éléments nécessaires au calcul du taux de combustion d'un réacteur de puissance.

Sur un même échantillon de combustible, elle rend possible la détermination de

- la quantité totale de plutonium formé au cours de l'irradiation,
- la composition isotopique de ce plutonium,
- la composition isotopique de l'uranium permettant de connaître la quantité de ^{235}U détruit pendant la fission.

TABLEAU IV

ÉCHANGES CEA - UKAEA

Echantillon	71.05.06.0P/1	22.35.08.0P/5	FE I	FE II
$10^3 \cdot$ Pu/U (poids) CEA	0,415 0,421 $0,418_5$ 0,415	3,40 $3,39_5$ $3,40_5$	2,476 2,50 2,47	5,07 $5,13_3$ $5,13_2$
moyenne	$0,417_4$	3,40	$2,48_2$	$5,11_2$
$10^3 \cdot$ Pu/U (poids) UKAEA	$0,421_7$ $0,419_8$	$3,39_2$ $3,38_1$	2,470 $2,50_4$	$5,13_5$ $5,12_6$
moyenne	$0,420_8$	$3,38_7$	$2,48_7$	$5,13_1$
$\frac{\text{UKAEA}}{\text{CEA}} - 1$ (%)	+ 0,8	- 0,4	+ 0,2	+ 0,4

RÉFÉRENCES

[1] TRETIAKOFF, O., Physique des combustibles irradiés, Actes 3e Conf. int. util. EAFP, Genève (1964) P/77.

[2] VIDAL, R., TRETIAKOFF, O. et ROBIN, M., « Mesure des sections efficaces effectives d'échantillons fissiles par une méthode d'oscillation dans les assemblages critiques», Exponential and Critical Experiments III AIEA, Vienne (1964) 141.

[3] CHENOUARD, J. et LUCAS, M., Dosage du plutonium par dilution isotopique dans les combustibles irradiés, Rapports CEA R-2563-R-2564 (1964).

[4] AIKIN, A.M., An Ion Exchange Process for the Recovery of Pu from Irradiated Fuels, Second Nuclear Engineering and Science Conference, Philadelphie (1957).

[5] WEBSTER, R.K., SMALES, A.A., DANCE, D.F. and SLEE, L.J., AERE R 3327-R3378 (1960).

[6] The Determination of the Plutonium/Uranium Ratio on the Feed Solution of the Windscale Primary Separation Plant (1962).

[7] PREVOT, I., CORPEL, J. and REGNAUT, P., Final Treatment of Plutonium at the End of the Fontenay-aux-Roses Pilot Plant, Proc. 2nd UN Int. Conf. PUAE 17 (1958) 96-106.

[8] JONES, R.J., Selected Measurement Methods for Plutonium and Uranium in the Nuclear Fuel Cycle, TID-7029 - USAEC (1963).

QUELQUES MÉTHODES D'ESSAIS NON DESTRUCTIFS APPLICABLES AUX MATÉRIAUX FRITTÉS

ELENA LĂBUŞCĂ, I. MIRION, N. ANDREESCU,
M. ALECU ET I. BÎSCOVEANU
INSTITUT DE PHYSIQUE ATOMIQUE, BUCAREST, ROUMANIE

Abstract — Résumé — Аннотация — Resumen

SOME NON-DESTRUCTIVE TESTING METHODS APPLICABLE TO SINTERED MATERIALS. Bearing in mind the specific granular structure of sintered materials produced from powders, whose compaction process is linked with the sintering treatment, we have experimented with methods of checking the degree of sintering and certain other properties. The non-destructive methods used include:

(1) Examination of the crystalline structure of solid sinters, using metallography and electron microscopy. These methods show the homogeneity of the structure, the grain size and orientation, the presence of various flaws such as inclusions and pores, and the actual course of the sintering process, including crystal formation, grain growth, etc. In certain cases the microscopic examination can be combined with micro-hardness tests. This examination of the microcrystalline structure is one of the principal methods of checking the quality of sintered materials, and is irreplaceable by any other method.

(2) The degree of compaction, which is the main factor in determining the quality of sintered materials, can also be checked by measuring certain properties such as electrical and thermal conductivity in relation to density, since for sintered materials conductivity is directly proportional to the degree of sintering. We have also tested and found satisfactory a method for checking porosity, and have obtained interesting experimental data, especially on free porosity, which is susceptible to gaseous inclusions.

The paper gives experimental data on the application of these methods to certain sintered materials of importance in nuclear technology.

QUELQUES MÉTHODES D'ESSAIS NON DESTRUCTIFS APPLICABLES AUX MATÉRIAUX FRITTÉS. En tenant compte de la structure spécifique granulaire des matériaux frittés, élaborés à partir de poudres, pour lesquels le procès de consolidation évolue en fonction du traitement de frittage, on a expérimenté des méthodes de contrôle du degré de frittage et de quelques propriétés. Parmi les méthodes non destructives utilisées, les auteurs citent les suivantes:

1. Examen de la structure cristalline des corps solides frittés, à l'aide de la métallographie et de la microscopie électronique. Ces méthodes mettent en évidence l'homogénéité de la structure, les dimensions et l'orientation des grains, la présence de défauts divers (inclusions, pores) et l'évolution même du processus de frittage, y compris la formation des cristaux, la croissance granulaire, etc. Dans quelques cas, on peut combiner l'examen microscopique à des essais de microdureté. Cet examen de la structure microcristalline représente l'une des méthodes principales de contrôle qualitatif des matériaux frittés, et ne peut être remplacé par aucun autre moyen d'investigation.

2. Contrôle du degré de consolidation, qui détermine essentiellement la qualité des matériaux frittés. Ce contrôle est effectué par la mesure de quelques propriétés, telles que la conductibilité électrique et thermique, en corrélation avec la densité, étant donné que la conductibilité des matériaux frittés est directement porportionnelle au degré de frittage. On a essayé aussi une méthode adéquate de contrôle de la porosité; on a obtenu des données expérimentales intéressantes, surtout au point de vue de la porosité libre, laquelle est susceptible aux inclusions gazeuses.

Le mémoire contient des données expérimentales concernant l'application de ces méthodes de contrôle à quelques matériaux frittés intéressants pour la technologie nucléaire.

НЕКОТОРЫЕ МЕТОДЫ НЕДЕСТРУКТИВНЫХ ИСПЫТАНИЙ, ПРИМЕНИМЫЕ К СПЕЧЕННЫМ МАТЕРИАЛАМ. С учетом специфичной зернистой структуры спеченных материалов, разработанных на основе порошков, для которых процесс уплотнения зависит от спекания, использовались методы контроля за степенью спекания и за некоторыми свойствами. Использовались следующие методы без разрушения:

1. Изучение кристаллической структуры спеченных твердых тел с помощью металлографии и электронной микроскопии. Эти методы позволяют обнаружить однородность структуры, размеры и ориентацию зерен, наличие различных дефектов (вкрапления, пустоты), а также развитие процесса спекания, включая образование кристаллов, увеличение зерен и пр. В некоторых случаях можно совмещать микроскопическое исследование с испытаниями на микротвердость. Такое исследование микрокристаллической структуры представляет собой один из основных методов качественного контроля за спеченными материалами, и он не может быть заменен никаким другим методом исследования;

2. Степень уплотнения, которая и определяет главным образом качество спеченных материалов, также контролируется путем измерения некоторых свойств, например электро- и теплопроводимости, с поправкой на плотность, поскольку в случае с спеченными материалами проводимость прямо пропорциональна степени спекания. Применялся также адэкватный метод контроля за пористостью, который позволил получить интересные экспериментальные сведения, особенно с точки зрения свободной пористости, пригодной для газовых включений.

Приводятся экспериментальные данные относительно применения этих методов контроля к некоторым спеченным материалам, представляющие интерес для ядерной технологии.

ALGUNOS METODOS DE ENSAYO NO DESTRUCTIVO APLICABLES A LOS MATERIALES SINTERIZADOS. Teniendo en cuenta la estructura granular específica de los materiales sinterizados, elaborados a partir de polvos, cuyo proceso de consolidación se desarrolla en función del tratamiento de sinterización, los autores han estudiado algunos métodos para verificar el grado de sinterización y controlar ciertas propiedades. Entre los métodos no destructivos utilizados, se mencionan en la presente memoria:

1. Examen de la estructura cristalina de los sólidos sinterizados por metalografía y microscopía electrónica. Estos métodos ponen de manifiesto el grado de homogeneidad estructural, la dimensión y orientación de los granos, la presencia de defectos diversos (inclusiones, poros), y también la evolución misma del proceso de sinterización, incluyendo la formación de los cristales, el crecimiento granular, etc. En algunos casos, el examen microscópico se puede combinar con ensayos de microdureza. Este examen de la estructura microcristalina representa uno de los principales métodos de control cualitativo de los materiales sinterizados, y ningún otro medio de investigación puede reemplazarlo.

2. El grado de consolidación, factor esencial que determina la calidad de los materiales sinterizados, se verifica también midiendo algunas propiedades, por ejemplo la conductividad eléctrica y térmica, en función de la densidad, teniendo presente que en el caso de los materiales sinterizados, la conductividad es directamente proporcional al grado de sinterización. También se ha ensayado un método adecuado para verificar la porosidad, obteniéndose datos experimentales interesantes, sobre todo desde el punto de vista de la porosidad libre, que es afectada por las inclusiones gaseosas.

La memoria contiene datos experimentales sobre la aplicación de estos métodos de control a algunos materiales sinterizados, de interés para la tecnología nuclear.

Le développement des matériaux frittés, qui sont utilisés dans la plupart des domaines de la technique moderne y compris la technologie nucléaire, est dû principalement aux progrès notables de la technologie de la métallurgie des poudres. On peut à l'heure actuelle obtenir des matériaux aux structures homogènes et très fines et, par suite, des corps solides ayant une bonne isotropie, maintenir les propriétés dans des limites étroites et obtenir des corps compacts à partir de substances qu'il serait impossible d'agglomérer par d'autres procédés (par exemple une substance réfractaire, carbure, etc., avec un liant plus fusible).

D'une façon générale, la complexité des propriétés d'un matériel fritté en fonction des paramètres spécifiques du procédé technologique est connue. Les propriétés de deux corps frittés ayant la même composition chimique peuvent différer considérablement, en raison de leur histoire technologique. Cette différence est due, dans l'ensemble, au degré de consolidation des particules des corps solides respectifs. Alors que les solides obtenus par la fusion des composants ont une densité relativement constante, caractéris-

tique de leur composition chimique, les corps solides frittés ayant la même composition peuvent présenter une gamme étendue de densités, en fonction du degré de consolidation obtenu. Ce degré de consolidation dépend de toute une série de paramètres spécifiques importants, tels que la structure et la granulation des poudres, la pression d'agglomération, la température et la durée du frittage, etc.

Les matériaux frittés ont des propriétés très sensibles à la modification de tout détail technologique. On peut donc faire varier largement ces propriétés, en faisant varier les différents paramètres technologiques. La métallurgie des poudres présente ainsi des avantages notables, mais elle pose en même temps des problèmes très sérieux de reproductibilité des caractéristiques et d'homogénéité de la qualité.

Pour cette raison nous sommes obligés de considérer pour l'étude des matériaux frittés deux types de propriétés.

- propriétés découlant de la nature (composition) des corps frittés,
- propriétés spécifiques déterminées par la technologie métallo-céramique.

Etant donné la complexité des influences subies par un matériel fritté en cours de fabrication, il est nécessaire d'effectuer un contrôle rigoureux des propriétés à différentes étapes. Le contrôle final est également indispensable et nous considérons que c'est la connaissance du degré de frittage qui permet le mieux de déterminer les propriétés, dans des conditions expérimentales données.

Le mémoire donne quelques exemples de méthodes non destructives de contrôle des corps frittés. Ces méthodes sont généralement des méthodes de référence servant à vérifier les méthodes de contrôle destructives et pouvant les remplacer dans une certaine mesure, ou même complètement, lorsqu'on veut éviter de détruire le corps étudié. Ces méthodes non destructives exigent cependant que certains principes soient respectés dans la corrélation des données expérimentales; on doit également tenir compte du procédé de préparation du corps et des conditions dans lesquelles il sera utilisé.

EXAMEN AU MICROSCOPE

L'étude granulométrique et de la structure à l'aide d'un microscope optique et d'un microscope électronique est l'une des principales méthodes de contrôle qualitatif non destructif, méthode qui ne peut être remplacée, dans ce cas, par aucun autre moyen d'investigation. Elle est considérée généralement comme une méthode de référence servant à vérifier les procédés moins directs [1]. Nous avons considéré trois étapes principales du contrôle microscopique des matériaux frittés:

1. L'étude de la structure des poudres utilisées pour préparer les corps frittés - nécessaire pour mieux déterminer et conditionner les propriétés finales. La microscopie permet de déterminer la forme et la grandeur des grains et leur distribution granulométrique [2]. On utilise la microscopie optique ou électronique selon la dimension des grains. Les figures 1 à 3 montrent des images obtenues, à l'aide d'un microscope électronique, de particules ayant des formes d'aiguilles (fig. 1a et 1b), des formes poly-

édriques (fig. 2) ou des formes irrégulières (fig. 3). La microscopie peut être également utilisée pour l'étude du mécanisme de formation de quelques poudres; nous donnons quelques exemples (fig. 4) de la formation du graphite par cristallisation en forme d'aiguilles. Au microscope électronique on peut même distinguer (fig. 4c) la croissance en spirale de ces aiguilles et la formation des filaments de graphite [3].

2. Le processus de consolidation des poudres et de cristallisation est également mis en évidence par la microscopie [4, 5, 6, 7]. On peut ainsi identifier a) la croissance des grains en fonction de la température de frittage, (fig. 5); b) la forme spécifique des cristaux (fig. 6); c) l'orientation de la structure en fonction du procédé technologique (fig. 7); d) la présence de deux ou plusieurs phases (fig. 8); e) l'apparition des défauts divers, tels que des dislocations (fig. 9), et f) l'homogénéité ou la non homogénéité de la granulation (fig. 10). Généralement, on met aussi en évidence des défauts tels que pores, inclusions, déformation des cristaux, etc.

3. Les modifications de la structure dues à l'irradiation présentent un très grand intérêt, surtout pour les matériaux nucléaires, et peuvent être mises en évidence nettement à l'aide de la microscopie électronique. Nous donnons quelques exemples de structures obtenues après irradiation des matériaux oxydiques par des flux de l'ordre de 10^{18} n/cm^2 [8]. On peut ainsi suivre les diverses étapes de destruction de la structure des cristaux (fig. 11a à 11m).

Les méthodes de préparation des échantillons pour l'examen microscopique varient en fonction de la nature des matériaux. Généralement nous avons utilisé des répliques en deux couches. Pour la corrosion superficielle des échantillons, on utilise la corrosion chimique ou thermique, on peut aussi utiliser la corrosion par bombardement ionique [9], cette dernière méthode pouvant apporter des avantages notables, lorsqu'elle est appliquée de façon rigoureuse.

Nous mentionnons ici la possibilité de coupler l'examen microscopique avec des essais de microdureté. L'essai normal de dureté est destructif; néanmoins, on peut le considérer comme non destructif, si l'on tient compte du fait que la sollicitation mécanique est très limitée (valeur et zone d'application). Cette méthode met en évidence, par exemple, la différence de dureté entre les deux phases d'un échantillon, et la variation de la microdureté en fonction de la composition chimique qui est très intéressante, surtout pour les cermets.

DÉTERMINATION DE QUELQUES PROPRIÉTÉS PHYSIQUES

Le degré de consolidation, qui détermine essentiellement la qualité des matériaux frittés, est aussi contrôlé par les mesures non destructives de quelques propriétés physiques, parmi lesquelles nous avons retenu en particulier les mesures de la densité, des propriétés magnétiques, de la conductibilité électrique et thermique, et de la porosité libre des corps frittés.

1. La mesure des propriétés magnétiques fournit des indications très intéressantes sur les matériaux ferromagnétiques. Lorsque cette méthode est applicable, les données expérimentales obtenues sont très utiles, par exemple, pour constater les effets de l'irradiation; les propriétés magnétiques sont en effet généralement très sensibles. En vue de l'utilisation éventuelle de quelques matériaux magnétiques oxydiques frittés dans des champs de radiations, nous avons étudié les propriétés magnétiques avant et après irradiation, en mettant en évidence la sensibilité de quelques types de ferrites (PGM) pour lesquels on a constaté un accroissement allant jusqu'à 50% de la perméabilité par rapport aux valeurs avant irradiation (fig. 12a). Pour d'autres types de ferrites (PB), on a mis en évidence, par contre, un décroissement de la perméabilité magnétique allant jusqu'à 30 à 35% (fig. 12b). Pour d'autres types encore, notamment pour les ferrites à cycle d'hystérésis rectangulaire, on a mis en évidence une bonne stabilité [8].

L'influence de l'irradiation croît avec le flux de neutrons, qu'il s'agisse d'un accroissement ou d'un décroissement de la perméabilité magnétique (fig. 12c).

2. Conductibilité électrique. Pour déterminer la conductibilité électrique, nous avons adopté une méthode appropriée à l'étude des corps frittés ayant des dimensions relativement réduites et une résistivité électrique comprise entre $1{,}5 \cdot 10^{-6}$ et $10^{6}\ \Omega \cdot \mathrm{cm}$. La méthode diffère des procédés usuels en ce sens qu'on utilise quatre électrodes de contact disposées symétriquement (fig. 13). Nous avons utilisé des échantillons, soit en forme de disque d'une épaisseur uniforme (fig. 13a), soit prismatiques (fig. 13b), et des électrodes très pointues, pour réaliser un contact intime dans toute l'épaisseur. Si nous établissons, à l'aide des contacts A et B (fig. 13), un courant électrique I_{AB} traversant l'échantillon, nous obtenons entre les contacts D et C une tension électrique U_{DC}. Lorsque les contacts A, B, C et D sont disposés symétriquement [10], on peut écrire la relation

$$\rho = \frac{\pi d R_{AB,DC}}{\ln 2},$$

où d représente l'épaisseur de l'échantillon et $R_{AB,DC} = U_{DC}/I_{AB}$.

La méthode présente les avantages suivants:

a) Il est facile d'assurer un bon contact par une faible pression des quatre électrodes, notamment pour des échantillons de faible épaisseur.

b) La relation de calcul de la résistivité ne comprend qu'une seule dimension géométrique de l'échantillon, ce qui élimine une source d'erreur.

c) Le montage des échantillons entre les contacts est facile et permet l'application de la méthode à des essais en série.

Le désavantage de la méthode consiste dans le fait que des erreurs peuvent apparaître par suite d'un arrangement non symétrique de l'échantillon entre les électrodes de contact. L'importance de ces erreurs peut diminuer si les dimensions des échantillons mesurés consécutivement diffèrent peu, et si les contacts sont soigneusement fixés.

En utilisant pour la mesure de U_{DC} – selon les matériaux étudiés –, soit un microvoltmètre à résistance intérieure minime (20 Ω), soit un potentiomètre couplé à un galvanomètre de $5 \cdot 10^{-9}$ A/div avec une résistance in-

térieure équivalant à 400 MΩ, nous sommes parvenus à effectuer les essais avec des erreurs inférieures à 4 à 5%, et même 1 à 2%.

Les mesures de résistivité ont montré l'utilité de la méthode, notamment

a) Pour des matériaux du type cermet, dont la résistivité varie sensiblement en fonction du degré d'agglomération, de la température de frittage et de la teneur en oxyde (fig. 14).

b) Pour le contrôle en série des briques de graphite; la méthode est appropriée, car elle révèle la présence des défauts intérieurs (fissures, pores, etc.) et, selon nous, elle indique aussi les différences du degré de graphitisation. Dans la figure 15 nous donnons l'exemple d'une courbe normale de variation de la résistivité en fonction de la densité, déterminée pour un type de graphite. Lorsque les briques mesurées ont des défauts intérieurs, on obtient, pour les mêmes densités, des valeurs plus grandes pour la résistivité, valeurs qui peuvent dépasser d'un ordre de grandeur les valeurs normales. Pour quelques briques avec défauts, nous avons indiqué les valeurs obtenues dans la partie supérieure de la figure 15.

c) Pour les matériaux oxydiques frittés tels que l'UO_2; on a mis en évidence des différences très sensibles de résistivité d'échantillons ayant la même histoire technologique, différences dues aux défauts de structure ou à quelque influence locale, que reflète bien la variation de la résistivité.

3. Détermination de la surface spécifique des poudres et des porosités ouvertes. On a aussi étudié la surface spécifique des poudres initiales déterminée par la méthode de Lea et Nurse fondée sur la théorie de Kozeny et sur les recherches de Carman [1], c'est-à-dire la méthode dite fluométrique, adéquate sur certains points. Dans la figure 16 nous donnons un exemple de variation de la résistance mécanique à la flexion et de la densité en fonction de la surface spécifique, pour Al_2O_3 fritté.

En se fondant sur la même méthode, on a déterminé la perméabilité aux gaz ainsi que la surface totale des pores libres (ouverts), valeurs qui donnent une bonne image du comportement des matériaux dans des milieux fluides.

La figure 17 donne un exemple de variation de la surface des pores libres et de la perméabilité aux gaz en fonction de la porosité.

CONCLUSIONS

En se fondant sur les résultats expérimentaux décrits ci-dessus, on peut conclure que, entre autres méthodes non destructives, l'examen microscopique et la mesure de propriétés physiques telles que densité, conductibilité électrique, propriétés magnétiques, surface spécifique et perméabilité aux gaz, peuvent donner des indications précieuses. Il faut mentionner que, pour chaque type de matériau, il est nécessaire d'établir à partir d'essais destructifs des diagrammes de la variation des propriétés en fonction des paramètres qui peuvent être déterminés à l'aide d'un ou de plusieurs essais non destructifs; à l'aide de ces données de référence, on peut déduire les propriétés, par l'étude non destructive seulement.

RÉFÉRENCES

[1] L'HERMITE, R., Méthodes générales d'essai et de contrôle I, Paris (1959).
[2] DALLAVALLE, J. M., Micromeritics - The Technology of fine particles, London (1948).
[3] LĂBUŞCĂ, E., TEODORESCU, I. and MIRION, I., The Study of Carbon Block Graphitisation, Rev. Phys. Bucureşti, VI 1 (1961).
[4] HUGI, W., Le microscope électronique appliqué à l'étude des matériaux, Rev. BBC 49 11/12 (nov. - déc. 1962).
[5] SUMINO, K., KAWASAKI, Y. et al., Electron Microscopical Study, Acta metall. II II (nov. 1963).
[6] TRILLAT, J.J. et SAULNIER, A., Le microscope électronique et la métallurgie moderne, Nucleus, Paris 3 (mai-juin 1962); 4 (juillet-aout 1962).
[7] LĂBUŞCĂ, E., TEODORESCU, I. et MIRION, I., Rev. Phys., Bucureşti V 2 (1960); Rev. Roum. Métall. VI 2 (1961).
[8] LABUŞCA, E., ANDREESCU, N. et MOTOC, C., «Effets de l'irradiation aux neutrons sur la structure et les propriétés magnétiques des ferrites de manganèse et de lithium à grande perméabilité», Radiation Damage in Solids, III AIEA, Vienne (1963) 103; Rev. Phys. Bucureşti IX 4 (1964).
[9] TEODORESCU, I., Effets du bombardement ionique sur la corrosion des surfaces métalliques, Thèse 1965 (à paraître dans Rev. Phys., Bucuresti).
[10] PAUW, L.J. van du., Rev. tech. Philips 20 8 (1959).
[11] VASILIU, S., Méthode de mesure de la conductivité thermique des échantillons de petites dimensions, (à paraître dans Studii si Cercetari de Fizica, Ed. Acad. R.P. Romine (1965).

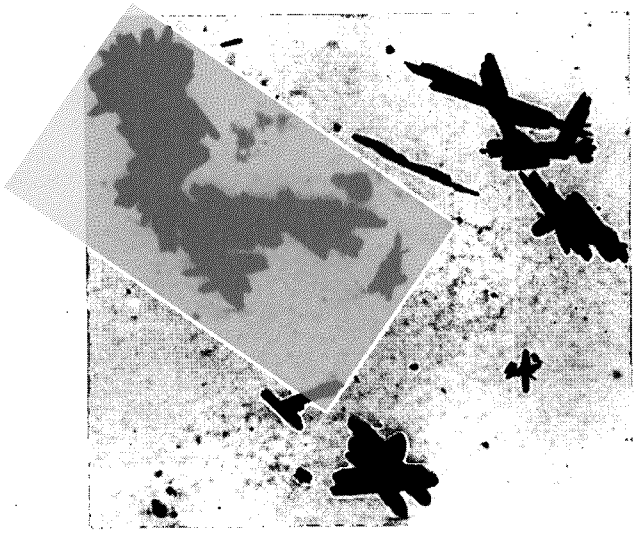

a)

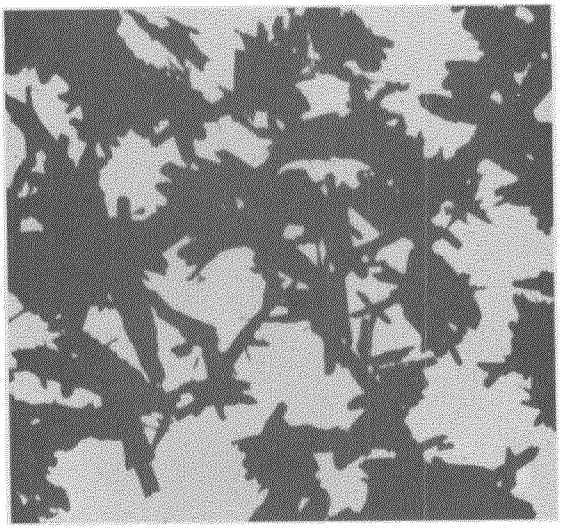

b)

Figure 1

Poudre métallique à particules en forme d'aiguilles (× 18 000).
(réduite de 25% à l'impression)

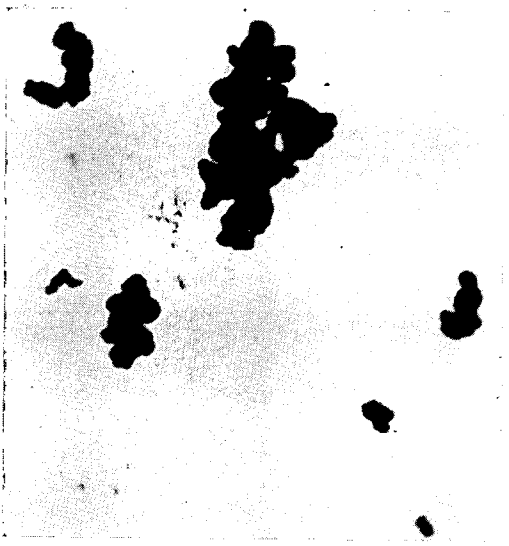

Figure 2

Poudre métallique à particules de forme polyédrique (× 18 000).
(réduite de 25% à l'impression)

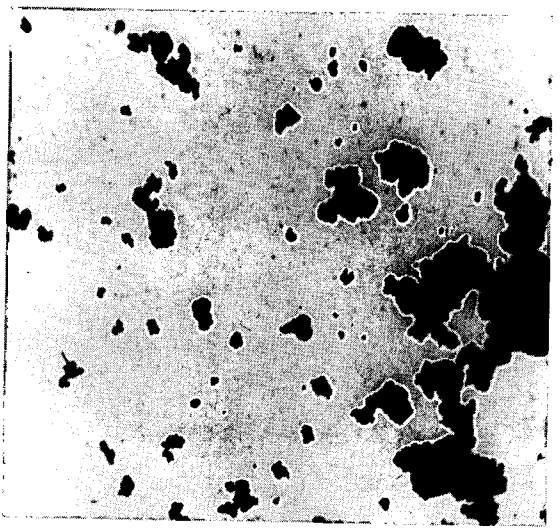

Figure 3

Particules agglomérées de forme irrégulière (× 18 000).
(réduite de 25% à l'impression)

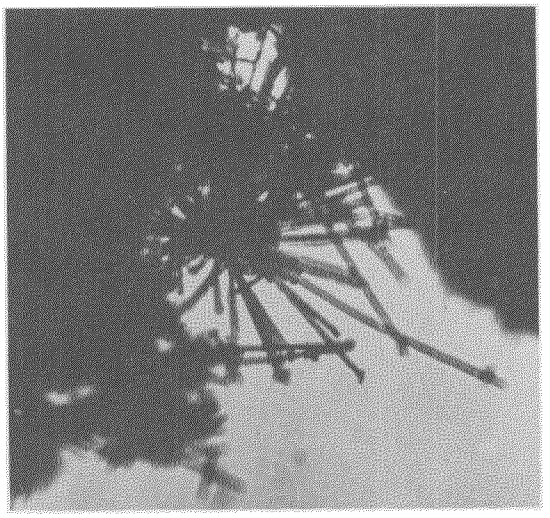

a)

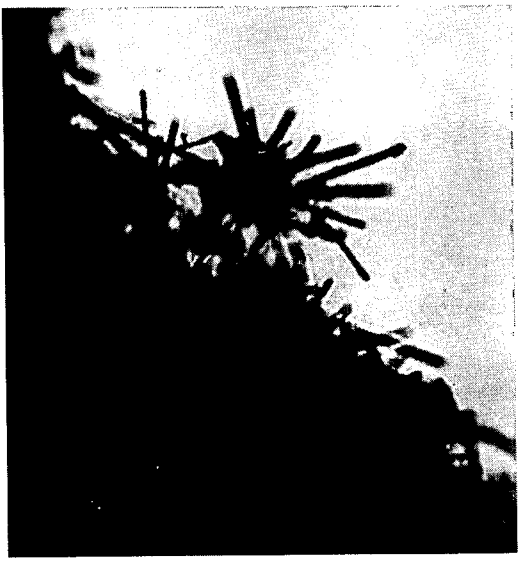

b)

Figure 4

Croissance granulaire du graphite, en forme d'aiguilles :a), b) ×300, (réduite de 25% à l'impression)

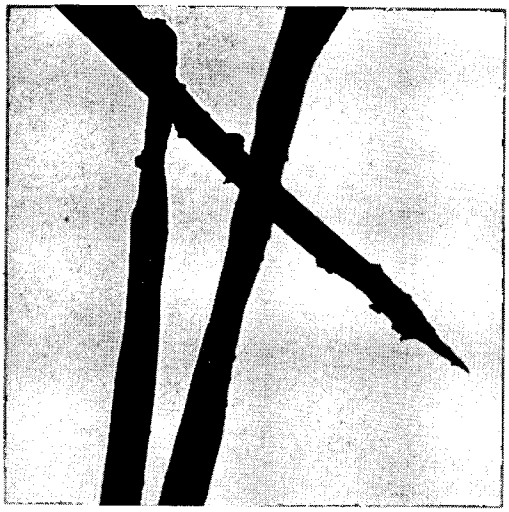

c)

Figure 4 (suite)

c) (× 18 000)
(réduite de 40% à l'impression)

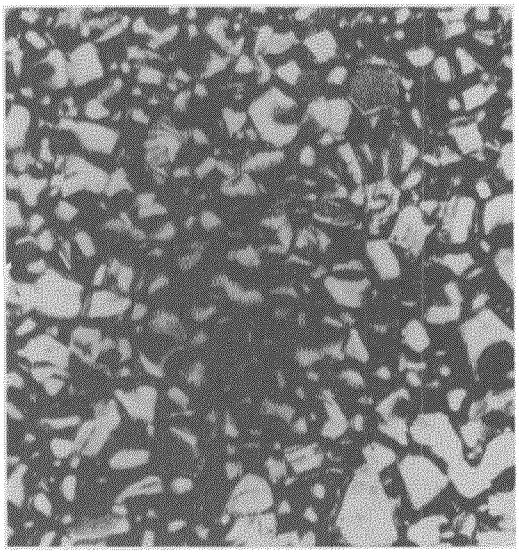

a)

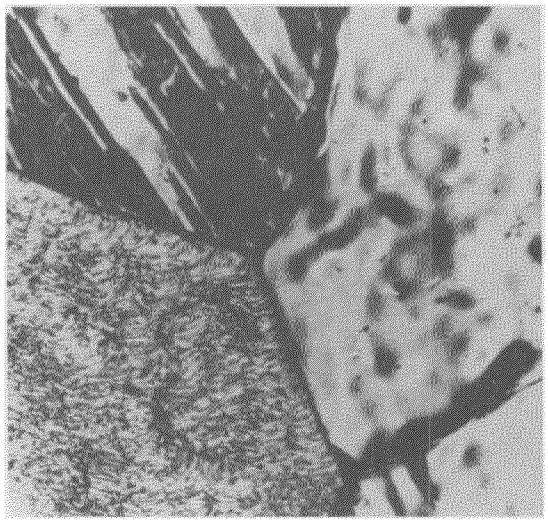

b)

Figure 5

Croissance granulaire des oxydes métalliques en fonction de la température de frittage
(× 900, a) 1200 °C; b) 1400 °C).
(réduite de 25% à l'impression)

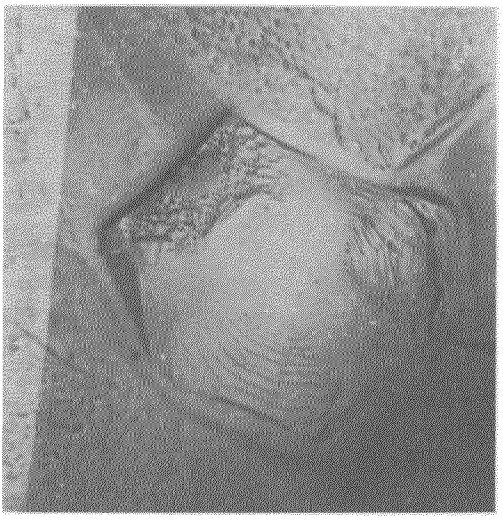

a)

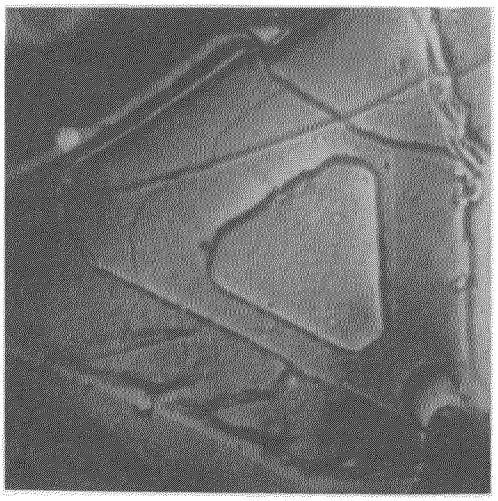

b)

Figure 6

Formation des cristaux de Al_2O_3 fritté: détails de structure (× 18 000), (réduite de 25% à l'impression)

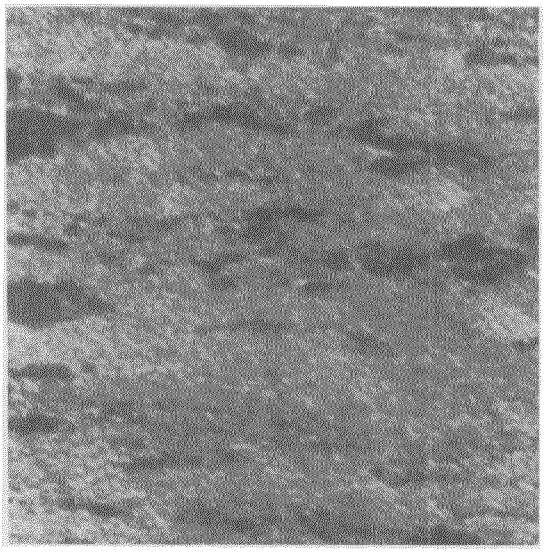

Figure 7

Orientation des grains et des défauts, déterminée par le laminage d'un matériel métallique (×900), (réduite de 25% à l'impression)

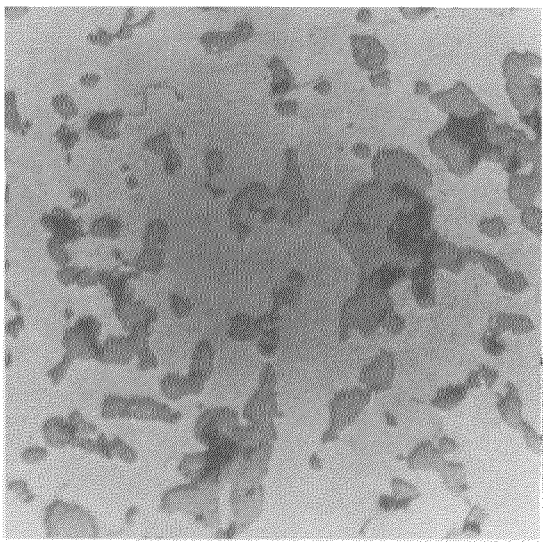

a)

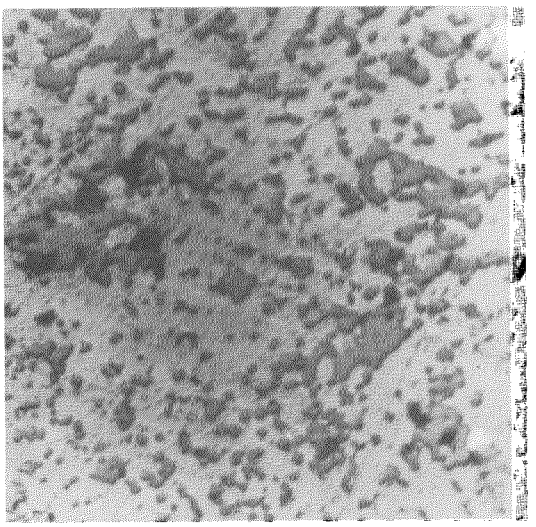

b)

Figure 8

Structure des matériaux de type cermet à deux phases distinctes
(oxyde + métal) (×900).
(réduite de 25% à l'impression)

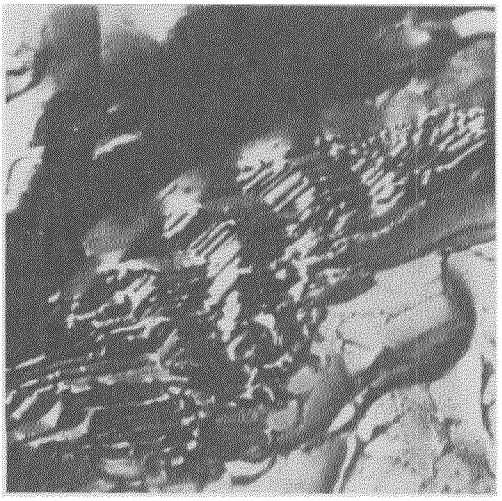

a)

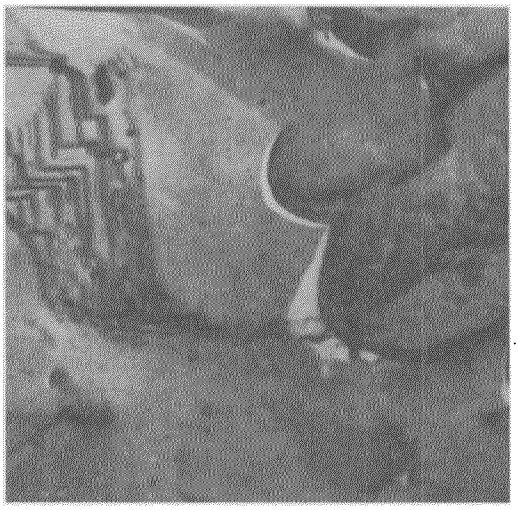

b)

Figure 9

Dislocations dans Al_2O_3 fritté (× 18 000).
(réduite de 25% à l'impression)

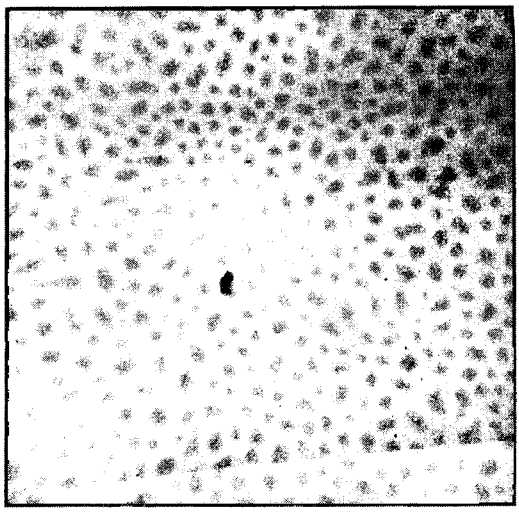

a)

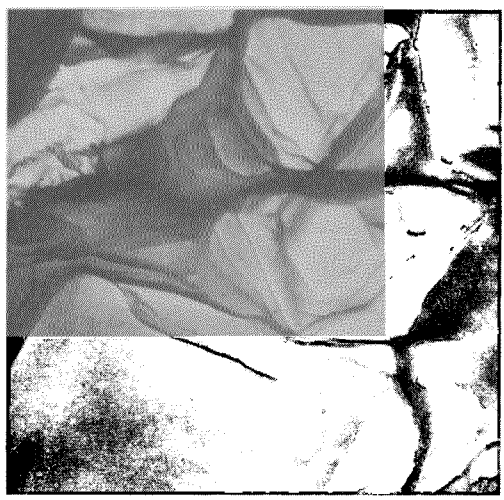

b)

Figure 10

Matériau oxydique fritté à granulation a) homogène, et b) discontinue (×18 000). (réduite de 40% à l'impression).

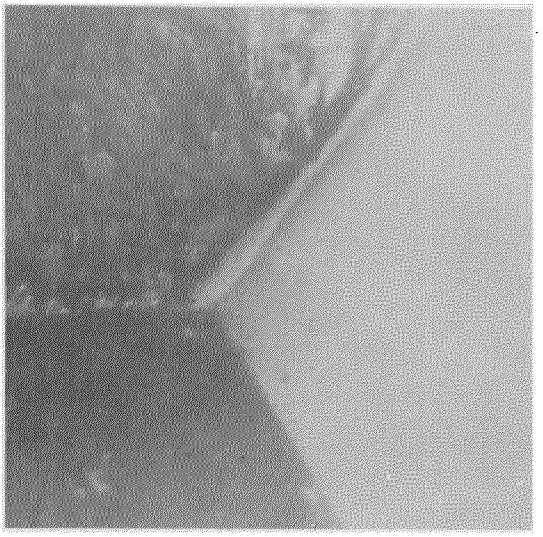

a)

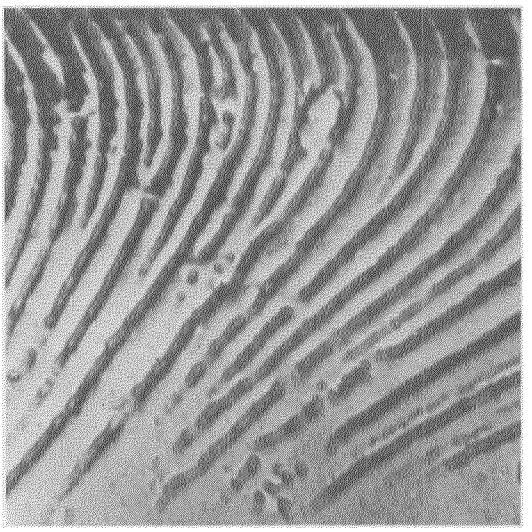

b)

Figure 11

Structure d'un matériau oxydique fritté (× 18 000).

a) cristal à forme parfaite, avant irradiation
b) couches lamellaires de croissance d'un cristal, avant irradiation

(réduite de 25% à l'impression)

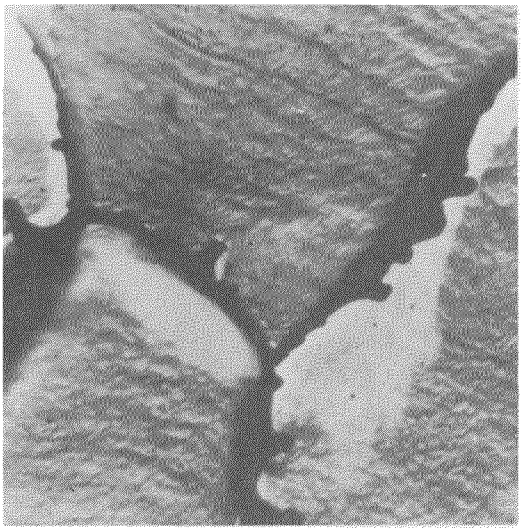

c)

Figure 11 (suite)

c) à m) défauts d'irradiation aux neutrons
c) déformation des cristaux

(réduite de 25% à l'impression)

d)

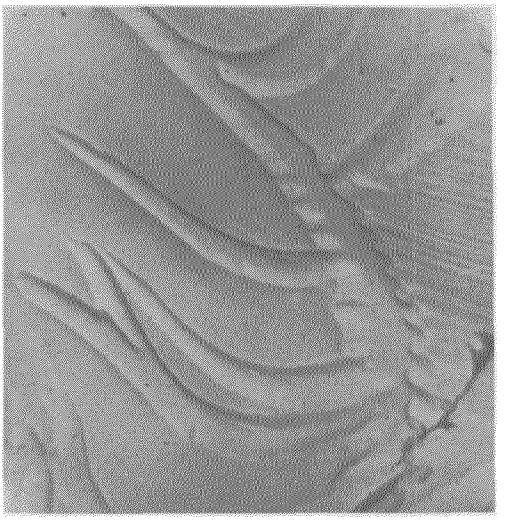

e)

Figure 11 (suite)

d), e) infiltration de la phase vitreuse à l'intérieur des cristaux

(e) réduite de 40% à l'impression)

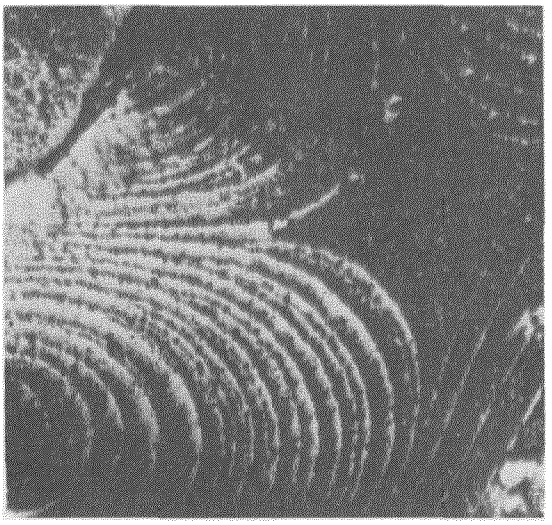

f)

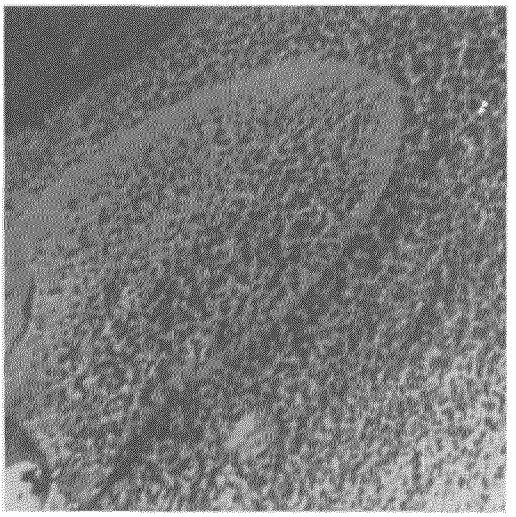

g)

Figure 11 (suite)

f), g) destruction de la structure lamellaire et apparition de la structure granulaire

(réduite de 25% à l'impression)

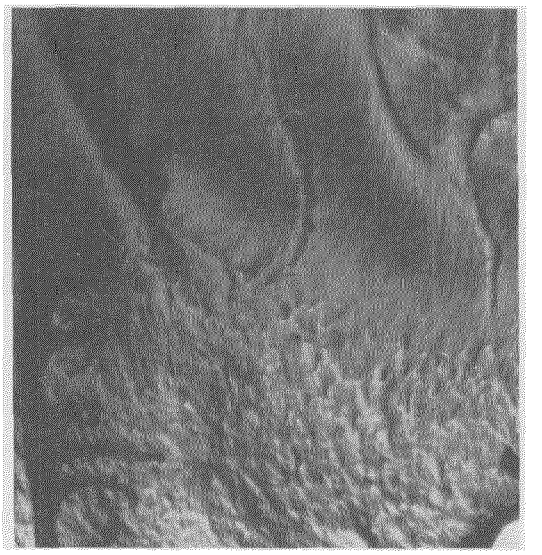

h)

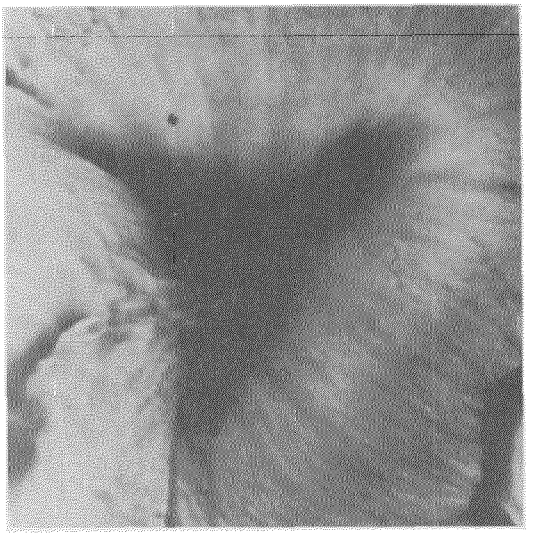

i)

Figure 11 (suite)

h), i) structures fibreuses

(réduite de 25% à l'impression)

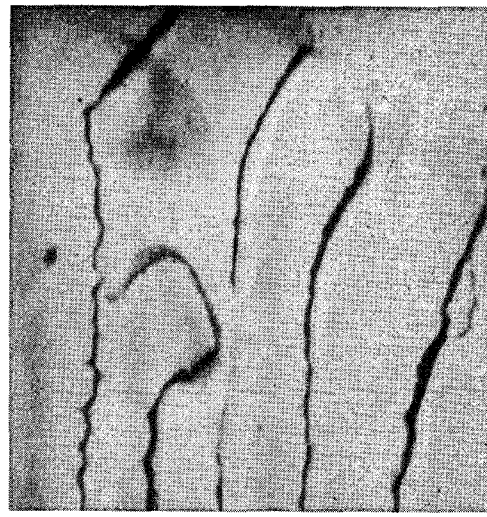

j)

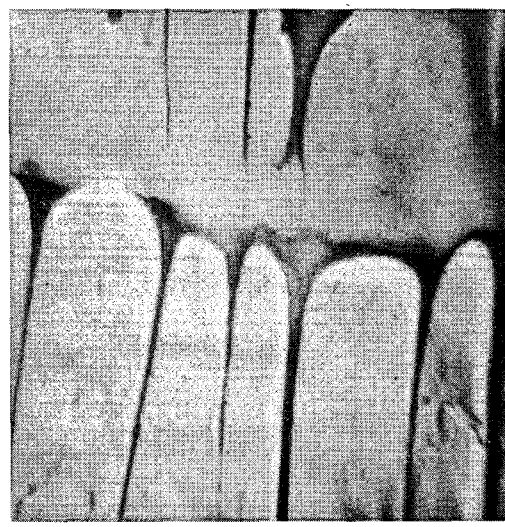

k)

Figure 11 (suite)

j), k) boucles de dislocations

(réduite de 40% à l'impression)

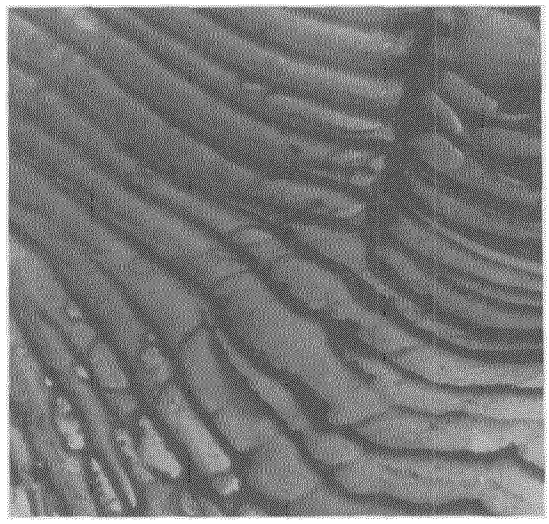

l)

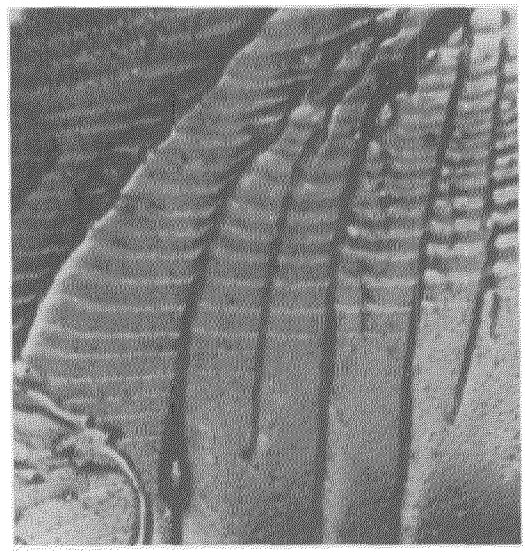

m)

Figure 11 (suite)

l), m) défauts complexes, dislocations

(réduite de 25% à l'impression)

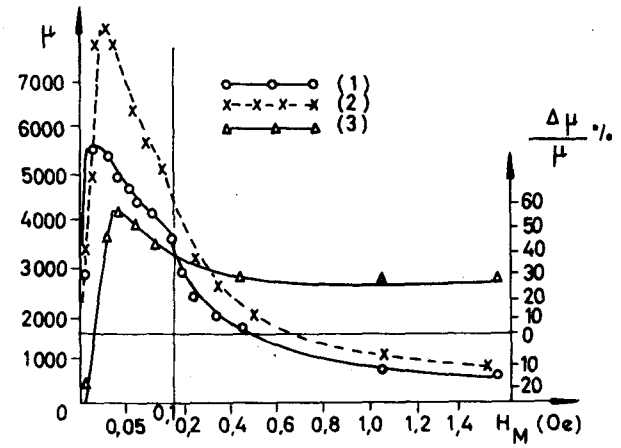

a)

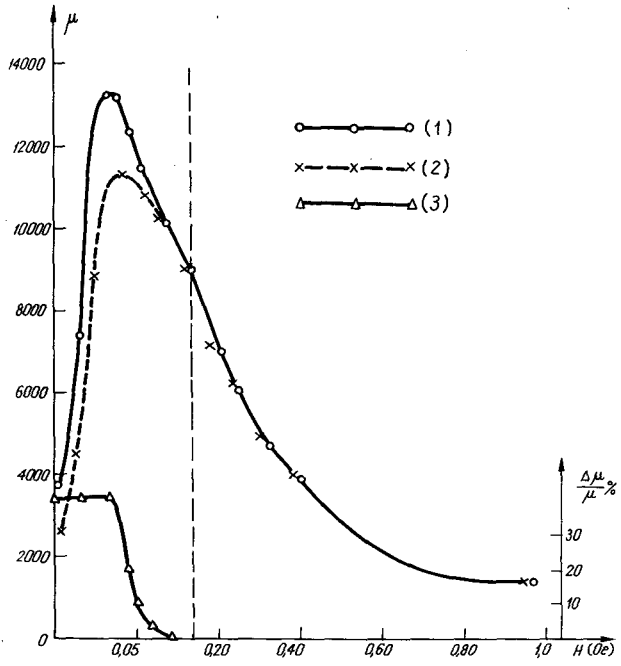

b)

Figure 12

Variation de la perméabilité magnétique des ferrites après irradiation aux neutrons.

a) accroissement de la perméabilité
   1) avant irradiation,
   2) après irradiation,
   3) variation relative $\Delta\mu/\mu\%$;

b) décroissement de la perméabilité;

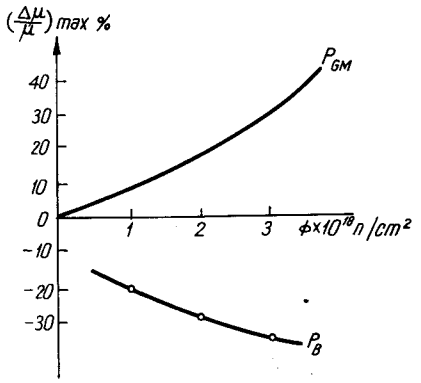

c)

Figure 12 (suite)

c) variation de la perméabilité en fonction du flux de neutrons.

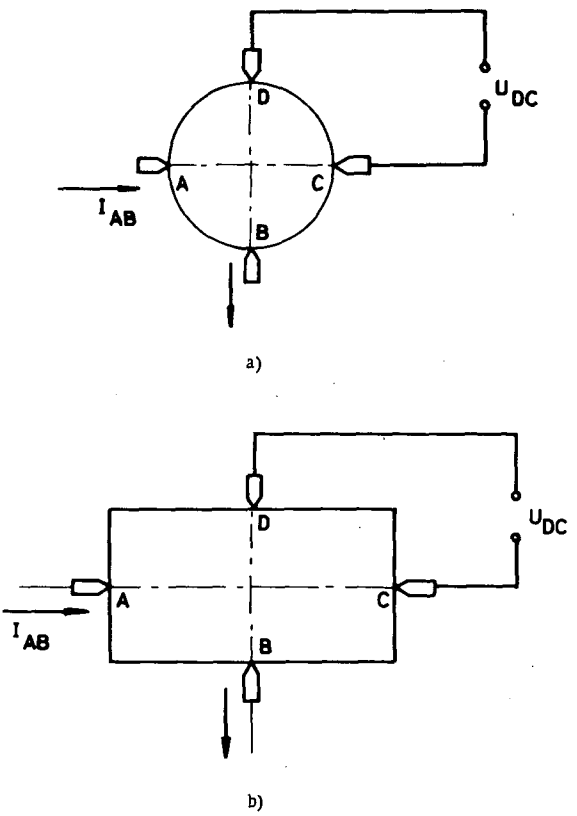

Figure 13

Schéma de la méthode de mesure de la résistivité.
a) échantillons cylindriques;
b) échantillons prismatiques.

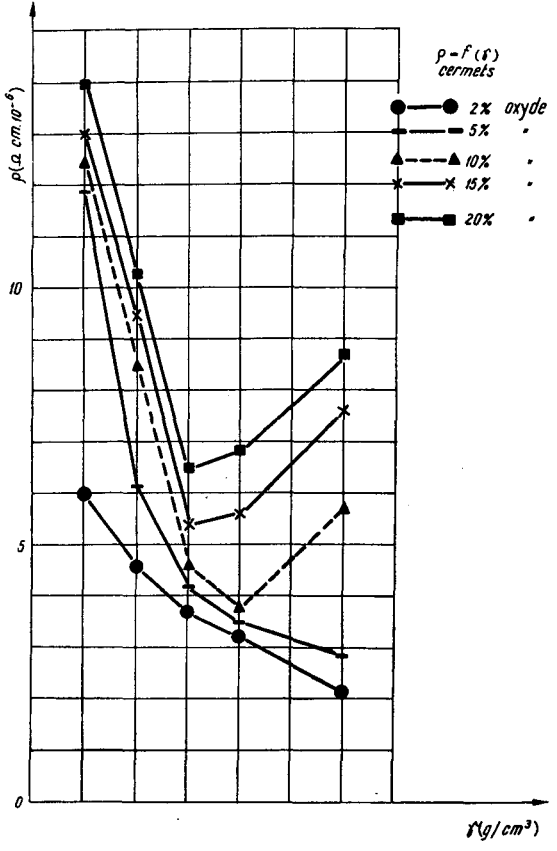

a)

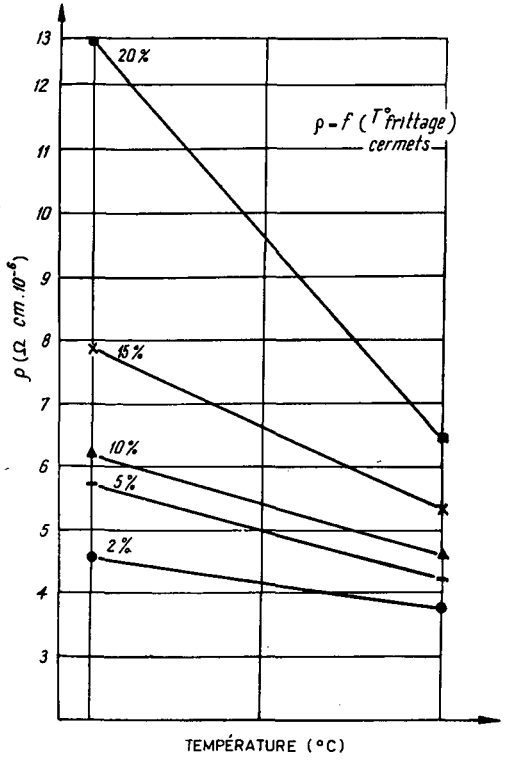

b)

Figure 14

Variation de la résistivité de quelques matériaux de type cermet en fonction
a) du degré d'agglomération et
b) de la température du frittage.

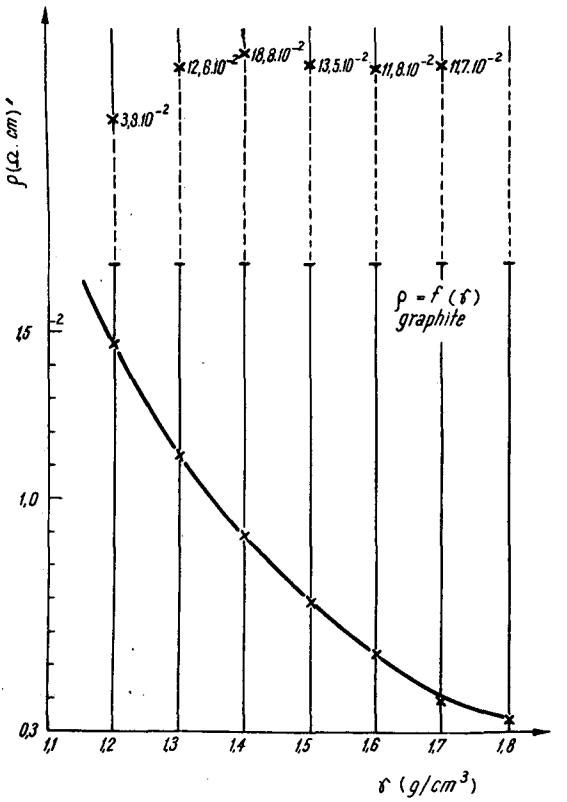

Figure 15

Variation de la résistivité des briques de graphite en fonction de la densité.

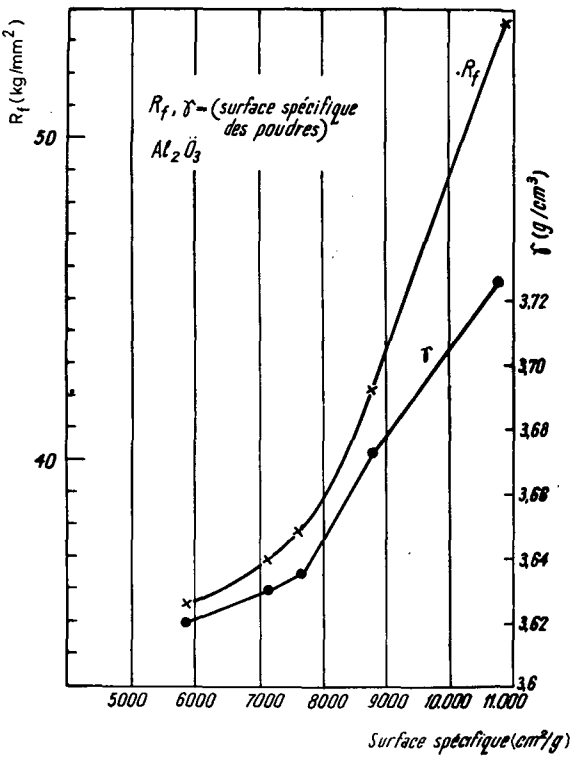

Figure 16

Variation de la résistance mécanique de Al_2O_3 fritté, en fonction de la surface spécifique des poudres.

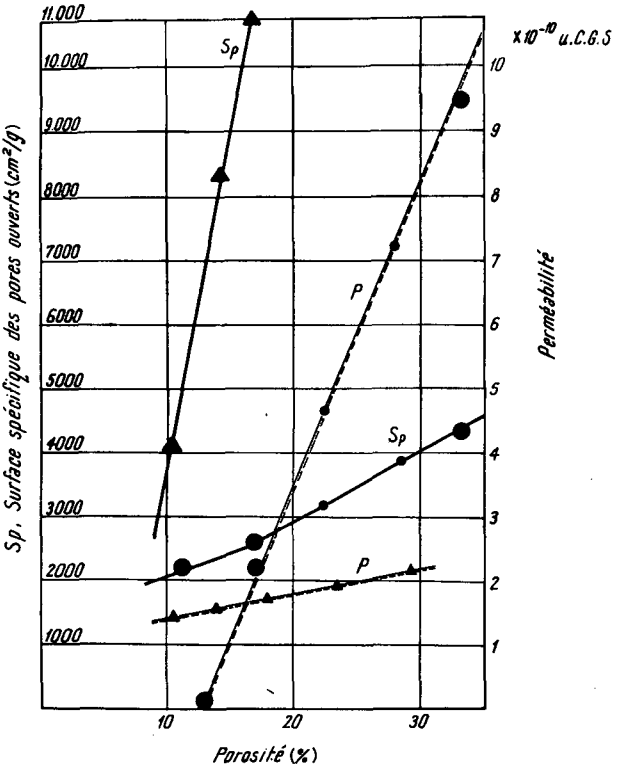

Figure 17

Variation de la surface spécifique des pores ouverts et de la perméabilité aux gaz en fonction de la porosité.

▲——▲ Aluminium métallique pressé

●——● Al_2O_3 fritté

DISCUSSION

J. GÉRARD: Do you think it is possible to determine sinterability completely from the physical characteristics of the powders alone? Which do you think are the most interesting parameters to examine?

E. LĂBUŞCĂ: With sintered material for which there is already a well-established technology in respect of all the technical parameters (pressures, temperatures, durations, sintering atmosphere etc.) the sinterability can be estimated with good accuracy from the characteristics of the powders alone. Of these characteristics I think the most representative and the most important to determine are: (1) the structure of the powder particles (shape); (2) the grain dimensions; (3) the specific surface; (4) the volume before and after compression. For a given powder, prepared under the same conditions, it is only necessary to control the dimensions and the specific surface to determine the quality.

G. TENNEY: What metal was used for the shadow-casting technique?

E. LĂBUŞCĂ: Gold, silver and chromium.

G. TENNEY: Since the scale was not shown I should like to ask what is the magnification.

E. LĂBUŞCĂ: The magnification for each photograph is indicated in the paper. For electron microscopy it was×18 000.

G. TENNEY: What kilovoltage was used for the electron beam?

E. LĂBUŞCĂ: 30-50 kV.

G. TENNEY: Do you have a hot stage?

E. LĂBUŞCĂ: We have not yet done any microscopic studies at high temperature.

P. de MEESTER: Since the magnification of the electron microscope photos was only ×18 000 do you regard the black lines shown in your last figure as simple dislocations or complex defects?

E. LĂBUŞCĂ: We regard the structures obtained after irradiation as agglomerations of dislocations, bearing in mind also that they are obtained for strongly irradiated materials. In other words, to use the terminology generally employed in specialized works, yes, we do regard them as "complex defects".

SESSION VI

THE ROLE OF NON-DESTRUCTIVE TESTING IN THE LOS ALAMOS REACTOR PROGRAMME *

G.H. TENNEY
UNIVERSITY OF CALIFORNIA, LOS ALAMOS SCIENTIFIC LABORATORY,
LOS ALAMOS, N. MEX., UNITED STATES OF AMERICA

Abstract — Résumé — Аннотация — Resumen

THE ROLE OF NON-DESTRUCTIVE TESTING IN THE LOS ALAMOS REACTOR PROGRAMME. The Los Alamos Scientific Laboratory, operated by the University of California for the United States Atomic Energy Commission, has been active for more than twenty years in developing, designing, and building nuclear reactors of four general types: research, power, rocket propulsion, and critical assembly.

The Non-destructive Testing Group serves practically all the activities and projects of the Laboratory; this paper describes some of the unique non-destructive testing techniques and applications developed for and used in the reactor programme.

LAPRE (Los Alamos Power Reactor Experiment) was based on the use of a uranium phosphate solution at high temperature. This solution is very corrosive, and all parts in contact with it were clad with gold. Special radiographic techniques were used to inspect the gold during the process of producing rolled sheet from cast ingot. The welded seams were similarly inspected. An electrode-potential inspection method was developed for checking the gold surfaces for imbedded impurities.

The fundamental concept of LAMPRE (Los Alamos Molten Plutonium Reactor Experiment) is the use of liquid - rather than solid - plutonium metal as fuel. Tantalum capsules contained the fuel. Novel non-destructive testing methods were used to check the soundness of base metal and welds during the production of the capsules, and to study the plutonium-loaded capsules before, during, and after melt-freeze tests. A molten plutonium pump experiment was followed with radiographic techniques, including a gamma-ray closed television circuit.

For UHTREX (Ultra High Temperature Reactor Experiment), now under construction, microradiographic and electron microscopic studies have been made on 150-μm-diam. pyrocarbon-coated uranium carbide beads, to evaluate uranium migration as a function of temperature. The amount, and uniformity, of the uranium loading in the UHTREX graphite elements are determined with specially designed scintillation counters. About 90% of the work on this subject has not been previously published.

RÔLE DES ESSAIS NON DESTRUCTIFS DANS LE PROGRAMME DE RÉACTEURS DE LOS ALAMOS. Le Laboratoire scientifique de Los Alamos, exploité par l'Université de Californie pour la Commission de l'énergie atomique des Etats-Unis, s'occupe depuis plus de vingt ans de l'étude, de la mise au point et de la construction de quatre types de réacteurs nucléaires: réacteurs de recherche, réacteurs de puissance, réacteurs pour la propulsion des fusées et assemblages critiques.

Le Groupe des essais non destructifs collabore à presque tous les projets et travaux du Laboratoire. Le mémoire décrit quelques-unes des méthodes inédites d'essais non destructifs qui y ont été mises au point et sont appliquées dans le cadre du programme de réacteurs.

Le réacteur de puissance expérimental LAMPRE est fondé sur l'utilisation d'une solution de phosphate d'uranium à haute température. Cette solution est très corrosive et toutes les parties en contact avec elle ont un revêtement en or. On a eu recours à des techniques radiographiques spéciales pour contrôler l'or pendant le processus de laminage d'un lingot coulé. On a procédé de la même manière à l'inspection des soudures. Une méthode d'inspection fondée sur les variations de potentiel aux électrodes a été mise au point, pour la détection d'impuretés sur les surfaces d'or.

Le réacteur expérimental au plutonium fondu LAPRE est fondé sur l'utilisation de plutonium métallique, sous forme liquide plutôt que sous forme solide, comme combustible. Le combustible est contenu dans des capsules en tantale. On a eu recours à des méthodes non destructives pour vérifier le bon état du métal de base et des soudures pendant la fabrication des capsules, ainsi que pour contrôler les capsules remplies de

* Work supported by the United States Atomic Energy Commission.

plutonium avant, pendant et après les essais de fusion et solidification. L'essai d'une pompe à plutonium fondu a été suivi par des méthodes radiographiques, en utilisant notamment un circuit fermé de télévision à rayons gamma.

Pour le réacteur expérimental à très haute température UHTREX, actuellement en construction, on a étudié par microradiographie et au moyen de microscopes électroniques des grains de carbure d'uranium enrobés de carbone pyrolytique, d'un diamètre de 150 µm, pour évaluer la translocation de l'uranium en fonction de la température. On détermine la quantité et l'uniformité de la charge d'uranium dans les éléments au graphite d'UHTREX au moyen de compteurs à scintillation spécialement conçus. Environ 90% des travaux effectués à ce sujet n'ont encore fait l'objet d'aucune publication.

РОЛЬ НЕДЕСТРУКТИВНЫХ ИСПЫТАНИЙ МАТЕРИАЛОВ В ЛОС-АЛАМОССКОЙ РЕАКТОРНОЙ ПРОГРАММЕ. Лос-Аламосская научная лаборатория, руководство которой осуществляет Калифорнийский университет для Комиссии по атомной энергии США, в течение более двадцати лет активно занимается разработкой, проектированием и строительством ядерных реакторов четырех общих типов: исследовательских, энергетических, реакторов для ракетных двигателей и критических сборок.

Группа недеструктивных испытаний материалов оказывает услуги на практике всем видам деятельности и проектам лаборатории; в этом докладе описываются некоторые из уникальных методов испытаний без разрушения и приемов, разработанных для реакторной программы и используемых в ней.

ЛАЭРЭ (Лос-Аламосский энергетический реакторный эксперимент) основан на использовании раствора фосфата урана при высокой температуре. Этот раствор является очень коррозийным, поэтому все части, находящиеся в контакте с ним, были покрыты золотом. Специальные радиографические методы позволяли контролировать золото во время процесса производства прокатанного листа из слитка. Осуществлялся также контроль за сварными швами. Был разработан метод проверки потенциала электрода для контроля золотых поверхностей для обнаружения содержащихся загрязнений.

Основная концепция ЛАРЭРП (Лос-Аламосский реакторный эксперимент с расплавленным плутонием) заключается в использовании в качестве топлива скорее жидкого, чем твердого металлического плутония. Танталовые капсулы содержали топливо. Были использованы новые методы контроля без разрушения для проверки прочности основного материала и сварок во время производства капсул, а также для изучения капсул, заполненных плутонием до, во время и после контроля методом охлажденной плавки. За экспериментом по перекачке расплавленного плутония наблюдали с помощью радиографических методов, включая гамма-лучи, связанные с контуром телеведения.

Для РЭУВТ (Реакторный эксперимент при ультра-высокой температуре), который в настоящее время находится в стадии строительства, были проведены микрорадиографические и электронно-микроскопические исследования на шариках диаметром 150 микрон из карбида урана, покрытых пироуглеродом, для оценки миграции урана как функция температуры. Количество и однородность урановой загрузки в графитовых элементах РЭУВТ определяются с помощью специально сконструированных сцинтилляционных счетчиков.

Примерно 90% работы по этой теме ранее не было опубликовано.

PAPEL DE LOS METODOS DE ENSAYO NO DESTRUCTIVO EN EL PROGRAMA DE REACTORES DE LOS ALAMOS. El Laboratorio Científico de Los Alamos, explotado por la Universidad de California por encargo de la Comisión de Energía Atómica de los Estados Unidos, viene ocupándose desde hace más de veinte años del proyecto, diseño y construcción de reactores nucleares de cuatro tipos generales; a saber, de investigación, de potencia, de propulsión espacial y para conjuntos críticos.

El llamado Grupo de ensayos no destructivos colabora prácticamente en todas las actividades y proyectos del laboratorio. En la presente memoria se exponen algunos de los métodos de ensayo no destructivo y sus aplicaciones, establecidos para uso en el programa de reactores.

El programa LAPRE (Los Alamos Power Reactor Experiment) se basa en el empleo de una solución de fosfato de uranio a alta temperatura. La solución es muy corrosiva y todas las piezas que entren en contacto con ella deben ir revestidas de oro. Durante el proceso de producción de chapa de oro laminada a partir de lingotes, se han utilizado procedimientos radiográficos especiales para inspeccionar el metal. Las juntas soldadas se examinaron del mismo modo, y además se estableció un método para comprobar la presencia de impurezas incrustadas en la superficie de la chapa de oro.

El concepto fundamental en que se basa el programa LAMPRE (Los Alamos Molten Plutonium Reactor Experiment) es la utilización como combustible de plutonio metálico líquido en vez de sólido. El combustible

está encerrado en cápsulas de tántalo, y durante la fabricación de éstas se aplicaron nuevos métodos de ensayo no destructivo para verificar la integridad del metal básico y de las soldaduras. También se aplicaron esos métodos durante los ensayos de fusión y enfriado y después de éstos. En un experimento realizado con una bomba mecánica de plutonio fundido, se utilizaron procedimientos radiográficos, entre ellos un circuito de televisión industrial de rayos gamma.

Para el programa UHTREX (Ultra High Temperature Reactor Experiment) actualmente en curso de ejecución, se efectuaron estudios microrradiográficos y al microscopio electrónico de las perlas de carburo de uranio revestidas de carbono pirolítico, de 150 μm de diámetro, con el fin de evaluar la migración del uranio en función de la temperatura. La masa y la uniformidad de la carga de uranio en los elementos de grafito del programa UHTREX se determinan mediante contadores de centelleo especiales.

INTRODUCTION

The University of California's Los Alamos Scientific Laboratory was established on 1 January 1943 to develop the first nuclear weapons. Despite this specific mission, the reactor development programme started only one year later, resulting in the development and construction of the world's first homogeneous reactor, the Water Boiler, and the world's first fast reactor, Clementine [1]. The reactor activities of the Laboratory then expanded into four distinct fields:

(1) Research reactors;
(2) Power reactors;
(3) Critical assemblies;
(4) Development of a reactor capable of propelling a rocket.

The Nondestructive Testing Group gives service to practically all the activities and projects of the laboratory. In this presentation are described some of the unique non-destructive testing techniques and applications developed for and used in the reactor programme.

THE LOS ALAMOS POWER-REACTOR EXPERIMENT (LAPRE)

In the mid-1950's, two reactors in the LAPRE series were constructed and operated at high temperatures with a uranium phosphate solution. This completely new concept, at that time, in nuclear-power reactor design allowed a homogeneous reactor to operate at temperatures and pressures far greater than those previously considered. At the same time, it was realized that this liquid fuel was highly corrosive. All reactor parts which were in contact with the uranium phosphate had to be gold cladded.

The reactor vessel was thoroughly radiographically inspected to guarantee the soundness of the walls in every respect (see Fig. 1, bottom). Because of the weight and the wall thickness of the vessel, a specially designed scaffold had to be constructed to hold the vessel at the same height from the floor as the horizontal X-ray beam emanating from the doughnut of the 24-MeV Allis-Chalmers Betatron. By using a 5-t crane, the vessel could be rotated about its axis, thereby making it possible to cover radiographically the entire circumference of the object under investigation [2].

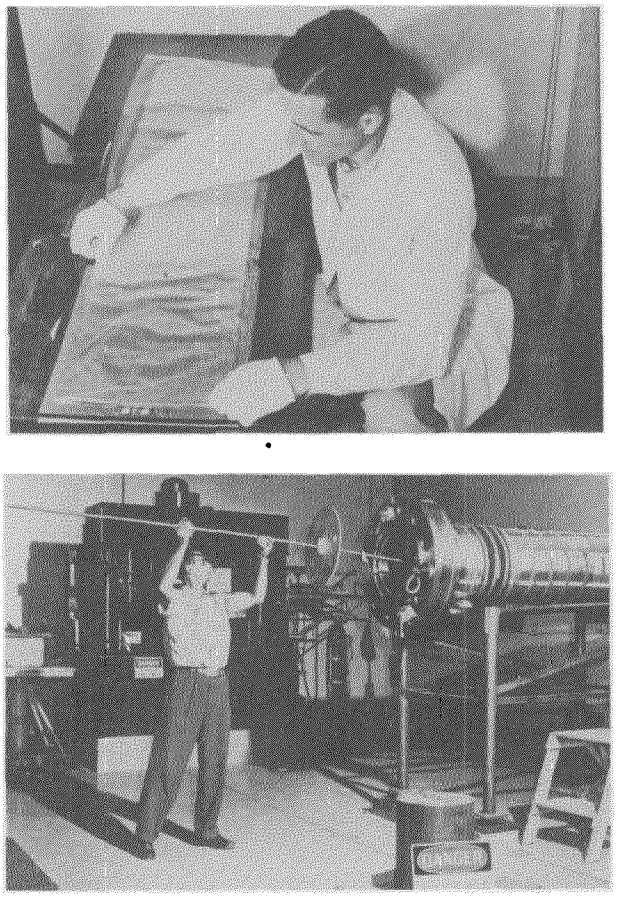

Fig. 1

Top: Gold sheet radiography for reactor liner
Bottom: Betatron and cobalt-60 radiography of LAPRE reactor vessel

Whenever permissible and possible, a cobalt-60 source was inserted along the axis of the vessel and radiographs taken of an entire 360° band of its cyclindrical portion [3, 4].

The gold to be used for cladding was rolled to size by the Metallurgy Department of the Laboratory. It was important to ascertain that no dust or debris infiltrated the gold during the rolling process. Two types of non-destructive inspection were therefore performed:

A. Radiography of the gold sheet after each rolling (see Fig. 1, top). The gold sheets were transported and kept in plastic containers. Lowest possible X-ray energies and fine-grain films were used to obtain highest radiographic contrast and quality.

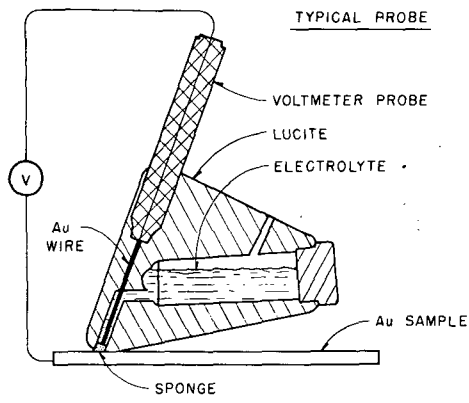

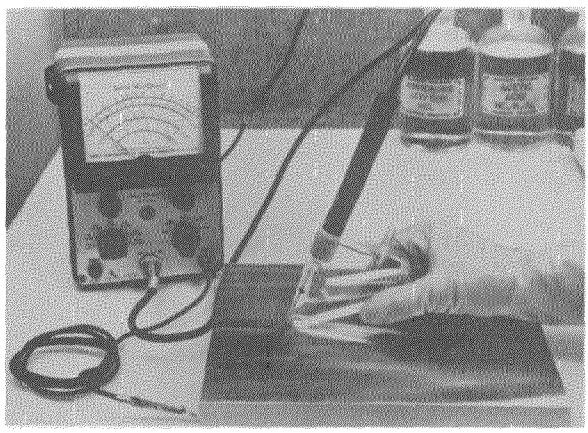

Fig. 2

Electrode potential tester

Top: Schematic cross-section of the tester
Bottom: Tester applied to gold slab

B. Electrode potential testing [5]. Since the gold sheets were rolled from a 1-in-thick slab down to a thickness of 0.015 inch, many rollings had to be performed. Despite extreme care and cleanliness during the rolling operation, it was impossible to prevent the pick-up of inclusions large enough to penetrate the finished product completely.

The Electrode Potential Tester (see Fig. 2) was developed by members of the Nondestructive Testing Group. The principle of this tester is based on the knowledge that one could detect an electric current or field produced by the action of an electrolyte in the region of a surface inclusion or pinhole. It is presupposed that the inclusion and matrix materials will pass in ionic form into the electrolyte and that the two reactions do not produce equal potential differences.

The first prototype tester, as illustrated in Fig. 2, consisted of a standard vacuum tube voltmeter, the DC probe of which was inserted into a Lucite holder. In it were embedded an electrolyte reservoir, and electrolyte feed channel, a gold wire electrode, and a $\frac{1}{4}$-in-diam. sponge used to confine the electrolyte (in this case HCl-H_2O-HAc, 2 : 2 : 1) on the test specimen. The tester was manually operated, as is seen in Fig. 2 (bottom).

This electrode potential scan of the gold sheet was applied after each rolling reduction to determine if pickling was necessary. Pickling operations of sufficient duration to dissolve all possible inclusions would have taken a prohibitively long time; therefore, the tester was used after each pickling cycle to determine if inclusions had been removed. By applying this tester, the estimated processing time with the prescribed pickling after each reduction was shortened from three months to two weeks.

THE LOS ALAMOS MOLTEN-PLUTONIUM EXPERIMENT (LAMPRE)

This experiment is based on the idea of using metallic plutonium as a fuel in the liquid rather than in the solid state. It was part of the concept of a fast-breeder reactor to produce power and at the same time manufacture more new fissionable material than it consumes.

Capsules of tantalum metal were used to contain the fuel in the core. Heat was removed from the fissioning fuel by a circulating stream of molten sodium. The operating temperature was about 950°F with a design power level of 1000 kW.

Some of the interesting non-destructive test methods developed for and applied to this reactor experiment are described in the following paragraphs.

Tantalum bar stock and thimbles

The bar stock was ultrasonically inspected for internal cracks. A Curtiss-Wright Immerscope was used for this purpose. The axis of the ultrasonic beam emanating from a line-focused lithium sulphate transducer was directed at the centre of the bar. A frequency of 5 Mc was used in this case.

The thimbles were impact-extruded from this bar stock to a wall thickness of about 0.030 in and a diameter of about 0.430 in. These thimbles could not contain any scores, pits, galls, and cracks, because of the danger of rapid corrosion when in contact with molten sodium.

Three types of non-destructive inspection were therefore developed for this purpose.

(1) Radiographic inspection

Three views were taken of each thimble (0°, 60°, and 120°) with its axis parallel to the film. 1000-kVP X-rays were utilized to penetrate both walls of the specimens. By using fine-grain films (double-film technique) and 0.005-in lead intensifying screens in vacuum cassettes, a radiographic resolution of 0.004 in was obtained.

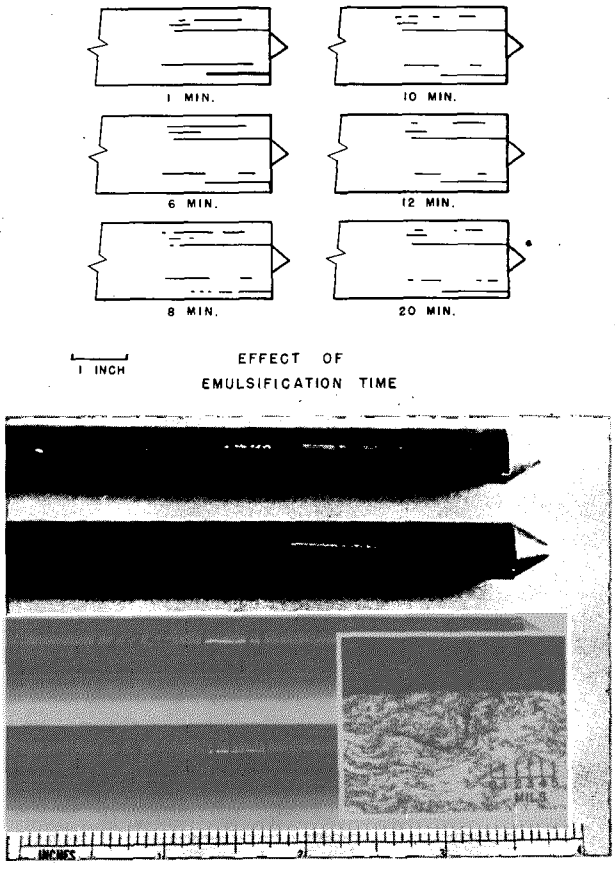

Fig. 3

Fluorescent penetrant inspection of tantalum thimbles

Top: Sketch of visualized longitudinal surface defects as function of emulsion time
Bottom: Photograph of tantalum thimbles taken under ultraviolet light
Insert: Photomicrograph of cross-section containing typical defect as detected by this surface inspection method

(2) Fluorescent penetrant inspection

Experiments had to be performed to establish the appropriate emulsification time, thereby visualizing under the ultraviolet light only those surface defects which could be harmful. In a sketch and photograph Fig. 3 shows the decreased lengths of longitudinal surface defects of increased emulsification time. The insert is a photomicrograph of a cross-section of such a rejectable defect (200 X). Based on these experiments the following technique was applied:

Penetrant:	ZL-22 for 20 min
Emulsifier:	ZE-2 for 20 min
Washing time using automatic rotary washer:	6 min at 95 to 100°F
Drying time:	10 min at 115 to 140°F
Developer:	ZP-4 for at least 10 min

Most of the surface defects uncovered by this fluorescent penetrant inspection could not be detected by visual or radiographic means.

(3) Electromagnetic method to measure wall thicknesses of thimbles

The thimble wall was inserted between two coaxial coils mounted on the ends of a U-shaped yoke. The variations in the wall thickness caused a linear phase shift in the signal induced in the receiving coil. This shift was displayed on an oscilloscope which was calibrated against known tantalum thicknesses. By moving the coils axially along the thimble and rotating the thimble, the minimum and maximum wall thicknesses and their locations could be obtained. The frequency range for this investigation was between 200 and 300 kc, depending upon the thickness range of the walls of the thimbles.

Highly-radioactive tantalum capsules filled with plutonium

Betatron radiography was used to ascertain the physical condition of these capsules after they were removed from the reactor (see Fig. 4). Remotely controlled handling devices were used for personnel safety reasons. A finite object-to-film distance utilizing the inverse-square law decreased the amount of undesirable radiation emanating from the specimen and exposing the film, thereby contributing to an increased radiographic contrast.

Molten-plutonium pump experiment [6]

This experiment was a subcritical mock-up of a reactor core in which a plutonium-iron alloy was circulated by means of a sodium lift pump. This type of circulation would permit continuous flushing of fission gases generated, and would create the potential for fuel re-processing during operation. Sodium for the lift pumping was circulated by an E.M. pump in an isothermal loop at 500°C. The purpose of this test was to study pump characteristics, instrumentation, sodium-fuel separation, and fuel-transfer systems.

Special non-destructive inspection methods were developed to observe the operational characteristics of the core and the fuel-transfer systems. Figure 5 illustrates the set-up of this experiment and a radiograph of the core showing the catch pan and the liquid plutonium level.

Radiographs were taken to study the test assembly involving static and steady-state conditions such as float location, fuel level, sodium in the lift pump annulus while pumping etc. Iridium-192 and cobalt-60 were the two sources of gamma radiation which lent themselves very successfully for this investigation. Iridium, because of its lower energy, produced better radiographic definition and contrast. The iridium sources were contained in tung-

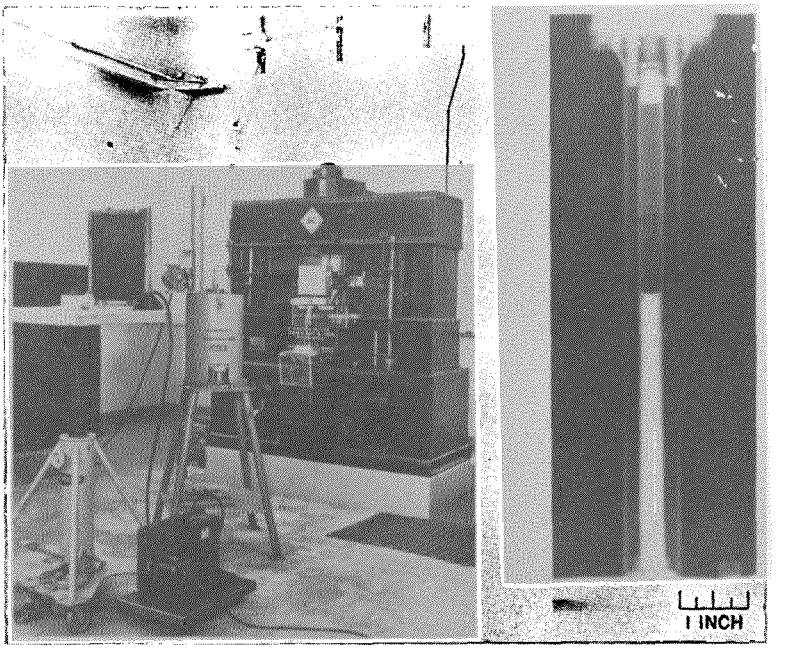

Fig. 4

Left: Radiographic set-up for inspecting highly-radioactive tantalum capsules filled with plutonium using the 24-MeV betatron
Right: Radiograph of such a capsule

sten collimators and exposed by removing the front plug. The shielding and collimation were sufficient to allow personnel to remain in the area behind the source during exposure.

The entire experimental set-up located behind the board was painted on the front, as is seen in the photograph. This painted sketch made it possible to place the isotope in the desired position to radiograph the area of interest. A gamma alarm was placed behind the test section; it activated a red light visible to the operators whenever the sources were exposed.

In addition to taking radiographs, a gamma-ray TV system was developed which made it possible to study on the screen the various events as they were taking place. The varying fuel flow, the starting of pump action, the fuel levels, and fuel-transfer operations could be readily observed. Movies were also taken of the TV screen, thereby permanently recording the various phases of this experiment.

THE ULTRA-HIGH-TEMPERATURE REACTOR EXPERIMENT (UHTREX)

This experiment now under construction at Los Alamos will use unclad highly refractory fuel in a gas-cooled reactor [7]. The fuel elements will be a mixture of "Triplex" pyrocarbon-coated UC_2 beads, with average dia-

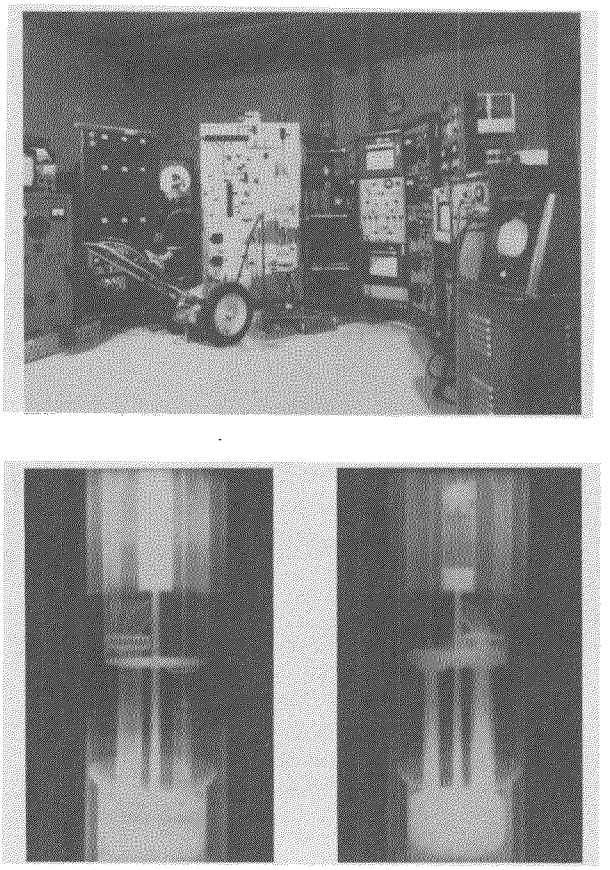

Fig. 5

Top: Photograph of the molten-plutonium pump experiment
Bottom: Radiograph of the core showing the liquid plutonium level

meters of 350 μm, and graphite. They will have cylindrical shapes with a diameter of about 1.2 in, and will be extruded and graphitized to size.

Again, various non-destructive test methods were developed and applied in order to study the behaviour of these beads when exposed to various temperatures. It is important to determine the degree of uranium migration through the pyrocarbon coatings as a function of temperature and time.

Figure 6 illustrates microradiographs of such beads as received from the manufacturer and after heat treatment for 4 h at 2300°C. These radiographs were taken under dark-room conditions by placing the beads directly on the photographic emulsion of spectrographic plates. Soft X-rays with an energy of about 6 kVP were utilized in a helium atmosphere. The X-rays penetrated the pyrocarbon layer and visualized clearly the migrated uranium after heat treatment.

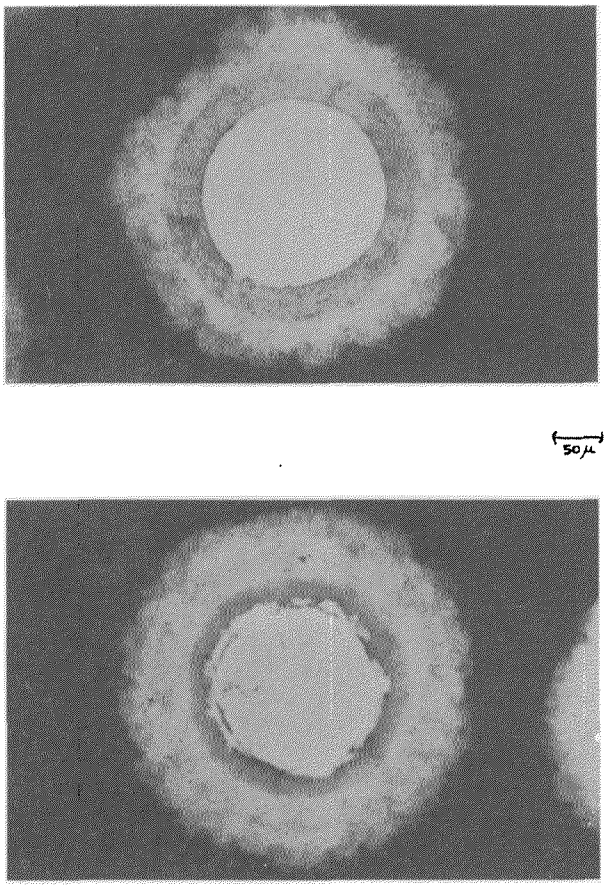

Fig. 6

Microradiographs of pyrocarbon-coated UC_2 beads, average diam. 350 μm

Top: Radiograph of bead as received
Bottom: Radiograph of bead after heat treatment for 4 h at 2300 °C

Some of these beads were sectioned and metallographic photographs taken, as seen in Fig. 7. Again, uranium migration could be observed as a result of heat treatment.

To study these phenomena in greater detail and beyond the range of optical microscopy, replicas were made of the sectioned surfaces of these beads. These replicas were then shadow-casted and transmission electron micrographs were taken. Figure 8 illustrates these 5500X electron micrographs. The boundaries between the UC_2 core and the surrounding pyrocarbon containing migrated uranium can be clearly seen.

The manufactured fuel elements must be inspected for uranium loading and homogeneity of uranium distribution. Ring-type sodium-iodide thalium-activated scintillators are used for this purpose. Figure 9 shows the model

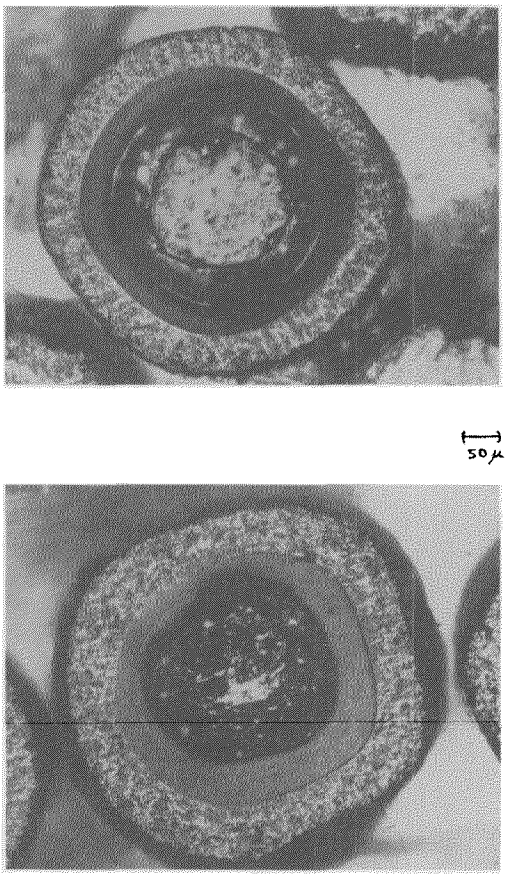

Fig. 7

Metallographic photographs of sectioned pyrocarbon UC_2 beads

Top: Bead as received
Bottom: Bead after heat treatment for 4 h at 2300 °C

of such a scintillation counter with one segment removed. The other half of this Figure shows the entire gamma-counting instrument with automatic read-out equipment. Data are recorded on punch tapes and fed into computers for final evaluation.

DISCUSSION

This paper has given a brief review of some of the various activities of the Nondestructive Testing Group of the Los Alamos Scientific Laboratory. To be of service to all the projects, many factors must be taken into consideration. Close communication and co-operation are the basis of successful service. The problems must be crystallized and discussed. All possible

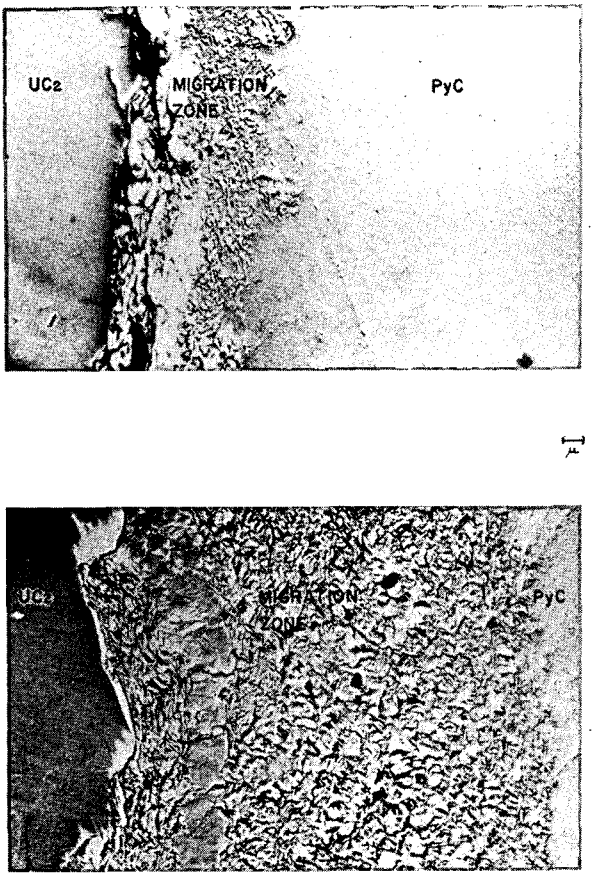

Fig. 8

Electron-micrographs of interface between UC_2 core and pyrocarbon coating of beads (5500X)

Top: Interface of bead as received
Bottom: Interface of bead after heat treatment for 4 h at 2300 °C

and probable non-destructive test methods, and especially their limitations, have to be fully understood. Last, but not least, the data obtained have to be analysed and evaluated to determine their usefulness with regard to establishing respective specifications.

ACKNOWLEDGEMENTS

The content of this paper is the result of the work of many members of the Nondestructive Testing Group over many years. They all deserve the credit. In addition, the progressive atmosphere of the Los Alamos

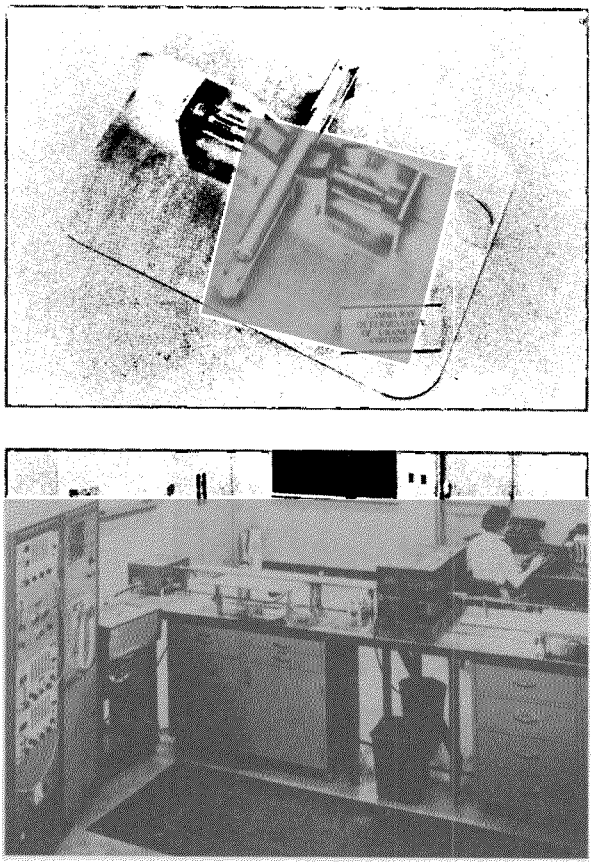

Fig. 9

Scintillation-counting equipment to determine uranium loading of fuel elements

Top: Model of scintillation counter with one segment removed
Bottom: Scintillation-counting instrument with automatic read-out equipment

Scientific Laboratory created and stimulated these evolutionary and fruitful activities.

REFERENCES

[1] Nuclear Reactors, Los Alamos Scientific Laboratory, March (1964).

[2] STEELY, J.D. and MILLER, N.C., "Some Experimental Findings and Operating Practices in Betatron Radiography", Nondestructive Testing, XI, No. 8 (1953) 35-40.

[3] TENNEY, G.H., "Survey of Radiation Techniques", from Symp. on Nondestructive Tests in the Field of Nuclear Energy, ASTM Special Technical Publication No. 223 (1958).

[4] DUTLI, J.W. and TENNEY, G.H., "A Preliminary Investigation of the Radiographic Visualization of Cracks", Nondestructive Testing, XII, No. 2, (1954) 13-15.

[5] BENDER, J.H. Jr., DUTLI, J.W. and EDWARDS, P.D., "Electrode Potential Testing", Nondestructive Testing, March-April (1960).

[6] DEVERALL, J.E. and CALDWELL, G.L., "Molten Plutonium Pump Experiment", Los Alamos Scientific Laboratory, Los Alamos, New Mexico, LA-2761, December (1962).

[7] Quarterly Status Reports on UHTREX, Los Alamos Scientific Laboratory, Los Alamos, New Mexico, LAMS-2623, 20 August (1961); and LA-3190-MS, 20 September (1964).

DISCUSSION

Z. PAWŁOWSKI: What was the wall thickness of the reactor vessel which you tested radiographically? What kinds of defect did you look for?

G.H. TENNEY: The wall thickness ranged from about 1 to 4.5 in. The radiographic sensitivity was between 0.020 and 0.080 in. We wished to avoid cracks and voids of about 0.080 to 0.090 in in diameter.

Z. PAWŁOWSKI: Did you also use ultrasonic inspection? It would be very interesting to have a comparison of the two methods and to know their limitations.

G.H. TENNEY: No, we didn't use ultrasonic inspection, seeing that we had the 24-MeV betatron and Co^{60} available. We preferred radiography because of the importance of the inspection and the consequent need to obtain permanent records.

Z. PAWŁOWSKI: Did you try to use the Lamb waves or any other waves for testing gold sheets after rolling?

G.H. TENNEY: Yes, we did, especially for inspecting the welds of the gold sheets.

Z. PAWŁOWSKI: What were the criteria for rejecting tantalum bars tested by means of the fluorescent penetrant method? What defects could be seen as harmful and why?

G.H. TENNEY: I described the types of defects in my paper. I should like particularly to refer to the insert to Fig. 3, showing the metallographic photograph. The specifications were established on the basis of corrosion rate studies.

O.A. KELLERMANN: In Figs. 6, 7 and 8 you have shown us excellent photographs of coated particles for the UHTREX. The importance of the coating for retaining fission products is well known. Do you perform tests in Los Alamos Laboratory to ensure the diffusion coefficients specified?

G.H. TENNEY: Yes, in Los Alamos, but not in the Nondestructive Testing Department. Therefore I can give no details.

P. de MEESTER: I would also like to ask a question on the UHTREX coated fuel particles. Could you tell us what was the fuel loading in the cylindrical elements in weight %? And what precision could you obtain in determining the amount of uranium? I assume that the fuel is highly enriched?

G.H. TENNEY: Yes, the element is highly enriched. The loading is 110-150 mg/cm^3 of uranium. The elements are made of these particles embedded in graphite. They are extruded and graphitized to size. The precision is $\pm$ 1.5%, bearing in mind that the width of the crystal is 3/4 in.

THE ECONOMICAL APPLICATION OF NON-DESTRUCTIVE TESTING TO REACTOR COMPONENTS, ESPECIALLY JACKET TUBING*

C.J. RENKEN
METALLURGY DIVISION
ARGONNE NATIONAL LABORATORY
ARGONNE, ILL., UNITED STATES OF AMERICA

(presented by D.C. WORLTON)

Abstract — Résumé — Аннотация — Resumen

THE ECONOMICAL APPLICATION OF NON-DESTRUCTIVE TESTING TO REACTOR COMPONENTS, ESPECIALLY JACKET TUBING. The ideal reactor design, in addition to its other desirable characteristics, would require no non-destructive testing. This ideal, like others, will probably never be attained. In any reactor design where cost is an important factor, the question of whether components can be economically tested should be proposed at the same time that questions of fabricability are being considered. Some development of these points as well as a discussion of the importance of non-destructive tests in specification writing is included in this section. Responsibility also rests on the fabricator to use the help provided by non-destructive testing in maintaining quality in the product through various stages in the fabrication process, and to use the test results to indicate those steps in the process most likely to introduce defects in the component. Often it develops that non-destructive testing in earlier stages of component fabrication cannot be replaced economically, if at all, by inspection of the component in finished or semi-finished form. Examples are cited to illustrate this point, particularly with regard to tubing for fuel jacket and heat-exchanger applications. The application of various non-destructive tests during a tube-fabrication development programme is described in some detail. The fabrication and inspection costs for some tubing used for jacket applications by Argonne National Laboratory are compared.

Although component inspection in finished form can be minimized by these procedures, it cannot in all cases be eliminated entirely.

The economical testing of plates and tubes, especially the latter, is discussed in detail. The discussion is centred around components of stainless steel, Zircaloy, and certain refractory metal alloys. It is shown through various examples that although the use of radiography and penetrants may be useful or even essential steps in the testing, critical inspection of thin-wall tubing must usually be made by either an ultrasonic or an electro-magnetic method for technical as well as economic reasons. The optimum area of application of these two methods is explained as well as the large area of overlap where results produced by well-designed and properly operated equipment of both types are essentially equivalent. Spurious defect indications contribute directly to increased component costs, so an evaluation of these effects for both the ultrasonic and the electromagnetic test methods is included for several commonly encountered sources of spurious defect signals. The experience in the application of these methods at Argonne National Laboratory on relatively large quantities of tubing from various sources are recounted from the standpoint of the lowest possible inspection cost per unit-length of tubing. This section also summarizes experience gained at Argonne with the newer pulsed electromagnetic test methods. The critical but generally unappreciated role of tube diameter and wall thickness on tube inspection cost is discussed. Since the question of economical inspection is closely related to allowable defect levels, defect levels and standards in use at Argonne are covered. Finally, the practical and theoretical barriers to reduced component inspection costs are enumerated and a projection of what possible reductions in cost might be attainable in the future with the ultrasonic and electromagnetic test methods is attempted.

* Work performed under the auspices of the United States Atomic Energy Commission.

AVANTAGES ECONOMIQUES DU CONTROLE NON DESTRUCTIF DES PIÈCES DE RÉACTEURS, NOTAMMENT DES TUBES DE GAINAGE. Le réacteur idéal aurait entre autres caractéristiques celle de ne pas exiger de contrôles non destructifs. Cet idéal, comme tant d'autres, ne sera probablement jamais atteint. Dans l'étude de tout réacteur pour lequel le prix de revient constitue un facteur important, il faudrait envisager la question de savoir si les pièces de ce réacteur pourront être essayées de façon économique en même temps que l'on examine les possibilités de fabrication. Cette partie du mémoire contient quelques considérations à ce propos ainsi qu'un exposé de l'importance des essais non destructifs dans l'établissement des spécifications. Il incombe aussi au fabricant de tirer parti des avantages que présentent les essais non destructifs pour maintenir la qualité du produit au cours des divers stades de fabrication, et d'utiliser les résultats des essais pour déterminer les stades où l'apparition de défauts est le plus probable. Il arrive fréquemmennt que des essais non destructifs au début des opérations de fabrication ne puissent pas être remplacés, économiquement ou non, par une inspection du produit fini ou semi-fini. L'auteur cite des exemples à l'appui de cette considération, notamment en ce qui concerne les tubes de gainage du combustible et les circuits caloporteurs. Il décrit de façon assez détaillée l'application des divers essais non destructifs au cours de la mise au point de gaines et de canaux. Il compare les coûts de fabrication et d'inspection de plusieurs modèles de gaines de combustible utilisés par le Laboratoire national d'Argonne.

Bien que le contrôle du produit fini puisse être réduit à un minimum à la suite de ces essais, il ne peut pas être éliminé entièrement dans tous le cas.

L'auteur discute en détail, du point de vue des économies, les essais des plaques et des tubes, particulièrement des seconds. Son examen porte principalement sur les pièces en acier inoxydable, en Zircaloy et en certains métaux réfractaires. Il montre, par divers exemples, que si la radiographie et l'emploi de liquides pénétrants peuvent constituer des mesures utiles ou même essentielles au cours des essais, l'inspection critique des tubes à paroi mince doit être effectuée habituellement, soit par les ultrasons, soit par une méthode électromagnétique, pour des raisons à la fois techniques et économiques. L'auteur décrit le domaine optimum d'application de ces deux méthodes ainsi que la vaste gamme dans laquelle les résultats obtenus avec des instruments ultrasonores et électromagnétiques bien conçus et convenablement utilisés sont pratiquement équivalents. Des indications erronées de défauts contribuent directement à l'accroissement du prix de revient des pièces; c'est pourquoi le mémoire contient une évaluation de ces effets pour les méthodes ultrasonores et électromagnétiques en ce qui concerne plusieurs sources fréquentes d'indications erronées. L'auteur expose l'expérience acquise au Laboratoire national d'Argonne dans l'application de ces méthodes à des quantités relativement importantes de tubes d'origines diverses, du point de vue du prix minimum du contrôle par unité de longueur de tube. Cette partie du mémoire résume également l'expérience acquise au Laboratoire d'Argonne avec les méthodes électromagnétiques à impulsions les plus récentes. L'auteur discute l'influence primordiale, mais généralement trop négligée, du diamètre et de l'épaisseur du tube sur le prix de revient du contrôle. Comme la question de l'économie du contrôle est étroitement liée à celle des défauts admissibles, l'auteur expose les normes appliquées à cet égard au Laboratoire d'Argonne. Enfin, il énumère les obstacles pratiques et théoriques qui empêchent de réduire le prix de revient du contrôle des pièces et il s'efforce de faire une prévision des réductions possibles de ce prix grâce aux méthodes ultrasonores et électromagnétiques.

ЭКОНОМИЧЕСКОЕ ПРИМЕНЕНИЕ НЕДЕСТРУКТИВНЫХ ИСПЫТАНИЙ ДЛЯ РЕАКТОРНЫХ КОМПОНЕНТОВ, В ЧАСТНОСТИ ОБОЛОЧЕЧНЫХ ТРУБ. Идеальная конструкция реактора, помимо других желательных для нее характеристик, не потребует проведения испытаний без разрушения оболочки образца. Такого идеала, как и многих других, вероятно, никогда не добиться. При любом проектировании реактора, когда затраты являются важным фактором, вопрос о том, могут ли его компоненты испытываться экономически выгодно, следует выдвигать одновременно с рассмотрением вопросов изготовления. В настоящий раздел включены некоторые моменты разработки этих вопросов, а также обсуждение важности проведения испытаний без разрушения оболочки образца в письменных спецификациях. На изготовителя также ложится ответственность использовать помощь, предоставляемую проведением испытаний без разрушения оболочки для сохранения качества продукта на различных стадиях процесса изготовления, а также использование результатов испытаний для того, чтобы определить те моменты, которые вероятнее всего вызовут дефекты в компоненте в процессе изготовления. Чаще всего получается так, что испытание без разрушения оболочки в начальных стадиях изготовления компонента не может быть замещено экономически выгодно иначе, если вообще это возможно, как только путем обследования компонента в виде готового продукта или полуфабриката. Приводятся примеры для иллюстрации этой точки зрения, осо-

бенно в отношении системы труб для применения оболочки тепловыделяющего элемента и применений в теплообменниках. Применение различных испытаний без разрушения оболочки образца подробным образом описывается в программе разработок по изготовлению труб. Дается сравнение расходов на изготовление и обследование некоторых систем труб, использовавшихся Аргоннской национальной лабораторией для покрытия этих труб оболочкой.

Хотя обследование компонента в окончательном виде может быть сведено до минимума посредством таких процедур, однако нельзя все эти случаи устранить целиком.

Подробным образом обсуждается экономическое проведение испытаний пластинок и труб, в особенности последних. Обсуждение ведется главным образом о компонентах из нержавеющей стали, циркаллоя и некоторых огнеупорных металлических сплавах. На различных примерах показывается, что хотя использование радиографии и смачивающих реагентов может оказаться весьма полезным, а может быть даже и необходимым делом при проведении испытаний, однако обязательно, как правило, следует проводить тщательное обследование тонкостенных труб с помощью либо ультразвука, либо электромагнитного метода как с точки зрения технических, так и экономических аспектов. Объясняется оптимальная область применения этих двух методов, а также перекрываемая ими область, где полученные результаты благодаря хорошей конструкции и точно работающему оборудованию обоих видов являются в значительной степени эквивалентными. Ложные указания на дефекты ведут непосредственно к удорожанию компонентов, поэтому как при ультразвуковом так и при электромагнитном методе учитывается целый ряд обычно встречающихся источников сигналов ложных дефектов. Опыт по применению этих методов в Аргоннской национальной лаборатории в отношении сравнительно большого количества систем труб из различных источников излагается подробно с точки зрения наименьших возможных затрат на проверку единицы длины труб. В настоящем разделе также в кратце излагается опыт, приобретенный в Аргонне с помощью самых новых методов испытаний электромагнитной пульсации. Обсуждается критическая, но, как правило, нежелательная роль диаметра труб и толщины стенок в вопросе затрат при обследовании труб. Поскольку вопрос экономического обследования непосредственно связан с уровнями допустимых дефектов, затрагивается также вопрос об уровнях дефектов и стандартах, используемых в Аргонне. И, наконец, перечисляются практические и теоретические барьеры для снижения затрат, связанных с обследованием компонентов, и указываются перспективы возможного снижения расходов, которых можно добиться в будущем с помощью ультразвуковых и электромагнитных методов испытаний.

APLICACION EN CONDICIONES ECONOMICAS DE ENSAYOS NO DESTRUCTIVOS A LAS PIEZAS DE LOS REACTORES, EN ESPECIAL A LOS TUBOS DE REVESTIMIENTO. Además de las características que debe reunir el modelo ideal de reactor, hay que aplicarle métodos de ensayo que no tengan carácter destructivo. Como otros ideales, es probable que éste no se alcance nunca. Para cualquier modelo en el que el costo sea un factor importante, la cuestión de la posibilidad de ensayar las piezas en condiciones económicas debe plantearse al mismo tiempo que la de la posibilidad de fabricación. En la presente memoria se reseñan algunas observaciones al respecto y se examina la importancia que ha de atribuirse a los métodos de ensayo no destructivo al establecer las especificaciones correspondientes. El fabricante además es responsable de la utilización de métodos de ensayo no destructivo para mantener la calidad del producto durante las diversas etapas del proceso y de indicar, a base de los resultados obtenidos, en cuáles de esas etapas es más probable que la pieza adquiera defectos. A menudo ocurre que el ensayo no destructivo de la pieza en las primeras etapas de su fabricación no puede sustituirse, por la inspección de dicha pieza en forma acabada o semiacabada. Para demostrarlo se citan ejemplos, sobre todo relativos a los tubos para revestimiento del combustible y a las aplicaciones de los intercambiadores de calor. Se expone, en forma bastante circunstanciada, la aplicación de los diversos métodos de ensayo no destructivo durante el desarrollo de un programa de producción de tubos, y se comparan los costos de fabricación y de inspección de algunas clases de tubos utilizadas para revestimiento por el Argonne National Laboratory.

Aunque con esos procedimientos la inspección de las piezas acabadas tiene una importancia secundaria, no siempre puede eliminársela enteramente.

Se examina detenidamente el método económico de ensayo de placas y tubos, en especial de estos últimos, refiriéndose sobre todo a las piezas de acero inoxidable, zircaloy y ciertas aleaciones de metales refractarios. Con varios ejemplos queda demostrado que si bien el uso de la radiografía y de los agentes de penetración puede ser útil o incluso constituir una parte imprescindible del ensayo, en general, por razones de índole técnica o económica, es preciso proceder a una inspección crítica de los tubos delgados, ya sea

por métodos ultrasónicos o electromagnéticos. Se explica el campo de aplicación de esos dos métodos en condiciones óptimas y también la amplia zona de superposición en que los resultados obtenidos con equipo de ambas clases, bien concebido y manejado, son esencialmente equivalentes. La indicación falsa de defectos contribuye directamente a aumentar el costo de la pieza; por ello, se incluye una evaluación de ese efecto pernicioso de varias fuentes indicadoras de falsos defectos que seuelen existir tanto cuando se aplican los métodos ultrasónicos como los electromagnéticos. La experiencia adquirida en la aplicación de esos dos métodos por el Argonne National Laboratory a cantidades relativamente grandes de tubo de diversas procedencias se estudia desde el punto de vista del costo más bajo posible a que pueda efectuarse la inspección por unidad de longitud del tubo de que se trate. En la presente sección se expone además en forma concisa la experiencia adquirida en Argonne con los modernos métodos de impulsos electromagnéticos. Se examina la influencia crítica, pero generalmente inapreciada, que tienen en el costo de la inspección el diámetro y el espesor de pared del tubo. Teniendo en cuenta que el problema de la inspección en condiciones económicas guarda una estrecha relación con el número medio de defectos admisibles, se estudian asimismo los promedios y las normas que se aplican en Argonne. Por último, se enumeran los obstáculos de orden teórico y práctico para reducir el costo de la inspección de piezas sobre esa base, y se evalúan las posibles reducciones de costo que podrían lograrse en lo futuro aplicando los métodos de ensayo ultrasónicos y electromagnéticos.

THE APPLICATION OF NON-DESTRUCTIVE TESTING TO REACTOR COMPONENTS

The ideal reactor design, in addition to its other desirable characteristics, would require no non-destructive testing. In any reactor design in which cost is an important factor, the question of whether components can be economically tested should be considered at the same time that questions of fabricability are being considered. Inevitably, those designs which approach any type of limit, whether it be of temperature, life-time, mechanical strength, or lowest possible cost, require some form of non-destructive testing to ensure that the material or component under test does in fact possess the characteristics which the designer assumed. The required quality level and perhaps even the non-destructive testing method might ideally be written as part of the design specification. Of course, this would demand specialized knowledge on the part of the designer that he probably does not possess. In this case his only course of action would be to do the same thing that he does when he encounters problems in materials, or heat transfer for example, that he cannot answer, and that is to seek the most expert advice which is available to him. This procedure would avoid the impasses which still occasionally occur; a design has been completed, materials are on order, fabrication is underway and suddenly it develops that the necessary non-destructive testing technique or method is either simply not available, or is unexpectedly expensive.

The application of non-destructive testing during fabrication

The constructor also bears a responsibility to use the help provided by non-destructive testing in maintaining quality in the product through various stages in the fabrication process, and to use the test results to indicate those steps in the fabrication process most likely to introduce defects in the component. Often it develops that non-destructive testing in earlier stages of component fabrication cannot be replaced economically, if at all, by inspection of the component in finished or semi-finished form. For ex-

ample, it is very difficult to make high-quality tubing from defective extrusion blanks. One radiograph of such a blank could save a great deal of testing on the finished product as well as the time expended reducing the blank to finished tube size. These procedures, which are so obvious, are far from being universally used, even in those firms serving the nuclear industry in the United States of America. Moreover, it often develops that the organization buying the component has no direct control over the tests the fabricator chooses to apply to the product other than the quality requirements written in the specifications applying to the finished product. There still exists an unfortunate state of ignorance on part of the industrial community (at least in the United States of America) regarding the methods and capabilities of the non-destructive testing field. Firms coming into contact with the nuclear industry for the first time are often dismayed to find a literal interpretation of specifications relating to quality prevalent, and the methods available to disclose deviations from the specified quality. It might be suspected that contracts awarded on the basis of price are often won by those organizations most ignorant of non-destructive testing because, as will be discussed shortly, non-destructive testing costs can amount to a significant portion of the price of some types of components.

The inspection of tubing

From the standpoint of quality control, tubing for jacket and heat-exchanger applications represents one of the more critical components in many reactor designs. Tubing is a popular geometrical form for fuel-element cladding, and in most reactors it is highly desirable to maintain the integrity of this cladding throughout the life of the fuel element. Tube integrity in heat exchangers is nearly as important and in some cases, for instance sodium-to-water heat exchangers, absolutely essential. The nuclear industry pioneered the requirement of really high-quality tubing in considerable quantity. Since that time, the cost of tubing inspection has become an important consideration in the cost of the tubing itself. For the purposes of this discussion, interest will be centred about tubing with a wall thickness of 2 mm or less, and about the materials zirconium and its alloys, various alloys of steel, especially the austenitic stainless steels, and certain refractory metal alloys.

DEFECT SPECIFICATIONS

It has been the practice at Argonne National Laboratory to write allowable defect specifications on the basis of the maximum allowable defect depth expressed as a percentage of the tube wall. A defect is then defined as any undesirable reduction in effective wall thickness. Defect specifications have ranged from a maximum allowable defect of from 20% to 5%, depending upon the application. When standards are covered in a specification, some mention of defect length must be made, but in a statement of maximum allowable reduction in effective wall thickness, the length is not mentioned, the presumption being that this length will be the minimum that the test equip-

ment can detect. The 10% level is most commonly used. There is some evidence indicating that the effect of defects of less than 10% of the wall upon tube strength is small enough to be obscured by other factors [1].

THE METHODS AVAILABLE FOR TUBE TESTING

The methods available for non-destructive testing of tubing to the standards prevalent in the nuclear industry are the following: radiography, magnetic particle, penetrant, ultrasonics, and electromagnetic methods. Radiography is both more effective and cheaper in these applications than might be assumed. The electro-machined notches often used as standards for the ultrasonic and electromagnetic tests are invariably visible on good quality radiographs, even the 5% notches. An analysis of the cost per metre of tubing shows that radiographic inspection can often be accomplished for only slightly more than the cost of ultrasonic inspection. Deep, but very short defects and inclusions, which are a problem to the ultrasonic and electromagnetic methods, are easily detectable on radiographs, so much so that radiography makes an ideal supplement to the former methods. It cannot be used alone, however, because the method is not capable of detecting fine cracks in many cases if they intersect the tangent to the point on the tube surface where the crack terminates at a shallow angle. The magnetic particle and the penetrant methods cannot be in general considered applicable in those situations where the tests must in some degree be quantitative; in addition, the difficulty of checking the inside surface of small diameter tubing, the fact that most tubing used in the applications we are discussing (for the magnetic method) is not ferromagnetic, and that the penetrant method is totally incapable of detecting defects not open to a surface, remove the need for detailed comment on these two methods as applied to the inspection of large quantities of thin-walled tubing.

Both the ultrasonic method and the electromagnetic method are well adapted to production testing of large quantities of tubing. The electromagnetic (eddy-current) method is generally considered to have a great advantage in speed.

THE INFLUENCE OF NOISE AND INTERFERENCE ON ECONOMICAL INSPECTION

Inspection of tubing to the standards often specified in the nuclear industry became practical by ultrasonic and electromagnetic methods when the problem of suppression of spurious defect signals was brought under control. This was accomplished in the former, and more recently in the latter method by reducing the geometrical area being scanned at a given instant to the same order of magnitude as the area of the defects themselves and incorporating a form of time discrimination against spurious signals. Inevitably, this led to a reduction in the rate of inspection. Commercial eddy-current tube-test equipment of the phase sensitive-encircling coil type produced both in Europe and the United States of America is capable of inspecting tubing at 2 m/s. With this type of equipment, there is no economic

problem involved in the inspection of tubing, unless the equipment produces spurious defect signals. Tubes, which are rejected because of defects which do not exist, contribute directly to inspection cost. We will now examine the factors relating to the computation of inspection costs.

THE COMPUTATION OF COMPARATIVE INSPECTION COSTS

The direct inspection cost will be defined as the sum of the direct labour cost of the inspection plus the cost of the tubing which is wasted because of inadequacies of the test system. For reasons of simplicity we will disregard capital equipment costs[2], maintenance, the value of the scrap, scheduling and, in fact, many other factors. Suppose that the indicated reject rate produced by a certain system is x, with a probability of a given defect indication being correctly indicated p. We assume that the test system will find every defect that exceeds the maximum allowable, or at least that it will invariably detect the standard. The problem is that it also produces spurious defect indications. The probability that a defect indication is spurious is (1-p).

If the component being inspected is tubing, the amount that must be inspected to get 100 m of good tubing is then $100/1-x$ m. Of this quantity, $100/1-x\,(1-p)$ metres will be wasted because of bogus defect indications assuming a large amount of tubing is being inspected. If the tube cost (up to the point of inspection) is c/m, and if the direct inspection labour charge per hundred metres is S, total inspection cost is $c \times (1-p)(100/1-x) + 100/1-xS$ per hundred metres. As an example, we will compute the cost of inspecting austenitic stainless-steel tubing of 10-mm-diam. and 0.5-mm wall-thickness by two different methods, one an ultrasonic shear-wave test which is slow but quite reliable, ($p \sim 1$), the other very fast. By using a very fine ultrasonic beam size and an extremely short pulse, one can obtain a test of high reliability, but the longitudinal advancement of the tube passing the ultrasonic transducer may be on the order of 0.2 mm per revolution [2]. The inspection rate will be about 0.37 m/min, and at the labour rates prevailing in the United States, the direct labour cost will be about \$0.20/m. The other inspection method uses commercial eddy-current test equipment, inspecting at 2 m/s [3]. Compared to the ultrasonic method this system is so fast that labour costs are negligible.

The cost of welded tubing of this diameter can be expected to be about \$ 1.50/m. The amount of material that must be scrapped per defect will of course depend upon the lengths in which the tubes must be used, but for purposes of this example, we will assume that 5 m/100 must be scrapped for defects. This figure in based upon the testing of about 1000 m of this material at the 10% level is approximately 3.3-m lengths with a finished length of 1 m. By use of the formula, a cost of inspection of \$ 21.00/100 m is calculated for the shear-wave method. It might be asked how reliable must the eddy-current method be to be economically competitive. For the eddy-current method,

---

* The purchase price for new electromagnetic, ultrasonic and radiographic inspection systems are all of the same order of magnitude.

$xp = 0.05 \qquad S = 0$
$c = \$\ 1.50 \qquad p = ?$

Since $x_1 p_1 = x_2 p_2$, where the subscripts refer to the two different methods, it is possible to calculate $p = 0.3$. So, if in this case the eddy-current equipment is correct 30% of the time, it will be economically competitive. It is probably not necessary to point out that the true reject rate is most likely not related to the indicated reject rate by a simple constant. The quantity p is useful only in comparing the costs of two test systems. It is determined upon the basis of metallographic examination of allegedly defective components or by comparison with a system of known reliability. Evaluation of the performance of the test system itself sometimes proves to be a significant expense. Obviously such factors as the value of the scrap, expendable items, such as radiographic film, the cost of cutting out indicated defects, maintenance etc. could easily be included in the formula. The example illustrates that the most economical application of non-destructive testing may favour neither the most reliable or the fastest method. As material costs rise, the most economic method will shift toward the most reliable, and as labour costs rise, the opposite becomes true. In addition, scheduling or material shortages may override all economic considerations.

THE REDUCTION OF INTERFERENCE IN ELECTROMAGNETIC TESTING

A detailed description of the causes of the interference is beyond the scope of this article, but interference can be defined as any condition in the sample which is being tested which produces a signal which can confuse, or be mistaken as a signal produced by those conditions defined in the specifications as "defects". (Of course, electromagnetic methods are not the only methods plagued by interference.) Various methods have been used to reduce the interference in electromagnetic testing. Among these are phase discrimination and filtering [4]. Another approach has been similar to that used in ultrasonic methods; that is to reduce the area being actively scanned to as small a volume as possible. This has been done by shorter encircling coils, smaller probe coils or in the approach incorporated into the electromagnetic test equipment in use at Argonne Laboratory, the fields are restricted to small cross-sectional areas by means of masks [5]. This of course reduces the speed of the method to the same range as that obtained by the ultrasonic method. But it also increases the reliability and discrimination of this equipment to the same level as generally attained by carefully applied ultrasonic shear-wave testing. In fact, in tubing sizes and materials where both methods are applicable, results obtained with the two methods correlate almost exactly [6]. The choice between the two is based upon considerations of wall thickness, conductivity, and ultrasonic propagation characteristics of the material. Tubes with wall thickness greater than 0.75 mm are generally tested with ultrasonics, and those with wall thicknesses less than 0.5 mm are tested using the pulsed electromagnetic method. Usually, either method can be used between these two limits unless special conditions are present. In addition, on tubes with outer diameters less than about 0.6 cm and walls less than 0.75 mm, the electro-

magnetic method is used because it results in a simplification of mechanical problems such as maintaining the proper entrance angle etc.

PULSED ELECTROMAGNETIC METHODS

Pulsed fields have found little application in electromagnetic testing, probably because their use seemed to complicate the theory and instrumentation unnecessarily. However, the pulsed field equipment in use at Argonne has a bearing on the economical non-destructive inspection of tubing because of the simplicity and ease of application of the equipment. Its operation is briefly as follows: a strong pulsed induction field is generated in an enclosure constructed of copper or another high-conductivity material, near an aperture through which some of the flux passes. Typical aperture cross-sectional areas are in the range of 2 mm^2. This field impinges upon the tube. A small pick-up coil is used to detect the field reflected from the test specimen. The voltage developed across a pick-up coil in the presence of a tube is then a function of the field reflected from the metal surface and interior. Line drawings of two types of mask-aperture assemblies are shown in Fig. 1.

The diffusion rate of current into a good conductor is relatively slow, so that an apparent delay can be detected between the surface reflection from the outer surface of the tube and the reflections from inside, including the inside surface reflection. By sampling the voltage pulse developed by the reflected field at appropriate times during its duration, it is possible to enhance or suppress information from conditions at various depths in the metal. This amplitude sampling in the time domain is one of the simplest methods of extracting information from a broadband signal, and works particularly well in the case of defect detection in tubing. A block diagram of the test system is shown in Fig. 2. The amplified pulse from the pick-up is applied to the sampling circuit which permits independent amplitude sampling of the reflected pulse at two separate instants of time. The pulse length of these sampling points is usually chosen at some time early in the duration of the reflected pulse. This point provides a signal primarily sensitive to aperture-to-metal spacing, and so can be used to adjust automatically the sensitivity of the system for changes in this spacing. The other sampling pulse can be moved about over the duration of the reflected pulse to a point in time which provides the best sensitivity to whatever condition is to be detected. A voltage proportional to the amplitude of the reflected pulse at the sampling point is applied to a filter system which has become a common feature of nearly all eddy-current tube test equipment. The output of the filter section is available for whatever type of read-out device is to be used.

This type of equipment was used to inspect several hundred metres of stainless-steel tubing of 9.55 mm O.D. and 0.508 mm wall, much like that cited in an earlier example. Using only one mask aperture assembly, inspection was at a rate of 4 m/min. The standard was an I.D. longitudinal notch, 10% of the wall in depth and approximately 0.6 mm long. By means of adjustment of the sampling pulse, equal sensitivity to O.D. and I.D. notches could be attained. About one defect every 100 m of tubing was detected. Some of these defects were small indentations on the inner surface,

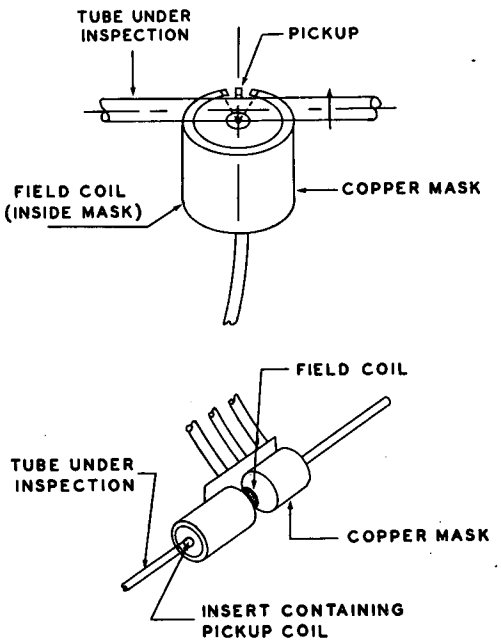

Fig. 1

Two types of mask-aperture assemblies

probably from chips being pressed into the surface by the mandrel. Direct labour costs for this inspection amounted to about $ 0.03/m, for tubing which costs in the neighbourhood of $ 1.50/m. The cost of the inspection equipment would be about the same as for ultrasonic equipment of comparable capability. Many thousands of metres of stainless-steel tubing of O.D. 4.46 mm and wall 0.229 mm were tested to the same standard at a number of different rates, but the optimum rate appeared to be about 10 m/min with the probability of being correct (p) of 0.75. Many of the defect indication areas which were sectioned and did not prove to be actual 10% reductions in the effective wall thickness were themselves deleterious, such as mill scale, projections on the inner surface caused by a pitted mandrel etc. The indicated reject rate was about 12%. This application of equipment of moderate speed and moderate reliability provided a very economical test even compared to the relatively low tubing costs of about $ 1.20/m.

THE QUESTION OF STANDARDS

The selection of standards for tube inspection depends upon the type of defect one wishes to detect, and this of course depends upon the type of service for which the tube will be used. If conditions which would reduce the effective wall strength and integrity are to be detected, and this is common in fuel-element and jacket applications, the electro-machined notch [7] is generally the most satisfactory standard. Its chief disadvantage is the ex-

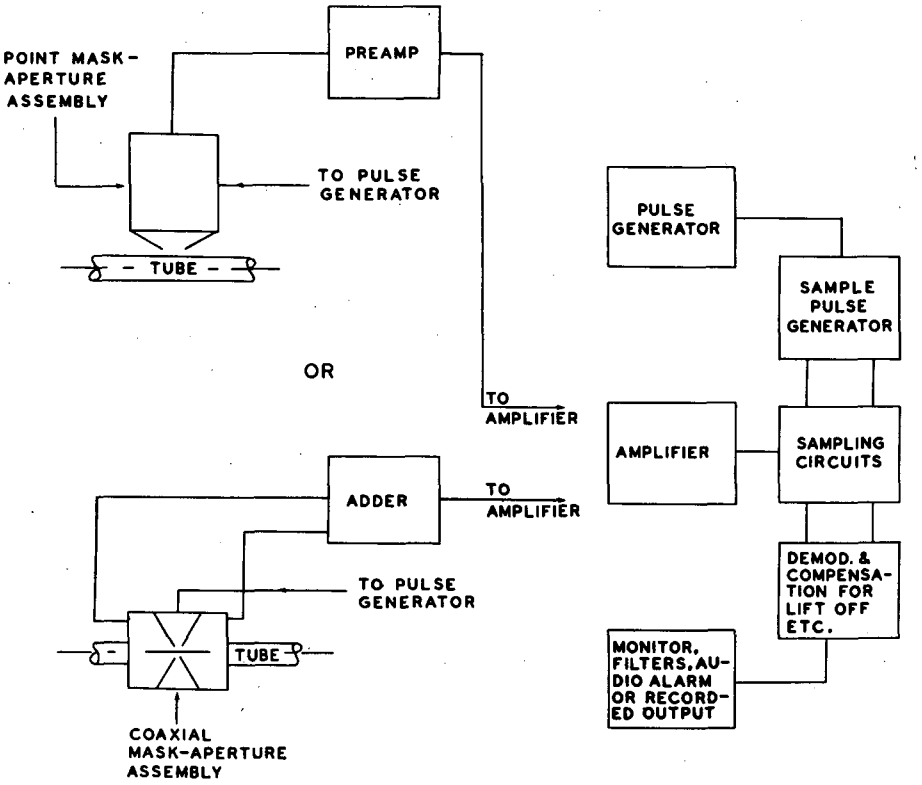

Fig. 2

Block diagram of a pulsed electromagnetic test system

pense. It is also possible to punch narrow notches in some types of tubing which approximate the notches obtained by electro-machining [8]. This is not possible when the tube is extremely hard, or brittle, as for example some types of refractory alloys. The notch depth and length should preferably be the result of a carefully planned and executed programme of long- and short-term creep and burst tests designed to simulate in-service conditions as closely as possible. This is practically never done. As a result the selection of standards boils down to selection of the type of artificial defect necessary to ensure fulfilment of an arbitrary specification. It is generally cheaper to test the tubing to a tighter specification than is really necessary than to execute the experiments necessary to obtain a reasonable idea of what is really required. Despite this ambiguous situation, there really is no excuse for using the long shallow I.D. and O.D. 60° notches used for so long as ultrasonic standards. These notches represent a very favourable situation compared to many natural defects, and about the only thing that can be said about tubing tested to a 1-cm-long 60° notch is that it probably does not contain any 1-cm-long 10% 60° notches. This same type of notch is often used on the outer surface of the tube as an eddy-current reject standard. This is worse, considering the excess sensitivity of most

eddy-current test equipment to surface defects. This is the type of standard in use by many tubing manufacturers, that is to say, those who are equipped at all. If this type of artificial defect produces too many defect signals, a practice known as "testing to the natural defect level" is initiated. This has been discussed before [9], and so will not be denounced here again. These practices will probably continue until equipment of greater discrimination between real defects and spurious signals can be obtained. There is no harm done unless the customer thinks he is buying a better test than he is in fact getting.

The discrimination and sensitivity of non-destructive tube-testing equipment has improved drastically within the past few years, mainly due to the use of focused transducers on ultrasonic equipment and filtering on electromagnetic test equipment. It appears that tubing testing could be reduced significantly in cost by an increased repetition rate of commercially available equipment. Significant cost reductions in testing by present-day commercial eddy-current test equipment must be by an increase in discrimination (the factor p must approach closer to unity). Non-destructive tubing-inspection costs are not a significant item in many reactor designs. For instance, for a relatively expensive material like the zirconium alloys, with tubing costs for the 1-cm O.D. × 0.75-mm wall-size, currently being quoted at about $10/m, it hardly seems worth while to reduce the cost of the non-destructive inspection. For reactors in which cheaper material, such as stainless steel, costing in the neighbourhood of $0.50/m, is used, reduced inspection costs would be beneficial, particularly if the reactor runs at a power level which makes frequent refuelling necessary.

REFERENCES

[1] KIRBY, R.F., GEAP-4095, General Electric Company, San Jose, California (1962).
[2] ZUETSCHEL, M.F. and DIXON, N.E., HW-81957, Hanford Atomic Products Operation, Richland, Washington (1964).
[3] FORSTER, F., Über Fortschritte der zerstörungsfreien Materialprüfung mit elektromagnetischen Verfahren, Materialprüf., Bd.4, Nr.11, Düsseldorf, (1962) 397-444.
[4] Ibid.
[5] RENKEN, C.J., ANL-6728, Argonne National Laboratory, Argonne, Illinois (1964).
[6] RENKEN, C.J. and SELNER, R.H., Refractory Metal Tubing Inspection Using Ultrasonic and Pulsed Eddy Current Methods, Materials Evaluation (to be published).
[7] BOWMAN, H.J., "A Standard for Eddy Current Tests", Metal Progress, 82 1 (1962) 78-79.
[8] ZUETSCHEL, M.F. and DIXON, N.E., HW-81957, Hanford Atomic Products Operation, Richland, Washington (1964) 5.
[9] HOLT, R.C., "Eddy Current Testing of Small Diameter Tubing," Proc. of the Third Ann. Symp. on Non-destructive Testing of Aircraft and Missile Components (1962).

DISCUSSION

R.S. SHARPE: The specification states that a defect is defined as any undesirable reduction in effective wall thickness. This suggests that the defect shape is not taken into consideration. Is this justified when considering fuel cans for reactor service, where cycling of thermal or mechanical stresses may occur during the life of the fuel element?

D.C. WORLTON: Certainly, the shape of a defect affects its degree of seriousness. The above definition is for convenience in preparing written specifications.

Z. PAWŁOWSKI: Are the defect specifications based on purely geometrical considerations, or also on observations of the operational behaviour?

D.C. WORLTON: They are written in terms of defect geometry.

POSSIBILITÉS OFFERTES PAR LA SPECTROMÉTRIE GAMMA DANS LE DOMAINE DES MESURES NON DESTRUCTIVES SUR LES ÉLÉMENTS COMBUSTIBLES

Ch. ENGELMANN, C. BREBANT, J. GOSSET, J. MONIER ET E. ROUSSEL
CENTRE D'ÉTUDES NUCLÉAIRES,
SACLAY, FRANCE

Abstract — Résumé — Аннотация — Resumen

POTENTIALITIES OF GAMMA-SPECTROMETRY IN NON-DESTRUCTIVE MEASUREMENTS ON FUEL ELEMENTS. For several years past we have been studying the application of gamma spectrometry to the problems of non-destructive determination of the burn-up of irradiated fuels. Research shows:

(1) That Pr^{144}, the daughter element of Ce^{144} with a half-life of 290 d, can be particularly recommended for determining the number of fissions ascribable to U^{235}. Its gamma radiation, of very high energy, is such that it can easily be detected in the presence of other fission products after a short cooling period.

(2) That in the same conditions, taking into account the fission yields, Rh^{106}, the daughter of Ru^{106} with half-life 370 d, can be used to measure the fissions characteristic of Pu^{239}. Thus, simultaneous measurement of the γ-ray intensities of Pr^{144} and Rh^{106} would make it possible to determine the burn-up of U^{235}; and the Pu^{239} content of the fuel.

The reasons which led to the choice of the two gamma emitters mentioned are discussed in the paper. The equipment which has been installed is described. An account is also given of the results already obtained, and of the practical possibilities and the limitations of the method.

POSSIBILITÉS OFFERTES PAR LA SPECTROMÉTRIE GAMMA DANS LE DOMAINE DES MESURES NON DESTRUCTIVES SUR LES ÉLÉMENTS COMBUSTIBLES. Depuis plusieurs années déjà, les auteurs étudient l'application de la spectrométrie γ aux problèmes de détermination non destructive des taux de combustion des combustibles irradiés. De leurs recherches, il découle que:

a) ^{144}Pr, produit de filiation de ^{144}Ce, avec une période de 290 j, est particulièrement indiqué pour les déterminations du nombre de fissions imputables à l'uranium-235. Son rayonnement γ de très grande énergie est tel qu'il peut être détecté aisément en présence des autres produits de fission émetteurs après une courte période de refroidissement.

b) Dans les mêmes conditions, compte tenu des rendements de fission, ^{106}Rh, produit de filiation de ^{106}Ru, avec une période de 370 j, peut être utilisé pour mesurer les fissions caractéristiques du plutonium-239. Il s'ensuit que des mesures simultanées des intensités des raies de ^{144}Pr et de ^{106}Rh pourraient permettre de déterminer la combustion en uranium-235 et la teneur du combustible en plutonium-239.

Dans le mémoire, les auteurs discutent les raisons qui ont guidé leur choix sur les deux émetteurs γ précités. Ils décrivent les équipements réalisés. Ils exposent les résultats déjà obtenus, les possibilités pratiques et les limitations de la méthode.

ВОЗМОЖНОСТИ, ОТКРЫВАЕМЫЕ ГАММА-СПЕКТРОМЕТРИЕЙ В ОБЛАСТИ НЕДЕСТРУКТИВНОГО КОНТРОЛЯ ТОПЛИВНЫХ ЭЛЕМЕНТОВ. В течение нескольких лет исследовали применение гамма-спектрометрии к проблемам недеструктивного контроля глубины выгорания облученных топливных элементов. Исследования привели к выводам:

1. Празеодим-144, являющийся продуктом распада церия-144 с периодом 290 дней особенно указывает на определение количества делений, приходящихся на уран 235. Его гамма-излучение с очень большой энергией таково, что оно может быть легко обнаружено в присутствии других излучателей, которые являются продуктами деления после короткого периода охлаждения.

2. В тех же самых условиях, с учетом выхода продуктов деления родий-106, являющийся продуктом деления рутения-106, с периодом 370 дней может быть использован для измерения характерных количеств делений плутония-239.

Таким образом, одновременные измерения интенсивностей лучей празеодина-144 и родия-106 могли бы позволить определить выгорание урана-235 и содержание плутония-239 в топливе.

В докладе обсуждаются причины, приведшие к выбору двух вышеупомянутых гамма-излучателей. Дается описание созданного оборудования. Приводятся полученные результаты, практические возможности, а также пределы применения нового метода.

POSIBILIDADES DE LA ESPECTROMETRIA GAMMA EN LA MEDICION NO DESTRUCTIVA DE ELEMENTOS COMBUSTIBLES. Desde hace varios años se viene estudiando en este Centro la aplicación de la espectrometría gamma a la determinación no destructiva del grado de combustión de combustibles irradiados. De esos estudios, se desprenden las siguientes conclusiones:

1. El ^{144}Pr, descendiente del ^{144}Ce, de período 290 días, es particularmente indicado para determinar el número de fisiones atribuible al ^{235}U.

Su radiación gamma de muy alta energía se puede detectar fácilmente en presencia de otros productos de fisión emisores gamma después de un breve período de enfriamiento.

2. En iguales condiciones, y teniendo en cuenta los rendimientos de fisión, las fisiones características del ^{239}Pu pueden medirse con ayuda del ^{106}Rh, descendiente del ^{106}Ru de período 370 días. Así, pues, midiendo simultáneamente la intensidad de los rayos gamma del ^{144}Pr y del ^{106}Rh, podría determinarse el grado de combustión del ^{235}U y la proporción de ^{239}Pu contenida en el combustible.

En la memoria se discuten los motivos a que obedece la selección de los dos emisores de rayos gamma arriba mencionados. Se describen los experimentos realizados; además, se exponen los resultados obtenidos, las posibilidades prácticas y las limitaciones del método.

1. INTRODUCTION

En technologie nucléaire les méthodes d'analyse non destructives sont certainement plus avantageuses encore que dans toutes les autres branches scientifiques ou industrielles.

Cela se conçoit quand on considère les très grandes activités radioactives mises en jeu et, par conséquent, les difficultés introduites par les opérations de prélèvements systématiques de petits échantillons.

D'autre part, et cela est plus important encore, les méthodes non destructives sont aptes à fournir des données sur toute une cartouche sans la détruire, de sorte qu'il est toujours possible de mesurer périodiquement le degré de consommation de matière fissile d'un élément combustible.

Rappelons que le taux de combustion d'un élément ne doit atteindre en aucun endroit une valeur supérieure à une limite imposée par des considérations métallurgiques. Si le gradient du taux de combustion le long de l'élément n'est pas négligeable, le rendement d'exploitation économique de l'élément se trouve diminué. Il est donc essentiel que la répartition du taux de combustion tout au long d'un élément soit uniforme, de façon qu'on puisse en tirer le maximum d'énergie.

Il est bien évident que dans un réacteur le flux de neutrons n'est pas le même partout, de sorte que certains éléments peuvent être irradiés dans des conditions très peu avantageuses.

Ainsi le fait qu'on puisse déterminer le gradient du taux de combustion le long d'une cartouche par des méthodes non destructives est très intéressant. En effet, en examinant systématiquement toutes les cartouches on peut les changer de place dans le réacteur en fonction des résultats de mesure obtenus, de façon que le taux de combustion soit partout le même, d'où une meilleure exploitation des barreaux de combustible.

D'ailleurs on pourra même éventuellement dessiner, d'après ces mesures, de nouveaux éléments, afin que ces conditions primordiales sur le plan énergétique et économique soient satisfaites.

On comprend ainsi que de tels équipements de mesure soient indispensables auprès de chaque installation nucléaire de recherche et de puissance.

2. APERÇU THÉORIQUE

La production totale de chaque produit de fission tout au long du séjour de l'élément dans le réacteur est directement proportionnelle à la consommation de matière fissile. De sorte que cette grandeur, donc le taux de combustion, peut se déduire de la mesure de la quantité totale produite pendant l'irradiation d'un produit de fission.

Dans le cas particulier, qui seul est intéressant d'ailleurs, où le produit de fission considéré est obtenu directement, ou en équilibre radioactif avec son ascendant, l'aspect mathématique du problème peut se résumer dans la relation suivante:

$$\frac{dN_i}{dt} = \alpha_i F - \lambda_i N_i - \psi_i(N_i), \tag{1}$$

où dN_i/dt est la vitesse de formation de l'espèce i;
α_i son rendement de fission;
λ_i sa constante de désintégration;
N_i le nombre d'atomes présents à l'instant considéré;
$\psi_i(N_i)$ un terme correctif qui tient compte de la disparition de l'espèce i par capture neutronique (pour les nucléides dont les sections efficaces sont inférieures à une centaine de Fermis, il peut être absolument négligé, ce qui est pratiquement le cas pour ceux qui nous intéressent);
F est le nombre de fissions par seconde.

2.1. Principe du calcul du nombre de fissions en première approximation

Le cas le plus simple est évidemment celui où α_i et F sont supposés constants tout au long de l'irradiation. De sorte que si l'on néglige le terme $\psi_i(N_i)$, l'intégration de (1) donne

$$N_{iT} = \frac{\alpha_i}{\lambda_i} F[1 - \exp(-\lambda_{it})] \exp(-\lambda_{iT}). \tag{2}$$

t est la durée d'irradiation;
T celle de refroidissement;
N_{iT} le nombre d'atomes de l'espèce i présents à l'instant T.

N_{iT} peut se mesurer, puisque l'activité radioactive qui s'y rattache est $N_{iT}\lambda_i$. Comme toutes les grandeurs figurant dans (2) sont connues sauf F, cette relation permet de calculer F, et par conséquent le nombre de fissions $F \times t$.

2.2. Cas général

La relation (2) ci-dessus ne peut être qu'approximative, pour diverses raisons. Tout d'abord F n'est jamais constant tout au long de la vie d'un élément dans le réacteur. Indépendamment des fluctuations locales de flux de neutrons, F varie en fonction de la combustion même. Mais la variation la plus importante est indiscutablement liée aux déplacements que peuvent subir les diverses cartouches dans le réacteur au cours de leur utilisation. Enfin le rendement de fission α_i dépend du spectre de neutrons; il varie donc avec l'évolution de ce dernier. Comme pour F, α_i dépend aussi de l'endroit du réacteur où est placée la cartouche. Néanmoins ses variations peuvent être négligées si l'on choisit convenablement le produit de fission sur lequel portent les mesures.

La relation simplifiée (2) doit donc être remplacée par l'expression plus générale

$$N_{iT} = \phi(\alpha_i F, t)\exp(-\lambda_i T). \tag{3}$$

Le calcul du nombre total de fissions devient alors très complexe. Le régime de fonctionnement du réacteur doit être connu. De toute façon ce calcul, s'il est possible, n'a de sens que dans la mesure où la durée d'irradiation n'excède pas deux à trois périodes du nucléide déterminé.

Si cette période est très supérieure au temps de séjour dans le réacteur (à un facteur 10 près, ou moins) l'expression (3) se simplifie et devient

$$N_{iT} = \int_0^t \alpha_i F \, dt \exp(-\lambda_{iT}), \tag{4}$$

de sorte que si l'on peut considérer α_i comme constant pendant la durée d'irradiation, le nombre total de fissions est donné par la relation

$$\int_0^t F \, dt = \frac{N_{iT}}{\alpha_i} \exp(\lambda_{iT}). \tag{5}$$

3. CRITÈRES INTERVENANT DANS LE CHOIX DU PRODUIT DE FISSION A DÉTERMINER QUANTITATIVEMENT

D'après les considérations développées ci-dessus, il faut que le produit de fission à choisir satisfasse aux conditions suivantes:

a) Section efficace de capture neutronique très faible.
b) Rendement de fission α_i très grand et très peu variable en fonction du spectre de neutrons.
c) Période de décroissance très grande. Les calculs sont d'autant plus simplifiés et exacts que les durées d'irradiations sont petites par rapport à la période.

d) Sa diffusion dans l'élément combustible et dans la gaine doit être très faible en fonction du temps, pour la température de fonctionnement existante. S'il migre vers des endroits privilégiés, les valeurs apparentes de taux de combustion ainsi déterminées peuvent être très différentes des valeurs réelles.

e) L'énergie du rayonnement γ émis doit être très élevée, d'une part pour que le pic photoélectrique sur lequel portent les mesures soit toujours nettement visible en présence des activités des autres produits de fission, d'autre part pour que l'absorption dans l'élément combustible lui-même du rayonnement à détecter ne soit pas trop importante.

Quand on considère l'ensemble des produits de fission, on s'aperçoit que les conditions impératives ci-dessus ne sont satisfaites pratiquement que pour deux éléments: ^{144}Pr, descendant de ^{144}Ce (période 290 j) et ^{106}Rh descendant de ^{106}Ru (période 370 j).

Le tableau I résume les principales caractéristiques nucléaires de ces isotopes. Ces constantes sont extraites de [1]. Deux spectres γ, de ^{106}Ru - ^{106}Rh et de ^{144}Ce - ^{144}Pr respectivement, ont été obtenus à partir de préparations particulièrement pures (fig. 1 et 2).

Ces valeurs montrent que le pic de ^{144}Pr à 2,18 MeV peut convenir aussi bien pour les combustibles à base d'uranium-235 que pour ceux à base de plutonium-239.

De toute façon une chose est évidente, d'après ces constantes et les spectres γ donnés, c'est que ^{106}Rh ne peut en aucune façon interférer avec ^{144}Pr.

Par contre, le fait que les rendements de fission de ^{106}Ru sont très différents pour l'uranium et le plutonium pourrait être exploité pour mettre au point des méthodes de mesures sélectives. En effet ^{106}Ru étant plus spécifique de la fission du plutonium, de sa mesure et de celle de ^{144}Pr on pourrait déduire

a) pour un combustible à uranium naturel ou peu enrichi, le taux de combustion de l'uranium-235 et celui dû au plutonium-239 formé pendant l'irradiation, de sorte que de cette dernière détermination découle la quantité de plutonium existant dans le combustible;

b) pour un combustible mixte contenant à la fois de l'uranium-235 et du plutonium-239, les taux de combustion individuels imputables à chaque type de matière fissible.

Afin de délimiter exactement le champ d'application des méthodes proposées ci-dessus, nous poursuivons actuellement des expériences relatives à des combustibles irradiés à des taux de combustion croissants, à base d'uranium et de plutonium avec des taux respectifs d'enrichissement divers.

4. DISPOSITIFS DE COMPTAGE

Les installations que nous avons utilisées dans nos études préliminaires sur les cartouches EL3 sont décrites dans une publication [2].

Rappelons brièvement que le barreau est introduit dans un château compteur spécial et défile devant un système de diaphragmes constitué par trois fentes de largeurs réglables disposées entre la zone mesurée du combustible et le compteur. Entre la deuxième et la dernière fente, des écrans amovibles

TABLEAU I

PRINCIPALES CARACTÉRISTIQUES NUCLÉAIRES DES ISOTOPES CONSIDÉRÉS

Nucléide	Période	Rendement de fission (%)		Energie du rayonnement γ (MeV)	
		^{235}U	^{239}Pu		
^{106}Ru	370 j	0,38	4,5	pas de γ	
^{106}Rh	30 s	-	-	2,45	0,25%
				1,55	0,5%
				1,045	2%
				0,87	1%
				0,624	11%
				0,513	21%
^{144}Ce	290 j	6,1	3,5	0,133	17,2%
				0,099	0,1%
				0,079	5,5%
				0,058	1,2%
				0,053	1%
^{144}Pr	17,5 min	-	-	2,18	0,8%
				1,49	0,26%
				0,69	1,6%
				0,61	1,34%
				0,48	1,34%

en plomb peuvent être interposés. Leur rôle est double: d'une part ils atténuent la composante de basse énergie du rayonnement émis par les produits de fission, d'autre part ils permettent de régler le flux de rayons γ arrivant sur le détecteur. Ce dernier fonctionne donc toujours dans des conditions reproductibles, bien que les activités des barreaux soient très diverses. Une pince spéciale permet enfin de faire tourner un barreau autour de son axe. Aussi est-il possible de déterminer des gradients de taux de combustion sur plusieurs génératrices.

Compte tenu de l'énergie des rayons γ de ^{144}Pr et de ^{106}Rh, nous utilisons des compteurs à scintillation avec des cristaux NaI(Tl) de grandes dimensions (80 × 100 mm).

Un sélecteur d'amplitude transistorisé à 400 canaux permet de tracer le spectre γ des produits de fission visibles et existant dans le barreau.

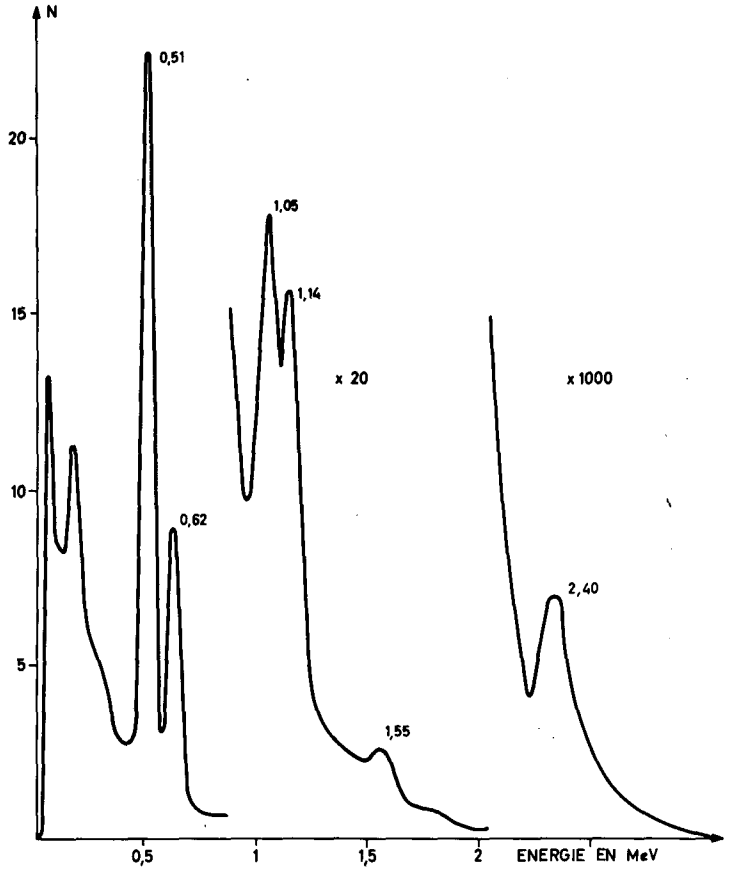

Figure 1

Spectre gamma du $^{106}Ru + ^{106}Rh$.

Enfin son utilisation en fonctionnement multi-échelle est particulièrement appréciable pour la détermination automatique des gradients, le défilement mécanique du barreau étant en synchronisme avec le déplacement des canaux. Il est bien entendu qu'un dispositif de sélection précède l'enregistrement, afin que les mesures portent sur le radionucléide prédéterminé.

Deux nouvelles installations sont en cours de réalisation, l'une au LECI à Saclay, la seconde au LECA à Cadarache. Leurs points communs sont les suivants:

a) Les mesures sont faites dans des cellules de très haute activité conventionnelles. Un tunnel percé dans la porte arrière contient le système de fentes et d'écrans absorbants. Le compteur placé au bout de ce tunnel est donc hors cellule.

b) Les barreaux défilent devant les diaphragmes à l'intérieur de la cellule. Il est donc possible de suivre la position du barreau à travers les vitres blindées en même temps que s'enregistre le taux de combustion.

c) Les barreaux peuvent se déplacer linéairement suivant deux directions

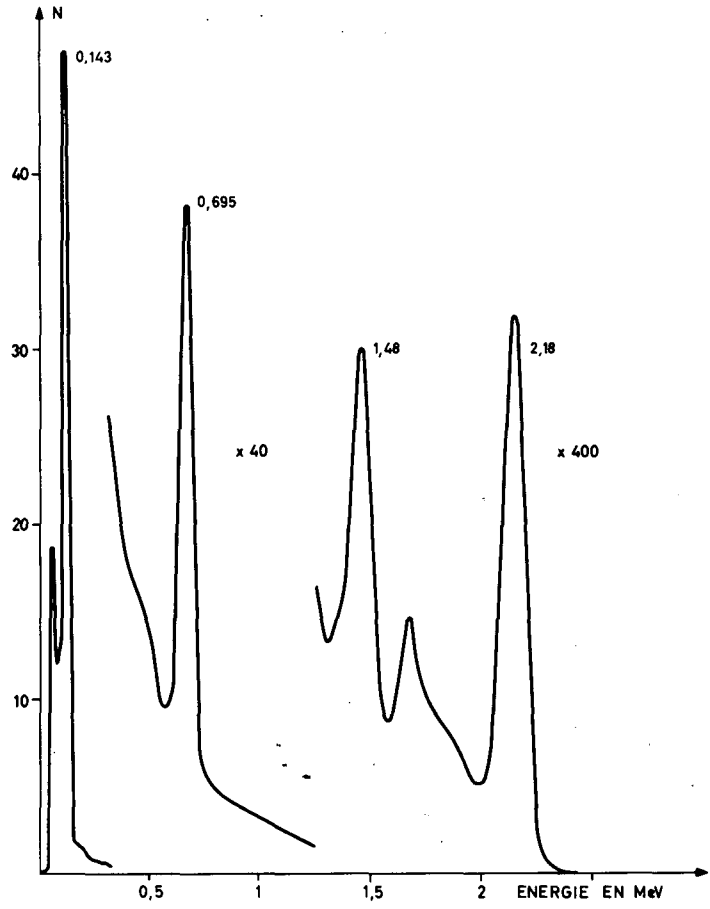

Figure 2

Spectre gamma du $^{144}Ce + ^{144}Pr$.

perpendiculaires XY. Ils peuvent également tourner autour de leur axe. La possibilité de faire tourner le barreau pendant son déplacement longitudinal est très précieux puisque, à partir de ce mouvement hélicoïdal, la courbe de répartition du taux de combustion obtenue est très représentative du taux de combustion global de l'élément.

d) Ces nouveaux dispositifs sont prévus avec deux systèmes de fentes réglables et perpendiculaires. Des mesures pontuelles sont donc possibles. L'appareillage peut également servir pour des mesures de taux de combustion sur des échantillons de petites dimensions.

Ainsi, avec ces installations qui possèdent de par leur construction un caractère d'emploi universel, il est possible de mesurer les gradients de tous les combustibles actuellement existants. En outre, puisque des mesures ponctuelles sont envisagées, il sera également possible de déterminer le gradient radial d'un barreau cylindrique en découpant des rondelles aux en-

droits intéressants. Ce genre d'expérience présente un intérêt évident. On sait en effet que dans un combustible à uranium naturel déjà, les couches superficielles font écran aux neutrons. Par ce mécanisme le taux de combustion doit passer par un minimum sur l'axe du cylindre si l'élément a cette symétrie. Cet effet est d'autant plus important que le taux d'enrichissement est plus élevé. Par conséquent des mesures du gradient radial deviennent indispensables, ne serait-ce que pour connaître avec précision la grandeur de la dépression de flux au cœur des éléments.

5. ÉTALONNAGE DES INSTALLATIONS

Deux types d'étalonnages peuvent être considérés:

a) Tout d'abord celui que nous utilisons couramment et qui consiste à découper une rondelle dans un barreau préalablement mesuré. Cette rondelle, pesée avec précision, est dissoute dans une solution acide et une analyse absolue de la quantité de ^{144}Ce ou d'un autre produit de fission est effectuée. L'efficacité de détection du dispositif s'en déduit. En faisant intervenir le rendement de fission α_i, on peut étalonner l'installation pour des conditions d'irradiation et de refroidissement données, directement en taux de combustion. Ce type d'étalonnage repose évidemment sur la validité des calculs, et surtout sur la bonne connaissance de α_i.

b) On peut aussi, et cela nous semble beaucoup plus rationnel, découper une rondelle après une première mesure, et, par spectrométrie de masse, déterminer la baisse de teneur en uranium-235 et éventuellement l'enrichissement en plutonium. Les activités mesurées avec le dispositif peuvent donc être reliées directement aux grandeurs qui nous intéressent.

Les expériences en cours reposent exclusivement sur cette dernière méthode d'étalonnage.

6. CONCLUSION

La spectrométrie γ sur des produits de fission comme ^{144}Pr et ^{106}Rh est donc apte à fournir aux spécialistes intéressés des renseignements très utiles sur l'irradiation des éléments combustibles. Les études complémentaires en cours nous permettront de montrer dans quelles conditions des mesures simultanées des pics de ^{144}Pr et de ^{106}Rh peuvent servir au calcul de l'appauvrissement en uranium-235 et de l'enrichissement en plutonium-239, par des méthodes non destructives.

Les méthodes de mesure proposées seront encore beaucoup plus intéressantes dans quelque temps, en raison du développement des détecteurs à semi-conducteur.

L'utilisation de dispositifs à anticoïncidence appliqués exclusivement au problème des mesures sur éléments combustibles [3] permettra de déterminer simultanément plusieurs produits de fission, compte tenu de la très haute résolution qui caractérise ces détecteurs.

Ces nouvelles techniques de mesure sont prévues pour l'exploitation des cellules dont nous avons esquissé le principe, conjointement avec le dépouillement automatique des résultats de mesure par calculateur électronique.

RÉFÉRENCES

[1] MALET, G., Rapport CEA n° 2226 (1962).

[2] ENGELMANN, Ch. et PETIT, J.F., Rapport CEA n° R 2542 (1964).

[3] HOLM, D.M. and SANDERS, W.M., «A Semiconductor Anticoincidence Detector System», Radiochemical Methods of Analysis II, IAEA, Vienna (1965) 81.

DISCUSSION

P. de MEESTER: What width of electron window do you use in order to avoid the influence of other peaks?

C. ENGELMANN: Before taking any measurement, we make a γ-spectrum with a multichannel selector. The single-channel selector which forms part of this equipment is then adjusted to the peak of the isotope concerned. The movement of the fuel rod is synchronized with the displacement of the channels of the selector working as a multichannel unit. The form of the burn-up profile along the length of the fuel element is thus directly recorded in the memory of the electronic apparatus.

P. de MEESTER: Is the measurement of the caesium peak representative of the burn-up distribution, in view of migration effects?

C. ENGELMANN: It is quite probable that Cs^{137} cannot be used to determine burn-up distribution, owing to the importance of migration, which itself depends on the temperature of the fuel element in the reactor. For this reason we use above all Pr^{144}, the daughter element of Ce^{144}, which is reputed to diffuse only to a small extent. It is incidentally part of the purpose of the present experiments to demonstrate this diffusion of Cs^{133} and make apparent the difficulties involved in using this isotope for non-destructive measurement of burn-up, especially for elements operating at high temperature.

P. de MEESTER: I believe the Commissariat à l'Energie Atomique is also carrying out radiographic tests on burn-up distribution. Have you compared the relative advantages of the two method?

C. ENGELMANN: I do not know the method you mention, and in fact do not see how radiography can be used to determine burn-up distribution.

R.S. FORSYTH: Did you notice any increase in the Pr^{144} peak due to pile-up of other gammas, say, the Zr^{95} 0.75-MeV activity?

C. ENGELMANN: As I explained in my paper, between the scintillator and the fuel element we insert, if necessary, lead absorbing screens, so that the radiation entering the NaI(Tl) crystal is filtered. Thus in the presence of very high activity of isotopes giving γ-rays of energy less than about 1 MeV, it is possible to attenuate this component of the radiation selectively in favour of the high-energy component containing the Pr^{144}. Since the summation pulses are produced solely in the counting equipment, the filtering

by the lead screens practically eliminates this effect if the activities become too considerable.

R. S. FORSYTH: What was the width of slit collimator used?

C. ENGELMANN: Our equipment is designed to permit continuous variation of the slit width from 0.1 mm to about 10 mm. This is done very accurately by a micrometer control.

MESURES DIMENSIONNELLES ET DÉTECTION DES DÉFAUTS

C. BREBANT, R. HUILLERY ET E. ROUSSEL
CENTRE D'ÉTUDES NUCLÉAIRES DE SACLAY, FRANCE

Abstract — Résumé — Аннотация — Resumen

DIMENSIONAL MEASUREMENTS AND FLAW DETECTION. Non-destructive tests on irradiated fuels are carried out in concrete cells in the very high-activity laboratories at Saclay and Cadarache. The equipment in use can be used for all types of fuel.

The cells used for these tests contain the following equipment:

Radiographic equipment scanning either around or along the sample; leak-testing equipment; observation equipment; and standard metrological equipment.

Radiography and leak testing are discussed.

For the rotary scanning equipment, the slugs are X-rayed with a Philips Majorix-300 projector and the films are introduced into the X-ray beam via an aperture in the rear door. The film exposure time is regulated by a rocker. The slug is placed in the beam by heavy remote-handling equipment. Several emulsions are available, the one most suited to the specific activity of the fuel being selected.

The results obtained to date are excellent, and it is hoped that they can be improved still further by the adoption of a new type of equipment scanning along the sample, whose operation is described in the paper.

The leak test is carried out in a transparent vessel which may contain either ethylene glycol or white spirit. Leaks are detected by progressive evacuation. Surface bubbling is eliminated by various methods of treating the surface of the slugs. For detecting microleaks the fuel is previously pressurized in a bath of helium at 35 kg(cm²). This equipment is satisfactory, and makes it possible to produce photographic record locating the leak.

MESURES DIMENSIONNELLES ET DÉTECTION DES DÉFAUTS. Les essais non destructifs sur combustibles irradiés sont effectués en cellule de béton dans les laboratoires de très haute activité de Saclay et de Cadarache. Les appareils utilisés s'adressent à tous les types de combustibles.

Les cellules réservées à ces essais contiennent les appareils suivants: un appareil de radiographie par basculement ou par défilement; un appareil de test d'étanchéité; des appareils d'observation; un outillage de métrologie de type classique.

Les auteurs traitent dans le mémoire la radiographie et le test d'étanchéité.

Pour les appareils par basculement, la radiographie des cartouches est faite à l'aide d'un projecteur Philips Majorix 300 et les films sont introduits dans le faisceau X par une ouverture de la porte arrière. Le temps d'exposition du film est réglé par un bascuteur. La cartouche est placée dans le faisceau par télémanipulateur lourd. On dispose de plusieurs émulsions dans lesquelles ont choisit celle convenant à l'activité spécifique du combustible.

Les résultats obtenus actuellement sont excellents et on espère les améliorer par l'adoption d'un nouvel appareil par défilement, dont le principe est décrit dans le mémoire.

Le test d'étanchéité est réalisé dans un récipient transparent pouvant contenir, soit de l'éthyl-glycol, soit du white spirit. Les fuites sont détectées par mise sous vide progressive. Les inconvénients des débullages parasites sont éliminés par divers traitements de surface des cartouches. Lorsqu'il importe de détecter des microfuites, on pratique la pressurisation préalable du combustible dans un bain d'hélium à 35 kg (cm²). Cet appareil est satisfaisant et permet la prise de documents photographiques localisant la fuite.

КОНТРОЛЬ РАЗМЕРОВ И ОБНАРУЖЕНИЕ ДЕФЕКТОВ. Испытания без разрушения образцов облученного топлива проводились в бетонной камере горячих лабораторий в Сакле и Кадараше. Использованные в процессе работы приборы предназначались для всех видов топлива.

В камерах, которые были отведены для этих опытов, имелись следующие приборы: прибор для радиографии при вращательном и плавном перемещении образцов; прибор для испытания на герметичность; приборы наблюдения; метрологическая аппаратура обычного типа.

Мы рассматриваем здесь радиографию и испытания на герметичность.

В отношении приборов скеннирования с помощью вращения, радиография топливных элементов производится проектором Филипс Маджорикс 300, когда пленки пропускают под пучком рентгенолучей через отверстие в задней дверце. Время облучения пленки регулируется опрокидывателем. Топливный элемент вводится в пучок тяжелым дистанционным манипулятором. Используется несколько эмульсий, из числа которых выбирается такая, которая соответствует удельной активности топлива. Полученные результаты являются отличными, однако есть возможность их улучшить с помощью нового прибора, который описывается в докладе.

Опыт проводится в прозрачной емкости, которая может содержать либо этилгликоль, либо спирт. Утечки обнаруживаются в результате постепенного создания вакуума. Помехи, связанные с вредными выделениями пузырьков, устраняются в результате различной обработки поверхности топливных элементов. Для обнаружения микроутечек используют предварительный наддув топлива с давлением 35 кг ($см^2$) в гелиевой ванне. Это устройство является удовлетворительным и позволяет получать фотодокументы с локализацией утечки.

MEDIDAS DIMENSIONALES Y DETECCION DE FALLAS. Los ensayos no destructivos de combustibles irradiados se llevan a cabo en celdas de hormigón, en los laboratorios de muy alta actividad de Saclay y de Cadarache. Los aparatos en servicio se utilizan para todos los tipos de combustible.

Las celdas reservadas para estos ensayos contienen los siguientes dispositivos: un aparato de radiografía por rotación o por avance lineal; un aparato para prueba de estanqueidad; aparatos de observación; instrumentos de medición del tipo clásico.

Esta parte de la memoria se refiere a la radiografía y a la estanquidad.

En los aparatos por rotación, la radiografía de los elementos combustibles se realiza con ayuda de un proyector Philips Majorix 300 y las películas se introducen en el haz de rayos X por una abertura de la puerta trasera. El tiempo de exposición de la película se regula mediante un contrapeso. El elemento se coloca en el haz con ayuda de un manipulador a distancia, del tipo pesado. Se dispone de varias emulsiones, entre las cuales se elige la que más se adapte a la actividad específica del combustible.

Los resultados obtenidos hasta la fecha son satisfactorios y se espera mejorarlos aún más adoptando un nuevo aparato de avance lineal, cuyo principio se describe en la memoria.

La prueba de estanquidad se realiza en un tanque transparente que puede contener etil-glicol, o bien esencia de trementina artificial. Los escapes se ponen de manifiesto aumentando gradualmente el vacío. Los inconvenientes derivados del desprendimiento de burbujas parásitas se eliminan mediante diversos tratamientos aplicados a la superficie de los elementos. Cuando se trata de detectar microescapes, se somete previamente el elemento combustible a una presión de 35 kg(cm^2), en baño de helio. Este aparato da resultados satisfactorios y permite tomar fotografías a fin de localizar los escapes.

I. RADIOGRAPHIE

1. Equipement de radiographie du LECI (fig. 1)

Principe

Il s'agit d'une projection conique. La source de rayons X, l'objet et le film sont fixes pendant la radiographie.

Description de l'appareillage

a) A l'intérieur de la cellule

La source de rayons X est constituée par un Majorix 300. L'objet à radiographier est posé sur un chariot mobile permettant de le mettre en position. Le film, placé dans une cassette, est introduit dans la cellule par la porte arrière. La cassette est placée à cet endroit sur un basculeur,

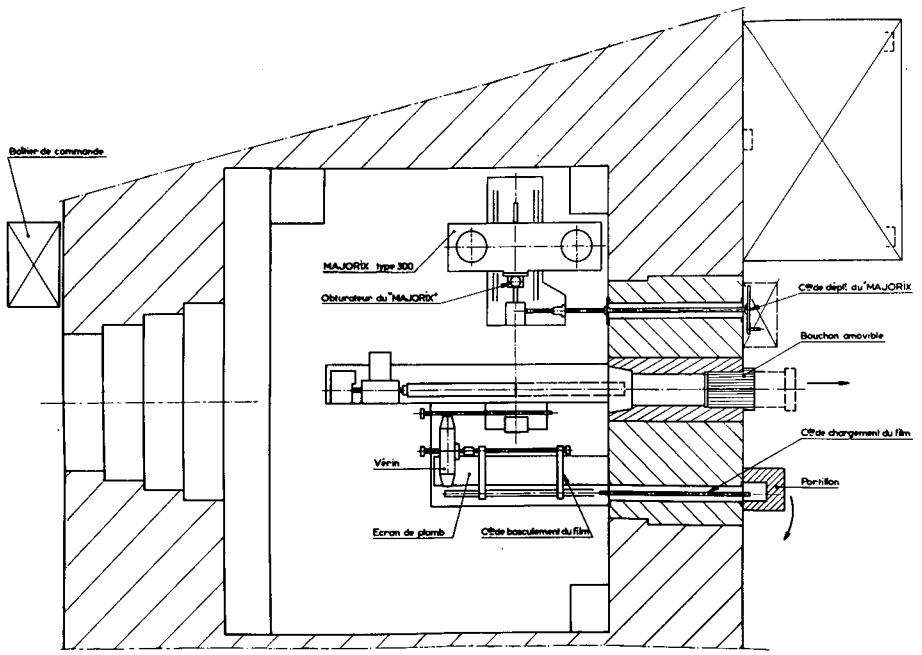

a)

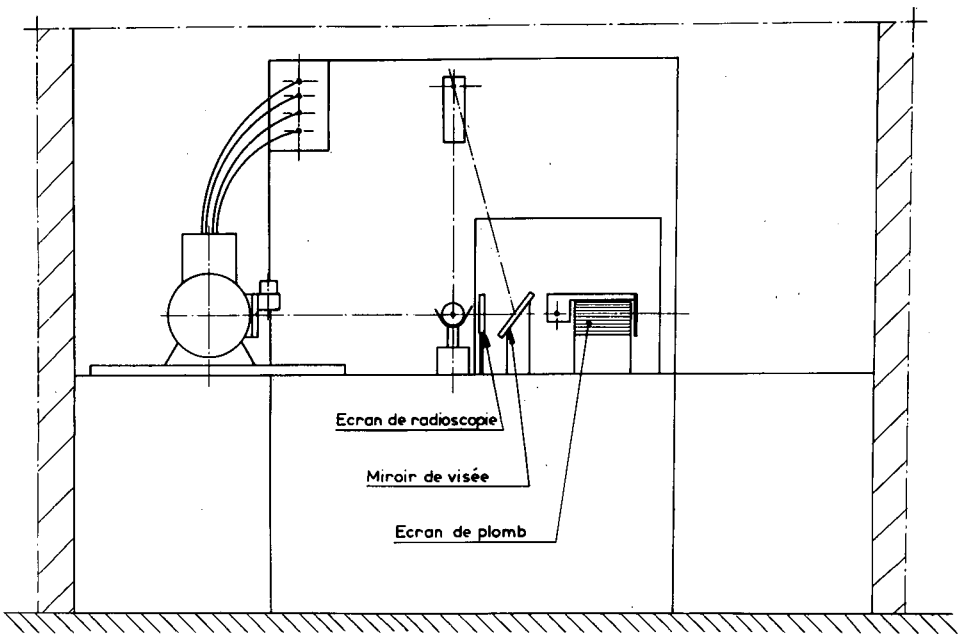

b)

Figure 1

Cellule de radiographie LECI.

derrière une forte épaisseur de plomb qui la protège du rayonnement émis par l'objet. Le basculeur amène le film à proximité de l'objet et actionne simultanément un contact électrique qui provoque l'effacement de l'obturateur de la source de rayons X. La radiographie terminée, le retour du basculeur est commandé soit par une minuterie, soit par l'opérateur.

b) A l'extérieur de la cellule

Nous avons placé à l'extérieur tous les appareillages annexe:
- les générateurs,
- la pompe à huile de refroidissement,
- le pupitre de commande du tube de rayons X,
- le pupitre de commande des déplacements du chariot.

Caractéristiques

- Tube Majorix 300: petit foyer = 4 mA, 300 kV,
  grand foyer = 10 mA, 300 kV,
- Dimensions des foyers: petit foyer = 1,5 × 1,5 mm,
  grand foyer = 4 × 4 mm,
- Distance foyer-film: 600 à 900 mm,
- Distance film-objet: 60 à 105 mm.

Types de films utilisés

Jusqu'à ce jour nous avons utilisé trois types de films:
- Structurix D 2 (Gevaert),
- JR 175-3 (Kodak),
- DX 685 (Kodak).

Le structurix D 2 est d'un emploi courant dans la radiographie ordinaire. Il est cependant utilisé avec succès jusqu'à des activités de 10 000 R/h et des temps de pose de l'ordre de 10 s. Au-delà, il est nécessaire d'utiliser des films dont la sensibilité au rayonnement γ est diminuée. Ce sont les films JR 175-3 et DX 685. Les temps de pose sont alors beaucoup plus longs (plusieurs minutes), mais les résultats sont bons. L'expérience que nous avons ne nous a pas permis de définir les limites exactes de ces films, mais on peut penser que le DX 685 permet de bonnes radiographies d'objets ayant une activité voisine de 40 000 R/h dans les conditions de notre appareillage.

Ces films peuvent être utilisés avec ou sans écrans renforçateurs.

Remarque: La firme Kodak continue ses recherches sur ce type de film et a déjà obtenu des résultats pour la radiographie d'objets ayant des activités supérieures à celles indiquées ci-dessus.

2. *Equipement de radiographie du LECA (fig. 2)*

Nous avions au LECA une installation analogue, que nous avons remplacée par une radiographie de défilement.

Dans ce dispositif, le film, placé en canette, défile en même temps qu'un barreau combustible; ils sont placés de part et d'autre d'une protection γ, devant une source X. Une fente étroite, placée verticalement dans

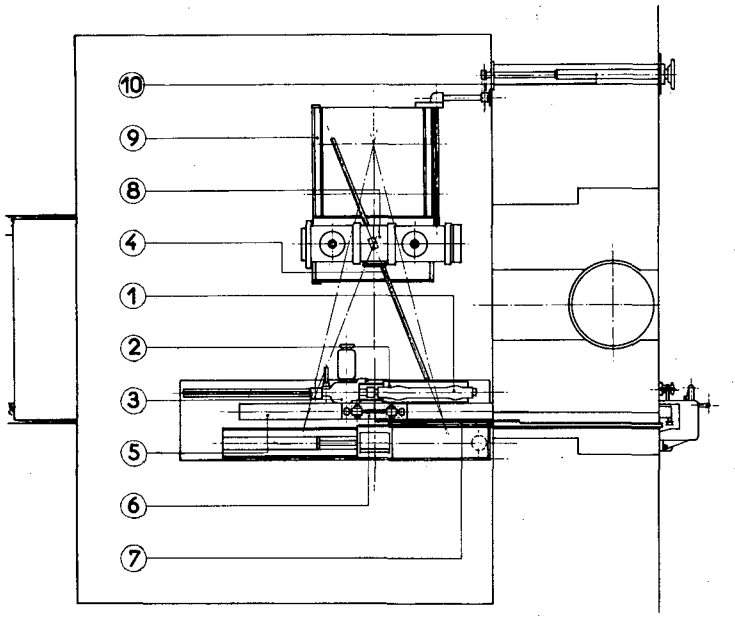

Figure 2

Radiographie par défilement.

1. Elément radioactif
2. Berceau
3. Bloc mécanisme à deux sorties
4. Tringlerie
5. Ecran en dénal
6. Fenêtre à ouverture réglable
7. Cassette
8. Générateur de rayons X
9. Chariot
10. Commande manuelle

la protection γ et située dans l'axe des X, laisse passer ceux-ci pour impressionner le film.

Caractéristiques principales

- Source X: 0 à 10 mA, 0 à 300 kV,
- Foyer de 1,5×1, 5 mm ou 4×4 mm,
- Distance des X à l'axe du combustible: 400 à 1200 mm,
- Distance du film à l'axe du combustible: 170 mm,
- Epaisseur de la protection: 100 mm,
- Largeur de fente: de 0 à 10 mm.

La fenêtre peut s'ouvrir jusqu'à 100 mm pour permettre l'examen radioscopique à l'aide d'un écran fluorescent et d'un périscope. La vitesse de défilement est d'environ 10 à 15 min pour un élément de 600 mm. Le barreau est réglable en hauteur sur son support.

3. Avantages et inconvénients des deux procédés

La radiographie globale par basculement laisse l'élément fixe sur son support. La prise de la photo radiographique est rapide. L'inconvénient

majeur est la projection conique du barreau sur le film. Les déformations vont croissant de part et d'autre de l'axe des X.

La radiographie par défilement nécessite la translation simultanée dans un rapport de vitesse constant du barreau et du film, ce qui est réalisé par une liaison mécanique. Le flou de défilement est donné par le rapport des distances, source d'X à film/source d'X à barreau. Le flou géométrique est fonction des dimensions du foyer. Le temps d'exposition est plus long.

On obtient par ce dispositif des films radiographiques sur lesquels l'on peut mesurer correctement des longueurs. Théoriquement la précision de la mesure est limitée par la valeur totale du flou, soit en moyenne 0,3 mm. En réalité, la réflexion et la diffraction des X sur les arêtes du métal lourd du barreau peuvent amener un grandissement optique de l'image de 1 à 3/10 de mm.

4. Conclusion

Pour diminuer le flou et améliorer la finesse de l'image, on a intérêt à avoir un générateur X à très petit foyer et une distance barreau-film réduite, donc à prendre pour écran γ un métal très lourd.

Il semble que la précision de mesure peut varier de 1 à 3/10 mm.

II. TEST D'ÉTANCHÉITÉ (fig. 3)

1. Test d'étanchéité du LECI

But

Nous désirons détecter et plus particulièrement localiser les fuites qui se produisent accidentellement sur les montages étanches.

Principe

Le montage est introduit dans un liquide au-dessus duquel nous créons une dépression. Le gaz contenu dans le montage s'échappe par la fissure sous forme d'un chapelet de bulles.

Equipement

a) A l'intérieur de la cellule

L'équipement est très simple. Il est essentiellement constitué par un récipient cylindrique transparent muni d'un couvercle dont la fermeture est assurée par un joint torique. Ce récipient, placé verticalement, peut à volonté tourner ou être bloqué au cours de l'opération, ce qui permet à l'opérateur de faire une observation complète du montage testé. Cet équipement intérieur peut être complété ou non par un piège à azote, selon le liquide utilisé.

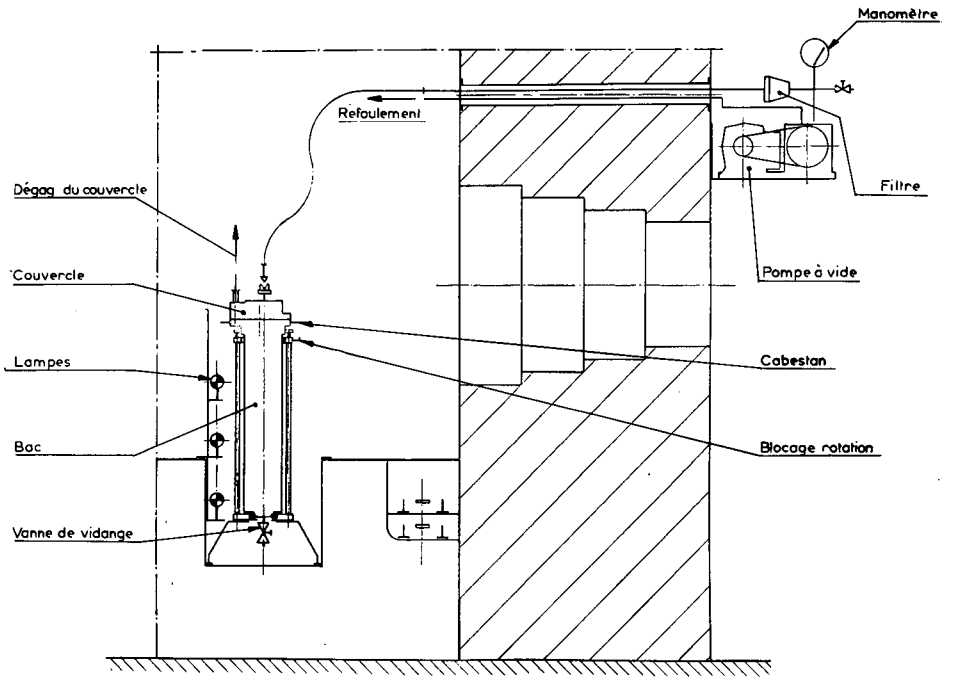

Figure 3a

Test d'étanchéité - LECI.

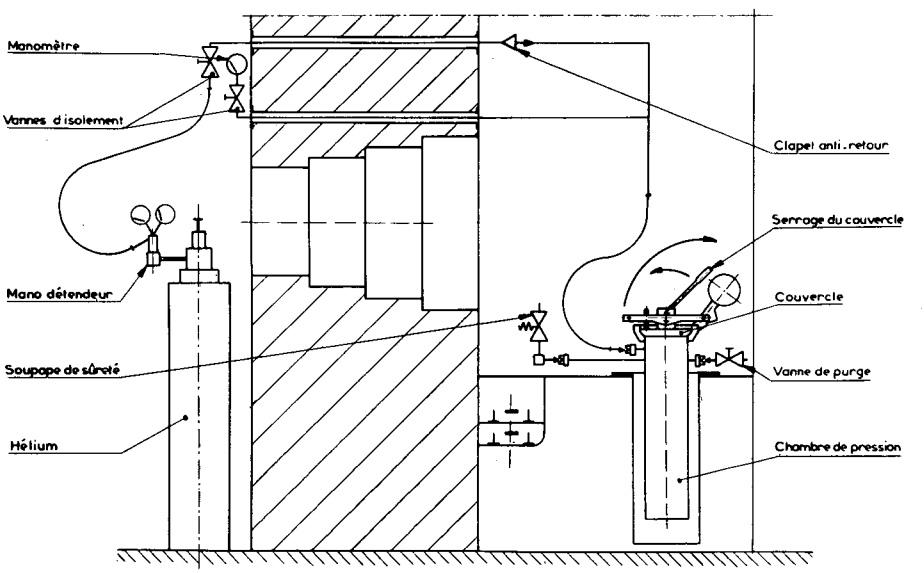

Figure 3b

Chambre de pression hélium - LECI.

b) A l'extérieur de la cellule

Nous avons placé une pompe à vide primaire équipée d'un robinet manuel de mise à la pression atmosphérique. Ceci permet à l'opérateur de faire varier la dépression dans le récipient de façon progressive et d'éviter parfois la présence de bulles parasites autour du montage.

c) Cuve de mise sous pression hélium (fig. 3b)

Pour augmenter la sensibilité de cet équipement nous avons aménagé à l'intérieur de la cellule une cuve permettant de placer les montages à tester dans l'hélium, sous une pression de 35 kg/cm^2 pendant 24 h ou 48 h.

Résultats

Cet équipement ne permet pas de détecter les fuites avec la même sensibilité que les dispositifs à ressuage d'hélium couramment utilisés pour tester les éléments combustibles avant utilisation dans les réacteurs.

Il permet avant tout de localiser le défaut. La possibilité de détecter les fuites est liée à un ensemble de facteurs qui favorisent ou non la sortie du gaz contenu dans le montage:

- surface de la fuite,
- forme de la fuite,
- pression résiduelle des gaz à l'intérieur du montage,
- liquide utilisé.

Jusqu'à ce jour, nous avons pu localiser les défauts de tous les montages ayant donné un signal DRG au cours de l'irradiation.

2. Autre modèle

Un nouveau modèle d'appareil (fig. 4) pouvant basculer à l'horizontale permet dès le début de l'opération de pompage, et lorsque l'on commence à voir apparaître les bulles de fuite, de placer le barreau dans la meilleure position pour l'observation. Les bulles dues au dégagement de surface ne brouillent plus l'émission détectée.

III. APPAREILLAGE D'OBSERVATION

1. Périscope binoculaire SRPI (fig. 5)

But

Observation et photographie des matériaux radioactifs à l'intérieur des cellules.

Description générale

Ce périscope se compose de trois tubes:

- le premier, situé dans la cellule, peut être placé soit horizontalement (grossissement 2 ou 4), soit verticalement (grossissement 7 ou 14);

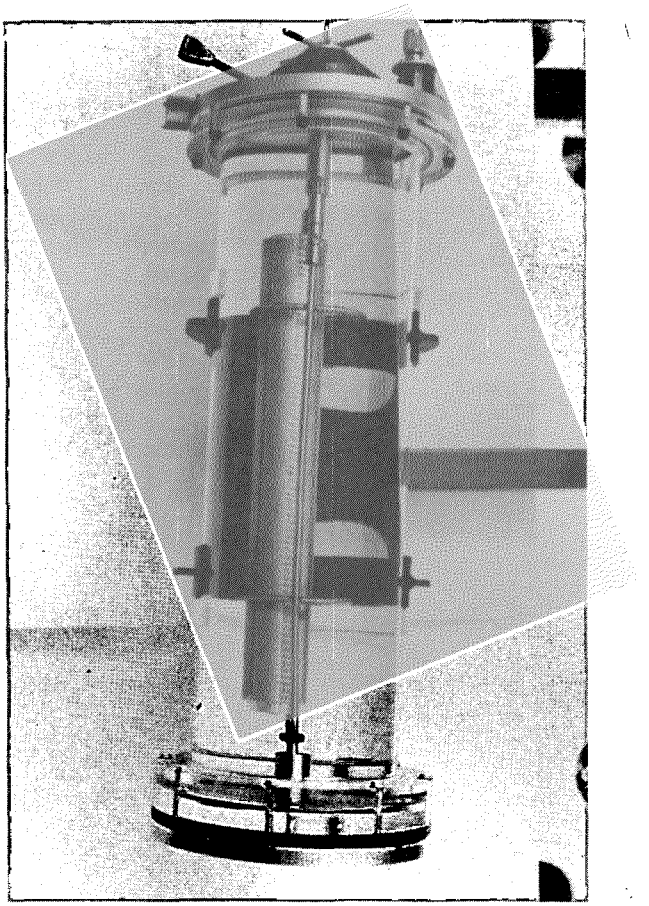

Figure 4

Test d'étanchéité de cartouche basculante.

- le deuxième est horizontal et traverse la paroi de protection à environ 2,60 m du sol;
- le troisième est vertical, à l'extérieur de la cellule. Il porte à la partie inférieure les diverses commandes et le dispositif photographique.

Emploi en observation visuelle

La vision binoculaire est obtenue par dédoublement du faisceau lumineux à l'aide d'un prisme semi-transparent. L'écartement des oculaires est réglable. La mise au point est obtenue par le déplacement d'une lentille située dans le tube extérieur. Un micromètre comportant une graduation millimétrique (champ: 38 mm) est placé dans le plan d'une image réelle, située dans le tube horizontal. Pour que le micromètre et l'image soient à la même échelle, il est nécessaire que le tube intérieur soit vertical. Pour obtenir les quatre grossissements, il faut utiliser deux jeux d'oculaires.

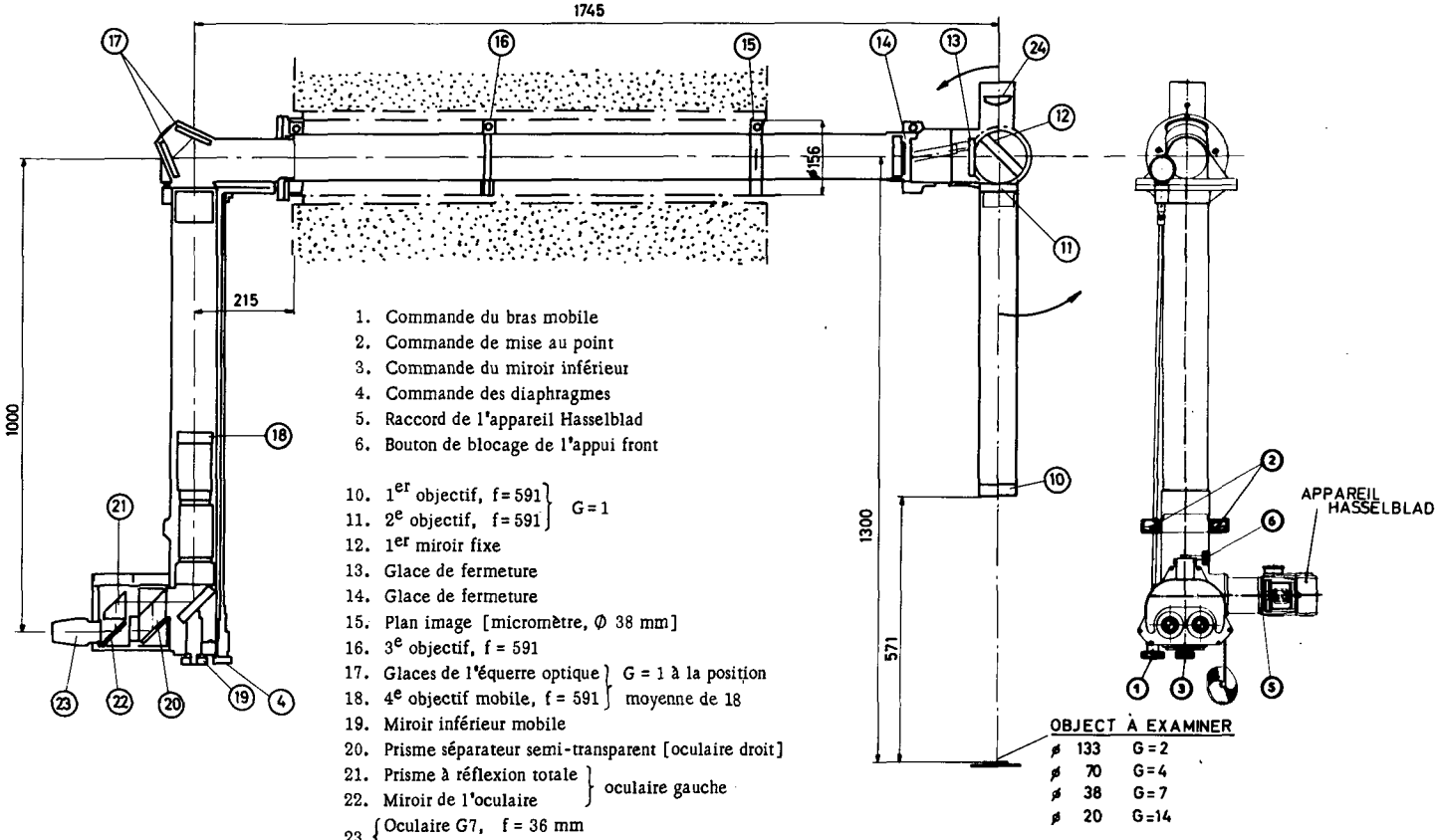

1. Commande du bras mobile
2. Commande de mise au point
3. Commande du miroir inférieur
4. Commande des diaphragmes
5. Raccord de l'appareil Hasselblad
6. Bouton de blocage de l'appui front

10. 1er objectif, f = 591
11. 2e objectif, f = 591
    } G = 1
12. 1er miroir fixe
13. Glace de fermeture
14. Glace de fermeture
15. Plan image [micromètre, Ø 38 mm]
16. 3e objectif, f = 591
17. Glaces de l'équerre optique
18. 4e objectif mobile, f = 591
    } G = 1 à la position moyenne de 18
19. Miroir inférieur mobile
20. Prisme séparateur semi-transparent [oculaire droit]
21. Prisme à réflexion totale
22. Miroir de l'oculaire
    } oculaire gauche
23. Oculaire G7, f = 36 mm
    Oculaire G14, f = 18 mm
24. Objectif G 1/3,5, f = 312 mm

Figure 5

Périscope binoculaire SRPI pour cellules à haute énergie radioactive.

	1er tube horizontal	1er tube vertical
1er jeu d'oculaires	grossissement 2	grossissement 7
2e jeu d'oculaires	" 4	" 14

Remarque: Si l'on observe simultanément le micromètre et l'objet lorsque le tube intérieur est horizontal, l'image et le micromètre sont dans le rapport 1/3,5.

Le champ et le diamètre de l'anneau oculaire correspondant à chaque grossissement sont les suivants:

grossissement	2	4	7	14
champ en mm	133	70	38	20
diamètre de l'anneau oculaire	4,2	2,1	4,2	2,1

Emploi en photographie

Le périscope est prévu pour recevoir une chambre photographique Hasselblad 6×6 réflex type 500c sur la partie inférieure droite du tube extérieur. Au niveau des oculaires, un miroir mobile permet de diriger les rayons lumineux soit vers les oculaires, soit vers la chambre photographique.

Lorsque le tube intérieur est vertical, la photographie de l'objet est à l'échelle 1. S'il est horizontal, l'image de la pièce est diminuée dans le rapport 1/3,5.

Pour faire varier la profondeur de champ, on a prévu cinq diaphragmes commandés par un bouton situé à la base du tube extérieur, ayant des diamètres de 1, 2, 3, 4 et 7 cm respectivement. Les profondeurs de champ obtenues sont 6, 3, 2, 1,5, et 1 mm respectivement, pour G = 1; et 72, 36, 24, 18 et 12 mm respectivement, pour G = 1/3,5.

2. Périscope stéréoscopique MONE

L'appareil est constitué par deux chemins optiques parallèles traversant le mur de la cellule. Il n'y a pas de coude dans le parcours. Les yeux de l'observateur sont protégés des rayonnements gamma par un jeu de deux chicanes avec prismes et une protection en plomb entre les chicanes.

A l'intérieur de la cellule, un miroir et un prisme sur chaque tube reportent l'axe de visée des objectifs à un écartement de 180 mm.

Du côté de l'observateur une disposition semblable amène les axes optiques dans les deux oculaires d'un appareil ZOOM à grossissement continu de 6 à 24. Au grossissement 6, le champ d'observation est de 20 mm de diamètre. La distance optimale entre l'objet et les objectifs est de 400 mm. Un appareil photographique stéréo permet de prendre un couple de photos.

IV. OUTILLAGE DE MÉTROLOGIE

1. Banc de mesure d'éléments gainés à ailettes (fig. 6)

Il est destiné à relever le profil dans le fond des ailettes, le long d'une génératrice du barreau. Le barreau est maintenu dans deux mandrins qui

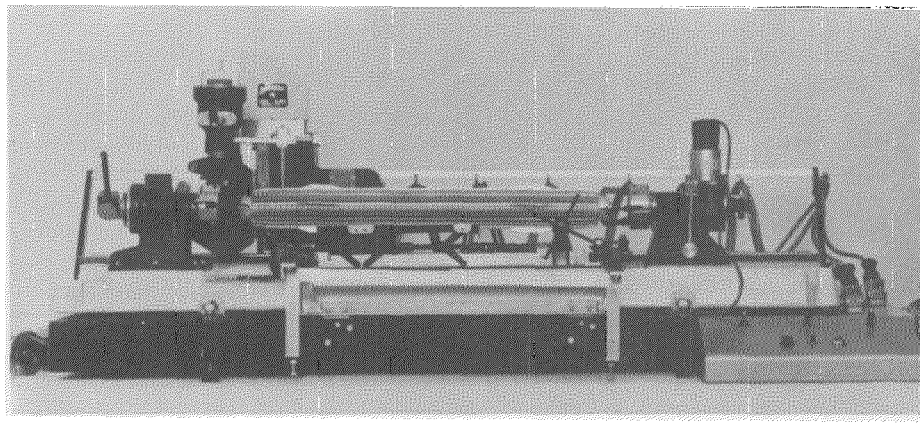

Figure 6

Banc de mesure pour élément gainé à ailettes.

matérialisent l'axe de référence. Parallèlement à celui-ci, un équipage mobile se déplace en entraînant un bras «porte-stylet». Ce bras est articulé dans deux plans suivant deux axes perpendiculaires (horizontal et vertical). Le stylet suit le profil du fond d'ailettes et fait osciller le bras suivant les deux axes. Les mouvements sont captés par deux goniographes qui transmettent les valeurs aux enregistreurs.

Dans le déplacement de l'équipage, la mesure de translation est donnée en comptant le nombre de tours de la vis de précision qui l'entraîne. Ce compteur asservit le déroulement du papier des enregistreurs. On obtient ainsi le relevé en X, Y, Z du profil.

Précision obtenue: en long ± 0,03 mm pour 800 mm;
en X et Y: ± 0,01 m.

2. *Banc de mesure de l'épaisseur de barreaux tubulaires (fig. 7)*

Après dégainage et ouverture des extrémités d'un barreau tubulaire, on veut mesurer les déformations et variations de l'épaisseur suivant une génératrice.

Le barreau est fixé verticalement sur un support. Au-dessous de celui-ci, un châssis porte une glissière sur laquelle se déplace verticalement un équipage de mesure. Cet équipage est constitué par deux tiges légèrement plus longues que le barreau. Celles-ci pivotent à leur base d'un angle faible autour de la verticale. L'extrémité supérieure des tiges est munie d'un stylet en carbure.

L'équipage est placé en position haute, une tige à l'intérieur du tube, l'autre à l'extérieur et dépassant le niveau supérieur du tube.

Dans cette position, on procède à l'étalonnage en plaçant un calibre entre les deux stylets. On descend alors lentement l'équipage. Les stylets suivent les profils intérieur et extérieur, car les deux tiges appuient légèrement sur la génératrice du barreau grâce à un ressort. Les mouvements d'oscillation des tiges sont enregistrés par un compteur à induction et transmis à un en-

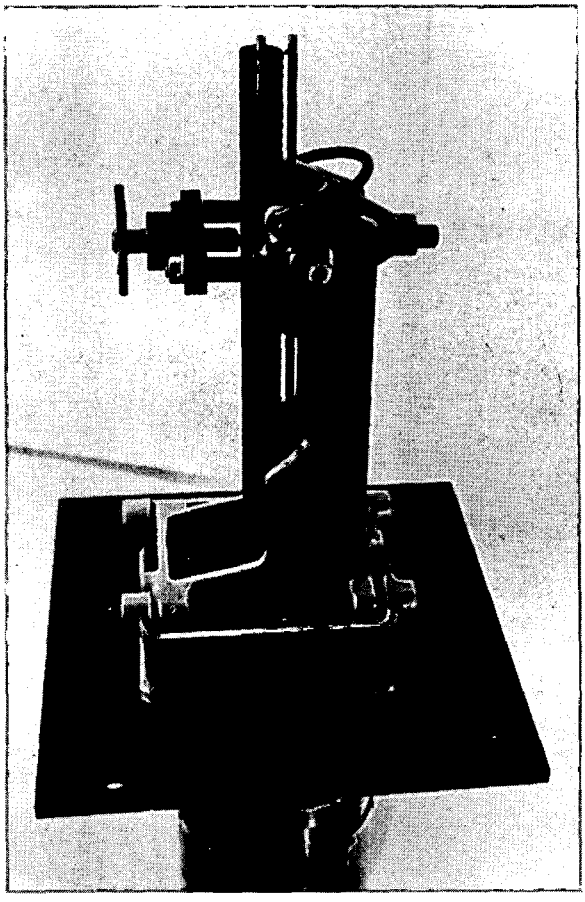

Figure 7

Banc de mesure d'épaisseur de barreau.

registreur. Le déroulement du papier de l'enregistreur est lui-même asservi à la vitesse de descente de l'équipage de mesure.

Précision obtenue = en long: ± 0,2 mm;
en épaisseur: ± 0,01 mm.

3. *Banc de métrologie pour les gros éléments combustibles dégainés et les grappes (fig. 8)*

a) Principe de la mesure

On mesure une dimension de l'élément placé horizontalement entre les palpeurs de deux comparateurs opposés dont les axes horizontaux sont confondus, puis on la compare à la mesure d'une pige de dimension connue.

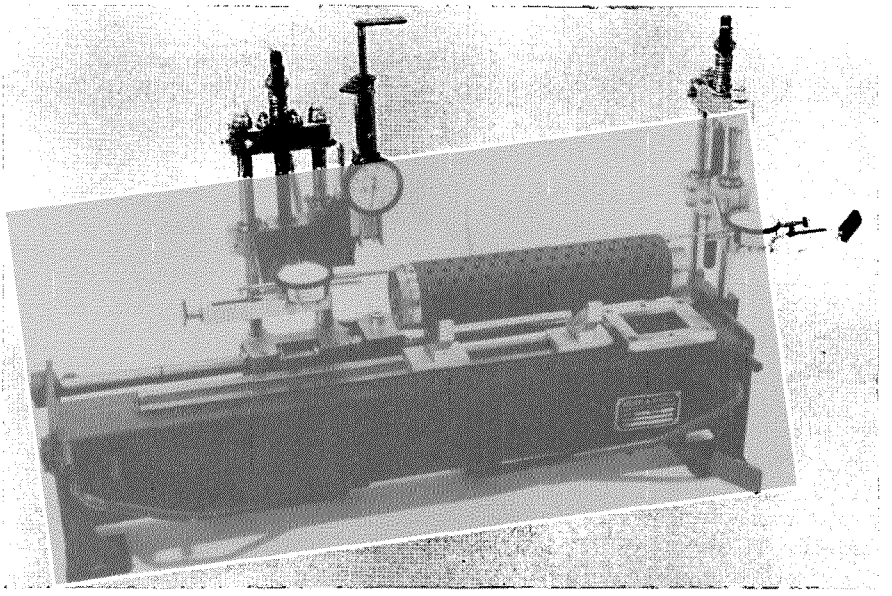

Figure 8

Banc de mesure pour gros éléments.

Nous préférons utiliser deux comparateurs opposés plutôt qu'un seul comparateur et une surface de référence pour les mesures de longueur et de diamètre, pour les raisons suivantes:

- Dans le premier cas nous savons exactement entre quels points s'effectue la mesure.
- Dans le deuxième cas, nous ignorons quel est le point en contact avec la surface de référence. De plus, si la surface de l'élément qui repose sur les vis-supports est rugueuse, nous ne sommes pas sûrs d'avoir un bon contact entre l'élément combustible et la surface de référence.

Les comparateurs sont de grande dimension, leur lecture est facile à travers un hublot de cellule.

b) Composition du banc

Le banc comprend une poutre horizontale ayant une rainure à la partie supérieure dans laquelle reposent et coulissent les vis-supports. A une extrémité se situe un guidage vertical permettant de monter et descendre un comparateur. Derrière le banc, sur un guidage horizontal parallèle à la rainure, se déplace un chariot. Ce dernier porte sur un guidage vertical deux comparateurs, l'un horizontal, l'autre vertical. A la base du guidage vertical fixe se situe un logement pyramidal qui permet de placer, soit un bras support horizontal perpendiculaire à l'axe du banc, soit une surface de référence verticale.

c) Possibilités de ce banc de mesure
- Mesure de longueur d'un élément entre deux points situés sur une même horizontale.
- Mesure de la planéité de l'extrémité d'un élément (pastille ou bouchon).
- Détermination de l'équerrage de l'extrémité des grappes du type EL4 en utilisant la surface de référence verticale. Nous sommes ainsi assurés, lorsque la grappe appuie contre la surface de référence, que chaque point reste dans un plan vertical lorsque la grappe tourne autour de son axe horizontal.
- Mesure des déplacements des crayons sur les grappes du type EL4.
- Mesure de la flèche: L'élément repose horizontalement sur deux vis placées à ses extrémités. Nous plaçons le comparateur vertical en contact avec l'élément dans la section où l'on désire mesurer la flèche. L'élément ayant effectué un tour complet, la moitié du déplacement indiqué par le comparateur représente la flèche.
- Mesure des diamètres: L'élément étant disposé sur le bras support perpendiculaire à l'axe du banc, nous plaçons les deux comparateurs horizontaux dans un plan diamétral.
- Mesure du parallélisme, de la planéité ou de l'épaisseur de certains constituants des éléments combustibles (bouchons de magnésium, pastilles d'aluminium, grilles des grappes).

La pièce à mesurer repose sur un marbre horizontal placé sur la rainure du banc. Les mesures se font à l'aide du comparateur vertical.

DISCUSSION

V.V. GORSKY: The method of checking the hermeticity of fuel elements which you have described is not in my opinion suitable for detecting cracks in the cans of fuel elements in which there are no unfilled spaces. What do you think?

E. ROUSSEL: We have not tested such elements. However, the first attempts at detecting defects by the helium penetrant inspection method, made on fuel elements in which all the space was occupied, gave good results, so there may be grounds for thinking that the hermeticity test can also be applied to elements of the type you mention. Further tests will be necessary to confirm this.

J.C. JANSEN: What voltage were the exposure curves of the selective films drawn for? Do you foresee considerable variations over the voltage range?

E. ROUSSEL: For 80 kV. No, we do not.

J.C. JANSEN: We have noticed that certain selective films showed, with the same total dose, blackening varying with the rate of irradiation (in r/min). Do the new films you have mentioned show any improvement in this respect?

E. ROUSSEL: This particular point does not arise, because of the way we use the films. I think these are defects which should disappear as the films are perfected.

D. BALLARD: For wall-thickness measurements, were the feelers part of a hydraulic, mechanical dial indicator, or of an electromagnetic system?

E. ROUSSEL: An electromagnetic system.

D. BALLARD: Have you attempted to use helium mass spectrometry after the high-pressure testing with helium penetration?

E. ROUSSEL: Not yet. We want above all to localize the defect.

R.S. SHARPE: We have also been working with British film manufacturers on the supply of experimental emulsions for "hot radiography". Have you any information on how these special characteristics are achieved, and whether further improvements can be expected?

E. ROUSSEL: We cannot yet give the characteristics of these films, as they are still a trade secret. I gather from my conversations with senior members of the Kodak Laboratory that the limit of the films has not yet been reached.

G.H. TENNEY: The emulsion sensitivity during the first moments of exposure is indeed a function of the radiation intensity if no additives to the emulsion are used. EK films which are not sensitive to this phenomenon are at present on the market in the USA.

The bubble technique is, I think, not satisfactory for determining the size of cracks in porous materials. I should be interested to know the standards used in this test.

E. ROUSSEL: I stated in my oral presentation that this test does not allow determination of the area or importance of the defect in the cladding. I simply expressed the wish that this test should be used in conjunction with helium penetrant inspection. I also said that the best procedure is to localize the defect by this test, and to study it by micrographic analysis.

P. BONNET: Could you tell me your cycle of operations when dealing with the EL4 cluster? I dot not imagine you perform radiography of the cluster.

E. ROUSSEL: We begin with visual inspection, followed by measurement, and finally by radiography of the pencils if we feel it is necessary. We never perform radiography of the whole cluster, since the overlapping of the pencils on the photograph would make analysis considerably more difficult.

THE APPLICATION OF NON-DESTRUCTIVE TECHNIQUES IN THE QUALITY CONTROL INSPECTION AND TESTING OF FUEL MATERIALS FOR THE DRAGON REACTOR EXPERIMENT

J.F.G. CONDÉ, R. POINTUD, J. HOLLIDAY AND P.D. GOOD
A.E.E. WINFRITH, DORCHESTER, DORSET, ENGLAND

Abstract — Résumé — Аннотация — Resumen

THE APPLICATION OF NON-DESTRUCTIVE TECHNIQUES IN THE QUALITY CONTROL INSPECTION AND TESTING OF FUEL MATERIALS FOR THE DRAGON REACTOR EXPERIMENT. The O.E.C.D. high-temperature gas-cooled reactor experiment, Dragon, is graphite-moderated and helium-cooled and employs fission product-retaining fuel of the coated-particle type. The development and use of this new type of fuel have required the application of a variety of non-destructive techniques for quality control, inspection and testing. This paper describes certain of the methods which are employed in the inspection of fuel materials both in the development phase and subsequently in production. Physical methods of analysis are used for control of the chemical analysis of fuel cartridges and assessment of fuel contamination of fuel-particle coatings, and particular gamma spectrometric and alpha-scintillation counting techniques are described. The general quality of coated particles is assessed and metrology of coatings performed by means of micro-radiography with the X-ray projection microscope; the procedure is outlined and typical results are presented. Fuel cartridges which consist of fuel particles in a graphite matrix are inspected for homogeneity of fuel distribution and freedom from defects by fluoroscopy and panoramic slit-scanning radiography. Colour radiography is also employed to a limited extent and the various techniques are presented together with illustrative examples of the results obtained. The fuel elements are fabricated almost entirely from various grades of graphite, and eddy-current non-destructive testing techniques are being developed to permit inspection of raw materials and finished machined components for freedom from significant defects. A brief description of these techniques is given.

APPLICATION DES MÉTHODES NON DESTRUCTIVES AU CONTRÔLE DE LA QUALITÉ A L'INSPECTION ET A L'ESSAI DES COMBUSTIBLES DESTINÉS AU RÉACTEUR EXPÉRIMENTAL DRAGON. Le réacteur expérimental Dragon de l'OCDE est un réacteur à haute température, ralenti au graphite et refroidi à l'hélium, qui utilise un combustible en capsule retenant bien les produits de fission. La mise au point et l'utilisation de ce nouveau type de combustible ont impliqué le recours à toute une gamme de méthodes non destructives pour le contrôle de la qualité, l'inspection et les essais. Le mémoire décrit certaines des méthodes appliquées dans l'inspection du combustible, tant dans la phase de mise au point que dans celle de la production. Des méthodes physiques d'analyse permettent de vérifier l'analyse chimique des cartouches de combustible et d'evaluer la contamination des capsules de combustible par les produits de fission retenus; les auteurs décrivent des méthodes spéciales de spectrométrie gamma et de scintillation alpha. La microradiographie au moyen du microscope à rayons X permet d'évaluer la qualité générale des particules encapsulées et de faire la métrologie des capsules; les auteurs expliquent la procédure et présentent des résultats caractéristiques. Les cartouches de combustible, composées de particules sous capsule enrobées dans une matrice en graphite, sont inspectées par fluoroscopie et radiographie panoramique pour déterminer l'homogénéité de la distribution du combustible et l'absence de défauts. La radiographie en couleur est également utilisée dans une mesure limitée; les auteurs décrivent les diverses techniques et donnent des exemples qui illustrent les résultats obtenus. Les cartouches de combustible sont faites presque entièrement en graphite de diverses qualités; on met au point des méthodes non destructives, fondées sur les courants de Foucault, pour contrôler l'absence de défauts dans les matières premières et les pièces fabriquées; les auteurs donnent une brève description de ces méthodes.

ПРИМЕНЕНИЕ МЕТОДА НЕДЕСТРУКТИВНОГО АНАЛИЗА ДЛЯ ПРОВЕРКИ КАЧЕСТВА ТОПЛИВНЫХ ЭЛЕМЕНТОВ ДЛЯ ПРОВЕДЕНИЯ ЭКСПЕРИМЕНТОВ НА РЕАКТОРЕ "ДРАГОН". Высокотемпературный реактор "Драгон" с газовым охлаждением, представляет собой реактор с графитовым замедлителем и гелиевым теплоносителем, который использует топли-

во, удерживающее продукты деления, в виде отдельных частиц с покрытием. Разработка и использование этого нового вида топлива потребовали применения различных методов контроля качества и испытания материалов без их разрушения.

Описываются некоторые методы, которые использованы при инспекции топливных материалов в фазе разработки и в производстве. Используются физические методы анализа для контроля химического анализа тепловыделяющих элементов и для оценки загрязнения покрытия топливных частиц, описываются конкретные гамма-спектрометрические и альфа-сцинтилляционные методы счета. Производится оценка общего качества покрытых частиц и осуществлена метрология покрытий с помощью микрорадиографии, с использованием рентгеновского проекционного микроскопа; излагается процедура, представлены типичные результаты. Тепловыделяющие элементы, которые состоят из топливных частиц в графитовых матрицах, подвергаются проверке в отношении гомогентности распределения топлива и свободы от дефектов с помощью флюроскопии и панорамной щелевидной радиографии развертывания. Применяется также цветная радиография в ограниченной степени, представлены различные методы вместе с помощью флюроскопии и панорамной щелевидной радиографии развертывания. Применяется также цветная радиография в ограниченной степени, представлены различные методы вместе с иллюстративными примерами полученных результатов. Топливные элементы изготовляются из различных сортов графита, разрабатываются методы недеструктивного контроля, чтобы дать возможность контролировать строительные материалы и производить проверку механических компонентов с целью выявления значительных дефектов. Дается краткое описание этих методов.

APLICACION DE TECNICAS NO DESTRUCTIVAS AL CONTROL DE CALIDAD, INSPECCION Y ENSAYO DE COMBUSTIBLES DESTINADOS AL REACTOR EXPERIMENTAL DRAGON. El reactor experimental Dragon, de la OCFE, de alta temperatura y refrigerado por gas, utiliza grafito como moderador, helio como refrigerante y partículas combustibles con revestimiento para retener los productos de fisión. El desarrollo y uso de este nuevo tipo de combustible exigió aplicar diversas técnicas no destructivas para proceder al control de calidad, inspección y ensayo. El presente trabajo describe algunos métodos empleados para inspeccionar materiales combustibles, tanto en la etapa de desarrollo como en la subsiguiente de producción. Se emplean métodos físicos para verificar los resultados del análisis químico de los elementos combustibles y evaluar la contaminación sufrida por el revestimiento de las partículas de combustible; se describen técnicas especiales de espectrometría gamma y métodos para recuento de partículas alfa por centelleo. Se evalúa la calidad general de las partículas revestidas y se mide el espesor de los revestimientos mediante microrradiografía en el microscopio de proyección de rayos X; se describe el procedimiento en líneas generales y se presentan algunos resultados característicos. Empleando fluoroscopia y radiografía con exploración mediante colimador panorámico, se verifican la homogeneidad de la distribución del combustible y la ausencia de defectos en elementos formados por partículas de combustible en una matriz de grafito. Se emplea también, en grado limitado, la radiografía cromática; las diversas técnicas se presentan juntas, con ejemplos ilustrativos de los resultados obtenidos. Los elementos combustibles se fabrican casi totalmente con diversas calidades de grafito; se desarrollan en la actualidad técnicas no destructivas de ensayo con corrientes de Foucault, a fin de inspeccionar las materias primas y los componentes terminados, y verificar la ausencia de defectos importantes. Se presenta una breve descripción de estas técnicas.

1. INTRODUCTION

The Dragon Reactor Experiment is a 20-MW high-temperature gas-cooled reactor and has been constructed as a joint O. E. C. D. Project at the U. K. A. E. A., Atomic Energy Establishment, Winfrith, Dorset, England. The reactor is graphite moderated and helium cooled; graphite is also used for the structural and cladding material of the fuel elements.

The fuel for the reactor is in the form of carbide and the core is homogeneous, both the fuel and moderator being incorporated in the fuel elements. The fuel elements are designed so that the whole core, including the graphite moderator and the top and bottom reflectors is removable and is replaced when the fuel is changed.

In the initital design concept of Dragon it was anticipated that the fuel would release a significant proportion of its fission products and the fuel elements would have a purge system to remove fission products from inside the fuel rods. The original objective of the purge system was to de-poison the fuel and to maintain the activity in the coolant circuit at an acceptable level. The fuel elements are also suitable for testing fission-product-retaining fuels and the rapid development of coated particle fuels of this type both within the Project laboratories and elsewhere has led to the use of these fuels for the first core of the reactor.

The reactor charge consists of 37 fuel elements of the type shown in Fig. 1. Each of the elements consists of 7 fuelled rods, the rods being of tubular form and machined from low permeability graphite. The fuelled portion of each rod is 1600 mm (63 in) long and the fuel is contained in 30 cartridges each a right hollow cylinder approximately 53.5 mm (2.1 in) × 44 min (1.7 in) outer diameter × 23 mm (0.9 in) bore.

The fuel is in the form of approximately spherical coated particles of 500 to 700 μm total diameter including the coating which is about 100 μm thick. The fuel elements are arranged within the reactor to form a two-zone core, the inner zone being fuelled with thorium/uranium carbide (Th/U ratio 10 : 1 by atoms) and the outer annular zone with zirconium/uranium carbide (Zr/U ratio 8 : 1 by atoms).

The fuel particles are manufactured by a powder metallurgical process giving sintered kernels of controlled density and approximate sphericity. The coating for fission-product retention is applied by a fluidized bed process. The zirconium-containing fuel is coated with a multi-layer pyrolytic carbon coating and the thorium fuel with a triplex pyrocarbon, silicon carbide, pyrocarbon coating. The coated particles are incorporated into a matrix consisting substantially of graphite by mixing and warm pressing in a die. The resulting cartridges are then heat-treated and out-gassed by high-temperature vacuum treatment.

The development and use of coated-particle fuel materials have required the evolution and application of a variety of non-destructive techniques for quality control, inspection and testing. This paper describes briefly certain of the methods which are used in the evaluation of fuel materials both in the development phase and subsequently in production for the reactor fuel elements.

2. PHYSICAL METHODS OF FUEL ASSAY

2.1. Gamma-spectrometric analysis

2.1.1. General

Physics requirements for the fuel loading of the Dragon reactor limited variations in the U^{235} content of the fuel to ± 5% from the theoretical values. Furthermore, the rate of fuel production required at least three uranium analyses per day for purposes of process control and fissile material movement. The radiometric method which is easy, rapid and non-destructive and of sufficient accuracy for the physics requirements has been applied.

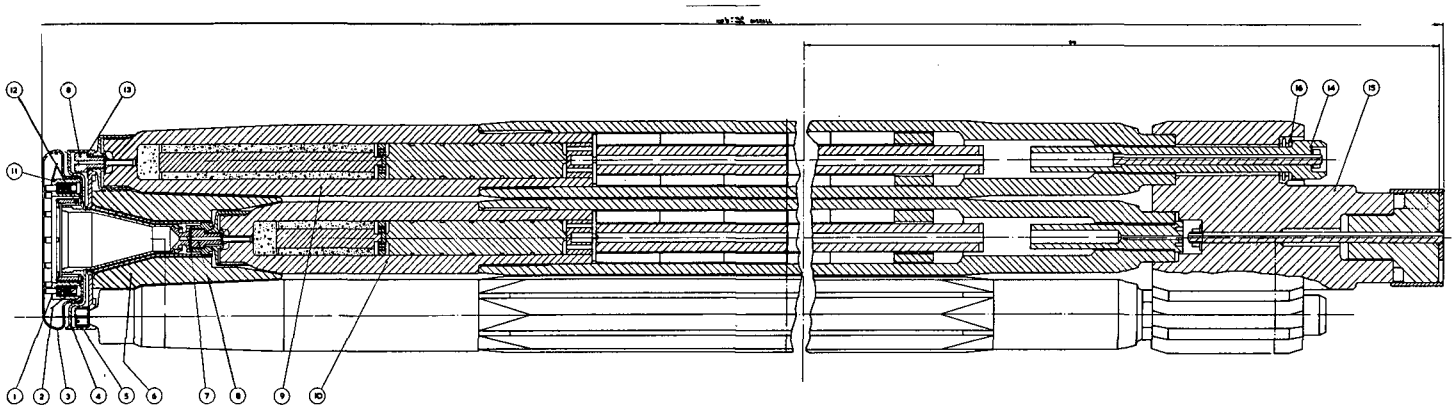

Fig.1

Fuel element for the Dragon reactor

1. Nut
2. Spacer
3. Guard
4. Inner Core Assembly
5. Outer Core Assembly
6. Fairing
7. Locker Tab Washer
8. Hollow Screw
9. Outer Fuel Rod Assembly
10. Centre Fuel Rod Assembly
11. Thermocouple Connector Type 'A' - Upper
12. Locking Sleeve
13. Locking Washer
14. Fuel Tube Bolt Subassembly
15. Top Block Subassembly
16. Bellows

2.1.2. Basis of method

A typical composition of a 93%-enriched uranium is as follows:

U^{235} = 93%; U^{238} = 5.5%; U^{234} = 1.2%; U^{236} = 0.25%; and $U^{232} = 5 \times 10^{-7}$%.

The examination of the gamma-ray spectra of the different uranium isotopes, taking into account their relative proportions, shows that U^{235} is the main source of gamma radiation, particularly at the 184-keV energy level. Even if thorium is mixed with the enriched uranium up to an atomic ratio $Th/U^{235} = 10$, there is no significant interference with the 184-keV photopeak of U^{235} and this has been used to measure the uranium content of the samples.

2.1.3. Method of measurement

The gamma detector (Fig. 2) is a counting assembly consisting of a 44.5-mm × 50-mm NaI (Tl) crystal and photomultiplier tube feeding a type-1430A amplifier followed by a single-channel pulse-height analyser, type 1168B. A Honeywell-Brown recorder, type 1387A, enables the complete spectrum to be plotted and a selection of the required photopeak. Figures 3 and 4 show respectively typical spectra obtained on an enriched uranium and a thorium sample.

A timer-type 2041 and a scaler-type 2112 allow comparison of the gamma activities in a sample with that of a standard of the same shape, weight and approximately similar composition. These identities between sample and standard avoid the need for corrections for self-absorption and geometrical variations. For analysis the pulse-height analyser is set to (184 ± 15) keV to cover about 68% of the photopeak. Counting times are maintained such that the relative error made in the ratio of the gamma activity of the sample to the gamma activity of the standard is less than 1.5% at the 3σ level of confidence.

When testing cartridges, a centralizing jig mounted on top of the NaI crystal ensures accurate positioning. A standard cartridge is tested every 12 cartridges (the test duration for one cartridge being 100 s) to allow for drift of the photopeak due to input voltage and temperature variation effects on the components of the gamma detector.

2.1.4. Precision of method

The results of two series of gamma measurements made seven days apart on the same cartridges are given in Table I. The data indicate that the relative error in comparing the uranium content of the test samples with that of the standard was always less than 1.5%.

However, the actual quantity of U^{235} contained in the standard is known with a relative error of about 1.7% which implies that in the test sample this quantity will be known with a relative error of 3.2% at the 3σ level of confidence. In practice this relative error has been found to be better than 2.5%.

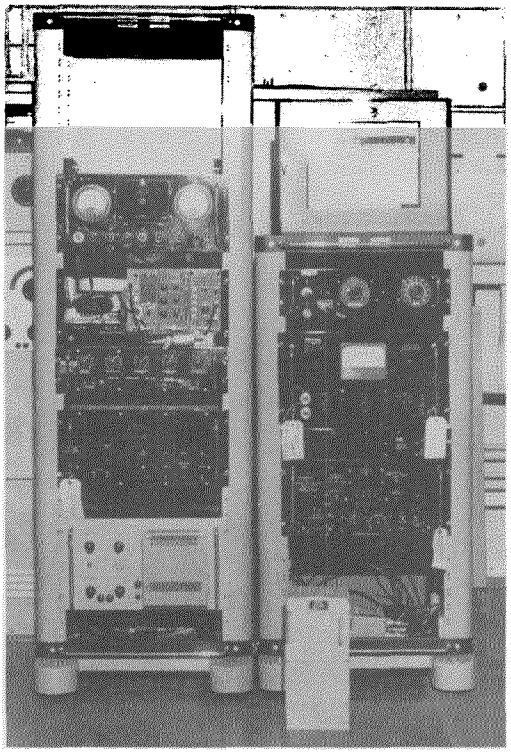

Fig.2

Gamma-spectrometer with lead castle containing sodium iodide crystal and photomultiplier

2.1.5. Extension of the method to thorium

A similar method can be applied for determining the thorium content in samples by using the complex 581-MeV photopeak displayed by Tl^{208}, a daughter product of Th^{232}. However, this method has limitations because of the volatility of the Th^{232} daughter products at high temperatures. Thus, a delay of at least one month after each heat treatment is necessary before any measurements can be made. This delay allows the Tl^{208} to reach its equilibrium activity.

2.2. Alpha scintillation

2.2.1. General

The aim of the coated-particle fuel in the Dragon reactor is to retain fission products. The retention properties of these coated particles can be impaired by the presence of uranium atoms, as impurities, in the pyrolytic coating. It is necessary therefore to detect the level of such pollution.

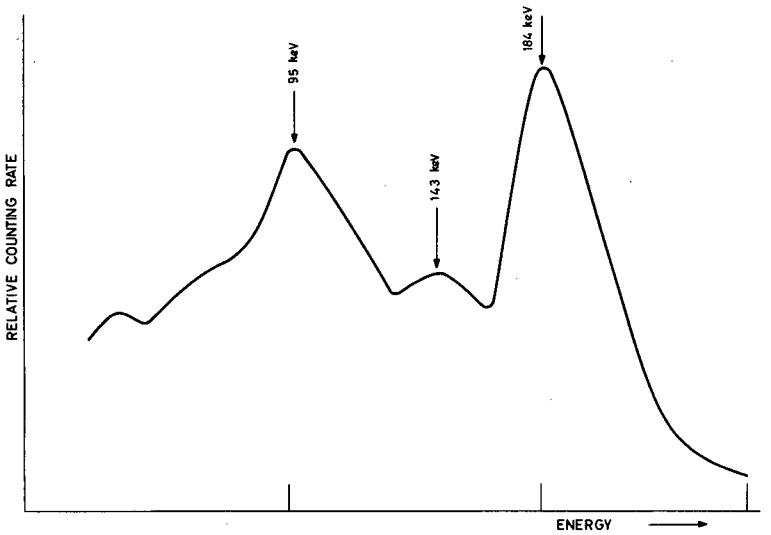

Fig. 3

Gamma-spectrum of enriched uranium (93%)

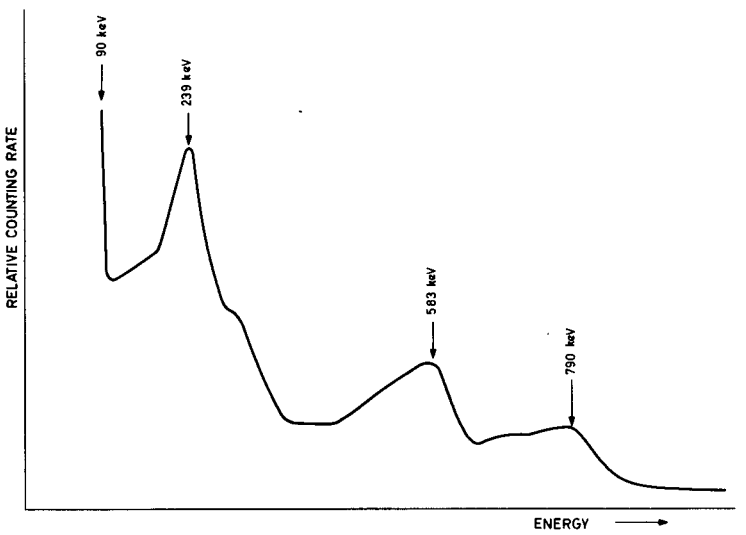

Fig. 4

Gamma-spectrum of thorium

2. 2. 2. Basis of the method

If the 93% enriched uranium composition given in section 2. 1. 3 is considered, it may be seen that 97. 5% of the alpha activity is given by the U^{234} isotope; the remainder being due to U^{235}. Even in a mixture of uranium

and thorium with an atomic ratio $Th/U^{235} = 10$, the contributions of thorium to the alpha activity will vary from 1.3% to 8% according to the ageing of the thorium. Therefore, the alpha activity represents mainly the activity of U^{234} and hence of the enriched uranium as a whole.

In spherical particles the fraction of alpha particles recoiling out of the sphere is given by [1]:

$$F = \frac{3}{4}\left(\frac{\lambda}{r}\right) - \frac{1}{16}\left(\frac{\lambda}{r}\right)^3 ,$$

with

$$\frac{\lambda}{r} < \frac{1}{2}$$

where λ is the range of the alpha particles in the medium constituting the sphere (here pyrocarbon) and r is the radius of the sphere.

The range of alpha particles in pyrocarbon is 3.10 mg/cm^2 for alpha particles of energy 4.70 MeV (corresponding to the U^{234} alpha emission) or about 17 μm for a pyrocarbon of 1.8-g/cm^3 density. Thus the alpha-scintillation test is able to detect alpha particles coming from the outer 15 to 20-μm layer of the pyrocarbon coating. In fact because of self-absorption the main contributions to the alpha activity which is detected will be from surface contamination.

2.2.3. Method of measurement

The alpha detector shown in Fig. 5 is a counting assembly consisting of a ZnS alpha-scintillation counter, type 1588A, followed by an automatic scaler EKCO, type N 530G. A schematic diagram of the equipment is given in Fig. 6. The coated particles are poured into an aluminium sample holder of 2-cm-diam. and 1.5-mm depth. The sample holder is shaken gently and levelled up giving a plane surface of hexagonally ordered spheres. The counting time is kept to 1000 s to record at least 200 to 300 counts and hence decrease the relative statistical error of counting.

2.2.4. Precision of the method

The reproductibility of the counts recorded on the same sample is within the 3σ level of confidence. However, it is not possible to obtain an accurate correlation between the alpha-counts recorded and the actual uranium pollution owing to the fact that the source is very thick and hence it is difficult to account for self-absorption. Accordingly alpha-counting can be used only as a method for comparing the contamination level of different batches of coated particles.

2.2.5. Limitations

When coated particles are treated at high temperature, mobile daughter products of Th^{232} and U^{232} diffuse from the kernel to the pyrocarbon coating

TABLE I

GAMMA-SPECTROMETRIC ANALYSIS OF THE FUEL CARTRIDGES

Cartridge No.	Mean U Content Compared to Standard No. 8	U Content Deviation ±
4413	0.95_3	0.00_3
4430	0.96_2	0.00_2
4431	0.97_0	0.00_1
4432	0.96_8	0.00_4
4444	0.94_9	0.00_3
4447	0.93_3	0.00_2
4450	0.94_6	0.00_3
4455	0.95_5	0.00_4
4459	0.96_8	0.00_3
4460	0.96_7	0.00_7
4461	0.97_2	0.01_3
4462	0.96_8	0.00_1
4463	0.95_3	0.00_0
4464	0.95_4	0.00_6
4465	0.96_1	0.00_1
4466	0.97_5	0.00_7
4467	0.96_9	0.00_4
4469	0.97_2	0.00_6
4470	0.96_6	0.00_4
4471	0.96_9	0.00_4
4472	0.99_0	0.00_4
4473	0.98_9	0.00_1
4474	0.94_8	0.00_2
4475	0.97_8	0.00_6
4476	0.96_4	0.00_0
4477	0.95_4	0.00_5
4478	0.98_1	0.00_2
4479	0.97_2	0.00_1
4480	0.97_3	0.00_5
4481	0.95_6	0.00_3
4482	0.98_1	0.00_1
4483	0.91_1	0.00_1
4484	0.97_1	0.00_1
4485	0.97_1	0.00_0
4486	0.96_8	0.00_2
4487	0.94_9	0.00_1
4488	0.95_0	0.00_1
4489	0.97_0	0.00_3
4490	0.96_8	0.00_4
4491	0.96_0	0.00_4
4492	0.96_1	0.00_5
4493	0.94_3	0.00_1
4494	0.94_1	0.01_1
4495	0.96_1	0.00_7
4496	0.97_3	0.01_1
4497	0.96_8	0.01_3
Maximum permissible scatter	-	0.01_5

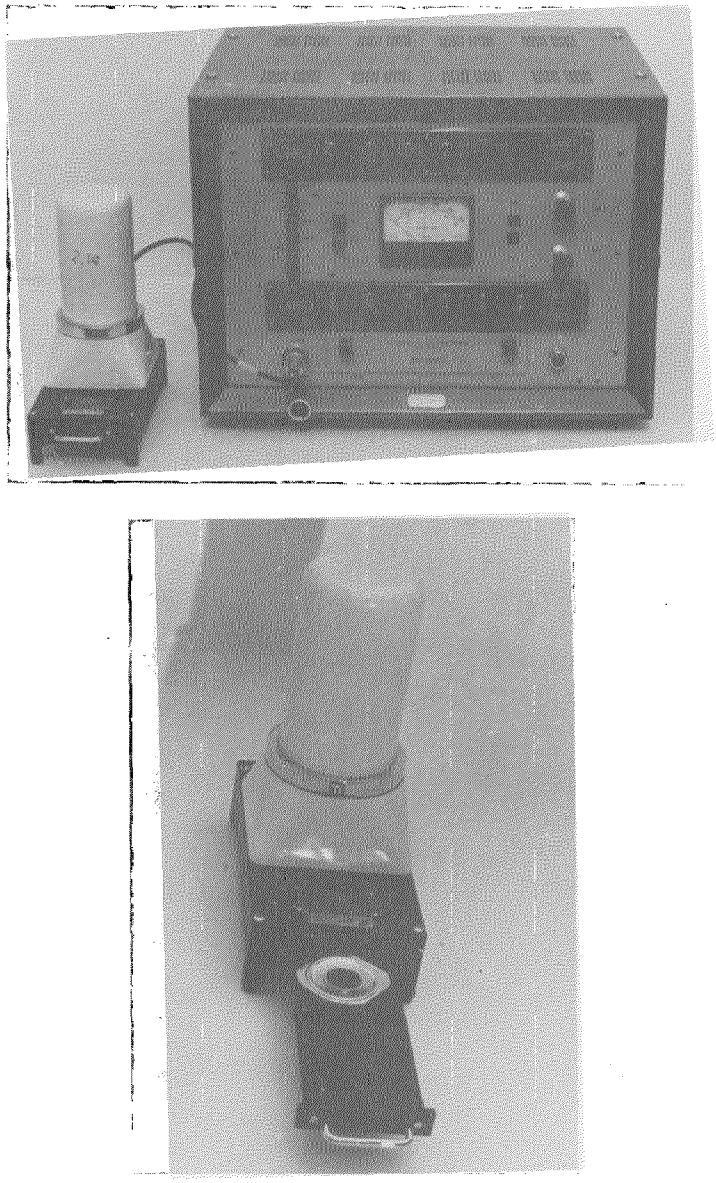

Fig. 5

Alpha scintillation apparatus showing sample in position in drawer

faster than uranium or thorium atoms. The alpha activity detected is therefore mainly due to these daughter products and a delay of at least one month is necessary to detect the true alpha activity due to uranium and thorium pollution. Two decay curves illustrating the effect are shown in Fig. 6.

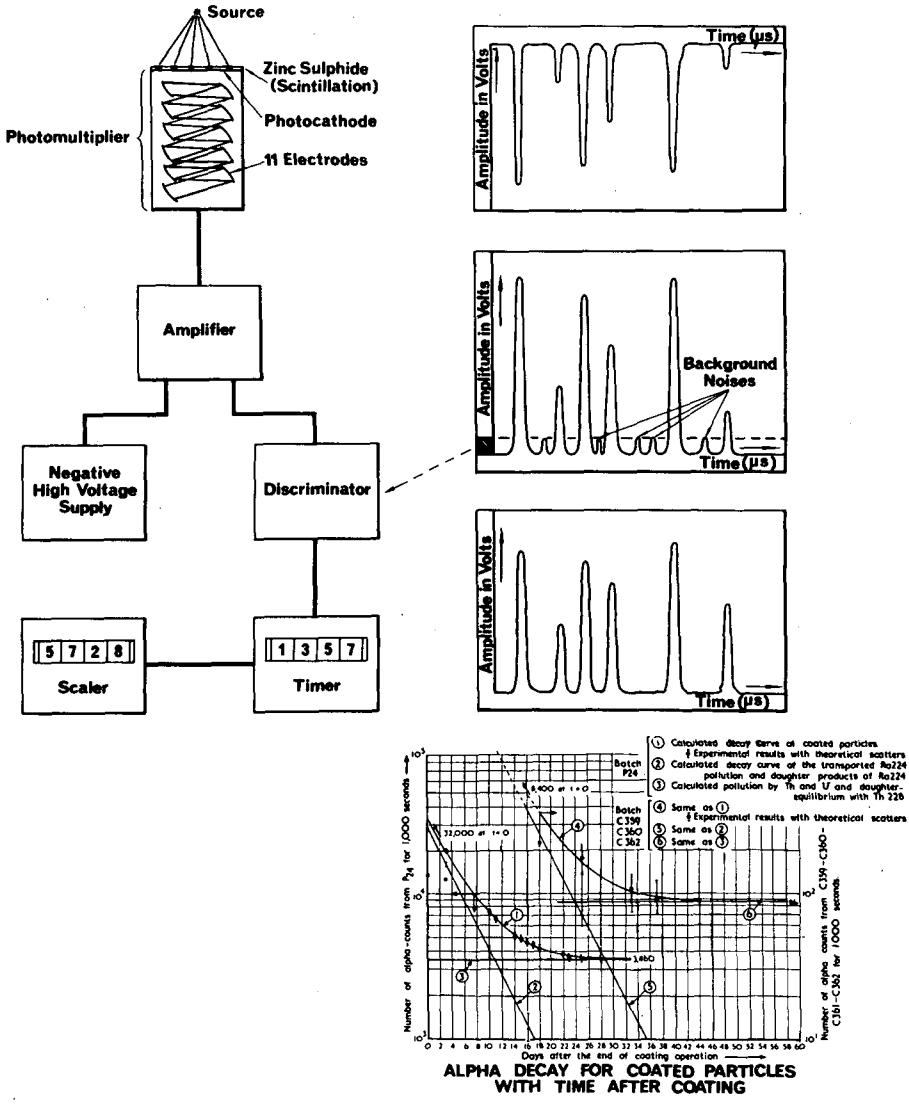

Fig. 6

Estimation of uranium pollution by alpha scintillation

2.3. *Alpha-spectrometry and alpha autoradiography*

Alpha-spectrometry and alpha autoradiography have been used as complementary techniques to enable interpretation of the results of alpha-scintillation counting. Alpha-spectrometry permits the determination of the energy of alpha particles and thus the identification of the atoms undergoing alpha decay. This test has been found useful in the instance of alpha activity due to Th^{232} and U^{232} daughter products.

The alpha spectrum is obtained using a silicon semiconductor as an alpha-radiation detector followed by a hundred-channel analyser. The spectrum obtained from a thin source is shown in Fig. 7 while Fig. 8 illustrates the deformed spectrum of a thick source simulating a coated-particle sample. In spite of a resolution loss it is still possible to separate the alpha activity resulting from U^{232} daughter products.

Alpha autoradiography permits the nature of the pollution, e.g. uranium diffusion, dust pollution, cracked particles etc., to be determined from the patterns obtained from coated particles.

About 2000 particles are laid, in a mono-layer, on an AR-10 Kodak photographic plate and left for a period of days dependent on the alpha activity of the coated particles. Five days are sufficient exposure for an alpha activity corresponding to 120 cpm/g of coated particles.

Examples of the effect produced by dust contamination are shown in Fig. 9.

3. THE INSPECTION AND METROLOGY OF COATED-PARTICLE FUELS BY PROJECTION X-RAY MICROSCOPY

3.1. Description

The X-ray projection microscope provides a quick and precise method for the non-destructive examination of the internal structure of coated particles and metrology of particles, kernels and coatings. A commercial instrument [2], see Fig. 10, based on the COSSLETT and NIXON [3] design is used, and consists of two magnetic lenses which focus a stream of electrons, produced by an electron gun, on to a transmission target. Vacuum pumps maintain a pressure of less than 3×10^{-5} Torr in the microscope column. The electron-beam accelerating potential can be varied from 4.5 to 30 kV, the electron gun being raised or lowered to suit the conditions. The tube current is controlled and can be biased to cut-off by a potential applied to the bias cup of the electron gun.

Samples are placed above the target on 15-μm-thick aluminium holders. A photographic plate is mounted over the sample on a support the height of which, together with the target sample distance, determines the magnification of the image. The plate is surmounted by a lead glass disc to reduce back-scatter, and the whole volume around the target and plate is enclosed in a light-tight lead box which also provides biological shielding.

3.2. Operating conditions

Work on X-ray microscopy of coated particles, by SHARPE at Harwell [4] was carried out using copper targets at 10 kV. This was very suitable for carbon coatings, but radiographs of duplex pyrocarbon-silicon-carbide coatings could not be printed satisfactorily owing to the contrast limitations of photographic paper [4]. To avoid making separate prints to show the two coatings of different densities, it was decided to adopt aluminium targets

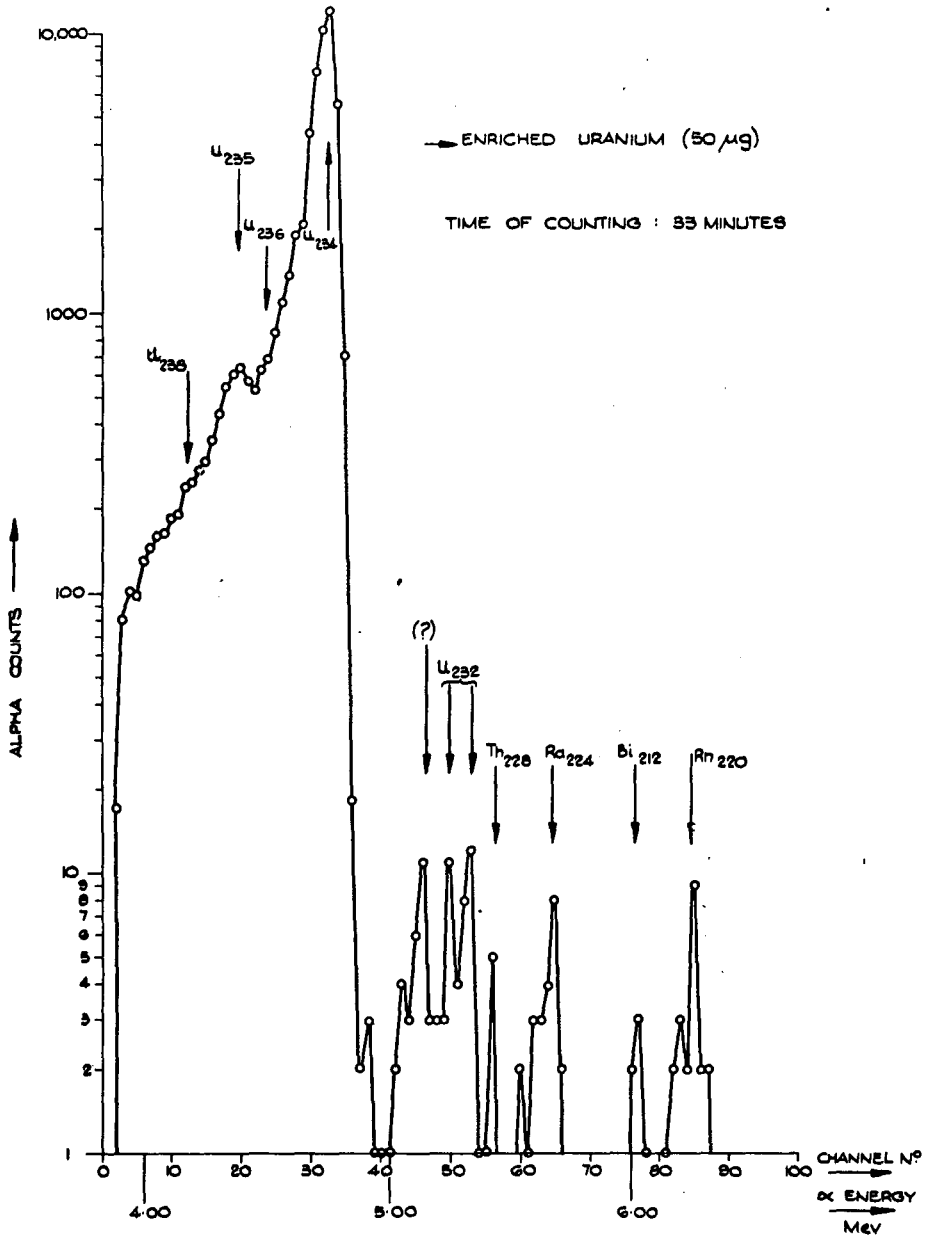

Fig. 7

Alpha-spectrum obtained from thin source

and thereby reduce the density difference in the X-ray negative. Operating at the low tube potential necessary to excite monochromatic aluminium K_α radiation gave rise to exposure times of unacceptable length, and high ab-

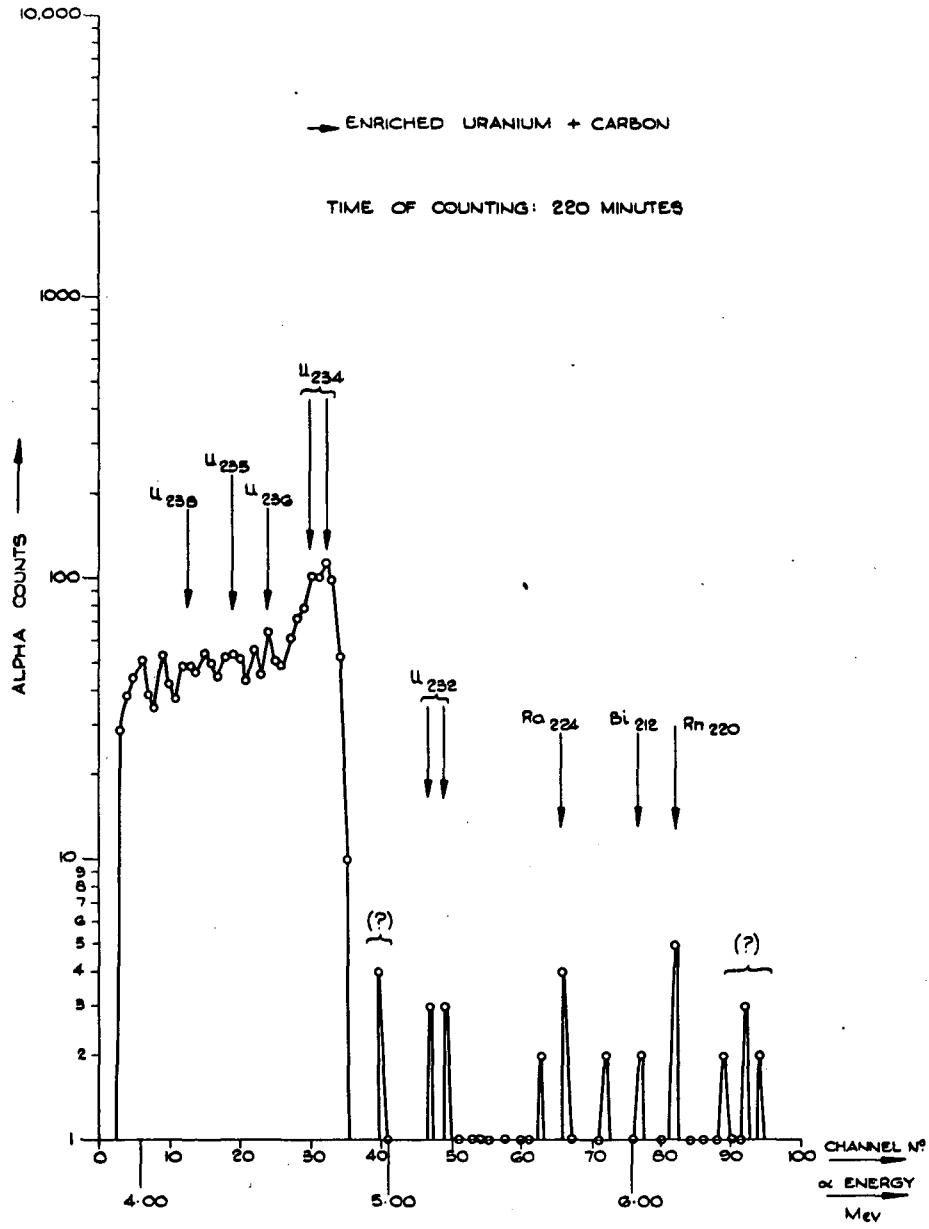

Fig. 8

Alpha spectrum obtained from thick source

sorption of X-rays in air and hence the accelerating potential was increased to 10 or 15 kV according to the subject. As the total magnification of samples rarely exceeds 100X the resulting deterioration in resolution is of little importance.

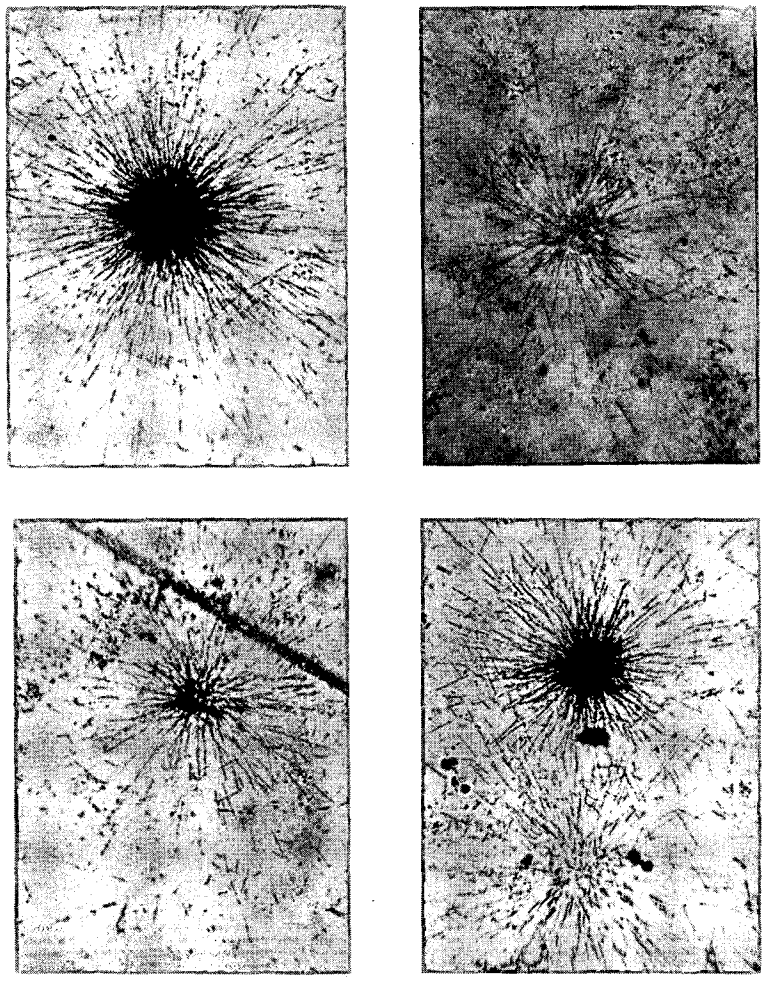

Fig. 9

Autoradiographs showing dust contamination on surfaces of coated particles

The targets are made of 9-μm aluminium foil of 99.2% purity. The sample holders are also made of similar material, and give an even background to the plates. Recently, much thicker silicon-carbide coatings have been deposited, and the tube potential has been increased to 20 kV to reveal the underlying pyrocarbon coatings. In these cases a copper target has been used because the tube potential is close to that necessary to excite the copper K_α radiation, and also to take advantage of the better resolution due to the smaller penetration of electrons in the copper target.

In all work the tube current is maintained at 35 to 40 μA, and with a target-to-photographic-plate distance of 50 mm, the exposures vary between 30 s and 3 min according to the type and thickness of the coatings on the

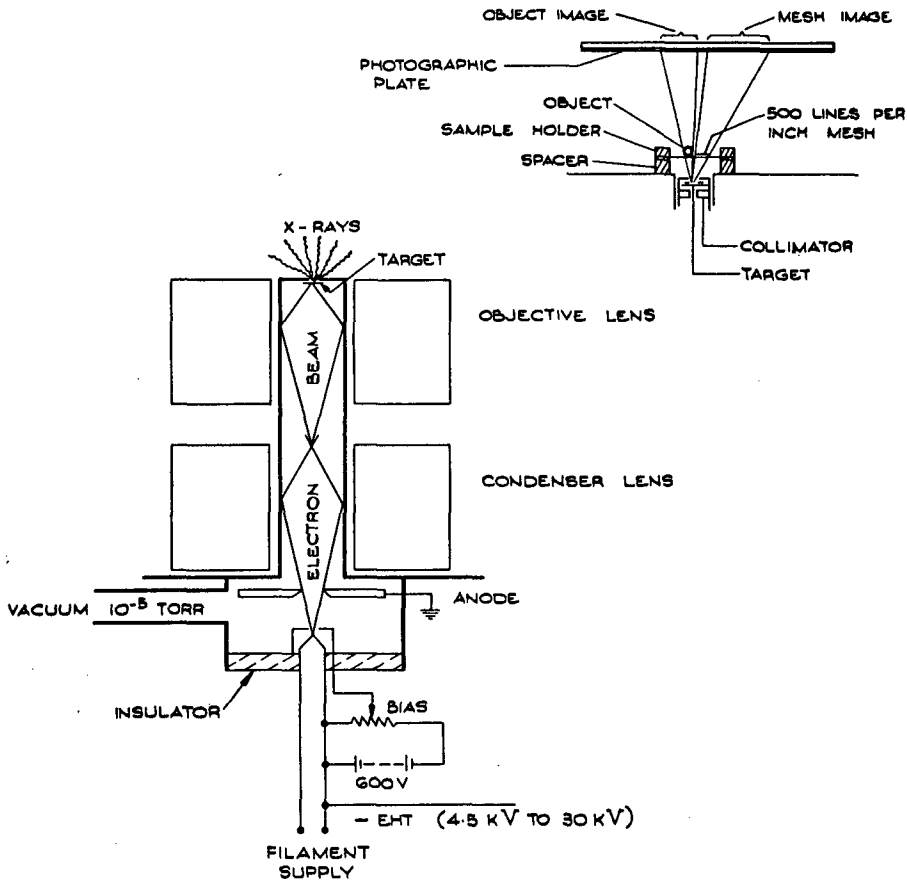

Fig. 10

X-ray projection microscope

fuel particles. The initial magnification is not increased beyond about 14X as this would entail correspondingly longer exposures. It has been the aim to radiograph, process and evaluate a sample within 40 min. It is then possible to check the deposition rate of pyrocarbon in a fluidized bed several times during the coating process. This procedure provides valuable information during proving runs to establish coating parameters.

Radiographs have been recorded on 50-mm-square Ilford Special Contrasty Lantern plates which are developed for one minute in Johnson's F. F. Contrast Developer.

3.3. Metrology of coatings

All sample holders have a strip of 500 lines per inch (20 lines/mm) mesh adhesive bonded to the surface of the aluminium foil. This enables the magnification of the sample to be established. The plates are projected

on to a ground-glass screen at a total magnification of 100X using a conventional slide projector. The magnification is checked by making the image of the 500 lines per inch mesh coincide with graduated marks on a scale calibrated in 0.2 in (5 mm) increments. Measurements of the images on the screen are made with vernier calipers.

Three sources of error must be considered when measuring images of spherical or nearly spherical particles.

(i) Only those particles on the X-ray axis are imaged without distortion, and therefore only these may be measured with any accuracy.

(ii) The image is not of the equatorial plane but of a chord plane of the sphere, unless a large target-object distance is employed.

(iii) Since the equators of the particles are not in the same plane as the standardizing mesh they do not receive the same magnification.

Mathematical analyses of these errors and their correction have been made both by SHARPE [4] and within the Project, but for routine work the following approximate method has been evolved. Precision steel spheres covering the same size range as the coated particles, e.g. 400 to 1000 μm, are bonded to a sample holder carrying a 500-lines-per-inch mesh. This standard sample is radiographed whenever the relation between target, sample and plate is altered, e.g. a change of target height due to a change in tube potential. The X-ray plate of the standard is projected at 100X and the images of the spheres measured. A graph is then drawn of the measured size of the spheres against the true size. This graph is used to determine the true diameter, and hence the magnification of objects radiographed under these conditions. It also assists interpretation of the radiographs as it shows the degree of ovality of images of non-axial particles. Analysis of error has shown that measurements are made to ± 2 μm, with a resolution of 2 μm.

3.4. Microradiographic results

Although the microscope is used primarily for routine metrology of coatings and particles such as are shown in Figs. 11 and 12, it provides information on irregularities in coatings and contamination of coatings by fuel materials (see Fig. 13).

This equipment has also proved valuable for studying graphite corrosion, since widely distributed impurities, which do not yield to conventional techniques of chemical analysis, can be readily identified on the radiographs. Radiography of corroded samples has shown that the impurities in the graphite act as nuclei for corrosion as shown in Fig. 14.

The effects of heat treatment and thermal cycling on the stability of the fuel kernel has been examined, and microradiographs have shown clearly the diffusion of fuel into the coating layers under certain conditions. A typical example is shown in Fig. 15.

The X-ray projection microscope is known to be capable of ten to twenty times better resolution than is gained with the mode of operation described in this report. It is felt, however, that work with this instrument in the Dragon Project has established it as being capable of providing a valuable,

Fig.11

Microradiograph of fuel particles coated with pyrocarbon layers of different density

Fig.12

Microradiograph of typical Dragon uranium/thorium carbide fuel particles coated with PyC/Sic/PyC coating

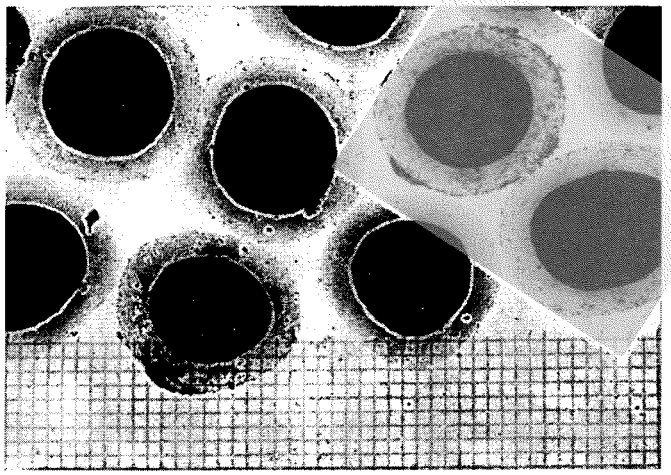

Fig.13

Microradiograph showing fuel contamination on the surfaces of coated particles

Fig.14

Fine-grained graphite showing corrosion pits centred around impurity sites

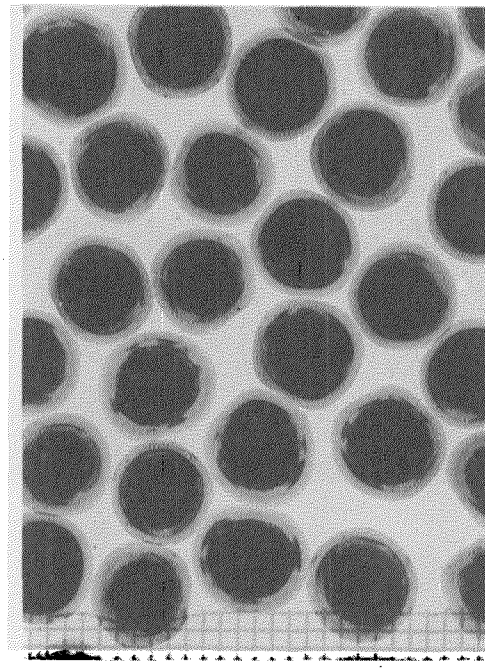

Fig.15

Diffusion of UC_2 fuel into a duplex pyrocarbon coating after 200 h at 1600°C

non-destructive method for the quality and process control of batch production of coated-particle fuel materials.

4. RADIOGRAPHY AND FLUOROSCOPY OF FUEL CARTRIDGES

4.1. General

In the Dragon fuel element the fuel cartridge, owing to its high fuel-particle loading contains relatively little matrix material. Provided that the original mixing batch of fuel particles plus matrix is homogeneous and remains so during pressing, gross inhomogeneity is unlikely to occur in the pressed fuel cartridge after its final heat treatment. However, in view of the need to demonstrate that segregation did not occur either in mixing or during subsequent pressing and to investigate the relative efficiencies of different mixing and pressing procedures it was considered necessary to carry out a 100% non-destructive examination of all fuel cartridges produced to check their homogeneity.

In addition, it was also desirable to examine the fuel cartridges for freedom from flaws such as cracks, voids, inclusions, or changes in density. A radiographic method was selected for this purpose, and a development of the original panoramic slit-scanning technique developed at A.E.R.E., Harwell, England was used.

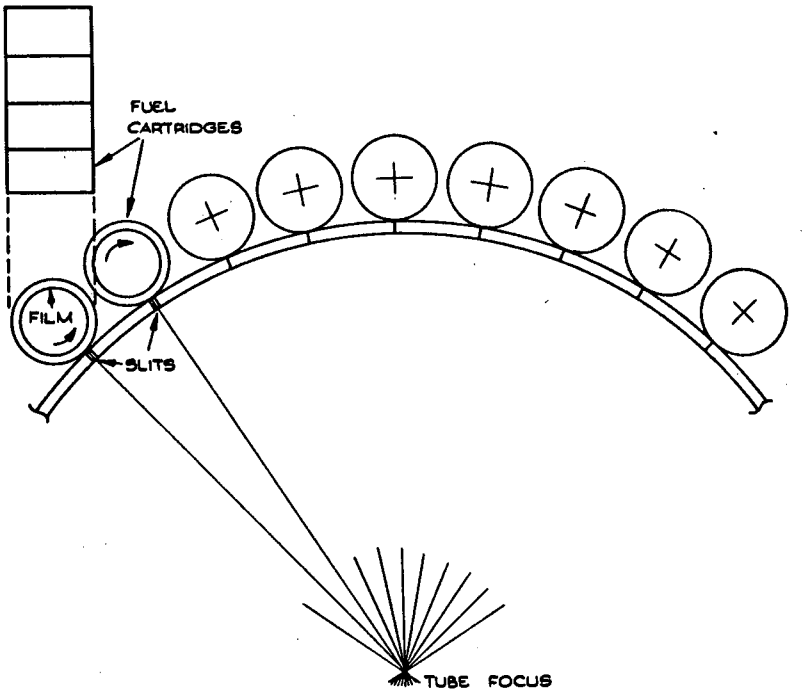

Fig.16

Multiple slit-scanning technique

As it was expected that up to 100 fuel cartridges per day would have to be examined, it was necessary to radiograph as many cartridges at one time as was possible. The slit-scanning technique, was suitably engineered and modified, to test one heat-treatment batch (45 cartridges), and to cope with up to 135 fuel cartridges per day.

4. 2. The panoramic slit-scanning apparatus

A lead shield is mounted on an arc of 760 mm radius from the focus of a 360° beam rod-anode X-ray tube. Twelve slits 1 mm in width by 310 mm long are machined at regular intervals through the lead shield as shown in Fig. 16. The constant potential rod anode, X-ray tube is electrostatically focused, is rated at 150 kV 15 mA and has a 5-mm focal spot.

Twelve cylindrical cassettes of 24-SWG aluminium tubing to fit within the bore of the fuel cartridges are mounted over the slit. Within each cassette is a brass rod 13 mm in diam., which acts both as a mounting spindle and beam trap. The X-ray film specially cut to size, is loaded into each cassette, so that being coiled it naturally assumes a position in contact with the aluminium tube walls, with about 6 mm of film overlapping. Each cassette will take four fuel cartridges; thus a total of 48 fuel cartridges can be mounted for each loading. The cassettes are rotated through a train of

gears driven by an electric motor suitably geared to give a speed range of 0-5 rpm. When loaded with fuel cartridges there is about 1 mm clearance from the lead shield, thus minimizing the risk of scatter from the collimated X-ray beam. Each cassette mounting bearing is spring-loaded, and thus loading and unloading of the equipment is simple and only about 3 min are necessary to load or unload the 12 cassettes. The whole equipment is contained in a shielded cabinet, the X-ray tube entry point and the lid being electrically interlocked to the control console so that accidental exposure of the operator to X-radiation when the lid is open, is impossible. Another important advantage of the panoramic slit-scanning method is that the cartridge wall-thickness is scanned continuously to give single-image exposure to the film moving past the slit. The brass rod (beam trap) passing through the centre of the cassette absorbs the X-rays, preventing double-image exposure of the film on the opposite diameter of the cassette. Figure 17 shows the top of the equipment within its shielding cabinet and the cassette assembly is illustrated in Fig. 18.

4.2.1. Evaluation

After the exposed films are processes and dried they are removed for examination on a viewing screen, to evaluate the degree of homogeneity and to detect the presence of flaws. To simplify reporting, an arbitrary scale of values has been used to assess the degree of homogeneity, and to include details of any flaws which may be present. The grading system in use is set out in Table II.

Over a period of months several thousand fuel cartridges have been produced and tested by this method. The results of the homogeneity evaluations are shown in Tables III and IV.

It is interesting to note that out of more than 8000 cartridges so far examined those of Grade "C" do not exceed 2.5% and the greatest proportion tested are Graded A-.

During the production of the Dragon First-Fuel Charge an average of 90 cartridges per day were radiographed, evaluated and fully reported upon without difficulty over a period of months. Occasionally 135 cartridges per day or three furnace batches were dealt with.

The results obtained so far have shown that this is a reliable and comparatively inexpensive test enabling full X-ray inspection to be carried out on a production basis. The detection of flaws and evaluation of homogeneity has shown a high degree of sensitivity and quite small defects are easily observed. This is partly because of a low degree of unsharpness, long full focal distance (F. F. D), and small focus, together with short exposure of the film. Early tests with D. I. N. penetrameters showed that the 0.05-mm wire was clearly seen, and the 0.025-mm wire could be clearly seen when the total F. F. D. exceeded 660 mm. At the normal working F. F. D. of 760 mm, the 0.025-mm wire was very clearly seen.

4.3. Fluoroscopic examination

In addition to the radiographic slit-scanning technique described above, each cartridge was subjected to an X-ray fluoroscopic examination. This

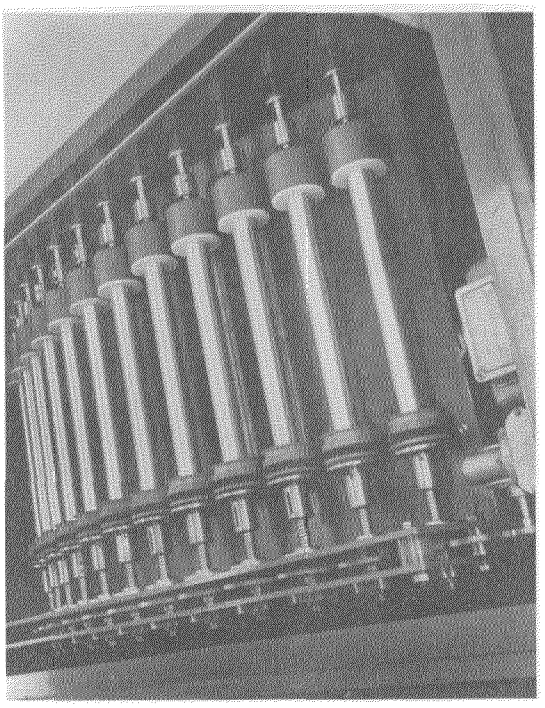

Fig.17

Multiple slit-scanning radiographic equipment

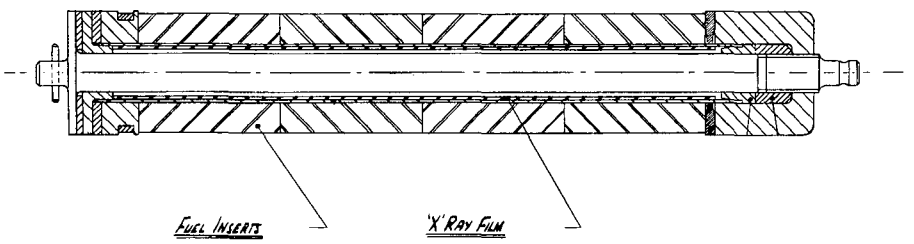

Fig.18

Cassette assembly

examination is a useful adjunct to the panoramic radiography in that it acts as a double check on the radiographic technique, and in itself is a rapid test to carry out. It takes less than 30 s to examine a cartridge by this technique, even when using an image intensifier. If the normal viewing screen is used (i.e. no image intensifier) then the testing time is about 15 s per cartridge.

The equipment used is a Seifert 150-kVP X-ray tube having dual focal spots, the available power being:

TABLE II

GRADING SYSTEM

Grade	Evaluation
A+	Very good fuel dispersion, no defects of any consequence.
A	Good fuel dispersion, may have very slight variations in density.
A-	Fair fuel dispersion. Could contain cracks, cavitation, porosity, variable density, segregation all in minor forms.
B	Moderate fuel dispersion. Could contain major cavities, cracks, porosity, clumps of fuel, density variation.
C	Poor fuel dispersion. Would contain very large clumps of fuel with possibly severe 360° cracks. Large cavities etc.

TABLE III

HOMOGENEITY OF URANIUM/ZIRCONIUM FUEL CARTRIDGES

Grade	(%)
A+	3.29
A	18.14
A-	54.69
B	21.38
C	2.5

TABLE IV

HOMOGENEITY OF URANIUM/THORIUM FUEL CARTRIDGES

Grade	(%)
A+	0.29
A	4.1
A-	54.4
B	38.95
C	2.26

150 kV at 3 mA on the 0.4-mm focal spot, or
150 kV at 12 mA on the 2.5-mm focal spot.

The X-ray tube is housed in a shielded fluoroscopic viewing cabinet, having a 380-mm-square viewing window. In addition a 130-mm Mullard Image Intensifier is installed on the face of the unit. The X-ray tube window has double-acting shutters which may be moved by power drive, at right angles to each other, and hence the X-ray beam may be collimated at source to any rectangular or square form.

4.4. Colour radiography

A satisfactory colour radiographic technique has been developed along lines suggested by work at A. E. R. E., Harwell, England [5]. At first Ektacolour Print Film was used, but more recently Ektachrome "B" sheet film, has been employed as being much faster. It is, however, slightly more expensive than the print film. The technique of X-ray exposure is fairly simple, and insofar as fuel cartridges are concerned the exposure time is increased by a factor of four, assuming that the kV, mA and F. F. D. remain constant. Thus a thorium/uranium-fuelled cartridge requiring a normal exposure of 3 min, at say 95 kV and 3 mA at 760 mm F. F. D., using load screens and normal black and white X-ray film, will require 12 to 15 min using Kodak Ektacolour Print Film. The film-processing technique is normally the Kodak-five Bath C. 22 process as recommended by PARRISH and PULLEN [5]. It was found, however, that Kodak Process P. 122 gave better colour contrast and had certain advantages over the C. 22 process. If Ektachrome "B" film is used, then the X-ray exposure time is no greater than for black and white, unfortunately the colour process (Kodak E2, E3) is rather slower and rather offsets the advantage of the faster film, except that the X-ray tube running time is appreciably less. For colour panoramic radiography the X-ray exposure time using Ektacolour Print is prohibitively long and for this technique Ektachrome "B" film and the E2, E3 colour process is recommended. (See Table V for exposure and processing changes).

4.5. Colour fluorography

The poor contrast obtained from black-and-white fluorography of fuel cartridges led to the need to develop a colour fluorographic technique. A pair of wide-angle Schneider Lenses-Xenon 1 : 2/75 and 1 : 1.5/55 was substituted for the binoculars in the Mullard-Image intensifier. The lens system was linked to a 35-mm Robot camera, mounted on an adjustable precision platform attached to the image intensifier as shown in Fig. 19. The film finally chosen for this work was Ektachrome "B". This colour film is very sensitive to the green fluorescent light as seen through the image intensifier, and photographs may be taken at speeds of up to 1/250 s with very good results. The effective film speed can be increased still further by altering the exposure and processing as follows. The normal film speed (A. S. A.) is 125.

The colour processing time of 58 min is rather slow but up to 60 fluorographs may be processed at one time.

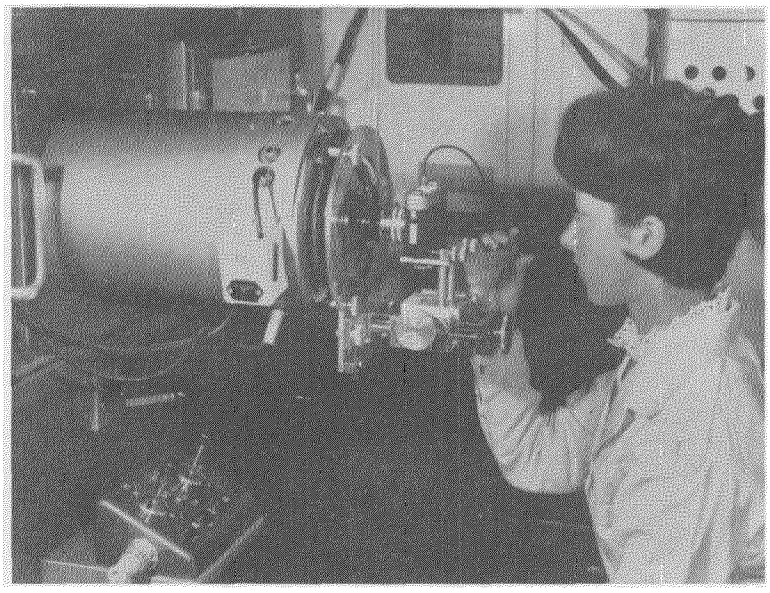

Fig.19

Robot camera in position on image intensifier

Colour is advantageous particularly when there is a need to look for minor changes in density or variations in fuel loading. Colour fluorography is cheap, rapid and provides an easy method of preparing a permanent record, e.g. a colour transparency, and is easier to evaluate than its black-and-white counterpart.

5. EDDY-CURRENT INSPECTION OF GRAPHITE FUEL-ELEMENT COMPONENTS

The structural components of the fuel element are machined from low-permeability graphite and, in view of the cost of the machining operations and the need for high integrity, it is desirable to test the material at various stages to ensure that the material is free from cracks and other defects which might lead to failure during final machining, assembly or in service.

A variety of inspection methods including radiography, ultrasonic, and eddy-current techniques have been investigated with the object of establishing an acceptable non-destructive procedure. Radiography was found to be too expensive and time-consuming and ultrasonic methods were abandoned because of the difficulty of using a non-liquid coupling medium which would not be absorbed in the pores of the graphite. A method of eddy-current inspection of graphite core rods and fuel tubes has been developed under extramural contract by the non-destructive testing group at A.E.R.E., Harwell. The method is known as "Eddyfax" inspection. A coil built into a probe is spring-loaded against the graphite surface. The axis of the sample is

TABLE V

EXPOSURE AND PROCESSING CHANGES

Exposure	Effective film speed (B.S. arithmetical)	1st developer Time min	Addition to colour developer per litre
1 stop under	320	13	2.1 cm^3 of 20% sulphuric acid
2 stops under	640	16	1.0 cm^3 of 20% sulphuric acid

scanned by the probe while the test sample is being rotated. A "Mufax" facsimile recorder is mechanically linked to the scanning speed and thus provides a record of the signals received. At present this work is in an early stage, but preliminary results suggest that the method is suitable for the detection of structural flaws in graphite.

The method is being adopted experimentally as a technique for inspecting the structural graphite components for the fuel elements of the second charge of the Dragon reactor. It is hoped to correlate the results of inspection with irradiation behaviour since at present no absolute standards of significance can be attached to various types of defect and hence the formulation of inspection standards must depend, to a large extent, on trial and error.

6. CONCLUSION

The inspection methods which have been described constitute a selection of the non-destructive techniques which are used for process control, evaluation and provision of data for correlation with post-irradiation examination. With the exception of the eddy-current inspection of graphite components the methods described utilize the properties of various types of radiation, i.e. alpha, gamma and 'X' radiation. In certain tests the characteristic decay properties of the fissile and fertile materials have been used to provide relatively simple testing procedures. All the techniques have proved to be suitable for routine application in batch-production processes.

A final assessment of the efficiency of such techniques in evaluating fuel quality will only be possible when the irradiation behaviour of the fuel materials is established from performance in the reactor core and post-irradiation examination. The methods of evaluation which have been employed will be kept under review in the future with a view to determining the minimum standard of testing necessary to define fuel of acceptable quality. It is the objective to establish those parameters which characterize fuel having adequate fission-product retention at high burn-up.

ACKNOWLEDGEMENTS

Acknowledgement is made to Mr. C. A. Rennie, Chief Executive, Dragon Project for permission to present this paper and to Mr. R. A. U. Huddle, under whose direction the work was carried out, for constant encouragement and support. The assistance of all those members of the staff of Dragon Project and associated organizations who have contributed to the programme of work is also gratefully acknowledged.

REFERENCES

[1] McDOLE, C.J., "Escape of Fission Products from Slurry Particles", WCAP-277 (1956).
[2] Electron-Physical Instrument Ltd., Hendon, London, England.
[3] Cavendish Laboratory, Cambridge University, England.
[4] SHARPE, R.S., "X-ray Microscopy Applied to the Examination of Coated Nuclear Fuel Particles", Reactor Science and Technology, 17, Nos.11/12, December (1963).
[5] PARRISH, R.W. and PULLEN, D.A.W., Brit. J. non-dest. Test. 6, No.4.

DISCUSSION

R. NEIDER: I would like to ask what advantage colour radiography has over black and white radiography? Would not a somewhat less contrasting black and white film do the same job?

J. F. G. CONDÉ: I am not advocating the use of colour radiography for general applications, only giving examples of some of the techniques which are employed. It has certain advantages, particularly in colour fluorography, where the results in conjunction with an image intensifier are superior to black and white.

EDDY-CURRENT TESTING OF THIN-WALLED CLADDING TUBES

C. VERSTAPPEN, R. DEKNOCK, R. NEIDER, M. BRABERS AND P. de MEESTER
STUDIECENTRUM VOOR KERNENERGIE, MOL, BELGIUM

Abstract — Résumé — Аннотация — Resumen

EDDY-CURRENT TESTING OF THIN-WALLED CLADDING TUBES. In view of an extended programme on the evaluation of properties and defects of stainless-steel and Zircaloy thin-walled tubes, a basic study has been made of the optimum test conditions for applying eddy-current test methods.

An electronic apparatus has been built to define these conditions for a great variety of test problems. Therefore, it was necessary to have the possibility of changing the frequency over a wide range and to measure the two components of the complex impedance of the test coil separately. This has the advantage over a measurement of the absolute value of the impedance change since this value has little meaning in view of the change of the properties of the test object. The actual apparatus allows the precise and sensitive measurement of the real and imaginary components of any test coil in a frequency range from 0.1 - 500 kHz. A special type of modulation device has been developed. The apparatus is not considered as an actual testing apparatus; by determining optimum conditions for each case, it enables a relatively simple and specific apparatus to be built.

Up to now, a detailed study of relationships between physical and electrical properties of a specimen and the test-coil impedance has been performed for tubular fuel-cladding materials. Frequency and coil configurations are established for wall-thickness measurements and a particular apparatus has been constructed; the accuracy is better than 1% and changes between inner and outer diameter variations can be discriminated. Other specific apparatus are studied and proposed.

CONTRÔLE PAR COURANTS DE FOUCAULT DES TUBES DE GAINAGE A PAROI MINCE. Dans le cadre d'un vaste programme visant à évaluer les propriétés et défauts des tubes de gainage à paroi mince, en acier inoxydable et Zircaloy, on a procédé à une étude fondamentale pour déterminer les meilleures conditions d'application des méthodes de contrôle par courants de Foucault.

On a construit un appareil électronique permettant de définir ces conditions pour une grande variété de problèmes de contrôle. A cet effet, il fallait pouvoir modifier la fréquence dans une gamme étendue de valeurs et mesurer séparément les deux composantes de l'impédance complexe de la bobine d'essai. Ce procédé est préférable à celui qui consiste à mesurer la valeur absolue de la variation de l'impédance, cette valeur absolue étant peu représentative du fait des modifications que subissent les propriétés de l'objet examiné. L'appareil en question permet de mesurer avec précision et une grande sensibilité les composantes réelles et imaginaires pour toute bobine d'essai dans une gamme de fréquences de 0,1 - 500 kHz. On a mis au point un dispositif de modulation d'un type spécial. Celui-ci n'est pas considéré comme un appareil de contrôle proprement dit; mais, en déterminant les conditions optimales pour chaque cas, il permet de construire un appareil relativement simple, spécialement adapté au cas considéré.

Jusqu'à présent, on a procédé à une étude détaillée des relations entre les propriétés physiques et électriques d'un spécimen et les modifications de l'impédance de la bobine d'essai pour les matériaux servant au gainage tubulaire du combustible. On a établi la fréquence et les configurations des bobines pour la mesure de l'épaisseur des parois; un appareil spécial a été construit à cet effet; la précision est supérieure à 1% et il est possible de déceler des écarts entre les variations du diamètre intérieur et celles du diamètre extérieur. Les auteurs étudient et proposent d'autres appareils spécialisés.

ИСПЫТАНИЕ ТОНКИХ ТРУБЧАТЫХ ОБОЛОЧЕК С ПОМОЩЬЮ ТОКОВ ФУКО. В связи с расширенной программой оценки свойств и дефектов тонких трубок из нержавеющей стали и циркаллоя изучены оптимальные условия испытаний для применения методов испытаний с помощью токов Фуко.

Был изготовлен электронный аппарат для определения этих оптимальных условий применительно к самым разнообразным проблемам испытаний. Поэтому было необходимо иметь возможность изменения частоты в широком диапазоне, а также измерить отдельно два компонента импеданса пробной катушки. Это имеет преимущество перед измерением абсолютной

величины импедансного изменения, поскольку эта величина имеет небольшое значение ввиду изменения свойств испытуемого объекта. Современный аппарат позволяет произвести точное и чувствительное измерение действительных и мнимых компонентов любой пробной катушки в диапазоне частот от 0,1 до 500 кгц. Было разработано специальное модуляционное устройство. Аппарат не рассматривается в качестве действительного испытательного устройства; определяя оптимальные условия для каждого случая, можно изготовить сравнительно простой аппарат специально для данного случая.

Вплоть до настоящего времени подробно изучается связь между физическими и электрическими свойствами образца и импедансными изменениями катушки применительно к материалам для трубчатых оболочек, например к нержавеющей стали и циркаллою.

Частота и конфигурации катушки устанавливаются для измерений толщины оболочки; был изготовлен специальный аппарат. Точность измерения составляет менее 1%, и можно определить изменения в соотношениях между внутренними и внешними диаметрами. Предлагаются и другие специальные аппараты, которые находятся в стадии изучения.

ENSAYO DE VAINAS DELGADAS MEDIANTE CORRIENTES DE FOUCAULT. Como parte de un programa ampliado de evaluación de las propiedades y defectos de los tubos delgados de acero inoxidable y zircaloy, se ha efectuado un estudio preliminar de las condiciones óptimas para la aplicación de métodos de ensayo basados en las corrientes de Foucault.

Se ha construido un aparato electrónico que permite determinar las condiciones más favorables para el estudio de muchos de los problemas que plantea el ensayo de materiales. Para ello, era necesario poder variar la frecuencia en un amplio margen y medir por separado los dos componentes de la impedancia de la bobina de ensayo. Es preferible ese método al que consiste en medir el valor absoluto de la variación de impedancia causada por el objeto que se ensaya, porque la modificación de las propiedades del objeto resta importancia a ese valor. El aparato permite medir con precisión y sensibilidad los componentes reales o imaginarios de la impedancia de cualquier bobina, en una gama de frecuencias que abarca de 10 kHz a 1 MHz. Se ha construido un dispositivo de modulación de tipo esencial. Aunque ese aparato no constituye propiamente un instrumento de prueba, al determinar las condiciones óptimas en cada caso, permite construir uno relativamente sencillo que sea el adecuado.

Hasta ahora, el estudio detallado de la relación entre las propiedades eléctricas y otras características físicas de una muestra, y las variaciones de impedancia de la bobina se ha realizado únicamente para ciertos materiales de revestimiento, como el acero inoxidable y el zircaloy. Adaptando la frecuencia y la estructura de la bobina a la medición de espesores de pared se ha construido un aparato especial. El error en la medición es inferior a 1%, y pueden distinguirse las diferencias en la variación del diámetro interior y del exterior. Los autores proponen y estudian otros aparatos especiales.

1. INTRODUCTION

In the scope of a non-destructive testing programme on cladding materials of the fuel elements of the BR3 power reactor a study has been made with the aim of investigating the range of utility and the possibilities of eddy-current testing methods.

The general theory and several detailed studies of specific test methods by eddy-currents are well known and have been described in the literature [1-5].

In a basic study on thin-walled cladding tubes, which aims at a critical examination of fabrication specifications, tolerances imposed and their necessity for safe fuel-element operation, several problems arise. A better accuracy is needed than for mere quality control on a given fabrication, and one should obtain as much information as possible to know and understand the physical properties and anisotropy involved in the assay of the materials and the manufactured products. The economic interest of such studies is evident, especially with the increasing number of pressurized water-power reactors.

A part of this study concerns eddy-current testing, which is performed in the laboratories of S.C.K./C.E.N. - Mol, and is described in this paper. The improvements to be made resulted from the measurements with an apparatus of classical design. The range of application with a newly built apparatus has been explored.

2. TOTAL IMPEDANCE MEASUREMENTS

2.1. Principle

Since the impedance of a coil is influenced by the test object it will be possible to regard the total impedance change as the quantity to be measured for quite a number of cases of non-destructive testing. It is well known, however, that different material parameters will influence the total impedance in the same way. So, the total impedance change measurements caused by a specific parameter can only be of use if all other factors are known or can be controlled. In one of our early cases, namely wall-thickness inspection of stainless-steel tubes, the impedance change of the coil permitted an accurate thickness measurement, since in that case the effect of possible changes in diameter and in conductivity of the tube could be neglected. In general, however, these parameters cannot be considered as known.

2.2. Apparatus and results

The apparatus formerly used in our laboratory is of classical design; it measures the relative impedance variations of two feed-through coils which are incorporated in a bridge circuit. One of the coils contains a reference tube, while the tube to be tested is passed through the second one.

Figure 1 shows a recording of a standard tube with several well-defined wall-thickness reductions on the external side of the stainless-steel tube as obtained with this method. These reductions in thickness have been artificially made by electrochemical milling. The wall thickness deviates some 5 to 15 μm from the original wall thickness of 500 μm. The results obtained with this apparatus permit measurements of the thickness fluctuation within 1% of the total wall thickness.

2.3. Limitations of this method

The principle of total impedance measurements which has worked satisfactorily in the case of wall-thickness measurements of a given fabrication batch of tubes is unfortunately not suited for a wide general-purpose application.

From theory as well as from actual experimental results it is known that several disturbing side effects influence the coil impedance and thus inhibit a clear distinction between these side effects and the actual quantity to be measured [5].

To determine the optimum test conditions for a specific eddy-current testing apparatus, it is possible to refer to theoretical treatments and to a quantity of published curves. However, it should be noted that most of these curves have been calculated and are not always representative for actual test

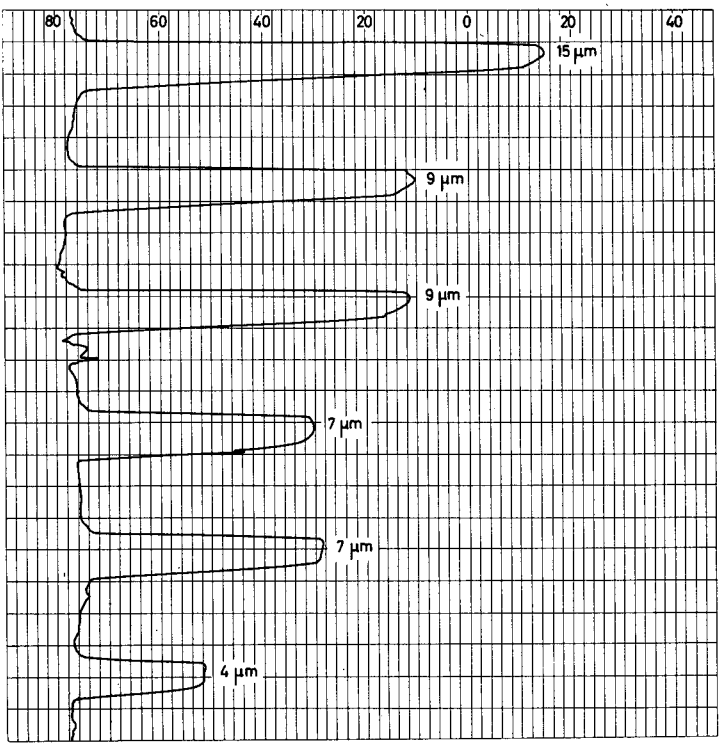

Fig. 1

Recording of the absolute impedance variation of a standard tube with wall-thickness reductions of 15-9-7-4 µm

conditions. The reasons for this are not only the complex mathematical translation of variables but also a restriction in the literature data concerning specific coil types and dimensions. From the foregoing one must draw the conclusion that, for the development of a specific test apparatus which should be applicable only to one certain testing problem, it is more logical to use a general-purpose test apparatus. This latter apparatus should be able to distinguish between the interesting factors influencing the coil impedance and the side effects. Further, it must be able to measure not only the changes of the total coil impedance caused by the test object but also the two components of this impedance, that is the imaginary part ωL and the real part, R. Moreover, this analysis should be done over a wide range of frequencies and for a variety of coil types and geometries.

3. IMPEDANCE ANALYSER

A new type of impedance analyser with a continuously variable frequency has been built by one of the authors; a detailed description of this apparatus

is given in Ref. [6]. A block diagram of this apparatus is represented in Fig. 2. A brief description of its principle of operation follows.

The output voltage of a sinusoidal oscillator is fed to the primary of a transformer Tr1. The secondary is floating and is loaded by the test coil

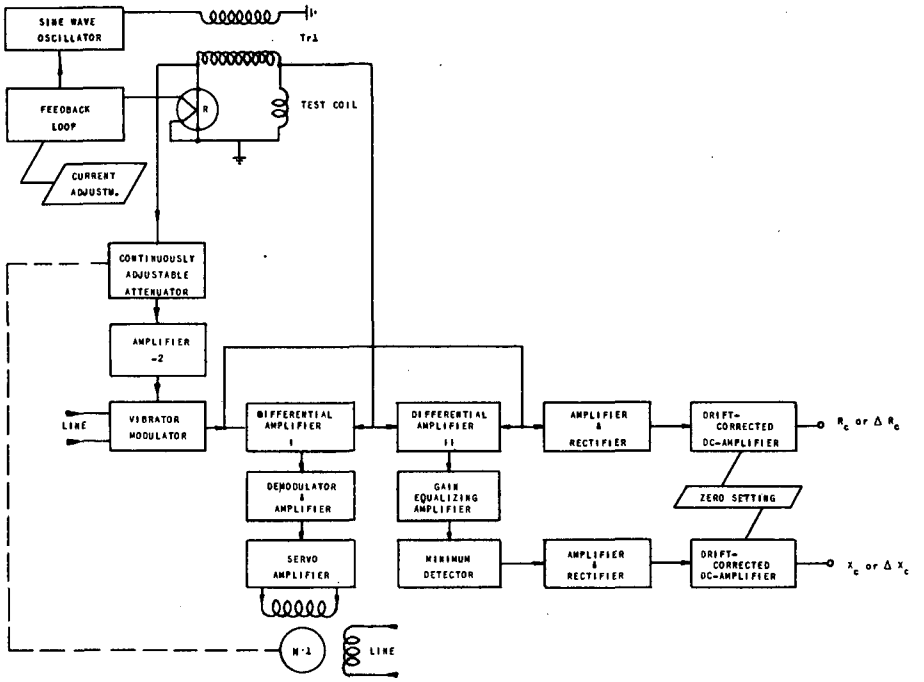

Fig. 2

Block diagram of eddy-current test-coil impedance analyser

in series with the heater resistance R of a vacuo-junction thermocouple. The thermocouple EMF controls the voltage at the primary of the transformer so as to keep a constant current through the test coil. Since the feedback loop contains an integrator, the apparent internal current resistance is, as measured, greater than 200 MΩ.

Two single-ended voltages are available from the secondary of the transformer (Fig. 3): the voltage $IR\,(\vec{PA})$ in phase with the current I through the coil, and a voltage $IZ_c\,(\vec{PB})$ where Z_c is the absolute value of the complex test-coil impedence $Z_c = R_c + jX_c$. These two voltages have a relative phase shift φ, and are applied to a highly degenerative differential amplifier with a single-ended output. The gain is stabilized and within 1% of unity over a frequency range of 500 to 0.1 kHz. The output voltage equals the vector difference of the two input voltages. By phase reversal of the vector $IR\,(\vec{PD})$ and proper attenuation of its amplitude to a value equal to the resistive component IR_c of the coil voltage $(\vec{PC})$, this vector difference reaches a minimum $(\vec{BC})$ which is equal to the imaginary component IX_c of the coil voltage.

As seen in Fig. 3, manual adjustment and readjustment of $\vec{PC} = IR_c$ for

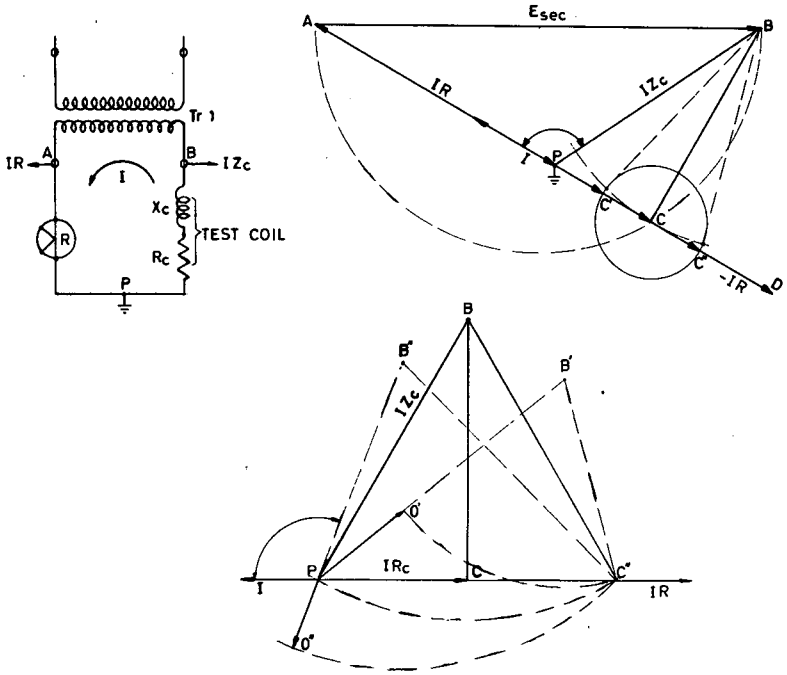

Fig. 3

Circuit of the test-coil and vector diagrams

minute phase and/or amplitude variations of the coil impedance are very cumbersome and inaccurate (the ratio $\Delta CB/\Delta PC$ is generally very small). Therefore, an automatic adjustment of the exact IR_c value is necessary, and has been developed in our laboratory. The principle is not widely known and could be original.

A chopper relay operated at power-line frequency switches alternately the IR input terminal of the differential amplifier between a |2 PC| level (PC''in Fig. 3) and ground potential. In this manner, the vector difference at the output of the differential amplifier respectively equals BC'' and $BP = IZ_c$. If PC is adjusted to a value equal to the resistive component of the coil, (BC'') equals (BP) and no amplitude modulation appears at the output of the differential amplifier. Also, a change in amplitude and/or phase of the test-coil impedance produces a square-wave-modulated carrier. After demodulation, the resulting square wave is AC-coupled to a servo-amplifier, the output of which controls the two-phase induction motor M1. The shaft position of the motor determines the attenuation of the voltage IR. This voltage is reversed in polarity and doubled.

To measure the imaginary component of the coil voltage, the chopped voltage $PC = IR_c$ and the coil voltage are applied to a second identical differential amplifier. The output voltage is also a square-wave-modulated carrier and a minimum-voltage detector was needed since the voltage $BC = IX_c$ is always smaller than the test-coil voltage PB.

4. PRELIMINARY RESULTS WITH THE IMPEDANCE ANALYSER

4.1. General procedure

The procedure followed for developing an appropriate apparatus for a well-defined testing problem will be demonstrated by means of a problem for cladding materials, namely the determination of wall thickness of thin tubes.

The influence of a change in wall thickness on the imaginary and real component of the impedance is measured for a series of variable coil types in a certain range of frequencies. The effect of possible interfering parameters is investigated, such as variable fill factor, lift-off and conductivity changes. The results obtained are then summarized in the normalized impedance plane (X/X_0 and $R-R_0/X_0$). From these curves it may be concluded which requirements the apparatus for the problem should meet.

4.2. Coils

For determining the tube wall-thicknesses, two different types of coils may be used: the feed-through coil and the probe coil.

The theory and the applications of feed-through coils has been thoroughly reported in the literature [1, 2, 5] and this type of coil is extensively used in many eddy-current test apparatuses. Figure 4 shows the normalized impedance plane for the frequency range 3-60 kHz of a stainless-steel tube for three different fill factors. According to the theory, wall-thickness variations at constant outer diameter move along these curves. Experimental results, however, have shown that at constant inner diameter the wall thickness causes the impedance to deviate from these curves. This makes it possible to distinguish between variations in wall thickness at constant inner diameter and at constant outer diameter.

The feed-through coils have an intrinsic disadvantage; namely, the information obtained is determined by the complete cross-section of the tube. In practice, application of the feed-through coil is still possible for wall-thickness measurements if the sensitivity of the apparatus is sufficiently high to detect deviations from the nominal value, which are smaller than the tolerances set by fabrication processes of tubes.

If the expected deviations from the normal properties of the material permit application of the feed-through coil, this is a rapid and efficient way of non-destructive testing.

On the other hand, the probe coil permits wall-thickness measurements on a part of the tube circumference. Figure 5 shows the measured impedance plane of a probe coil ($d/h = 1.9$; d = medium coil diam., h = coil height) for stainless-steel plates of 0.5; 1.0 and 2.0 mm thickness. Each measured value corresponds to a certain frequency, and sheet thickness as indicated. For one certain frequency the point with the smallest X/X_0 value corresponds to the greatest sheet thickness. According to theory the limit frequency fg should be proportional to

$$\frac{1}{\sigma . \mu_{rel} . D . A .}$$

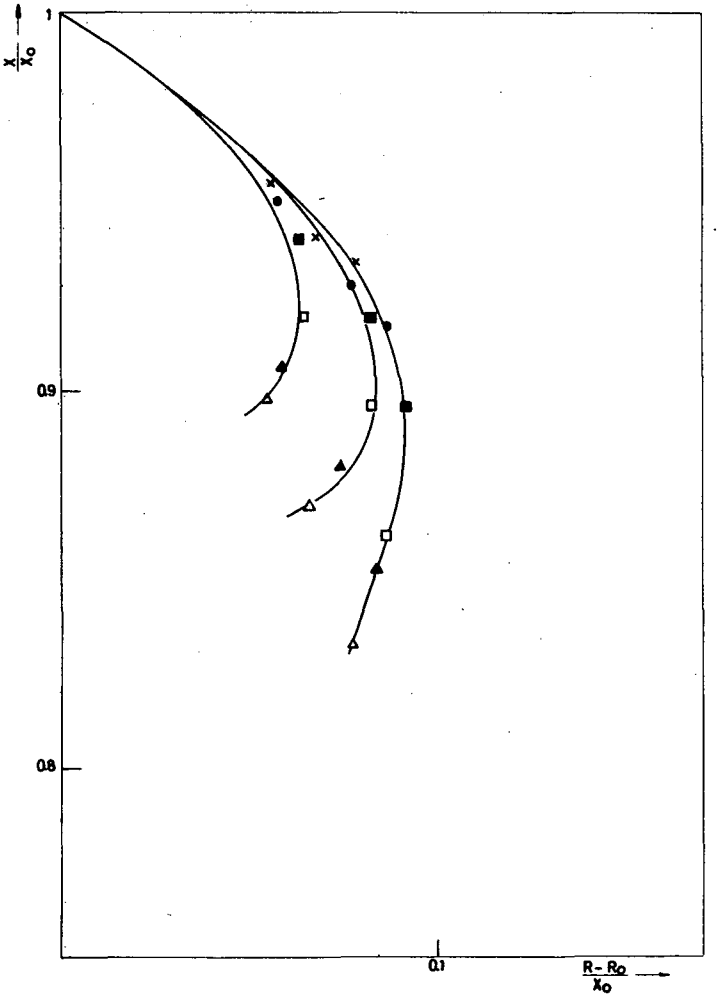

Fig. 4

Normalized impedance plane of a feed-through coil for various fill factors.
Test object: stainless steel (I. D. 6 mm; O. D. 10 mm).

X 20 kHz
● 25 kHz
■ 30 kHz
□ 40 kHz
▲ 50 kHz
△ 60 kHz

where

σ : electrical conductivity of the tested material, m/Ω mm;
D : thickness of the material in cm;
μ_{rel} : relative magnetic permeability of the sheet;
A : factor depending on the coil geometry.

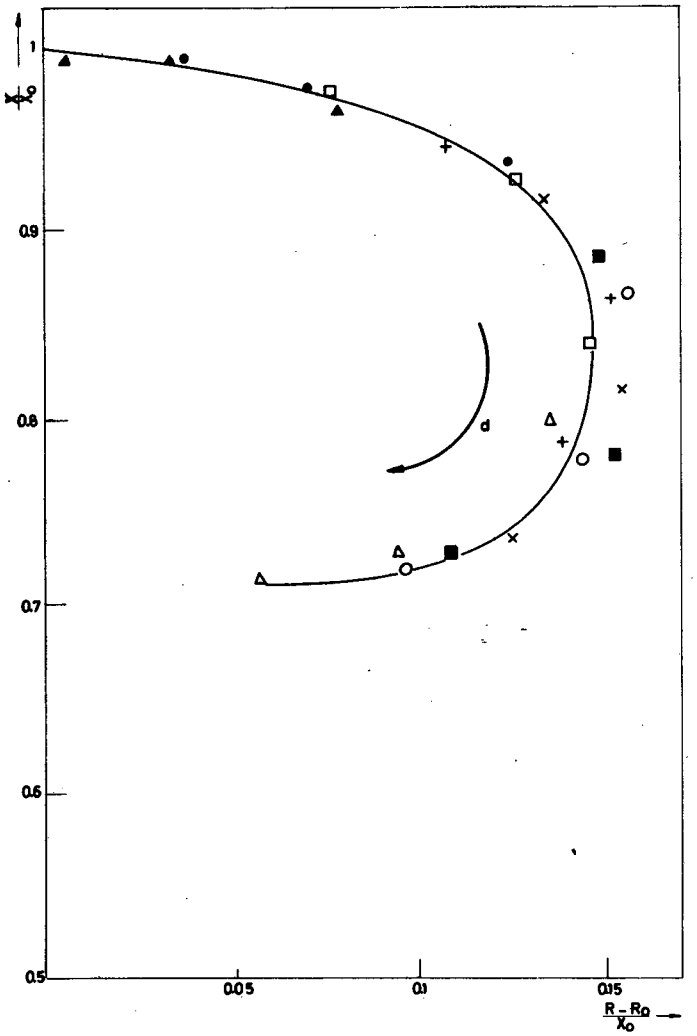

Fig. 5

Normalized impedance plane of a probe coil (d/h = 1,9) for various sheet thicknesses (0.5 1 and 2 mm) of stainless steel.

d : plate thickness
0. 5 - 1 - 2 mm
STAINLESS-STEEL 304
d/h = 1. 9

▲	3 kHz	×	20 kHz
●	5 kHz	■	25 kHz
□	10 kHz	○	30 kHz
+	15 kHz	△	50 kHz

Thus, it is clear that the ratio f/fg increases with increasing sheet thickness D and vice versa. The accuracy of a measured point in Fig. 5 was determined to be 3%.

The measurements by means of probe coils are very much affected by a variation of the distance between coil and test object, namely the well-known lift-off effect. This is clearly shown in Fig. 6, where the variations in the impedance are plotted for lift-off values of 0.5, 1 and 2 mm at constant sheet thickness (2-mm stainless steel). The lift-off has an effect on both components ωL and R for all frequencies. The value of this effect is frequency dependent.

Figure 7 shows the lift-off effect as a function of the frequency for different lift-off values. Measurements are relative to the value at 0 mm lift-off. It is seen that the effect is pronounced at low frequencies (< 10 kHz). At higher frequencies the lift-off effect is nearly constant. It is remarkable that for low frequencies the value of L decreases below the value of L for 0-mm lift-off as found in experimental results. The generally known fact that a small lift-off causes a large variation in L and R components and that the influence of lift-off decreases with increasing lift-off values is clearly shown in these curves. At a frequency of 30 kHz/0.5-mm lift-off causes an R variation (with respect to 0-mm lift-off) of 18%, and a 2-mm lift-off causes an R deviation of only 24%.

From these experimental values it may be concluded that, when probe coils are used, it is desirable to apply a certain lift-off in spite of the fact that this reduces the sensitivity. Reduction in sensitivity is shown in Fig. 8 and one can see that the effect is most pronounced on the R component of the impedance.

These orientating measurements have been carried out in the case of probe coils on flat plates of the material to be tested, to avoid undesirable effects of a wrong centring of the tube with respect to the coil, resulting in a kind of lift-off.

Because the finite dimensions of the coil used with respect to the tube diameter, the published curves cannot directly be applied to tubes. In Fig. 9 the effect of the transition from plate to tube with tubes of decreasing diameters is shown in the normalized impedance plane. The effect is to be attributed to a partial lift-off. A certain value for the ratio of coil diameter to tube diameter must exist for optimum test conditions. This value, however, has not yet been determined.

5. CONCLUSIONS

A general-purpose eddy-current test apparatus with a wide frequency range and an accuracy of better than 3% permits the precise analysis of the impedance as measured with different coil types and under a variety of test conditions. This prototype is used to develop other eddy-current test equipment for specific practical problems. The empirical method for determining the optimum test conditions has a great advantage over the theoretical method. The influence of different interrelated parameters, which are not revealed by a purely theoretical examination, can be determined.

The effect of the coil type on the measured impedance has been investi-

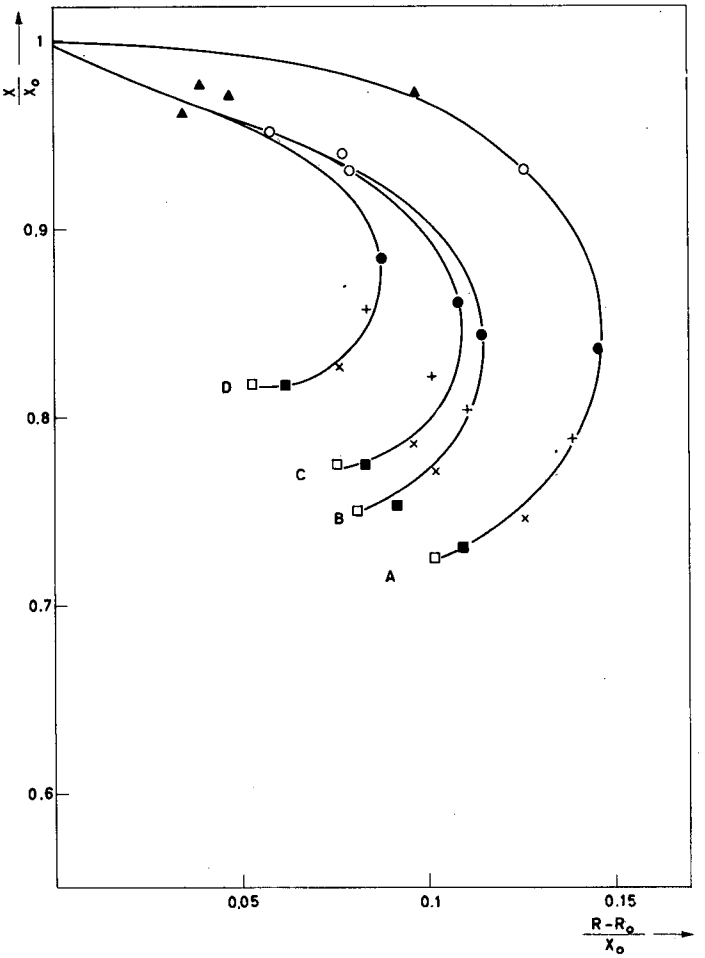

Fig. 6

Normalized impedance plane of a probe coil with various lift-off factors (0.5, 1 and 2 mm) at a constant sheet thickness of 2-mm stainless steel.

LIFT-OFF VALUES

A 0 mm
B 0.5 mm
C 1 mm
D 1.5 mm

▲ 3 kHz
○ 5 kHz
● 10 kHz
\+ 15 kHz
× 20 kHz
■ 25 kHz
□ 30 kHz

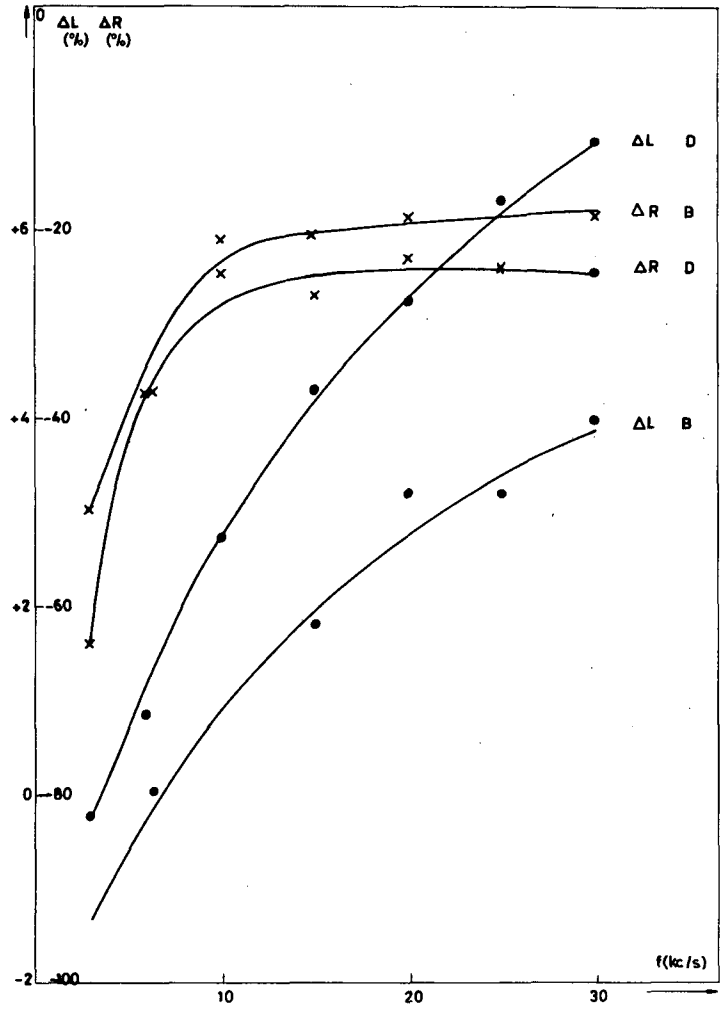

Fig. 7

Effect of lift-off as a function of the frequency for different lift-off values (0.5 and 2 mm) at a constant sheet thickness of 2-mm stainless-steel. Measurements are relative to 0-mm lift-off.

LIFT-OFF VALUES
B 0.5 mm
D 2 mm

gated for the case of wall-thickness measurements of cladding materials. An eddy-current apparatus using a feed-through coil has been constructed, particularly for wall-thickness determination. The measurements are accurate within 1% of the total wall thickness. However, probe coils offer more possibilities than feed-through coils. The lift-off effect inherent to probe coils has been investigated. The results indicate the requirements for an electronic circuit adapted to a probe coil.

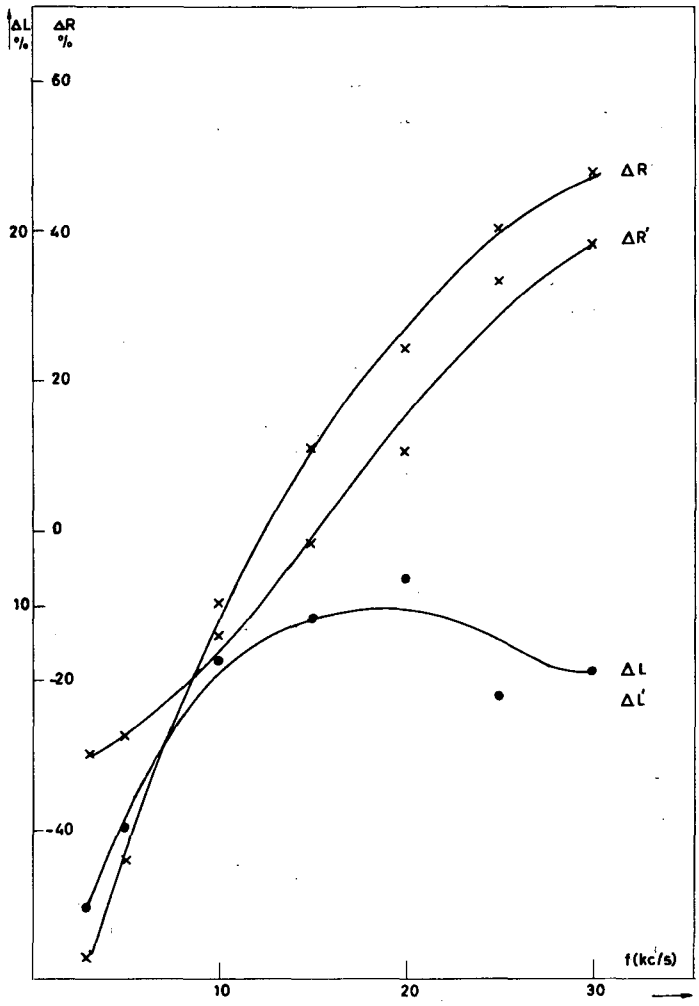

Fig. 8

Influence of a 2-mm lift-off on the sensitivity as a function of frequency.

$\Delta R = R_{(2\text{ mm sheet})} - R'_{(1\text{ mm sheet})}$ (0 mm lift-off)

$\Delta R' = R_{(2\text{ mm sheet})} - R'_{(1\text{ mm sheet})}$ (2 mm lift-off)

analogous for ΔX and $\Delta X'$

ACKNOWLEDGEMENTS

The authors are grateful to Mr. Huet for his encouragements and for supplying the means for this work. One of the authors (R. N.) thanks S. C. K. for making his stay at S. C. K. possible and the Bundesminister für Wissen-

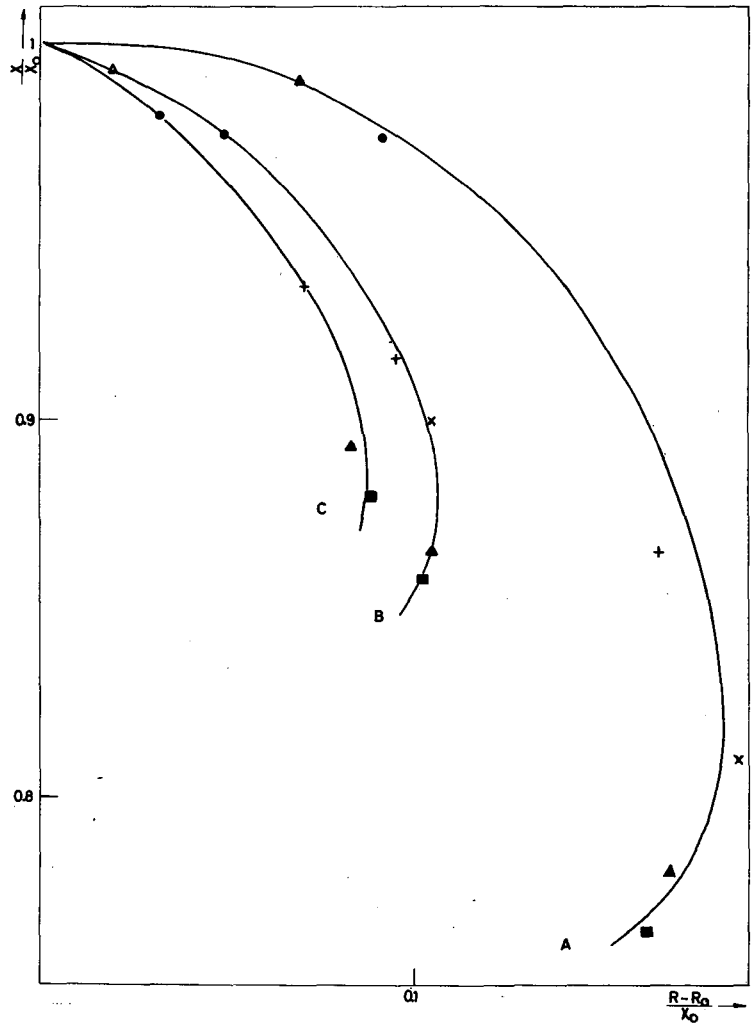

Fig. 9

Normalized impedance plane of a probe coil (d/h = 1.9)
at the transition from plate to tube with decreasing tube diameters.

A = plate
B = tube with 31-mm diam.
C = tube with 20-mm diam.

Δ 3 kHz
● 5 kHz
\+ 15 kHz
× 20 kHz
▲ 25 kHz
■ 30 kHz

schaftliche Forschung, Bad Godesberg, Federal Republic of Germany, for financial support. They acknowledge the technical assistance of Messrs. M. Van Doorslaer and F. Vreys. Thanks are also due to Mrs. Heylen and Mr. Boddou for providing the electrochemically milled standards.

REFERENCES

[1] FÖRSTER, F., Handbuch der Werkstoffprüfung, Erster Band Springer Verlag Berlin/Göttingen/Heidelberg (1958).
Beiträge in Z. für Metallkde.

[2] HOCHSCHILD, R., "Eddy Current Testing by Impedance Analysis", Non-destr. Test. 12, No. 3 (1954).

[3] DODD, C. V. and DEEDS, W. E., Eddy Current Coil Impedance Calculated by a Relaxation Method, Paper presented at the Symp. of Phys. and Non-destructive Testing, Texas (1963).

[4] RENKEN, C. J., Progress Report on Non-destructive Testing by Electromagnetic Methods. ANL-6414.

[5] McMASTER, C., Non-destructive Testing Handbook, II, Eddy Current Testing Principles Sec 36-40, New York, The Ronald Press Company (1959).

[6] DEKNOCK, R., An Eddy Current Test Coil Impedance Analyser, (to be published in Electronic Engineering).

DISCUSSION

V. GERASIMOV: Did you set up any definite apparatus to measure the thickness of tube walls, or just experimental laboratory equipment for measuring changes in coil impedance?

G. VERSTAPPEN: We have one apparatus for measuring industrial wall-thickness variations in stainless-steel tubes, using feed-through coils. The second apparatus we built enables us to look for the right measuring conditions to be applied in a wide range of eddy-current test problems. For this reason it has to be very versatile, with an especially wide frequency range, from 100 Hz to 500 kHz, and a high accuracy.

V. GERASIMOV: Did you use single-coil or two-coil probes?

G. VERSTAPPEN: In the first apparatus we have differential measurement with two feed-through coils. The measurements with the impedance analyser were carried out with feed-through coils and pick-up coils.

V. GERASIMOV: What is the fill factor?

G. VERSTAPPEN: The fill factor is given by:

$$N = \left(\frac{D}{d}\right)^2$$

D = diameter of tube
d = mean coil diameter

SESSION VII

LIMITS TO THE RECOGNIZABILITY OF FLAWS IN NON-DESTRUCTIVE TESTING STEAM-GENERATOR TUBES FOR NUCLEAR-POWER PLANTS

A. KUHLMANN AND F.-J. ADAMSKY
TECHNISCHER ÜBERWACHUNGS-VEREIN REINLAND e. V.,
COLOGNE, FEDERAL REPUBLIC OF GERMANY

(Presented by E. MORGNER)

Abstract — Résumé — Аннотация — Resumen

LIMITS TO THE RECOGNIZABILITY OF FLAWS IN NON-DESTRUCTIVE TESTING STEAM-GENERATOR TUBES FOR NUCLEAR-POWER PLANTS. In the Federal Republic of Germany there are nuclear reactors under construction with steam generators inside the reactor pressure-vessel. As a result design repairs of steam-generator tubes are very difficult and cause large shut-down times of the nuclear-power plant. It is known that numerous troubles in operating conventional power plants are results of steam-generator tube damages. Because of the high total costs of these reactors it is necessary to construct the steam generators especially in such a manner that the load factor of the power plant is as high as possible.

The Technischer Überwachungs-Verein Rheinland was charged to supervise and to test fabrication and construction of the steam generators to see that this part of the plant was as free of defects as possible. The experience gained during this work is of interest for manufacture and construction of steam generators for nuclear-power plants in general.

This paper deals with the efficiency limits of non-destructive testing steam-generator tubes. The following tests performed will be discussed in detail:

(a) Automatic ultrasonic testing of the straight tubes in the production facility;
(b) Combined ultrasonic and radiographic testing of the bent tubes and tube weldings;
(c) Other non-destructive tests.

LIMITATIONS DE L'EFFICACITÉ DE LA DÉTECTION DES DÉFAUTS PAR ESSAIS NON DESTRUCTIFS DE TUBES DE BOUILLEURS POUR CENTRALES NUCLÉAIRES. En Allemagne, on construit actuellement des génératrices nucléaires dans lesquelles les bouilleurs sont installés à l'intérieur du caisson étanche du réacteur. Il s'ensuit que les réparations des tubes des bouilleurs sont très difficiles et provoquent de longs arrêts des centrales nucléaires. On sait que de nombreuses perturbations du fonctionnement des centrales classiques sont dues à des dommages dans les tubes des bouilleurs. C'est en grande partie en raison du prix de revient élevé de ces réacteurs qu'il est nécessaire de construire les bouilleurs notamment de sorte que le facteur d'utilisation de la centrale soit aussi élevé que possible.

C'est le « Technischer Überwachungs-Verein» de Rhénanie qui a été chargé de surveiller et de contrôler la fabrication et le montage des bouilleurs, pour garantir que cet élément de la centrale soit aussi exempt que possible de défauts. L'expérience acquise dans l'exécution de ces travaux peut être très utile pour la fabrication et le montage des bouilleurs de n'importe quel type de centrale nucléaire.

Le mémoire traite des limitations de l'efficacité des essais non destructifs de tubes de bouilleurs. Les auteurs discutent plus particulièrement les essais ci-après:

a) Contrôle automatique par ultrasons de tubes droits dans l'usine de production;
b) Contrôle combiné, par ultrasons et par radiographie, de tubes coudés et de soudures;
c) Autres contrôles non destructifs.

ПРЕДЕЛЫ ЭФФЕКТИВНОСТИ НЕДЕСТРУКТИВНОЙ ДЕФЕКТОСКОПИИ ТРУБ ПАРОГЕНЕРАТОРОВ ЯДЕРНЫХ ЭЛЕКТРОСТАНЦИЙ. В ФРГ строятся ядерные реакторы с парогенераторами внутри корпуса реактора под давлением. При такой конструкции очень трудно ремонтировать трубы парогенераторов, что ведет к большим простоям ядерной электро-

станции. Известно, что многочисленные неисправности, встречающиеся на обычных электростанциях, являются результатом повреждений труб парогенераторов.

Ввиду высоких общих затрат необходимо строить парогенераторы так, чтобы загрузка их по возможности была высокой.

Объединению технического контроля Рейнланд поручено осуществлять наблюдение и контроль за изготовлением парогенераторов, чтобы эта часть электростанций была, по возможности, свободна от каких-либо недостатков. Полученный при осуществлении этой работы опыт представляет в общем интерес для производства и строительства парогенераторов для ядерных электростанций.

Доклад касается пределов эффективности контроля труб парогенераторов без их разрушения. Обсуждаются в деталях следующие выполненные виды контроля:

а) автоматическая ультразвуковая проверка прямых труб на производящей установке;
б) комбинированная ультразвуковая и радиографическая проверка гнутых труб и сварок труб;
в) другие виды недеструктивного контроля.

LIMITES PARA DISTINGUIR LOS DEFECTOS EN EL ENSAYO NO DESTRUCTIVO DE TUBO PARA GENERADORES DE VAPOR DESTINADOS A CENTRALES NUCLEARES. En la República Federal de Alemania se están construyendo reactores nucleares con generadores de vapor situados en el interior del tanque de presión. Las características de este modelo dificultan considerablemente la reparación de los tubos del generador que puede llegar a paralizar la central nuclear por largos perfodos. Como es bien sabido, muchas de las dificultades para mantener en funcionamiento las centrales nucleares de tipo clásico provienen de averías en los tubos del generador de vapor. Por ello, y teniendo también en cuenta como razón no menos importante el elevado costo total de esos reactores, es preciso construir los generadores de vapor de tal manera que el factor carga de la central sea lo más elevado posible.

El Technischer Überwachungs-Verein Rheinland se encarga de dirigir e inspeccionar la fabricación y la construcción de generadores de vapor para que esa parte de las instalaciones carezca en lo posible de defectos. La experiencia adquirida a ese respecto ofrece además interés para la fabricación y construcción de los generadores de vapor que se destinan a las centrales nucleares en general.

En la presente memoria se examinan los límites de rendimiento del ensayo no destructivo de los tubos para generadores de vapor. Se describen minuciosamente los siguientes ensayos:

a) ensayo ultrasónico automático de los tubos rectos en la fábrica misma;
b) ensayo combinado, ultrasónico y radiográfico, de los tubos curvados y de las soldaduras;
c) otros ensayos no destructivos.

If the steam generator of a nuclear-power plant is located inside the reactor pressure-vessel, the design will be so compact that accessibility and replaceability are limited only to a very small degree. The risk of expensive repairs and long down-times justifies the requirements for a better quality of the structural members, particularly for flawless tubes and their connections – and evidence of lack of flaw through a thorough inspection.

The Technischer Überwachungs-Verein Rheinland was authorized to inspect and to supervise the manufacture and the assembly of a steam generator, sited in a very narrow space. The inspection was carried out within time limits whereby expenses were not narrowed down. This paper deals with the applied test methods, the limits of their statements and the experiences gained in rejecting flaws, because this is of general interest for the fabrication and the assembly of such steam generators.

The way to maximum operating reliability begins in the design stage, which must above all consider the manufacturing methods which will result from the design. The tube manufacturers and constructors must apply their simplest and most reliable methods of manufacturing. The assembly must be carried out by trained experts who bear a large share of the responsi-

bility because, when the steam generator is installed, a qualitative flaw check is no longer possible, either during operation or in an integral test.

The many tests and examinations interspersed in the whole manufacturing process must be planned by persons who have a well-founded ability to judge, based on a thorough knowledge of the manufacturing methods and the demands made on the unit in operation. Those examinations which serve to assess the durability by supplying numerical values (e.g. tensile strength, pressure test, leakage test) are easy to judge and will not cause misunderstandings even for laymen, since the results need only be compared with the reference values laid down in the regulations or standards. Even the extremely subjective mode of judgement applied in visual inspection or in the ring-drifting test will only rarely cause serious differences of opinion. The same is to be applied to the surface-testing methods (dye penetration and magnetic powder methods), and in fact for all testing methods which furnish a reliable illustration of the flaw and reserve the possibility of a simple control check.

This is also true for the ultrasonic test as long as it is used as a measuring unit only (wall thickness). However, this method is to be used for locating flaws, and for sorting out the usables and the rejects, with the aim of obtaining the highest degree of flawlessness, after which a number of concessions may be made in regard to the recognizability of flaws and especially to the rejections during testing. For the eddy-current test, the same applies within its range of application. Both these methods are real mass-testing methods when applied to tube testing. Both methods do not give an actual illustration of the flaw, and their indicating sensitivity depends considerably on the location and nature of the flaw. Confirming tests can only be made occasionally as spot checks. In the case of internal flaws, this requires expensive macro-ground sections, which nevertheless can only give an incomplete demonstration of the flaw since it will only become visible in one cross-sectional plane. It will only very rarely be possible to make several closely-spaced cuts through the flaw.

X-ray testing occupies a special position. While this method will supply the experienced tester with a real illustration of the flaw, misinterpretations are also possible with this method when the quality requirements are increased. It is known that X-ray tests have a low sensitivity for unfavourably located separations. If the flaw lies inside the tested cross-section of the material, only the ultrasonic method can be used as a check test.

It is not surprising that even today, after many years' experience with the various non-destructive testing methods, long discussions still ensue, particularly among experts, about the interpretation of flaw indications. This could be avoided if the principle were always followed of using the testing methods, not only because of their applicability, but more important, according to their ability to indicate flaws which experience has shown to occur during the various manufacturing steps. The more reliable the test result is to be, the higher will also be the frequent apparently unjustified rejections during testing. What is justified in such a case can be decided only by the value of the object and by the consequences which may possibly result from an undetected flaw.

If we examine the possibilities one by one, the manufacture and consequently the testing of steam generators can be divided into three main sections:

(1) Straight pipe (Manufacture)
(2) Pipe bends (Fabrication)
(3) Welding seams (Assembly)

In the following, these three sections will be discussed successively.

1. Straight pipe

Testing of the straight pipe is aimed at detecting flaws which run predominantly in a longitudinal direction. It is inherent in the nature of the manufacturing process that the greatest flaw frequency lies in this direction. In view of the numerous pipes to be tested, only those methods can be considered which permit a high speed in testing, otherwise such mass testing could not be carried out economically. Two testing methods are suitable: ultrasonic testing in immersion technique and the eddy-current testing method. The latter has by far the highest testing speed, but with the limited experience available up to now, this method is applicable with sufficient reliability only to the smaller pipe dimensions. Besides, this method has not yet been proven sufficiently in practice, and is therefore not yet universally applicable.

In the Federal Republic of Germany, two different systems for ultrasonic testing in immersion technique are at present being applied. In both, the bundle of ultrasonic waves is introduced into the pipe simultaneously in both circulating directions in order to be able to detect flaws located unfavourably in relation to the ultrasonic direction. However, the two systems differ basically in their design and construction. In one case, a testing block in which are mounted two probe pairs in two testing levels, connected in T/R circuit (separate transmitter and detector), rotates around the pipe at 3000 rpm; the pipe is moved through the testing equipment in such a manner that it is spirally probed over its whole length. The probes are tightly imbedded in the testing block.

In the second method, three probes are mounted in a testing block adjustable parallel to their own axis and vertically to the pipe axis. The testing block is spring-mounted. The pipe is moved through the testing block in a rotating manner. The probes operate on the impulse-reflection system, i.e. they are at the same time transmitter and detector. Two of the three probes are arranged for the emission of transverse waves directed at the pipe circumference, while the third probe emits surface waves, also directed at the pipe circumference. With a sufficiently good pipe surface, this arrangement makes it possible to distinguish between external and internal flaws.

In both testing methods, adjustable monitors permit an automatic signal evaluation. These monitors control spray guns which mark the flaw on the pipe. As a check for the operator of the testing plant, an acoustical signal is given in addition to the light signal on the monitor whenever an indication exceeds the pre-set tolerance level.

The sensitivity setting is made with the aid of a test flaw with defined outer and inner grooves. The use of such a test flaw for checking the sensitivity is the only possibility for reproducibly testing larger quantities of pipes of one dimension at the same sensitivity level.

For testing the pipes of our steam generator, the second method was used. The sensitivity level was increased to such an extent that in many

cases the normal surface roughness of the pipe, caused during the manufacturing process, gave indications above the tolerance level. Therefore, a large part of the pipes had to be surface-ground before the final ultrasonic test could be made.

Radial external longitudinal flaws of 0.1 mm depth could usually be detected with sufficient reliability. Through the examination of numerous ground samples it was shown that an internal flaw located in radial direction had to have a slightly greater depth to give the same indication as the external flaw. However, dish-shaped flaws located at an angle in the pipe wall required a multiple of this borderline depth if they were to be reliably indicated. The radial flaw will be sure to reflect the ultrasonic wave bundle from both sides. The flaw located around under about 45° to the pipe wall will reflect the wave bundle from one side only. For this reason, ultrasonic testing of tubes must always be made in both directions. A flaw having a very shallow course will hardly be detectable, since the wave bundle will be reflected off one side and will peter out from the other side without giving an echo.

Equally difficult to detect – and frequently not detectable at all – are flaws located at an angle or vertically to the pipe axis. Fortunately, serious flaws of this type occur only singly. If they are major flaws, some indication of them will usually be given in one of the other tests made. In this steam generator, one such flaw, slanted at about 45° to the pipe axis, was discovered by a helium leakage test which was interposed during the assembly, when the faulty pipe had already been installed. The pipe could not be removed again without endangering the neighbouring pipes, so that examination was not possible. The corresponding length of pipe was by-passed.

If such flaws are to be eliminated, then this dead area must also be subjected to inspection through the arrangement of additional probes. This increases the installation costs and also increases the complexity of the testing equipment but it will, in the final analysis, yield more complete test results. The final uncertain factor which would remain would be the dish-shaped flaw lying at an angle in the pipe wall, apart, of course, from incidental errors and disturbances in the testing equipment itself. The conclusion drawn from all this is that even with a refined method for ultrasonic testing of pipes, a complete test result cannot be expected in every respect.

2. Pipe bends

Because of the generally required close packing of tubes in steam generators for nuclear-power plants, very small bending radii usually result, depending on the design. In the present case, pipe bends with a radius/diameter ratio of about 1.0 were used.

Since pipe dimensions of 28 to 42.5-mm outer diam. and 3.5 to 4-mm wall thickness were used, cold-bending was out of the question for these tight-bending radii. To stay within the required limits of pipe ovality, the bends had to be made in several steps, in part with sand filling. The final bend shape was obtained by a final pressing in a die. Then the complete bend was normalized. The scale caused by the hot-bending and the annealing was to be removed by simultaneous internal and external pickling of the pipes.

It is understandable that, with such a large number, almost 6000, reversing bends for this order and with such an extreme deformation, a large flaw

occurrence was to be expected. The tests to be carried out were planned with this in mind.

First, a wall-thickness measurement was taken with ultrasonic waves over the whole drawn bend zone. The measurement was made with a transmitter-receiver probe which permitted determination of the wall thickness to within ± 0.1 mm. All bends, which were below a certain minimum wall thickness, were rejected. Such a measurement with the tolerance given can be designated as reliable, since the tester checked the calibration of the testing unit after each bend by comparing it with a reference piece whose wall thickness was known. The tolerance range of the unit was compensated by being adding on to the required minimum wall thickness.

More difficult was a test of the bend for separations created during the bending operation, a distinct possibility in view of the large amount of deformation taking place and the difficulty of proper heat application during the bending operation. Because of its shape, the compressed inner side of the bend cannot be ultrasonically tested. The curves of the saddle-shaped surface are too tight to permit a positive guiding of the probe and sufficiently good coupling. But this examination could be justifiably dispensed with since separations are not expected to occur in the compression zones.

In the drawn area of the bend, i.e. from the neutral grain to the drawn outer grain, such an examination can, however, not be dispensed with. But this zone could not be covered by one single testing operation. The all-in-planes curved surface of the pipe bends required the use of various differently ground probes to obtain sufficient coupling.

Easiest to test was the outer grain, since the probe ground to fit this surface could be moved along the longitudinal direction of the bend without hindrance. More difficult was the testing of the zones pointing towards the neutral grain. Here, in every case there were unfavourable coupling conditions because of the almost linear contact of the probe.

The testing unit adjustment was such that a 0.5-mm-deep rectangular cut on the inside of the bend at a distance of 30 mm from the angle-probe showed a full-scree deflection on the viewing screen. It was agreed that all indications which exceeded half the screen height at this setting should be followed up by subjecting the corresponding bends to closer examination.

At first such a sensitive setting of the testing unit caused difficulties; especially with the 42.5-mm-outer-diam. pipe which, because of its radius/diam. ratio of less than 1.0, had to be bent with sand filling. Many significant indications were found, but closer examination revealed that they were caused by scale which tightly adhered to the inner-pipe surface. A separation of these indications from true flaw indications proved most difficult. The removal of the scale was not only necessary for proper testing, but had already been ordered previously with a view to trouble-free operation. Because of a partial sintering of a layer of bending sand to the inner surface of the bend, the annealing scale acquired a glazed consistency which resisted complete removal through pickling. The only remedy was to change the signalled points through mechanical treatment (sandblasting of the inside, jogging or hammering from the outside) in such a way that a clear conclusion could be drawn concerning their origin. A check test was the X-ray examination which, with a correspondingly good picture quality, under

certain circumstances makes the recognition of scale deposits on the inside of the pipe possible.

One X-ray examination had already been made before the ultrasonic test in one direction (vertically to the bend plane) to remove the uncertainties of the ultrasonic test in regard to the neutral zone. This revealed short but very deep individual breaks in three bends; the flaws were located radially and started on the inner surface of the pipe. After a thorough examination they were recognized as breaks due to copper diffusion which came into being because of copper traces which happen to be present in the bending sand. From the characteristics of such breaks it could be concluded that these were probably individual cases. Because of their natural depth, a fairly certain recognition on X-ray examination could be assumed.

During the ultrasonic tests, a series of small separations were discovered on the bend surface which had a depth of only a few tenths of a millimetre. These flaws were corroborated by the magnetic powder test. After grinding out these flaws, under continuous check through the magnetic powder test, the remaining wall thickness was re-measured ultrasonically.

For the sake of completeness, it should also be mentioned that during the X-ray examinations a series of internal flaws were distinctly indicated. An inspection with suitable internal viewing units also showed an alarming flaw picture. But when macro-ground sections were made of some of these spots, it was found that the flaw depth was a maximum 0.1 mm and were thus acceptable.

The final test was an internal water-pressure test with only 1.1-fold safety against the cold yield point of the pipe material. The purpose was to remove uncertainties which might still have existed after completion of the other tests. No flaws were discovered with this test. To summarize, the following can be said regarding the testing of pipe bends:

The flaws which were found, particularly the deep, very short internal cross-tears caused by copper diffusion, have shown that such a thorough examination was necessary. It is understandable that, when flaws were found, the examination was even more thorough. The testing costs were very high, since only a manual examination of each individual piece could be made. But it is this very fact which makes the completeness of the test result very strongly dependent on the thoroughness of the tester. Fatigue and waning attention to work cannot be excluded when so many parts must be examined. No doubt the water-pressure test at high internal pressure has supported the reliability of the tests, but it is questionable if it has removed all doubts. It is a known fact that pipes with serious flaws can sometimes withstand tests of unbelievably high internal pressures. It must also be kept in mind that this is a static stress, which can never fully replace the varying stresses occurring in actual operation.

3. Welding seams

The non-destructive testing of welding seams has always posed certain problems. It is well-known that, as far as fusion leaks and fine tears are concerned, the X-ray examination is a poorer indicator than the ultrasonic test, while it has distinct advantages in the demonstration of other faults.

When applied to a search for flaws with more serious consequences, the ultrasonic test may thus be considered the more sensitive testing method. But, on the other hand, it causes some uncertainties, particularly in that it very easily gives excessively strong indications for unimportant form echos (root sagging, final run). This is particularly true when the method is applied to welding seams on thin-wall thicknesses, where surface indications are more difficult to distinguish from really serious faults because of the slight differences in the sound-path length. In the round welding seams on the pipes of the steam generator to be tested, there were a few factors present which could cause some uncertainty. The accessibility for X-ray examination was often poor, and the pipe wall thickness was within a range of only a few millimetres. Therefore, it was necessary at the very beginning to remove the hindrances existing under normal conditions for non-destructive testing.

It is known that a welding seam on such pipe dimensions as in this case can only be considered completely X-ray examined if it has been X-rayed from various directions, taking into consideration the location of the seam flanks. Only then can a lack of fusion be reliably shown on the film. This, however, results in very high testing costs because, among other reasons, such an examination can only be made outside the normal working hours because of the radiation danger. An examination in this thorough manner was not possible because, for construction reasons, it was impossible to create the necessary accessibility to the welding seams. Because of the poorer picture quality, the use of radioactive isotopes was out of the question. Thus, it only remained to apply ultrasonic testing by excluding, as far as possible, the particularly pronounced interference echos to be expected with this wall thickness.

To obtain a smooth root sagging, all welding seams (about 5000) were made with the tungsten inert gas method, the pipe being filled with inert gas. Even with this welding method, a certain amount of training of the welders to make such a test-acceptable root was necessary, the more so as care had to be taken that, when gas-welding the covering beads, the root would after all sag through to the inside. The final run was ground to create the best possible conditions for ultrasonic testing.

At first efforts were made to record the ultrasonic tests, which could only be carried out manually, on a recording strip. But this soon turned out to be impractical, since, for example, at the high sensitivity level of the unit small double indications in the range of the monitor shutter added up and caused a reading above the tolerance level, which led to the unjustified rejection of that particular welding seam.

The whole examination went off rather smoothly in that the ultrasonic test was carried out first. If indications resulted, then the possible flaw at that point was examined more closely by means of a well-aimed X-ray. In addition, welding seams without ultrasonic indications were X-rayed from one constant direction. Of course, in line with the value of the object, the standard of judgement was set very high. After a certain time, the welders became used to the increased demands and the rejects stayed within acceptable limits. Thus, in this case everything possible was done from the design and construction side to make a complete test result possible. Of course, also in this case the previously mentioned uncertainties inherent in

the manual ultrasonic testing method were present. But the ultrasonic tests were always immediately followed by the X-ray examination.

The greatest value must be placed on the importance of the direct time-sequence of manufacture, testing and check-test, in view of the educational effect, which cannot be over-emphasized. Summing up, it must be said that it is very difficult to achieve the stipulated complete freedom from flaws on such a complicated and poorly accessible construction as the above-cited steam generator. However, through the carefully planned use of the non-destructive testing methods throughout the manufacturing process, and with consciously chosen extremely severe standards, an optimum can be achieved which would, as far as can be judged, seem to warrant the safety of the construction.

Below is a short sketch about how the high testing costs required for a largely trouble-free steam generator are to be evaluated from an economic viewpoint.

Based on our experience and adjusted to the conditions prevalent in the Federal Republic of Germany, we have shown in Fig. 1 the additional testing costs (curve a) for a steam generator as a function of the electrical output of an atomic-power plant. These costs are the difference between the normal testing costs for steam generators of conventional boiler construction and the increased expenditures for atomic-power-plant steam generators. Of course, curve a is valid only in the case where the steam required for generating electric power is obtained totally from steam generators. Our analysis showed that the essential part of the testing costs for steam generators is practically proportional to the length of pipe installed. In a second curve c we have plotted the break-down costs per day as a function of the electrical output. As an average of various statements received, we have calculated at a rate of 0.03 DM/kWh for the costs engendered through a breakdown in current generation. The relationship between curves a and c is also shown in Fig. 1 and states how many breakdown days must be saved during the life of the installation to cover the additional testing costs. It will be evident from the chart that, for electrical outputs of above 100 MW, this relationship is fairly constant and amounts to only about two to three days.

It should be realized that, at a theoretical operating time of 7000 h/yr and an assumed life of the atomic-power plant of 10 yr, i.e. 70 000 h, a breakdown for three days influences the degree of availability of the plant by only about 0.1%.

Figure 2 shows the relationship between the additional testing costs and the costs of the installation as a function of the electrical output. Within the range of accuracy possible here, this relationship is also constant and amounts to about 0.1 to 0.2%.

Summing up, we would like to conclude from these figures, which understandably are only approximately correct, that the high testing costs for steam-generator pipes seems quite justified from an economic point of view. Our experience has shown that, owing to the extensive testing procedure, quite a number of flaws were discovered which cannot be detected with less extensive tests, and can then lead to considerable breakdown periods for an atomic-power plant.

The statement made in the preceding paragraph seems justified because generally, in atomic power plants, damage through poor quality of the coolant,

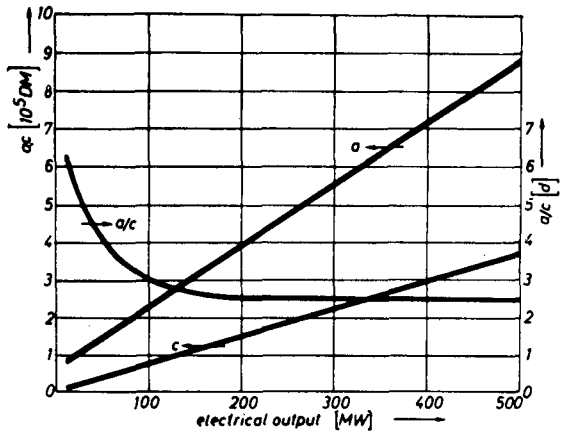

Fig. 1

Additional testing cost (a), lost generated power cost per day (c) and ratio of additional testing cost to lost generated power cost per day versus electrical output of a nuclear-power plant

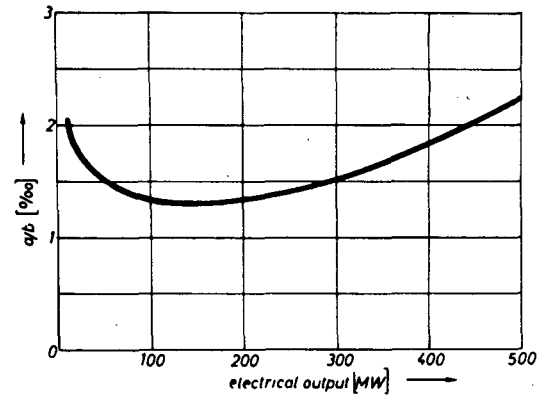

Fig. 2

Ratio of additional testing cost (a) to plant cost (b) versus electrical output of a nuclear-power plant

localized overheating of the steam-generator pipes, or other influences favouring corrosion, are not to be expected. As a rule, damage can only be expected on such pipes or pipe connections, which already have a flaw which originated in the manufacturing or construction process.

It was stated that, in spite of all test requirements, it still would not be possible to exclude all material flaws on steam generators. For this reason, among others, we are therefore inclined to conclude that large atomic-power plants should be so designed that the steam generator and atomic reactor are separated from each other and ample possibilities for repairs are provided.

The results of our tests have also shown that, in the case of compact reactor construction, which may be desirable for small outputs and mobile

units, the steam generator can be built with sufficient safety against breakdowns if a sufficiently extensive testing procedure is followed, and that the expenditure for such extensive testing is quite justifiable economically.

DISCUSSION

Z. PAWŁOWSKI: For checking the pipe bends, what was the frequency of the ultrasonic shear waves used, and what was the refraction angle of the probe?

E. MORGNER: The frequency was 4 MHz and the refraction angle of the probe was 45°. This angle was used because of the higher sensitivity in detecting cracks which begin in the inner or outer surface of the tube bends.

Z. PAWŁOWSKI: What was the refraction angle of the probe for checking the welded seams, and what was the wall thickness of the tube?

E. MORGNER: The wall thickness of the tubes was 3.5 to 4 mm, and the refraction angle of the probe was 60°.

Z. PAWŁOWSKI: Did you not find that probes with this angle have poor sensitivity for crack detection?

E. MORGNER: We agree with you that the sensitivity for detecting cracks with the 60° angle is not the best in general. We selected this angle for two reasons. The sensitivity level was very high, and therefore we could expect that even with a 60° angle cracks would be detected. This was established in previous tests. Also, welding preparations lead to the assumption that lack of fusion will appear at an angle of 30° to the radial direction. Hence the 60° refraction angle was the best for detecting this severe welding fault.

HIGH-VOLUME NON-DESTRUCTIVE TEST APPLICATIONS AT THE HANFORD ATOMIC PRODUCTS OPERATION

D. C. WORLTON
PACIFIC NORTHWEST LABORATORY,
BATTELLE MEMORIAL INSTITUTE,
RICHLAND, WASH., UNITED STATES OF AMERICA

Abstract — Résumé — Аннотация — Resumen

HIGH-VOLUME NON-DESTRUCTIVE TEST APPLICATIONS AT THE HANFORD ATOMIC PRODUCTS OPERATION. Safety and efficiency of critical Hanford processes are assured with rapid, reliable, and automatic non-destructive tests. High-sensitive eddy-current and ultrasonic inspection systems are in routine use in the field and in manufacturing production processes to provide maximum quality assurance of large volumes of material in minimum inspection time.

This paper describes inspection systems being used to ensure quality of Hanford's production nuclear-fuel manufacturing processes. Operated as regular in-line manufacturing equipment, these systems employ ultrasonic attenuation measurements to monitor grain structure of bare uranium fuel cores, ultrasonic and eddy-current techniques to ensure adequate bonding and thickness of 0.040 in aluminium cladding on canned elements, and novel wide-band, high-resolution ultrasonic inspection techniques to detect defects in the fuel end-weld closures. Combined eddy-current and ultrasonic tests are applied simultaneously to perform a complete fuel-element inspection on a nine-second cycle; defective elements are automatically segregated from the process stream.

Emphasis is given to advanced ultrasonic test methods of inspecting thin-walled, fuel-sheath tubing. Special highly focused transducers are used with wide-band circuitry to generate pure shear waves in 0.015-in-thick wall tubing. Lamb and other complicated wave motions are excluded so that tests results are readily interpreted and reproduced. Novel, economical methods of producing defect standards have been developed, as have critically important methods of ensuring uniform operating characteristics of the transducers themselves. Automatic tubing inspection equipment has been developed, and results of its routine use in testing some 30 000 ft of tubing are summarized.

Finally, eddy-current techniques developed specifically for inspecting installed heat-exchanger tubing are reviewed. The technique employs novel read-out features which plot defect indications as oscilloscope patterns whose size and shape reveal defect magnitude, location within the tube wall, and depth. Probe wobble and harmless tube kinks and bends are plotted with a characteristic pattern readily distinguishable from genuine defects. Results of applying the test to 750 000 ft of installed tubing under difficult field conditions are summarized.

APPLICATIONS INDUSTRIELLES DES ESSAIS NON DESTRUCTIFS A L'ÉTABLISSEMENT NUCLÉAIRE DE HANFORD. On a recours à des essais non destructifs — rapides, sûrs et automatiques — pour assurer la sécurité et l'efficacité des opérations critiques à Hanford. On utilise couramment des méthodes de contrôle très sensibles, fondées sur les courants de Foucault et les ultrasons, pour vérifier avec le maximum d'assurance et dans le minimum de temps la qualité d'importants volumes de matières et produits.

Le mémoire décrit les appareils de contrôle utilisés pour s'assurer de la qualité de la fabrication des combustibles nucléaires à Hanford. Ces appareils, qui font partie intégrante de l'équipement de fabrication, appliquent le principe de l'atténuation des ondes ultrasonores pour contrôler la structure granulaire de barreaux d'uranium non gainé, les ultrasons et les courants de Foucault pour contrôler la liaison entre l'uranium et sa gaine en aluminium ainsi que l'épaisseur de cette dernière (1 mm), et une nouvelle méthode ultrasonore (large bande, haute résolution) pour la détection des défauts dans les soudures aux extrémités des cartouches de combustible. Des méthodes combinées (courants de Foucault et ultrasons) sont appliquées simultanément pour l'inspection complète d'un élément combustible en neuf secondes; les éléments défectueux sont rejetés automatiquement.

Le mémoire expose en détail les méthodes ultrasonores perfectionnées pour le contrôle des gaines de combustible à parois minces. Des traducteurs spéciaux à forte focalisation sont utilisés avec un circuit à bande

large pour produire des ondes de rotation pures dans un tube de 0,37 mm d'épaisseur. Les ondes de Lamb et autres mouvements ondulatoires complexes sont exclus, de sorte que les résultats peuvent être facilement interprétés et reproduits. On a mis au point des méthodes nouvelles et économiques de production d'étalons de défauts, ainsi que des méthodes permettant de donner aux traducteurs eux-mêmes des caractéristiques uniformes de fonctionnement. On a également mis au point un appareil d'inspection automatique des tubes; le mémoire résume les résultats de l'utilisation courante de cet appareil pour contrôler quelque 10 000 m de tubes.

Enfin, le mémoire passe en revue les méthodes fondées sur les courants de Foucault qui ont été mises au point spécialement pour l'inspection des tubes des échangeurs de chaleur après montage. On a recours à un système inédit de lecture qui enregistre graphiquement les indications de défauts de la même manière qu'un oscillographe: l'amplitude et la forme du signal indiquent l'importance du défaut, son emplacement dans la paroi du tube et sa profondeur. Les petits mouvements de la sonde et les déformations sans importance de la surface du tube sont enregistrés selon une courbe caractéristique, facile à distinguer de celle que produisent les véritables défauts. Le mémoire résume les résultats de ce mode de contrôle pour 250 000 m de tubes installés.

ПРОВЕДЕНИЕ БОЛЬШОГО ЧИСЛА НЕДЕСТРУКТИВНЫХ ИСПЫТАНИЙ В "ХЕНФОРД АТОМИК ПРОДАКТС ОПЕРЕЙШЕН". Безопасность и эффективность критических процессов Хенфорда гарантируется быстрым, надежным и автоматическим способом испытания образцов без разрушения оболочки. Высокочувствительные токи Фуко и ультразвук находят свое обычное применение в этой области и в процессах изготовления изделий для того, чтобы обеспечить максимальную гарантию качества больших количеств материала за минимальный период времени.

Описываются системы, используемые для того, чтобы обеспечить качественность процессов Хенфорда по изготовлению изделий ядерного топлива. Действующие как обычное оборудование эти системы используют измерения ультразвукового затухания для того, чтобы проконтролировать структуру зерна активных зон неэкранированного уранового топлива, а ультразвуковой метод и метод токов Фуко для того, чтобы обеспечить соответствующую полосность и толщину 0,040 дюйма алюминиевого покрытия элементов в кассетах, и новый широкополосный метод с высокоразрешающей способностью ультразвукового обследования для обнаружения дефектов в сварных швах на стыках оболочки. Объединение испытаний с помощью ультразвука и токов Фуко применяется одновременно для того, чтобы провести полное обследование топливного элемента в девятисекундном цикле. Элементы с дефектом автоматически удаляются с поточной линии производства. Особый упор делается на усовершенствованные методы испытаний с помощью ультразвука по обследованию тонкостенных оболочных труб для топливных элементов. Используются специальные прерыватели с высокой фокусировкой вместе с широкополосной схемой для того, чтобы получить чистый срез волны в трубах толщиной 0,015 дюйма. Простейшие и более сложные волновые движения исключаются, поскольку результаты испытаний легко истолковываются и воспроизводятся. Разработаны новые экономические способы получения стандартов по дефектам, поскольку имеются чрезвычайно важные методы, обеспечивающие единообразие действующих характеристик самих преобразователей. Разработан прибор по автоматическому обследованию труб, и вкратце излагаются результаты его обычного использования по испытанию труб, общей длиной почти 30 тыс. футов.

И, наконец, рассматривается метод токов Фуко, разработанный специально для обследования установленных труб теплообменника. Этот метод несет в себе новые особенности, он регистрирует указания о дефектах на шкале осциллографа, размеры и конфигурация которого вскрывают величину дефекта, его расположение в стенке трубы и глубину. На диаграмме регистрируются колебания щупа и неопасные петли труб и изгибы вместе с характерным образцом, четко отличающимся от настоящих дефектов. Вкратце излагаются результаты применения этих испытаний для труб общей длиной 750 тыс футов, установленных в трудных полевых условиях.

ENSAYOS NO DESTRUCTIVOS EN GRAN ESCALA APLICADOS EN HANFORD. La seguridad y la eficiencia de las operaciones críticas efectuadas en Hanford se logran por medio de ensayos no destructivos rápidos, seguros y automáticos. Tanto in situ como en los procesos de fabricación se emplean normalmente sistemas de inspección de alta sensibilidad, ultrasónicos y por corrientes de Foucault, que aseguran la calidad máxima de grandes cantidades de material en un tiempo de inspección mínimo.

La memoria describe los sistemas de inspección que se emplean en Hanford para mantener la calidad de los procesos de fabricación de combustibles nucleares. Están intercalados en la cadena de producción y emplean

mediciones de atenuación ultrasónica para comprobar la estructura granular de barras de uranio sin revestimiento, técnicas ultrasónicas y de corrientes de Foucault para verificar la correcta unión y el espesor (0,040 pulg) del revestimiento de aluminio de otros elementos combustibles, y un nuevo sistema de inspección de banda ancha y elevada resolución que emplea ultrasonidos para detectar fallas en las soldaduras que cierran los elementos combustibles. Los ensayos por corrientes de Foucault y ultrasonidos se combinan aplicándolos simultáneamente para efectuar una inspección completa del elemento combustible en un ciclo de 9 s; los elementos defectuosos se retiran automáticamente de la cadena de producción.

La memoria destaca los métodos avanzados de ensayo ultrasónico para inspeccionar tubos de revestimiento de paredes delgadas. Se emplean transductores de alto enfoque, con circuitos de banda ancha, para generar ondas transversales puras en tubos de 0, 015 pulg de espesor de pared. Se excluyen las ondas de Lamb y otras ondas complicadas, de manera que es fácil interpretar y reproducir los resultados de los ensayos. Se han perfeccionado métodos nuevos y económicos para producir defectos tipo, así como métodos de importancia fundamental para asegurar la uniformidad de las características de funcionamiento de los transductores mismos. Se ha construido equipo para la inspección automática de tubos y la memoria resume los resultados obtenidos en el ensayo de unos 10 000 m de tubería. Por último, la memoria revisa la aplicación de las corrientes de Foucault que se han desarrollado específicamente para inspeccionar tubos ya montados en intercambiadores de calor. Emplea nuevos métodos de lectura que en un osciloscopio indican los defectos como perfiles cuyo tamaño y forma revela la magnitud, la posición dentro de la pared del tubo y la profundidad a que se encuentra el defecto. Las inestabilidades de la probeta y las deformaciones y pliegues inofensivos de los tubos aparecen con un perfil característico que se distingue netamente de los defectos reales. La memoria resume los resultados obtenidos con este método de ensayo, que se ha aplicado en condiciones difíciles a 250 000 m de tubería instalada.

INTRODUCTION

Industrial applications of non-destructive testing are most economically profitable when they can be applied to large volumes of material under rapid, reliable and routine operation. For maximum benefit, tests must be applied in the field or in a competitive manufacturing process where laboratory conveniences do not exist. The need for inspection techniques with these capabilities has promoted the growth of X-ray, fluorescent penetrant, magnetic particle, and similar methods even though they are intrinsically slow and difficult to automate. The newer electronic methods, such as eddy current and ultrasonic, while being extremely fast and readily adapted to automatic operation, are hampered by their susceptibility to instrument drift and faulty calibration, necessity for skilled data interpretation, sensitivity to trivial specimen parameters and other factors. These tests have thus been slow to be applied in those areas where they offer the greatest potential - the routine inspection of large quantities of material under difficult field conditions.

At the Hanford Operations of the United States Atomic Energy Commission (USAEC), a major effort has been devoted over the past several years to accelerate transition of these tests from laboratory to field use. This paper describes results in two major areas: The inspection of thin-wall tubing, and the automatic inspection of nuclear fuel.

I. THIN-WALLED TUBING TESTS

Modern technology uses tubing with diameters less than one inch and wall thickness less than 0.050 inch in tremendous quantities. The heat-

exchanger system of one Hanford nuclear installation alone uses about a million feet of this material. Typically, the quality of the tubing must be high, necessitating careful non-destructive inspection before installation. During operation, the tubing is normally subjected to rigorous environments. Since efficiency and safety of major installations is often critically dependent upon the continued integrity of its installed tubing, periodic inspection of this tubing is essential.

Tests are therefore necessary for the inspection of tubing both before and after installation. At Hanford, eddy-current tests have been developed for the inspection of installed tubing, and ultrasonic tests are used for the inspection of as-fabricated tubing. Each is discussed below.

1. Eddy-current test

The eddy-current test is particularly useful for inspecting installed tubing having restricted access. It readily scans with an internal probe the inside surface of long tubes where only the ends are accessible. It can also be readily adapted to a scan of the outside surface in instances where this is more convenient [1].

Its novelty with respect to existing tests lies in the increased information it provides regarding the defects which it detects, and the convenient manner in which this information is displayed. In essence, its principle of operation is based upon two key points: The impedance locus of a coil in motion with respect to a defect is a curve rather than a straight line, and the shape of this locus uniquely describes (to a first approximation) the nature of the defect, i.e., its position with respect to the outer and inner tube surface, its depth, and its size. An important related point is that probe wobble and its associated "lift-off" signal has, with proper instrument adjustment, a unique and readily identifiable characteristic locus.

These concepts are readily demonstrated experimentally. The impedance of a coil approaching a tubing irregularity varies non-linearly because of the apparent change of wall thickness and the difference in phase of the eddy currents with distance from the coil. It follows that two concentric differentially connected coils, one slightly displaced to the other, will provide an output which varies in magnitude and phase as the two coils pass over an irregularity.

The vectors shown in Fig. 1 demonstrate that these vector signals provide information regarding the nature of the defect. Here the vectors represent the peak output of two differentially connected 130-turn, 0.5-in-diam. coils as the coils move past various irregularities in a 5/8-in outside diameter (O.D.) 304 stainless-steel tube with 0.054-in wall. The coils are spaced 1/10 in apart and are driven at 200 kc. It is apparent that inner-surface flaws are readily distinguishable from outer flaws by the vector position, and that the vectors rotate as the defects increase in depth. It is noted that the probe wobble, or lift of signal, so troublesome to many eddy-current tests, has its own characteristic position easily distinguishable from the defect signals.

Useful application of these results requires the data be put in a form readily observed and interpreted by unskilled operators. This is accomplished by displaying the information as Lissajou patterns on a cathode-ray tube.

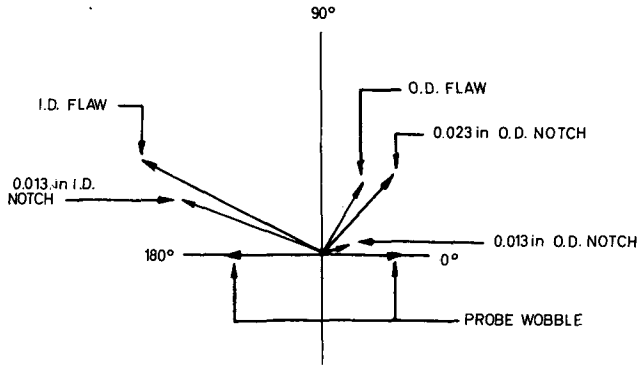

Fig. 1

Impedance vectors of coil corresponding to various tubing defects

In essence, the output signal is separated into quadrature components and separately fed on to the horizontal and vertical plates of a cathode-ray tube. The spot is deflected in first one direction and then the other as the two-coil probe passes over an irregularity. Because of the curvature of the impedance locus, and the physical displacement of the coils with respect to the irregularity, the spot motion is non-linear. The net result is a "figure-8" whose shape and axis of tilt approximately define defect depth and location. Signals arising from harmless tube conditions such as kinks, bends etc. degenerate the "figure-8" into a straight horizontal line.

Origin of the "figure-8" is illustrated in more detail in Fig. 2. The complex impedance locus f(d) of a single coil was plotted with measurements made at 0.025-in intervals as the coil moved past a 0.013-in deep by 1/8-in-long inner-surface notch. $d = 0$ is the coil starting-point where the defect makes no measurable effect on the coil, and $d = 0.175$ represents the coil centred over the notch. Test-coil wobble is in this case along arrow A. If now a second identical coil, separated from the first a distance d_1, is also moved along the tube it generates a signal $f(d - d_1)$. The differential output in this case is $f(d - d_1) - f(d)$. Point C on the curve of Fig. 2 is derived by letting vector OA represent the negative of the first coil output at $d = 0.150$. Since the output of the second coil is a function of $d - d_1$, its value at this point is $0.150 - 0.075 = 0.075$, assuming the coils are separated by 0.075 in. In the Figure this value is represented by the vector OB. The terminus of vector OC, the sum of OA and OB, locates a point on the "figure-8". Other points generated in a similar manner plot the complete figure. Actual oscilloscope traces for representative tubing irregularities are shown in Figs. 3 and 4. Correspondence of pattern shape to defect geometry is obvious. Figure 5 illustrates the arrangement of the coil inside the tube and response patterns for various defects.

An important application of the technique was made in inspecting ten heat exchangers of the type illustrated in Fig. 6 [2]. Each unit contained two thousand 60-ft-long tubes. The tubes were "U" shape, with the ends piercing a 5-ft-diam., 5-in-thick carbon steel tube sheet. The probe was blown into each tube end with a few pounds air pressure and manually with-

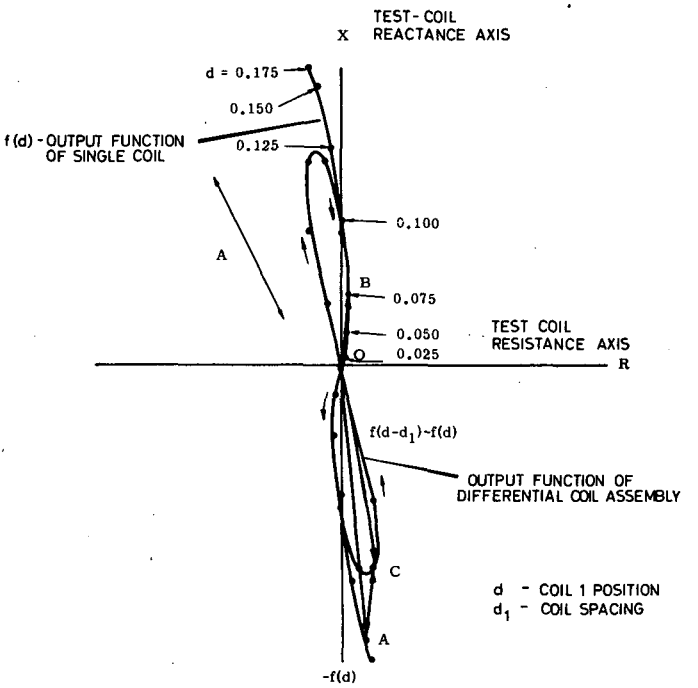

Fig. 2

Construction of "figure-8" from response of two differentially connected coils to 0.013-in-deep tubing defect

drawn at about 20 ft/min as the scan was made. Some six thousand tubes were tested in a 30-d period on a round-the-clock basis. Serious instances of intergranular corrosion were detected, an example of which is shown in the Figure.

In this application, it was desired to identify defects whose depth extended greater than 50% of the tube wall. Defect depth was estimated on the basis of the "figure-8" display with good precision in view of the difficult conditions under which the test was made. In no case did destructive examination fail to reveal defects predicted by the eddy-current test.

2. *Ultrasonic tests*

Although ultrasonic methods of inspecting uninstalled thin-wall tubing have been in use for years, results in many respects have not been satisfactory. Signal response is often dependent upon defect size and shape rather than being linearly dependent upon severity; uniform day-to-day calibration of test equipment is difficult, and satisfactory standardization of separate inspection installations is not possible with existing test methods. Full beneficial use of ultrasonic methods has been hampered by an incomplete understanding of basic propagation mechanisms of stress waves in thin, curved sections. Anomalies exist in data obtained with conventional practices which

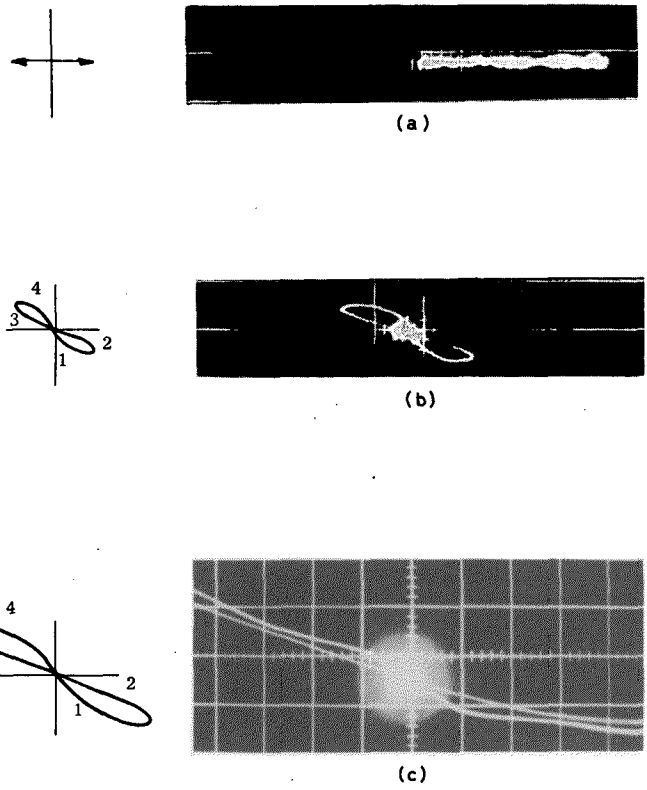

Fig. 3

Typical signal patterns
(a) Probe wobble
(b) 0.013-in I. D. notch
(c) Shallow I. D. ring

clearly demonstrate inadequacies of simple theories. Lamb-wave concepts are approximately valid for waves propagating in a direction parallel to the longitudinal axis of the tube, but are involved when curvature is taken into account for waves travelling in a circumferential direction. Complexity of the latter case is reflected in the fact that its mathematical solution has not been developed, so far as is known.

At Hanford, long-range research efforts have developed improved ultrasonic inspection techniques and have provided strengthened understanding of their technical operation. Very briefly, a major contribution of this study has been to side-step complete solution of the theoretical problem by developing experimental techniques which extend validity of simple shear-wave theories to the thin-wall case (wall thickness greater than 0.012 in). Complicated wave motions which resonate the tube wall, distort signal response depending upon defect orientation and shape, and make test results critically dependent upon incident beam angle and ultrasonic frequency, are avoided by

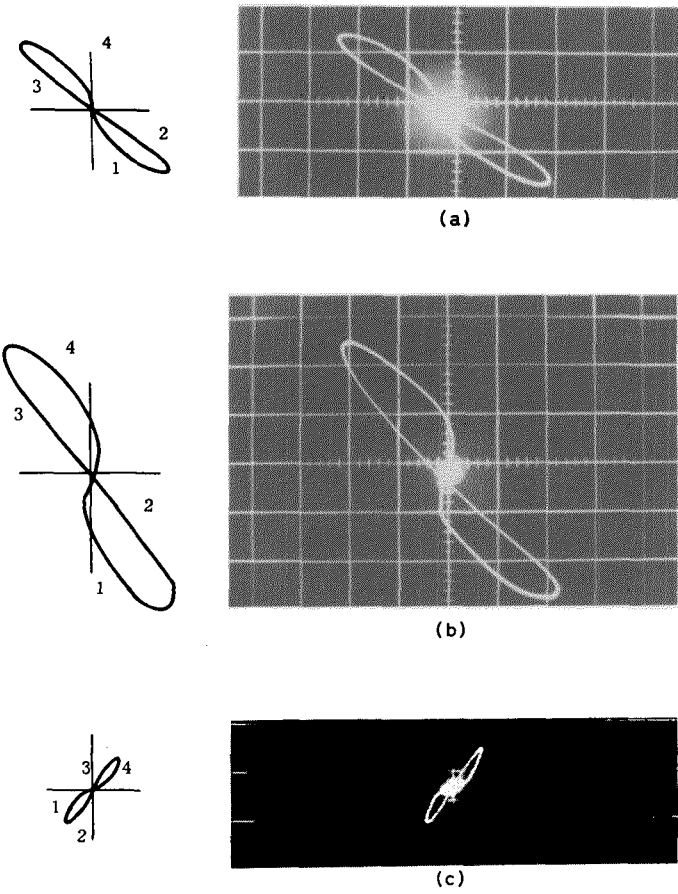

Fig. 4

Typical signal patterns
(a) 0.023-in I. D. notch
(b) 0.040-in diam. drill hole
(c) 0.023-in O. D. notch

use of small, highly focused, transducers whose diameters are less than one-half of the wall thickness. 3/16-in-diam. transducers with 0.008-in focused beam diameters are commonly used. Frequency band-widths are made as wide as possible; a 15-Mc centre frequency is employed, although this value is not critical [3].

Figure 7 illustrates the key point in the experimental approach. The data demonstrate that, under the given experimental conditions, shear waves only propagate in the tube wall in an uncomplicated zig-zag manner entirely analogous to the way shear waves travel in thicker sections. Waves impinge upon the inner- and outer-tube surfaces at discrete points only. Response amplitude to standard defects increases linearly as the discontinuity approaches the beam entry point. These data were obtained with the in-

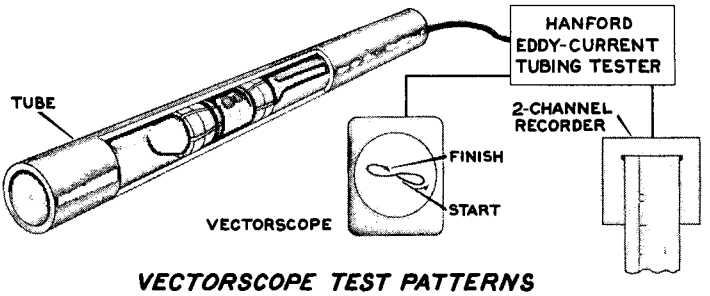

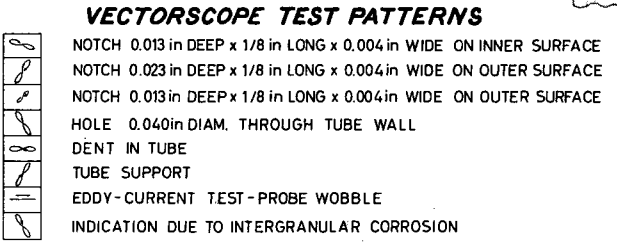

Fig. 5

Steam-generator tubing-test eddy-current tester arrangement

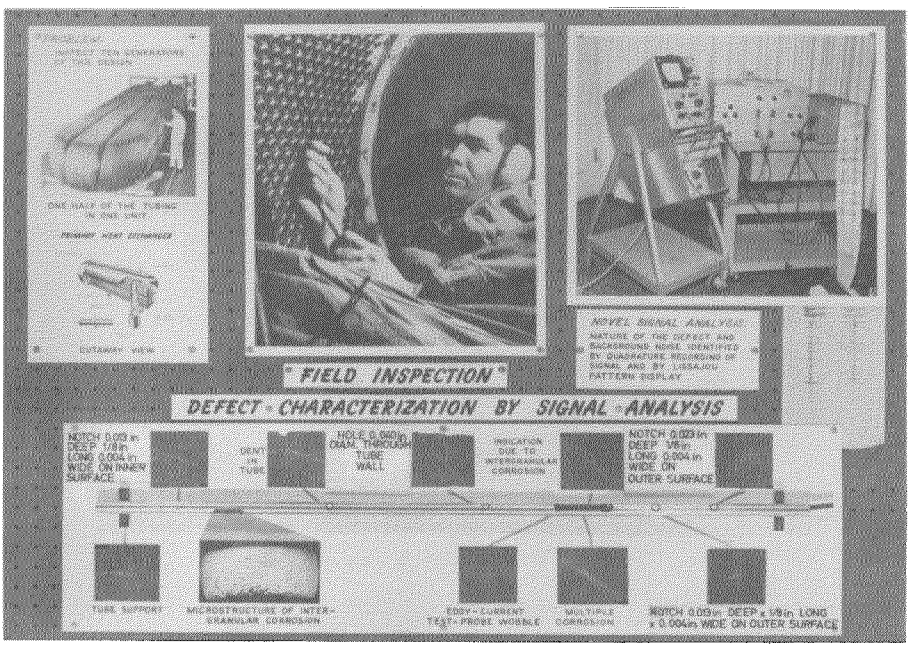

Fig. 6

Eddy-current testing N-reactor steam generators

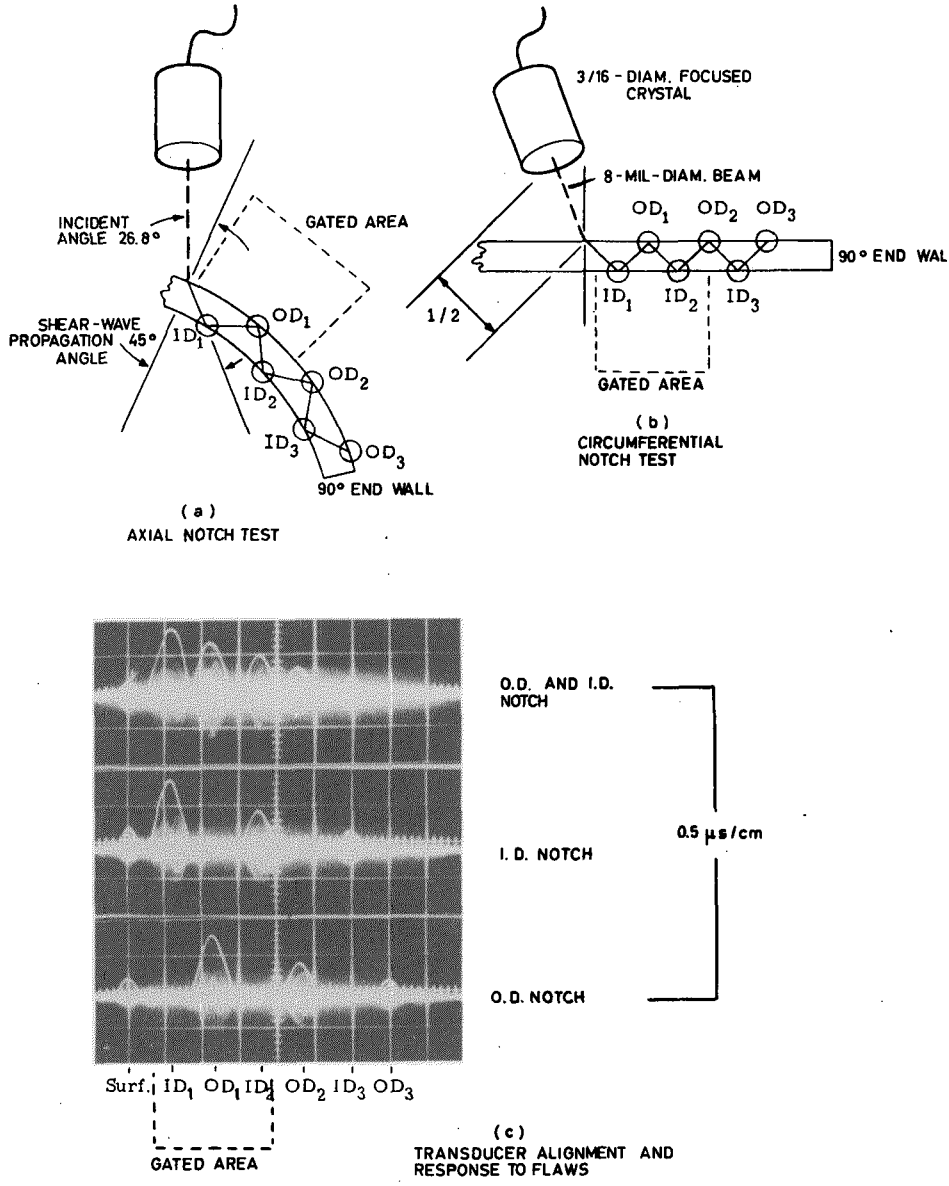

Fig. 7

Experimental arrangement of ultrasonic tubing test

cident beam angle purposely set to exclude the generation of longitudinal waves.

Data-defect-signal response as a function of defect-depth location with respect to inner and outer surface, and incident beam angle are shown in

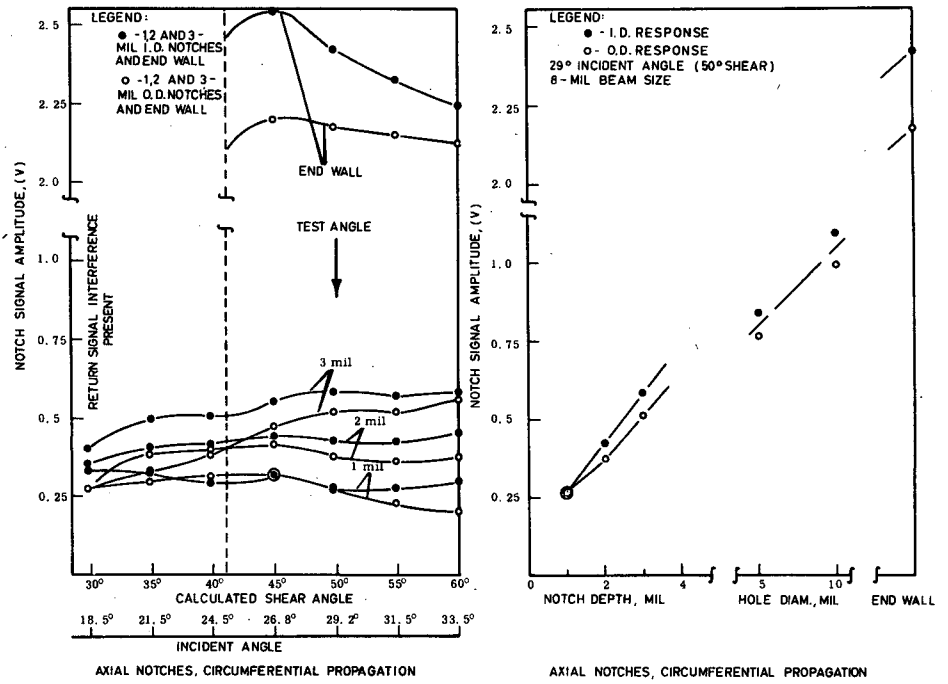

Fig. 8

Signal response as of defect depth,
position and incident beam angle for 0.012-in-thick Zircaloy tubing

Fig. 8 for axially-oriented defects in 0.012-in-thick Zircaloy tubes. Data from defects oriented in a perpendicular direction are essentially identical. It is noted that response increases with defect depth, and that notches located on the inner and outer surface respond with nearly equal amplitude. Sensitivity is capable of detecting notches 0.001 in deep, and amplitude response is not critically dependent upon incident beam angle. The important conclusion to be drawn from these data is that wide-band electronic circuitry, small transducers, and highly-focused beams make possible the inspection of thin-wall tubing with the same confidence and readily interpreted results as are obtained on thicker sections. This fact guided the development of equipment for routine inspection of fuel-sheath tubing. Summarized in Table I are extensive data which define optimum test procedures for tubing of various geometries and materials.

We proceed to a description of the equipment ultimately developed with a review of work done in evaluating transducer performance and the possible importance of transducer variables on the quality of test results achieved [4]. It was observed early that test-data anomalies were often traceable to inconsistencies in the transducers themselves. Supposedly identical transducers operating in a given experimental arrangement did not necessarily give equivalent results. A study made to explain these effects has led to the development of a novel method of measuring transducer frequency, efficiency,

TABLE I

GENERAL TUBING TEST DATA

Tube material	Wall thickness	Diameter-to-thickness ratio	Minimum notch depth and orientation	Entry angle	Beam size	Pitch
Zircaloy	12	31	1 axial	29°	8	6
	12		1 circumferential	29°	8	6
Stainless	12	31	2 axial	22°	8	6
	12		2 circumferential	22°	8	6
Aluminium	12	31	1 axial	22°	8	6
	12		1 circumferential	22°	8	6
Zircaloy	17	35	1 axial	26.8°	8	6
	17		1 circumferential	26.8°	8	6
Zircaloy	25	15	1 axial	26.8°	8	6
	25		1 circumferential	26.8°	8	6
Stainless	25	15	2 axial	18°	8	6
	25		2 circumferential	19.9°	8	6
Aluminium	25	15	1 axial	18°	8	6
	25		1 circumferential	19.9°	8	6
Zircaloy	45		2 circumferential	26.8°	20	15
	45	10	1 axial	24°	20	15
	45		1 circumferential	26.8°	8	6
Stainless	45	10	2 axial	17°	20	15
	45		2 circumferential	19.9°	8	6
Aluminium	45	10	2 axial	17°	20	15
	45		1 circumferential	19.9°	8	6
Aluminium	65	7.7	1 axial	16°	20	15
	65		2 circumferential	19.9°	20	15
Zircaloy	65	7.7	1 axial	21.5°	20	15
	65		1 circumferential	26.8°	8	6
Stainless	65	7.7	2 axial	16°	20	15
	65		1 circumferential	19.9°	8	6
Aluminium	65	7.7	2 axial	16°	20	15
	65		1 circumferential	19.9°	8	6

Note: All dimensions in mils unless otherwise stated.

damping factor, focal length and radiated beam profile. Obviously, each of these parameters affects transducer performance. Unfortunately, however, subtle transducer irregularities affect this performance in a way that is not

readily observable from use of the transducers in regular test equipment, yet markedly degrades quality of results obtained. Existence of such irregularities was found to be not uncommon in the commercial transducers examined.

Figure 9 illustrates an experimental arrangement especially designed to measure the transducer parameters listed above. As applied to small

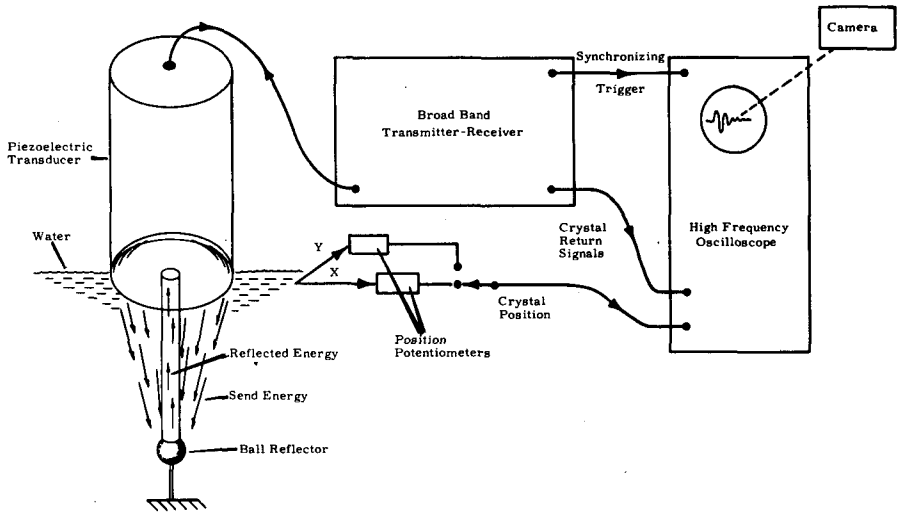

Fig. 9

Experimental arrangement for measuring transducer parameters

highly-focused units, 0.025-in ball reflector is translated through the focal point in two perpendicular directions designated X and Y. Motion of the ball in either direction rotates a potentiometer which generates a linearly increasing voltage. Fed on to the horizontal plates of an oscilloscope, this voltage deflects a spot across the face of the scope in one-to-one correspondence with reflector displacement. A broad frequency-band electronic system excites the transducer with a sharp voltage spike, receives and amplifies pulse echoes returning from the reflector, and displays them on the vertical plates of the oscilloscope.

Results obtained from a well-made 15-MHz, spherically focused, commercial transducer are shown in Fig. 10. The one exception to the excellent performance of this unit is that its actual frequency is 17 MHz instead of the rated 15 MHz - an acceptable deviation for this application. The radiated beam profile shown in the lower two wave traces are very important, however. The amplitude of each half-cycle of radiated energy is shown as a function of X in the middle photograph, and as a function of Y in the lower photograph. It is noted that the profile is approximately equal in width in both directions. These curves also show that the radiated energy is symmetrical about the midpoint. A damping factor of three (defined as the number of positive half-cycles greater in amplitude than the first half-cycle) is measured. Transducers with these characteristics readily reproduce

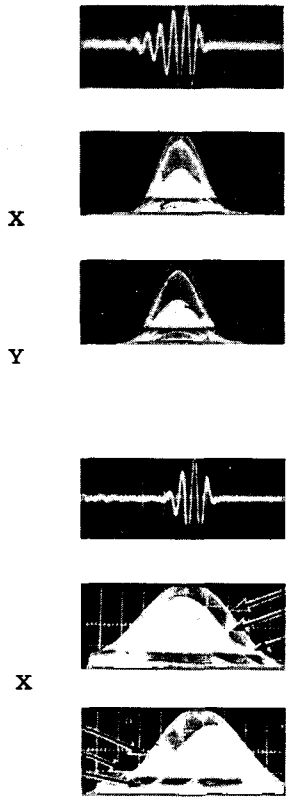

FREQUENCY	1 Mc
FOCAL LENGTH	19 μs
BEAM DIMENSIONS	
X	8 MIL
Y	8 MIL
DAMPING FACTOR	3

FREQUENCY	17.5 Mc
FOCAL LENGTH	34.9 μs
BEAM DIMENSIONS	
X	17.1 MIL
Y	16.5 MIL
DAMPING FACTOR	2

Fig. 10

Ultrasonic transducer characteristics

data earlier reported in Fig. 8 and provide consistent results in practical application.

The same measurements applied to a supposedly equivalent transducer reveal typical manufacturing imperfections shown in the lower half of Fig. 10. In this case the actual frequency is 17.5 MHz and the damping factor is 2. The beam profile width in both the X and Y directions is nearly twice as broad as the former case, revealing reduced sensitivity to small defects. The lower two waveforms are not symmetrical, showing that the focusing lens is improperly aligned on the transducer face. Attempts to use this practical tube-testing equipment would give erratic results. Similar tests applied to an extensive number of units have revealed that regions of faulty bonding between crystal and backing member, density variations of the backing, and faulty alignment of the focusing lens, are readily apparent. On the basis of these tests, specifications have been developed to insure accurate and reproducible results when applied to routine tubing inspection.

These specifications are as follows:

Centre frequency	+ 10% - 0% of specified value (normally 15 MHz)
Damping factor	3.5 ± 0.5
Beam width	0.008 ±0.001 in (at 3-db points)
Beam symmetry	Peak amplitude of each half-cycle within 0.004 in of beam centre
Focal point	19 ± 1 μs

An important outgrowth of this activity has been a general upgrading of the quality of transducers marketed in the United States of America. At least one leading vendor has adopted the practice of inspecting each unit manufactured with an arrangement equivalent to Fig. 9 as a final step in its manufacture. Transducers made to the specifications prescribed above have thus became available for the first time.

Equipment for inspection of thin-walled tubing has been developed and put to routine use [5]. In practice, two transducers are used; one sends a beam circumferentially around the tube, the other is directed down the longitudinal axis of the tube. This ensures the detection of defects regardless of their orientation, and eliminates the necessity for repeat tests as is sometimes required. As shown by the sketch in Fig. 11, the arrangement passes the tubes through a 6 in × 8-in "weir" tank which is translated along the tube as the scan is made. Water is continuously filtered and circulated through weir tank. Special bearing design permits free passage of the tube through the tank without appreciable wear to the tube or the bearing.

Tubes rotate at 1800 rpm, pulse repetition rate is 10 kc, and one foot of tubing is inspected per minute. The equipment shown was developed under the United States/Canadian Co-operative Programme on Heavy-Water Reactors, and is at present applied to the inspection of nuclear-fuel-sheath tubing in Canada. Similar equipment has been in routine one and two-shift use at Hanford for the past two years inspecting United States fuel-sheath tubing.

II. AUTOMATIC FUEL TESTING

Hanford's nuclear-fuel inspection practices are a good example of the beneficial returns that result from the use of non-destructive methods in routine, automatic production lines. Here the high cost of charging failure-prone fuel into a reactor makes it essential that the quality of each element is non-destructively ensured before use.

Hanford has had automatic test equipment operating in fuel-manufacturing lines for a number of years. While at the time of their development these test techniques were novel and in the forefront of NDT technology - at this time they are more representative of well-accepted practices. For this reason, the following discussion gives the main emphasis to the automatic features of the equipment rather than to the physics of the tests themselves. More detailed information on the latter subject is available from numerous references [6-9].

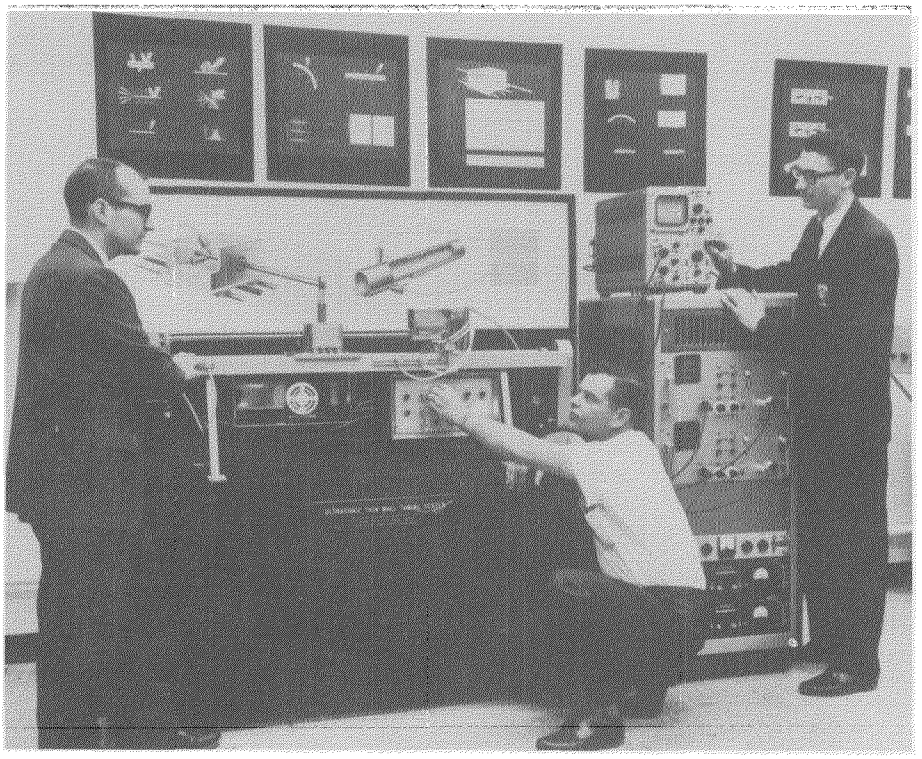

Fig. 11

Ultrasonic tubing tester

Fully-automatic ultrasonic and eddy-current inspection systems have been developed to ensure the integrity of Hanford production fuel elements on a routine, production line, basis. The uranium-fuel cores are cylindrical in shape, roughly 1 - 1/3 in in diam. by 8 in long, with a 3/8-in hole down the central axis. The cores are clad in a 0.030-in aluminium jacket with an aluminium silicon braze alloy which metallurgically bonds the jacket to the core. The fuel elements are closed with aluminium end-caps which are Heli-arc welded to the side jacket at one end and a central aluminium spine at the other.

Three separate systems have been developed to inspect the bare uranium core, the cladding, and the closure. In each system, fuel is brought to the test station, submerged in the test tank, separated into acceptable and unacceptable categories on the basis of the non-destructive test performed, and transferred down a continuous production line by automatic conveyor.

Uniform grains of the correct average diameter are ensured in the bare fuel cores by a 5-Mc through-transmission ultrasonic test. Unacceptable grains which are too large or too small incorrectly attenuate the beam and thereby provide an identifying signal. The bases of the test are shown in the extreme right of Fig. 12. Correspondence of grain size to wave attenuation is graphically illustrated in the right centre photograph.

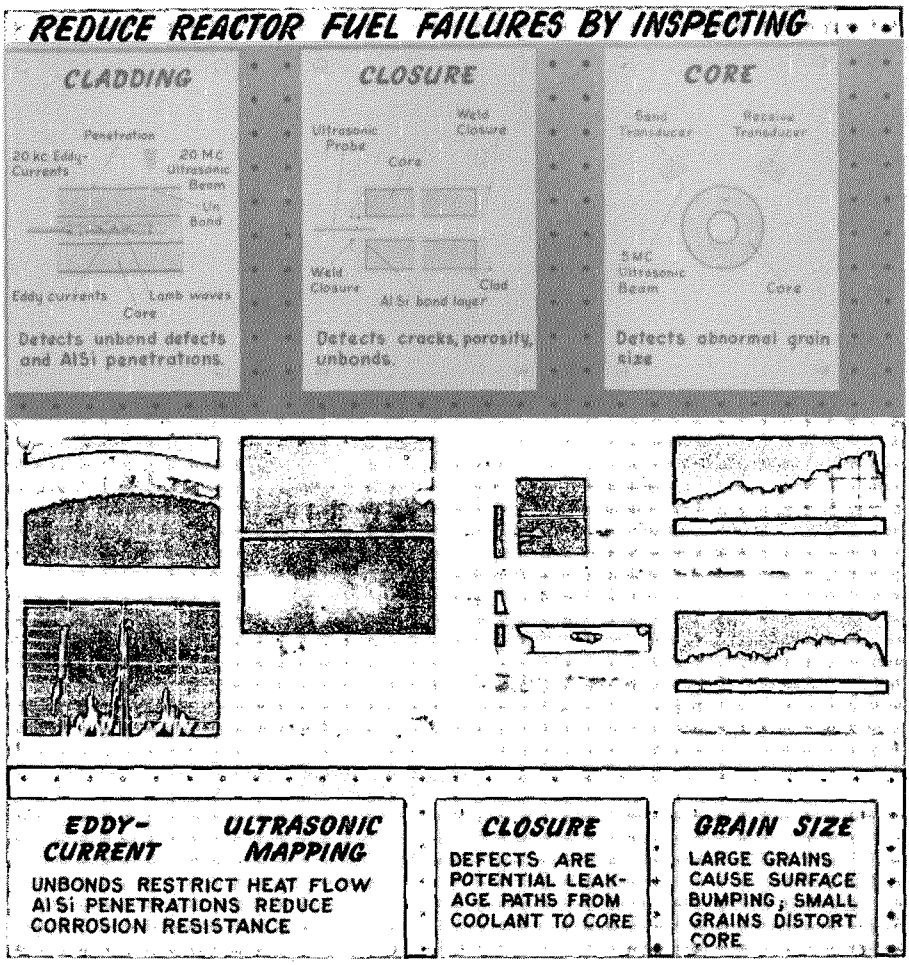

Fig. 12

Principle of operation of automatic fuel testers

Defects in the weld closure offer potential leakage paths for the reactor coolant to contact the fuel core. Such defects between the core and the extreme ends are detected with an ultrasonic system of high defect resolution capabilities. As illustrated in the upper centre diagram, tests are simultaneously applied to both weld closures. Sensitivity is sufficient to detect a hairline crack or 0.020-in-diam. porosity 0.020 in below the surface. Electronic memory techniques distinguish continuous from scattered defects.

Combined ultrasonic and eddy-current tests ensure that cladding braze porosity is within acceptable limits, and that the cladding is free from erosion penetrations of its under surface by the braze alloy. Both tests are simultaneously applied to the inner and outer surface. The inner probe uses a send-and-receive transducer to generate what are presumed to be Lamb

Fig. 13

Automatic fuel-test station

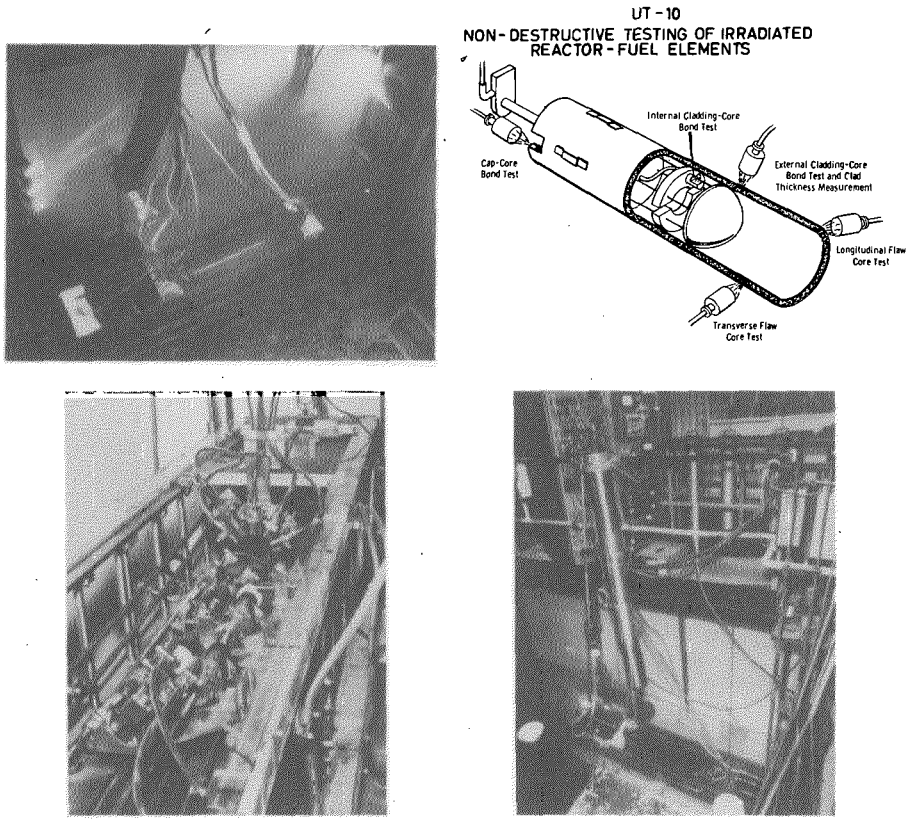

Fig. 14

Inspection of irradiated fuel

waves in unbonded regions of the cladding. The external bond test uses a conventional 20-Mc pulse-echo technique. Braze porosity or non-bond defects as small as 0.030 in are reliably detected, and AlSi penetrations reaching within 0.015 in of the surface are revealed by the eddy-current test. The eddy-current test operates at 20 kc with each probe consisting of a primary and secondary winding. In the external eddy-current test, a thin film of plastic tape is continuously passed between the test coil and the rotating fuel element. Its purpose is to eliminate wear of the probe and to minimize variation in the spacing of probe and fuel surface. Typical AlSi penetrations with their corresponding detecting signal are shown in the centre of Fig. 12. Also shown is an ultrasonic map of typical unbond defects with autoradiograph results of the same element. The under surface of the cladding after destructive removal from the element is also shown.

All systems rotate the fuel cores at about 1000 rpm with a complete scan completed in a few seconds. Figure 13 shows the automatic test station incorporating ultrasonic and eddy-current tests for the fuel cladding. As the external and internal fuel surfaces are inspected simultaneously, each

station includes two ultrasonic and two eddy-current tests. A close-up of an element under test is shown in the lower right of the upper photograph. The lower photograph illustrates the various ultrasonic probes used by the fuel-inspection equipment.

Although not applied to such large numbers, non-destructive tests have also been developed for the inspection of irradiated fuel after reactor exposure. For this application, techniques similar to the unirradiated case are employed, except that provision for remotely conducting the test are necessary. At Hanford, tests are applied approximately 20 ft under water. Figure 14 sketches tests applied to radiated fuel of different design in the upper right. Fuel properties inspected are identified in the sketch. Equipment used to mechanically support the fuel and transducers and provide the necessary scanning motions are shown in the two lower photographs. A fuel element under test is shown in the upper left.

REFERENCES

[1] LIBBY, H. L., An Improved Eddy-Current Test, HW-81780, May 7 (1964).
[2] CHOCKIE, L. J., Nondestructive Testing Nuclear Steam Generators After Installation, HW-SA-3245, October 21 (1963).
[3] ZEUTSCHEL, M. F., Thin-Walled Tubing Test Using Ultrasonic Shear Waves, Part II Production Test Equipment: Its Operation and Test Results, HW-81957, June 30 (1964).
[4] ZEUTSCHEL, M. F., The Measurement of Ultrasonic Transducer Characteristics, HW-81955, June (1964).
[5] ZEUTSCHEL, M. F., Thin Walled Tubing Test Using Ultrasonic Shear Waves, Part I Theory of Ultrasonic Waves Propagation, Experimental Data and Standard Fabrication, HW-81956, June 12 (1964).
[6] FREDERICK, C. L., Ultrasonic Grain Size Testing of Hanford Fuel Elements, HW-64971, May 11 (1960).
[7] LIBBY, H. L., Electromagnetic Detection of AlSi Penetrations, HW-29730, October 23 (1953).
[8] WORLTON, D. C., An Ultrasonic Method for Bond Testing Reactor Fuel Elements, HW-47017, November 27 (1956).
[9] ZEUTSCHEL, M. F. and HUNTER, D. O., UT-4- An Automatic Ultrasonic Tester for Closures of Hanford I & E Fuels, HW-74625, May (1963).

DISCUSSION

A.D. McEACHERN: During the discussion of Mr. McKane's paper* in which he mentioned some apparent limitations of ultrasonic bond testing, you indicated that Hanford had a better method. Could you now give us some details?

D.C. WORLTON: We use a 20-MHz wide-band pulse-echo system. The higher frequency provides higher sensitivity to non-bond defects and eliminates variations in the uranium core. This system is satisfactory for the Hanford canning process, but it is not certain that it would be better for other canning processes.

A.D. McEACHERN: In your oral presentation you brought up a very important point about the unpredictable characteristics of commercial ultrasonic transducers. Can you comment on whether the time is coming when

* These proceedings, (SM-63/43).

we will be able to order a specific type of transducer and expect to get what we order?

D.C. WORLTON: Our system of analysing transducers has been adopted by commercial transducer manufacturers, and the quality of their transducers has thereby been improved. I think that is all I can say at the moment.

R.S. SHARPE: I would like to support your move to provide more precise data on the characteristics of your ultrasonic transducers. I would suggest, however, that you should also measure the frequency of the wave in the medium (for example by a Schlieren method).

D.C. WORLTON: The measurement you suggest would be an excellent one for basic study, but we have not performed it.

Z. PAWŁOWSKI: You showed two patterns obtained with the device for testing piezoelectric transducers (crystals). The first was symmetrical, i.e. the transducer was good, while the other was asymmetrical, which you interpret as bad.

Could you say a little more about the possible reasons for "good" and "bad" behaviour of the transducers.

Also, did you measure the displacement pattern on the surface of the transducer?

D.C. WORLTON: The main difficulties with commercial transducers are variations in bonding between crystal and its backing member and bonding between crystal and lens, and improperly mounted lenses.

No, we have not measured the displacement pattern.

R. NEIDER: I would like to ask two questions on the eddy-current measurement of fuel-element cladding material. Could you please explain the construction and material of the fuel elements tested?

D.C. WORLTON: The cladding is bonded to the uranium core with a braze alloy which melts at lower temperatures than the aluminium jacket. Serious defects occur in those cases when this alloy has eroded the under side of the aluminium jacket, thus reducing its thickness.

R. NEIDER: Did you use a feed-through coil, and did you measure the absolute impedance or make an impedance analysis?

D.C. WORLTON: No, a point coil was used. We made a phase analysis, and also a relative, not absolute, impedance measurement. Variation in impedance was correlated with the defect being detected.

F.H. WELLS: In the case of the eddy-current testing of heat-exchanger tubes, for how long is the Lissajou figure derived from a defect available for view on the oscilloscope?

D.C. WORLTON: The probe passes the irregularity at about 20 ft/min. The data are also recorded on a strip chart recorder.

V. GERASIMOV: For what detectors did you obtain amplitude phase characteristics of the "figure-8" type, and how did you use them for defect inspection?

D.C. WORLTON: In the eddy-current inspection of installed tubes the complex impedance of a coil moving past an irregularity varies non-linearly. That is, the locus is a curve. By differentially connecting two coils one obtains a "figure-8"-shaped curve, whose shape and orientation are used to give additional information.

W. FRANCIS: How do you get the eddy-current probe around the tube bend in the heat-exchanger tube, and how did you correlate the defect location with the position along the tube?

D.C. WORLTON: We did not inspect around the bend of the tube.

NON-DESTRUCTIVE TESTING TECHNIQUES FOR RESEARCH AND PROCESS CONTROL*

D. A. DOUGLAS, Jr., R. W. McCLUNG, B. E. FOSTER AND C. V. DODD
METALS AND CERAMICS DIVISION,
OAK RIDGE NATIONAL LABORATORY, OAK RIDGE, TENN.,
UNITED STATES OF AMERICA

Abstract — Résumé — Аннотация — Resumen

NON-DESTRUCTIVE TESTING TECHNIQUES FOR RESEARCH AND PROCESS CONTROL. Non-destructive test methods have been used primarily for the detection of defects and the rejection of faulty materials. The Oak Ridge National Laboratory has found it valuable to employ special non-destructive testing techniques as aids in materials research, component development, and process control. This paper gives three recent examples of the evolution of non-destructive testing techniques from research to process control.

A current fuel-element design contains fuel pins filled with vibratorily compacted uranium and thorium oxide powder. A gamma-attenuation technique was developed to allow the homogeneity of fuel loading to be measured and was used to aid the development of fabrication techniques and equipment. Later an inspection device was built to operate remotely in a hermetically sealed and shielded facility and used for production process control.

Another fuel element required fuel plates containing a uranium oxide-aluminium dispersion core with a programmed variation in the fuel loading across the width. A continuous scanning, X-ray attenuation technique was developed and used to measure fuel inhomogeneities and conformity to design contour. The technique assisted the development for both core pressing and plate-rolling practices. A system was constructed for rapid automatic evaluation of production fuel plates.

These fuel plates were pressed into involute shape and assembled with alternate cooling channels. Stringent heat-transfer requirements imposed a tight tolerance on the channel dimensions. A unique eddy-current device using the "lift-off" characteristic was invented to insert in the very narrow channel and allow recording of dimensions both during fabrication development and actual manufacture.

Another approach to fuel elements is the use of minute fuel-bearing particles coated with pyrolytic carbon to retain the fission products. Of concern are the core diameter, coating thickness and integrity, and presence of fuel in the coating. Development of microradiographic techniques has provided a powerful tool to evaluate the many variables in the coating process for optimum fabrication. Further application allows the evaluation of the effects of service including heat treatment and in-reactor testing. Results of these studies assist the realistic evaluation of production lots and the recycle of information to correct discrepancies.

MÉTHODES D'ESSAIS NON DESTRUCTIFS APPLIQUEES DANS LA RECHERCHE ET DANS LE CONTRÔLE DE LA FABRICATION. On a recours aux essais non destructifs principalement pour la détection de défauts et le rejet des matières et produits défectueux. Le Laboratoire national d'Oak Ridge a constaté qu'ils sont également précieux dans la recherche de nouveaux matériaux, la mise au point de pièces et le contrôle de la fabrication. Le mémoire expose trois exemples récents de l'évolution des méthodes d'essais non destructifs, du stade de la recherche à celui du contrôle de la fabrication.

Un modèle courant d'éléments combustibles est constitué d'aiguilles de combustible en poudre d'oxyde d'uranium et d'oxyde de thorium compressée par vibration. On a mis au point une méthode fondée sur l'atténuation gamma pour mesurer l'homogénéité du combustible; elle a été appliquée au cours de la mise au point des procédés et du matériel de fabrication. On a construit ensuite un appareil de contrôle télécommandé, devant fonctionner dans un dispositif hermétiquement scellé et blindé; il est utilisé pour le contrôle de la fabrication.

Un autre type d'élément combustible est constitué de plaques de combustible avec une âme en oxyde d'uranium en dispersion dans de l'aluminium, la teneur en combustible variant de manière pré-établie dans la

* Research sponsored by the United States Atomic Energy Commission under contract with the Union Carbide Corporation.

largeur de l'élément. On a mis au point une méthode d'exploration continue, fondée sur l'atténuation des rayons X, pour vérifier si la répartition du combustible est conforme aux prévisions. Cette méthode de contrôle a facilité la mise au point des procédés de compression du combustible et de laminage des plaques. On a construit un appareil pour l'évaluation automatique rapide des plaques de combustible fabriquées.

On a donné par emboutissage à ces plaques de combustible une forme involutée et on les a assemblées en ménageant entre elles des canaux de refroidissement. Les exigences sévères du transfert de chaleur imposaient une très faible tolérance pour les dimensions des canaux. On a inventé un appareil à courants de Foucault, fondé sur la caractéristique du «décrochement», qui peut être inséré dans ces canaux très étroits pour mesurer les dimensions, aussi bien au stade de la mise au point qu'au stade de la fabrication.

Un autre type d'élément combustible consiste en petites pastilles de combustible enrobées de carbone pyrolytique retenant bien les produits de fission. Le diamètre de la pastille de combustible, l'épaisseur et l'intégrité du revêtement et la présence de combustible sous le revêtement présentent une grande importance. La mise au point de méthodes de microradiographie a été un excellent moyen d'évaluer les nombreuses variables des procédés de revêtement des pastilles, en vue d'une fabrication optimum. Une autre application consiste à évaluer les effets d'opérations telles que le traitement thermique et l'essai en pile. Les résultats de ces études renforcent l'évaluation réaliste des produits fabriqués et permettent de rectifier les erreurs éventuelles des contrôles antérieures.

ТЕХНИКА НЕДЕСТРУКТИВНЫХ ИСПЫТАНИЙ ДЛЯ ИССЛЕДОВАТЕЛЬСКИХ И ПРОИЗВОДСТВЕННЫХ ЦЕЛЕЙ. Методы испытаний без разрушения оболочки использовались, главным образом, для определения дефектов и отсортировки бракованных материалов. Окриджская национальная лаборатория нашла весьма ценным применение недеструктивных методов испытаний в качестве дополнительного средства при исследовании материалов, разработке компонентов и процесса контроля. В докладе приводятся три последних примера развития этих методов для исследовательских и производственных целей.

Существующая конструкция топливных элементов состоит из тепловыделяющих элементов в виде тонкого стержня, заполненного ураном и порошком окиси тория, которые уплотняются вибраторами. Был разработан метод ослабления гамма-лучей для того, чтобы измерить однородность топливной загрузки, и он использовался для того, чтобы оказать содействие разработке изготовления аппаратуры и оборудования. Позднее было построено обследующее устройство, могущее действовать на расстоянии в герметически закупоренном и экранированном помещении и которое можно использовать для контроля производственного процесса.

Другой топливный элемент потребовал топливные пластинки, содержащие в себе активную зону с диспергированным ураном и окисью алюминия с помощью запрограммированного разнообразия в загрузке топливом по ширине. Был разработан способ затухания рентгеновского луча и непрерывного сканнирования для измерений неоднородности топлива и при наметке контура. Этот метод пригодился как в разработке прессовки активной зоны, так и при прокатке пластин. Система конструировалась для быстрой автоматической оценки качества изготовления топливных пластин.

Эти пластины сложных форм собирались и прессовались вместе с чередующимися каналами для охлаждения. Строгие требования теплопередачи повлекли за собой жесткий допуск в размерах канала. Уникальное устройство с применением токов Фуко, использующее характеристику "лифт-офф", было приспособлено для помещения в самый узкий канал, чтобы контролировать размеры деталей в процессе изготовления и после.

Другим решением проблемы контроля топливных элементов является использование частиц покрытых пиролитическим углеродом. Интерес представляют размер активной зоны, толщина и целостность покрытия и наличие топлива в покрытии. Разработка микрорадиографических способов дала сильное средство для оценки многих вариаций в процессе покрытия топливных элементов оболочкой. Дальнейшее применение позволило сделать оценку эффективности способа, включая тепловую обработку и проведение испытаний в реакторе. Результаты этих исследований повышают реальную ценность массового производства и дают новый толчок сведениям для соответствующих поправок.

TECNICAS DE ENSAYO NO DESTRUCTIVO PARA LA INVESTIGACION Y EL CONTROL DE PROCESOS DE FABRICATION. Los métodos de ensayo no destructivo se vienen empleando en primer lugar para la detección de fallos y para rechazar materiales defectuosos. El laboratorio nacional de Oak Ridge ha encontrado útil emplear técnicas especiales de ensayo no destructivo como ayuda en las investigaciones sobre materiales,

én el perfeccionamiento de componentes y en el control de los procesos industriales. La memoria expondrá tres ejemplos recientes de la evolución de las técnicas de ensayo no destructivo desde la fase de investigación hasta su empleo en el control de los procesos.

Uno de los tipos de elementos combustibles de uso corriente consiste en agujas rellenas de óxidos de uranio y de torio en polvo, compactados por vibración. Se desarrolló una técnica de atenuación gamma que permite medir la homogeneidad de la carga combustible y que contribuyó al perfeccionamiento de los procedimientos y del equipo que se emplea en la elaboración. Más adelante, se construyó un dispositivo de inspección que se maneja a distancia en un recinto herméticamente cerrado y blindado, y que sirve para controlar el proceso de producción.

Otro elemento requiere placas de combustible con un alma de óxido de uranio disperso en aluminio, en las que la carga de combustible varía transversalmente según valores prestablecidos. Se desarrolló una técnica de exploración continua por atenuación de rayos X que se emplea para medir la heterogeneidad del combustible y comprobar si su distribución es correcta. Esta técnica se utilizó para perfeccionar los procedimientos de preparación de las almas por prensado o por laminado de placas. Se construyó un sistema para evaluar rápida y automáticamente la elaboración de placas de combustible.

Estas placas se prensan en formas complejas y se montan alternando con canales de refrigeración. Las prescripciones para la transmisión de calor son muy estrictas y admiten muy poca tolerancia en las dimensiones de los canales. Se inventó un dispositivo especial de corrientes de Foucault que se inserta en el estrechísimo canal y registra las dimensiones durante todo el proceso de fabricación en escala experimental e industrial.

Otro tipo de elemento emplea pequeñas partículas de combustible revestidas de carbono pirolítico que retienen los productos de fisión. En este caso es fundamental medir el diámetro del alma, el espesor y la integridad del revestimiento y la presencia de combustible en el mismo. Las técnicas microrradiográficas son sumamente útiles para medir las múltiples variables del proceso de revestimiento y contribuyen a la obtención de un producto óptimo. Otras aplicaciones permiten evaluar los efectos del desgaste durante el empleo o en ensayos por tratamiento térmico y en el reactor. Los estudios confirman la utilidad objetiva de los métodos empleados en el control industrial y reafirman la importancia de emplear datos registrados en ocasiones anteriores para corregir posibles discrepancias.

INTRODUCTION

Non-destructive test methods have been used primarily for the detection of defects and rejection of faulty materials. There is a growing trend toward the application of these methods to monitor the quality of manufactured products and use the information obtained in turn to modify or control the manufacturing process. The Oak Ridge National Laboratory (ORNL) has found it valuable to develop and use special non-destructive testing techniques as aids in materials and research and component development for nuclear-power reactors. Frequently the data obtained from these techniques could not be derived in any other way. After serving to obtain basic information and assisting in the determination of optimum fabrication procedures, the techniques can frequently be adapted for process control and product evaluation during actual manufacture.

The non-destructive test development programme at ORNL encompasses many methods. Examples of recently completed work include gamma-ray attenuation techniques for examining homogeneity in fuel rods, X-ray attenuation to measure the content and distrubtion of uranium in fuel plates, eddy-current devices for fuel-element coolant-channel spacing, and a low-voltage microradiographic approach to the evaluation of minute fuel particles. In each cited case the programme started with materials research and component development and continued into the support of a manufacturing process.

EVALUATION OF FUEL RODS

About five years ago our Laboratory was faced with the problem of fabricating reactor fuel elements of thoria and urania (containing U^{233}). These elements would need to be fabricated entirely inside a shielded alpha-tight enclosure. A conceptual design for a complete process flow-sheet was formulated and ultimately over 1000 fuel rods were produced to very rigid specifications [1]. One of the key developmental tasks involved encapsulating the ceramic fuel in Zircaloy tubes. It was decided that the best remote fabrication process would be to crush, size, and blend the fuel and pour the ceramic powders into tubes. They would be compacted by either electrodynamic or pneumatic shakers. Many questions were to be answered during the development of this technique. What particle-size distribution would provide the best compaction density? Which shaker is superior, the pneumatic or the electrodynamic? How much does the density vary along the length of fuel column in the tube? Foremost in the mind of the engineer was how could he measure what occurred as he changed the fabrication variables. We analysed this problem and decided that the attenuation of the gammma rays emitted by a Co^{60} source would provide a sensitive measurement of changes in the compacted density of the fuel. Using a collimator to produce a focal spot of 3.2 mm (1/8 in) and a NaI crystal with a photomultiplier tube as the detector, we measured the fuel-density changes that occurred as the vibratory compaction research progressed. Figure 1 illustrates the simple arrangement constructed to aid in the fabrication research. The Co^{60} source is in the large lead block and the detector is in the smaller overhead shielding. Using our measurements to guide him, the engineer determined the optimum particle-size distribution, learned that pneumatic shakers produced higher densities than electrodynamic devices, and proved that fuel densities 90% of theoretical could be routinely achieved.

General principles

Lambert's Law is the basic principle of this inspection system, although we prefer to use a modified coefficient which is based on mass and is independent of the physical state of the absorber, rather than the linear attenuation factor in Lambert's equation. Thus, for our purposes we use

$$I/I_0 = \exp(-\mu_m x \rho),$$

where I_0 is the incident intensity of the photon beam, I the transmitted intensity of the photon beam, x is the thickness of the sample, μ_m is the linear attenuation coefficient divided by the density of the absorber, and ρ is the density of the absorber.

In the detection system, the sodium-iodide crystal produces a visible scintillation when struck by a transmitted photon. This scintillation is detected by the photosensitive cathode of the photomultiplier tube. Electrons are ejected and multiplied many thousand times, producing a current pulse. This signal is integrated and fed to a strip-chart recorder. The data are not readily interpretable unless they can be compared with a standard. At

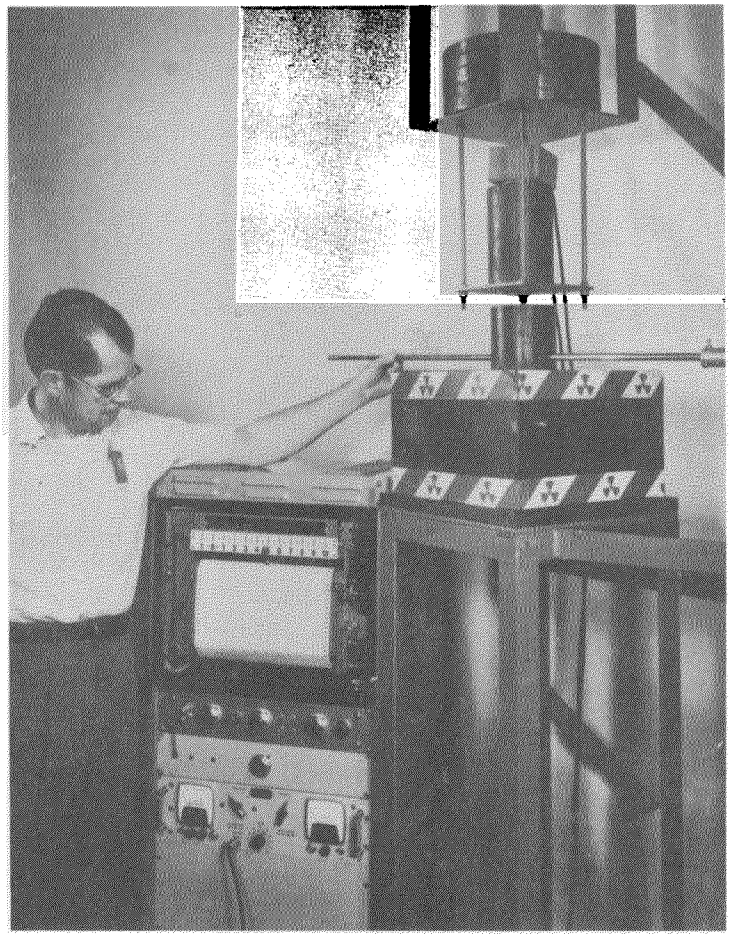

Fig. 1

Gamma-attenuation device used to assist fabrication development of fuel rods

first, an exact quantitative measurement of the density was not needed, so we calibrated the system with a gold foil whose thickness was calculated to provide an attenuation equivalent to a 2% change in density.

Process control

Once the fabrication engineers had fixed their parameters, the second phase of the work commenced. One specification was that no single rod should deviate in average fuel density by more than 2% from the mean density of the total lot. The mean density was selected as 89%. A stricter requirement was that no area along the length of the fuel column should deviate by more than 2% in density from the average for the rod. To meet these requirements a scanner was obviously needed, as part of the process line,

to detect the rods that did not meet these specifications. Thus, our objective changed from evaluation of research to quality control.

Several new problems emerged when we needed to design a device for process control. The gold foil was no longer an adequate standard. A method was needed to integrate the signal at the recorder to provide the engineer with data he could rapidly interpret, tests were needed to determine the maximum scanning speed commensurate with the desired sensitivity, and finally the system had to be mechanized so that it would operate in a shielded facility. Figure 2 shows the finished equipment ready for installation.

The mechanical design for automatic indexing and traversing of the rods was not difficult. We integrated the signal to obtain the average density by attaching a mechanical device to the slide wire of the strip-chart recorder; also, an audible signal was added to assist the operator in recognizing undesirable rods. One of the most difficult tasks was to prepare exact standards that would enable us to quantitatively measure the density. We needed a size that would fit into a Zircaloy tube of the same dimensions as the fuel tube. Thus, the combined attenuation effects of the cladding and the fuel would be reproduced. To vary the density of a ceramic or a metal exactly and homogeneously was a difficult task. Finally, our Ceramics Group was able to isostatically press satisfactory pellets of thoria-urania, which ranged in density from 85 to 93% in incremental changes of 2%.

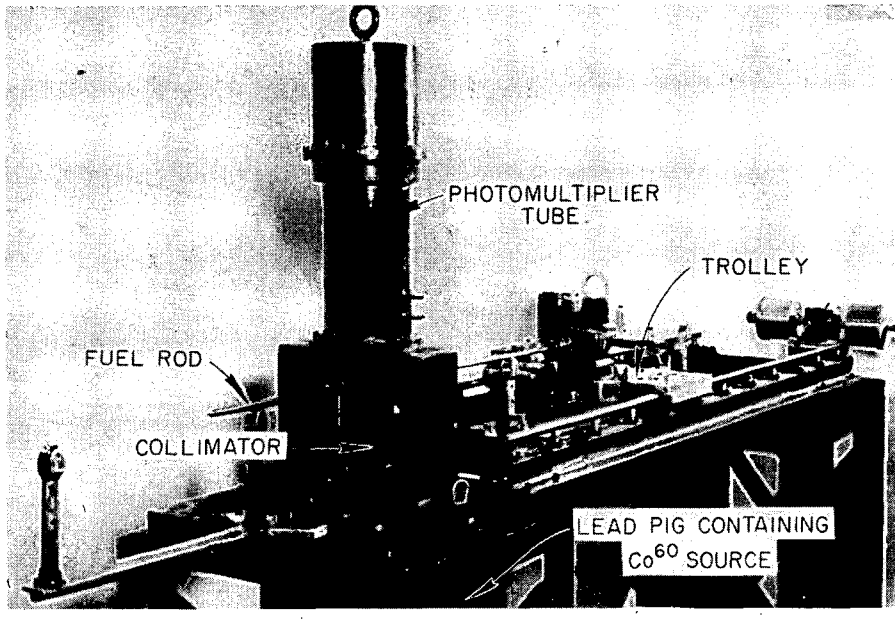

Fig. 2

Gamma-attenuation device used for process control during manufacture of fuel rods

We decided that two scans would be made on each rod 90° apart. Because of the large number of rods to be inspected, scanning them very rapidly was desirable. However, our scanning speed is limited by the recorder

response time and by the beam intensity at the detector. The latter is the most serious restriction, particularly in this case, because approximately 1.3 cm (0.5 in) of very dense material was the absorber. The statistical accuracy of the system for any spot on the rod is related to the accumulated radiation as determined by the dwell time and the intensity of the transmitted beam. One technique we used to increase the effective scanning speed was to enlarge the collimator and make a rectangular slot 3.2×9.5 mm (1/8×3/8 in). This smoothed out many of the irregularities produced by variations in fuel-particle size but did not appear to reduce the sensitivity. Nevertheless, we had to limit the speed to 10 cm/min (4 in/min) to achieve an over-all accuracy of 1%.

The scanner operated very successfully for over a year as one unit of quality control in the process. The only operational difficulty occurred when the photomultiplier tube rapidly lost sensitivity over a period of only a few weeks. We thought that the level of gamma activity in the cell might have curtailed its life. However, when we substituted the same type of tube used in our laboratory machine no further difficulty was encountered.

The use of our simple laboratory device for density measurement helped the engineer solve his fabrication problems. It also provided us with sufficient knowledge to optimize the design of a quality control machine with very little extra development. The production unit demonstrated its worth in routinely determining the quality of compacted fuel rods.

FUEL HOMOGENEITY IN DISPERSION-CORE FUEL PLATES

During fabrication development for the High Flux Isotope Reactor (HFIR) fuel element [2] we studied, developed, and applied several non-destructive testing methods to the evaluation of various fuel-element properties. The basic fuel-bearing unit is a 0.127×61-cm by approximately 10-cm (0.050×24×4 in) plate with a non-symmetrical fuel-bearing section as shown in Fig. 3. The fuel is in the form of minute particles of U_3O_8 interspersed with aluminium. This core section is then completely encased and bonded within an aluminium frame and cladding. Each fuel plate is formed into an involute in the width direction and 540 of these plates are assembled into two annular assemblies. This fuel element, designed to develop a very intense neutron flux in the centre of the core, will generate approximately 100 MW of thermal power. Because of this large rate of heat production, one of the requirements for a non-destructive testing technique was to give assurance that the generation of heat would be uniform, thus enhancing the reliability of the reactor core. During fabrication development, a number of variables could affect the achieved fuel homogeneity. These included the particle-size distribution, the particle blending, the die top design, techniques for filling the die and pressing a core, and the detailed practices for rolling the finished plate. Again we chose a radiation attenuation method [3] as the optimum approach to evaluate the effect of each of these variables and assist the selection of the proper fabrication procedure. The homogeneity evaluation required on the HFIR fuel plates included inspections to ensure that no 2-mm- (5/64-in) diam. spot exceeded the nominal fuel loading by more than 30% as well as to ensure that the average fuel loading within any 2-mm- (5/64-in) wide by

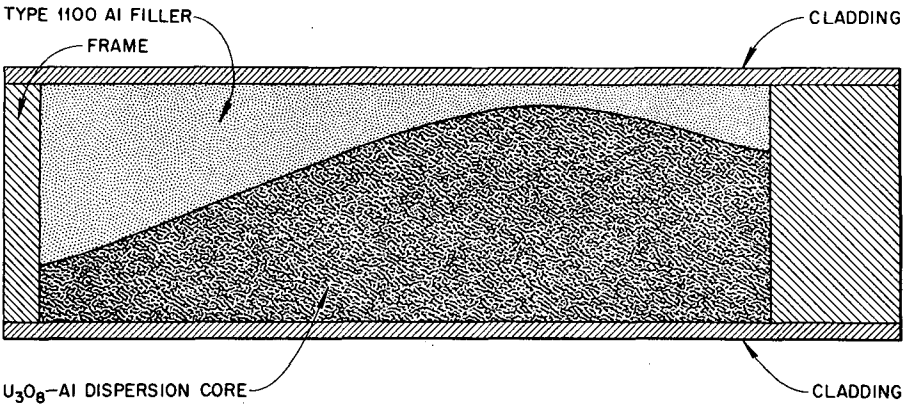

Fig. 3

Cross-section of the High Flux Isotope Reactor fuel plate

1.3-cm- (1/2-in) long section along the core length did not deviate from the nominal by more than ±10%. This stringent homogeneity requirement for such a small area, 3.1 mm^2 (0.0048 in^2) far exceeded that of any other known specification. The necessity for 100% inspection of numerous plates each day demanded a rapid inspection method.

Theory

As noted earlier, X-rays transmitted through a material are attenuated in accordance with the relation:

$$I = I_0 \exp(-\mu_m \rho x).$$

The mass attenuation coefficient, μ_m, increases with increasing atomic number and, in general, decreases with increasing X-ray energy. Under constant operating conditions, therefore, as the amount of high atomic number material (uranium) in the dispersion core changes, the intensity of the transmitted radiation will change. Appropriate calibration techniques allow correlation of intensity change to fuel concentration change.

Equipment

We used industrial X-ray equipment for the irradiation source. Careful control of all operating conditions resulted in a very stable and reproducible operation. The detection system for monitoring the X-ray intensity changes consisted of a NaI(Tl) crystal optically coupled to a photomultiplier tube. Figure 4 shows the system.

The collimator array restricts the primary beam to an appropriate spot size on the specimen and prevents scattered radiation from reaching the detector. Thus, as either the fuel concentration or the thickness of the specimen changes, a corresponding fluctuation in the amount of transmitted radiation is detected, amplified, and recorded.

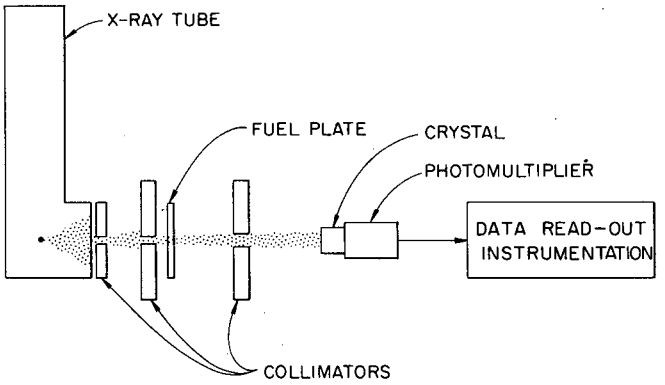

Fig. 4

Block diagram of the gamma-scintillation detection system

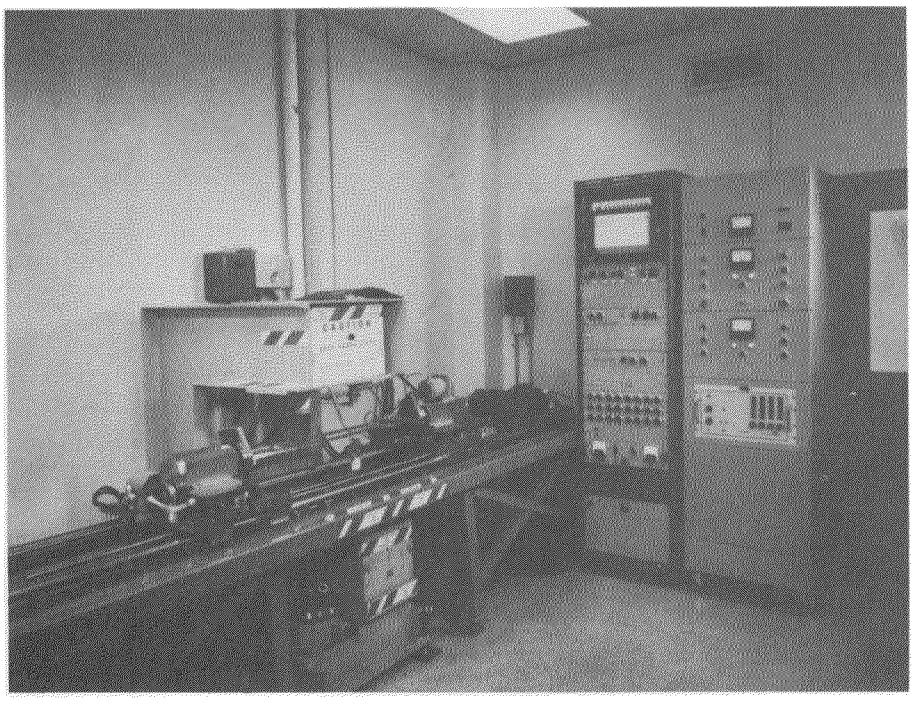

Fig. 5

Mechanical scanning system for inhomogeneity measurement in fuel plates

Mechanical X-Y scanning of the plate was necessary to evaluate the entire surface area. Figure 5 shows the system that we designed and assembled to mount the radiation source and detector and to allow the horizontal plate to be driven longitudinally through the radiation beam. Trans-

verse indexing was automatically programmed at the end of each longitudinal scan.

Of course, the useful longitudinal scanning speeds are limited by the instrumentation-response time and the beam intensity that can be accurately sensed by the detector. The latter is a major consideration in the determination of the statistical accuracy. Fuel plates have been scanned for go-no-go inspections at a linear speed as high as 6.1 m/min (240 in/min), but for strip-chart recording with full response for all 2-mm- (5/64-in) diam. variations, the scanning speed has been approximately 1.6 m/min (64 in/min). We selected wide-chart instruments despite their slower response because of the need for extreme sensitivity over the wide range of fuel concentration.

Calibration and standards

As is true with most non-destructive tests, the measurement of inhomogeneity required special standards to establish and calibrate the technique. We had to establish a quantitative relationship between changes in fuel concentration and X-ray attenuation. Pressed compacts of U_3O_8-Al were rolled into thin foils of different thickness having various amounts of U_3O_8 per unit area. We then combined these foils with an appropriate thickness of aluminium to simulate total thickness of a fuel plate at discrete points across the fuel-concentration gradient in the core. Although these standards were not completely homogeneous, extensive scanning and integration of attenuation values coupled with chemical analyses produced a relatively smooth curve relating fuel content to instrument response. The fuel-concentration gradient of the HFIR plate, the concomitant requirement for re-calibration at each integral position across the width of the plate, and the need for single-point standardization for go-no-go inspections demanded the use of materials for standards that were very homogeneous and readily machinable. We investigated several materials including tool steel, Al-13% U alloy and 6061-T6 aluminium. The aluminium was selected because of its good homogeneity, its ease of machining and the relaxed machining tolerances that resulted from increased thicknesses for equivalent attenuation. Each standard, since it was related to the changing values of attenuation across the width of the fuel plate, had a contour that resembled the non-symmetrical core shown in Fig. 3. These standards which were fabricated to be equivalent in attenuation to the respective fuel concentrations of nominal and +30% and ±10% from nominal, were placed by each end of the fuel plate. Thus, immediately before each successive scan was made, the attenuation value for the go-no-go conditions was recorded on the strip chart and/or used to set an alarm circuitry. Then direct comparisons could be made between the reference levels and the actual values on the plate.

Results

We used the scanning system throughout the latter stages of the development of the fuel plates, where it proved quite useful in evaluating the effect of changes in the fabrication procedure. The system was instrumental in

altering the fabrication technique to reduce the excessive accumulation of fuel at the ends of the finished fuel plate. The effect of changing the particle size was graphically illustrated. The system was used to obtain the values necessary to correct the die tops in which the fuel cores are pressed. The scanner is also used for rapid location of any fuel that is outside the maximum core outline.

Frequent checks with primary attenuation standards and occasional comparison of predicted fuel content with chemical analyses indicate a system accuracy of approximately ± 1%. The design criteria that we developed on the versatile laboratory model enabled the building of one pilot and two production scanners for an evaluation of the HFIR production cores. These latter three scanners incorporated X-Y plotters to allow a recording of out-of-tolerance conditions on a plan view.

COOLANT-CHANNEL SPACING

Another problem facing the fabrication engineer on the HFIR fuel element was the assembly of the large number of plates while maintaining careful control on the coolant-channel space between plates. If this spacing deviates excessively from the intended value, it would affect the coolant flow and could cause excessive fuel-plate temperature and possible failure. We selected an eddy-current approach [4, 5] as being best for this measurement.

Principles

When an electrical coil is excited by a high-frequency alternating current, it produces an electromagnetic field. This field will induce the flow of eddy currents in nearby electrical conductors. The eddy-current flow, which is influenced by the electrical properties of the specimen and the coil-to-specimen distance, will be a factor in determining the electrical impedance of the eddy-current coil. Thus, as the coil-to-specimen spacing changes, the coil impedance changes correspondingly. Figure 6 shows a cross-sectional view of the probe designed to use this principle for the measurement of coolant-channel spacing. The coil is mounted on a long thin metal strip which serves as the insertion handle. Attached to the end of the tape is a metal leaf spring, which is curved so that it overhangs the coil. When inserted in a channel as thin as 0.875 mm (0.035 in), the tape presses against one surface and the spring pushes against the opposing surface. The electrical excitation of the coil generates the eddy currents in the spring. Thus, as the channel spacing varies, the movement of the leaf spring towards or away from the coil will generate a change in the coil impedance that can be calibrated in terms of the channel thickness.

Application

We used elementary hand-held probes throughout fabrication development for measuring experimental fuel elements to reveal poor dimensional control and to assist corrective measures. Figure 7 shows a probe being

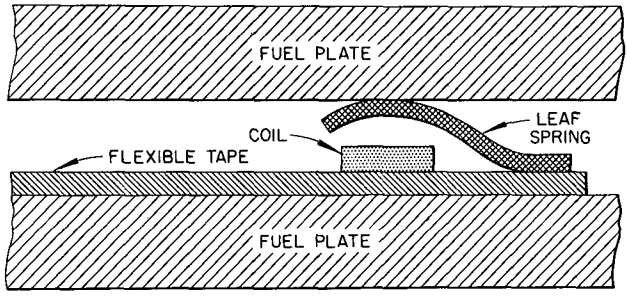

Fig. 6

Probe for measuring coolant-channel spacing between fuel plates

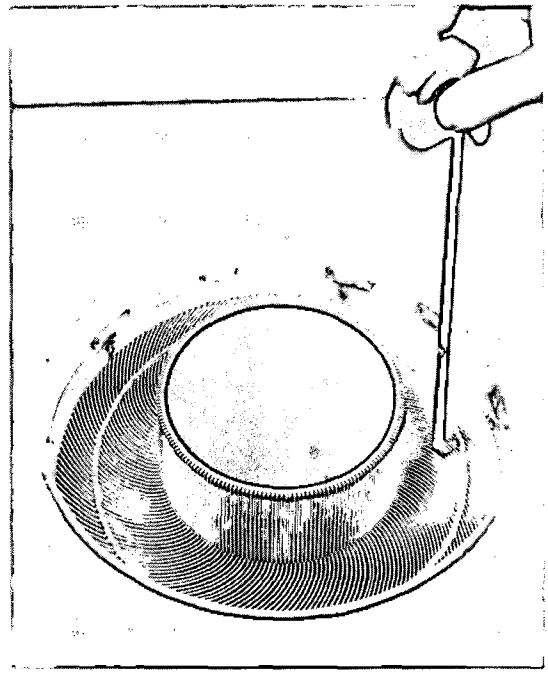

Fig. 7

Measuring probe inserted in coolant channel of prototype High Flux Isotope Reactor fuel core

inserted into a channel of a prototype HFIR fuel core. For dimensional control on production cores a motor-driven inspection station was built containing five probes for simultaneous multipoint measurement and continuous recording in a channel cross-section. The accuracy of measurement is a function of the total range of measurements but has been demonstrated to be better than 0.025 mm (0.001 in) in this particular application.

MICRORADIOGRAPHY OF MINUTE FUEL PARTICLES

Another approach to fuel elements is the use of minute fuel-bearing particles that have been coated with pyrolytic carbon to retain the fission products. These materials seem very promising to the nuclear industry because of their high-temperature capabilities and good neutron economy. Typical dimensions for such a specimen are a 0.15-mm (0.006-in) core and a 0.05-mm (0.002-in) coating thickness. The coating is intended to prevent the fission products produced during reactor operation from escaping into the coolant. To establish the overall quality of these minute particles, new non-destructive testing techniques were necessary for evaluating the coating thickness, fuel-particle shape, presence of fuel in the coating, and integrity of both coating and core. A microradiographic technique [6, 7] has been shown to be a powerful tool for this. We have used the method to inspect fabricated particles for acceptability and to evaluate the results of changes in manufacturing procedure and of thermal and radiation proof-testing.

General principles

The application of radiography to the evaluation of very small coated particles required extensive modification of conventional techniques. The radiographic method records on film the variation in radiation absorption (which is energy dependent) across a specimen. To be useful the absorption must vary enough for an interpretable contrast of density to be achieved on the film or other detector. The very small dimensions of the coated particles and the low absorption of radiation by the pyrolytic carbon coating required the use of low-energy (low-voltage) radiation.

Equipment and materials

In the programme we used commercial radiographic instrumentation modified to provide better control over X-ray energy and exposure time. The use of very low-energy X-rays made the presence of absorbers other than the specimen most undesirable. Therefore, we needed to remove all extraneous material that could cause absorption, scattering, or uneven filtration of the soft X-ray beam between the target and the detector film. The radiation-absorbing material was removed by use of an X-ray tube head containing a beryllium window only 0.2 mm thick and a helium-filled chamber between the X-ray head and the specimen, since even air effectively attenuates the X-rays at the energy level required. The helium was retained in the chamber by 0.0125-mm (0.0005-in) polyethylene diaphragms, which had no measurable effect on the X-ray transmission. Figure 8 shows the 107-cm- (42-in) high chamber that we used in the programme. With the 1.5-mm (0.06-in) focal spot, the effective penumbral shadow contribution to unsharpness is approximately 0.3 μm. Later we made a 47-cm- (18.5-in) high chamber that reduced the exposure time to one-fourth but increased the penumbral shadow only to 0.6 μm. Also we reduced unnecessary absorption by the use of bare photographic plates (without cassettes

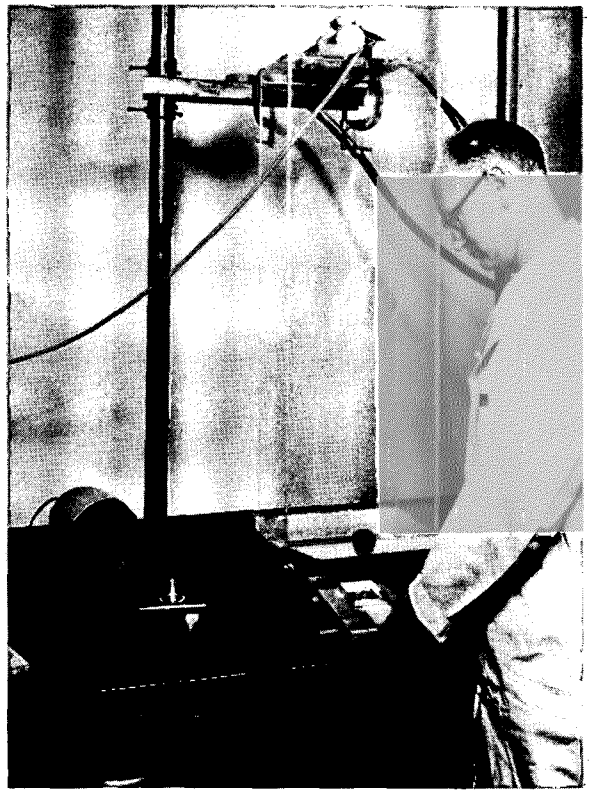

Fig. 8

Equipment arranged for microradiography of coated particles. *Note helium chamber

or film holders). This change necessitated the use of darkroom exposure techniques.

We evaluated several different detectors and showed that the optimum was high-resolution plates coated with an emulsion having a reported resolution capability of 1500 lines/mm (38 000 lines/in). We viewed radiographs on these plates at magnifications up to 500X with little difficulty caused by emulsion grain-size.

Of the several high-contrast fine-grained developing solutions tested for the high-resolution plates, we found the standard X-ray film developer to be as good as or better than any other solution tested and to have the added advantage of being near the X-ray exposure room. Considerable care was exercised in handling and drying the high-resolution plates to prevent undesirable artifacts caused by contamination.

Procedure

The particles were placed directly on the radiographic plate beneath the helium chamber. The helium atmosphere was maintained in the chamber

with a very slight positive internal pressure retained by the thin diaphragm. Since the specimens and film were in the room outside the helium chamber, they were easily changed before and after exposure without disturbing the helium in the chamber. With the available X-ray exposure field, samples from a number of batches could be radiographed simultaneously. The energy levels used for particle evaluation varied up to about 10 kVP. A typical exposure included the following values: 10-kVP, 30-mA, 50-cm (20-in) film-to-focus distance, and 15-min exposure time. For the small specimens and penumbral shadow, we feel that the detail or resolution in the plates is limited by electron diffusion in the emulsion, which is rated at about 1 μm at the energy level being used.

Transmitted light microscopy is used for viewing the radiographs and for preparing photomicrographs.

Results

The technique has become a vital link in the development of fuel particle technology. It is now regularly used in the evaluation of as-fabricated particles for coating thickness and core diameter with an accuracy better than 1 μm. Qualitative information is obtained about the shape and integrity of the core and coatings and whether fuel has migrated into the coating during fabrication. Figure 9 is a microradiograph of particles selected to show many of these characteristics. When particles are evaluated during and immediately after manufacture, the desired information is used to make appropriate correction to coating-gas mixture, the coating time, or temperature. This has been particularly valuable when particles have been made with layers of coating of different densities. Other applications have included the evaluation of all particles intended for in-pile testing. They are examined to assure the removal of all imperfect particles to give added assurance of a successful test. The technique has also assisted in determining the effects of service testing such as heat treatment or in-pile testing. Figure 10 shows fuel migration detected after heat treatment in a batch of particles.

Several fuel particles that had undergone as much as 6 at. % burn-up were microradiographed. The radiation levels at contact were as high as 3000 r/h of beta and 120 r/h of gamma. Slight modification of the standard technique allowed valuable evaluation with only slight loss of detail on these highly radioactive particles.

CONCLUSIONS

The projects that have been discussed show some of the benefits that have been obtained at ORNL through the use of specially developed nondestructive techniques. The valuable information derived during the early stages of material research and the assistance provided in revealing the effects of process variation in prototype component development make this technology indispensable in research and development. In addition there is usually much destructive analysis during process development that can

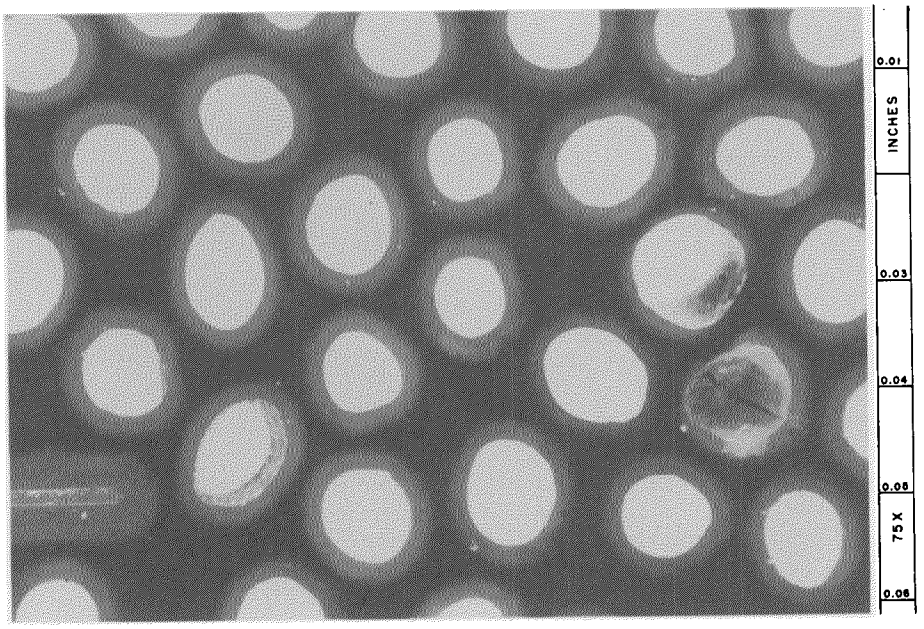

Fig. 9

Microradiograph of coated particles selected to show different qualities of interest

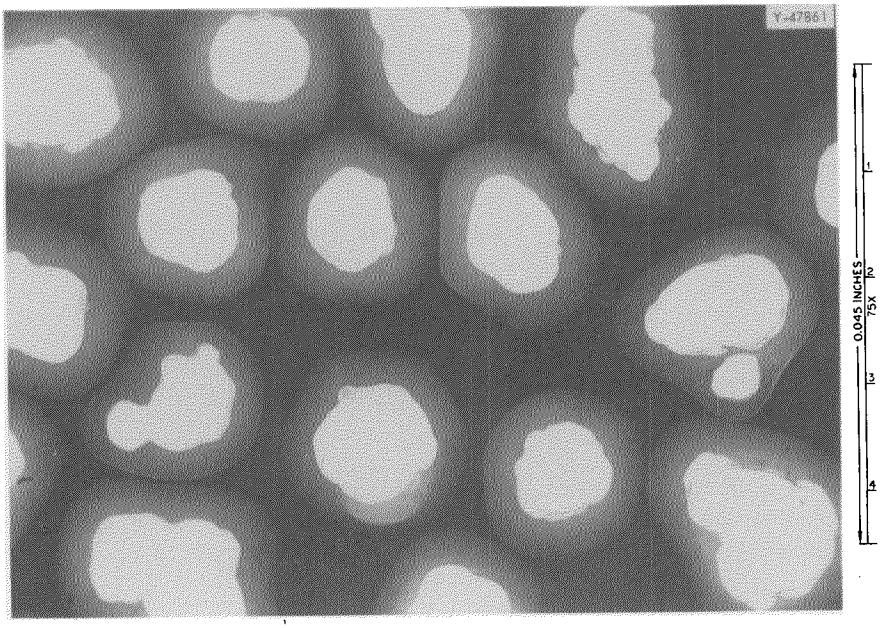

Fig. 10

Microgradiograph of fuel particles showing fuel migration after heat treatment

be correlated with non-destructive test results. Therefore, when these tests are adapted for production control, the correlation will allow more intelligent interpretation of data. As newer test methods are developed, these benefits will become even more apparent in the future.

REFERENCES

[1] HAWS, C. C., MATHERNE, J. L., MILES, F. W. and VANCLEVE, J. E., Summary of the Kilorod Project - A Semiremote 10-kg/day Demonstration of $^{233}UO_2$-ThO_2 Fuel Element Fabrication by the ORNL Sol-Gel Vibratory-Compaction Method, ORNL 3681 (1964).

[2] MARTIN, M. M., ERWIN, J. H. and LEITTEN, C. F., Jr., Fabrication Development of the Involute-Shaped High Flux Isotope Reactor Fuel Plates, Research Reactor Fuel Element Conference, September 17-19, 1962, Gatlinburg, Tenn., TID-7642 (1962) 268-289.

[3] FOSTER, B. E., SNYDER, S. D. and McCLUNG, R. W., Continuous Scanning X-Ray Attenuation Technique for Determining Fuel Inhomogeneities in Dispersion Core Fuel Plates, ORNL-3737 (1965).

[4] DODD, C. V. and McCLUNG, R. W., Fuel Element Coolant Channel and Other Spacing Measurements by Eddy-Current Techniques, ORNL-TM-129 (March 1962).

[5] DODD, C. V., Design and Construction of Eddy-Current Coolant Channel Spacing Probes, ORNL 3580 (1964).

[6] Gas-Cooled Reactor Program Quarterly Progress Report March 31, 1962, ORNL-3302 (1962) 165-167.

[7] McCLUNG, R. W., BOMAR, E. S. and GRAY, R. J., Use of Microradiography Combined with Metallography for Evaluation of Coated Particles, ORNL-3577 (1964).

DISCUSSION

P. KNUDSEN: Why was the eddy-current method preferred to other techniques (for example, ultrasonics, air gauge, strain gauge) for measuring coolant-channel spacing?

R. W. McCLUNG: For four reasons. We did not think that we could readily mount an ultrasonic probe in the very narrow (0.035 in) curved channels; the wide range of possible dimensions during development (0.035-0.075 in) precluded air gauging; users of strain gauges for similar purposes found the ease of breakage of the probes inconvenient; and our experience with eddy currents made us confident that this was a reasonable approach. Later experience with this type of probe on a number of projects has confirmed our decision.

P. de MEESTER: At what voltage did you work when measuring the fuel homogeneity by X-ray absorption?

R. W. McCLUNG: The voltage was 50-kV constant potential.

P. de MEESTER: Did you not have trouble with fuel-content evaluation, caused by variations in enrichment from one bath to another?

R. W. McCLUNG: The last calibration curve for the manufacture of reference standards was prepared by making a chemical analysis of inspected sections of fuel plates containing the same enrichment as the manufactured plates. We did not feel that the slight change in attenuation due to minor changes in isotopic enrichment would be significant when compared with the potential inaccuracies in the production test equipment. The accuracy of our laboratory system was found to be approximately 1%. It is felt that the accuracy of the production scanner may be about 2%.

P. de MEESTER: What was the activity of your Co^{60} source?

R. W. McCLUNG: A one-curie source of Co^{60} was used in the laboratory device, and a two-curie source of Co^{60} for the production "scanner".

J. GÉRARD: Is there any difficulty involved in using the coil designed for measuring the space between fuel-element plates to measure the space between tubular fuel pencils in a cluster?

R. W. McCLUNG: The same type of probe has been used at Oak Ridge National Laboratory for measuring tube-to-tube spaces both in concentric annular (coaxial) arrangements and in parallel arrays. The shape of the probe head may need to be changed according to the specific problem.

R. NEIDER: Did you not have difficulties with instability of output of the X-ray tube used to measure the fuel plates? If so, how did you circumvent these difficulties?

R. W. McCLUNG: We used an external voltage regulator on a commerical X-ray machine and operated the machine at the milliamperage found to offer the most stable operation. We were pleasantly surprised at the stability. For the production scanners, special high-stability X-ray equipment was designed and built.

R. S. SHARPE: We were also discouraged from using an X-ray tube as the source of transmitted radiation, owing to voltage variation and focal spot shift. How often do you find you need to recalibrate against your standards?

R. W. McCLUNG: For the evaluation of the HFIR fuel plates, with the standards at each end of the fuel plates, re-standardization is performed before each linear scan of the fuel plate. At production speeds this is every 10-15 s. Of course, this was necessary because of the variable fuel gradient across the plate width. In practice we have found that our equipment can operate for several hours without need for recalibration.

In the beginning of our work we were not sure that our stability would be adequate. However, we knew that we could use a secondary radiation detector to monitor the initial radiation and correct our instrument response. As is evident, this was not needed.

V. GERASIMOV: What was the accuracy you obtained with the coil probe, and by what was it limited?

R. W. McCLUNG: We used a commercial eddy-current instrument containing a bridge circuit. The accuracy of our measurements on the HFIR fuel assembly was approximately 0.0005 inches. As this was adequate, no attempt was made to improve upon it.

In the simplest case (where a meter on the face of the instrument is read), the accuracy is a percentage of the total range of measurements. For instance, the accuracy will be better if all measurement values cover only a very small range.

ASSESSMENT OF END-PLUG WELDING OF FUEL ELEMENTS

Y. NAKAMURA AND T. AOKI
TOKAI REFINERY, ATOMIC FUEL CORPORATION
JAPAN

Abstract — Résumé — Аннотация — Resumen

ASSESSMENT OF END-PLUG WELDING OF FUEL ELEMENTS. It is very important to correlate the testing results with the performance in reactor service, as well as to develop non-destructive testing techniques themselves. However, it is rather difficult to obtain these correlations because of high expense and radioactivity.

Several kinds of assessments in out-of-pile state were carried out simulating the in-reactor conditions.

Some details of these assessments on JRR-3 fuel elements are described. The reactor is a heavy-water-moderated and cooled research reactor of 10-MW capacity, with aluminium-clad metallic uranium fuel-elements. As the elements have only mechanical bonding between cladding and core, there might be a tensile stress at the end plug as a result of irradiation growth of the uranium core. Thermal cycling will cause a similar stress in the welds. Preferential corrosion by hot water might occur in the vicinity of the welds because of the difference of micro-structure.

It is essential to keep leak-tightness during and after the reactor service. Specially designed specimens were used for tensile testing, high-temperature creep testing, thermal cycling and corrosion testing. Many sorts of weld characters were examined non-destructively before the tests and leak-checked at intervals of the tests. Evaluations of these results may be used for the establishment of inspection standards such as X-ray radiography and visual inspection of the end-plug welding. Some other results on Magnox-clad and Zircaloy-clad fuel elements will also be described.

ÉVALUATION DES SOUDURES TERMINALES DES ÉLÉMENTS COMBUSTIBLES. Il est très important de mettre en corrélation les résultats d'essais et les performances d'un réacteur en service, et d'améliorer les méthodes d'essais non destructifs. Toutefois, cette corrélation est souvent difficile à obtenir du fait des dépenses élevées nécessaires et de difficultés tenant à la radioactivité.

Plusieurs sortes d'évaluations ont été faites hors pile en simulant les conditions en pile.

Le mémoire donne certains détails des évaluations faites pour des éléments combustibles du réacteur JRR-3. Il s'agit d'un réacteur de recherche de 10 MW, ralenti et refroidi à l'eau lourde, avec des éléments combustibles en uranium métallique sous gaine d'aluminium. Comme ces éléments n'ont qu'une liaison mécanique entre la gaine et l'âme, il peut exister une contrainte de traction aux bouchons de la gaine sous l'effet du gonflement de l'uranium par suite de l'irradiation. Le traitement thermique provoquera une contrainte analogue dans les soudures. Une corrosion préférentielle provoquée par l'eau chaude peut se produire dans le voisinage des soudures, à cause de la différence de microstructure.

Il est essentiel d'assurer l'étanchéité pendant et après l'utilisation dans le réacteur. Des spécimens spécialement conçus ont été utilisés pour les essais d'élasticité, les essais de fluage à haute température, les essais thermiques et le contrôle de la corrosion. Plusieurs sortes de soudures ont fait l'objet d'essais non destructifs avant les contrôles proprement dits et ont été vérifiées quant à l'étanchéité à diverses périodes entre les contrôles. L'étude critique des résultats obtenus peut permettre de fixer des normes d'inspection, telles que la radiographie par rayons X et l'inspection visuelle des soudures des bouchons. Le mémoire donne également d'autres résultats pour les éléments combustibles avec gaine en Magnox ou en Zircaloy.

ОЦЕНКА КАЧЕСТВА ПРИВАРКИ КОНЦЕВОЙ ПРОБКИ ТОПЛИВНЫХ ЭЛЕМЕНТОВ. Очень важно установить соотношение между результатами испытаний и использованием их в реакторе, а также разработать сами методы испытания без разрушения испытываемого объекта. Однако сделать это довольно трудно, так как это связано с большими расходами и большой радиоактивностью.

Было произведено несколько видов оценок во внереакторном состоянии с имитацией внутриреакторных условий.

Описываются некоторые детали этих оценок в отношении топливных элементов исследовательского реактора JRR-3. В этом реакторе установленной мощностью 10 мгвт с тяжелой водой в качестве замедлителя и теплоносителя используются топливные элементы из металлического урана с алюминиевым покрытием. Поскольку в элементах между покрытием и сердцевиной существует только механическая связь, концевая пробка может испытывать растягивающее напряжение в результате увеличения облучения урановой сердцевины. Температурные колебания вызовут аналогичное напряжение в сварных швах. Вследствие неоднородности микроструктуры вблизи сварных швов там может произойти усиленная коррозия под воздействием горячей воды.

Во время работы реактора и после его остановки необходимо обеспечить герметичность. Для проведения испытаний на прочность на разрыв, испытаний на ползучесть при высокой температуре, испытаний температурных колебаний и коррозии были разработаны специальные образцы. Многие характеристики сварных швов были изучены без разрушения испытываемого образца до проведения испытаний и проверены на герметичность в промежутках между испытаниями. Эти результаты могут быть использованы для установления стандартов проверки, таких как рентгеновская радиография и визуальная проверка качества приварки концевой пробки. Будут также описаны некоторые другие результаты, полученные по топливным элементам, покрытым магноксом или циркаллоем.

INSPECCION DE LA SOLDADURA DEL TAPON TERMINAL DE LOS ELEMENTOS COMBUSTIBLES. Es muy importante establecer una correlación entre los resultados de los ensayos y el rendimiento en los reactores en servicio, así como perfeccionar los correspondientes métodos de ensayo no destructivo. Ahora bien, resulta algo difícil lograr la correlación indicada a causa de los elevados gastos que ello supone y de la intensa radiactividad.

Se han efectuado varios estudios fuera del reactor simulando las condiciones que reinan en el interior de éste.

En el presente documento se exponen algunos datos sobre los ensayos con elementos combustibles del reactor japonés de investigación Nº 3 (JRR-3). Ese reactor de 10 MW es moderado y refrigerado por agua pesada, y tiene elementos combustibles de uranio metálico revestidos de aluminio. Como entre el revestimiento y el alma hay solamente una unión mecánica, puede producirse una tensión en el tapón terminal como resultado del crecimiento del alma de uranio debido a la irradiación. El ciclo térmico produce tensiones análogas en las soldaduras. Como resultado de la diferencia de microestructura, las proximidades de éstas que dan especialmente expuestas a la corrosión producida por el agua caliente.

Mientras el reactor está en servicio, es imprescindible asegurar su estanqueidad. Se han utilizado probetas especiales para estudiar la resistencia a la tracción, la fluencia a alta temperatura, los efectos del ciclo térmico y la corrosión. Antes de hacer esos ensayos, y periódicamente durante su realización, se sometieron a examen no destructivo muchas clases de soldaduras y se verificó si había escapes. La evaluación de los resultados obtenidos puede servir para establecer normas de inspección, por ejemplo, mediante radiografía y examen visual de la soldadura del tapón. En la memoria se describen algunos otros resultados de ensayos efectuados con elementos combustibles revestidos de Magnox y Zircaloy.

1. INTRODUCTION

It is very important to correlate testing results of welding techniques on reactor fuel elements with the performance in reactor service, as well as to develop non-destructive testing techniques themselves. However, it is difficult to obtain these correlations because of high expense and difficulties of handling radioactive materials.

Several kinds of assessments of end-plug welding techniques for reactor fuel elements were made in out-of-pile tests, simulating reactor conditions.

Helium leak testing is used for the final check in the fabrication of fuel elements and its specifications can be decided according to the permissible

radioactivity released from the defects into the reactor coolant. However, inspection standards for visual inspection and radiography on the welds is difficult. No leakage should occur during and after the designed service in the reactor even if the fuel element is leak tight in the as-fabricated state. However, in economic and routine production there are no fuel elements without any indications of defects in visual inspection and radiography. Therefore it is necessary to assess the qualities of the welding by such indications.

There will be a tensile stress at the end-plug welding as a result of irradiation growth of the uranium core and the different elongations of core and cladding, and thermal cycling will give some accumulative action on the welds. Corrosion will be accelerated in the vicinities of the welds because of uneven micro-structures. The welds should maintain leak tightness under these stresses and reactions.

2. ALUMINIUM END-PLUG WELDING

Specially designed specimens were used for the assessment. Many samples of various weld qualities were examined non-destructively in the as-fabricated state and separated into several classes.

The fuel element of the Japan Research Reactor (JRR-3), which is a heavy-water-moderated and cooled research reactor of 10 MW capacity, is metallic uranium mechanically clad with aluminium by drawing, and may be susceptible to the tensile stress at the welds. The fuel element is shown in Fig. 1 and test specimen is shown in Fig. 2. X-ray radiography was conducted according to following conditions

Equipment:	Müller-type MG 150 with beryllium window
Focus size:	0.7 mm diam.
X-ray film:	SAKURA R
Lead foil:	none on front, back 0.03 mm
Distance:	600 mm
X-ray tube voltage:	62 kVP
X-ray tube current:	4 mA
Exposure time:	5 min
Penetrameter:	detectable 0.2 mm diam. of aluminium wire
Correction block:	aluminium masking
Film developing:	CONIDOL, 20°C, 5 min

Aluminium masking and X-ray protective barrier liquid (ASL) were effective to improve the detectable limit, as shown in Table I.

The results of radiography on welds were classified into the following five groups.

Defect index 1:	defects of 0.1 - 0.3 mm equivalent in diameter
Defect index 3:	defects of 0.4 - 0.6 mm equivalent in diameter
Defect index 10:	defects of 0.7 - 1.2 mm equivalent in diameter
Defect index 20:	defects of 1.3 - 2.0 mm equivalent in diameter
Group A:	total defect index 0 - 2
Group B:	total defect index 3 - 9
Group C:	total defect index 10 - 19
Group D:	total defect index 20 -
Group E:	tungsten spots

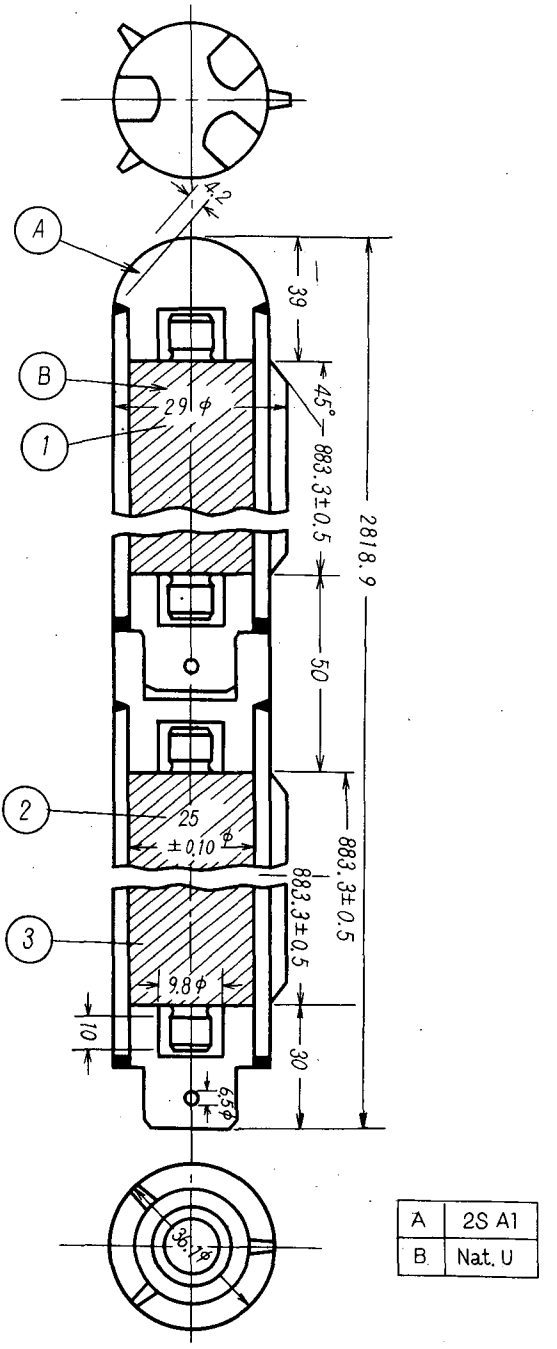

Fig. 1

JRR-3 fuel element

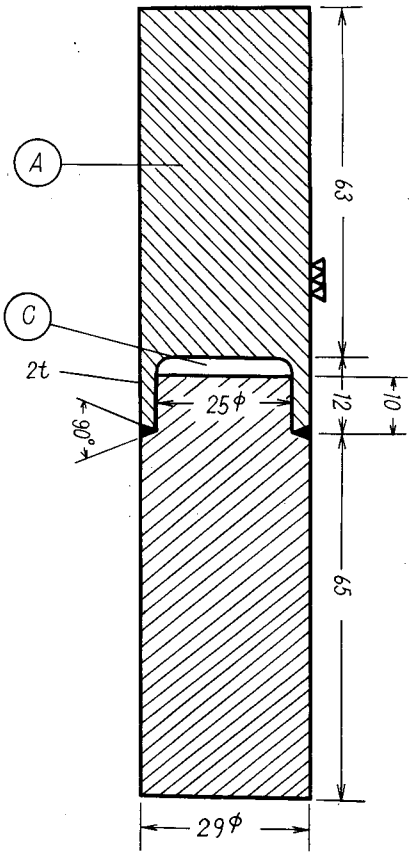

A	2S A1
C	He Gas

Fig. 2

End-plug welding specimen (aluminium)

Tensile stress was induced gradually until the specimen was broken. Helium and glycol leak tests were applied at many intervals of stress. Evaluation of the results was done at the stress level that is calculated from the designed permissible elongation of the fuel element; for instance, the permissible elongation of a JRR-3 fuel element, which consists of three fuel rods in one line, is 50 mm in a total length of 2650 mm, and then the critical loading to the specimen was calculated to be 400 kg from the mechanical properties of the cladding.

The loading for creep testing was selected to obtain a local elongation of 2% in 1000 h at the designed maximum temperature at the inside surface of the cladding. Some acceleration testing was also conducted. In both cases

TABLE I

COMPARISON OF MASKING EFFECT ON X-RAY RADIOGRAPHY

Items / Methods of masking	Conditions of exposure				Developing conditions of film		Film density at the centre	Figure quality
	Type of film	Tube voltage (kVP)	Lead foil					
			front (mm)	back (mm)	Temperature (°C)	Time (min)		
Aluminium masking	Fuji	70	no	0.03	20	5	1.56	good
ASL liquid masking	Sakura R	78	0.03	0.03	20	6	1.60	good
Without masking	Sakura	78	0.03	0.03	20	6	1.70	poor

leak testing was carried out at several intervals during the test. The maximum temperature in the thermal cycling test was selected to cause recrystallization in the cladding rather than the maximum design temperature of the reactor. The specimens were leak tested at several intervals of the cycling. Corrosion testing was carried out at a higher temperature in a simulated environment of the reactor coolant.

Leak testing was applied at various times during the corrosion test.

Results of tensile testing

Fifty-five specimens were tested, and none caused leakage until the loading was increased to 400 kg. Average rupture of the specimen occurred at a loading of 1530 kg and some specimens, which contained poor welding quality, leaked at a loading of 1000 kg or 1200 kg. The results are listed in Table II.

Results of creep testing

Four specimens each from group A, C and D were tested at 150°C with 700 kg loading for 1000 h, but none of them leaked. Further creep testing was continued at 150°C with 910-kg loading for an additional 1000 h.

One specimen of group A ruptured at a total of 1284 h. Two of group C caused leakage at 1200 and 1209 h. All the specimens of group D ruptured at 1263, 1366, 1412 and 1724 h.

TABLE II

RESULTS OF LEAK TEST UNDER TENSILE LOADING ON THE SPECIMENS WITH KNOWN DEFECTS IN THE WELD

Class	No. of specimens tested	No. of specimens which leaked		
		1[1]	2[1]	3[1]
A	10	8	2	0
B	11	3	7	1[2]
C	13	4	7	2[3]
D	12	4	6	2[4]
E	9	6	3	0

[1] Group 1: Leaked only when the specimen ruptured
Group 2: Leaked just before rupture
Group 3: Leaked at low loading
[2] 1000 kg
[3] 1000 kg, 1200 kg
[4] 1000 kg, 1350 kg

Results of thermal cycling

Thermal cycling tests were carried out between room temperature and 220°C with 12 specimens (four each from group A, C, and D). No leakage was observed after 500 cycles. Furthermore the cycle was continued between room temperature and 500°C, but no leakage was observed after an additional 500 cycles.

Results of corrosion testing

Hot-water immersion corrosion testing was conducted at 100-117°C for 50 d with 29 specimens (A-8, C-9, D-6, E-6). No leakage was observed after the test.

Conclusion

It may be concluded that:

(1) The probability of leakage at the weld by the tensile stress increases with the decreased weld quality.
(2) There is no difference of the probability of leakage caused by thermal cycling and corrosion with different qualities of the welds.
(3) Welding qualities of group A and B and even C will be leak-proof during actual operation conditions of the reactor, but group A and B are recommendable for routine application.
(4) The results suggest further reduction of welding specifications if the element-fabrication method is improved to include metallic bonding.

3. MAGNOX END-PLUG WELDING

A Calder-Hall-type power reactor of 585 MWt is now under construction in Japan. Since the Magnox can is pressure-bonded on uranium core, the tensile stress in the welds is very much reduced compared with the JRR-3 type, because of the anti-ratchetting grooves and a machined screw at the interface of can and end-plug. However Magnox is much more susceptible to weld defects than aluminium.

A series of testing on Magnox welds was carried out similar to the above-mentioned tests on aluminium end-plugs. Two kinds of specially designed specimens, one of them with a screwed end-plug and the other with no screw, are shown in Fig. 3. A particular system arrangement was necessary to obtain good radiographs as shown in Fig. 4.

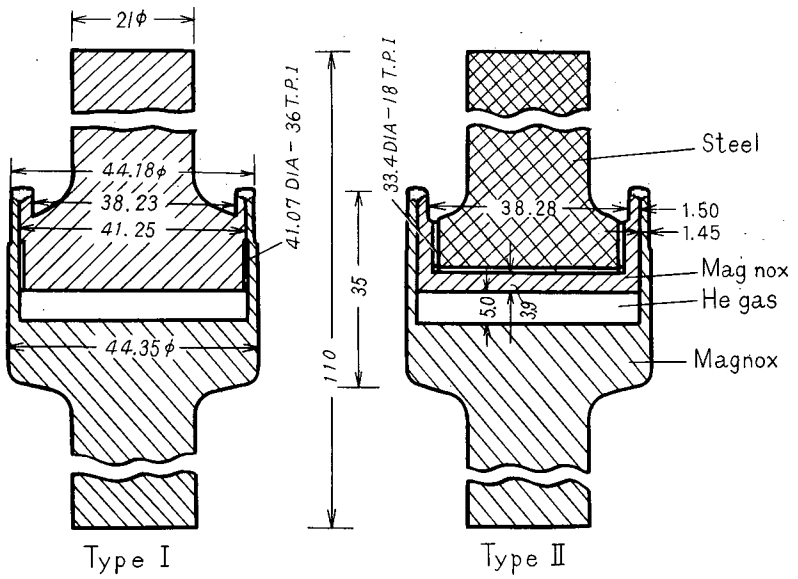

Fig. 3

End-plug welding specimen (Magnox)

Radiographs were very much improved by the specimen rotation method as shown in Table III, but the poor penetration in the welds was still hard to detect.

The conditions of X-ray radiography are as follows,

Equipment:	Müller-type MG 150 with beryllium window
Focus size:	0.7 mm diam.
X-ray film:	FUJI No. 80
Lead foil:	none
Distance:	300 mm
X-ray tube voltage:	30 kVP
Exposure time:	10 min
Penetrameter:	detectable 0.2 mm diam. of magnesium wire
Film developing:	LENDOL, 20°C, 6 min

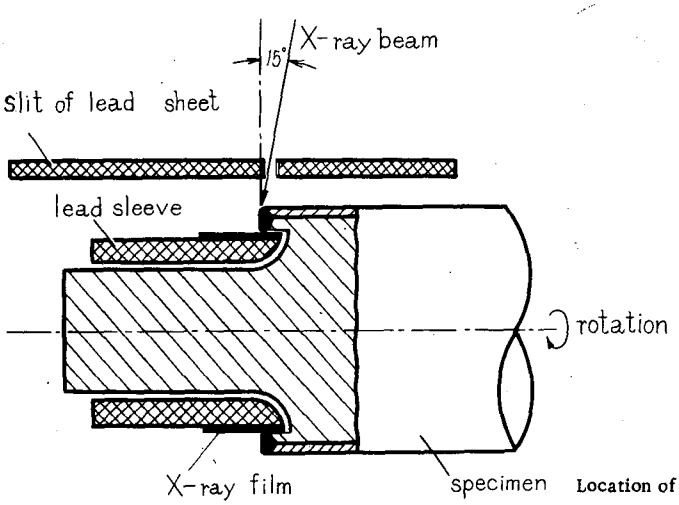

Fig. 4
Location of rotatory X-ray radiography

TABLE III

CONDITIONS OF X-RAY RADIOGRAPHY AND THEIR RESULTS

No.	X-ray radiography test condition				X-ray film	
	X-ray beam wide (mm)	Tube voltage (kVP)	Exposure time (min)	Filter	Penetrameter 0.1 mm-diam. Al	Sharpness of image
1	4	30	2.5	no	-[1]	×[2]
2	2	30	5	no	±	Δ
3	1	30	10	no	+	o
4	0.5	30	20	no	+	◉
5	0.5	25	56	no	+	◉
6	1	25	28	no	+	o
7	1	35	5	no	+	o
8	1	40	3	no	±	Δ
9	1	30	14	Al 0.5 mm	+	o
10	1	35	7	Al 0.5 mm	+	o

Other test conditions: F.F.D.: 300 mm
Rotation: 6 rpm
Tube current: 4 mA

[1] -: no detection +: detectable
[2] ◉: excellent o: good
Δ: medium ×: poor

The classification of weld quality is similar to that for the aluminium welds.

Results of tensile testing

The tests were carried out with six of type I (with end-plug screw) and ten of type II (without end-plug screw) at 250°C and 450°C. The results are shown in Table IV.

TABLE IV

RESULTS OF TENSILE TESTING

No.	Type of specimen	Welding quality	Penetration of welds	Test temperature (°C)	Load where leakage was found (kg)
1	I	B	good	250	915
2	I	B	good	250	965
3	II	B	poor	250	780
4	II	B	poor	250	665
5	II	B	poor	250	775
6	II	C	good	250	800
7	II	C	good	250	850
8	II	D	good	250	600
9	I	B	good	450	360
10	I	B	good	450	350
11	I	B	poor	450	200
12	I	C	good	450	240
13	II	B	good	450	250
14	II	B	poor	450	220
15	II	B	poor	450	225
16	II	C	good	450	206

Results of creep testing

Six specimens of type II were creep-tested with the loading of 10 kg at 450°C in CO_2 atmosphere. Each one of welding quality A and B did not leak in 1000 h. Poor penetration and welding quality reduced the duration until the leakage was found.

Results of thermal cycling

The testing was carried out with 12 type-I specimens of B welding quality in argon atomosphere. The cycling was done between room temperature and 500°C. Four specimens did not leak until 500 cycles, but five specimens leaked before 100 cycles, three of which were found to contain a poor penetration of the welds.

Results of corrosion testing

Nineteen specimens were heated to 450 ± 25°C in CO_2 gas with a pressure of 20 ± 2 kg/cm^2 for 90 d. One specimen, which had poor penetration, showed a leakage of the order of 10^{-5} μs after 30 d. Twenty-two specimens were corroded in hot water (pH 10 - 12, added Cl ion 2 ppm, 60°C) for 90 d. One specimen which had poor penetration leaked after 60 d.

Conclusion

As the testings are time-consuming and the numbers tested are limited, it is difficult to make a conclusion, but the results suggest that:

(1) X-ray radiography is much improved by the specimen rotation method, but it takes a longer exposure time to get the finest radiograph, and further improvement will be necessary for mass production.
(2) Magnox is more susceptible to weld defects than aluminium, and a higher specified grade of welding quality will be required.
(3) Since poor penetration of the welds is difficult to detect by radiography, process controls of welding are particularly important.
(4) A screw of the end-plug is effective to maintain leak-tightness.

Similar experiments are being planned with Zircaloy and stainless-steel end-plug weldings.

DISCUSSION

V. V. GORSKY: Did the X-ray photographs show unfused sections in the joints due to the presence of a film of aluminium oxide?

R. H. McKANE: If I may comment on the question, many welds of this type are made at the Savannah River plant, and we have been unable to find oxide films in the welds by means of X-rays, particularly when the films are normal to the X-ray beam.

T. AOKI: I agree with Mr. McKane. We were also unable to detect the aluminium oxide by metallography.

P. BONNET: I can give further details. In argon arc welds on SAP (sintered aluminium powder) fuel-element pencils, when an aluminium ring is placed between the plug and the can, it is impossible to detect the difference between SAP and Al on the radiographs.

I also have a question. Was the choice of test temperature (e.g. 480°C in the case of Magnox) guided by the normal operating temperature, or by the possible temperature of the hottest point of the pencil in the pile?

T. AOKI: The test temperature was selected for maximum operating conditions or for accelerative conditions. The maximum operating temperatures are about 80°C on the surface of the aluminium can (JRR-3 fuel elements) and about 450°C on the end-plugs of the Magnox (Calder Hall-type reactor of the Japan Atomic Power Company).

NON-DESTRUCTIVE EXAMINATION OF THE HEAT-AFFECTED ZONE OF WELDED Zr-Nb ALLOY

R. F. HANSTOCK AND D. C. B. WALKER
U. K. A. E. A. REACTOR MATERIALS LABORATORY,
CULCHETH, UNITED KINGDOM

Abstract — Résumé — Аннотация — Resumen

NON-DESTRUCTIVE EXAMINATION OF THE HEAT-AFFECTED ZONE OF WELDED Zr-Nb ALLOY. An alloy of zirconium, 2½% niobium has advantages for pressure containment in water-moderated reactors owing to the strength attainable by heat treatment. The corrosion resistance of the alloy under reactor operating conditions is also sensitively affected by heat treatment and zones of low corrosion resistance may be produced in the heat-affected zones of fusion welds. The zones susceptible to corrosion may be identified by autoclave treatment but this is not convenient when extensive pressure circuits are being assembled by welding. It has been found that heat-affected zones susceptible to corrosion can be detected non-destructively by measuring the thermo-electric potential between a heated metallic point probe in contact with particular regions of the weld and adjacent metal. The construction of the thermo-electric probe is similar to one devised by the British Non-ferrous Metals Research Association for measuring plating thickness on metal substrates and a commercially available instrument incorporating this type of probe is, with simple modification, suitable for testing welds in Zr-Nb alloys. An example is given of the variation of probe response across the heat-affected zones of a weld and is compared with an autoclave test for corrosion.

CONTRÔLE NON DESTRUCTIF DE LA ZONE D'UN ALLIAGE Zr-Nb AFFECTÉE PAR LA CHALEUR LORS DU SOUDAGE. Un alliage zirconium-niobium à 2, 5% Nb présente des avantages pour les circuits sous pression des réacteurs ralentis par de l'eau, du fait de la résistance mécanique que l'on peut obtenir par traitement thermique. La résistance à la corrosion de l'alliage dans les conditions de fonctionnement du réacteur est sensiblement affectée par le traitement thermique et des zones de faible résistance à la corrosion peuvent se produire au voisinage des soudures par fusion. On peut identifier ces zones par traitement en autoclave, mais cette méthode n'est pas applicable dans le cas de longs circuits sous pression que l'on assemble par soudage. On a constaté que les zones affectées par la chaleur qui sont susceptibles de corrosion pouvaient être décelées par contrôle non destructif, en mesurant le potentiel thermoélectrique aux bornes d'une sonde métallique chauffée, en contact avec des parties déterminées de la soudure et le métal adjacent. La sonde thermoélectrique est similaire à celle mise au point par l'Association britannique de recherches sur les métaux non ferreux en vue de mesurer l'épaisseur des revêtements de plaques de métal; un instrument en vente sur le marché et muni de ce type de sonde peut être utilisé, après une légère modification, pour le contrôle des soudures dans les alliages Zr-Nb. Le mémoire donne un exemple de la variation de la réponse de la sonde dans des zones affectées par la chaleur lors du sondage; les résultats sont comparés à ceux d'un examen en autoclave.

НЕДЕСТРУКТИВНОЕ ИСПЫТАНИЕ ЗОНЫ СВАРНОГО ШВА ИЗ ЦИРКОНИЙ-НИОБИЙ СПЛАВА, КОТОРЫЙ ПОДВЕРЖЕН ТЕПЛОВОМУ ВЛИЯНИЮ. Использование сплава из циркония и 2,5% ниобия для оболочки высокого давления в реакторах с водным замедлителем имеет ряд преимуществ, связанных с прочностью этого сплава благодаря термообработке. Термообработка также чувствительно влияет на коррозионную стойкость сплава в условиях работы реактора, и в зонах сварки плавлением, которые подвержены тепловому влиянию, могут появиться зоны низкой коррозионной стойкости. Зоны, подверженные коррозии, можно установить путем обработки в автоклаве. Однако этот метод является неудобным в тех случаях, когда путем сварки собираются крупногабаритные контуры высокого давления. Пришли к выводу, что зоны теплового воздействия, чувствительные к коррозии, можно обнаружить путем измерения термоэлектрического потенциала между нагретым металлическим точечным зондом, контактирующимся с определенными областями сварного шва, и примыкающим к нему металлом. Термоэлектрический зонд изготавливается так же, как зонд, который создан Британской ассоциацией по исследованиям цветных металлов для измерения толщины покрытия металлических субстратов. Имеющийся в продаже прибор, который включает такой

зонд с незначительными видоизменениями, можно использовать для испытания сварных соединений из цирконий-ниобий сплавов. Приводится пример изменения зондовой чувствительности по зонам сварного шва, подверженным тепловому воздействию, и этот пример сравнивается с проведенным в автоклаве испытанием на коррозию.

EXAMEN NO DESTRUCTIVO DE LA ZONA DE SOLDADURA AFECTADA POR EL CALOR EN LAS ALEACIONES DE CIRCONIO Y NIOBIO. Las aleaciones de circonio con 2½% de niobio ofrecen, gracias al tratamiento térmico, la ventaja de resistir la presión en los reactores moderados por agua. Por otra parte, ese tratamiento afecta considerablemente a la resistencia a la corrosión en las condiciones de funcionamiento del reactor, siendo de señalar que pueden surgir puntos especialmente vulnerables en las zonas de las soldaduras sometidas al calor. Las zonas susceptibles de corrosión pueden localizarse mediante tratamiento en autoclase, pero no es conveniente aplicarlo cuando extensos circuitos de presión se arman mediante soldadura. Se ha comprobado que las zonas afectadas por el calor que son vulnerables a la corrosión pueden localizarse por métodos no destructivos consistentes en medir el potencial termoeléctrico entre la punta de una sonda metálica caliente en contacto con determinadas partes de la soldadura y el del metal adyacente. La sonda es análoga a la que ha diseñado la British-ferrous Metals Research Association para medir el espesor del chapado de sustratos metálicos. Los instrumentos comerciales equipados con ese tipo de sonda sirven con una sencilla modificación, para examinar las soldaduras en las aleaciones de circonio y niobio. Se da un ejemplo de las variaciones en la respuesta de la sonda en las distintas partes de una soldadura afectadas por el calor, y se las compara con los resultados del estudio de la corrosión efectuado en autoclave.

1. INTRODUCTION

The low neutron absorption cross-section and good corrosion resistance of zirconium favours its use as the basis of strong alloys for the fabrication of in-core sections of pressure circuits of pressure-tube-type reactors. An acceptable alloy for this purpose is cold-worked Zircaloy-2 but substantially higher strength is obtainable in an alloy of zirconium with 2½% niobium. However, the strength and corrosion resistance of this alloy depends on its heat-treatment. When rapidly cooled, e.g. by quenching in water-from ≈1000°C, its strength is below the optimum and its corrosion resistance to high-temperature steam is relatively low. Strength and corrosion resistance increase on ageing at a temperature of 500°C from the quenched state but prolonged ageing reduces the ductility of the alloy. Annealing at ≈700°C allows the alloy to be cold-worked to give satisfactory strength and corrosion resistance.

2. WELDING OF Zr-2½% Nb ALLOY

Fusion welds in Zr-2½% Nb alloy may be made by the tungsten-arc process in an atmosphere of argon. Being responsive to heat-treatment the properties of the alloy are affected where fusion occurs and in a zone where the weld heat produces high temperatures. For the purpose of evaluating welding procedures it has been customary to test the corrosion resistance of experimental welds by subjecting them to steam at 400°C and 500 lb/in^2 in an autoclave for 72 h or at 300°C in water for 7 d. On a good weld the corrosion product is dark grey and adherent. Poor corrosion resistance is indicated by either the formation of a white, less-adherent deposit arising from atmosphere contamination or a "tramline" effect as in Fig. 1 arising from a variation in a metallurgical condition. Obviously these tests are not

Fig. 1

Autoclave corrosion test on Zr-2½% Nb alloy fusion weld

convenient for the examination of welds during the fabrication of a large pressure circuit.

3. NON-DESTRUCTIVE TESTS

A method is required which will indicate quickly the metallurgical condition at various points in the heat-affected zone and which will not be influenced by the geometry of the weld. To assess the sensitivity of several possible test methods, samples of Zr-2½% Nb alloy were heat-treated to conditions designated as follows:

Q - heated at 1000°C for ½ h and quenched in water,
QA_1 - Q followed by ageing at 500°C for 5 h,
QA_2 - Q followed by ageing at 500°C for 24 h.

3.1. Hardness and electrical resistivity

Conventional methods for measuring hardness and electrical resistivity might be used to explore the condition of a weld. However, Table I shows that these properties are not particularly sensitive to variations in heat-treatment. Their use entails certain disadvantages, e.g. indentation of the metal, and in the measurement of resistivity, difficulty in defining a small enough region over which the measurement is made.

3.2. Thermo-electric potential

It is well known that a thermo-electric potential is developed at a hot junction of two dissimilar metals or alloys. Table II shows the magnitude

TABLE I

HARDNESS AND ELECTRICAL RESISTIVITY OF Zr-2½% Nb ALLOY

State (see text)	Hardness (V.P.N.)	Resistivity ($\mu\Omega$-cm)
Q	258	60
QA_1	276	56
QA_2	287	53

of this effect for couples between zirconium and Zr-2½% Nb or Zircaloy-2. It is seen that the thermo-electric potential discriminates between zirconium and the zirconium alloys and that a junction between Zr-2½% Nb alloys in different conditions will, when heated to about 100°C above the cold junction of the thermo-electric circuit, produce a voltage that can be easily measured.

4. THERMO-ELECTRIC PROBE FOR WELDS

A simple thermo-electric probe for examining welds is shown diagrammatically in Fig. 2, where A and A^1 represent two plates of Zr-2½% Nb alloy welded together in the zone B. The probe P, which for simplicity may be regarded as metallurgically similar to the material of A, is heated near its pointed end by a small coil, C, so that a hot junction is made at X, the point of contact between the probe and the weld. The thermo-electric circuit is completed through an instrument V, measuring microvolts, and a cold junction which may be on the plate A at a point sufficiently far from X to avoid heating by conduction from the probe. If, initially, the probe is placed at X^1 outside the heat-affected zone of the weld no thermo-electric potential is developed but, as the probe is moved to point X, a potential difference appears if the condition of the weld is different from that of the plate.

A probe constructed for preliminary trials of the method consisted of an annealed Zr-2½% Nb rod, approximately 6 mm diam., formed with a conical end to a point radius of ≈ 0.5 mm. A small coil heater wound near the conical point raised the temperature at this end of the rod to ≈ 250°C. The probe was held in contact with the test sample to form the hot junction and the cold junction was made by attaching a wire to the sample by a clip. The thermo-electric potential, amplified by a chopper-type high-gain amplifier, operated a meter calibrated to read microvolts. This simple equipment demonstrated the feasibility of the method.

Subsequently, all tests have been made with modified commercially available[1] equipment based on the design[2] of an instrument for determining the thickness of metallic coating [1, 2]. In this instrument, the probe has

[1] Nash and Thompson Ltd. Tolworth, Surrey, England.

[2] By the British Non-ferrous Metals Research Association, Euston Street, London, N.W.1. England.

TABLE II

THERMO-ELECTRIC POTENTIALS BETWEEN ZIRCONIUM AND ALLOYS

Material	Zirconium	Zirconium 2½% Niobium				Zircaloy-2
		Annealed	QA_2	QA_1	Q	
Thermo-electric potential μV/deg C	0	1.38	1.62	2.16	2.66	4.33

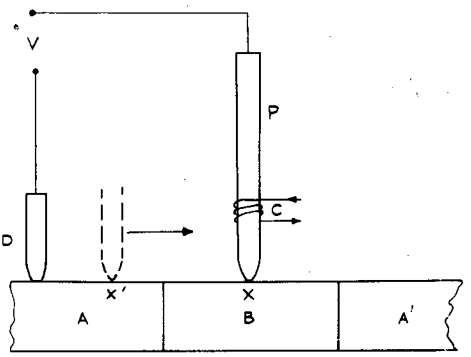

Fig. 2

Principle of the thermo-electric probe

a steel point about 0.5 mm radius and a large thermo-electric potential is developed when this is placed in contact with zirconium alloy. Thus it is necessary to apply a backing-off potential to obtain a zero reading on the alloy away from the weld in order to be able to amplify the smaller potential difference that arises when the probe is moved into the weld zone. A schematic design of the probe and a block diagram of the measuring circuit is shown in Fig. 3. The thermal capacity associated with the probe tip is sufficiently large for its temperature, about 100°C above ambient, to be relatively unaffected by the small heat leak through the point contact on the test weld. The heat transferred at the weld by the point probe produces a very localized hot spot without increasing the general temperature of the weld metal. The response of the probe is moderately sensitive to the contact pressure. A helical spring compressed to a constant amount limited by the contact of a thermally insulating end-cap with the weld surface ensures a reproducible pressure. The measuring circuit of the instrument has been modified by replacing the normal voltage backing circuit provided for zero setting by a more accurate potential divider and by the addition of a potentiometer for measuring this backing voltage. This allows the thermo-electric

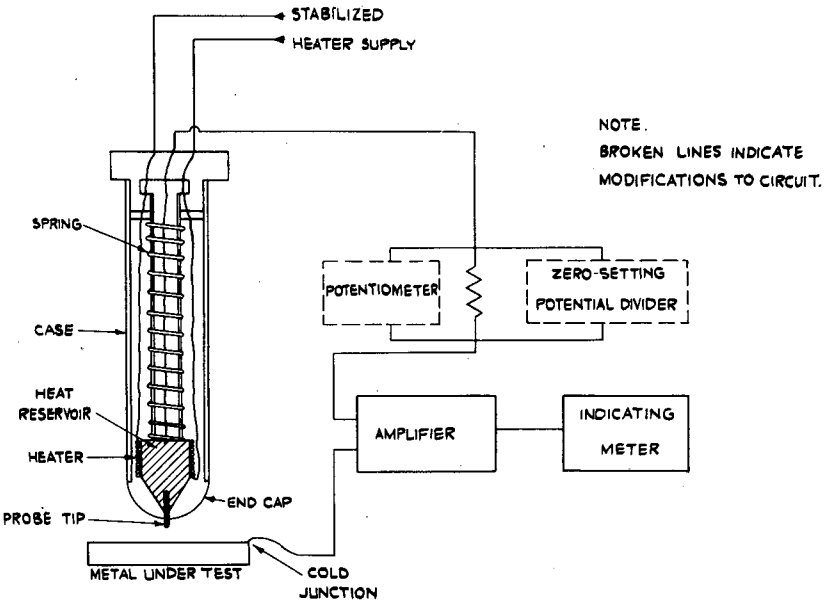

Fig. 3

Thermo-electric probe and associated circuits

potentials to be measured when scanning across a weld. For a quick assessment of the weld condition the out-of-balance of the meter, after setting the zero on the plate material, is sufficient for routine tests.

5. WELD TESTS

The thermal probe is very simple to use, the only precaution necessary being to ensure that the weld is clean and free from electrically insulating oxide. Before use, the probe must be allowed enough time to reach temperature equilibrium, after which potential readings may be made quickly, allowing a few seconds to elapse between each reading.

The results of the examination of some fusion welds of Zr-2½% Nb alloy are shown in Fig. 4, curves A and B. The weld to which curve A refers was produced by fusing together the abutting edges of two pieces of 1.10-mm-thick plate by means of a tungsten arc in an enclosure filled with argon at about atmospheric pressure. The plates were cold-rolled with 20% reduction from the annealed condition and had a thermo-electric potential slightly less than that of material in the state QA_2 as defined in section 3. The variation of thermo-electric potential across the heat-affected zone, Curve A, shows that the metallurgical condition of the weld approaches but does not reach the state QA_1. It was concluded that this weld would have good corrosion resistance and this was confirmed by the autoclave test. It is interesting to note that the nearest approach to the state QA_1 is at the outer boundaries

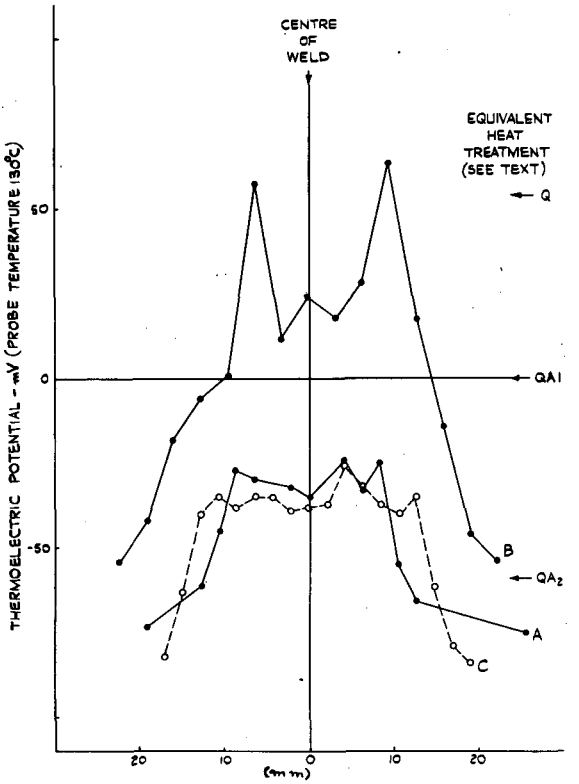

Fig. 4

Thermo-electric potential in heat-affected zones of welds in Zr-2½% Nb alloy

of the heat-affected zone, where the rate of cooling of the weld by the unheated parts of the plate is highest.

The weld to which Fig. 4, Curve B, refers was produced by fusing abutting edges of two pieces of 3.2-mm-thick plate which had been heat-treated to the state QA_2. The variation of the thermo-electric potential across the heat-affected zone shows that the quenching effect of the cold parts of the plates was very severe at the boundaries of the zone and produced regions which have a metallurgical condition corresponding approximately to the Q state. These regions would be expected to have low corrosion resistance and a subsequent autoclave test produced the "tramline" effect in positions corresponding to the peaks in Curve B. The width of the heat-affected zone of weld B made in 3.2-mm plate is considerably greater than that in weld A made in 1.1-mm plate, presumably because more heat input is required to weld the thicker plate. In a weld where a filler rod is used to fill a gap between abutting plates the heat input required to fuse the filler and the plate edges is also higher than in a simple fusion weld. Curve C in Fig. 4 shows the variation of thermo-electric potential across a filler-type weld between plates of the same thickness and condition as those used in producing weld A. It is seen that the heat-affected zone is wider in the filler-type weld. In

applying the test to filler-type welds it is necessary to ensure that the filler rod is of the same composition as the plate material since it is evident from Table II that the thermo-electric potential is sensitive to composition as well as to heat-treatment.

6. CONCLUSIONS

The use of a thermo-electric probe to measure variations of thermo-electric potentials in fusion welded Zr-2½% Nb alloy is a simple and practical non-destructive technique for defining the heat-affected zone. If the thermo-electric potential at any point in the zone is near to that of the alloy in the state induced by rapid quenching from 1000°C, then the weld is likely to have unsatisfactory corrosion resistance in steam environment.

ACKNOWLEDGEMENTS

The assistance of Messrs. F. S. Dickinson, P. Lees and C. P. Pennington in the preparation of welds and autoclave testing is gratefully acknowledged. The authors also wish to thank Mr. J. M. Hutcheon, Head of the Reactor Materials Laboratory and Mr. R. V. Moore, Managing Director of the Reactor Group, U. K. A. E. A. for approval to contribute this paper to the Symposium.

REFERENCES

[1] HEATH, A. R., Metal Finishing J. 1 (New Series) (1955) 145-50.
[2] British Patents 768,448 and 858,345.

NEW FRONTIERS FOR NON-DESTRUCTIVE TESTING IN THE NUCLEAR AGE

D. W. BALLARD
SANDIA LABORATORY
ALBUQUERQUE, N. MEX.,
UNITED STATES OF AMERICA

Abstract — Résumé — Аннотация — Resumen

NEW FRONTIERS FOR NON-DESTRUCTIVE TESTING IN THE NUCLEAR AGE. Much of the fantastic growth in non-destructive testing since World War II can be attributed to the more demanding quality requirements for highly reliable components in the nuclear industry. System complexity and overall costs of service failures have become so great that it is imperative that more effective non-destructive test methods be developed and used throughout the "cradle-to-grave" product cycle.

While the capabilities of well-known test methods such as radiography, ultrasonics, and electromagnetic testing are being greatly extended in an attempt to satisfy the accelerating technical demands for perfection, new testing concepts are being developed specifically to test both static and dynamic performance requirements. These high-speed, high-resolution methods are truly "new frontiers" for non-destructive testing and constitute the basis for this paper.

Among the newer test methods to be discussed are the use of infra-red testing for determining the integrity of weldments. Cineradiographic testing of structures during vibration testing to examine their dynamic behaviour is covered. Another area of extreme importance to obtaining reliable reactor fuel is effective leak detection. A method for inspecting canned components is discussed which uses a radioactive gas and which is capable of measuring leak rates as low as 10^{-12} cm^3/s or 1 cm^3 leakage in 500 yr.

In-motion radiography at high magnifications using X-ray sensitive vidicon tubes is another valuable new tool. A similar new method (cinesonography) using ultrasonic imaging rather than radiography is covered.

Finally, there is a discussion of the next generation of fully automatic, high-speed equipment that must be developed for rapid scanning applications. Such systems will incorporate several non-destructive test methods applied simultaneously. Infra-red, electromagnetic, and microwave test methods coupled with tape-controlled scanning will be adapted to produce output images suitable for remote television displays and recording. Test parameters, display capabilities, and continuous monitoring systems are discussed. These possibilities have already been demonstrated in laboratory testing and their use must be extended to production testing if a new level of reliability of components in the nuclear industry is to be achieved.

PERSPECTIVES DES ESSAIS NON DESTRUCTIFS A L'ÈRE NUCLÉAIRE. On peut attribuer en grande partie l'extraordinaire développement des essais non destructifs depuis la deuxième guerre mondiale aux spécifications extrêmement strictes imposées aux matériaux et produits de l'industrie nucléaire. La complexité des installations et de leurs éléments et les incidences financières des arrêts de fonctionnement ont atteint des proportions telles qu'il est impérieux de mettre au point des méthodes plus efficaces d'essais non destructifs et de les appliquer tout au long de la durée de vie des produits, depuis leur mise en fabrication jusqu'à leur déclassement.

En même temps que, pour tenter de satisfaire aux impératifs techniques de perfection, on développe considérablement les possibilités offertes par des méthodes d'essais confirmées, comme la radiographie, les ultrasons et l'électromagnétisme, on met au point de nouveaux principes d'essais destinés expressément au contrôle des performances statiques et dynamiques. Le mémoire porte sur ces méthodes particulièrement rapides et sensibles qui ouvrent vraiment de nouvelles perspectives aux essais non destructifs.

Au nombre des méthodes d'essais les plus récentes discutées dans le mémoire figure le contrôle par les infrarouges de l'intégrité des soudures. Le contrôle cinéradiographique des structures au cours des essais de vibration, pour étudier leur comportement dynamique, est également traité. La détection des fuites est extrêmement importante pour assurer la qualité des éléments combustibles. Le mémoire décrit une méthode de contrôle des éléments combustibles sous gaine, qui est fondée sur l'utilisation d'un gaz radioactif et qui permet de mesurer des fuites de l'ordre de 10^{-12}cm^3/s, soit 1 cm^3 en 500 a.

La cinéradiographie à fort grossissement, au moyen de tubes Vidicon à rayons X, constitue un nouveau procédé fort utile. Le mémoire décrit aussi une nouvelle méthode similaire (cinésonographie), dans laquelle la formation de l'image est fondée sur les ultrasons et non sur la radiographie.

Enfin, l'auteur étudie la prochaine génération d'appareils entièrement automatiques et à grande vitesse qu'il faudra mettre au point pour procéder à des explorations rapides. Ces appareils permettront l'application simultanée de plusieurs méthodes non destructives. Il faudra adapter des méthodes d'essais par les infrarouges, l'électromagnétisme et les micro-ondes à l'enregistrement continu des résultats, de manière à obtenir des images pouvant être retransmises par télévision et kinescopées. Le mémoire discute les paramètres des essais, les possibilités de transmission des résultats et les possibilités de contrôle en continu. Ces possibilités ont déjà été démontrées au cours d'essais en laboratoire; il faudra en tirer profit sur le plan industriel si l'on veut atteindre un niveau encore plus élevé de la qualité dans l'industrie nucléaire.

"НОВЫЕ РУБЕЖИ" НЕДЕСТРУКТИВНЫХ ИСПЫТАНИЙ В ЯДЕРНЫЙ ВЕК. После второй мировой войны колоссально возросло число методов недеструктивных испытаний, что можно в значительной степени объяснить тем, что в ядерной промышленности предъявляются все более строгие требования к качеству и надежности оборудования. Сложность системы и общие расходы, связанные с повреждениями, настолько возросли, что существует настоятельная необходимость в разработке более эффективных методов недеструктивных испытаний, а также в их использовании на всем протяжении производственного цикла.

В настоящее время значительно расширяются возможности применения хорошо известных методов испытаний, например с помощью радиографии, ультразвука и электромагнитных колебаний, для удовлетворения все возрастающих требований технического усовершенствования. Одновременно разрабатываются новые принципы испытаний специально для того, чтобы проверить те требования, которые предъявляются к статическим и динамическим характеристикам. Эти быстродействующие методы с высокой разрешающей способностью, являющиеся поистине "новыми рубежами" недеструктивных испытаний, положены в основу настоящей работы.

В число новейших методов, которые рассматриваются в докладе, входит использование инфракрасных лучей для определения прочности сварных соединений. Рассматривается испытание структур методом кинорадиографии во время вибрационного испытания с целью изучения их динамического поведения. Другой областью, которая имеет исключительно важное значение для получения надежного реакторного топлива, является эффективное нахождение места течи. Рассматривается метод проверки заключенных в оболочку компонентов, при котором используется радиоактивный газ и который позволяет измерять скорости утечки, составляющие 10^{-12} см^3/сек, или 1 см^3 в течение 500 лет.

Другим ценным методом является радиография в движении при больших увеличениях с использованием видиконов, чувствительных к рентгеновским лучам. Освещается новый аналогичный метод (киносонография), при котором используется не радиография, а ультразвуковое изображение. В заключение работы рассматривается новый вид полностью автоматического быстродействующего оборудования, разрабатываемого для использования при быстром сканировании. Такие системы будут включать несколько методов недеструктивных испытаний, которые применяются одновременно. Приборы использующие инфракрасные лучи, электромагнитные колебания и токи высокой частоты в сочетании со сканнирующими устройствами, управляемые с помощью магнитной пленки, соответствующим образом приспасабливаются для получения выходных изображений, которые пригодны для дистанционного телевизионного воспроизведения и записи. Рассмотрены испытательные параметры, воспроизводящие способности и непрерывные системы контроля. Эти возможности уже выявлены в ходе лабораторных испытаний и их следует также использовать и при заводских испытаниях, если мы хотим добиться большей надежности оборудования в ядерной промышленности.

NUEVAS POSIBILIDADES DE LOS ENSAYOS NO DESTRUCTIVOS EN LA ERA NUCLEAR. El extraordinario desarrollo de los ensayos no destructivos que se ha registrado desde la segunda guerra mundial puede atribuirse en gran parte a las mayores exigencias en cuanto a la calidad del material que, en la industria nuclear, ha de ofrecer un alto nivel de seguridad. La complejidad de las instalaciones y los gastos que en general entrañan las fallas en su funcionamiento han aumentado de tal forma que se impone establecer métodos más eficaces de ensayo no destructivo, aplicables al material desde que sale de la fábrica hasta que queda en desuso.

Al mismo tiempo que se procura atender las exigencias cada vez mayores de perfección técnica mejorando los métodos de ensayo conocidos, por ejemplo los radiográficos, ultrasónicos y electromagnéticos, se establecen otros nuevos para comprobar si el equipo reúne los requisitos necesarios tanto en el aspecto estático como en el

dinámico. Esos métodos ultrarrápidos y de elevado poder de resolución constituyen en realidad las nuevas fronteras del ensayo no destructivo, y a ellos se refiere fundamentalmente la presente memoria.

Entre los modernos métodos de ensayo que se estudian se cuenta el uso de rayos infrarrojos para verificar el estado de las soldaduras y la inspección cinematorradiográfica de las estructuras durante los ensayos de vibración para verificar su comportamiento dinámico. Hay que tener también muy en cuenta la importancia de una localización eficaz de los escapes para que el combustible de los reactores pueda utilizarse en condiciones de seguridad. Se examina un método de inspección de piezas revestidas, basado en el empleo de gas radiactivo, con el que se pueden medir fugas de incluso 10^{-12} cm³/s, esto es, de 1 cm³ cada 500 años.

Otro medio eficaz que puede utilizarse actualmente es la radiografía dinámica con gran ampliación, basada en el uso de tubos vidicón sensibles a los rayos X. Se estudia asimismo un nuevo método análogo al indicado, (cinesonografía); con este método, la obtención de imágenes se realiza por medios ultrasónicos y no radiográficos.

Para terminar, se procura estudiar el equipo totalmente automático y ultrarrápido que habrá de prepararse para exploración a gran velocidad. Ese equipo supone la aplicación simultánea de varios métodos de ensayo no destructivo. Los métodos basados en el empleo de rayos infrarrojos, los electromagnéticos y los de microondas combinados con la exploración gobernada por cinta magnética se utilizan para obtener imágenes de la producción; esas imágenes pueden ser televisadas o registradas a distancia. Se examinan los parámetros de ensayo, las posibilidades de indicación y los sistemas de comprobación continua. Esas posibilidades se han estudiado ya en laboratorio y ahora hay que aplicarlas a la producción si se quiere lograr un mayor nivel de seguridad en el empleo del equipo nuclear.

1. INTRODUCTION

In October 1965, the American Society for Nondestructive Testing will celebrate its silver anniversary as a technical society. Twenty-five years ago the significant impact that non-destructive testing was to have on everyone's life was not foreseen when a group of nine technicians met in Boston to exchange some early experiences in industrial radiography.

Non-destructive testing (NDT) is now playing a critical and widely recognized role in the quality control operations of modern industry. Tests such as radiography, ultrasonics, magnetic particle and electromagnetic testing have earned their reputation on the production lines as vital tools which help to ensure the reliability of products [1].

Much of the tremendous growth of non-destructive testing since World War II can be directly attributed to the more demanding quality requirements imposed on military ordnance and, more recently, for more reliable space and nuclear components [2].

If these dynamic advances are to continue we must consider the needs of the rapidly changing world of ten to twenty years hence. As we enter the second quarter-century of NDT in the United States of America, it is appropriate to speculate about the "new frontiers" for non-destructive testing in the nuclear age.

This paper presents seven predictions of new frontiers for non-destructive testing that should represent a distinct challenge to those now engaged in this profession.

These predictions are based on my experiences during the past seven years that I have served as a National Director and Officer of the American Society for Nondestructive Testing. It is hoped that this review will encourage each of the members of this distinguished audience to consider his own use of NDT methods as related to these new frontiers.

2. NEW FRONTIERS FOR NON-DESTRUCTIVE TESTING

As the emphasis on reliability of parts, equipment and systems continues to grow, the tools of non-destructive testing will be modified or refined to meet the challenge of the following six new fields.

Material properties testing; Research and development tools; Dynamic NDT applications; Multiple non-destructive testing; Electronic component and systems testing; and infra-red and micro-wave tests.

Each of these fields deserves closer study. Examples will be used in the following sections to reinforce each prediction.

3. MATERIAL PROPERTIES TESTING

3.1. Identification with defect detection

By nature of their conception and development, most established non-destructive tests have been concerned solely with detecting material discontinuities [3]. This almost universal identification with defect detection and inspection has had the unfortunate effect of creating artificial and restrictive boundaries of non-destructive testing. While defect detection is obviously important, information on material properties and structural uniformity should receive equal emphasis [4].

Non-destructive testing will, therefore, undergo a re-direction with the emphasis on quantitative properties measurements.

Already, examples of current applications are appearing in the literature on non-destructive material property testing. For example, the March 1965 issue of Materials Evaluation featured the following: "Ultrasonic attenuation test for improper heat treatment of steels" [5], "Radiography for metallurgical troubleshooting" [6]; and "Ultrasonic velocity for ultimate tensile strength of resin-ceramic heat shield" [7].

3.2. Ultrasonic hardness tester

Another example of the application of NDT methods to material property testing is a recently announced ultrasonic hardness tester for steel which gives a direct read-out in three seconds of Rockwell C 10 to 70 range with a claimed accuracy of $\pm$ 1 point [8].

3.3. Ultrasonic attenuation tests

SHARPE [9, 10] of Harwell has reported the use of ultrasonics for studying the coarse microstructure of uranium bars as well as for accurate wall-thickness measurements of stainless-steel fuel-element sheeting.

3.4. Electromagnetic conductivity test

Eddy-current measurements of conductivity of the newer alloy steels have shown a closer correlation with tensile strength than does the traditional hardness testing.

3.5. Guide for test selection

CARLTON H. HASTINGS [11], a past-president of SNT, gave the following guide for selecting the proper tests for physical properties: "If you want to measure a list of properties, the first step is to translate them to a list of independent material variables. The next step is to determine what kind of test energy to use". Applying these guides led to the layout of Table I.

4. RESEARCH AND DEVELOPMENT TOOLS

4.1. Basis for prediction

Closely related to the previous application is the predicted increased usage of NDT methods as important tools for the design stages [12]. The designer's problems have increased enormously in recent years. Examples include the need to design for higher strength-to-weight ratios, ability to withstand split-second shock loading, radiation and thermal stresses.

4.2. Benefits to designers

Proper use of NDT techniques during development will provide the designer with five major benefits, all of which are related to a better understanding of the capabilities and limitations of his design, and to a higher degree of assurance in the performance of his product during production. Specifically, these benefits of an active non-destructive testing programme to the designer are as follows:

(a) Valid correlation: Provides a valid basis for correlating design prove-in tests with subsequent acceptance tests during production.
(b) More information: Allows the designer to derive more useful information on destructive and/or environmental tests with very little additional cost.
(c) Fewer expensive tests: Reduces the number of expensive destructive tests.
(d) New source of data: Provides a source of unique information that often cannot be obtained by other test methods.
(e) Better designs: Permits better design by earlier "trouble-shooting" and justifiable reduction of design safety factors.

4.3. Possible savings

At the beginning of the design programme, a definite effort should be made to correlate the findings of non-destructive tests with the destructive tests that are so essential to the development of a design satisfactory to the customer. Formulating the acceptance criteria for production tests during the design stage can save many frustrating man-hours for both the production and quality control departments. Valid correlation studies also enable the designer to work closer to the true yield and ultimate stresses of his materials. An estimate of $150 000 penalty for each additional pound of

TABLE I

NON-DESTRUCTIVE TEST PARAMETERS MATERIAL INTERACTIONS

NDT Technique	Interaction	Related Material variables
1. Ultrasonics		
(a) Velocity	Stress-wave Propagation	A: Elasticity, Density/porosity, Crystal structure, Grain size, Anisotropy
(b) Attenuation	Energy scattering	A plus flaw content and less density
(c) Flaw detection	Reflection at impedance mismatch	Elasticity, Density, Flaw content, Anisotropy
(d) Thickness resonance	Stress-wave Propagation	Elasticity, Density/porosity, Crystal structure, Grain size, Composition/purity, Flaw content, Anisotropy
2. Radiography	Absorption/scattering	Density/porosity, Crystal structure, Composition/purity, Flaw content
3. Electrical		
(a) Resistivity	Resistance to current flow	Porosity, Crystal structures, Composition/purity
(b) Conductivity	Resistance to eddy currents	Flaw content, Anisotropy
4. Thermal		
(a) Infra-red scan	Heat-absorptivity, Diffusion, Velocity of heat-pulse transmission, Radiation (emissivity)	Density/porosity, Crystal structure, Composition/purity, Flaw content, Anisotropy
(b) Thermal comparitor	*Conductivity*	

weight on one space vehicle of the 1960's strikingly underlines the need for a more definitive design.

5. DYNAMIC NON-DESTRUCTIVE TESTING

5.1. Indirect static testing

Non-destructive testing has been limited in the past because most of the available methods gave only indirect qualitative results which were difficult to correlate with product serviceability or function [13]. Moreover, these tests were invariably applied to static structures not under service stresses.

5.2. Direct dynamic testing

More recently, these severe limitations have been studied and I predict that dynamic non-destructive testing will be a strong new frontier of our profession. Nearly all our classified NDT methods, including even liquid penetrant testing, have been collated for valid cross comparison of data and retention of test observation [14]. Moreover, stroboradiography, ultrasonic inspection of on-stream pipe lines as hot as 1200°F, in-motion radiography, combined vibration/fluoroscopy, and infra-red measurements of energized components under actual stress demonstrate the practicability of this new frontier. I personally feel that the inherent advantages of NDT will not be fully utilized until our ability to perform dynamic testing rather than static bench testing is demonstrated.

5.3. Cineradiography

An example of a dynamic non-destructive test set-up is shown in Fig. 1. Vibration is applied to a structure or component while undergoing simultaneous examination by fluoroscopy. This cineradiographic technique has enabled the designer to study frame by frame the behaviour of their components during vibration simulating service conditions [15].

5.4. Leak detection

Dynamic leak detection is another example of a non-destructive test method that has been virtually ignored. Ironically, the prime inpetus in the leak-detection field was generated by the need to manufacture atomic fuel elements [16]. Recently, the need for even tighter environmental controls on nuclear-reactor components has brought about more rigid leak-detection requirements. This environmental control can best be achieved by hermetic sealing, and the adequacy of this seal under service conditions must be measured.

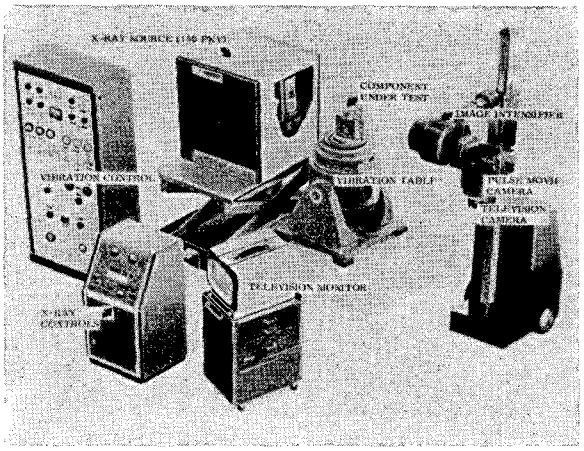

Fig. 1

Dynamic cine-radiography system

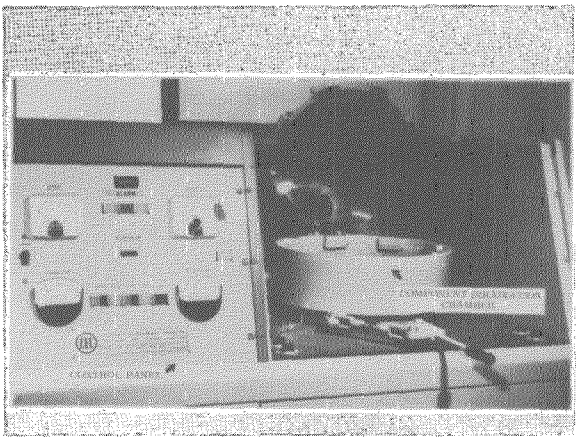

Fig. 2

Precision leak detection using krypton-85 gas

5.5. Radioactive gas testing

Grading of leakage rates from sealed components before and subsequent to simulated service environments has been used to set valid leak-test criteria for production acceptance. Figure 2 shows a relatively new precision leak detector which utilizes a radioactive gas (Krypton-85) under pressure to infiltrate hermetically-sealed components through any microscopic leakage path. After the sealed part is decontaminated to remove surface count, a detector is used to measure leakage rates as low as 10^{-12} cm^3/s, or 1 cm^3 leakage in 500 yr. This is truly a dynamic NDT method with quantitative information [17].

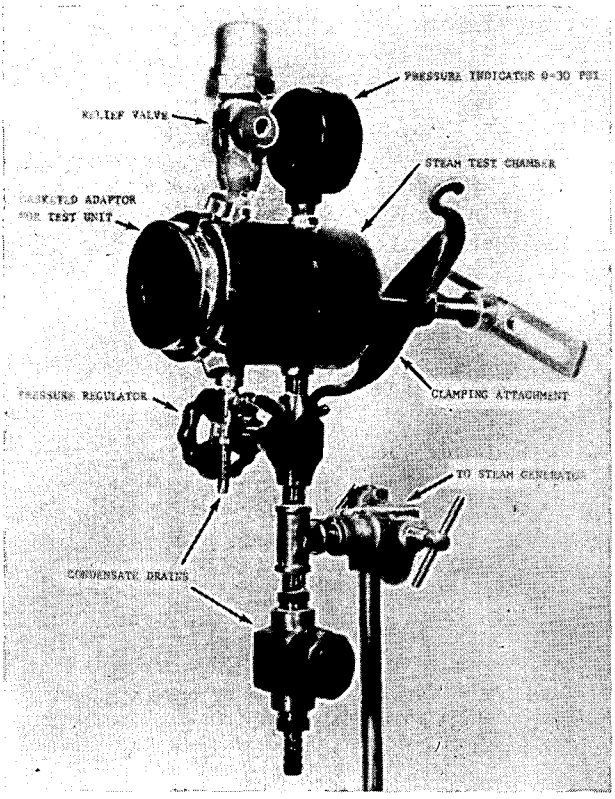

Fig. 3

Non-destructive paint tester

5. 6. Paint-finish testing

At Sandia Laboratory a dynamic paint surface tester was recently developed and is shown in Fig. 3 [18]. Saturated steam is used at a closely controlled and timed pressure against the painted surface under test. An unsatisfactory finish will blister or peel, but coating systems with good film integrity and good adherence will not be destroyed by a 10-min test (simulating 500 h in a humidity cabinet test.)

5. 7. Other examples of dynamic testing

Other examples of dynamic non-destructive tests were reported at the 1965 Spring Convention of the Society for Nondestructive Testing in Los Angeles. These included cinefluorography of small ablative thrust chambers during hot firings [19], and the evaluation of integrated microcircuitry under load by infra-red examination [20].

6. MULTIPLE NON-DESTRUCTIVE TESTING

6.1. Basis for prediction

Another new field for non-destructive testing will involve the simultaneous or successive exposure of the object being examined by multiple NDT methods. This development, which has been slow in coming, reflects a growing maturity of our profession. Even the most enthusiastic radiographer (or ultrasonics practitioner) has been forced to recognize the inherent as well as state-of-the-art limitations of his speciality. Sacrifices in sensitivity, time and cost are inevitable if attempts are made to use one test method exclusively. Therefore, I predict a large increase of multiple test set-ups with the NDT methods selected to optimize the sensitivity of the test of each parameter.

6.2. Examples of multiple testing

The testing of thick-wall weldments by ultrasonics and radiography is a well-known example of multiple NDT usage. The use of thermal, radiography and ultrasonics for inspecting canned reactor fuels has been widely documented.

One recently reported combination test, "CEBM", included corona discharge, eddy-current, beta-ray backscattering and micro-wave testing - all applied simultaneously when inspecting a composite structure [21]. Each NDT method was tailored to provide optimum information on such parameters as dimensions, dielectric constants and internal defects.

7. ELECTRONIC COMPONENTS AND SYSTEMS TESTING

7.1. Background

Any survey of present non-destructive test methods reveals one outstanding and seemingly self-imposed limitation - the almost total absorbtion in the detection of discontinuities and flaws in structural parts. Probably 90% of our testing costs are applied to structures, whereas considerable statistical evidence proves that the mechanical structures are inherently the most reliable parts of an over-all product, whether it be a reactor, aeroplane or automobile. The vast majority of failures of components and systems have occurred in those elements of the product for which non-destructive testing has been minimal, namely electronic and electromechanical components and sub-systems.

7.2. Prediction

A major re-evaluation of the use of non-destructive testing is underway to solve the very serious reliability problems of electronic components and entire systems. This is another major new field for the foreseeable future.

7.3. Examples of electronic NDT methods

Amplification systems: Many of the older NDT methods have been extended to new sensitivities and capabilities in an attempt to provide better information on critical electronic components. For example, in-motion radiography of components at 30X to 50X with detail resolution of 10 μm is now feasible by using X-ray-sensitive vidicon tubes. As shown in Fig. 4, the components are viewed on a 19-in closed-circuit television monitor. This method has demonstrated its effectiveness for the examination of transistors and diodes, printed-circuit electronic assemblies, thin-wall weldments and brazed honeycomb structures [22]. A similar test method (cinesonography), using ultrasonic imaging rather than radiography, was announced recently [23] and is shown in Fig. 5.

Extension of present tests: Eddy-current tests have been used to locate butt welds in insulated electrical wiring that must be weld-free for critical system interconnections. Pulsed X-ray systems have been packaged for safe use on the production line with Polaroid Type 52 film. Figure 6 shows a unit used for quality control testing of semiconductors and printed-circuit sub-assemblies.

Radio frequency fault detection: A new technique for locating incipient malfunctions and intermittent electronic faults in entire systems is being effectively used [24]. The technique is based on the discovery that imperfections in solder joints and minute breaks or discontinuities in internal component connections generate a radio-frequency (FR) noise which is superimposed on the regular power-supply voltage. Most of the RF energy occurs at 25 Mc, where it is 5 to 40 db higher than the steady-state background noise of the circuit. This RF noise method has been used to discover and screen out faulty components in a group of amplifier-demodulator circuits which had successfully passed normal acceptance testing. The systems would have failed under exposure to mechanical and thermal shocks.

Infra-red detection: The use of infra-red surveillance testing of electronic components from resistors to complete sub-systems is being rapidly expanded. The directness of this technique is a real advantage; see section 8.7 for additional information.

Leak detection: Virtually all sealed components are now being nondestructively tested for seal integrity. Test methods range from simple air-pressure and soap-bubble tests to mass-spectrography testing with helium-gas tracers and to radioactive isotope testing; see section 5.5.

8. INFRA-RED AND MICRO-WAVE TESTING

8.1. Basis for prediction

Two exciting new fields for non-destructive testing, involving the use of infra-red and micro-wave techniques are in the early stages of development. The potential applications of these two methods (which are at the same stage of development as ultrasonics in 1942) for materials testing will affect almost everyone in the process industries.

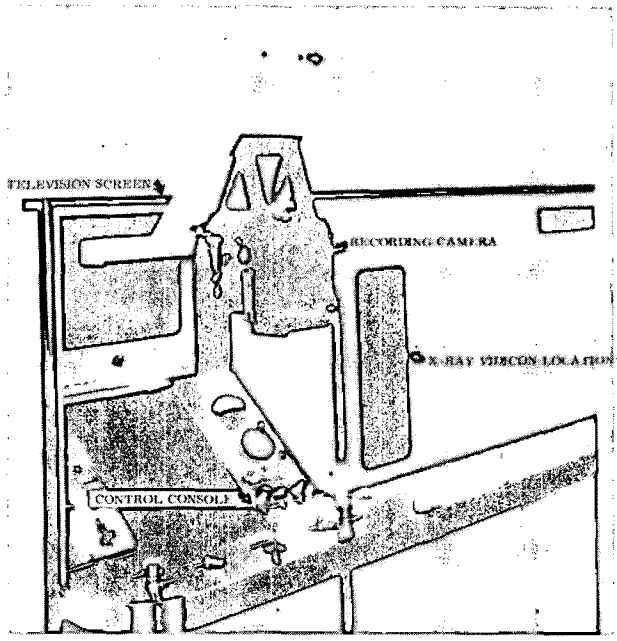

Fig. 4

In-motion radiography and high magnifications

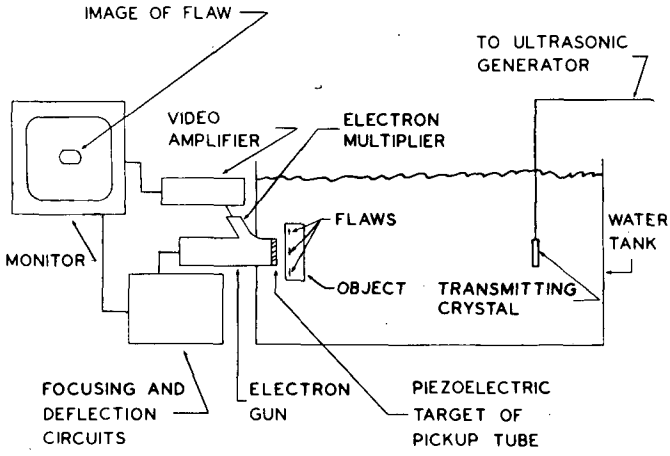

Fig. 5

Cine-sonography test set-up

As shown in Fig. 7, micro-waves and infra-red occupy the electromagnetic spectrum at frequencies between those of radio waves and visible light. Thirty years ago, this portion of the spectrum was mostly regarded as a curiosity, studied by a few individuals in the USA and Europe. During World

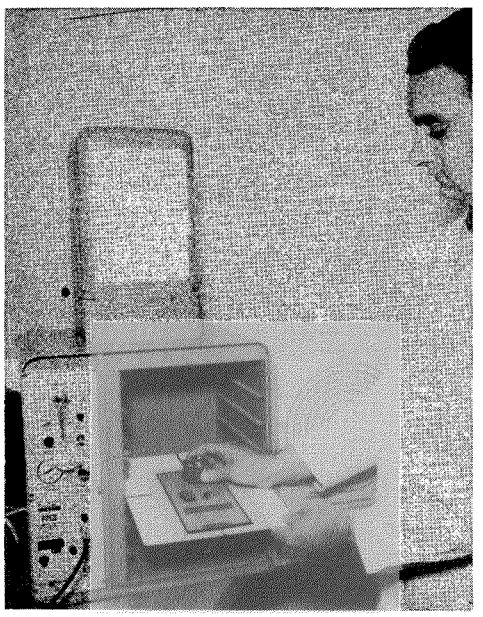

Fig. 6

Portable radiographic system using polaroid film

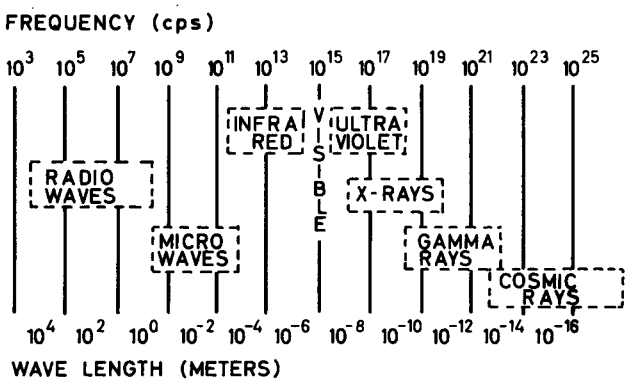

Fig. 7

Electromagnetic spectrum

War II, micro-wave technology expanded enormously in the development of radar and telemetry. More recently, attention has been focused on the use of micro-waves and infra-red for the non-destructive testing of materials and components.

8.2. Micro-wave testing

Common micro-wave test procedure is to direct a narrow beam of micro-waves - 10 Gc is a popular test frequency - at the test object and,

with suitable instrumentation, analyse the reflected beam for information regarding the material parameter for which the test was designed.

8.3. Materials for micro-wave testing

Essentially all solid and liquid non-metals can be tested, e.g. plastics, ceramics, rubber, fibreglass, wood, petroleum etc. Information about the structure, composition, physical properties, moisture content, thickness and other dimensions can be obtained. Under certain conditions, micro-waves may also be used for flaw detection [25].

8.4. Micro-wave thickness testing

While it is beyond the scope of this paper to discuss all the possible applications of micro-waves, one example will demonstrate the versatility of this new NDT method. A typical micro-wave thickness gauge for a non-metallic application is shown in Fig. 8. This set-up operates on the through-transmission principle. Similar thickness gauges can operate on the pulse-reflection principles. It is interesting to note that while all metals are opaque to micro-waves, metal-thickness gauging may develop into one of the most important applications for micro-waves. This anomalous application depends on the use of two sensing heads which beam micro-waves from set distances apart to the metal sheet being measured. Standing wave patterns are produced by the reflections. The instrumentations measure both the path lengths of the standing waves, add them electronically and then subtract them from the known total distance between the two sensing heads. The difference is the thickness of the piece of metal.

8.5. Advantages of micro-wave testing

The micro-wave thickness gauges described offer six decided advantages, namely:

Wide range: A single gauge can cover a thickness range from a fraction of a millimetre to 25 cm or more.

Constant accuracy: Accuracy is not dependent on thickness - a 25-cm plate can be measured to the same over-all accuracy as one which is only a millimetre thick.

Variety of metals: Metals of all types can be gauged with the same instrumentation since micro-waves do not penetrate the metal.

Safety: Micro-wave radiation at the level used (mW) is harmless.

Instant response: Response speed is essentially instantaneous with the ability to record chatter even at material speeds of 5000 ft/min.

Adaptive control: Micro-wave gauges are readily adaptable to automatic process control which will be so vital on future production lines.

8.6. Extent of prediction

In the foreseeable future, micro-waves may control some part of the manufacture and inspection, not only of critical materials such as those used

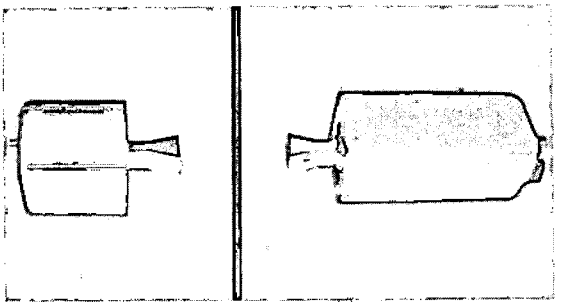

Fig. 8

Micro-wave thickness measurement system

in nuclear and space applications, but also the everyday products of the chemical, paper, textile and metal industries. However, it will require a tremendous amount of application engineering to fully realize the potential of micro-waves for materials testing.

8. 7. Infra-red testing

Another new addition to non-destructive testing is the use of infra-red which is really in its infancy. The pioneering work of R. VANZETTI [26] at Raytheon Manufacturing and others established the ability to map non-destructively an infra-red profile of electronic components and sub-assemblies. This profile is as distinctive as a fingerprint and can be used to "trouble-shoot" development models and set acceptance criteria for production testing. A strong indication concerning the interest being given this NDT method in the USA is obtainable by reviewing the content of technical papers presented at the 1965 Spring National Convention of SNT. Twenty-two of the fifty-two papers involved some phase of infra-red testing, with fourteen of these papers aimed at non-destructive testing of electronic components and assemblies, and the remaining eight on structural and welding infra-red applications. (It is interesting to note that more than 90% of the papers presented at the SNT convention twenty years ago were devoted exclusively to applications of penetrating radiation).

8. 8. Basis for infra-red interest

Infra-red testing has several attractive advantages, especially in the inspection of electronic microcircuitry, namely:

Non-contacting: No physical contact with test object.

Rapid response: High speed of response, permitting scanning.

Repeatable: Better repeatability than thermocouples.

Directness: Record data on heat output during operation which is the variable most closely correlated with performance of electronic circuitry.

Adaptable: Compatible with adaptive controls.

Simple: Can be used by semi-skilled labour.

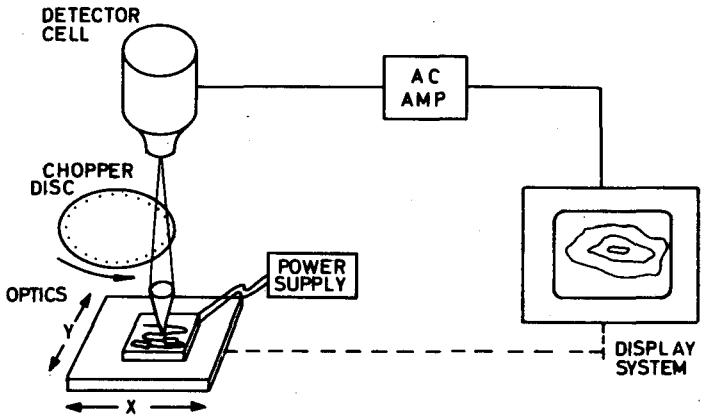

Fig. 9

Infra-red scanning set-up

8.9. Typical applications

A typical infra-red scanning arrangement is shown in Fig. 9. The test object can be energized by normal power if a part of an electronic circuit, or artificially heated or cooled if it is part of a structure. Spot sizes as small as 0.7 mil are used to read out the radiant energy.

The increased use of composite structures has focused attention on infra-red testing of the integrity of bonding between materials. A nuclear-fuel element will not function correctly if there is not a good thermal bond between the fuel and the cladding; sandwich structures will not distribute stress efficiently if there is not a good structural bond between the skin and the honeycomb core; and solid propellant will not burn evenly if the bond between the fuel and the motor casing is not continuous. All three applications of infra-red testing have been recently reported by investigators in the USA [27].

8.10. Weldment testing

Dynamic infra-red test methods are being developed for quality control of thin-wall weldments and resistance welds of critical wiring. Sandia Corporation reported a test set-up [28] which shows great promise in eliminating destructive tests for resistance welds as shown in Fig. 10. The heat output of the resistance weld is observed during a non-destructive pulse of electrical energy. A high degree of correlation between weld strength and heat output was shown and the test method enabled the investigators to predict weld strength with a 90% confidence. LEE and LEONARD [29] of Lockheed Missiles recently reported data on a similar test which used the heat generated at the interface of the weld head and the weldment during welding. D. R. MALEY [30] reported recently on an effective infra-red test using the set-up shown in Fig. 11. Discontinuities detected with this technique included laminar inclusions, internal voids and transverse cracks.

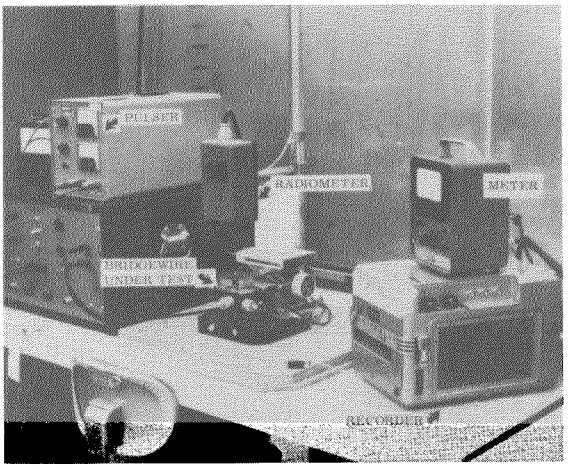

Fig. 10

Set-up for infra-red testing of microwelds

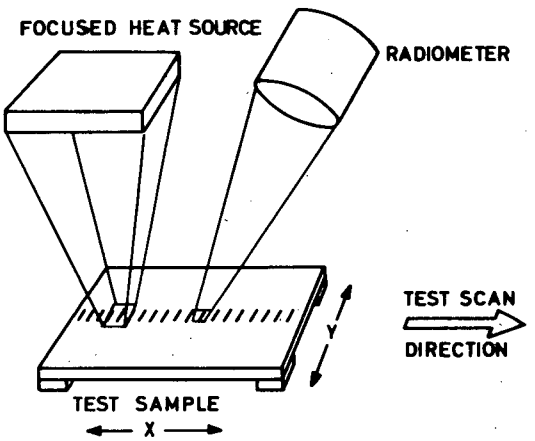

Fig. 11

Scan heat technique

8.11. Infra-red fibre optics

Infra-red transmitting glass fibres are being actively investigated. The piping of heat indications without losses from deep inside a sealed or encapsulated component would open new vistas for quality control and surveillance. Fibres transmitting infra-red in the 6 to 10-μm frequency (25°C to 225°C) have defied fabrication so far, although some success has been reported by American Optical Company [31] and Simms of Optics Technology [32] with arsenic tri-sulphide glass (As_2S_3). Additional significant im-

provements in usable infra-red light pipes are anticipated in the not-too-distant future.

CONCLUSION

Today's pressing demands for higher product reliability make it imperative that the most effective test methods be used throughout the product-development cycle. Tomorrow's increasing demands will make it mandatory. Each of the six predicted new frontiers for non-destructive testing discussed in this paper present unique opportunities for increasing our contributions to product reliability in the nuclear age.

REFERENCES

[1] Time Magazine, 81, No. 26, p. 77.
[2] McMASTER, R.C., "Nondestructive Testing", Proc. ASTM (1952) 52.
[3] SHARPE, R.S., "Nondestructive Testing in Perspective", Brit. J. non-destr. Test. 5, No. 3 (1963) 83-89.
[4] JUDGE, John F., "Nondestructive Testing Fundamental to Advanced Materials Development", Missiles and Rockets Magazine, February 22 (1965) 27-32.
[5] PAPADATIS, E.P., "Ultrasonic Nondestructive Test for the Detection of Improper Heat Treatment of Steel, Materials Evaluation XXIII, No. 3, (1965) 136-139.
[6] PETERS, B.F., "Radiography for Corrosion Evaluation", Materials Evaluation XXIII, No. 3 (1965) 129-135.
[7] LOCKYER, G.E., "Evaluation of a Resin-Ceramic Heat-Shield Material by Ultrasonic Methods", Materials Evaluation, XXIII, No. 3 (1965) 144-148.
[8] Branson Instruments Bulletin 4-101, "Ultrasonic Hardness Tester", U.S. Patent 3153338, March (1965).
[9] Ref. [3], p. 85
[10] Ref. [3], p. 84
[11] Ref. [4], p. 30
[12] BALLARD, D.W., "Nondestructive Testing's Role in Reliability Programs", Proc. 11th Nat. Symp. on Reliability and Quality Control, January 12-14 (1965) IEEE.
[13] Ref. [2] pp 8-9.
[14] THOMAS, W.E., "An Analytic Approach to Penetrant Performance", Proc. 4th Int. Conf. Nondestructive Testing, September (1963) 1-15.
[15] ARMSTRONG, J.H., "A Stroboscopic X-Ray Photographic System Undergoing Evaluation", Spring Convention of SNT, February (1965).
[16] KING, J.G., "Production Leak Testing of Large Pressure Vessels", 1961 Tran. of the Eighth Vacuum Symp. and Second Int. Cong. (1961) 1100-1105.
[17] Ref. [12], pp 8-9.
[18] ARNOLD, V.E., "Accelerated Testing for Humidity Resistance of Paint Films - A Nondestructive Method", Sandia Report SC-TM-64-1656, February (1965).
[19] HAGEMAIER, D.J., "Cinefluorography of Small Ablative Thrust Chambers During Hot Firing", Spring Convention of SNT, February (1965).
[20] COLLINS, D.J., Evaluation of Infrared for Integrated Circuit Reliability by Detection and Rejection of Potential Early Failures", Spring Convention of SNT, February (1965).
[21] Plastics Design and Processing, September (1963).
[22] McMASTER, R.C., "New Techniques in Aerospace Nondestructive Testing", 1963 Annual Air Transport Association Engineering and Maintenance Conference, Washington, D.C., October 30 (1963)
[23] JACOBS, J.E., BERGER, H. and COLLIS, W.J., "An Evaluation of an Ultrasonic Inspection System Employing Television Techniques, 1963 SNT National Convention, Cleveland, Ohio, October (1963).
[24] MAKI, C.E. and HAGERT, F.W., "Radio Frequency Fault Detection Techniques", 1963 SNT National Convention, Cleveland, Ohio, October (1963).
[25] HOCHSCHELD, R., "Principles and Applications of Microwaves in Materials Testing", Fall Convention of SNT, October (1964).

[26] VANZETTI, R., "Infrared-Another Medium of Evaluation", Quality Assurance 2, No. 12 (1963) 25-28.
[27] McGONNACLE, W. and PARK, F., "Nondestructive Testing". Materials Evaluation XXII, No. 12 (1964) 561-574.
[28] KLAMERUS, L.J., "Development of a Nondestructive Test for Resistance Welds", Spring Convention of SNT, March (1964).
[29] LEE, J.K.S. and LEONARD, S., "Evaluation of the Resistance Micro-welding Process by Infrared Energy Measurements", Spring Convention of SNT, February (1965).
[30] MALEY, D.R., "Two Thermal Nondestructive Testing Techniques", Spring Convention of SNT, February (1965).
[31] EISNER, L., "Infrared: What's Ahead", Electron. Products, 7, No. 9, (1965) p.F23.
[32] SIMMS, J., "Infrared Fiber Optics and Infrared Nondestructive Testing", Spring Convention of SNT, February (1965).

DISCUSSION

C.A. MANN: Is the use of the concept of redundancy not an alternative to the search for 100% reliability, which is strictly unattainable?

D. BALLARD: Yes, in fact we are using redundancy a good deal in our electronics now just because of the electronics "reliability problem". This solution may not be acceptable for aerospace components because of the weight problem.

R.S. SHARPE: When introducing new non-destructive testing equipment, one must be careful to ensure that its characteristics and capabilities are well known to those who have to use it and interpret the results.

The ultrasonic hardness tester may lead to ambiguity, now that it is possible to measure hardnesses over such small areas of surface.

D. BALLARD: I agree, but should like to point out that care should be exercised in this respect in all hardness testing, since we can only sample the area being tested.

P. de MEESTER: I have been most impressed by the wide new frontiers you have described, and feel in the light of what we have heard that international meetings such as the present one will become increasingly necessary in order to co-ordinate effort.

It seems in fact highly desirable to bring production people, quality control experts and reactor operators together to discuss points such as the type and nature of specifications (too many aspects are unknown and may be over-stressed), what tests are necessary and sufficient, and what accuracy is required. An extensive international programme on the irradiation of defective or suspect fuel elements might prove useful in this respect.

SESSION VIII

MEASUREMENT OF INTERNAL FRICTION ON NUCLEAR MATERIALS

R. R. HASIGUTI, N. IGATA AND R. TONOMAE
UNIVERSITY OF TOKYO
AND
Y. NAKAMURA, N. SASAO AND K. DOMOTO,
TOKAI, REFINERY, ATOMIC FUEL CORPORATION, JAPAN

Abstract — Résumé — Аннотация — Resumen

MEASUREMENT OF INTERNAL FRICTION ON NUCLEAR MATERIALS. The internal friction measurement is applicable to the inspection of metallic uranium, uranium-diodixe pellets and zirconium alloys. This is because of its great sensitivity to the concentration of point defects and impurity atoms, to the density of dislocations and also to the micro-structure of crystals.

We found a relaxation peak at about 100°C from internal friction measurements of as-cast uranium, at various temperatures with free decaying method. The peak height increases by quenching and decreases by annealing after quenching. The peak temperature is almost the same in commercial and in high-purity uranium, but it shifts a little to higher temperature by the addition of a small amount of aluminium, and much more by the addition of 1% molybdenum.

The amplitude dependent internal friction of uranium was also measured. As the Granato-Lücke relation is satisfied in this case, we can calculate the dislocation density and the dislocation loop length. These quantities were obtained, as the uranium specimens were cold-rolled, annealed and quenched.

The internal friction measurements of UO_2 pellets were performed using ultrasonic attenuation in the region of maximum concentration. From the temperature dependence of internal friction, a new relaxation peak was observed at low temperatures.

In the measurements on zirconium alloys, the snoek peak of hydrogen was found.

Above are some examples which are applicable to the inspection of nuclear materials, and now we intend to apply these methods to the study of the structural changes of irradiated or fission-damaged materials.

MESURE DE LA FRICTION INTERNE DANS LES MATIÈRES NUCLÉAIRES. La mesure de la friction interne intervient dans l'inspection de l'uranium métallique, des pastilles en bioxyde d'uranium et des alliages de zirconium, en raison de sa grande sensibilité à la concentration des défauts ponctuels et des impuretés, à la densité des dislocations et à la microstructure des cristaux.

Au cours de mesures de la friction interne dans des spécimens d'uranium moulé, à différentes températures, par la méthode de la libre désintégration, les auteurs ont observé un pic de relaxation aux alentours de 100°C. La hauteur du pic augmente après la trempe et diminue si la trempe est suivie d'un recuit. La température de pic est pratiquement la même pour l'uranium de pureté commerciale et l'uranium de pureté nucléaire, mais elle augmente légèrement après addition d'une petite quantité d'aluminium et augmente plus sensiblement après addition de 1% de molybdène.

Les auteurs ont également mesuré la friction interne de l'uranium en fonction de l'amplitude. Etant donné que dans ce cas la relation de Granato-Lücke est satisfaite, on peut calculer la densité de dislocation et la longueur de la boucle de dislocation. Ils ont obtenu ces données avec de l'uranium laminé à froid, recuit et trempé.

La friction interne de pastilles de UO_2 a été mesurée par la méthode de l'atténuation des ultrasons dans la région de la concentration maximum. En faisant varier la température, on a observé un nouveau pic de relaxation à basse température.

En effectuant des mesures sur des alliages de zirconium, on a observé un pic secondaire pour l'hydrogène.

Les auteurs donnent quelques exemples d'applications au contrôle de matières nucléaires. Ils se proposent d'appliquer les mêmes méthodes à l'étude des changements de structure dans les matières irradiées ou endommagées par la fission.

ИЗМЕРЕНИЕ ВНУТРЕННЕГО ТРЕНИЯ В ЯДЕРНЫХ МАТЕРИАЛАХ. Измерение внутреннего трения можно использовать для прверки металлического урана, таблеток из двуокиси урана и циркониевых сплавов. Это объясняется его большой чувствительностью к концентрации точечных дефектов и атомов примесей, к плотности дислокаций, а также к микроструктурам кристаллов.

Обнаружен пик релаксации примерно в точке 100° С путем измерения внутреннего трения кованого урана при различных температурах методом свободного затухания. Высота пика увеличивалась при закалке и уменьшалась при отжиге после закалки. Пиковая температура почти одинакова для промышленного урана и урана высокой чистоты, но она сдвигается немного в сторону увеличения при добавлении небольшого количества алюминия и значительно сильнее сдвигается при добавлении одного процента молибдена.

Было также измерено зависящее от амплитуды внутреннее трение урана. Поскольку для данного случая подходит отношение Гранато-Луке, мы можем рассчитывать плотность дислокации и длину петли дислокации. Эти характеристики были получены после холодной прокатки, отжига и закалки образца урана.

Для измерения внутреннего трения таблеток из UO_2 было использовано ослабление ультразвука в мегагерцевой области. На основании температурной зависимости внутреннего трения был получен новый пик релаксации при низких температурах.

Выше мы привели несколько примеров, которые могут быть использованы для проверки ядерных материалов, а теперь мы намереваемся использовать эти методы для изучения структурных изменений в облученных или поврежденных делением материалах.

MEDIDA DE LA FRICCION INTERNA EN MATERIALES NUCLEARES. El procedimiento de medida de la fricción interna es utilizable para la inspección del uranio metálico, pastillas de dióxido de uranio y aleaciones de circonio, debido a su gran sensibilidad a la concentración de defectos puntiformes y átomos impureza, a la densidad de las dislocaciones y a la microestructura cristalina.

Midiendo a varias temperaturas por el método de la atenuación libre la fricción interna del uranio fundido, el máximo de relajación se encontró a 100°C. Ese máximo aumenta por enfriamiento y disminuye por recocido ulterior. La temperatura máxima es casi la misma en el uranio comercial que en el de alta pureza, pero aumenta ligeramente añadiendo aluminio en baja proporción y mucho más si se agrega 1% de molibdeno.

También se ha medido la fricción interna del uranio, que depende de la amplitud. Como en ese caso se cumple la relación de Granato-Lücke, puede calcularse la densidad de la dislocación y la longitud de ciclo de la misma. Esas cifras se obtuvieron al laminar en frío, recocer y enfriar bruscamente probetas de uranio.

La medida de la fricción interna de las pastillas de UO_2 se efectuó mediante atenuación ultrasónica en la banda del megaciclo. Como la fricción interna depende de la temperatura, pudo observarse un nuevo máximo de relajación a baja temperatura.

En la medida de aleaciones de circonio se halló un máximo correspondiente al hidrógeno.

Se han citado algunos ejemplos aplicables a la inspección de materiales nucleares, y ahora se procura aplicar los métodos correspondientes al estudio de las alteraciones estructurales del material irradiado o dañado por fisión.

1. INTRODUCTION

Most nuclear materials are used under irradiation. As the irradiation effect itself is an atomic process, the inspection of the atomic structure becomes very important, apart from the ordinary inspection methods. Recently much development has been made in the field of internal friction studies. The authors tried to develop its application to non-destructive testing because of its great sensitivity to failure in the atomic structure, for instance, minor interstitial solute impurity atoms, point defects or dislocations, and also because of the possibility it gives of measuring the elastic module and yield stresses very accurately, which are directly connected to the mechanical properties of materials. This method would become in-

creasingly important as the physical meaning of the atomic structure to the strength of materials becomes clear.

2. EXPERIMENTAL METHOD AND SPECIMEN

In the internal friction measurements different kinds of apparatus are now developed in accordance with the required temperature ranges, frequency and strain amplitude. Among these the authors used two kinds, i.e. the automatic measurement apparatus for transverse (or longitudinal) vibration and the "ultrasonic comparator" of the pulse-echo method. A block diagram of these is shown in Figs. 1 and 2.

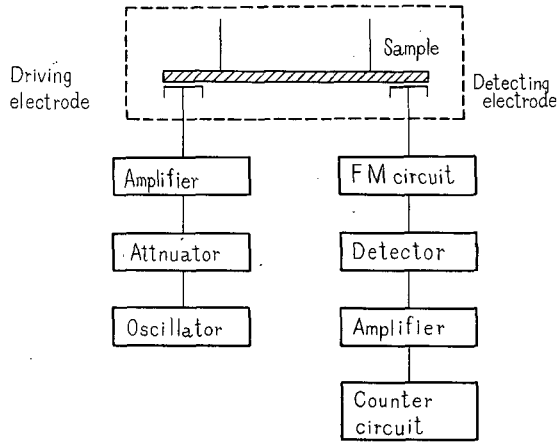

Fig. 1

Block diagram of internal-friction measurement apparatus of transverse vibration method

In Fig. 1 the specimen is supported with thin metallic wires on the two nodal points so as to vibrate in the fundamental mode. An electrostatic method is used* for driving and detecting the vibration. The control of the strain amplitude is performed with the attenuater. The counter circuit is driven with the timer for measuring the resonant frequency f_0, and with the reference voltage for measuring the half-decay wave-numbers, n. Young's modulus E and internal friction Δ of the specimen are derived from the following equations:

$$E = 0.96535 \times 10^{-8} \left(\frac{\ell}{a}\right)^3 \frac{g}{b} \quad (kg/mm^2) \tag{1}$$

and

$$\Delta = \ell n 2/n, \tag{2}$$

* In the larger strain amplitude region, an electro-magnetic method is used.

where ℓ, a and b are the specimen length, thickness and width, respectively, and g is the weight of the specimen.

In Fig. 2, a quartz crystal is attached with silcone grease to the specimen. The sound waves are transferred to the specimen using the piëzoelectricity of the quartz. A multi-pulse echo can be detected through the same quartz. The sound velocity v is measured from the interval of the multi-reflected echo on the cathode-ray tube. The attenuation α is measured

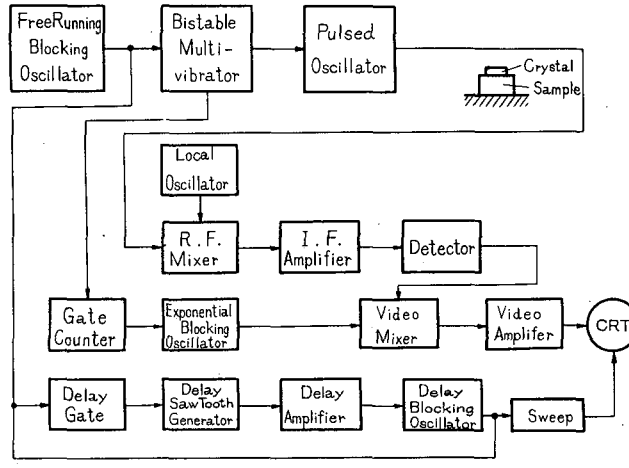

Fig. 2

Block diagram of "ultrasonic comparator"

from the exponential decay curve of the multi-reflected echo. Young's modulus E and internal friction Δ are obtained from the following equations for the isotropic materials:

$$E = v_e^2 \rho \frac{(1+\sigma)(1-2\sigma)}{1-\sigma} = 2v_t^2 \rho (1+\sigma)\rho \tag{3}$$

and

$$\Delta = \alpha\lambda = \alpha v/f, \tag{4}$$

where v_e is the sound velocity of longitudinal wave (in the case of X-cut quartz), v_t is that of transverse wave (in the case of Y-cut quartz), ρ is the density, σ is the Poisson's ratio, λ is the wave-length, f is the frequency of sound wave and α is expressed by the following equations:

$$\alpha = \frac{1}{2(m-n)\ell} \log\left(\frac{A_n}{A_m}\right) \text{ neper/cm} = \frac{1}{2(m-n)\ell} \log_{10}\left(\frac{A_n}{A_m}\right) \text{db/cm}, \tag{5}$$

where A_n and A_m are the pulse height of nth and mth reflected waves respectively.

Temperature dependence is measured, in both methods, in the cryostat between room temperature and liquid-nitrogen temperature, in a vacuum of 10^{-3}-10^{-4} mm Hg. The strain amplitude ϵ_{max} is calculated by using the Eq. (6) from the vibrational amplitude h, which is calibrated by the detector circuit (Fig. 1), or by an optical microscope,

$$\epsilon_{max} = \frac{\pi^3 hd}{4\ell^2}, \tag{6}$$

where d and ℓ are the thickness and length of the specimen. Frequency dependence is measured using higher harmonics of the sound wave induced in the quartz crystal.

Nuclear materials, which were measured, are uranium, uranium alloys, UO_2 and Zircaloy-2, whose compositions are shown in Table I. The specimen sizes, the type of internal friction and the methods and ranges of the measurements are summarized in Table II.

3. SIGNIFICANCE OF THE EXPERIMENTS

Internal friction is phenomenologically divided into three categories, i.e. relaxation, resonance and hysteresis. The internal friction due to relaxation is expressed by the following equation:

$$\Delta = \Delta_0 \frac{w\tau}{1 + w^2\tau^2}, \tag{7}$$

where τ is the relaxation time, w is the angular frequency of vibration. When the relaxation is assisted by a thermally activated process, for instance with atomic diffusion or dislocation motion over the barriers, it is written by the Arrhenius equation as follows:

$$\tau = \tau_0 \exp H/kT, \tag{8}$$

where H is the activation energy of the process and k is Boltzman's constant. Thus, the relaxation peak is observed in the temperature dependence of the internal friction. As $w\tau = 1$ must be satisfied at the peak maximum, the activation energy of the peak process is obtained from the peak shift from T_1 to T_2 using Eq. (9), if the measurements are performed at two frequencies, w_1 and w_2:

$$\ell n \frac{w_1}{w_2} = \frac{H}{k}\left(\frac{1}{T_2} - \frac{1}{T_1}\right). \tag{9}$$

The mechanism of a relaxation can be identified from the activation energy, the time constant τ in Eq. (8) and/or the behaviour of the peak. When the mechanism is clarified, we understand the atomic behaviour of impurities or the crystal defects in the materials. From the relaxation measurement,

TABLE I

COMPOSITIONS OF MATERIALS USED

Materials	Treatment	Compositions (Impurities (ppm))
U I	Derby	Ni: 27, Al: 13, C: 50, Fe: 45, N: 10, Si: 8, Cu: 3, Cr: 8, Mn: 3, H: 9
U II	Ingot	N: 67, Al: 12, C: 605, Fe: 160, Si: 39, Cu: 55, Cr: 8, Mn: 3.5, H: 6.8
U III	Derby	Ag: < 0.2, Al: 12, B: < 0.1, Cd: < 1.2, Cr: < 8, Cu: < 3, Fe: 62, Mn: < 3, Mg: < 2 Ni: 11, Si: < 10, V: < 10, Zn: < 10, C: 152, N: 26
U IV	Rolled	Ag: <0.2, Al: < 10, B: < 0.1, Cd: < 0.2, Cr: < 8, Cu: 4, Fe: 74, Mn: < 3, Mg: < 2, Ni: 13, Si: 27, V: < 10, Zn: < 10, C: 700, N: 30
U-Mo I	as-cast	Mo 1.2 wt.%
U-Mo II	as-cast	Mo 4.5 wt.%
UO_2 (I and II)	Pellets Sintered O/U = 2.016 ρ = 10.55	Ag: < 0.2, Al: 48, B: 0.13, Cd: < 0.2, Co: < 5, Cr: < 8, Cu: < 3, Fe: < 10, Mg: 4, Mn: 3, Ni: < 10, Si: 10, V: < 10, Zn: < 50, Ca: 10 Cl: < 5, N: 7
Zircaloy-2	Rolled and annealed	Sn: 1.40 wt.%, Fe: 0.119 wt.%, Cr: 0.112 wt.%, Ni: 0.063 wt.%, Al: 68, C: 20, Hf: 57, N: 21, Sample I H : 100 Sample II H : 300

important information is received about the diffusion constant, the solubility limit and the content of minor solute impurity atoms or point defects, and further the barriers of dislocation motion which have direct connections to the mechanical properties of the materials.

Now the internal friction due to hysteresis, which is observed in amplitude-dependent internal friction, comes from the hysteresis motion

TABLE II

SPECIMEN SIZES, TYPES OF INTERNAL FRICTION, METHODS AND RANGES OF THE MEASUREMENTS

Materials	Specimen size (mm)	Type of internal friction	Type of method	Range		
				Temperature	Frequency	Amplitude
U I U II	2.5 × 10.0 × 110.0	relaxation	transverse vibration	room-temp. ~300°C	600 ~700 Hz	$\sim 10^{-7}$
U III U IV	ibid.	hysteresis	ibid.	room - temp.	~700 Hz	10^{-6} $\sim 5 \times 10^{-4}$
U-Mo I U-Mo II	ibid.	relaxation	ibid.	room - temp. ~300°C	600 ~700 Hz	$\sim 10^{-7}$
UO_2	diam.: 12.50 length : 10.380	relaxation reasonance	pulse-echo method	room - temp. ~ -190°C room -temp.	5 ~ 35 Mc	$\sim 10^{-6}$
Zircaloy-2		relaxation hysteresis	transverse vibration	room - temp. ~ - 190°C room - temp.	~500 Hz	10^{-5}-10^{-3}

of dislocations. The critical stress amplitude, at which internal friction begins to increase, gives the microscopic yield-point. The amplitude-dependent internal friction Δ_H was analysed by GRANATO and LUCKE [1] with the string model of dislocations and some more assumptions. According to the Granato-Lücke theory Eq. (10) is derived:

$$\Delta_H = \frac{\Omega \Lambda L_N^3}{\pi^2 L_c} \cdot \frac{K\eta a}{L_c \epsilon_o} \cdot \exp\left(\frac{-K\eta a}{L_c \epsilon_o}\right), \tag{10}$$

where Δ_H is amplitude-dependent part of Δ, and Ω is the orientation factor, Λ is the dislocation density, L_c is the mean length of dislocation segments pinned with impurity atoms or point defects, L_N is the length between nodes of dislocation network, K is the strength for unpinning, η is the misfit factor of pinning atoms or point defects, a is the inter-atomic distance, and ϵ_o is the strain amplitude. Eq. (10) shows

$$\ln \Delta_H \epsilon_o \propto \epsilon_o^{-1}. \tag{11}$$

When Eq. (11) (Granato-Lücke relation) is satisfied, we can obtain the information on the dislocation density, the dislocation loop length or the pinning of dislocation which are directly connected with the pre-yield process [2] and the yield process.

Finally, the internal friction due to resonance Δ_I is expressed by the following equation:

$$\Delta_I = \Delta_o \frac{\omega \tau_r}{1 + \omega^2 \tau_r^2}, \tag{12}$$

where τ_r is the constant for the resonance mechanism. This can be measured in the frequency-dependent internal friction. Granato and Lücke also analysed the resonance damping of dislocations assuming the string-like motions of dislocation segments pinned down with impurity atoms or point defects. When the frequency at Δ_{max} is denoted by ω_r, in the region of $\omega \ll \omega_r$, the Eq. (13) is derived:

$$\Delta = \frac{\Omega \Lambda L_c^4 B \omega t_1}{\pi^3 C}, \tag{13}$$

where the notations Ω, Λ and L_c are the same as in Eq. (10), t_1 is the constant which is determined from the distribution of dislocation loop-lengths, B is the frictional constant, and C is the force constant of line tension of dislocations. Eq. (13) shows that

$$\Delta \propto w. \tag{14}$$

This relation is very important in the interpretation of internal friction. When Eq. (14) is satisfied, information is obtained on the dislocation density, the dislocation loop-length and the frictional force of dislocations under some

assumptions, which are also directly connected to the pre-yield process and the yield process.

Thus,from the atomic standpoint, information is obtained on impurity atoms, point defects or dislocations from the measurements of internal friction. This is why this method is powerful for the non-destructive testing of nuclear materials.

The correlation between the atomic structure and the irradiation effects such as swelling, irradiation growth, irradiation creep, irradiation brittleness and release of fission-gas products is the most important problem to be solved in the future.

4. EXPERIMENTAL RESULTS AND DISCUSSIONS

Uranium and uranium alloys

(a) Relaxation

The temperature dependence of the internal friction of U I, U II, U-Mo I and U-Mo II specimens are observed between room temperature and 300°C. Figure 3 shows the result on U I after the treatments of β-quenching and

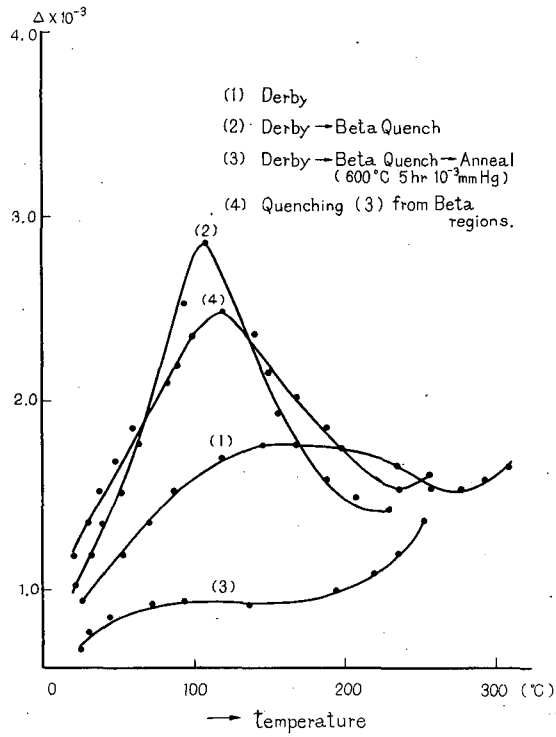

Fig. 3

Temperature dependence of internal friction of U I before and after β-quenching

annealing. The peak is reached around 100°C and it is found that this peak is independent of strain amplitude. The peak height increases with β-quenching and decreases with annealing at 600°C. Figure 4 shows the effect of successive α-quenching after β-quenching. The peak height increases

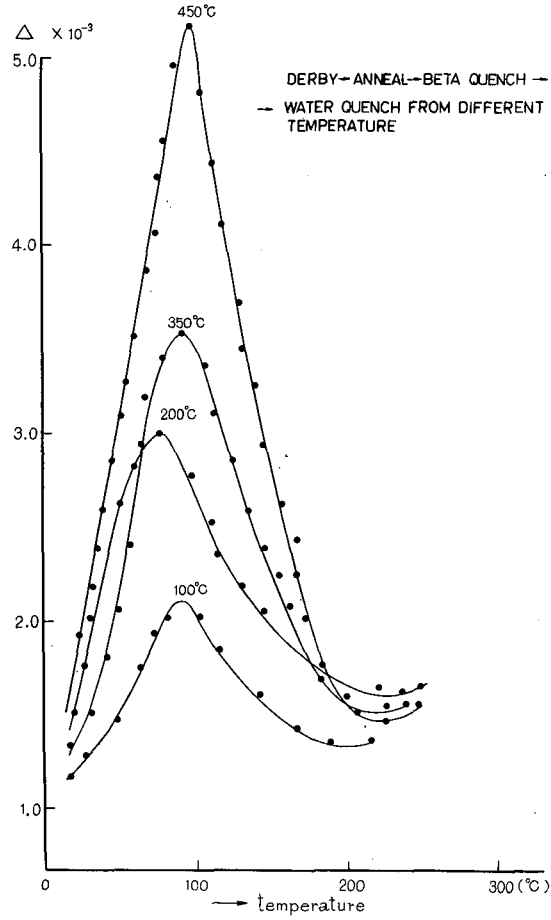

Fig. 4

Temperature dependence of internal friction of U I α-quenched after β-quenching

with the quenching temperature. The change of the peak height by successive α-quenching following β-quenching is shown in Fig. 5. The height decreases with time and seems to saturate. The straining of 1-3% before and after α-quenching does not affect the peak height, and the peak does not appear by the straining of annealed specimens.

With U II the peak height is larger than with U I after the same treatment. The peak temperature shifts with the vibrational frequency. The activation energy, that is obtained from the peak shift, is 21 kcal/mol, which is about half that of self-diffusion, and the frequency factor is about 10^{14}/s. The effect of hydrogen on this peak was investigated, but the result showed

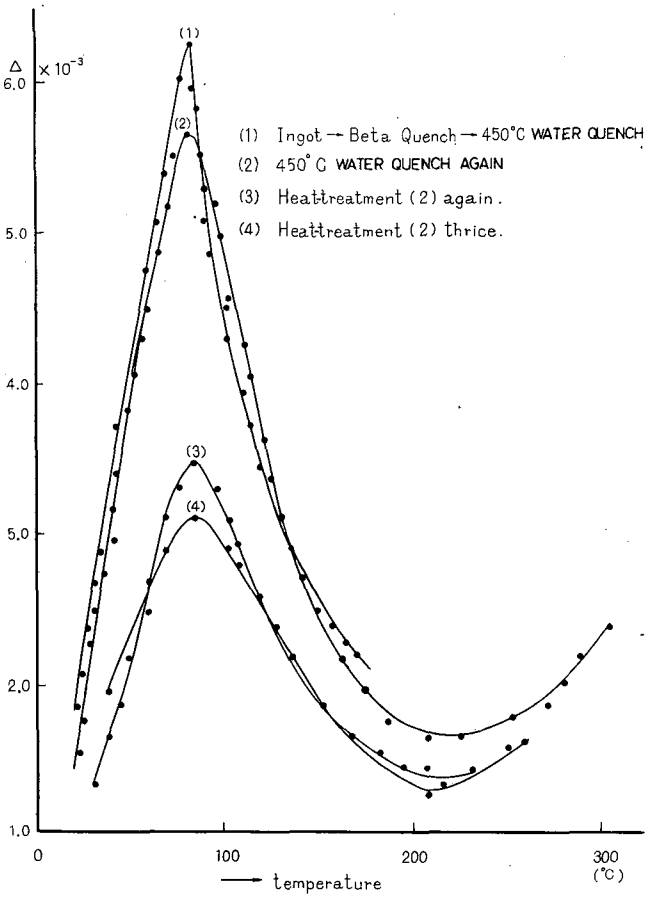

Fig. 5

Temperature dependence of internal friction of U II β-quenched and successive α-quenching

that the peak behaviour was independent of hydrogen content. From the above results, the mechanism of this peak would be the diffusion of interstitial impurity atoms, of which the solute concentration would be changed by α-quenching.

With U-Mo I and U-Mo II a similar peak is observed at a little higher temperature as shown in Figs. 6 and 7. When the specimens are quenched from 800°C, no peak was found between room temperature and about 400°C, instead of which the rise of internal friction was observed near room temperature in the case of U-Mo I, and near room temperature and 220°C in the case of U-Mo II.

(b) Hysteresis

The amplitude dependence of internal friction is observed between the strain amplitudes of 10^{-6} and 5×10^{-4} on the specimens of U III and U IV under

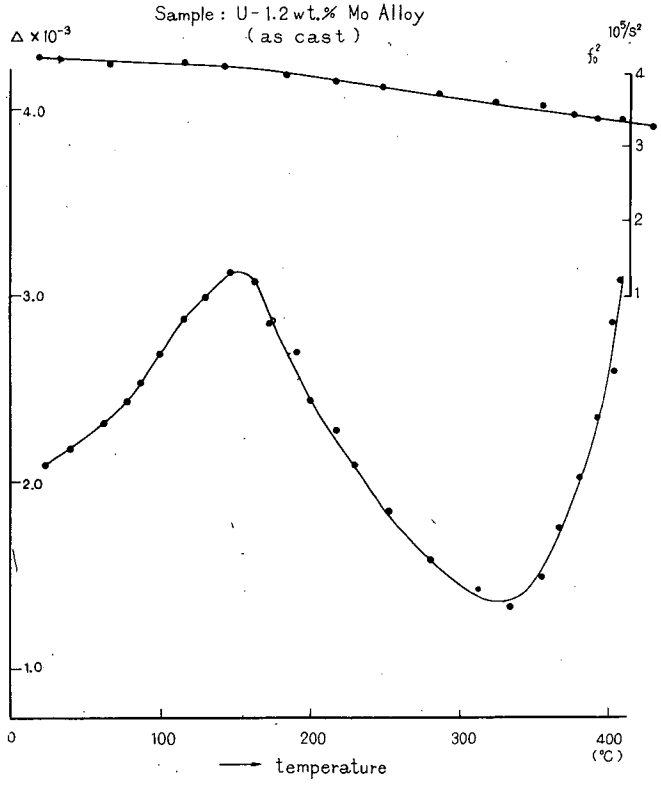

Fig. 6

Temperature dependence of internal friction of U-Mo I as cast

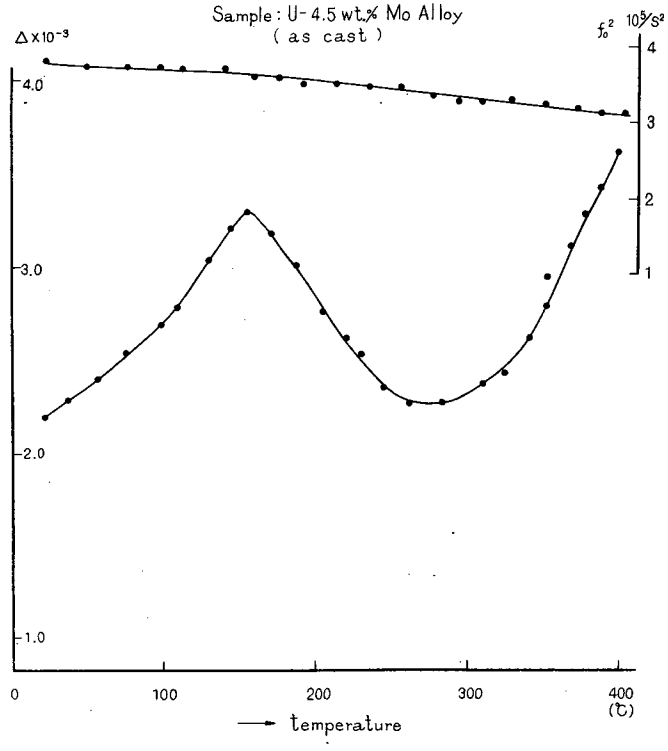

Fig. 7

Temperature dependence of internal friction of U-Mo II as cast

various conditions of straining, annealing and quenching. These results are shown in Figs. 8, 9 and 10.

The break-away strain increases with the degree of cold-work, and upon annealing and quenching it increases a little at a low annealing temperature

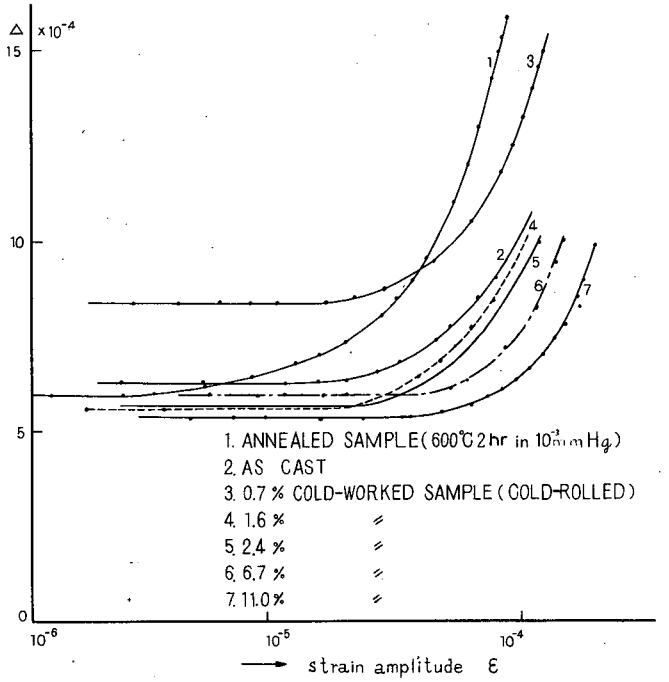

Fig. 8

Amplitude dependence of internal friction of U III before and after cold-work

and decreases as the annealing or quenching temperature becomes higher. As the Granato-Lücke relation, viz. Eq. (11), is satisfied, dislocation densities and dislocation loop-lengths L_c are obtained from Eq. (10), assuming the values of constant Ω, K and η. The number of pinning points along dislocation lines is also calculated from dislocation densities and dislocation loop-lengths L_c. These values are shown in Figs. 11-13, corresponding to Figs. 8-10 respectively. Dislocation densities increase with the degree of cold-work and decrease with annealing or quenching temperature except for β-quenching. Dislocation loop-length decreases with the degree of cold-work, but both on annealing and quenching it decreases a little at about 200°C and increases at higher temperatures. The decreases of dislocation loop-length corresponds to the increase of the break-away strain in both annealing and quenching. This is an example of low-temperature hardening. The number of pinning points along dislocations increases with the degree of cold-work, which shows the production of point defects in plastic deformation, and it recovers with annealing. That the number of pinning points rather decreases with the quenching temperature shows that the quenching is not complete owing to the low thermal diffusivity of uranium.

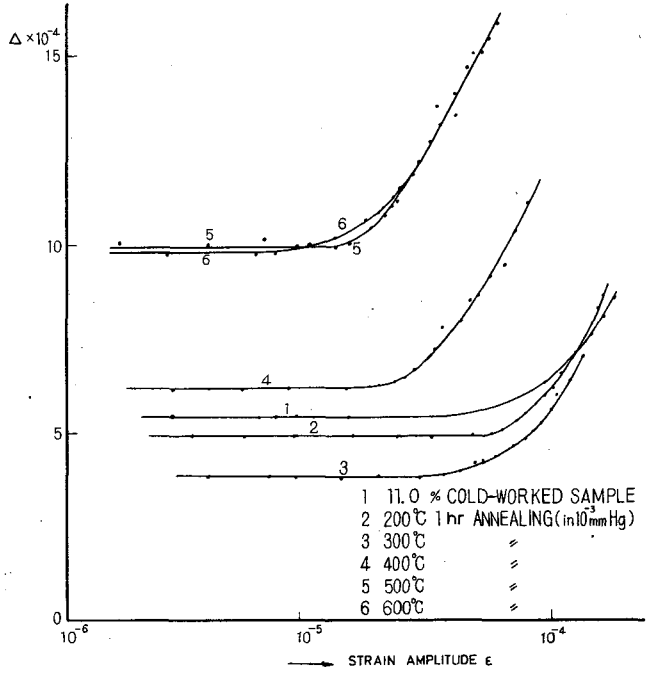

Fig. 9

Amplitude dependence of internal driction of U III before and after annealing

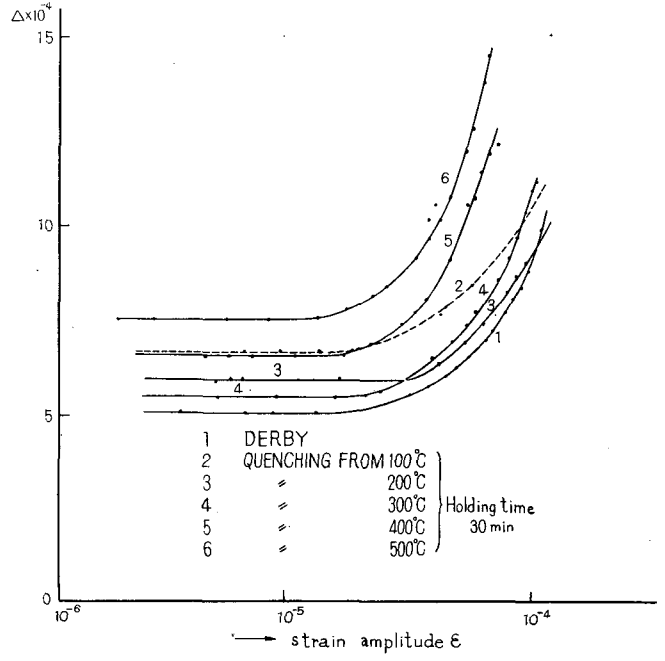

Fig. 10

Amplitude dependence of internal friction of U IV before and after quenching

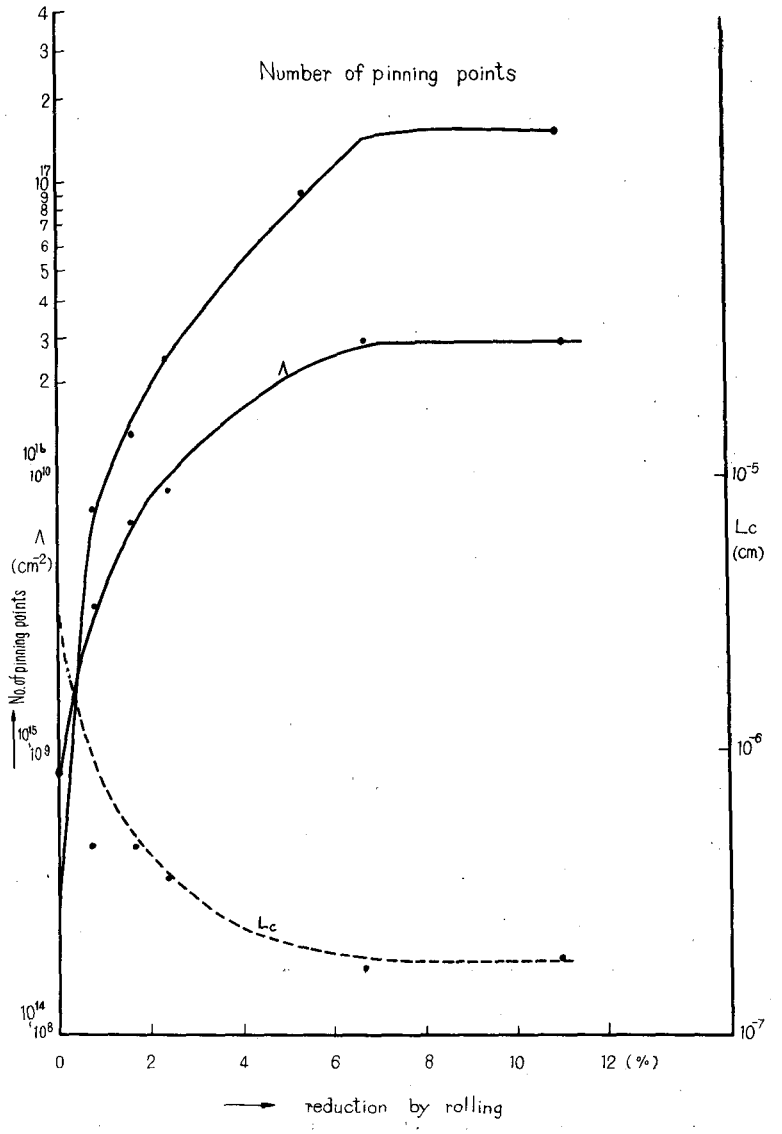

Fig. 11

Dislocation density, dislocation loop length and the number of pinning points along dislocation lines of cold-worked U III

Uranium oxide

(a) Relaxation

Temperature dependence of ultrasonic attenuation is observed from -130°C to +150°C at 5, 7 and 9 MHz. The result of 5 MHz is shown in Fig. 14. A new peak is found at about -40°C. This peak is broad, and the peak

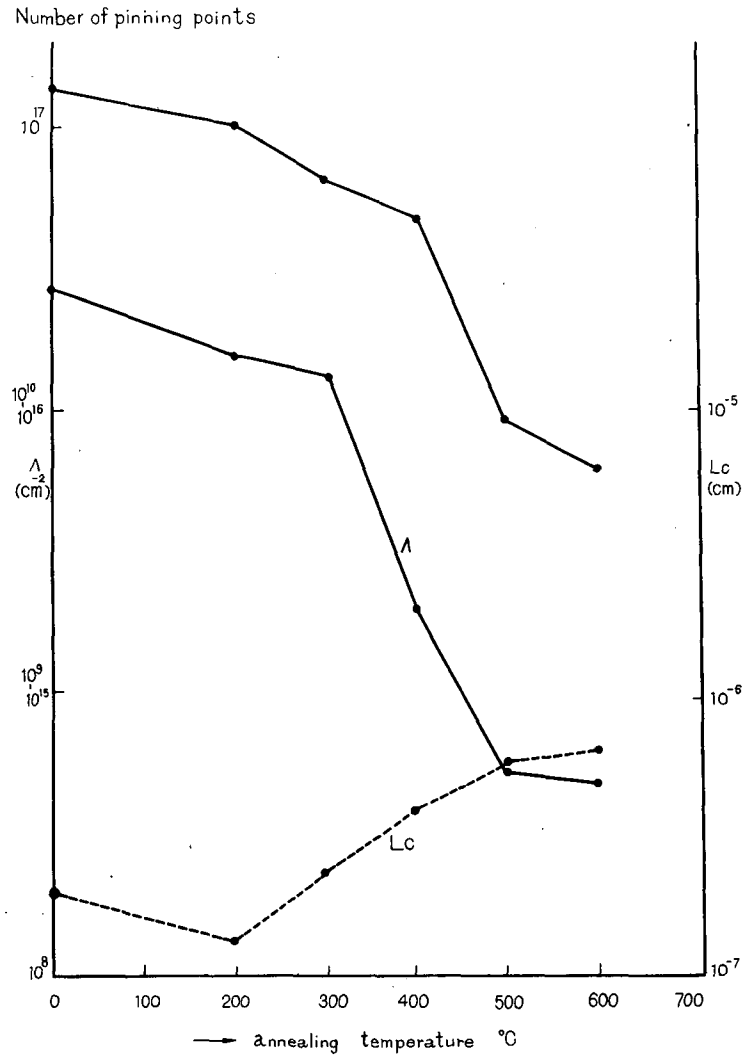

Fig. 12

Dislocation density, dislocation loop length and the number of pinning points along dislocation lines of annealed U III

temperature is not observed clearly in some cases. Therefore, the activation energy of this peak is not determined exactly, but seems to be below 0.1 eV. As the activation energy is very small and the frequency factor is smaller than the Debye frequency, the mechanism of this peak is not considered to be due to the diffusion of any point defects including impurity atoms, but may be considered to be due to the dislocation relaxation such as that observed in magnesium oxide or in other metal oxides.

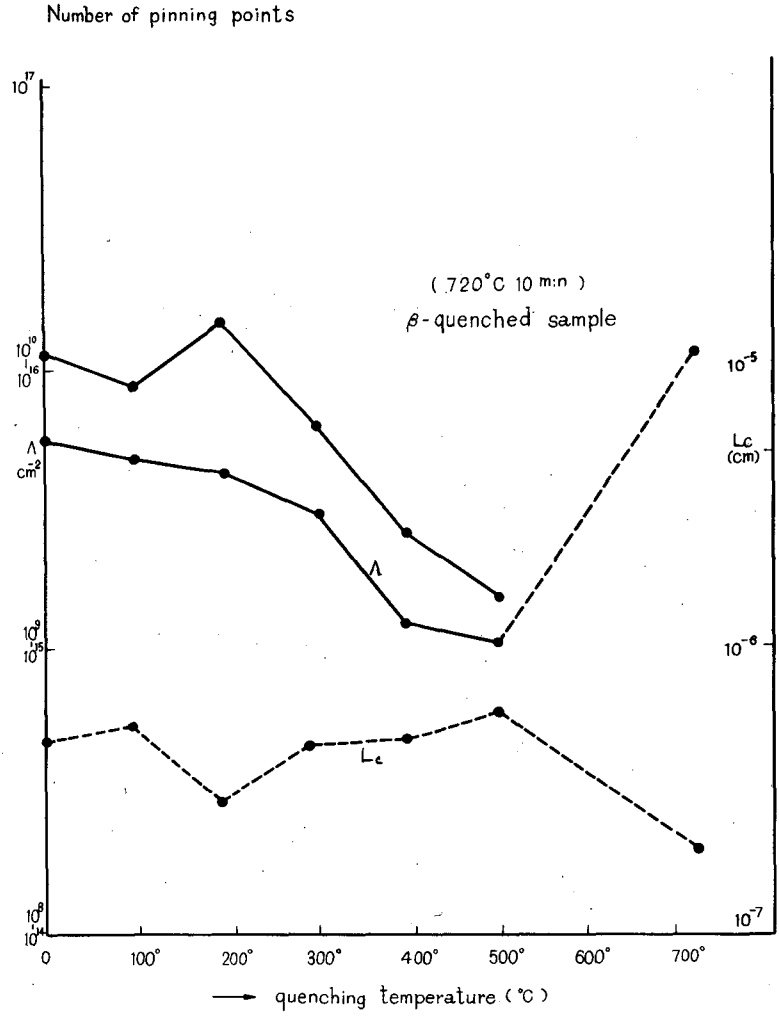

Fig. 13

Dislocation density, dislocation loop length and the number of pinning points along dislocation lines of quenched U IV

(b) Resonance

Frequency dependence of ultrasonic attenuation is measured in the frequency range of 5 MHz-35 MHz. The experiment is performed before and after compression on the sintered UO_2. The results are shown in Figs. 15 and 16. The internal friction due to crystal defects are estimated from the difference between the measured values before and after the compression, because the obtained values themselves include other factors which come from, for example, the size effect of the specimen, the quartz loss and so

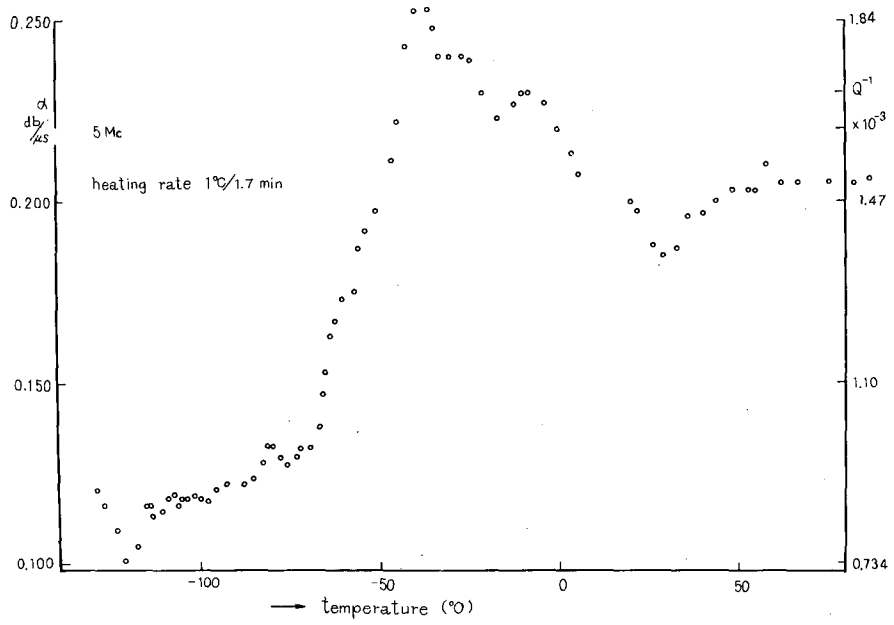

Fig. 14

Temperature dependence of ultrasonic attenuation of UO_2 I

on. This differential value is shown in Figs. 17 and 18, in which it is seen that the internal friction increases with the vibrational frequency, overlapped by the peak around 15 MHz, which is interpretated as the relaxation peak observed at -40°C at 5 MHz (Fig. 15). In Fig. 18 the over-damped region (the decrease of internal friction with the vibrational frequency) was observed as with LiF. This is an exact evidence of resonance of dislocations as was predicted by GRANATO and LÜCKE [1].

The proportion of this internal friction to the vibrational frequency shows that this difference is due to the string-like motion of dislocation which is suggested by the Granato-Lücke theory, because another mechanism which is proportional to the frequency, for example electronic or electromagnetic contribution, is excluded in this experimental condition. If this is the case, this method is very sensitive for detecting minor plastic deformation at room temperature, which is directly connected to the strength of UO_2.

Zircaloy-2

(a) Relaxation

The internal friction of Zircaloy-2, which is hydrogen charged, is measured between room temperature and liquid-nitrogen temperature by a transverse vibration-free decaying method. In an annealed specimen, relaxation peaks are observed at 250-260°K and at about 160°K, and when quenched

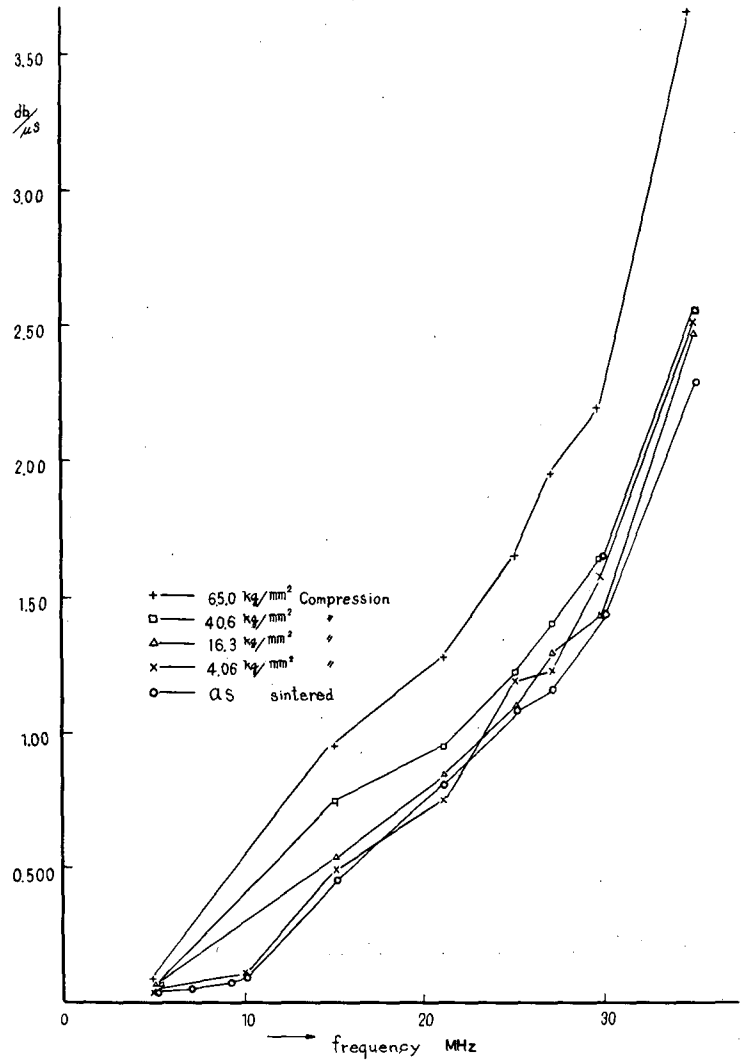

Fig. 15

Frequency dependence of ultrasonic attenuation of UO_2 I before and after compression

from 300°C, the height of 260°K peak increases. These results are shown in Fig. 19 and in Table I. After quenching the 260°K peak becomes higher as the hydrogen content increases. This peak is of single relaxation and the activation energies, which are obtained from the peak width and from the peak temperature, coincide very well and its value is almost the same as the BUNGARDT et al. [3] results on pure zirconium.

For the above reasons this peak is believed to be Snoek's peak of hydrogen which comes from the stress-induced diffusion of hydrogen between

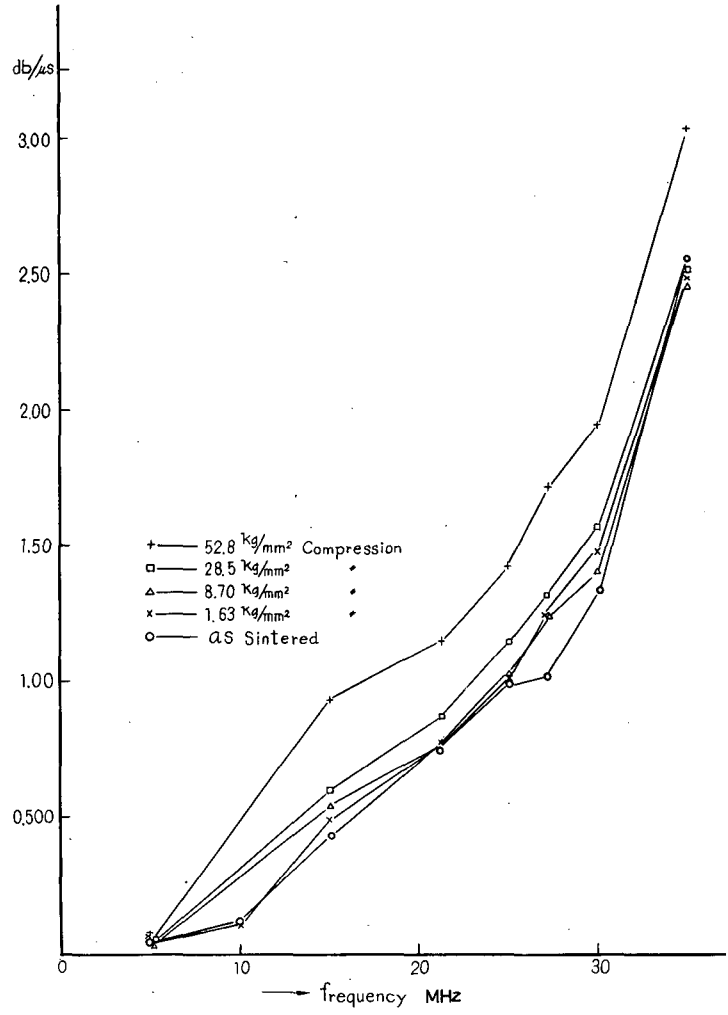

Fig. 16

Frequency dependence of ultrasonic attenuation of UO_2 II before and after compression

tetrahedral and octahedral sites. Such a peak is also observed in hydrogen-charged titanium [4]. This peak may be used for inspecting hydrogen pick-up.

(b) Hysteresis

The amplitude dependence is also observed here. In this case the Granato-Lücke relation is satisfied in the higher amplitude region, but it deviates in the lower amplitude region. The values of dislocation densities and dislocation loop-lengths are calculated from the higher amplitude region, and are shown in Fig. 20. This shows that the dislocation density increases with

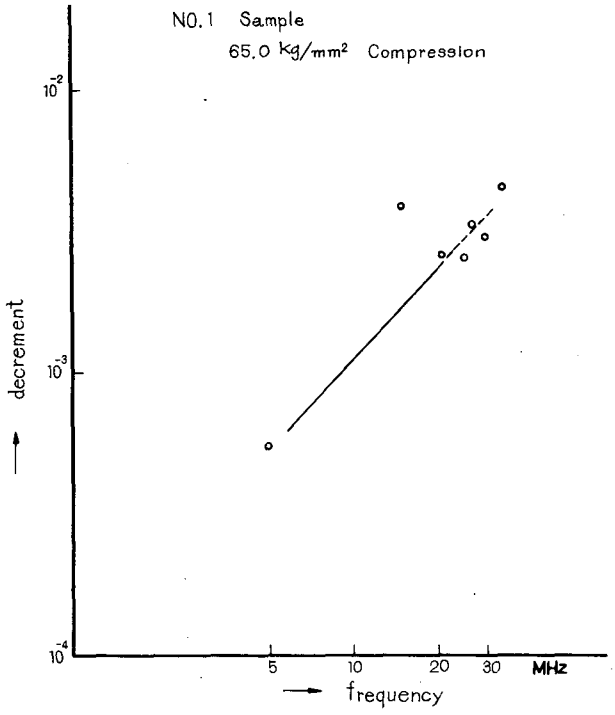

Fig. 17

The differential internal friction versus vibrational frequency of compressed UO_2 I

hydrogen content, which would be connected to the hydrogen brittleness of Zircaloy-2.

5. CONCLUSIONS

From experimental results in part 4, it is concluded that the internal friction measurements are applicable to the non-destructive testings of nuclear materials for the following cases:

(i) The change of solute impurity concentration brought forth by quenching in uranium and uranium alloys.
(ii) Dislocation density and dislocation loop-length of cold-worked, annealed and quenched uranium.
(iii) Dislocation behaviour in UO_2.
(iv) Detection of minor plastic deformation of UO_2 at room temperature.
(v) Solute hydrogen in Zircaloy-2.
(vi) Dislocation density and dislocation loop-length in Zircaloy-2.

Thus, these atomic measurements would be useful for inspecting nuclear materials. The authors intend to investigate the irradiation processes of nuclear materials the near future.

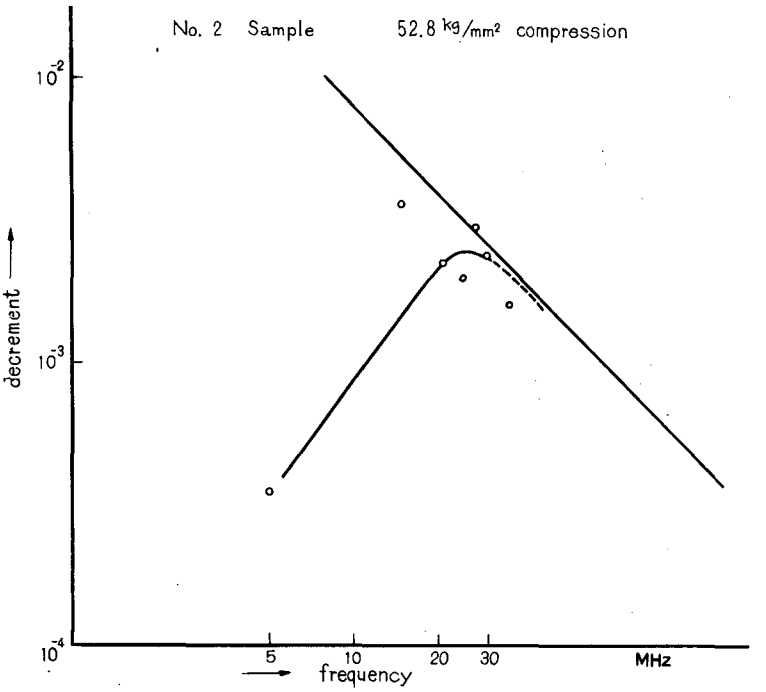

Fig. 18

The differential internal friction versus vibrational frequency of compressed UO_2 II

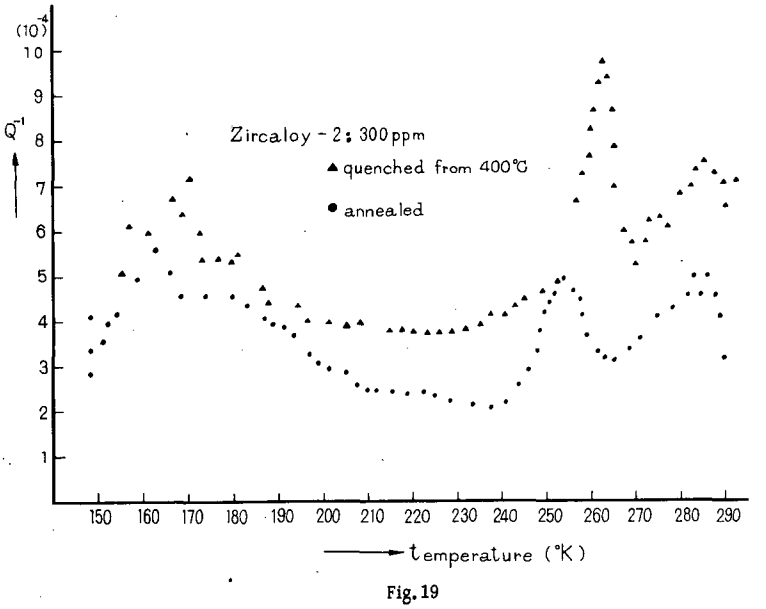

Fig. 19

Temperature dependence of internal friction of Zircaloy-2 II quenched from 350°C

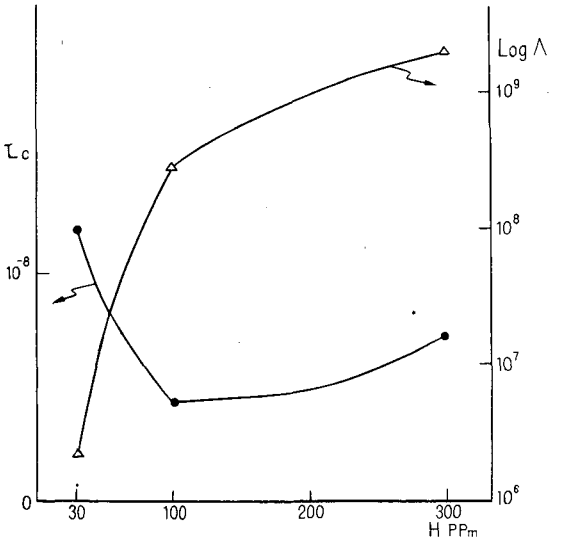

Fig. 20

Dislocation density and dislocation loop length of Zircaloy-2 I and II versus hydrogen content

REFERENCES

[1] GRANATO, A. and LÜCKE, K., J. appl. Phys. 27 (1956) 583, 789.
[2] HASIGUTI, R.R., IGATA, N. and UEKI, M. (to be published).
[3] BUNGARDT, K. and PREISENDANZ, H., Z. Metallk. 51 (1960) 280.
[4] KÖSTER, W., Z. Metallk. 47 (1956) 564.

DISCUSSION

A. VAN DER LINDE: I have three questions concerning Fig. 20 of your paper, showing the logarithm of the dislocation density of Zircaloy-2 as a function of hydrogen content in ppm. Is the curve valid for quenched or annealed Zircaloy-2?

N. SASAO: It is valid for quenched Zircaloy-2.

A. VAN DER LINDE: The shape of the log. Λ curve is such that at about 500 ppm hydrogen content a saturation value can be expected. Can such a saturation condition be explained theoretically?

N. SASAO: I think that the saturation condition is due to the formation of hydrogen compounds.

A. VAN DER LINDE: Is there a theoretical explanation of the minimum in the L_c curve?

N. SASAO: We cannot explain it at present because there are only a few measured points.

F. H. WELLS: In the electrostatic method of measuring resonance frequency (Fig. 1) is any special surface preparation or conductive coating needed on the specimen?

N. SASAO: No, none at all.

THE ROLE OF NON-DESTRUCTIVE TESTING IN TEST-REACTOR OPERATION AT THE NATIONAL REACTOR TESTING STATION*

W. C. FRANCIS, E. S. BROWN, E. E. BURDICK, G. W. GIBSON AND F. H. TINGEY
PHILLIPS PETROLEUM COMPANY, ATOMIC ENERGY DIVISION,
IDAHO FALLS, IDAHO,
UNITED STATES OF AMERICA

Abstract — Résumé — Аннотация — Resumen

THE ROLE OF NON-DESTRUCTIVE TESTING IN TEST-REACTOR OPERATION AT THE NATIONAL REACTOR TESTING STATION. The huge investment (well over $100 000 000) in the Nuclear Test Reactors at the National Reactor Testing Station and the need to operate them safely requires the highest order of quality control for reactor and test components, especially for fuel and control elements. Non-destructive testing has, therefore, assumed a very vital role in establishing the quality of these components before their use in the Test Reactors. Although many of these non-destructive tests follow well-established procedures, many unique techniques have been developed and new uses made of conventional equipment.

Ultrasonic techniques have long been used at this site for detecting voids, non-bonding and internal cracking. More recently this work has been extended to the automated scanning of curved plates and to the inspection of irradiated fuel plates in the storage canals. A very interesting work has been the application of the ultrasonic technique to the detection of brittle core fracture which may occur in forming operations.

A gamma-scanning technique to establish the U^{235} content of fuel elements has proved so reliable that it is the basis for assessing financial penalties for out-of-specification material. Radiographs of fuel plates provide core dimensions and, with densitometer scans, determine fuel distribution. Radiographing of welds is standard procedure for reactor and test loop components.

Burnup of fuel and poison in test specimens may be determined each reactor cycle by the use of the Advanced Reactivity Measurement Facility (ARMF). A somewhat unusual application for a critical facility is the measurement of the boron content of fuel in the Engineering Test Reactor Critical Facility (ETRC).

Eddy-current and mechanical probing of fuel-plate spacing and eddy-current gauging of oxide film thickness (corrosion) on irradiated plates have given excellent results. Additional techniques, which have proved valuable, include liquid penetrant inspection and liquid nitrogen tests for surface cracks, thermal anneal tests for blistering, and gamma-scanning of irradiated plates. Hydraulic testing of statistical sampling of fuel elements is used to confirm structural integrity, particularly the fuel plate-side plate-joint strength. A continuous effort is made to improve existing techniques and to develop new non-destructive inspection procedures.

RÔLE DES ESSAIS NON DESTRUCTIFS DANS L'EXPLOITATION DES RÉACTEURS D'ESSAI AU CENTRE NATIONAL D'ESSAIS DE RÉACTEURS. Les investissements très importants (plus de 100 millions de dollars) consacrés aux réacteurs d'essai du Centre national d'essais de réacteurs et la nécessité d'exploiter ces réacteurs en toute sécurité exigent un contrôle extrêmement strict de la qualité des réacteurs et de leurs parties constitutives, notamment des éléments combustibles et du dispositif de commande. Les essais non destructifs ont donc joué un rôle essentiel dans le contrôle de la qualité de ces pièces avant leur utilisation dans les réacteurs d'essai. Bien qu'un grand nombre de ces essais non destructifs soient exécutés selon des procédures bien établies, on a mis au point de nombreuses méthodes inédites et introduit de nouvelles utilisations du matériel classique.

On applique depuis longtemps au Centre d'essais les méthodes ultrasonores pour la détection des cavités, des défauts de liaison et des craquelures internes. Récemment, on a étendu ces méthodes à l'exploration automatique des plaques courbes et à l'inspection des éléments combustibles irradiés dans les canaux de stockage. Des travaux très intéressants ont permis d'appliquer la méthode des ultrasons à la détection des fractures qui peuvent se produire dans l'âme lors du façonnement.

* Work performed under the auspices of the United States Atomic Energy Commission.

Une méthode d'exploration par rayons gamma, pour déterminer la teneur d'éléments combustibles en ^{235}U, s'est révélée tellement fiable qu'elle a été adoptée pour calculer les pénalisations financières pour les articles non conformes aux spécifications. Les radiographies de plaques de combustible donnent les dimensions de l'âme et, associées aux explorations à l'aide d'un densimètre, permettent de déterminer la distribution du combustible. On a habituellement recours à la radiographie des soudures pour les parties constitutives des réacteurs et des boucles d'essai.

Le dispositif perfectionné de mesure de la réactivité (Advanced Reactivity Measurement Facility, ARMF) permet de déterminer, pour chaque cycle de réacteur, l'irradiation du combustible et l'empoisonnement dans des spécimens. Une application assez peu courante pour un assemblage critique est la mesure de la teneur en bore du combustible dans l'assemblage critique d'essai en genie des réacteurs (Engineering Test Reactor Critical Facility, ETRC).

Le contrôle par courants de Foucault et par des procédés mécaniques de l'espacement des plaques de combustible et la mesure par courants de Foucault de l'épaisseur de l'oxydation (corrosion) sur les plaques irradiées ont donné d'excellents résultats. Des méthodes complémentaires qui ont fait leurs preuves sont l'inspection par liquide pénétrant et les essais à l'azote liquide pour les craquelures superficielles, les essais par recuit thermique pour les soufflures et l'exploration par rayons gamma des plaques irradiées. On a recours à l'essai hydraulique d'un échantillon statistique d'éléments combustibles pour vérifier l'intégrité structurale, notamment la résistance de la liaison entre les plaques de combustible et la gaine. Des efforts constants sont déployés pour améliorer les méthodes actuelles et mettre au point de nouveaux procédés de contrôle non destructif.

РОЛЬ НЕДЕСТРУКТИВНЫХ ИСПЫТАНИЙ ПРИ ЭКСПЛУАТАЦИИ ИСПЫТАТЕЛЬНЫХ РЕАКТОРОВ НА НАЦИОНАЛЬНОЙ СТАНЦИИ ПО ИСПЫТАНИЯМ РЕАКТОРОВ. Большие капиталовложения (более 100 млн. долл.) в ядерные опытные реакторы при Национальной лаборатории по испытанию реакторов и необходимость эксплуатировать их безопасно требуют высококачественного контроля за реакторами и опытными компонентами в особенности за топливом и управляющими стержнями. Поэтому недеструктивные испытания играют очень важную роль в определении качества этих компонентов до того, как они используются на опытных реакторах. Хотя многие из этих опытов проводятся по хорошо отработанным программам, тем не менее было разработано много уникальных способов и широко используется обычное оборудование.

Долгое время использовались ультразвуковые методы в целях обнаружения раковин, недиффузиозности тепловыделяющих элементов и внутренних трещин. В последнее время эта работа была распространена на автоматическое сканнирование кривых пластин и для обследования облученных топливных пластин в каналах для хранения. Весьма интересная работа была проведена в деле применения ультразвука для обнаружения разрыва хрупких активных зон, который может возникнуть в процессе изготовления.

Метод гамма-сканнирования для определения содержания урана-235 в топливных элементах оказался настолько надежным, что он является основой для подсчета финансовых затрат на материал, числящийся вне спецификации. Рентгеновские снимки топливных пластинок дают размеры активных зон и с помощью развертки денситометра определяют распределение топлива. Рентгеновская съемка сварных швов является стандартной процедурой для реакторов и компонентов опытных петель.

Выгорание топлива и отравление в опытных образцах может быть определено в каждом цикле реактора путем использования усовершенствованного устройства по измерению реактивности (ARMF). В какой-то степени необычное применение для критического устройства является измерение содержания бора в топливе на критической установке по технологии испытательных реакторов (ETRC).

Токи Фуко и механическое зондирование расстояния топливных пластинок и измерение толщины окиси пленки (коррозия) с помощью токов Фуко облученных пластинок дали отличные результаты. Дополнительные способы, которые оказались весьма ценными, включают обследование жидких проникновений и опыты по жидкому азоту для трещин на поверхностях, опыты по тепловому отжигу для окалин и гамма- сканнирование облученных пластин. Гидравлическое испытание стабильных образцов топливных элементов используется для того, чтобы подтвердить структурную целостность, в особенности, силу соединения топливных пластинок. Ведутся дальнейшие работы по улучшению существующих методов и по разработке новых недеструктивных методов обследования.

PAPEL DE LOS METODOS NO DESTRUCTIVOS EN LA EXPLOTACION DE LOS REACTORES DE LA NATIONAL REACTOR TESTING STATION. Los reactores de ensayo de la National Reactor Testing Station suponen

una enorme inversión (superior a 100 millones de dólares) y la necesidad de explotarlos en condiciones de seguridad obliga a proceder a un control de calidad muy estricto de los componentes nucleares y de ensayo, especialmente en lo que respecta a los elementos combustibles y de control. Por tanto, los métodos no destructivos son fundamentales para determinar la calidad de estos componentes antes de emplearlos en los reactores. Aunque muchos de estos ensayos no destructivos se efectúan según procedimientos bien establecidos, se han desarrollado numerosas técnicas especiales y se ha encontrado aplicaciones originales para diversos instrumentos clásicos.

Desde hace tiempo se vienen aplicando técnicas ultrasónicas a la detección de cavidades, uniones defectuosas y grietas internas. Más recientemente, estos trabajos se han ampliado a la exploración automática de placas curvas y a la inspección de placas combustibles irradiadas que se encuentran en los canales de almacenamiento. Particular interés reviste la aplicación de técnicas ultrasónicas para detector fracturas en núcleos frágiles que se pueden producir durante las operaciones de conformado.

Se ha observado que la técnica de exploración con rayos gamma para determinar el contenido en uranio-235 de los elementos combustibles es tan precisa que puede emplearse como la base para determinar la cuantía de las indemnizaciones que se han de pagar por materiales que no cumplan ciertas especificaciones. Las radiografías de las placas combustibles indican las dimensiones del núcleo, y si se exploran densitométricamente, la distribución del combustible. La radiografía de soldaduras constituye un procedimiento corriente para comprobar las piezas del reactor y de los circuitos de ensayo.

El grado de combustión de las especies fisionables y de los venenos en las muestras a ensayar se pueden determinar en cada ciclo del reactor empleando la Advanced Reactivity Measurement Facility (ARMF). Una aplicación poco corriente para una instalación crítica es la medición del contenido de boro del combustible en el Engineering Test Reactor Critical Facility (ETRC).

Se han obtenido excelentes resultados con la aplicación de corrientes de Foucault y del sondeo mecánico para determinar el espaciamiento de las placas combustibles, así como en el calibrado del espesor de las películas de óxido (corrosión) de placas irradiadas empleando corrientes de Foucault. Otras técnicas que han demostrado su utilidad son la inspección por penetración de líquidos, los ensayos con nitrógeno líquido para detector grietas superficiales, los ensayos de recocido térmico para determinar ampollas, y la exploración gamma de placas irradiadas. Muestras de elementos combustibles tomadas estadísticamente se ensayan por métodos hidráulicos para confirmar su integridad estructural, especialmente la estabilidad de la unión entre la placa combustible y la placa lateral. Constantemente se intenta mejorar las técnicas actuales y perfeccionar nuevos procedimientos de inspección de carácter no destructivo.

The nuclear test reactors at the National Reactor Testing Station (NRTS) represent a capital investment of well over $ 100 000 000. The annual fuel costs and the value of the hundreds of experiments in the reactors would add many millions more to this total. When the Advanced Test Reactor comes on-stream later this year it is expected that the three test reactors will consume an average of 115 fuel elements each month. It is essential, therefore, that the quality control of initial and replacement components, especially of fuel and control elements and of test samples, be of the highest order. Non-destructive testing of these components before their use in the test reactors assumes a very vital role in establishing the quality and providing important pre-irradiation data. It is the purpose of this paper to describe some of the non-destructive testing techniques in use at the NRTS and especially to present some of the more unique developments and applications which have evolved through extensive experience.

1. USE OF ULTRASONICS

Ultrasonic techniques have been used at the NRTS for over eight years for pre-irradiation inspection of specimens for voids, non-bonding, and

internal cracking. These procedures have also been used for inspecting irradiated fuel plates as well as for scanning full-size Materials Testing Reactor (MTR) fuel plates which had been formed to the final curved configuration. The purchase specifications for the Advanced Test Reactor (ATR) fuel elements now require that the plates be ultrasonically scanned by the manufacturer to detect undesirable imperfections.

1.1. Description of equipment

A Model 424-A "Immerscope" manufactured by the Curtiss-Wright Corporation has been the basic instrument for this work. Most items are inspected by through-transmission techniques in a water medium. A choice of frequencies from 2 to 25 MHz is available, pulsed at 100-500 Hz.

The information thus obtained was originally displayed on a 7-in cathode-ray tube as "pips". A flaw-alarm control on the instrument made it possible to trigger a circuit which would operate a light or pen when the "pip" height dropped below an arbitrarily chosen value. To provide permanent records of the ultrasonic scans the "Immerscope" was combined with an X-Y recorder. To do this, two electrical measuring and balancing systems were used: one system operates the pen travel on the horizontal axis (X-axis), the other operates the chart movement on the vertical axis (Y-axis). The alarm circuit of the "Immerscope" was used to actuate a solenoid-operated pen lifter in the recorder. The record is produced on a strip chart and provides a $9\frac{1}{2} \times 9\frac{1}{2}$-in record which is easily detached for filing. Provision is made for changing the recorder magnification so that scans of full-size (3 in×24 in) fuel plates may be recorded on the 9-1/2×9-1/2-in chart space.

1.2. Pre-irradiation inspection of samples

Under the Reactor Fuels and Materials Programme conducted at the NRTS, small specimen fuel-plates of a variety of compositions are fabricated, inspected, irradiated, and examined. These plates range in thickness from 0.030 - 0.150 in. As part of the pre-irradiation inspections, the plates are ultrasonically scanned.

1.3. Automated scanning of curved plates

Since the fuel plates used in the MTR and the ATR-type fuel elements are curved it was necessary to provide a means of inspecting these plates after forming to ensure that this operation had not disrupted the metallurgical bond between the fuel-plate core and cladding. A special fuel-plate scanner was designed and built for this purpose.

In this scanner a pair of transducers are passed longitudinally down the plate. The fuel-plate holder is automatically rotated after each pass of the transmitting-receiving crystal pair. This procedure keeps the surface of the plate always perpendicular to the sound beam. Fig. 1A shows the ultrasonic scanning tank together with the transducer crystals and the holder for the inspection of curved plates. The electrical linkages between the crystals scanning the plates, the plate-rotating mechanism, and the re-

corder pen are adjusted so that the scans can be recorded on the 9-1/2× 9-1/2-in chart area. An example of a very practical application of this automated scanner for curved plates is given in the following section.

1.4. Detection of brittle core fracture in forming

By making use of an interesting concept involving the dispersion of fuelled glass fibres in an aluminium matrix, the Clevite Corporation [1] developed a potentially useful reactor fuel. Fabrication development, mechanical property studies, and irradiation of test samples, all substantiated the promise of this material and led to the fabrication of an MRT prototype fuel element. The element satisfactorily passed all acceptance tests, which had included blister testing of the fuel plates, and was awaiting insertion in the MTR when an extra fuel plate which had been provided along with the prototype element was given an ultrasonic inspection. This plate had been blister-tested after hot-rolling and then was cold-rolled to final thickness and cold-formed to MTR curvature. Since no ultrasonic scanner was available at the time for curved plates the ultrasonic test was, at best, somewhat crude. However, areas of especially poor sound transmission were suspected as indicating unbonded or void areas and the plate was examined metallographically to reveal cracks similar to those shown in Fig. 1C. Since flat plates prepared for irradiation and mechanical property measurements had indicated some brittleness but no cracking, it was concluded that the cracks observed in the small plate were initiated by the shear forces associated with curving of the plates. Because of concern for the in-pile performance or the prototype element, should its plates also have similar separations in the cores, it was decided to disassemble the element and ultrasonically scan each plate. The transducers used for both transmitting and receiving were 10-MHz Li_2SO_4 crystals with 0.56-in focal lengths. The standard used for simulating flaws in the plates was a pair of lead washers. Some typical scans of plates in which flaws were indicated are shown in Fig. 1B. A composite photomicrograph of the "flaw" area of Plate No. 3 is shown in Fig. 1C. A pronounced separation in the core is visible at the top edge and a smaller crack is observed at the lower edge of the core.

In working with very brittle materials such as this fibreglas fuel element it is possible, by ultrasonic means, to detect not only the soundness of the finished plate but also to determine if the forming operation is causing brittle cracking.

1.5. Irradiated inspection

The ultrasonic inspection equipment has also been adapted for use in the inspection of irradiated fuel plates. The only major change in the equipment required for this use was to construct a pair of 10-ft-long search tubes. No appreciable changes were noted in the operating conditions of the transducers used for this application after exposure ranging up to 120 h.

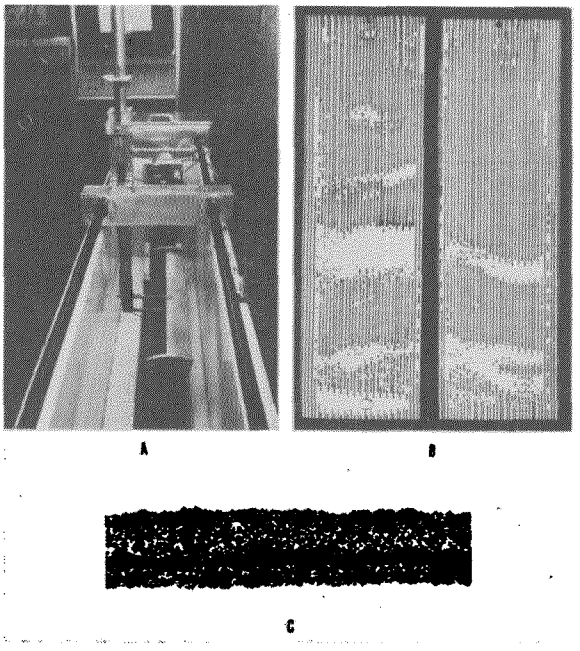

Fig. 1

Ultrasonic scanning of fuel plates
A. Scanner for curved plates
B. Scan records
C. Photomicrograph of core separation

2. FUEL SCANNING

In addition to the requirement for accurate U^{235} material accountability, safe operation of the reactors depends on good knowledge of U^{235} quantity and distribution.

2.1. U^{235} assay by beam of thermal neutrons

In the early days of MTR operation an attempt at fuel assaying was made through the use of a beam of thermal neutrons emanating from the MTR reactor. The fuel element to be assayed was placed in the beam. Fast-fission neutrons consequently generated were detected by counters placed on opposite sides of the fuel element and in a plane 90° to the thermal beam. A specially fabricated track and motor-driven carriage were used to propel the fuel element to be scanned across the neutron beam at a constant rate.

To avoid the complication of an absolute calibration, a reference element was periodically introduced into the scanning sequence of production elements. The fission-neutron counting-rates of the production elements were then compared with that of the reference element.

Although this procedure was used for many years, certain obvious disadvantages were recognized. First, the technique was available only to

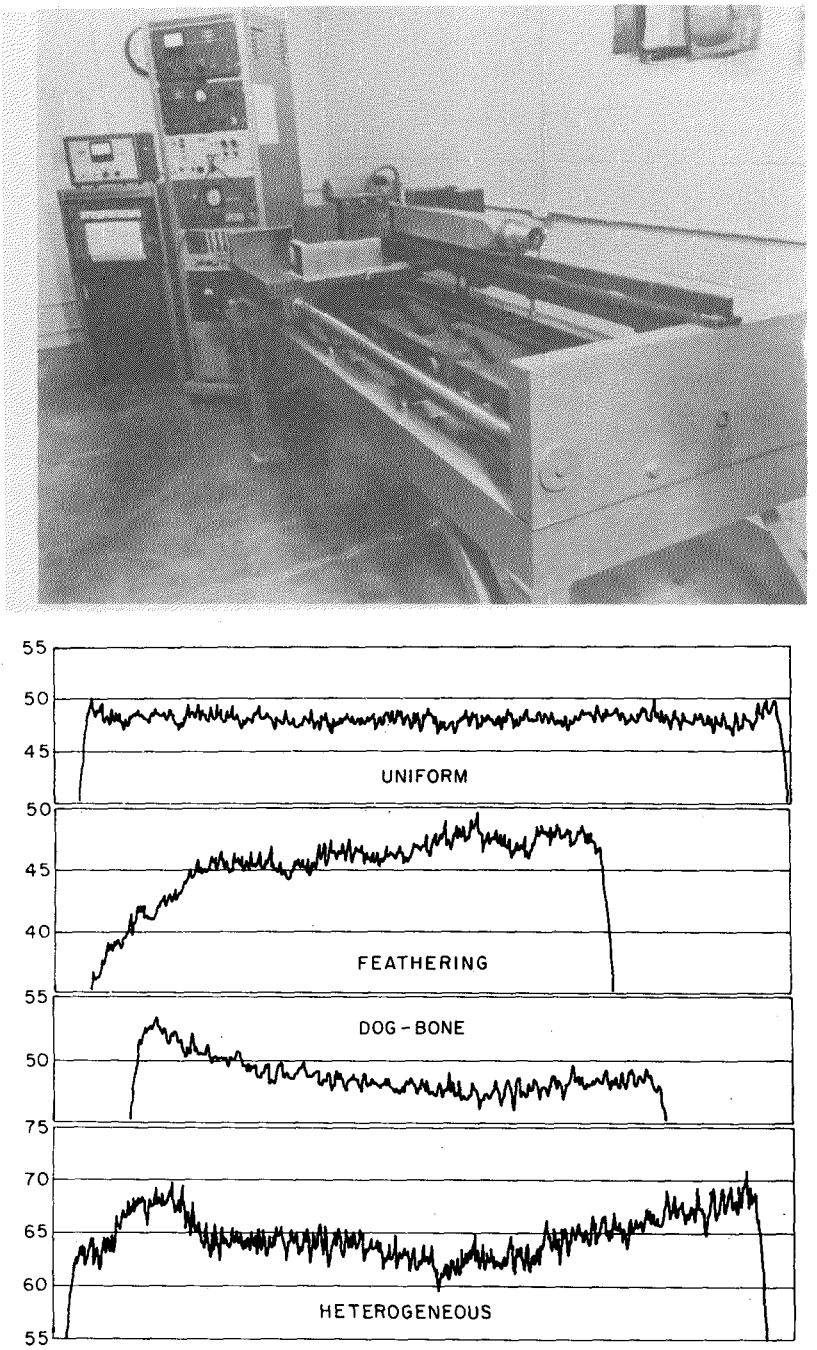

Fig. 2

Fuel scanner and typical profiles

those who had generous supplies of thermal neutrons, namely reactor operators, and only then when the reactor was operating. Second, in our application, the neutron beam used for scanning emanated from the top of the MTR reactor and consequently the scanning equipment interfered with the insertion and removal of experiments. Third, and probably most important, the reproducibility of results was extremely sensitive to the density of neutrons in the beam, and thus even small perturbations in the reactor flux during operation tended to make the data difficult to interpret.

2.2. Natural gamma-activity counting

In a large measure many of these problems were solved by use of a non-destructive assaying device fabricated by the Westinghouse Electric Corporation [2]. The apparatus is illustrated in Fig. 2.

The complete system employs four complementary methods of non-destructive assay: counting of natural gamma activity, thermal neutron attenuation measurements, epithermal neutron absorption, and weight and volume measurements. Our experience has been mainly with the first method; limited work in neutron absorption has not produced results comparable to the reactivity measurements discussed in a later section.

Since U^{235} emits gamma radiation, the measurement of the gamma rays emitted by a fully-enriched fuel element provides information on the amount of fuel contained. To use this method for an accurate determination of U^{235} in rather dense objects such as fuel elements, it is necessary to minimize the effects of counting geometry, self-absorption within the materials and the non-uniform uranium distribution. The basic procedure employed in the natural radioactivity device is to scan the element between a pair of NaI(Tl) scintillation counters and compare the resultant count with that from "standard" elements whose U^{235} contents are known and bracket that of the unknown. Linear interpolation with reference to the U^{235} content of the standards provides a measure of the U^{235} content of the element. This method is used for assaying fuel plates as well as fuel elements. Different detection geometries are needed for plate and for element assays to compensate in part for the different amounts of self-absorption.

For the fuel plates, the configuration consists of two opposed 1×3-in rectangular scintillation crystals which scan the fuel plate at a constant rate. The plate-assay system is modified for the assay of elements by retracting the detectors and inserting collimators which effectively reduce the crystals to 1×1-3/4-in rectangles. Elements are scanned one direction, rotated 90° and scanned back, and the sum of the counts determined. Typical scans of acceptable and unsatisfactory plates are shown in Fig. 2. The detection efficiency of this system would be independent of position within the element if there were no attenuation. However, the attenuation is considerably greater along the centre of an element than along the edges. This non-uniformity is compensated by the insertion of the gamma collimator so that the crystals "see" the edges of the elements less effectively.

The principal sources of variation which contribute to the over-all uncertainty of this assay method are the electronic drift of the instrument, variation in aluminium content of elements, and error in uranium values

assigned to the standards. The effect of variation in aluminium and instrument drift is minimized through the use of a filter made of 20-mil cadmium sheet which covers the 1-in slit in the collimator. For the particular geometry employed, aluminium contributes a net loss of counts in the high (> 180-keV) and the low (< 60-keV) energy ranges and a net gain in counts through the medium energy range. By setting the "window" discriminator to accept pulse heights only in the energy 60 keV to 250 keV, and by the use of the filter, variations in aluminium content must be considerably larger than one would expect from the fabrication tolerances to be of any consequence.

To date we have individually assayed through gamma scanning the following:

800 MTR elements;
2000 Engineering Test Reactor (ETR) elements;
420 ETR control-rod fuel sections;
50 Advanced Reactivity Measurement Facility (ARMF) elements; and
8500 Miscellaneous plates.

From an analysis of all pertinent errors, both random and systematic, to be associated with this technique of assay, it is estimated that the uncertainty (95% confidence limit) on an individual item determination does not exceed 1.0%.

Use is made of the data obtained in the fuel assay both with regard to fissile material accountability and payment for fabrication services. Contractually, off-loaded elements and plates are purchased at a sliding scale price keyed to the amount off-loaded and the resultant utility of the item to Phillips. (Off-loaded elements require special handling and can only be used in certain locations in the reactor). It is interesting to note that, as a result of this provision, fuel-fabrication services sub-contracts have been penalized in excess of $ 100 000 over the past three years.

2.3. Gamma scanning of irradiated fuel plates

Gamma scanning of irradiated fuel plates from both the MTR and ETR has been accomplished by passing the plate at a controlled rate in front of a 1/8-in opening in a plug through a hot-cell wall. The relative gamma intensities through the opening are recorded and correlated with distance along the plate. Calibration is accomplished by means of a Cs^{137} source. The discrimination voltage is set to accept only energies above 0.7 MeV. A photographic reduction of a typical ETR plate scan is shown in Fig. 3A. This scan verifies that the peak flux remains somewhat below the reactor core midplane for most of the cycle and that there is indeed some effective peaking of fission rate at the fuel ends; but appreciably less than the flux peaking measured by wires in the water channels. Corroboration of the gamma-scan results was obtained by punching specimens from the plate and analysing them for U^{235} content. A typical plot of 2% iso-burnup contours is shown in Fig. 3B. This Figure shows the distribution skewed towards one edge and towards the lower half of the plate.

Gamma scanning as a non-destructive technique has also found considerable application to improve homogeneity of fuel cores during fabrication. Vendors supplying fuel elements for the test reactors currently gamma scan

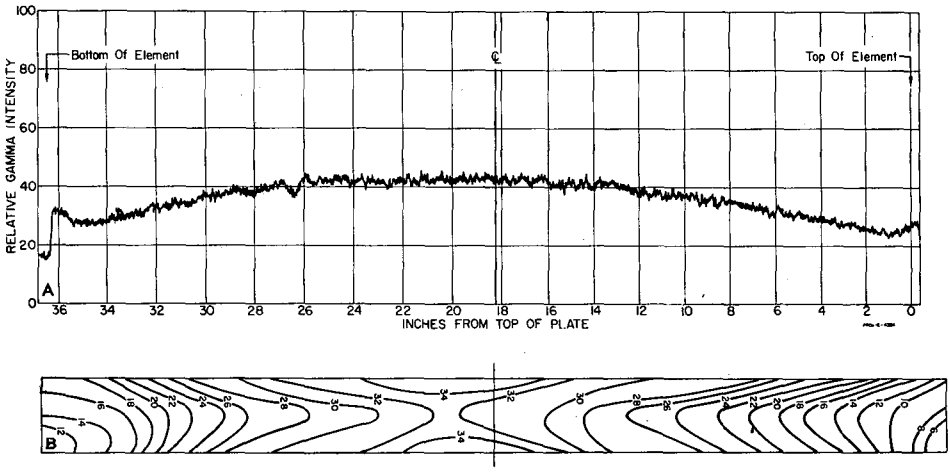

Fig. 3

Gamma scan of irradiated ETR fuel plate and corresponding burnup contours

the punched or compacted cores before assembling in the picture frame and cover plates for roll bonding. This results in improving the distribution of uranium in the finished fuel plates and reduces reject or re-work material after final rolling.

3. RADIOGRAPHY

3.1. Description of equipment

Fuel-plate radiography at the NRTS is used to determine fuel-plate core dimensions and location, and hot stripes, segregation and "dogboning" which may affect the heat-transfer conditions of the plate.

The basic equipment consists of a 200-kVP, 5-mA ANDREX X-ray set, a darkroom for development of film under controlled conditions suggested by the film manufacturer, and a Photovolt Transmission Densitometer Model 501-A and Photometer.

The X-ray set is generally used for the non-destructive testing of welds and sample fuel plates fabricated for fuel-element development. Radiographs of production fuel plates are furnished by the fuel-element vendor.

The densitometer and photometer are used to determine film densities of radiographs by measuring the light transmission through the radiograph.

3.2. Fuel-plate inspection – core outline and homogeneity

The core outline is distinctly observed by a visual inspection of the radiograph and thus provides a reliable method of determining whether or not the core location within each plate is within the specified tolerances.

Fuel concentration and/or segregation is also determined from the same radiographs used in determining the core outline. Film density readings

are taken using the densitometer. These readings are then used in determining the difference in uranium content between two locations on the film. It has been found that there can be a marked difference in density readings of different radiographs taken of the same fuel plate. It has also been determined that there may be a significant variation in readings taken several inches apart even though the uranium content may be uniform (one reason for this is because of the variation in X-ray beam intensity). Because of these variables, a single densitometer reading cannot be used to determine the uranium content. Therefore, a uniform method has been established to determine the per cent variation between two locations of a single radiograph. A brief outline of this procedure is as follows.

Variations in fuel concentration are usually of three types: streaking, spot concentration, and "dogboning" – thickening at the ends of the core caused in the rolling process. The radiograph is first visually inspected for non-uniformity. A density reading is then taken at the worst spot; and within 2 or 3 in, an average reading is taken across the plate. To reduce the "beam" effect caused by the variation in X-ray intensity when the radiograph was taken, two additional readings are taken along the aluminium edge adjacent to the core readings. The difference between these two "edge" readings is used in correcting the final values of the core readings. The difference in uranium content is then read from a calibration curve obtained from a variety of Al-U plate samples of known fuel density. The per cent difference in uranium content between the two locations can thus be determined, using the nominal fuel concentration called out in the specifications.

Fuel-element assembly specifications now used at the NRTS require that the range of light transmission through plate radiographs, using a densitometer with a 1/16-in-diam. aperture, shall not exceed 10% of the average for all core locations of any plate.

At present a method is being investigated which may eliminate the beam-effect consideration in film-density measurements and also allow the determination of the uranium content of a point in the plate directly. This would be done by radiographing alongside the fuel plate an aluminium strip the length of the plate. If the thickness of the strip corresponded to a plate of known uranium content, then the difference in densitometer readings at a particular level of the strip and plate would correspond to a difference between a plate of known fuel concentration and that of the plate in question. If the X-ray conditions were well controlled, a maximum allowable difference in the film density between the strip and plate could be established which would correspond to the maximum fuel-density variation allowable by the specification.

4. EDDY-CURRENT INSPECTION

Eddy-current inspection techniques have been applied to three very important operations at the NRTS: (1) That of measuring channel thickness between plates in fuel elements, (2) determining cladding and coating thickness, and (3) identifying temper in metal alloys.

4.1. Channel-thickness measurements

Fuel-element plate-spacing measurements are obtained by the use of a probe developed by the Oak Ridge National Laboratory [3] and a commercial instrument (Dermitron) which furnishes the high-frequency current to the coil in the probe and in turn measures the effect of the eddy-current-induced magnetic field which opposes the inducing current. Such a test arrangement is shown in Fig. 4. Long probes of the type illustrated are capable of measuring the fuel channel in our longest element. Rapid measurements can be made on a go-no-go basis with the high and low limits set to correspond to the required specifications. These limits are set by use of accurately machined test blocks. It is also conceivable that the indicated response could be converted to a recorder for automated scanning. To date our work involving these measurements has been confined primarily to static measurements. Channel-spacing measurements, using this system under dynamic conditions (flowing water at temperatures up to 200°C), have not been successful because of probe failure.

4.2. Cladding and coating thickness

Using the same instrument described in the preceding section, but with a commercially manufactured probe shown in the insert to Fig. 4, measurements are made of aluminium cladding over uranium fuel cores and of anodized coatings on aluminium. An interesting evolution of the anodized coating measurements, however, came about when it was observed that these coatings under reactor test conditions underwent considerable change – both increasing in thickness and spalling (film stripping). To measure these changes a Dermitron probe was set up in the hot cell and connected to the instrument outside the cell through long lead wires emerging through a hot-cell plug. Very accurate measurements were then taken over the entire surface of the plate. The measurements so obtained have been verified through extensive dimensional measurements before and after stripping and by metallography.

These measurements are also adaptable to corrosion determinations. Eddy-current measurements of corrosion film, by means of the Dermitron instrument, on fuel samples being tested for the ATR were an outstanding success.

4.3. Temper determination in aluminium

Preliminary work has indicated another potentially important application of the eddy-current technique for non-destructive testing of metal alloy temper. Fuel specifications for the test reactors call for cold-worked fuel plates and solution heat-treated and artificially aged (T6) side plates. Because of the structure and thinness of the plates, it is almost impossible to obtain good hardness measurements by superficial testers to check on the condition of these items once assembled. The electrical conductivity of these materials is dependent on the temper (and alloy composition) and, therefore, should be amenable to eddy-current measurements. By use of

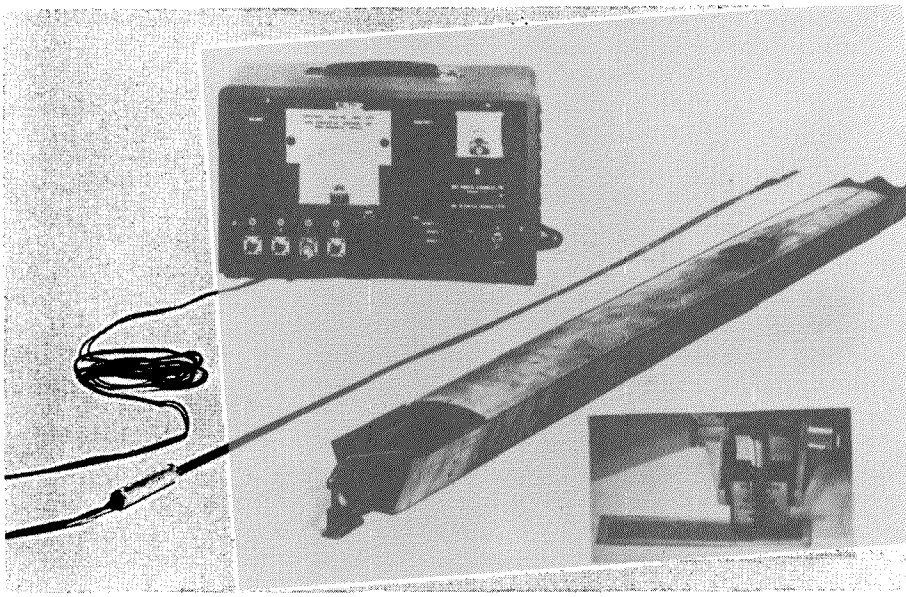

Fig. 4

Eddy-current inspection of fuel-element channels and coating thickness

a suitable 6061-T6 aluminium standard, several fuel-element side plates have been measured with the Dermitron. Good correlations have been obtained in this manner. Obviously this technique has a potentially much wider application and further work along these lines is in progress.

5. CRITICAL FACILITIES FOR NON-DESTRUCTIVE TESTING

5.1. Advanced reactivity-measurement facilities (ARMF-I and ARMF-II)

ARMF-I and ARMF-II [4] are nearly identical critical facilities and are used almost exclusively for measuring reactor physics parameters, such as reactor-spectrum cross-sections and resonance integral cross-sections. These facilities are swimming-pool-type reactors having light-water-moderated cores made up of plate-type fuel elements containing fully-enriched U^{235}.

One ARMF ability, which is somewhat unique and highly beneficial, is that of non-destructively determining the macroscopic cross-sections (or quantity) of both fuels and poisons combined in a single sample. Measurements of this nature have been conducted to determine the U^{235} and boron content of ETR fuel-element core-alloy samples [5, 6] and to determine fuel and boron burnup after high-flux irradiations in a fuel-element development programme [7].

Simultaneous assaying of fuels and poisons in a single sample is possible because the ARMF-I loading is arranged so that it contains several experi-

mental positions (see Fig. 5) in which the relative importance of fission and thermal neutrons are markedly different. Determination of the fuel and poison content of a specimen is accomplished by measuring it in two of these positions. For each position the reactivity effect of the specimen can be written in a simplified form as follows:

$$P_i = W_{fi}\,\Sigma_f + W_{pi}\,\Sigma_p$$

where W_f and W_p are the weighting functions for fuel and poison, Σ_f and Σ_p the macroscopic cross-sections for fuel and poison present in the sample, and i identifies the experimental position. A simultaneous solution of the equations for measurements made in the two positions yields the values of Σ_f and Σ_p which in turn can be converted to mass of fuel and boron, or boron equivalence if the poison is other than boron.

The weighting functions used in the equation are determined experimentally. For small quantities (approximately 2 cm^2) of materials this is straight forward and can be accomplished with a small number of calibrating samples because the reactivity response is nearly a linear function of material content. However, for larger quantities the calibration becomes more complex because particle self-shielding and neutron-flux-perturbation effects are experienced. Of significance, is the fact that the weighting function of one material is dependent on the quantity of the other material. It is conceivable that the accurate assaying of specimens with widely diverse quantities of fuels and poisons would require calibrating standards with one hundred different combinations of fuels and poisons. Some work [8] has been done to attain analytical expressions which describe the interacting effects. When completed this work should minimize the number of calibrating standards required.

Because the ARMF is a precision instrument (error for a single 4.5-min measurement is 10^{-7} $\Delta k/k$), the accuracy of an assay measurement is principally limited by the accuracy of the calibrating standards but is capable of assays accurate to better than a milligram of each material.

5.2. Engineering Test Reactor Critical-Facility boron determination

Beginning with the first fuel elements fabricated for the ETR, considerable difficulty has been encountered by all fabricators in controlling the amount of boron included in the elements. Consequently, it has been necessary to assay the elements for boron to maintain reactivity control of ETR core loadings. All boron assaying has been done in the ETR Critical Facility (ETRC) [9]. The ETRC is a low-power, swimming-pool-type reactor, which is a full-scale nuclear duplicate of the core and reflector of its parent reactor, the ETR.

Assuming that the U^{235} content is the same in all elements the boron content of an element can be determined from its reactivity worth relative to elements with known boron contents. The relative reactivity worths are determined from the position of a shim rod which is manually adjusted to make the reactor critical. The calibration is accomplished by plotting a curve of shim position versus fuel-element boron-content from data obtained

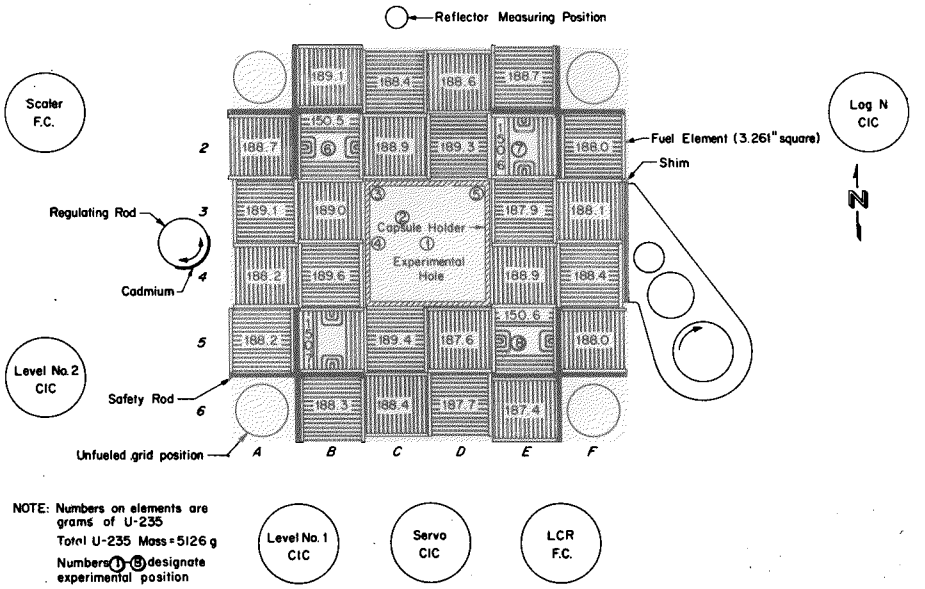

Fig. 5

ARMF-I core loading (2-26)

in measurements on fuel-element standards containing known amounts of boron. These standards consist of unborated elements with boron-impregnated polyethylene tape distributed uniformly in their coolant channels.

Because the shim and safety rods need to be inserted each time to ensure reactor safety, the time required to make a measurement is 30 min. This is equivalent to a cost of $ 50. Although this cost is high no other less expensive method has proved satisfactory.

There are a number of factors which affect the accuracy of boron-content assays. The method does not permit an absolute determination if the boron is segregated such that particle self-shielding exists. With segregation, which tends to be the case with the alloying technique of fabrication, the critical facility assay gives only an effective boron content. This proves to be an advantage, however, when the assay is to be used in conjunction with reactivity control of ETR fuel loadings. Systematic errors, which can arise from the boron in the tapes not being equivalent to the boron in the fuel plates, are avoided or corrected through careful distribution of the tapes and disadvantage factor corrections (3%). Sources of error which are random and cannot be corrected arise from uncertainties in U^{235} contents and non-reproducibility of shim-rod position at criticality. Because U^{235} uncertainties are only ± 2 g and its weighting function (expressed in grams) is only 1/50 that of boron, the U^{235} uncertainty contributes a small error to the boron assay. This error combined with shim-rod non-reproducibility yields a net error of ± 0.1 g for boron assaying in the ETRC. ETRC measurements of boron fuel elements have resulted in vendor penalties on about 40% of the ETR elements received.

6. HYDRAULIC TESTS

A statistical sampling plan is used to select representative fuel elements from each batch of elements received from the vendor. These elements are hydraulically tested, one at a time, in a facility capable of producing flow rates of 140% of the normal reactor operating flow rate through a fuel element (Fig. 6A). This 140% test effectively doubles the pressure differentials acting on the various areas of the element. An analysis of fuel-element-failure distribution provides the assurance that an element which successfully passes such a flow test has a probability of failure in the reactor of 0.000. The hydraulic test helps to establish the maximum operating limits for new elements or modifications to existing elements and thus in turn to establish adequate acceptance test criteria. In addition, it has proved a sensitive test to disclose poorly assembled elements, especially in the strength of the fuel plate-side plate joint. Examples of failed elements due to faulty brazing and roll-swaging are shown in Fig. 6B and C. In the past

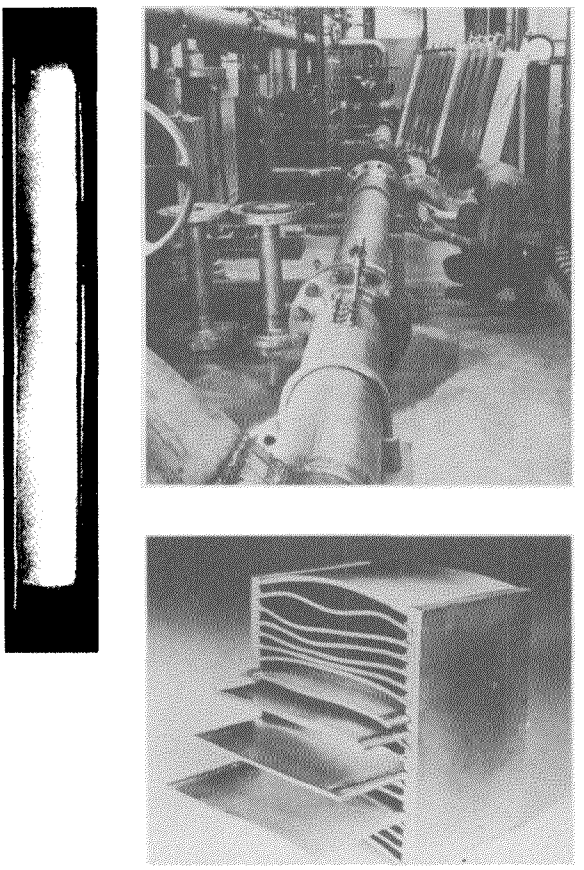

Fig. 6

Hydraulic test facility and examples of failed elements

three years of this type of testing, 2595 MTR and ETR elements have been received of which 421 have been hydraulically tested; 18 have failed. Since the cause of failure was poor swaging of fuel plates into the side plates, the vendor was required to make restitution. This penalty clause is now a standard part of all MTR and ETR fuel specifications.

7. OTHER NON-DESTRUCTIVE TESTS

Several other tests are routinely used to ensure that irradiation samples as well as reactor fuel plates are safe for use.

All aluminium-clad reactor fuel-element plates and irradiation specimens are blister-tested by heating for one hour at 500°C. Irradiation samples and welds have been inspected by the well-known liquid-penetrant inspection procedures. Liquid-nitrogen leak-testing is frequently used for inspecting irradiation specimens before insertion into the reactor. In this procedure [10] the samples are immersed in a bath of liquid nitrogen until the bubbling of the nitrogen has stopped. The sample is then quickly transferred to a bath of alcohol. Bubbles of nitrogen gas streaming from the test piece indicate imperfections.

REFERENCES

[1] BASKEY, R.H., Fuel Bearing Fiberglas in Aluminium-Base Fuel Elements Final Report, TID-16847, June (1962).

[2] BABCOCK, R.V. and RUBY, S.L., Phase II Nuclear Materials Control System. The Fuel Assay Scanner, "A Device for the Non-Destructive Assay of Highly Enriched Fuel Elements", WCAP-6039, February 1 (1960).

[3] DODD, C.V., Design and Construction of Eddy-Current Coolant-Channel Spacing Probes, ORNL-3580, April. (1964).

[4] BURDICK, E.E., Fast, E. and KNIGHT, D.W., The Advanced Reactivity Measurement Facilities, IDO-17005, October (1964).

[5] FAST, E. et al., "Use of the RMF for Non-destructive Assay of Fuel-Bearing Samples", Reactor Fuel Measurement Techniques Symposium, TID-7560, June 18-20 (1958) 139-152.

[6] KNIGHT, D.W. and FAST, E., "Simultaneous Nondestructive Analysis of Engineering Test Reactor Core Samples for Boron and U-235 in the Reactivity Measurement Facility", Trans. Amer. nucl. Soc. 1 No. 1, June (1958) 38.

[7] GIBSON, G.W. and FRANCIS, W.C., Annual Progress Report on Fuel Element Development, IDO-16799, August (1962) 81.

[8] MILLSAP, D.A. and NISLE, R.G., "Analysis of Reactivity Measurements", MTR-ETR Technical Branches Quarterly Report, IDO-16977, October 1-December 31 (1963) 14-18.

[9] De BOISBLAND, D.R. et al., The Engineering Test Reactor Critical Facility Hazards Summary Report, IDO-16332, March (1957).

[10] WATSON, M.B., "The Assembly and Testing of Experimental Fuel Elements for Irradiation Testing", Chalk River, Ontario, AECL-1288, April (1961).

DISCUSSION

J. GÉRARD: In gamma counting on complete elements do you interpolate the results linearly with respect to one standard, or do you use several standards to plot a curve?

W. FRANCIS: We use standards bracketing the desired value and interpolate between them. There are, of course, different standards for MTR, ETR and ATR. Arriving at these standards is quite an elaborate process: many plates are scanned, one is selected, and many are dissolved chemically to establish the true uranium content versus the scan count. Plates are then built up in a loose-leaf array to establish the fuel content of the assembly.

J. GERARD: In ultrasonic inspection of plates for ETR elements, what is the actual dimension of the unacceptable defect?

W. FRANCIS: We can "see" a 0.0625-in defect and we specify that any defects of this size, or larger, should entail rejection

D. HORVAT: You mentioned that the range of light transmission through plate radiographs should not exceed 10% of the average for all core locations of any plate. Do you not think that is a dangerous specification, because the density differences in the plate radiographs depend on various factors such as the gradation of the emulsion, the energy of the radiation applied, the ratio of primary to secondary radiation, etc? I very much doubt whether these parameters would be held constant, even with very strict definitions of the technique to be used.

W. FRANCIS: Yes, I agree. We carefully specify film type and exposure, yet we find variation over the radiograph which does not represent a difference in fuel content. By scanning the radiograph across the short dimension and using a statistical approach for the difference in density (maximum minus minimum) we obtain a corresponding difference in fuel content – not absolute values.

A. VAN DER LINDE: What is the measuring range and accuracy of the Dermitron instrument you used for measuring the coating and corrosion film thickness on aluminium-clad fuel plates?

W. FRANCIS: The accuracy of measurement is about 10% of the coating thickness i.e. 0.2 to 0.3 mil in the range of 2.0 to 3.0 mil. For very thin corrosion films, of course, the accuracy is not so good.

P. KNUDSEN: Your paper describes various kinds of inspection of plate elements. Are these tests performed by the fuel-element vendor, or do you perform them yourselves at the cost of the vendor?

W. FRANCIS: I believe all the tests I have described are performed by us at the National Reactor Testing Station. Generally, we specify acceptance criteria but do not say how the vendor shall meet them. For example, most vendors do not have fuel scanners or ultrasonic equipment. However, for ATR fuel we are specifying an ultrasonic test by the vendor.

I. PURICA: I have two questions on the method you use with the Advanced Reactivity Measurement Facility. Firstly, do you only use the danger coefficient method, that is reactivity measurements, or do you also use the oscillation method?

W. FRANCIS: Just the reactivity measurements. At one time we considered using a pile oscillator, or more precisely a sample oscillator, but this has not been found necessary. The accuracy of 10^{-7} is perfectly acceptable for our work.

I. PURICA: What is the sensitivity of the method you use to separate the effects of fuel and absorbent? In other words, what are the minimum

amounts of fuel and absorbent that you can measure with the reported sensitivity of 10^{-7} for reactivity measurements?

W. FRANCIS: Perhaps I can answer that best by saying that for the ARMF we consider that the poison statistical weight is 2.8×10^{-2} δk/k per gram of natural boron. The equivalent number for U^{235} is 6.36×10^{-4}.

Z. PAWŁOWSKI: Your paper states that by means of ultrasonics it was not only possible to detect the soundness of the finished plate but also to determine whether the forming operation is causing "brittle cracking". Are you thinking of detection of fine cracks caused by the forming operation or do you mean that you can predict the tendency of the material to brittle fracture? If so, what testing technique did you use?

W. FRANCIS: As higher fuel loadings and reactors of higher power density come into use, we become more concerned about the brittleness of the core material. Originally, this was not a problem but it becomes one with the use of cermet cores. It is, therefore, not sufficient to scan the flat plate ultrasonically after rolling; it is necessary to examine the plate after forming to the required curvature. This technique is really a final acceptance test. If we found that cracking was occurring we would initiate a development programme and use other means, such as bend tests and "pre-post irradiation" examinations, to determine the nature of the brittleness.

THE DEVELOPMENT OF FLAW-DETECTION TECHNIQUES AT HARWELL

R. S. SHARPE
METALLURGY DIVISION,
UKAEA RESEARCH GROUP,
ATOMIC ENERGY RESEARCH ESTABLISHMENT,
HARWELL, UNITED KINGDOM

Abstract — Résumé — Аннотация — Resumen

THE DEVELOPMENT OF FLAW-DETECTION TECHNIQUES AT HARWELL. In the context of materials inspection a flaw demands a definitive interpretation. It should be taken to signify any structural deviation that can impair or modify the performance of a component. With this reference point established the significance and scope of the subject can be more perspectively portrayed. This paper draws on Harwell experience to emphasize the value and importance of a strong research and development programme in support of materials inspection in the nuclear-power industry.

New and improved non-destructive testing techniques are continually being demanded. They are essential to ensure the maintenance of quality and conformity in production components and they can also usefully be introduced to provide data to assist in design and development. At an earlier stage they are called upon to assist in categorizing and standardizing materials, and to ensure material uniformity in irradiation experiments. During laboratory research they can be designed to monitor physical properties so that structural variables likely to affect the service performance of nuclear components can be more precisely evaluated.

In the field of radiography, attention at Harwell recently has been directed towards high-speed techniques, methods of dealing with highly active components and X-ray microscopy. Panoramic radiography, projection fluoroscopy, and a radiopaque penetrant technique have been developed to meet the particular needs of reactor components.

The characteristics of an image converter system for radiography are described and the results of applying a novel design of ultrasonic converter tube to fuel-plate bond evaluation are illustrated. Other ultrasonic techniques described have been developed for detecting structural and dimensional flaws in thin-walled fuel sheathing.

It is shown how emphasis has been placed on improving inspection techniques by concentrating attention on data presentation. Facsimile recording of test signals has been widely applied to ultrasonic and eddy-current methods of inspection. By a novel form of signal processing (quantizing) it is shown how these recordings have been made considerably more informative.

DÉVELOPPEMENT DES MÉTHODES DE DÉTECTION DES DÉFAUTS A HARWELL. Dans le contrôle des matériaux, tout défaut décelé doit être interprété de façon sûre. Il faut considérer que l'on se trouve en présence d'un défaut lorsqu'il y a modification structurelle de nature à réduire ou altérer les performances d'une pièce. Sur la base de cette définition, on peut mieux délimiter la signification et la nature du problème. Se fondant sur l'expérience acquise à Harwell, l'auteur met en évidence la valeur et l'importance d'un programme rigoureux de recherche et de développement pour le contrôle des matériaux dans l'industrie nucléaire.

Il faut sans cesse créer des méthodes plus perfectionnées d'essais non destructifs. Elles sont indispensables pour assurer le maintien de la qualité et de la conformité des pièces fabriquées et elles peuvent également être utiles pour fournir des données aux bureaux d'études. A un stade préliminaire, elles servent à classer et à normaliser les matériaux et à assurer l'uniformité des matières dans les expériences d'irradiation. Dans la recherche en laboratoire, elles peuvent servir à contrôler les propriétés physiques, ce qui permettra d'évaluer avec davantage de précision les variables structurelles pouvant affecter les performances des pièces.

En matière de radiographie, on s'est récemment attaché à Harwell aux méthodes à grande vitesse d'exécution, aux méthodes de contrôle des matières fortement radioactives et à la microscopie aux rayons X. Pour résoudre les problèmes particuliers que posent les pièces de réacteur, on a mis au point des méthodes de radiographie panoramique, de fluoroscopie par projection et de pénétration de fluides radio-opaques.

Le mémoire décrit les caractéristiques d'un convertisseur d'image pour la radiographie et expose les résultats obtenus avec un type nouveau de convertisseur ultrasonore dans l'évaluation de la liaison des plaques

de combustible. D'autres méthodes ultrasonores, décrites dans le mémoire, ont été mises au point pour déceler des défauts structurels et dimensionnels dans des gaines de combustible à paroi mince.

Le mémoire montre comment on s'est attaché à perfectionner les méthodes de contrôle en accordant la plus grande attention à la présentation des données. L'enregistrement fac-similaire des signaux a été largement utilisé dans les méthodes de contrôle par les ultrasons et les courants de Foucault. Grâce à une forme nouvelle de traitement des signaux (quantification), les enregistrements donnent des informations très supérieures.

РАЗРАБОТКА МЕТОДОВ ДЕФЕКТОСКОПИИ В ХАРУЭЛЛЕ. В связи с проверкой материалов требуется дать определенное объяснение тому или иному дефекту. Это объяснение необходимо для оценки любого структурного отклонения, которое может ухудшить или изменить рабочую характеристику компонента. Только с учетом этого можно с большей перспективой определить значение и рамки данного вопроса. В публикуемой работе используется опыт Харуэлла для того, чтобы подчеркнуть значение, которое имеет эффективная программа исследований и разработок для проверки материалов в атомной энергетике.

Существует постоянная необходимость в новых и усовершенствованных методах недеструктивных испытаний. Они нужны для обеспечения качества и соответствия компонентов продукции и могут также найти полезное применение для получения данных, которые содействуют решению вопросов, связанных с конструкцией и разработками. На более ранней стадии они должны содействовать распределению материалов по категориям и их стандартизации, а также обеспечить однородность материалов в экспериментах по облучению. Во время лабораторных исследований они могут служить для измерения физических свойств, так что структурные переменные, которые, вероятно, повлияют на эксплуатационные качества ядерных компонентов, можно будет оценить с большей точностью.

В Харуэлле недавно стали уделять внимание быстродействующим методам, методам, связанным с высокоактивными компонентами и рентгеновской микроскопией. Были разработаны панорамная радиография, проекционная флуороскопия и метод проникновения жидкости, непроницаемой для излучения, в целях удовлетворения определенных требований, предъявляемых к реакторным компонентам.

Дается характеристика электронно-оптического преобразователя для радиографии и иллюстрируются результаты применения новой конструкции ультразвукового преобразователя к оценке сцепления сердечника с оболочкой. Другие описанные ультразвуковые методы разработаны для обнаружения структурных дефектов и отклонений размеров в тонких топливных оболочках.

Показывается, каким образом был сделан упор на улучшение методов проверки за счет того, что главное внимание уделялось представлению данных. Точная запись изображений сигналов испытаний широко применялась к проверке методами ультразвука и вихревых токов. С помощью нового вида обработки сигналов (квантование) показывается, каким образом в этих записях содержится значительно больше информации.

TECNICAS DE DETECCION DE FALLAS DESARROLLADAS EN HARWELL. En la inspección de materiales, toda falla exige una interpretación definitiva; debe considerarse falla toda desviación estructural capaz de menoscabar o modificar el comportamiento de un componente de reactor. Establecido este criterio de referencia, es posible definir con mayor objetividad la significación y el alcance del tema.

La presente memoria se basa en la experiencia adquirida en Harwell para subrayar el valor y la importancia de un programa intenso de investigación y desarrollo que sirva de base a la inspección de materiales en la industria de la energía nuclear.

Existe una demanda continua de nuevas y mejores técnicas de ensayo no destructivo. Estas técnicas son esenciales para mantener la calidad y uniformidad de los componentes, siendo también posible uttilizarlas con provecho para reunir datos útiles en los trabajos de proyecto y desarrollo. En una etapa anterior, esas técnicas pueden contribuir a la clasificación y normalización de materiales, como también a asegurar la uniformidad del material en experimentos de irradiación. Durante las investigaciones de laboratorio, se las puede aplicar para medir propiedades físicas y de esa manera evaluar con precisión las variables estructurales susceptibles de ejercer influencia sobre el comportamiento de los componentes nucleares en servicio.

En la estera de la radiografía, durante los últimos tiempos se ha prestado atención en Harwell a las técnicas de alta velocidad, al manejo de componentes muy radiactivos, y a la microscopía con rayos X. Para satisfacer las necesidades particulares en materia de componentes de reactores, se han desarrollado métodos de radiografía panorámica, fluoroscopía por proyección y una técnica con agentes penetrantes radiopacos.

Se describen las características de un sistema convertidor de imágenes para radiografía y se ilustran los resultados obtenidos al aplicar un nuevo diseño de tubo convertidor ultrasónico a la evaluación de la unión

entre placas de combustible. Otras técnicas ultrasónicas descritas en el presente trabajo se han desarrollado para descubrir defectos estructurales y dimensionales en vainas de pared delgada.

El autor hace hincapié en el mejoramiento de las técnicas de inspección y dedica especial atención a la presentación de los datos. El registro facsimilar de señales de ensayo se ha aplicado ampliamente a los métodos clásicos de inspección por ondas ultrasónicas y corrientes de Foucault. Mediante una nueva forma de sistematización de la señal (« cuantización ») se pone de manifiesto la información considerablemente mayor contenida en estos registros.

1. INTRODUCTION

A section of the Metallurgy Division at Harwell is devoted to development work in non-destructive testing. The bias of the work is closely aligned to the inspection requirements of the United Kingdom Atomic Energy Authority (U.K.A.E.A.) reactor programme. However, since Harwell is in the Authority's Research Group, emphasis is placed on the study and understanding of basic physical principles, on the assessment of new ideas, new instruments and new techniques and on the development of inspection procedures to anticipate possible future Authority requirements.

The purpose of this paper is to review progress made in this Section at Harwell in recent years and show how the various facets of the programme fit into a logical pattern when the scope of flaw detection is realistically defined. A list of references at the end of the paper covers the published work of the Section.

2. THE SCOPE OF FLAW DETECTION

In any industry, the overriding purpose of introducing non-destructive tests is to ensure that each and every component has achieved a certain standard of quality, so that they will perform satisfactorily over the period of service, and under the conditions of service, for which they were designed. The level of confidence written into the specification will depend, in a complex way, on such factors as the consequences of premature failure, the design factors-of-safety, manufacturing economics and commercial prestige. A very high level of confidence has been demanded for the nuclear-power industry and this has led to the development of more sensitive and more selective tests than are generally considered necessary in other industries.

Structural variations or defects of one sort or another may be introduced at various stages during component fabrication. Any variation, or defect, that will impair service performance constitutes a flaw in the context of quality inspection and the ability to detect flaws of one kind or another is the common factor demanded of all non-destructive tests. The majority of interest is generally directed towards dimensional flaws (metrology) and the more obvious structural flaws (crack detection). The fact is sometimes overlooked that the more insidious variations in microstructure that can occur may also constitute flaws of comparable significance under particular conditions of service.

There are three reasonably distinct stages in fuel-element manufacture where flaws-detection techniques need to be applied if the fullest use is to be made of non-destructive testing procedures.

(a) In the laboratory, the techniques can be incorporated into programmes of materials research to complement those that required destructive means to prepare suitable specimens. For example, in the examination of coated fuel particles, non-destructive X-ray microscopy is providing the type of structural information that tends to be destroyed or masked during surface preparation for optical microscopy.

Non-destructive methods of studying microstructural uniformity are still generally regarded as laboratory techniques. Elastic-wave propagation is the basis for a wide range of such techniques. Attenuation is influenced by a number of microstructural features such as grain-size distribution, porosity and dislocation loop length, whilst velocity measurements can be used to monitor elastic constants, preferred orientation and internal stress. By means of such techniques potential flaws, arising from structural heterogeneity, can be pin-pointed at a very early stage in fuel-element design. Being non-destructive, sequential studies can be made on the same sample so that the tests can, if necessary, be extended to include a progressive study of irradiation behaviour.

(b) In the development and pre-production stages, flaw-detection techniques can help to categorize materials and compare equivalent or competitive products. The data can be used to feed information back to manufacturers concerning any material or structural non-uniformity. This can usually provide a basis for improving the final product. For product assessment in this way to be effective, maximum information is required from the tests, calling for particular emphasis to be placed on data recording and information analysis. These detailed, and often painstaking, studies (closely supported by destructive tests) are also required to classify defects likely to occur in a given product so that more objective decisions can be taken on flaw levels and specifications. These preliminary investigations can then be used to design and set up suitable inspection procedures to cope with the subsequent production requirements. It is to these particular aspects of flaw detection that many of the Harwell programmes are primarily directed.

(c) The third field of application of flaw detection is the production inspection of components. This calls for carefully engineered installations, test simplicity, clear and simple data presentation and complete unambiguity in flaw interpretation. In general, this application to full-scale production is beyond the terms of reference of the Harwell N.D.T. (non-destructive testing) programme and is not discussed in this paper. The allied problems of post-irradiation component inspection have received some attention at Harwell. The aim here is to devise procedures to duplicate, where necessary, production inspection techniques so that material deterioration and the behaviour of "defects" can be directly studied after reactor service.

Looking forward, there is a further objective in any industry where automated production methods are envisaged. Instead of using non-destructive testing in a purely passive role to detect flaws and reject scrap, the techniques should be designed as monitoring procedures at a point in the production line where corrective action can be automatically initiated to avoid scrap. For example, the continuous non-destructive monitoring of microstructures might be developed to control heat treatments in the same way that feed-back from radiation thickness gauges is being used to control roll pressures in sheet production.

In defining the scope and objectives of non-destructive testing it is easy to foster an impression that it has blossomed into a subject standing in its own right. It should not, of course, be considered in isolation in this way and in order to develop fully must be recognized and accepted as a conjunctive theme to the over-all plattern of component design development and production [1, 2, 3].

3. TECHNIQUES BASED ON X-RAYS AND γ-RAYS

The attenuation of photon radiation by electron interaction in passing through materials has led to the widespread use of radiography to detect flaws. Techniques have been developed to pin-point cracks and porosity, locate regions of non-homogeneous distribution in multi-phase systems and measure internal dimensions non-destructively. Work at Harwell has been directed to various problems of this type with the underlying aims of improving the range of applications, sensitivity, resolution and radiographic contrast. The special problems presented by post-irradiation radiography have also led to a variety of methods for discriminating against high levels of ambient gamma radiation that would otherwise tend to mask the image detail.

3. 1. High definition radiography

A number of factors contribute to the unsharpness of a radiographic image. The predominant factor with conventional X-ray equipment is usually the penumbra attributable to the finite size of the X-ray focal spot. By focusing the electron beam before it impinges on the anode an X-ray microscope design has been perfected and equipment is now commercially available[1] with a focal spot size as small as 1 μm. With a thin-foil transmission anode the sample can be brought very close to the source of X-rays and, by a combination of image projection and subsequent photographic enlargement, magnifications are possible to make the fullest use of a resolution down to 1 μm [4].

Applications to which the X-ray microscope has been put at Harwell include the examination of coated nuclear-fuel particles, the distribution of the fissile constituent in fuel plates, the study of micro-cavitation in fuel cans and a comparison of pore-size distributions in reactor graphites. The fact that the microradiographic image is obtained by projection has enabled post-irradiation studies of fuel particles to be made and hot-stage sequential studies of the progression of catalytic oxidation in graphite [5, 6, 8].

When single-crystal specimens are examined in the same way Kossel line diffraction conics are superimposed on the microradiograph. These can be indexed in terms of lattice planes and used to determine accurate unit-cell dimensions [7].

In the present equipment up to 1 W is dissipated in the 2-μm-thick metal-foil target, corresponding to a focal spot loading of 10-100 kW/mm² at the

[1] XM30 X-ray Microscope, Hilger & Watts Ltd. (EPI Sales Division).

surface. A modified design of micro-focus X-ray source is now under test at Harwell with a solid reflection target capable of dissipating 15 W on a slightly degraded focal spot[2]. The uprated output of this equipment opens up a completely new field of conventional radiography where the highest definition and resolution are required without the need for the high magnification necessary for microstructural observation. The target assembly is rotatable in vacuum and is constructed of different metals so that a range of monochromatic radiations is available for analysing constitutent elements in alloy specimens by a differential absorption technique.

3.2. Direct-view X-ray techniques

When a permanent photographic record is not essential; when production-line film radiography is uneconomic, or when a moving subject needs to be examined radiographically, direct-image viewing techniques are an attractive alternative.

Images can be viewed directly on a fluorescent screen although the image unsharpness is greater than with film recording because of the finite size of the fluorescent crystals and the diffuse spreading of the fluorescent light. By using an X-ray equipment with an 0.2-mm focal spot a projection fluoroscopic technique has been developed capable of resolving 80-mesh brass gauze [10]. This equipment was engineered at Harwell to provide an inspection procedure for locating cores in M.T.R. fuel plates to a positional accuracy of ± 0.02 in.

More recently, solid-state electro-luminescent screens have been made available[3] which retain a useful fluorescent image for about 15 min, with slowly decaying intensity. This provides a cheap alternative to film radiography for detecting the alignment and positioning of internal components and leads in rigs and assemblies [2].

Direct viewing by the use of an electronic image converter largely overcomes the limitation set by fluorescent screen unsharpness. The system being investigated at Harwell uses a selenium-layer image-converter tube that is now commercially available[4]. The high inherent definition and the image magnification with the TV monitor presentation makes the system ideally suited to applications such as the inspection of fuel-element end-welds. The converter tube requires radiation dose-rates of 200-400 r/min at the tube face to produce sufficient image contrast. This unfortunately limits the range of application of the technique by restricting the materials and section thickness that can be examined [2]. A method of increasing the effective contrast by introducing circuitry to quantize the video signal is currently being examined and this might be expected to overcome some of the present difficulties. Penumbral unsharpness is also a problem because of the small focus-to-sample distances that are required to obtain an adequate radiation dose-rate at the sensitive face plate of the converter tube. Initial tests, however, indicate that the output of the uprated X-ray microscope previously

---

[2] Variable Target XM30 Unit. Hilger & Watts Ltd. (EPI Sales Division).

[3] Thorn Electrical Industries Ltd. Enfield, Middlesex.

[4] Dynamicon ML589. The Machlett Laboratories Inc. Stamford, Conn.

referred to (section 3.1) is sufficient to operate the converter tube. The specimen can then be brought up very close to the X-ray source without introducing any detectable unsharpness.

3.3 Quantitative radiography

Interpreting data from radiographs is usually limited to a visual appraisal of detail, using the image of a stepped or wire image-quality indicator as a reference standard. The attenuation processes in materials, however, are sufficiently well defined to warrant a more detailed analysis of radiographic density in terms of structural homogeneity. A particularly relevant application of this quantitative approach is the use of transmission radiography to check the uniformity of fuel loading in the cores of nuclear-fuel plates.

The technique of scintillography has been developed at Harwell in which a facsimile record of the isodose contours of radiation transmitted through a fuel plate are obtained. The scanning beam is a 2-mm narrowly collimated pencil of radiation from an Am^{241} source which is mechanically scanned over the whole surface of the plate [14, 15].

By virtue of the attenuation processes the transmitted radiation contains essential information concerning the point-by-point variation in the uranium loading of the core. The radiation is collected in a scintillation counter linked to the source-scanning mechanism. To facilitate data analysis the integrated count-rate is quantized into predetermined levels which are presented on a facsimile recorder in discrete shades of grey. By suitable calibration the quantized levels can be directly linked to the tolerance levels of uranium content defined in the fuel-plate specification.

This radiation-scanning technique is not likely to improve the radiographic detection of discrete structural defects such as cracks or weld porosity. However, it extends the range of radiography into areas of inspection that are beyond what is normally considered to be the scope of film recording.

3.4. Contrast enhancing techniques

Two inspection problems have arisen where straight-forward radiography provides insufficient contrast to reveal adequate detail.

In the first case, the heterogeneous nature of 1-in-square graphite struts gave a radiographic background pattern in which it was difficult to detect fine cracks. Carbon tetrachloride was found to be a very suitable liquid to use as a radiopaque penetrant. By dipping the graphite struts into the liquid for a few seconds immediately before radiography, preferential absorption into cracks opening to the surface greatly increased the radiographic contrast [13]. The carbon tetrachloride evaporates away completely after the exposure and has no deleterious effect on the graphite. The absorption coefficient of carbon tetrachloride also makes it a suitable radiopaque penetrant for beryllium, beryllia and magnesium samples and it has been shown that it can successfully be used to accentuate detail and study surface profiles in thin microradiographic samples [18].

In the second case, the inspection of graphite-compacted coated fuel particles for layered segregation in HTR fuel sleeves presented problems of image superposition when radiographed in the normal way across a diameter. By threading the fuel sleeves on to cylindrical cassettes and rotating them over narrow slits in a lead mask, through which the X-rays pass, single-tube panoramic radiographs of the fuel tubes were obtained. This greatly enhanced contrast and enabled the uniformity of fuel loading to be assessed without difficulty and provided the basis for a production-inspection procedure [12].

3.5. Post-irradiation radiography

The main problem with in-cell radiography of active specimens is that of overcoming autoradiation blackening of the recording film. Work in this field at Harwell originally stemmed from the requirement in 1949 to inspect the profiles of uranium fuel bars from the BEPO reactor to detect distortion and growth. The technique developed used lead shutters and a lead masking strip to reduce the level of background radiation.

When the emphasis changed to the radiography of active irradiation rigs, their construction and more highly concentrated activities led to the development of a panoramic technique in which the rig and film were synchronously moved in parallel paths on opposite sides of a 9-in lead shielding block. The block had a central 2-mm slit in it through which the X-rays were directed to produce the radiographic image [11].

Use can be made of the energy dependence of film emulsions to discriminate to a certain extent against the higher energy background gamma radiation. The spectral sensitivity of a wide range of emulsions has been determined at Harwell and in one case (an experimental Kodak emulsion V6035) the sensitivity to 100-kVcp X-rays was found to be 100 times greater than that to Co^{60} γ-rays [17]. With this emulsion test radiographs have been obtained when the superimposed background gamma radiation dose at the film was as high as 400 r. This implies that, with simple projection, a suitable choice of emulsions and perhaps some form of image recovery after processing a very wide range of active specimens can be radiographed without the need for complex installations.

Electronic methods of energy discrimination using pulse-height analysis has also been used to differentiate between high-energy background radiation and the lower-energy radiation used for the radiographic exposure. A practical system of building up a panoramic radiograph with a scanning scintillation counter has already been referred to (section 3.3) and with this equipment an X-ray scintillograph has been obtained of an encapsulated Ir^{192} source using a single-channel analyser to process the counts and, in this way, to reject the radiation emitted by the iridium source [15].

Fine-focus field emission X-ray tubes are now commercially available[5] and experiments are being conducted with them at Harwell with a view to developing a radiographic technique for extremely active specimens where

[5] Fexitron X-ray equipment. Field Emission Corporation. McMinnville, Ore, United States of America.

other methods are inadequate [16]. It is necessary to use salt intensifying screens with the films because of the comparatively low X-ray dose from each pulse and the salt-screen/film combination will tolerate only a low dose of background radiation. Since, however, the exposures are made in 0.05-0.1 μs, the film or object may be moving at high speed during the exposure. In this way, the background dose at the film can be kept very small during an exposure.

4. ULTRASONIC AND EDDY-CURRENT TECHNIQUES

Ultrasonic and eddy-current methods of inspection can complement radiography in detecting flaws [28]. Ultrasonic energy suffers less attenuation than X-rays and consequently, far thicker sections of metals can be examined. In addition, both ultrasonic and eddy-current techniques are sensitive to the finer types of crack and laminations that are not readily detected by X-rays. However, as generally applied, the presentation of the information is less direct than with radiography and interpretation of test signals is open to greater ambiguity. Consequently much of the Harwell effort has been directed towards methods of improving data presentation so as to provide a basis for more reliable and more informative inspection techniques. As well as their ability to detect the discontinuity type of flaw, both ultrasonic and eddy-current techniques can be designed to monitor a number of microstructural deviations which are also liable to constitute a flaw. Work along these lines is in progress although this is an aspect of flaw detection where there is considerable potential for further development.

4.1. Tube inspection

In a pre-production assessment of reactor-grade tubing for fuel-element sheathing the inadequacies of eddy-current testing became apparent [23]. Because of interference from high background signals caused by slight variations in wall thickness, the technique failed to detect fine surface cracks and, in addition, tended to reject tubing unnecessarily. Ultrasonic flaw-detection techniques were found to be more sensitive and more selective, although at the expense of speed of inspection. It was also shown that the use of artificial flaws as calibration standards for the ultrasonic test were not a satisfactory compromise and that efforts should be made to locate suitable natural defects as standards. The ultrasonic test should be supported by a visual examination of the tubing. On the outer surface this is best carried out with the aid of a fluorescent penetrant and, for the bore, a special 360° Borescope was developed that was subsequently found to be satisfactory for production inspection[6].

A wall-thickness variation can constitute a dimensional flaw in fuel-element sheathing. A very sensitive ultrasonic micrometer has been developed at Harwell that is capable of measuring wall thicknesses over 1 mm² of surface [22]. A 50-μs pulse of ultrasound is focused, through a water coup-

[6] Developed by Mr. C. F. Smith, Wood End Close, Farnham Common, Bucks. UK.

lant, on to the surface of the tubing. By adjusting the frequency of the ultrasound in the pulses, values can be found where there is zero reflection back to the probe over the central portion of the pulse. The effect occurs at frequencies very close to the fundamental and harmonic resonances of the tube wall and it is suggested that at these frequencies the energy is transferred along the tube away from the incident point as slowly propagating Lamb-wave modes, which rapidly re-radiate in a non-normal direction [35]. The accuracy by which these reflection nulls can be set is equivalent to wall-thickness variations of approximately 0, 5 μm.

For the measurement of a wall thickness of hollow uranium fuel tubes with a 0.35-in wall, a commercial precision ultrasonic pulse-echo instrument has been used which is capable of resolving individual cycles of the ultrasonic pulse[7]. The transit time of the pulses across the wall is approximately 5 μs and it was found possible to measure this with an accuracy of 1%. To avoid errors due to variations in water-couplant path-length a gating system was used so that the time measurement could be initiated by the front surface echo and terminated by the arrival of the back wall echo. Since individual measurements of wall thickness are possible with each pulse, 2000 measurements a second could be achieved which provided an extremely high inspection speed [24].

The uniformity of tube bore is important in sheathing into which fuel pellets must be loaded with a minimum resultant peripheral clearance. Air gauges are accurate, but have a poor response time. Work at Harwell has been directed towards improved forms of capacitance gauge, and probe beads have been designed to reduce errors arising from lateral movements of the capacitance probe about the tube axis during the spiral scan through the tube The possibility of using a porous metal plug to act as an internal air bearing for a capacitance probe is currently being examined [24].

4.2. Quantized facsimile recording

It is obviously an advantage to have the facility to record test data as comprehensively as possible. With the quantized facsimile recording system developed at Harwell, signal strengths can be recorded as discrete and predetermined shades of grey at points on a facsimile record that automatically define two positional co-ordinates in the sample [21, 27]. In ultrasonic testing this has enabled the shapes of individual defects to be examined and the pattern of scatter from anisotropic microstructures to be studied [19]. In addition, scanning with a small received probe in the vicinity of an immersed ultrasonic transducer has enabled contoured polar diagrams to be produced from which the radiation characteristics of the transducer can be seen at a glance [20]. All of this is of value in the laboratory and development stages of non-destructive testing application and should help to provide a more basic understanding of materials, test equipment and inspection procedures.

With eddy currents, quantized facsimile recording can help to improve the selectivity of the tests. With graphite and stainless steel, where excessive "noise" is often a problem, a facsimile presentation can form a recog-

[7] Microradar Unit. Réalisations Ultrasoniques, Meaux, France.

nizable pattern from the background noise against which signals from discrete defects are readily distinguished [24]. The two-dimensional method of recording eddy-current signals has also been used to display the exact size and location of voids in the sodium interlayer or irradiation capsules. This has provided a technique to enable the mechanism of sodium filling to be studied and the variables controlled [25].

4. 3. The ultrasound camera

Image-converter tubes are of interest in a number of fields and work has been in progress at Harwell for a number of years to try to perfect an inspection system based on an ultrasonic image-converter tube [29, 30, 31]. A converter-tube design has been developed using a 1. 5-in-diam. quartz face plate resonant at 4 MHz [32]. The sequence of operation is that the quartz plate is first brought to earth potential. A piëzoelectric charge pattern is then built up on it by virtue of the ultrasound image thrown on it by an acoustic lens in the inspection tank. The charged plate is then scanned with a low-velocity electron beam and the pattern of deposited electrons induces a corresponding charge pattern on an adjacent signal plate which is connected through a filter and amplifier to a TV monitor display. The surface is then restored to earth potential by residual ion bombardment and the operating sequence repeated.

In this way a direct-view facsimile type of presentation is obtained, but because of the speed of the operating sequence the object can be moved during inspection. The fairly coarse scan pitch also provides a more rapid rate of inspection than the conventional probe-scanning technique.

The system suffers from aberrations and has still not been transformed into a fully engineered inspection equipment. However, it shows promise as a means of scanning fuel plates for unbonded areas between the core and cladding. The sensitivity appears to be superior to probe scanning and the speed of inspection is more compatible with production rates [33, 34]. As a result the work at Harwell is being directed primarily with this particular application in mind.

5. CONCLUSIONS

This paper has purposely not attempted to highlight any particular flaw-detection technique. Instead, as a review, it has provided the Harwell interpretation of the range and scope of non-destructive flaw detection and served as a means of summarizing the programmes and published reports of recent years.

REFERENCES

The following list of references covers all the unclassified publications dealing with the N. D. T. development work of the Metallurgy Division at Harwell.

General review articles

[1] SHARPE, R.S., Future Developments in Non-Destructive Testing, Brit. J. non-destr. Test. 3 (1961) 111.
[2] SHARPE, R.S., Non-Destructive Testing in Perspective, Brit. J. non-destr. Test. 5 (1963) 83.
[3] SHARPE, R.S., The Physicists Approach to Non-Destructive Testing, Bull. Inst. Phys. 15 (1964) 223.

Microradiography

[4] SHARPE, R.S., X-Ray Microscopy, Progr. in non-destr. Test. 3 (1961) 191.
[5] SHARPE, R.S., Some Applications of Microradiography to Fuel Element Inspection, Fuel Element Fabrication 2, IAEA, Vienna (1960) 45.
[6] SHARPE, R.S., X-Ray Microscopy applied to the Examination of Coated Nuclear Fuel Particles, Harwell Report AERE - R.4252 March 1963, and React. Sci. Tech. A/B 17 (1963) 505.
[7] SHARPE, R.S., Divergent Beam X-ray Diffraction and its Application to Irradiated MgO, Harwell Report AERE - R.4452 October 1963, and Appl. Mat. Res. April 1965 (to be published).
[8] SHARPE, R.S., Divergent Beam X-ray Microscopy and Crystal Analysis, Proc. 4th Symp. on Physics and NDT (1963) (published by S.W. Research Institute) 193.

Radiographic techniques

[9] THEWLIS, J. and DERBYSHIRE, R.T.P., Neutron Radiography, AERE MT/N 37. July 1956, and Progr. in non-destr. Test. 1 (1958) 113.
[10] THEWLIS, J. and DERBYSHIRE, R.T P., Non-Destructive Testing of Fuel Elements for DIDO, J. Amer. Soc. non-destr. Test. 16 (1958) 154.
[11] DERBYSHIRE, R.T.P., Radiological Examination of Highly Active Specimens, E.A.N.S. Symp. on reactor materials, Paper UK 26 (1959).
[12] DERBYSHIRE, R.T.P., A Multiple Panoramic Apparatus for Radiographic Examination of H.T.R. Fuel Sleeves, Harwell Report AERE - R.3855 Dec. (1961).
[13] COTTERELL, K. and SHARPE, R.S., The Use of Carbon Tetrachloride as a Radiopaque Penetrant. Harwell Report AERE - R.3785 Sept. 1961 and Amer. J. non-destr. Test. 20 (1962) 234.
[14] COTTERELL, K., Scintillography as an Alternative to Radiography, Harwell Report AERE - R.4293, May (1963).
[15] COTTERELL, K., Scintillography as a Means of Recording Radiographic Information, Appl. Mat. Res. 3 (1964) 102.
[16] DERBYSHIRE, R.T.P., HEWITT, G.F. and NICHOLLS, B., X-Radiography of Two-Phase Gas-Liquid Flow, Harwell Report AERE - M.1321, Jan. (1964).
[17] SHARPE, R.S., DERBYSHIRE, R.T.P. and PARISH, R.W., The Development of Active Radiographic Inspection Techniques at Harwell, E.N.E.A. Conference on Working Methods in High Activity Hot Laboratories, Grenoble, June 1965, Paper No. 7 (to be published).
[18] JACKSON, R. and SHARPE, R.S., Radiographic Techniques Applied to Carbons, Chapter in "Porous Carbon Solids" (to be published).

Ultrasonics and eddy-current techniques

[19] SHARPE, R.S. and AVEYARD, S., The Visualisation of an Ultrasonic Extinction Network in Coarse Grained Uranium, Appl. Mat. Res. 1 (1962) 170.
[20] AVEYARD, S., Radiation Patterns from Ultrasonic Probes, Brit. J. non-destr. Test. 4 (1962) 120.
[21] AVEYARD, S., A High Definition Ultrasonic Recording System, Inst. Welding Select Conf. on Ultrasonic Testing 1963, Memo No. 10.
[22] AVEYARD, S. and SHARPE, R.S., Applications of Pulse Interference, Proc. 4th Int. Conf. on Non-Destr. Test., Butterworth (1964) 150.
[23] SHARPE, R.S. and AVEYARD, S., The Inspection of Thin Walled Stainless Steel Reactor-Grade Tubing, J. Iron and Steel Inst. 201 (1963) 856.
[24] AVEYARD, S., Rapid Methods of Tube Measurement, Harwell Report AERE - M.1431, July (1964).

[25] AVEYARD, S., Plotting the Position of Voids in a Sodium Heat Transfer Layer, Harwell Report AERE - M. 1391, June (1964).
[26] SHARPE, R.S. AVEYARD, S. and SAYERS, J. F., The Inspection of Fuel Element Bonding, Harwell Report AERE - R. 4605, April (1964).
[27] HODGKINSON, W.L., A Quantised System of Facsimile Recording, Harwell Report AERE - R. 4688, July (1964).
[28] SHARPE, R.S., Low Power Ultrasonic Techniques for Materials Inspection, Ultrasonics 3 (1965) 25.

The ultrasonic camera

[29] SAYERS, J. F., Epoxy-Resin Joints for Sealed Off High Vacuum Tubes, J. sci. Instrum. 37 (1960) 203.
[30] SMYTH, C.N. and SAYERS, J.F., Improvements in or Relating to Ultrasonic Viewing Devices, Brit. Patent No. 841025, July (1960).
[31] SMYTH, C.N., POYNTON, F.Y. and SAYERS, J.F., The Ultrasound Image Camera, Proc I.E.E. 110 (1963) 16; and J. I.E.E. 9 (1963) 26.
[32] SAYERS, J.F., The Ultrasound Camera: Part 1, The Instrument Constructed at A.E.R.E., Harwell Report AERE - R. 4356, Nov. (1963).
[33] SAYERS, J.F., The Ultrasound Camera, Progr. in appl. Mat. Res. 7 (to be published).
[34] SAYERS, J.F., The Ultrasound Camera, Proc. 5th Symp. Physics and N.D.T. (to be published).

Supporting and supported work

[35] ALDRIDGE, E.E., (Electronics Division), An Investigation into the Mode of Working of the Ultrasonic Micrometer used in Thickness Measurements of Thin Wall Stainless Steel Tubing, Harwell Report AERE-M. 1510, (1965).
[36] MOTT, G., A Study of Wave Propagation in Thin Sheets, University of London PhD Thesis, Jan.(1960).
[37] SMITH, R.T., The Propagation of Elastic Waves in Anisotropic Solid Media, University of London M.Sc. Dissertation, June (1961).
[38] FINNEY, D., Ultrasonic Field Investigations, University of London PhD Thesis, June (1964).
[39] BARTON, J.P., (University of Birmingham), Contrast Sensitivity in Neutron Radiography, Appl. Mat. Res. (to be published).
[40] BARTON, J.P., (Univeristy of Birmingham), Radiographic Examination through Steel Using Cold Neutrons, (to be published).

DISCUSSION

J. DORY: What is the resolution of the acoustic image converter?

R. SHARPE: In the object plane we find that the resolution is better than 1.5 mm at 4 MHz using a lens systems It is quite surprising that such a high resolution can be obtained for a piëzoelectric image impressed on the thin quartz face-plate of the converter tube.

J. DORY: Are you not troubled by interference through continuous operation?

R. SHARPE: Yes. This is one of the major problems, especially interference effects within the sample. We hope to develop a pulse-sensitive converter tube to overcome this spurious effect.

J. DORY: What acoustic power is necessary?

R. SHARPE: Between 0.1 and 10 W at the transmitter, depending on the attenuation in the sample.

V.V. GORSKY: Did I understand correctly that to obtain relief on the facsimile the voltage on the eddy-current detector is changed for two or three surface scans?

R. SHARPE: To obtain the contours on the facsimile record the signal voltage from the eddy-current equipment is quantized into discrete amplitude levels, each of which can be displayed in a predetermined writing shade.

V.V. GORSKY: What defect do you regard as permissible in the wall (can) of the fuel element and what is the permissible area of poor bonding, for instance in flat fuel elements?

R. SHARPE: We are not directly responsible at Harwell for setting material specifications for reactor components, so I am not the best person to quote current defect tolerances. Until more experimental evidence of defect significance is available our standards are inevitably based on conservative estimates and previous operational experience.

V. GERASIMOV: With what accuracy do you measure the tube-wall thickness using the eddy-current method?

R. SHARPE: We are not using an eddy-current method for any routine measurement of tube-wall thickness. On the slide I showed during my oral presentation to illustrate what we call the Eddyfax technique, each contour in the facsimile record corresponded to a thickness change of about 0.0002 in for a stainless-steel tube, with a 0.015-in wall.

V. GERASIMOV: Have you eliminated the effects of changes in the electrical conductivity of the component being inspected and changes in the distance between probe and tube?

R. SHARPE: To obtain this display the eddy-current scanning probe was spring-loaded against the wall of the tube to eliminate the lift-off effect. This naturally reduces inspection speed. We were in fact using speed, of about 60 rpm.

G. TENNEY: What are the size and intensity of the source for the Am^{241} radiation gauge?

R. SHARPE: Although the gamma radiation emanates from a flat encapsulated 200-mc source, 7 mm in diameter, only a fraction of the output is made use of, as it is necessary to mask the front face of the source to provide the narrow pencil of radiation (1 or 2 mm in diameter) needed to give adequate radiographic definition. Count rates in excess of 10^5/counts/s are obtained and this enables us to obtain an inspection speed of about one inch length of fuel plate per minute.

P. de MEESTER: What accuracy can you obtain in fuel homogeneity? With your quantized recording I assume that you are putting two or three quantized levels at both upper and lower tolerance limits. How far do you have to put these apart to get good accuracy?

R. SHARPE: In the present mode of operation we only use three intensity shades in the quantized recording of a fuel plate - one shade of grey for compositions within specification and two other shades to indicate uranium contents above and below specification. The method of standardizing and setting the quantized levels is naturally influenced by statistical considerations although the line-by-line correlation in the facsimile record helps to smooth out some of the statistical uncertainty.

THE NON-DESTRUCTIVE TESTING OF FUEL ELEMENTS AND THEIR COMPONENTS FOR THE UNITED KINGDOM POWER-REACTOR DEVELOPMENT PROGRAMME

C. A. MANN AND I. C. CAMPSIE
U. K. A. E. A., REACTOR FUEL ELEMENT LABORATORIES,
SPRINGFIELDS, SALWICK, PRESTON, LANCS., ENGLAND

Abstract — Résumé — Аннотация — Resumen

THE NON-DESTRUCTIVE TESTING OF FUEL ELEMENTS AND THEIR COMPONENTS FOR THE UNITED KINGDOM POWER-REACTOR DEVELOPMENT PROGRAMME. The test procedures are described which have been developed in the Reactor Fuel Element Laboratories as part of the Reactor Group's development programme on fuel pins for a number of reactor systems. The sheaths of these pins are tubes in the range 5 mm-15 mm diam; the materials are stainless steels and zirconium alloys.

(a) Flaw detection in tubes is decribed.

Ultrasonic inspection using two immersed probes. The tubes are traversed helically at high speeds through a stationary tank. Flaw signals are monitored and recorded. Spark-machined slots on the surfaces of tubes are used as references in setting up the system and in checking its stability.

Eddy-current inspection is also employed in some cases. Two tests are described: an encircling coil system with rapid throughput, and a surface coil with helical scan. Phase selection and filtering of the output from a bridge circuit is used, at frequencies between 30 and 60 kHz.

(b) Dimensional inspection of tubes and pellets is also discussed.

Various mechanical, pneumatic, nuclear and electronic methods of measuring the tube dimensions are compared and the arrangements to prevent the scratching of the tubes are described.

Techniques for measuring pellet diameter and circumferences are explained and it is suggested that with thin-walled tubes a more realistic approach to the pellet/gap problems can be obtained by comparing circumferences.

With the development of efficient tube-traversing equipment it has been possible to combine the above development technique to form a completely integrated tube-testing facility operated by semi-skilled labour. The laboratory's requirement for precise information of tube sizes has been met by the automatic recording of measurements, eliminating a time-consuming and somewhat inaccurate method of manual recording of the results.

For flaw detection in fuel pins, the techniques already mentioned can in general be applied to examine the sheaths of fuel pins, i. e. after fuel has been loaded and the ends closed. In addition, the integrity of end closures is established by radiography. Multiple exposures are commonly made to examine the whole of circumferential weld adequately. The disposition of the fuel can also be recorded accurately by using a panoramic technique. The use of colour radiography is also discussed.

Pins are normally tested for leakage after filling with helium, using a mass-spectrometer leak detector. Pins not filled with helium may be tested using a "back-pressurizing" technique. Conventional "probing" and "sniffing" methods are used when it is desirable to locate the sites of leaks. The bubble test in liquids is also used, as a cheap and simple test. The use of krypton-85 as a tracer gas is discussed.

CONTRÔLE NON DESTRUCTIF DES ÉLÉMENTS COMBUSTIBLES ET DE LEURS PARTIES CONSTITUTIVES DANS LE CADRE DU PROGRAMME DE DÉVELOPPEMENT DES RÉACTEURS DE PUISSANCE AU ROYAUME-UNI. Les auteurs décrivent les méthodes d'essai que les laboratoires chargés des éléments combustibles ont élaborées dans le cadre du programme établi par le « Groupe des réacteurs » en vue de mettre au point des aiguilles de combustible pour diverses filières de réacteurs. Ces aiguilles sont contenues dans des gaines de 5 à 15 mm de diamètre, les matériaux utilisés étant des aciers inoxydables et des alliages de zirconium.

a) Détection de défauts dans les gaines.

Examen par ultrasons à l'aide de deux traducteurs immergés. Les tubes sont animés d'un mouvement

hélicoïdal rapide dans un réservoir fixe. Chaque signal de défaut est vérifié et enregistré. Pour régler le dispositif et vérifier sa stabilité, on utilise comme témoins des fentes pratiquées à l'arc à la surface des tubes.

Dans certains cas, on a également recours au contrôle par courants de Foucault. Les auteurs décrivent deux procédés: l'un, à débit rapide, est fondé sur un système de bobines encerclant le tube; l'autre, à exploration hélicoïdale, utilise une bobine se déplaçant le long du tube. Les signaux fournis par un circuit à pont sont sélectionnés selon la phase et filtrés, pour des fréquences de 30 à 60 kHz.

b) Contrôle des dimensions de tubes et de pastilles.

Diverses méthodes mécaniques, pneumatiques, nucléaires et électriques permettant de mesurer les dimensions des tubes font l'objet d'une étude comparative. On décrit les mesures qui sont prises pour ne pas rayer la surface des tubes.

Les auteurs exposent les procédés employés pour mesurer le diamètre et la circonférence des pastilles; pour les tubes à paroi mince, les problèmes que pose le rapport entre le volume des pastilles et celui des vides pourraient être traités de façon plus réaliste en comparant les circonférences.

La mise au point d'un appareil efficace de rotation des tubes a permis de combiner les méthodes décrites ci-dessus et de construire un dispositif d'essai entièrement intégré dont l'utilisation ne nécessite pas un personnel hautement qualifié. Pour que le Laboratoire puisse obtenir rapidement des renseignements précis sur les dimensions des tubes, on procède à l'enregistrement automatique des mesures; on a ainsi supprimé l'opération, lente et quelque peu inexacte, d'enregistrement à la main.

En ce qui concerne la détection des défauts dans les aiguilles de combustible, les méthodes exposées sous le point a) peuvent, en règle générale, servir à examiner les gaines d'aiguilles de combustible après le chargement du combustible et l'obturation des extrémités. En plus, l'état des bouchons terminaux est vérifié par radiographie. On fait normalement des expositions multiples pour examiner convenablement toute la périphérie des soudures. On peut également déterminer avec précision la répartition du combustible par radiographie panoramique. Le recours à la radiographie en couleurs est également étudié.

L'étanchéité des aiguilles est vérifiée après remplissage d'hélium au moyen d'un détecteur de fuites à spectromètre de masse. Les aiguilles ne contenant pas d'hélium peuvent être contrôlées par immersion dans un milieu sous pression. Pour localiser les fuites, on peut appliquer, le cas échéant, des méthodes d'investigation classiques. On utilise aussi le procédé simple et peu coûteux qui consiste à plonger la pièce dans un liquide et à observer la formation de bulles. Enfin, les auteurs discutent l'emploi du krypton-85 comme radioindicateur.

НЕДЕСТРУКТИВНОЕ ИСПЫТАНИЕ ТЕПЛОВЫДЕЛЯЮЩИХ ЭЛЕМЕНТОВ И ИХ КОМПОНЕНТОВ ДЛЯ ОСУЩЕСТВЛЕНИЯ ПРОГРАММЫ СОЕДИНЕННОГО КОРОЛЕВСТВА ПО РАЗРАБОТКЕ ЭНЕРГЕТИЧЕСКИХ РЕАКТОРОВ. Описываются методы испытаний, которые разработаны в лабораториях реакторных тепловыделяющих элементов в порядке осуществления программы реакторной группы по разработке тепловыделяющих элементов в виде тонких стержней для ряда реакторных систем. Оболочка этих стержней представляет собой трубку диаметром 5-15 мм и изготавливается из нержавеющей стали и сплавов циркония.

а. Дефектоскопия в трубках

Ультразвуковая проверка с помощью двух погруженных зондов. Трубки перемещаются винтообразно с большой скоростью через неподвижный бак. Сигналы дефекта измеряются и регистрируются. Сделанные с помощью дугового разряда прорези на поверхностях трубок используются в качестве эталона при установке системы и проверке ее стабильности.

В некоторых случаях проверка осуществляется также при помощи метода вихревых токов. Описываются два испытания,одно с замкнутой катушечной системой с быстрой производительностью, а другое - с поверхностной катушкой с винтовой разверткой. Используется выбор фаз и фильтрация выходного напряжения из мостовой схемы в диапазоне частот от 30 до 60 килогерц.

б. Проверка размеров трубок и таблеток

Сравниваются различные механические, пневматические, ядерные и электронные методы измерения размеров трубок. Описываются меры по предотвращению царапин на трубках.

Объясняются методы измерения диаметра и длины окружности таблеток. Предполагается, что с помощью тонких трубок можно добиться более реалистического подхода к проблемам таблетка/зазор путем сравнивания длины окружностей.

Разработка эффективного оборудования для перемещения трубок позволила комбини-

ровать вышеупомянутые методы разработки в целях создания комплексного устройства для испытания трубок, которым управляют полуквалифицированные рабочие. Требование, которое предъявляется лабораторией в отношении точной информации о размерах трубок, удовлетворяется за счет автоматической записи измерений, что устраняет необходимость применять ручной метод записи результата, который требует много времени и является несколько неточным.

Дефектоскопия в общем применима для проверки оболочек тепловыделяющих элементов в виде тонкого стержня, т. е. после загрузки топлива и заделки концов. Кроме того, целостность закрытых концов определяется с помощью радиографии. Многократное облучение обычно производится для необходимой проверки всего сварного шва по длине окружности. Положение топлива также можно точно зарегистрировать с помощью панорамного метода. Рассматривается также использование цветной радиографии.

Стержни обычно испытываются на течь после наполнения гелием с помощью масс-спектрометрического течеискателя. Стержни, которые не наполняются гелием, можно испытывать методом повышения "обратного давления". Обычные методы зондов и "всасывания воздуха" используются в тех случаях, когда желательно найти места течи. Используется также проба на образование пузырей в качестве дешевого и простого испытания. Обсуждается вопрос использования криптона-85 в качестве индикаторного газа.

ENSAYO NO DESTRUCTIVO DE ELEMENTOS COMBUSTIBLES Y SUS COMPONENTES, EN EL MARCO DEL PROGRAMA DE REACTORES DE POTENCIA DEL REINO UNIDO. Los procedimientos de ensayo que se exponen han sido establecidos en el Laboratorio de combustibles nucleares, como parte del programa del Grupo correspondiente, relativo a varillas de combustible para reactores de distintos tipos. La vainas de esas varillas consisten en tubos de acero inoxidable o aleaciones de circonio de 5 a 15 mm de diámetro.

a) Se describe la localización de fallas o grietas en los tubos.

Inspección ultrasónica con dos sondas sumergidas. Los tubos se someten a un barrido helicoidal a gran velocidad en un tanque estacionario, con lo cual se observan y registran las señales que denotan la existencia de fallas. Para calibrar el sistema y comprobar su estabilidad, se usan como referencias unas ranuras practicadas por chisporroteo.

En ciertos casos se recurre también a la inspección mediante corrientes de Foucault. Los dos métodos que se describen emplean un sistema de bobina anular de pasaje rápido y una bobina superficial con exploración helicoidal. Para la selección de fases y filtrado de la señal de salida se una un circuito de puente, con frecuencias comprendidas entre 30 y 60 kHz.

b) Se discute además la inspección de las dimensiones de tubos y pastillas.

Se hace un estudio comparativo de diversos métodos mecánicos, neumáticos, nucleares y electrónicos de medición de las dimensiones de los tubos, y se explican las precauciones que han de adoptarse para impedir que éstos se rayen.

Se describen técnicas para medir el diámetro y la longitud de la circunferencia de las pastillas y se recomienda la comparación de las circunferencias, en el caso de tubos delgados, como método más ajustado a la realidad para el estudio de los problemas que plantea la existencia de huecos entre las paredes del tubo y las pastillas.

El perfeccionamiento de equipo para el desplazamiento transversal de tubos ha permitido, mediante una combinación de técnicas, instalar un dispositivo de ensayo que puede ser manejado por personal semiespecializado. Las necesidades del Laboratorio en cuanto a datos de precisión sobre las dimensiones de los tubos pueden satisfacerse con un sistema automático que registra los datos y permite prescindir del método laborioso y algo inexacto de anotación manual de los resultados.

En el caso de la localización de fallas en las varillas de combustible, el método expuesto en el párrafo a) puede utilizarse en general para examinar los tubos de revestimiento después de haber efectuado la carga del combustible y de haber cerrado los extremos del tubo; además, la integridad del cierre se comprueba radiográficamente. Para verificar adecuadamente el estado de una soldadura circular, se toman varias radiografías. Utilizando una técnica panorámica puede también registrarse con exactitud la disposición del combustible. Se estudia además la posibilidad de utilizar la radiografía cromática.

La detección de escapes en las varillas de combustible suele realizarse utilizando un espectrómetro de masas después de haber procedido al rellenado con helio. Si éste no es posible, puede aplicarse un procedimiento de contrapresión. Para localizar los escapes se utilizan los métodos ordinarios de sondeo o «rastreo». Un procedimiento sencillo y poco oneroso aplicable cuando se trata de líquidos, es el de burbujeo. Se estudia la posibilidad de utilizar el kriptón-85. como gas indicador.

1. INTRODUCTION

The reactor systems currently being developed by the Reactor Group U.K.A.E.A. have fuel elements in the form of clusters of fuel pins. The pins are, typically, stacks of uranium-dioxide pellets enclosed in metal tubes with welded closures at each end. This paper discusses the methods of non-destructive testing and measurement applied to the components of the fuel pin before assembly, and to the fuel pin after assembly. These will be considered under the following headings:

Flaw detection of the tubing.
Dimensional inspection of tube and fuel.
Checking the integrity of finished pins.

2. INSPECTING TUBING FOR FLAWS

2.1. Ultrasonic flaw-detection

All tubing for fuel elements is examined ultrasonically, either at the manufacturer's works or in U.K.A.E.A. laboratories. The apparatus in the Reactor Fuel Element Laboratories is in the now conventional form using two pulse-echo flaw-detection sets, with the transducer probes oriented, one to detect flaws extended parallel to the axis of the tube and the other to detect flaws extended around the tube wall (Fig. 1). The transducers are coupled to the tube by water in which they and it are immersed. The ultrasound enters the tube over a small area; it has been found advantageous for most tests to concentrate the energy by using a spherically concave crystal in the transducer. The tube must therefore be systematically scanned if every part is to be examined. In the apparatus used in these laboratories the tube is spiralled past the transducers, which are fixed (Fig. 2).

Commercial pulse-echo detector sets are used; the sets have however been modified by the makers so that the pulse repetition rates have been raised to 3000 pulses/s from 600 pulses/s. A higher scanning speed is thus possible. The pulse emission is also synchronized to eliminate cross-interference between the two transducers. The returning signals from flaws are detected by monitor units and passed through pre-amplifiers to a two-channel pen-recorder. The frequency of the pulsed ultrasound is in the range 2-12 MHz, with 4 and 6 MHz as the preferred frequencies. Conventional transducers using such materials as barium titanate, lead zirconate or lithium sulphate are used. It has been found convenient on occasion to make up transducers in the laboratory from crystal blanks [1]. The radiation patterns in water are plotted, using the system developed by AVEYARD [2] to confirm that the transducer is functioning satisfactorily.

Because of the variations between nominally identical transducers, it is necessary to set the exact positions of the transducers in the test tank empirically. A specimen piece of the tubing under test is used for calibration. Into this piece are spark-eroded standard square-section notches, typically 1.2 mm × 50 μm × 50 μm. Four such notches are normally machined

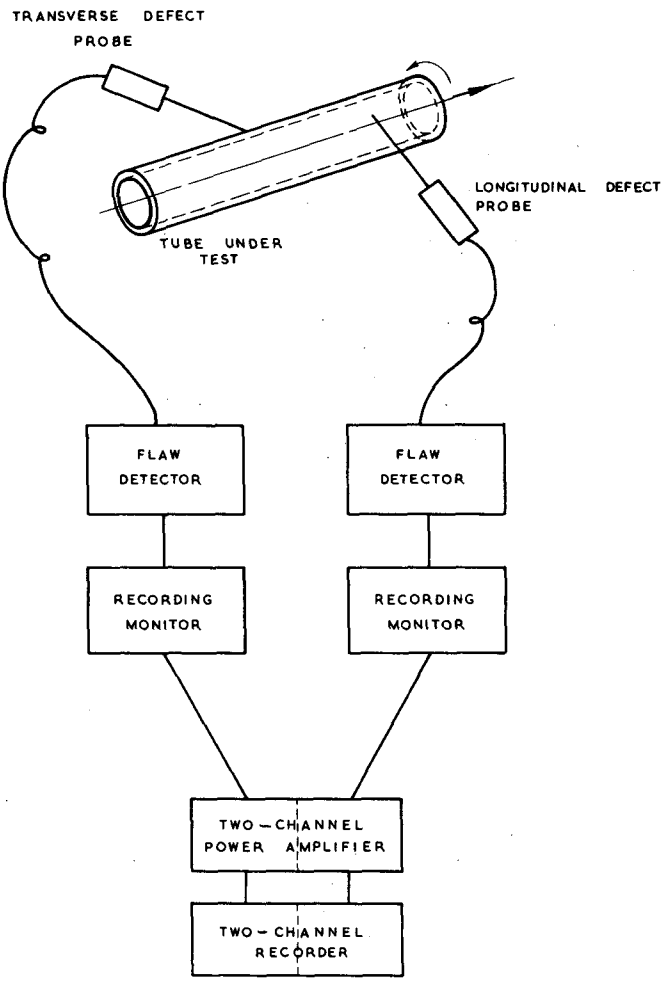

Fig. 1

Disposition of ultrasonic transducer probes

in each calibration piece. Two are on the outside surface and two on the bore, and of each of these pairs one is machined with its major dimension parallel to the axis of the tube while the other is machined circumferentially. The transducers are adjusted until an equal response is obtained on the recorder from each of the four notches as the calibration piece passes through the equipment, the two longitudinal notches appearing on one recorder channel, and the two circumferential ones on the other.

There is evidence that the mode of propagation of the ultrasonic pulses on entering the wall of the tubing is not simple, and that mode conversion occurs, as might be expected. The signal returned from any discontinuity varies markedly with distance from the point of entry of the ultrasound, with dissimilar variations for discontinuities on the inner and outer surfaces.

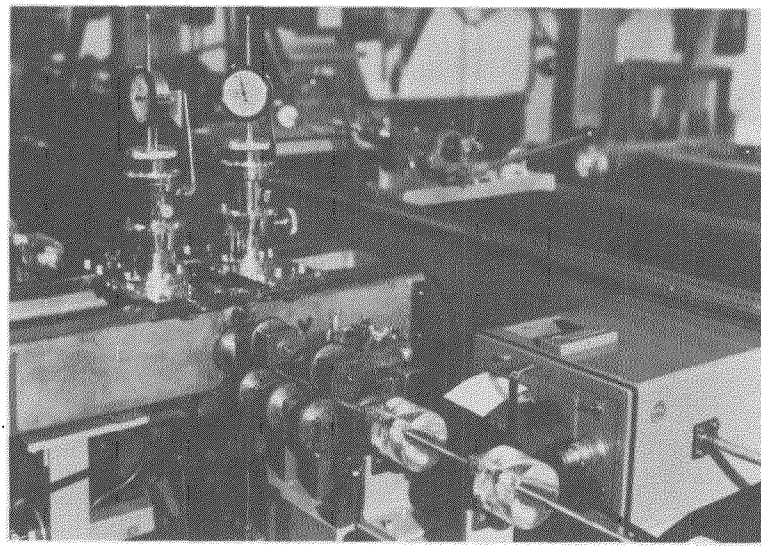

Fig. 2

Ultrasonic flaw-detection equipment

However, by monitoring the return pulses through gate circuits of high stability, accurately adjusted, equal pulse heights may be picked off whatever the position of the discontinuity.

It is essential to maintain the relative positions of transducers and tubing to close limits during testing. A small test tank is used, the tubing entering and leaving it through bushes which are a close fit on the tubing. These serve both to locate the tubing accurately and to minimize loss of water past the tubing. The bushes are machined from polytetrafluoroethylene, which has been found satisfactory even for such easily damaged metals as Zircaloy. The tubing and the whole apparatus must of course be kept clean to prevent pick-up of abrasive particles on the bushes. Distilled water is used in the tank to eliminate spurious signals from air bubbles. A fixed brush is used to wipe off any bubbles entrained during entry. Water escaping through the bushes is returned to a reservoir, from which a pump maintains the level in the tank through a filter.

Means of accurately adjusting the positions of the transducers and of firmly locking them in place during operation are provided. The positions relative to the tube are thus maintained. The length of tubing in the tank between the bushes is 10 cm; movement due to bow of the tubing over this distance is normally negligible. The tubing is simultaneously rotated and traversed by sets of angled wheels with rubber tyres. Surface speeds of up to 90 cm/s are used. The pitch of the spiral in which the tubes are driven is typically 0.15 mm, so that throughput speeds of 25-60 cm/min are usual.

Each piece of tubing is tested twice in reverse directions, since an asymmetrical flaw may return widely different echoes from pulses approaching from either side. Figure 3 shows such a flaw found in practice, with the traces of the two tests, and those of the calibration piece for comparison.

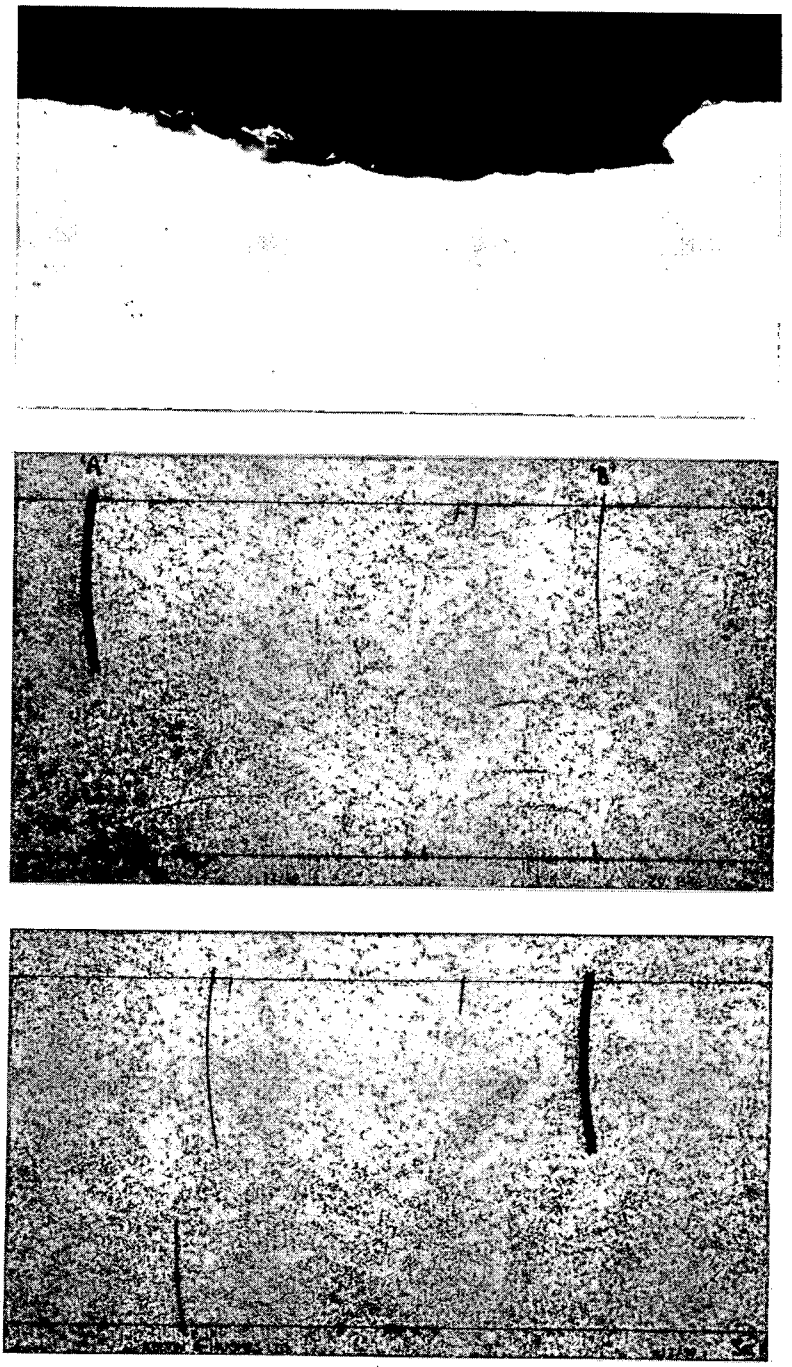

Fig. 3

Detection of a flaw

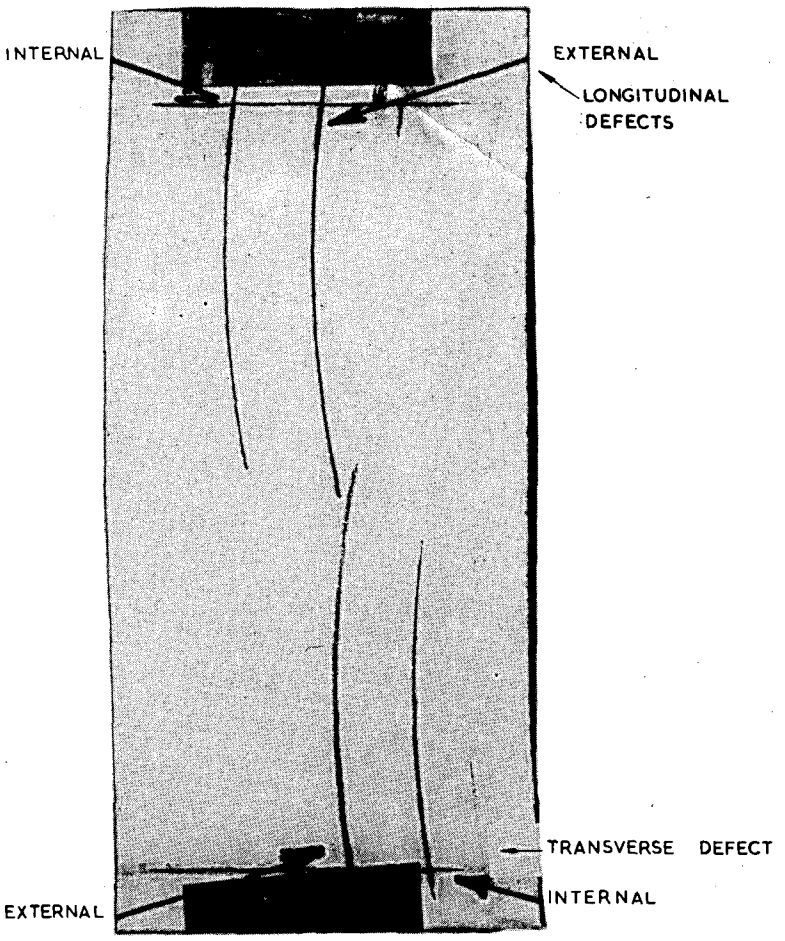

Fig. 3

Detection of a flaw

This differential sensitivity suggests that one of the weaknesses of the ultrasonic test method is the variation of its sensitivity to the shape and orientation of the flaw. However, it may be argued that such sharp-edged defects as cracks, which it detects sensitively, are likely to be the most deleterious in fuel-element sheaths.

The equipment, once set up, may be operated by semi-skilled personnel. The calibration piece is put through at stated intervals to confirm that the equipment is remaining in adjustment.

2.2. Eddy-current flaw-detection

This method is regarded as complementary, rather than an alternative, to the ultrasonic techniques just described. The eddy-current method is not,

for example, as sensitive to fine cracks as the ultrasonic method, but detects smooth-sided pits which the latter does not, because they do not reflect ultrasound significantly.

The shortcomings of the eddy-current technique when uncritically carried out are well known; spurious signals may originate from such sources as dimensional variations in the specimen, incidental local variations in resistivity of the specimen's material, and movement of the specimen relative to the test coils. Minimizing these spurious signals while combining simplicity and effectiveness has been achieved in two main ways; by phase selection of the output from the test coils and by further filtering of the selected signal.

Two systems have been developed for tube testing, one with an encircling coil arrangement and the other with a surface coil arrangement and helical scanning. The two systems are similar electrically, in that the eddy currents are generated by an exciting coil fed from a power oscillator. Two pick-up coils, fixed with respect to the exciting coil, form two arms of a Heydweiller AC bridge which is normally balanced when a sound specimen of tubing is in place. The passage beneath the pick-up coils of a discontinuity in a specimen temporarily unbalances the bridge; the unbalance voltage may be considered the input signal to the detection system. A phase-selective amplifier has been developed which has been found useful in discriminating between signals from defects and those from dimensional variations. The output from this amplifier after a further stage of amplification drives a conventional pen recorder.

In the encircling coil arrangement the pick-up coils are mounted symmetrically within the exciting coil, the coils being coaxial with the tubing under test. This is traversed through the coil block by a system of driven rollers, so that irregular movement is impossible. The speed of traverse is 15 cm/s. The phase-selection is chosen empirically after experiments with tubing containing known defects. Figure 4 shows the trace resulting from a tube containing the calibration notches for the ultrasonic test (Section 2.1) and also notches 2 mm × 200 μm deep × 100 μm wide. The smaller notches are barely detectable.

In the surface-coil arrangement, which is still under development, two pick-up coils whose arcs are normal to the surface of the specimen are surrounded by the exciting coil. The coils are mounted in a bush which is a close fit over the specimen. The latter is rotated while the bush is traversed along it; alternatively the specimen may be traversed through the bush as in the ultrasonic equipment. Figure 5 shows the trace from a tube containing calibration notches ranging from 50 μm - 200 μm deep.

2.3. A comparison of the methods of inspection

The ultrasonic method of flaw detection must be considered the prime technique of inspection, and it is the standard technique used by the U.K.A.E.A. for all reactor fuel-element tubing. There is a danger, however, in relying unquestioningly on any one test method, and it is for this reason that the eddy-current technique, though surpassed in sensitivity in recent years, has been considered worthy of continued development. The two techniques, as already indicated above, differ in their responses to defects of different

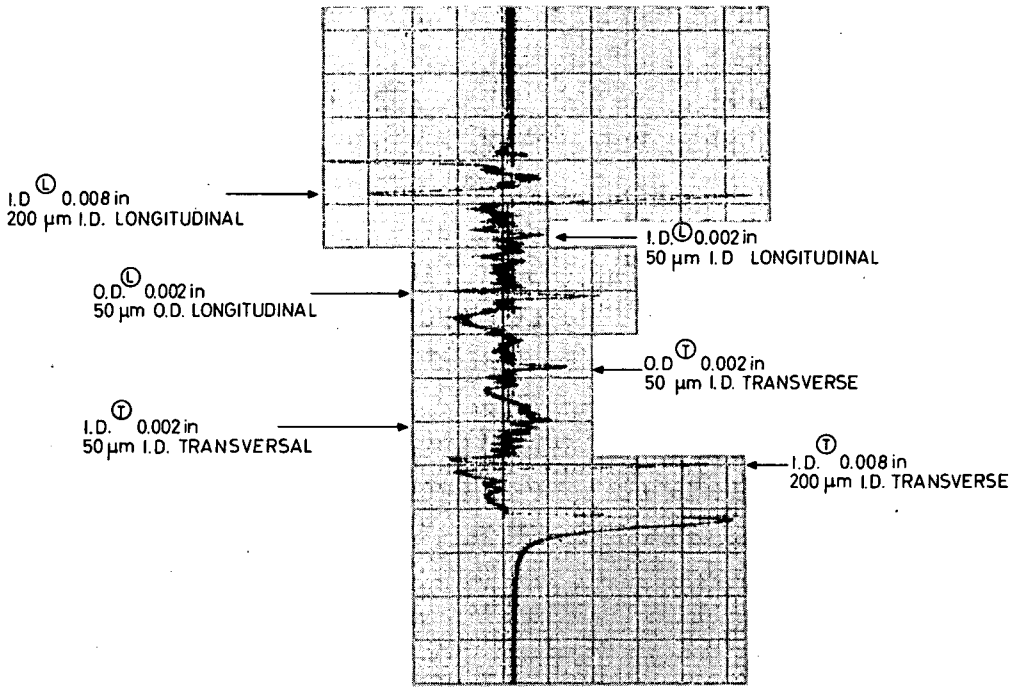

Fig. 4

Eddy-current response from tube containing notches
(encircling coil arrangement)

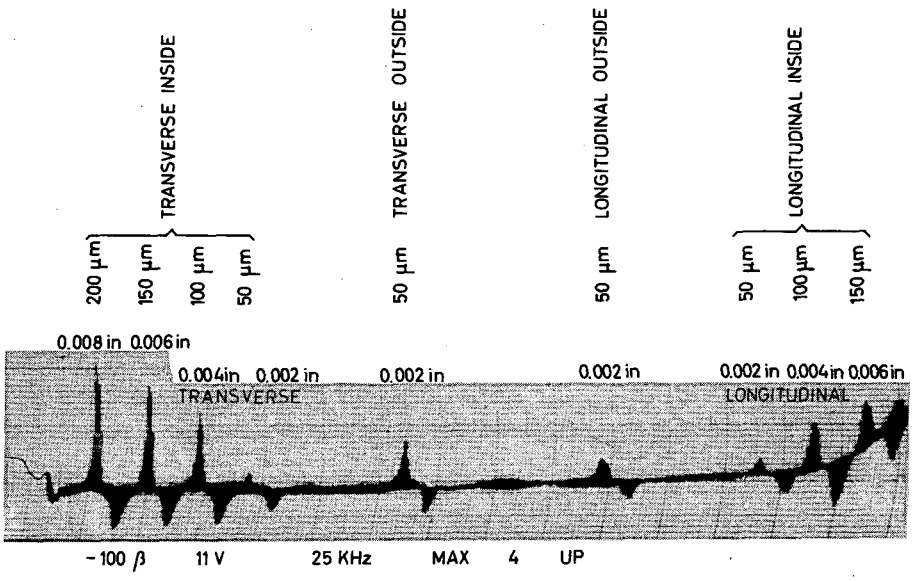

Fig. 5

Eddy-current response from tube containing notches
(surface coil arrangement)

types, while any particular test equipment will possess its own individual characteristics. It is therefore necessary, in specifying the test for any particular tubing, to assess carefully the requirements and the behaviour of the tubing on test equipment currently available.

3. DIMENSIONAL INSPECTION OF TUBING AND FUEL PELLETS

3.1. Tubes

The length-to-diameter ratio of tubes is usually greater than 100:1 and is commonly 500:1. The simplest method of inspecting inside and outside diameters to a given acceptance range is to pass plus gauges through the bore and ring gauges over the outside diameter. These are "go/no-go" tests, and little other information is obtained. Maximum forces on gauges must be specified, and care must be taken not to scratch or gall the tubes. Gauges of sintered alumina have been found advantageous. In general, however, it is preferred to measure tube dimensions; apart from the additional information provided, any size of tubing in the range of the measuring equipment may be dealt with without manufacturing new plugs or rings.

3.1.1. Measuring the inside diameter

Air-plug gauges are commonly used. Two-or three-jet plugs are used depending on whether it is required to measure local or average diameter.

Air gauging is accurate, usually linear, but the response speed is slow and depends upon the length and diameter of the air-gauge stem and the method of indicating or displaying the dimension being measured. High-pressure air gauges can accommodate diameter changes or ovality in the order of 0.2 mm. Pneumatic recorders currently available are slow, and linear inductive transducers have been coupled to the air-gauge control units to drive chart recorders or digital print-out units (see Fig. 6).

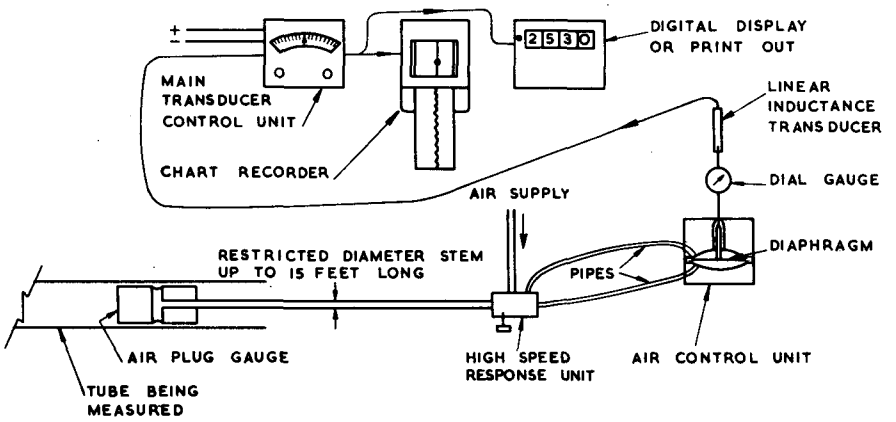

Fig. 6

System for recording measurements of inside diameters of tubing using air gauge

Capacitance gauges have not been widely used since those available had a smaller range (50 μm) than the air-plug gauge (200 μm). Greater ranges than these require complicated devices for centralizing the gauge inside the tube being measured. The speed of response is however very fast.

Mechanical methods are limited by the length-to-diameter ratio which is feasible. Again linear transducers have been used to give recorded measurements. For tubes of internal diameter greater than 10 mm the linear transducer is mounted on the gauge head (see Fig. 7).

3.1.2. Measuring the outside diameter

The dimension is readily measured by conventional equipment and air-ring gauges, adjustable air-gap gauges, and gap gauges using linear transducers are used.

3.1.3. Measuring the wall thickness

The measurement of the wall thickness remote from the end of long tubes has always been difficult until the development of ultrasonic and nucleonic gauges.

Initially the wall thickness was measured using a mandrel and a dial gauge but this technique gives poor results due to variable reflections of the mandrel. A later rig used a balanced lever arm and an inductance trans-

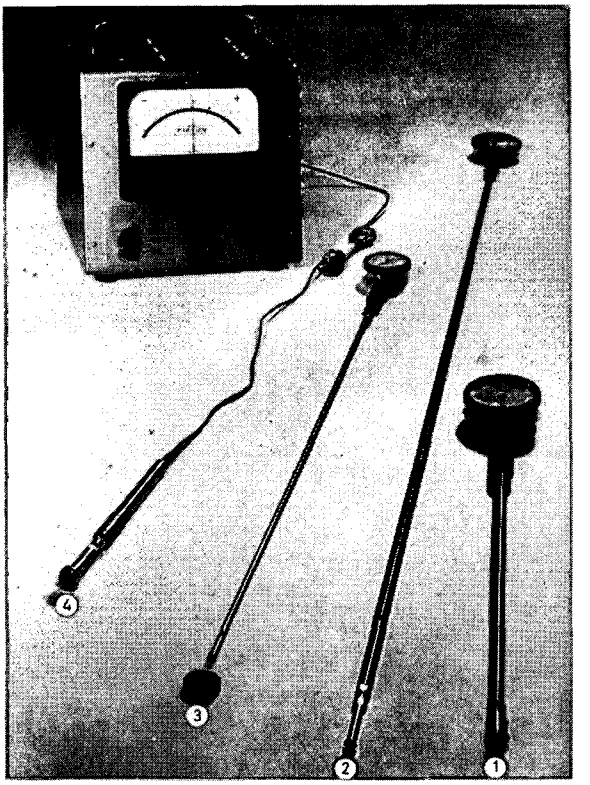

Fig. 7

Mechanical methods of measuring inside diameter of tubing.

1. Standard bore gauge
2. Bore gauge with extensions for measuring long tubes
3. Small bore gauge
4. Gauge for measuring long tubes. Head adapted to take linear inductance transducer with long cable connection to control unit.

ducer as a fiducial indicator; this equipment enabled tubes up to 1 m long to be measured to an accuracy of ± 2.5 μm, but the process of setting and using the equipment was slow and expensive.

A more successful approach to the measurement of long straight tubes was by the use of a micro-alignment telescope sighting on an illuminated target. This technique although somewhat tedious can measure wall thickness to better than ± 7.5 μm (see Fig. 8).

Nucleonic gauges, depending on the absorption of radiation from a source, have not been widely used because of their relatively slow response. Ultrasonic gauging is now regarded as the standard method for wall-thickness measurement. Two types of equipment are used; commercial swept-frequency sets which detect resonance of the tube wall when a beam of ultrasound is directed perpendicularly at it, and the more precise Harwell interferometer [3]. In the latter method pulsed ultrasound is similarly directed at the

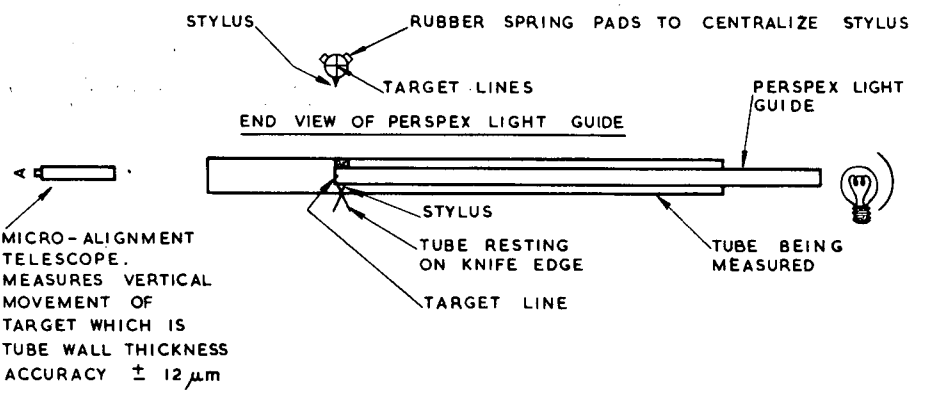

Fig. 8

Measurement of wall thickness of tubing using micro-alignment telescope

tubing; the form of the reflected pulse is very sensitive to thickness in the half-wave and multiple half-wave conditions. The ultrasonic transducers are coupled to the tubing through water in both instances (Fig. 9).

The ultrasonic method has the advantage that it requires no component to be inserted in the bore. It can thus be used in measurements on completed pins containing fuel. It has also been used on sheathing with external fins, where these are not more closely spaced than 2 mm.

3.1.4. Preventing damage during inspection

Care must be taken to avoid scratching tubing during inspection. Air gauges have had their working surfaces covered with polytetrafluoroethylene to prevent metal-to-metal contact. Air-plug gauges have also been developed with air-support bearings to centralize the plug in the tubing.

It has not been feasible to protect mechanical bore gauges in any way.

3.2. Fuel pellets

The prime dimension of the fuel pellet is its diameter, since the difference between this and the internal diameter of the tubing is an important factor in the design of the fuel pin. Too small a clearance makes it difficult to load the pellets, while too large a clearance is objectionable in service.

As lobing occurs when pellets are ground on their circumference, their maximum diameters are checked by a ring gauge, and the minimum diameter by a snap gauge (caliper gauge).

When pellets are loaded into thin-walled tubing the latter may distort to accommodate them. It may therefore be more realistic to compare the circumferences of the tubing and the pellets rather than their diameters.

Two techniques have been developed to measure circumferences. First, the diameter is measured successively at different angles and the results are averaged. This is done automatically with up to 12 000 measurements per revolution. Alternatively, a follower-wheel technique has been developed. This is accurate to ± 15 μm on circumferences of 45 mm (Fig. 10).

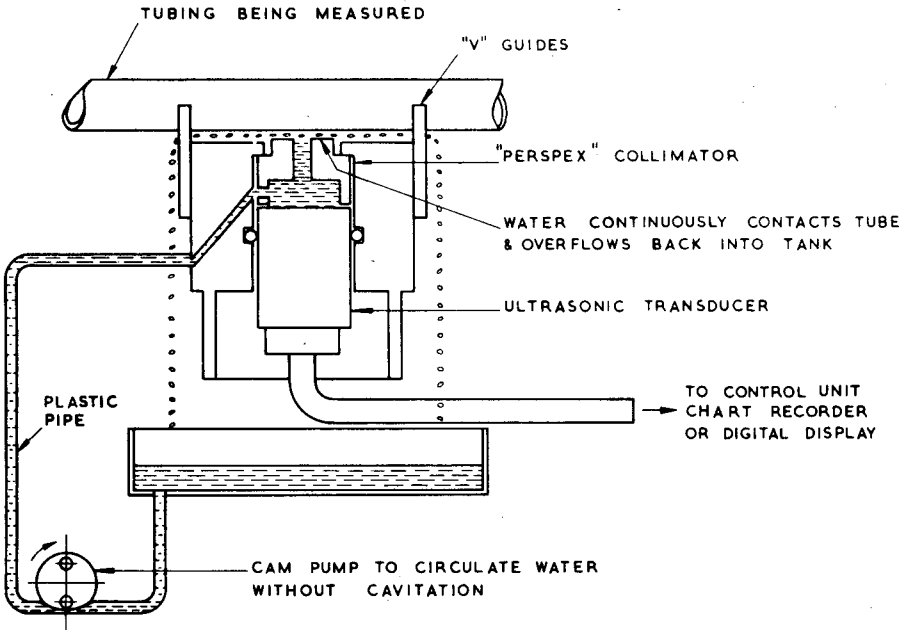

Fig. 9

Measurement of wall thickness of tubing ultrasonically

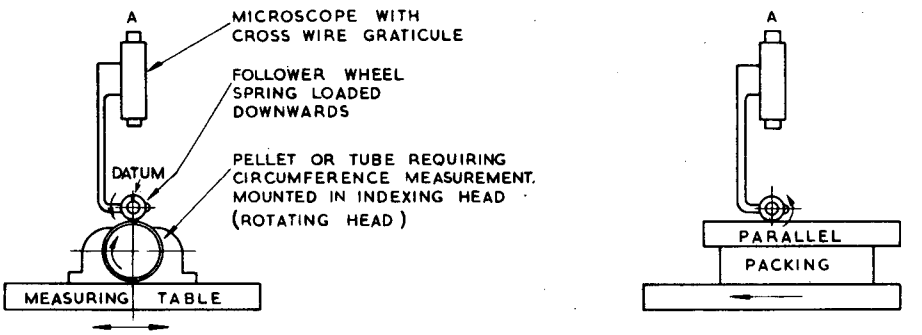

Fig. 10

Accurate measurement of circumference of pellet or tubing

Starting with the datum coincident with the graticule, the pellet is rotated accurately through 360°. The follower is raised and lowered again to a plane surface which is moved to return the follower to its original orientation. This movement is equal to the circumference of the pellet

These techniques have been used to measure external pellet and tube circumferences. Methods for measuring internal tube circumferences throughout the tube length are under development.

3.3. Complete semi-automatic tube inspection

With the development of efficient tube traversing equipment for ultrasonic flaw detection, it has been possible to develop similar equipment for the various dimensional measuring techniques. Rigs based on the equipment described above have been combined to form a complete tube-testing section which is operated by semi-skilled labour. The laboratories' requirements for precise information of tube sizes has been met by the automatic recording of measurements, eliminating a time-consuming manual method with its possibility of human error. The charts are then assessed and the tubes passed or rejected; the charts are stored should more detailed information later be required. Plans at present being discussed in the laboratory suggest that time and effort might be saved by having a central control unit capable of monitoring the various measuring rigs at the rate of several scans per rig per second. The results would be recorded on tape and then processed to give a complete collective assessment of the various measurements.

4. CHECKING THE INTEGRITY OF FINISHED FUEL PINS

Fuel pins are normally completed by welding end caps or plugs to the tubing containing the fuel. The integrity of these closures is assured by leak-testing the whole pin, and by radiographing the welds. It may also be noted that pins with welds which do not stand significantly proud of the sheath diameter may be tested for flaws, if required, on the same rigs as are used for tubing (sections 2.1 and 2.2).

4.1. Leak testing

The preferred method of test is to fill the pins with helium during manufacture and to test for leaks using a mass-spectrometer leak detector in the well-known way. Standards of tightness of 10^{-7} torr. 1 s^{-1} or better are commonly applied. The main precaution necessary in this test is to ensure that a pin with a large leak cannot be passed as sound because it has lost helium before the test is made. This can be ensured by imposing a limit to the time which elapses between filling and testing.

Pins which exceed this limit, or which were unavoidably made without helium filling, may be leak-tested by the "back-pressurizing" method [4, 5]. The pins are first immersed in the tracer gas (usually helium) at high pressure and then tested for the re-emission of the tracer from any leak. Sensitivities equal to those of the helium-filling technique may be obtained, though high pressures or long pressurizing times are needed if the internal volume of the pin is large.

The stipulation of a time-limit may also be avoided by filling with a radioactive tracer. If, for example, to the helium is added a small amount of krypton-85, the continued presence of the filling gas may be confirmed at any time by detecting the radiation from the Kr^{85} through the sheath of the pin. A helium leak-test may thus be given, following this confirmation, with

confidence that a zero result unambiguously indicates a sound element. If the pin cannot be gas-filled, the krypton may be added as a quinol clathrate – milligram amounts of quinol can carry an adequate activity – and the krypton-85 can also serve as the tracer gas.

The bubble technique of leak testing [6, 7, 8] is also used when stringent standards of tightness are not required, since its sensitivity cannot be assumed to be better than 10^{-4} to 10^{-5} torr.l s^{-1}. Its main use in U.K.A.E.A. laboratories has been in the location of leaks in elements rejected by other routine leak tests. For this purpose it is a cheap and rapid test, though not as sensitive as the "probing" or "sniffing" tests using helium and the mass spectrometer.

4.2. Radiography of end closures

The end-closure weld is normally circumferential; it is examined radiographically for adequate penetration and freedom from inclusions, blowholes etc. The end plug may be solid, in which case the region to be inspected is essentially the outer layer of a solid cylinder. A single radiograph, with the direction of radiation perpendicular to the axis of the pin, cannot be correctly exposed over the whole projected diameter of the pin. The weld is therefore normally examined by a series of such shots, the edges of the image being examined; the pin is rotated through a fixed angle, e.g. 20°, between each exposure. A rig is used to rotate a number of pins, radiographed simultaneously, and simultaneously to move the film between exposures. These actions are performed by pneumatic actuators controlled by the operator from outside the X-ray cell.

4.3. Radiography of complete pin

In the manufacture of experimental batches of fuel pins it is often desirable to radiograph the complete pin, to obtain information of the gaps between fuel pellets and the disposition of other components. To obviate perspective distortion, the pin and film are traversed beneath a slit to produce a "parallel-beam" radiograph. The pellet gaps are usually required to be the most sharply defined item, and it is possible to increase the width of the slit to say 3 cm for a source-film distance of 66 cm since gaps between pellets act themselves as collimating slits. Gaps down to 75 μm are detected in this equipment. The fuel pin presents the usual difficulty to the radiographer in accommodating components of widely differing absorptions in a single radiograph. The technique of colour radiography [9, 10] has been found useful in enabling a single radiograph to be produced of a pin which shows the tube, the gap between tube and fuel, gaps between fuel pellets, and some details of the fuel itself.

REFERENCES

[1] WALKER, D.C.B. and LUMB, R.F., Applied Materials Research (1964) 176-183.
[2] AVEYARD, S., Brit. J. non-destr. Test. 4 (1962) 120.

[3] AVEYARD, S. and SHARPE, R. S., in Proc. of the Fourth Int. Conf. on N. D. T., Butterworths, London (1964) 150-154.
[4] BLANC, B., D'ORIVAL, M. and CHOUMOFF, S., in Fuel Element Fabrications, 2, IAEA, Vienna (1961)3.
[5] HOWL, D. A. and MANN, C. A., R. F. L. Springfields U. K. A. E. A. (to be published).
[6] BIRAM, J. G. S., A. E. R. E. CE/R 2066 (1957).
[7] RATCLIFFE, R. T., Brit. J. appl. Phys. 15 (1964) 79-83.
[8] BIRAM, J. and BURROWS, G., Vacuum 14 (1964) 221-226.
[9] BEYER, N. S., ANL-6515 203-217.
[10] PARISH, R. W. and PULLEN, D. A. W., Brit. J. non-destr. Test. 6 (1964) 103-108.

DISCUSSION

P. de MEESTER: You also examine complete fuel pins by gamma scanning in your laboratory. From the technical and economic standpoints, do you prefer this technique or complete scanning on radiographic film?

G. MANN: I think the choice between the two methods depends on the information required. In production, including pilot-scale production, gamma-scanning with a chart record will usually be acceptable. If more information is required, for example on the distribution of fuel, a scanning radiograph may be considered desirable and worth the extra cost.

U. NYSTRÖM: What is the actual rotation speed when you test tubes ultrasonically for longitudinal and transverse defects, and why do you use a pitch of only 0.15 mm with the correspondingly low testing speed, which is a disadvantage from the economic point of view?

G. MANN: The speed depends on the diameter of the tube: small tubes may be rotated at several thousand rpm, larger ones at several hundred rpm. Reliable detection of the calibration notches is of course always a necessity. The pitch of 0.15 mm quoted is used for small tubes; larger tubes are tested with a larger pitch.

U. NYSTRÖM: I understand you use Branson commercial equipment for measuring the wall thickness of cladding tubes. From the harmonic resonance indications you showed on the screen during your oral presentation, I suppose you use the contact method. Why do you not use the immersion technique?

G. MANN: The immersion technique shown in Fig. 9 is normally used for tubes. Contact methods are used when necessary.

U. NYSTRÖM: In section 4.2 of your paper you say that a single radiograph of the welds of circular fuel rods cannot be obtained satisfactorily and that is the reason why you use the technique described. Have you tried using a block to compensate for the circular shape? If so, what is your opinion of the sensitivity which can be obtained with the two methods?

G. MANN: Multiple radiographs were used in our laboratories before the compensating block method was developed. Possibly because of the greater experience of our inspectors with the former method, we have preferred to continue using it. We see little difference in the sensitivities obtainable from the two methods.

U. NYSTRÖM: My last question relates to helium leak detection on fuel rods. I suppose you have a low rejection level so I wonder why you test the rods individually, as I understand you do, instead of testing larger batches.

G. MANN: No, in production on any scale we do indeed test pins in multiple batches.

G. VERSTAPPEN: Why do you use both ultrasonics and eddy currents in your laboratories, and what are the advantages of each method?

G. MANN: At the moment our normal flaw-detection test for thin-walled tubing is an ultrasonic test. We maintain an eddy-current flaw test because we think it dangerous to have only one test available. Sometimes, moreover, for example with experimental batches of tubing, the surface finish or the interference effects of intragranular products make ultrasonic testing difficult.

G. VERSTAPPEN: Do you then do the same tests with both methods and compare the results?

G. MANN: One must distinguish between tests on routine tubing which is being made in large quantities and development tests. We would not duplicate flaw tests on large amounts of tubing. Incidentally, we do not measure wall thickness using eddy currents.

SESSION IX

A FAST TEST FOR EXCESSIVE U^{235} CONCENTRATIONS IN ENRICHED FUEL ELEMENTS

A. D. McEACHERN
ATOMIC ENERGY OF CANADA LIMITED,
CHALK RIVER, ONTARIO, CANADA

Abstract — Résumé — Аннотация — Resumen

A FAST TEST FOR EXCESSIVE U^{235} CONCENTRATIONS IN ENRICHED FUEL ELEMENTS. This paper describes a new non-destructive method of detecting areas of enriched fuel elements containing excessive U^{235}, and an instrument designed to inspect uranium-aluminium alloy fuel for the NRU reactor using the new method. The new method is as precise as conventional methods but is much faster. The improvement in test speed depends on the application, but typically may be a factor of four. Alternatively, the method may be used to improve the precision of the test without increasing the testing time.

The method may be used when the U^{235} concentration in selected areas of a fuel element is estimated by measuring the intensity of 184-keV γ-rays (from the natural decay of U^{235}) and when an area is considered acceptable if the measured intensity from it is less than a limiting intensity equivalent to the maximum allowable U^{235} concentration. If the measured intensity is much less or much greater than the limiting intensity, much less time is required to make this decision than when they are nearly the same. The new method takes advantage of this. It thus inspects each area only as long as is necessary to make a decision with the required confidence. The average time taken in practical cases is less than that taken by conventional methods which inspect each area for a pre-selected time chosen to give the required confidence in the most difficult cases – when the measured and limiting intensities are nearly the same.

The new method is based on sequential sampling theory. It may also be used to detect areas with undesirably low U^{235} concentration.

DÉTECTION RAPIDE DES CONCENTRATIONS EXCESSIVES DE ^{235}U DANS LES ÉLÉMENTS COMBUSTIBLES EN URANIUM ENRICHI. Le mémoire décrit une amélioration des méthodes classiques de détection, dans les éléments combustibles en uranium enrichi, des zones qui contiennent une trop forte quantité de ^{235}U. On a conçu un instrument pour examiner, par cette méthode perfectionnée, le combustible en alliage uranium-aluminium destiné au réacteur NRU. Cette méthode est aussi précise que les méthodes classiques, mais beaucoup plus rapide. L'économie de temps dépend du mode d'application; elle peut être normalement de l'ordre du facteur quatre. On peut également appliquer cette méthode pour accroître la précision de l'essai sans en augmenter la durée.

La méthode est applicable lorsqu'on évalue la concentration de ^{235}U dans une zone donnée en mesurant l'intensité des rayons gamma de 184 keV (émis lors de la désintégration naturelle de ^{235}U) et que l'on considère une zone comme acceptable si l'intensité mesurée du rayonnement qui en émane est inférieure à une limite correspondant à la concentration maximum admissible de ^{235}U. Si l'intensité mesurée est sensiblement inférieure ou supérieure à cette limite, il faut beaucoup moins de temps pour se prononcer que lorsqu'elle lui est sensiblement égale. La méthode améliorée tire parti de ce fait. L'examen de chaque zone ne dure que le temps strictement nécessaire pour prendre une décision avec la confiance voulue. Dans la pratique, le temps moyen nécessaire à cet effet est inférieur à celui qu'exigent les méthodes classiques, qui consistent à examiner chaque zone pendant un temps prédéterminé de manière à pouvoir se prononcer avec confiance dans les cas les plus difficiles: intensité mesurée très voisine de la limite.

La méthode perfectionnée est fondée sur la théorie de l'échantillonnage continu. On peut également l'appliquer pour détecter les concentrations trop faibles de ^{235}U.

БЫСТРОЕ ОПРЕДЕЛЕНИЕ ИЗЛИШНИХ КОНЦЕНТРАЦИЙ U-235 В ОБОГАЩЕННЫХ ТОПЛИВНЫХ ЭЛЕМЕНТАХ. Описывается усовершенствование обычных методов обнаружения тех мест в обогащенных топливных элементах, в которых содержится излишнее количество урана-235. Разработан прибор для проверки топлива, изготовленного из сплава уран-

алюминий, для реактора NRU с использованием этого усовершенствованного метода. Усовершенствованный метод такой же точный, как и обычные методы, но значительно быстрее. Для типичного случая он дает результаты в четыре раза быстрее. Кроме того, усовершенствование можно направить на увеличение точности проверки без увеличения времени, необходимого для проведения такой проверки.

Метод можно применять, когда концентрация урана-235 в отдельных местах в топливных элементах определяется в результате измерения интенсивности гамма-лучей с энергией 184 кэв (в результате естественного распада урана-235) и когда считается, что это место *является приемлемым, если измеренная в этом месте интенсивность меньше*, чем эквивалент ограничивающий интенсивность в отношении максимально-допустимой концентрации урана-235. Если измеренная интенсивность значительно меньше или больше ограничивающей интенсивности, требуется значительно меньше времени для принятия решения, чем когда они почти одинаковы. Это и учтено при усовершенствованном методе. При этом методе проверяется каждое место, как только необходимо принять решение с необходимой уверенностью. Принимаемое в практических случаях среднее время меньше, чем при обычных методах, когда проверяется каждое место в предварительно определенное время с целью получения необходимой уверенности в наиболее трудных случаях, когда измеряемая и ограничивающая интенсивности почти одинаковы.

Усовершенствованный метод основан на теории последовательного отбора проб. Его можно также применять для обнаружения нежелательно низких концентраций урана-235.

ENSAYO RAPIDO PARA DETERMINAR CONCENTRACIONES EXCESIVAS DE ^{235}U EN ELEMENTOS COMBUSTIBLES ENRIQUECIDOS. El presente trabajo describe un perfeccionamiento introducido en los métodos corrientemente empleados para descubrir en elementos combustibles enriquecidos las zonas que contengan cantidades excesivas de ^{235}U. Se ha ideado un aparato para inspeccionar con este método el combustible a base de aleación uranio-aluminio, destinado al reactor NRU. El método perfeccionado es tan preciso como los corrientes, pero mucho más rápido. La reducción del tiempo necesario para la prueba depende de la aplicación, pero puede tomarse como valor típico una disminución a la cuarta parte de aquél. El mejoramiento puede aprovecharse asimismo para aumentar la precisión del ensayo, sin por ello prolongar su duración.

El método puede aplicarse cuando la concentración de ^{235}U en áreas seleccionadas de un elemento combustible se evalúa midiendo la intensidad de los rayos gamma de 184 keV (provenientes de la desintegración natural del ^{235}U) y cuando un área se considera aceptable si la intensidad medida en la misma es inferior a una intensidad límite equivalente a la máxima concentración admisible de ^{235}U. Si la intensidad medida es considerablemente menor o mayor que el valor límite, el tiempo necesario para tomar esa decisión es mucho más breve que el requerido cuando los valores son aproximadamente iguales. El método mejorado aprovecha esta característica inspeccionando cada área sólo el tiempo necesario para tomar una decisión con el grado de certeza requerido. El tiempo medio necesario en casos prácticos es inferior al que requieren los métodos clásicos, según los cuales, cada área se inspecciona durante un lapso predeterminado para obtener la certeza requerida en los casos más difíciles, o sea cuando las intensidades medida y límite son aproximadamente iguales.

El método mejorado se basa en la teoría de muestreo por secuencias. También puede aplicarse a concentraciones excesivamente bajas de ^{235}U.

INTRODUCTION

At Chalk River we inspect our enriched uranium-aluminium alloy fuel elements to detect areas with too much U^{235}. These areas are dangerous since they may get too hot in the reactor and cause fuel-element failure.

To detect them we measure the intensity of the 184-keV gamma-rays produced during the natural decay of U^{235} [1-3]. A sample of the fuel-element surface is viewed through a collimator by a gamma-sensor such as a scintillation crystal. It (with associated circuitry) produces electrical pulses with amplitude related to the energies of the gamma rays. The pulses corresponding to the energy of interest (184 keV in our case) are selected

and fed to an instrument which measures their rate of occurrence or "count-rate". Since the pulses occur randomly in time, the true average count-rate can only be estimated, and the accuracy of the estimate is increased only by observing the sample for a longer time so that more pulses are accumulated from each sample for the estimation of the average rate.

The test must decide whether the count rates from sampled areas of the fuel elements are greater or less than a limiting value, and the most efficient test makes these decisions with an acceptable accuracy in the shortest time. In order to compare different tests we can define two functions of interest.

The operating characteristic (OC)

The OC is the probability (P) of making a chosen decision for any test condition, and plotting it for different sample count-rates shows the accuracy of the test. For our purposes we are concerned with the OC curve showing the probability of deciding that a sample has a true count rate greater than a selected limiting value. If the limiting count-rate is N and the sample count-rate is fN, this is equivalent to deciding that f is greater than 1. I will refer to this as a "high" decision and to its alternative as a "low" decision.

THE AVERAGE SAMPLE TIME (AST)

The AST is the average time required to make either a high or a low decision for any given value of f or for an assumed distribution of f in a succession of samples. In general, increasing the accuracy of a test results in an increased AST.

I will first describe two conventional test methods which we have used for a number of years. They have acceptable OC curves but we have found them to be inconveniently slow. I will then describe our improved test method, which has a very similar OC curve but is much faster.

The physical size of the "sample" referred to depends on the collimator cross-section. When the fuel element is moved relative to the collimator (either in steps or continuously) so that adjacent samples are viewed in succession by the gamma-sensor, the scanning rate can be expressed in collimator-widths per second (if the width of the collimator cross-section is defined as its dimension in the direction of relative movement).

DIGITAL COUNTING FOR A FIXED TIME

This test counts the number of 184-keV gamma-rays emitted by each sample in a fixed time. It makes a high decision if the accumulated count in the selected time T is greater than TN, where N is the limiting count-rate. After time T the fuel element is moved to a new position and another sample is observed.

To compute the OC for this test, we first observe that for the tests of interest the results follow the Gaussian distribution curve with mean fNT

and standard deviation $\sqrt{fNT}$ [4]. We can compute the statistic

$$z = (NT - fNT)/\sqrt{fNT}. \quad (1)$$

Then

$$P = (1/\sqrt{2\pi}) \int_z^\infty \exp(-x^2/2)dx, \quad (2)$$

which is the Gaussian error function. The OC curve results from plotting P against f.

The AST for this test is constant and equal to T.

CONTINUOUS SCANNING WITH A COUNT-RATE METER

In this test the fuel element is moved past the collimator at a steady rate and the pulses are fed to a count-rate meter with a time constant t. The output of the count-rate meter is traced on a recorder chart, and a trace which goes above the level corresponding to N results in a high decision.

The standard deviation of the trace position resulting from a steady count-rate fN is $\sqrt{fN/2t}$ [5]. In this case a "steady" count-rate means one which has been observed by the count-rate meter for many time constants. This happens when changes in U^{235} concentration occur very gradually, and in this case

$$z = (N - fN)/\sqrt{fN/2t} \quad (3)$$

and P is calculated using equation (2). It is worth while noting that the OC of this test is identical to that for digital counting for a fixed time with T equal to 2t.

If there is a sudden change from a steady count-rate f_1N to a new one f_2N, at a time $1/R$ seconds after the change.

$$z = (N - M)/\sqrt{M/2t}, \quad (4)$$

where

$$M = f_1N + (f_2N - f_1N)(1 - \exp[1/Rt]). \quad (5)$$

If the sudden increase occurs in only a small spot, the maximum height of the trace indicating it is given by equations (4) and (5) with R equal to the scanning rate in collimator-widths per second. This limits the scanning rate if small spots are to be detected. We have found that setting R equal to $1/3t$ gives a reasonable compromise between the competing requirements of good discrimination and high scanning rate.

As for the fixed counting-time test, the AST is constant. It is the reciprocal of the scanning rate.

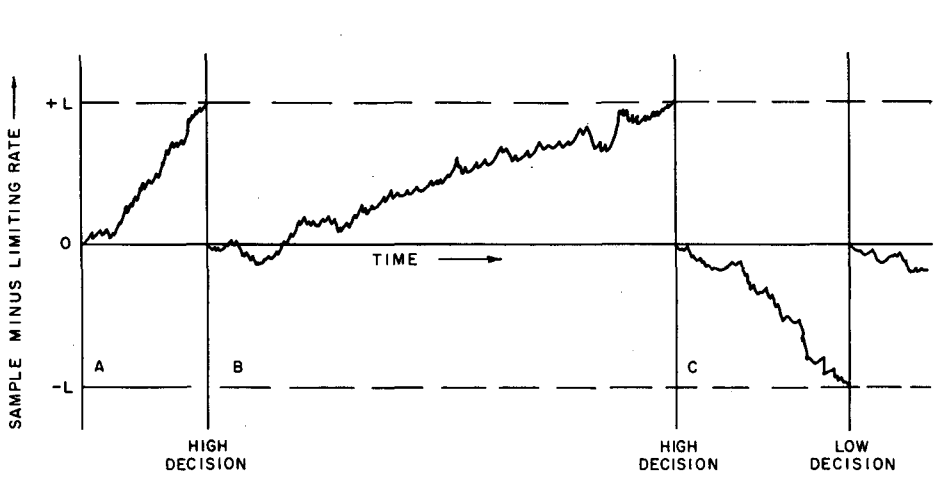

Fig. 1

Operation of sequential sampling circuit

DIGITAL COUNTING USING SEQUENTIAL SAMPLING

Sequential sampling techniques developed by WALD [6] have been used for a number of years in sampling inspection of manufactured products. COOKE-YARBOROUGH and BARNES applied developments of the theory [7, 8] to the problem of determining whether the intensity of radiation from a sample exceeds a limiting value, and our method is based on their treatment of the subject [9].

The difference between the sample count-rate fN and the limiting count-rate N is accumulated. If the difference reaches a preset limit L a high decision is made, and if it reaches -L a low decision is made. When either occurs, observation is stopped and the fuel element is moved to the next sample position. Figure 1 shows a sequence of events which might happen with this method. It shows that the time spent on successive samples is not constant but depends on their count rates.

To compute the OC function we first define a quantity q so that

$$(\ln q)/(q-1) = f. \tag{6}$$

Then when $f \neq 1$,

$$(1-q^{-L})/(q^{L}-q^{-L}) \geq P \geq (1-q^{-L})/(q^{L+1}-q^{-L}), \tag{7}$$

and when f = 1,

$$P = 0.5. \tag{8}$$

Three inequalities define the AST.
When f < 1,

$$(2LP - L)/(fN - N) \geq AST \geq ([2Lt1]P - L)/(fN - N). \tag{9}$$

When f > 1,

$$(2LP - L)/(fN - N) \leq AST \leq ([2L + 1]P - L)/(fN - N). \tag{10}$$

When f = 1,

$$L^2/N \leq AST \leq (L^2 + L + 0.5)/N. \tag{11}$$

Note that P for this test depends on f but not on N. Also, the AST is not constant but changes with both f and N.

A COMPARISON OF THE THREE METHODS

Figures 2 and 3 show OC and AST curves for the three methods, calculated using the relations described in the preceding sections. The limiting count-rate is 540 counts/s for the cases plotted. In Fig. 2, OC curves A and B have different shapes and so cannot be matched exactly, and I have chosen the parameters so that the two curves coincide where P equals 0.01 and 0.99. Below 0.01 curve A is slightly higher than curve B and above 0.99 it is slightly lower, although this is not evident from the graph.

Curve C is calculated from equations (4) and (5) and is included to show the effect on the count-rate meter test of small spots of high U^{235} concentration. Many examples could be plotted, but I have chosen one which is typical of our test conditions. This is a case where the limiting rate is a rejection level set 10% above the nominal U^{235} concentration. In our fabrication processes this nominal concentration is also the average and is therefore the most probable homogeneous matrix in which we may expect to find a small high-concentration spot. On the scale of Fig. 2 this nominal concentration corresponds to where f equals 0.91 and this is the value of f_1 which was used in equation (5). If a higher or lower value of f_1 is chosen curve C is shifted to the left or right respectively.

We used our sequential sampling instrument to get some experimental data for comparison with the theoretical curves for the sequential sampling test. The data are tabulated in Table I, and the resulting points are plotted in Figs. 2 and 3. As I will explain later, the instrument 'loses' about 8% of the sample counts at these count rates, so that for the sequential sampling test N is 500 counts/s to match the actual limiting rate of 540 counts/s. The points match the theoretical curves well within the measurement accuracy.

Figure 3 shows why the sequential sampling test is faster than the others. The test speed depends on the sample activities encountered in practice, and

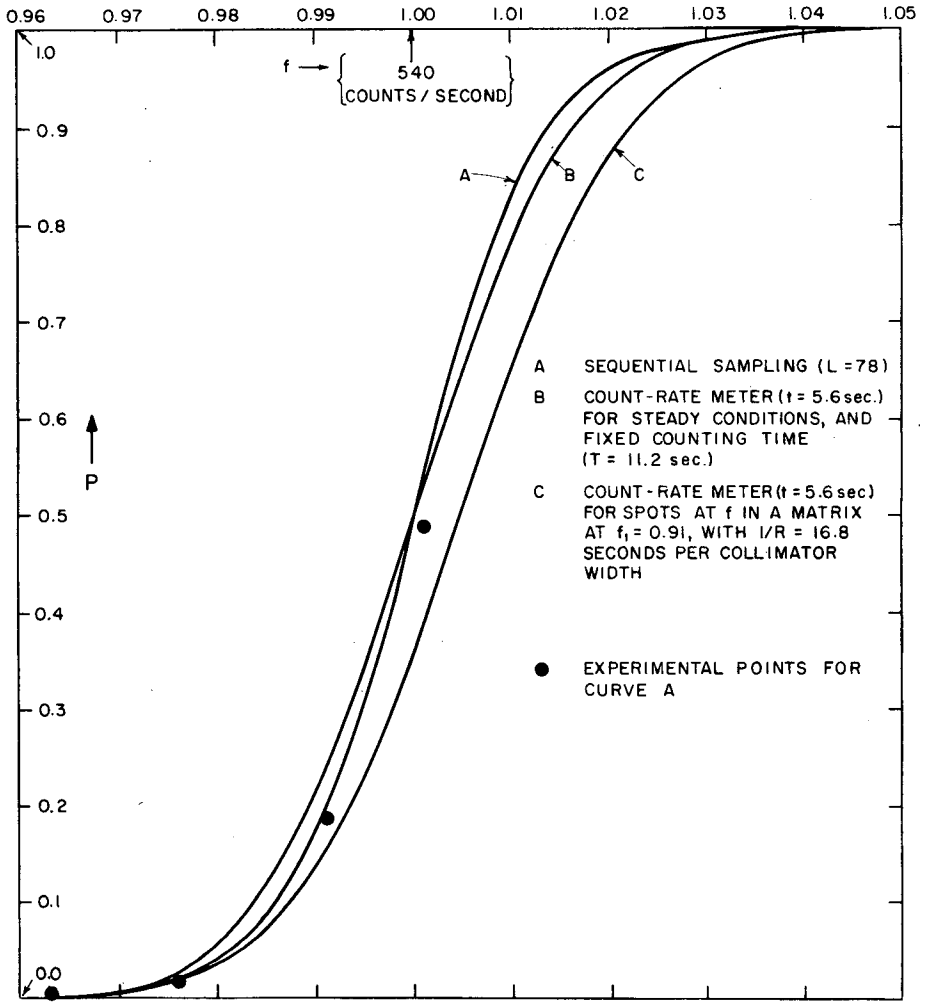

Fig. 2

Operating characteristic (OC) curves

estimates of it are subject to large errors. However, for our conditions where the limiting concentration is 10% above the nominal (and average) we can calculate two limiting cases:

(a) A rectangular distribution of concentrations from 10% below to 10% above nominal (from f = 0.83 to f = 1.00);

(b) A point distribution with all samples at the nominal value (f = 0.91).

In practice the U^{235} concentrations in the fuel elements may be represented by a Gaussian distribution around the nominal value more closely than by either of these cases.

An approximation of case (a) using an integration method described in Ref. [9] gives an average sample time of 3.35 s, and from Fig. 3 case (b)

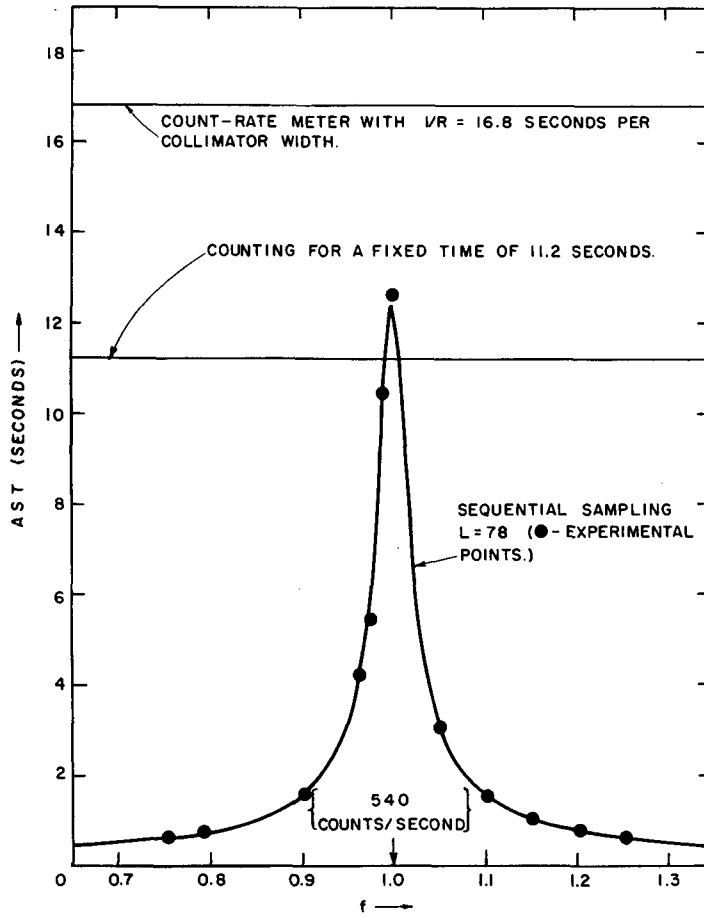

Fig. 3

Average sample time (AST) curves

gives 1.7 s. Comparing these figures to the 11.2-s sampling time for the fixed-time test gives increased test speeds of factors of 3.3 and 6.5 for the limiting cases, so that some increase between these limits will normally be realized in practice.

The purpose of all these tests is to decide whether samples have count rates above or below the limiting value. When the sample rate is close to the limit the measurement accuracy necessary to make this decision is greater than when it is much above or below it, and the sequential sampling test takes advantage of this. It spends only as long as is necessary on each sample, while the other methods spend as much time on each sample as is necessary only in the most difficult cases, when the sample and limiting rates are close together.

In this discussion I have considered cases where abnormally high U^{235} concentrations are of interest, but the same tests can be applied just as

TABLE I

DATA FOR THE SEQUENTIAL SAMPLING CURVES

Measured				Calculated		
Time (s)	fN* (counts/s)	Decisions High	Low	f	P	AST (s)
300	374.3	0	480	0.751	0.000	0.63
300	395.2	0	405	0.793	0.000	0.74
300	449.9	0	193	0.902	0.000	1.55
1000	480.5	2	236	0.964	0.008	4.20
1000	486.9	3	182	0.976	0.016	5.41
1000	494.4	18	78	0.991	0.188	10.42
3000	499.3	117	121	1.001	0.492	12.61
300	524.6	97	0	1.052	1.000	3.09
300	549.5	196	0	1.102	1.000	1.53
300	574.2	291	0	1.151	1.000	1.03
300	599.3	388	0	1.202	1.000	0.77
300	625.2	489	0	1.254	1.000	0.61

* N = 498.7 counts/s in all cases

well to inspection for low concentrations. If it is not worth while installing a special test for low concentrations, some qualitative information about them may be derived from the sequential sampling test described, since the inspection of a section of a fuel element in an unusually short time indicates that it has an unusually low average concentration.

A SEQUENTIAL SAMPLING TEST INSTRUMENT

We have built an instrument to inspect fuel elements using the sequential sampling test, and Fig. 4 shows a functional block diagram of it.

The heart of the instrument is the bi-directional scaler. This is a digital counter which adds one to its memory for a pulse at its forward input and subtracts one for a pulse at its reverse input. When its memory accumulates a value of L or -L (78 or -78 in the case we have considered) it provides an output pulse on the corresponding line. These pulses are recorded, and are also fed to an OR gate, which gives an output pulse for a pulse at either of its input lines. The OR gate output resets the scaler

SEQUENTIAL SAMPLING
CIRCUIT— BLOCK DIAGRAM

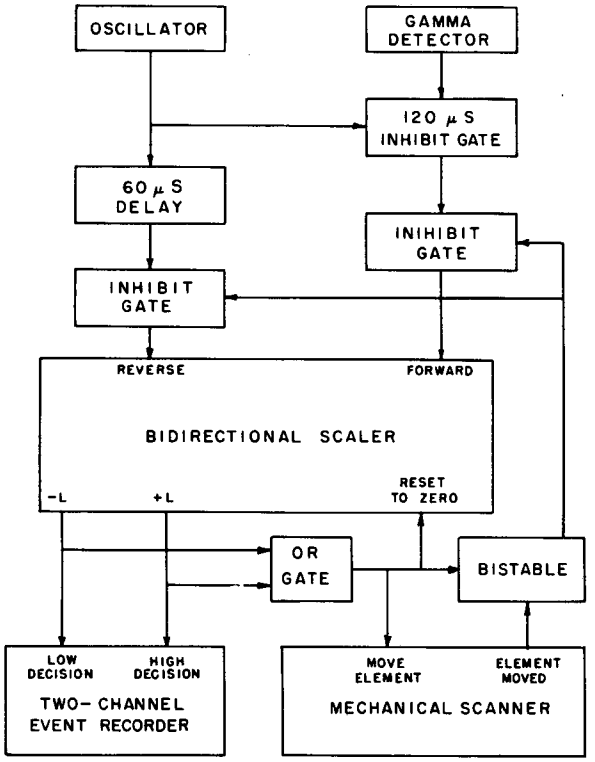

Fig. 4

Sequential sampling circuit - block diagram

to zero, signals the mechanical scanner to begin moving the fuel element to a new position, and sets a bistable switch. When the bistable is set in this way it provides an output which opens two inhibit gates in the inputs to the scaler, ensuring that no pulses enter it while the element is being moved. When the element is moved to the next sample position the mechanical scanner sends a pulse to the bistable to reset it. When it is reset the output to the inhibit gates is removed, so that pulses can again enter the scaler.

The pulses to the reverse input of the scaler come from a tuning-fork-controlled oscillator set to a frequency corresponding to the limiting count-rate, and the pulses to the forward input come from the gamma detector. A pulse on one input line which follows a pulse on the other one too closely can cause our scaler to make errors, so the 60-μs delay and 120-μs inhibit gate in the diagram were added to ensure that pulses on the two inputs are spaced by about 60 μs. In addition, the scaler will not register the second

of two pulses from the gamma detector which occur less than about 60 μs apart. Both these factors result in the loss of some of the sample pulses, and we have found that at count rates near 500 counts/s we lose about 8%. This does not affect the OC of the test, but it increases the AST.

With the exception of the recorder and the mechanical scanner, the instrument is made of solid-state circuit elements mounted on printed-circuit boards.

REFERENCES

[1] MORRISON, G. H. and COSGROVE, J. F., Analyt. Chem. 29 (1957) 1770.
[2] JUDD, W. C. and LEBOEUF, M. B., Report KAPL-1925 (1958).
[3] McEACHERN, A. D., Canadian Nuclear Technology 1, No. 3 (1962) 25-28.
[4] BEERS, Y., in Introduction to the Theory of Error, Addison-Wesley Inc., New York (1957) 46-9.
[5] ELMORE, W. C. and SANDS, M., in Electronics-Experimental Techniques, National Nuclear Energy Series, Div. V, 1, McGraw-Hill Inc., New York (1949) 252.
[6] WALD, A., Sequential Analysis, John Wiley and Sons Inc., New York (1947).
[7] KIEFER, J. and WOLFOWITZ, J., NRL Quarterly 3 (1956) 205-19.
[8] DVORETZKY, A., KIEFER, J. and WOLFOWITZ, J., Ann. Math. Stat. 24 (1953) 254-64.
[9] COOKE-YARBOROUGH, E. H., and BARNES, R. C. M., Proc. I. E. E. Part B 108 (1961) 153-66.

DISCUSSION

P. de MEESTER: If I understand Fig. 4 correctly, you are rather limited in count rate. From the inhibit gate working at 120 μs I assume that the maximum counting rate is between 1000 and 3000 counts/s. Is that right?

A. D. McEACHERN: You are correct. The main advantage of this method is realized when the count rate is low, as ours is (about 500 counts/s). If our count rate had been very much higher than the range you mention, it might not have been necessary to build this instrument.

THE NON-DESTRUCTIVE DETERMINATION OF BURN-UP BY MEANS OF THE Pr^{144} 2.18-MeV GAMMA-ACTIVITY

R. S. FORSYTH AND W. H. BLACKADDER
AB ATOMENERGI, STUDSVIK, SWEDEN

Abstract — Résumé — Аннотация — Resumen

THE NON-DESTRUCTIVE DETERMINATION OF BURN-UP BY MEANS OF THE Pr^{144} 2.18-MeV GAMMA-ACTIVITY. In recent years, gamma scanning has been used at several establishments for the determination of the burn-up profile along irradiated fuel elements, the 0.75-MeV gamma from Zr^{95}/Nb^{95} being most often used as the monitored radiation. Difficulties in establishing the geometry and the self-absorption of the gamma activity in the fuel have tended to prevent the application of the method to quantitative burn-up determination, which has usually been carried out by dissolution of selected portions of the fuel followed by conventional fission-product separation or by uranium-235 depletion methods.

The present paper describes experiments carried out to calibrate a gamma scanner for quantitative measurements by counting the 2.18-MeV gamma-activity due to Pr^{144}, the short-lived daughter of Ce^{144} ($T_{1/2}$ 285 d) from selected pellets in several UO_2 fuel specimens. Accurate burn-up values were then determined by dissolution and application of the isotopic dilution method using stable molybdenum fission products.

The elements, which were rotated about their longitudinal axes to minimize assymetry effects, were viewed by a sodium iodide crystal and a multichannel analyser through a suitable collimator. Correction for attenuation of the gamma activity (much less than for 0.75 MeV) in the fuel elements which were of different diameters (12.6 to 15.04 mm) was made by applying relative attenuation factors, and the effective geometry factor of the instrument was determined. In order to check the corrections applied, the counter factor was also calculated for the 0.75-MeV activity from Zr^{95}/Nb^{95}, and in certain cases for the 0.66-MeV activity from Cs^{137}. The results obtained demonstrate that, at least over the range of diameters and cooling times used, the method is suitable for quantitative determinations.

Preliminary experiments to explore the possibility of using the high-energy gammas (2.35, 2.65 MeV) from Rh^{106} as a method for estimating the fraction of fission events which have taken place in the Pu^{239} formed during irradiation have also been carried out. Determination of the relative intensities of the gammas suggests that the method is of only limited application.

DÉTERMINATION NON DESTRUCTIVE DE LA COMBUSTION MASSIQUE PAR MESURE DE L'ACTIVITÉ GAMMA (2,18 MeV) DE ^{144}Pr. Depuis quelques années, on a souvent recours à la gammagraphie pour déterminer le profil de la combustion massique le long des éléments combustibles irradiés; en général, on utilise pour cela les rayons gamma de 0,75 MeV émis par ^{95}Zr-^{95}Nb. Mais comme il est difficile d'établir la géométrie et l'auto-absorption de l'activité gamma dans le combustible, cette méthode se prête mal à la détermination quantitative de la combustion massique; on préfère habituellement procéder par dissolution de certaines portions du combustible et séparation des produits de fission ou par la méthode de l'appauvrissement en uranium-235.

Les auteurs décrivent les expériences faites en vue d'étalonner un appareil de gammagraphie pour permettre des mesures quantitatives par comptage de l'activité gamma ($T_{1/2}$ 2,18 MeV) de ^{144}Pr, produit de filiation à courte période de ^{144}Ce (285 j) dans les pastilles sélectionnées de divers spécimens de bioxyde d'uranium. On a ensuite déterminé les valeurs exactes de la combustion massique par dissolution et par dilution isotopique en utilisant les isotopes stables du molybdène produits de fission.

Les éléments combustibles, auxquels on imprime un mouvement de rotation suivant leur axe longitudinal pour diminuer les effets d'asymétrie, sont explorés par un cristal d'iodure de sodium et un analyseur multicanal muni d'un collimateur approprié. Pour tenir compte de l'atténuation de l'activité gamma (nettement moins marquée que pour 0,75 MeV) dans les éléments combustibles, qui étaient de diamètres différents (12,6 à 15,04 mm), on a fait une correction en appliquant des facteurs d'atténuation relative; on a ensuite déterminé le facteur de géométrie effectif de l'instrument. Pour vérifier les corrections appliquées, on a également calculé le rendement du détecteur pour l'activité gamma (0,75 MeV) de ^{95}Zr-^{95}Nb et, dans certains cas, pour

l'activité gamma (0,66 MeV) de ^{137}Cs. Les résultats obtenus montrent que, tout au moins pour la gamme des diamètres et des temps de refroidissement considérés, la méthode convient pour des mesures quantitatives.

On a également procédé à des expériences préliminaires pour étudier la possibilité d'utiliser les rayons gamma de haute énergie (2,35, 2,65 MeV) de ^{106}Rh pour évaluer la fraction d'événements de fission qui se produit dans ^{239}Pu formé pendant l'irradiation. Le résultat de la détermination des intensités relatives des rayons gamma donne à penser que cette méthode n'a qu'une application limitée.

ОПРЕДЕЛЕНИЕ СТЕПЕНИ ВЫГОРАНИЯ НЕДЕСТРУКТИВНЫМ МЕТОДОМ С ПОМОЩЬЮ ГАММА-АКТИВНОСТИ ПРАЗЕОДИМА-144 С ЭНЕРГИЕЙ 2,18 Мэв. В последние годы в некоторых научно-исследовательских центрах гамма-сканнирование применяли для определения профиля выгорания в облученных топливных элементах, при этом в качестве контролируемого излучения чаще всего использовали гамма-излучение циркоций-95/ниобий-95 с энергией 0,75 Мэв. В связи с трудностями установления геометрии и определения самопоглощения гамма-активности в топливе не представлялось возможным применять этот метод для количественного определения выгорания, которое часто осуществляется путем растворения отдельных частей топлива, после чего применяются методы обычного разделения продуктов деления или обеднения урана-235.

Описываются эксперименты, проведенные с целью калибрования гамма-развертывающего устройства для осуществления количественных изменений путем счета гамма-активности с энергией 2,18 Мэв, порождаемой празеодимом-144, короткоживущим продуктом церий-144 (период полураспада 285 дней), взятым из отдельных таблеток в некоторых образцах топлива, изготовленного из UO_2. Затем определяли точные значения выгорания путем растворения и применения метода изотопного разбавления с использованием устойчивых продуктов деления молибдена.

Элементы, которые вращались вокруг своих продольных осей с целью сведения к минимуму эффектов асимметрии, наблюдали с помощью кристаллов иодида натрия и многоканального анализатора через соответствующий коллиматор. Путем применения соответствующих коэффициентов ослабления брали поправку на ослабление гамма-активности (значительно меньшее, чем при энергии 0,75 Мэв) в топливных элементах, которые имели различные диаметры (12,6-15,04мм), и определяли коэффициент эффективной геометрии прибора. С целью проверки применяемых поправок рассчитывали также коэффициент счетчика для активности циркоций-95/ниобий-95 0,75 Мэв, и в некоторых случаях для активности цезия-137 с энергией 0,66 Мэв. Полученные результаты свидетельствуют о том, что по крайней мере в диапазоне выбранных диаметров и переходов охлаждения этот метод пригоден для количественных определений.

Проведены также предварительные эксперименты с целью изучения возможностей применения гамма-излучения рения-106 большой энергии (2,35 и 2,65 Мэв) как метода определения доли случаев деления плутония-239 во время облучения. Определение относительных интенсивностей гамма-излучения показывает, что этот метод имеет лишь ограниченную сферу применения.

DETERMINACION DEL GRADO DE COMBUSTION POR MEDIOS NO DESTRUCTIVOS UTILIZANDO LA RADIACION GAMMA DE 2,18 MeV DEL ^{144}Pr. En varios establecimientos se ha venido utilizando en los últimos años la exploración con rayos gamma para determinar la variación del grado de combustión a lo largo de elementos combustibles irradiados; la radiación empleada más a menudo para fines de medición ha sido la gamma de 0,75 MeV, emitida por el $^{95}Zr/^{95}Nb$. Las dificultades con que se tropieza para establecer la geometría y la autoabsorción de la actividad gamma en el combustible, han impedido aplicar ese método a la determinación cuantitativa del grado de combustión. Este suele determinarse disolviendo partes seleccionadas de combustible y separando por procedimientos clásicos los productos de fisión, o bien por métodos de agotamiento del ^{235}U.

El presente trabajo describe los experimentos realizados con miras a calibrar un dispositivo explorador de rayos gamma, destinado a mediciones cuantitativas por recuento de la actividad gamma de 2,18 MeV debida al ^{144}Pr, descendiente de período breve del ^{144}Ce ($T_{1/2}$ 285 d), presente en pastillas escogidas de varias muestras de UO_2. Los grados exactos de combustión se determinaron luego por disolución y aplicando el método de dilución isotópica, para lo cual se emplearon productos estables de la fisión del molibdeno.

Un cristal de yoduro sódico y un analizador multicanal «vefan», a través de un colimador adecuando, los elementos combustibles a los que se hacía girar alrededor de sus ejes longitudinales a fin de reducir al mínimo los efectos de asimetría. La atenuación de la actividad gamma (mucho menor que para el caso de 0,75 MeV) en los elementos combustibles de distintos diámetros (12,6 a 15,04 mm), se corrigió aplicando

factores de atenuación relativa, y se determinó el factor geométrico efectivo del instrumento. A fin de verificar las correcciones aplicadas, también se calculó el factor del contador para la actividad de 0,75 MeV emitida por el $^{95}Zr/^{95}Nb$, y en algunos casos para la actividad de 0,66 MeV del ^{137}Cs. Los resultados obtenidos demuestran que, al menos dentro del intervalo de diámetros y tiempos de enfriamiento utilizados, el método se presta a determinaciones cuantitativas.

También se han realizado experimentos preliminares destinados a explorar la posibilidad de usar los rayos gamma de alta energía (2,35 y 2,65 MeV) emitidos por el ^{106}Rh en la determinación del grado de fisión sufrido por el ^{239}Pu formado durante la irradiación. La determinación de las intensidades relativas de los rayos gamma sugiere que el método sólo posee una aplicación limitada.

1. INTRODUCTION

1.1. The determination of the burn-up of irradiated fuel, in the form of irradiation specimens, fuel elements or assemblies, has received increasing attention during the past few years. The earlier approach of dissolution followed by uranium-depletion analysis or by conventional radiochemical separation procedures for various fission products such as Zr^{95}, Cs^{137} or Sr^{89}, has been complemented and often superseded by the isotopic-dilution technique using stable molybdenum or neodymium fission products [1, 2]. This technique offers increased accuracy and precision, and independence of variation of fission rate throughout the irradiation period or detailed irradiation history. Growing interest in mass-spectrometric methods is reflected in the number of papers describing such methods at the recent Gatlinburg conference [3].

1.2. The use of gamma-spectrometry or gamma-scanning for the non-destructive determination of burn-up, which is considered in this paper, cannot at present reach the same accuracy as the destructive methods, but nevertheless offers obvious advantages in time and expense and, in certain circumstances where it is desirable to avoid fuel dissolution, it may be the most suitable method.

Gamma-scanning is used in several laboratories [4-7] including Studsvik for the determination of burn-up profile along irradiated fuel-elements, and the location of cracks or discontinuities. Usually the gamma activity at 0.75 MeV due to the Zr^{95}/Nb^{95} fission-product couple has been scanned by a shielded sodium-iodide crystal and the channel-output counting-rate presented on a recorder as the element is moved at a fixed speed past the collimator.

The method has several limitations: the short half-lives involved (Zr^{95}, 65 d: Nb^{95} 35 d) restrict the range of irradiation times to periods of a few months and correction for planned and un-planned reactor shut-downs involves cumbersome calculations. The difficulty of determining the geometry of the specimen and the self-absorption of the emitted gamma-activity in the fuel has prevented the method from being used quantitatively, and where this is desired the results have been put on a quantitative basis by the subsequent dissolution of selected parts of the fuel followed by radiochemical analysis, thus losing the major advantage of the method.

1.3. The use of more energetic gammas reduces the importance of self-absorption in the specimens, and the 1.6 MeV-gamma from La^{140} has

been used for specimens irradiated and cooled for short periods [8]. By using the 2.18-MeV gamma from Pr^{144}, the daughter of Ce^{144}($T_{\frac{1}{2}}$, 285 d) the problems of both half-life and attenuation are alleviated, and this has been considered by several authors [7, 9, 10]. In the latter reference, experimental work is described, but once again destructive analysis was performed to establish a quantitative basis for the results.

1.4. In the present paper, the calibration of a gamma-scanner for quantitative burn-up measurement is described. After an initial gamma-scan using the 0.75-MeV peak, the burn-up at fixed points along the length can be determined by means of the 2.18-MeV gamma-activity. We describe the calibration of the instrument by means of three fuel specimens of different diameters and cooling times and their subsequent dissolution and analysis by the stable molybdenum method. For other elements, the instrument geometry factor thus determined can be applied, together with a factor allowing for the relatively low self-attenuation of the gamma-activity in the specimen.

2. EQUIPMENT

2.1. Scanner

A schematic diagram of the gamma-scanner built at Studsvik [11] and used in this work is shown in Fig. 1. The apparatus is conventional: the fuel, usually in the form of UO_2 pellets in a Zircaloy can, suspended vertically, is moved at a controlled speed (6 cm/min) past a collimator situated in a steel-lined hole in the cell wall, a fixed position being maintained by a pair of roller guides. Another motor can be used to rotate the element about its axis at a speed of 0.5 rpm.

For scanning experiments, slit collimators of 0.5, 1 or 2-mm aperture can be used, but for the Pr^{144} counts a hole collimator of 2-mm diam., scanning across the fuel diameter was preferred, and the effective volume of fuel examined was considered to be a pencil of UO_2 of this diameter through the pellet. This is thought to be a reasonable approximation since the fuel-to-collimator distance is small.

To minimize the effect of extraneous gamma from the fuel streaming through the steel liner, the sodium-iodide crystal at the outer end of the hole is screened by a lead cap with a central hole. The results were further improved by determining and subtracting instrumentally the background counts with the fuel in position by replacing the collimator by a solid lead plug of the same dimensions.

2.2. Gamma spectrometry

The collimated pencil of gammas from the specimen were viewed by a sodium-iodide crystal ($1\frac{3}{4}$ in×2 in), the output being analysed by a nuclear-data 512-channel analyser, half of the memory being used for the specimen spectrum and half for the background. No temperature control

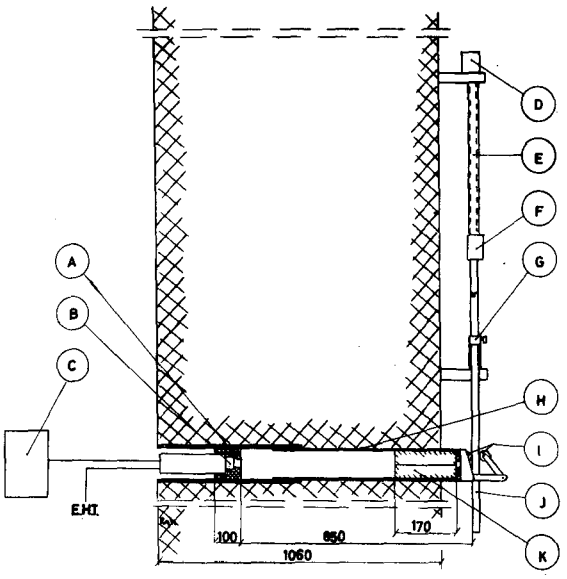

Fig. 1

Schematic diagram of the gamma scanner

A. Lead cap
B. Sodium iodide crystal
C. Multichannel analyser
D. Motor for vertical movement
E. Screw drive
F. Motor for element rotation
G. Pin coupling
H. Steel liner
I. Roller guides
J. Element
K. Collimator

was necessary since the ambient temperature in the building was sufficiently constant to prevent significant peak drift.

3. FUEL SPECIMENS

Only three fuel specimens were available for the calibration experiments, none with a shorter cooling time than five months. Brief details of the specimens are given below. Detailed information about reactor shutdowns is not given in order to save space, but these, of course, were taken into consideration in all calculation work.

Specimen 1: UO_2, fuel diam., 12.6 mm. Irradiation time, 8.05 d. Examined after cooling times of 155 and 181 d. Total fuel burn-up was 7.34×10^{17} fissions/g UO_2 at the position examined.

Specimen 2: UO_2, fuel diam., 15.04 mm. Irradiation time, 23.2 d. Examined after a cooling time of 373 d. Fuel burn-up was 1.10×10^{18} fissions/g UO_2.

Specimen 3: UO_2, fuel diam., 14.8 mm. Irradiation time, 19.5 d. Examined after cooling times of 508, 550, 625 and 646 d. Fuel burn-up was 1.60×10^{18} fissions/g UO_2.

4. METHOD

4.1. General

Although a form of calibration correlating the Pr^{144} counting rate with burn-up, allowing only for irradiation and cooling history, fuel geometry and gamma self-absorption can be carried out, in this work it has been preferred to extend the method to other gamma emitters, thus permitting a further check on the correction factors used and perhaps allowing more data to be available for scrutiny. For this purpose a knowledge of how the relative photo-peak efficiency of the detector crystal varies with incident gamma energy is required, together with data on gamma-branching ratios, half-lives and fission yields. All factors are considered more fully below.

4.2. Gamma counting-rates

Typical gamma spectra of the three specimens with background subtracted are shown in Figs. 2, 3 and 4, plotted to show the relative counts observed at low and high energies. The resolution of the 2.18-MeV gamma photo-peak was always between 5.5 and 6% (width at half-peak height). In each calibration experiment, the counting time was selected to give a total photo-peak count of not less than 4×10^4, giving a counting precision (3 σ) of 1.5% or better. For the Pr^{144} gamma peak this usually meant a counting time of several hundred minutes for the relatively low burn-up specimens examined.

Determination of the photo-peak counts was carried out by arithmetic addition of the appropriate channel counts and subtracting an arbitrary background considered as a straight line connecting the minimum on the high-energy side to half the height of the valley on the low-energy side. This procedure could not be used directly when peaks at 0.66 MeV (Cs^{137}) and 0.75 MeV (Zr^{95}/Nb^{95}) were both evident and the results from these spectra are, of course, less accurate.

4.3. Crystal efficiency

The gamma counting-rates as determined in 4.2 were then corrected for the photo-peak efficiency of the sodium-iodide detection crystal to enable counts at different energies to be compared directly. Data were obtained from the literature [12] and checked by isotopes calibrated by 4π counting, satisfactory agreement being obtained. All efficiencies were calculated with respect to the Cs^{137} 0.66-MeV gamma, which was given an arbitrary efficiency of 1. The relative crystal efficiency curve is shown in Fig. 5.

4.4. Gamma attenuation in can and fuel

The relative counting-rates were then corrected for attenuation in the Zircaloy canning, and self-absorption in the UO_2 fuel. Figure 6 presents curves showing the relative percentage transmission perpendicular to the surface of gammas of 2.18, 0.75 and 0.66 MeV from varying thicknesses

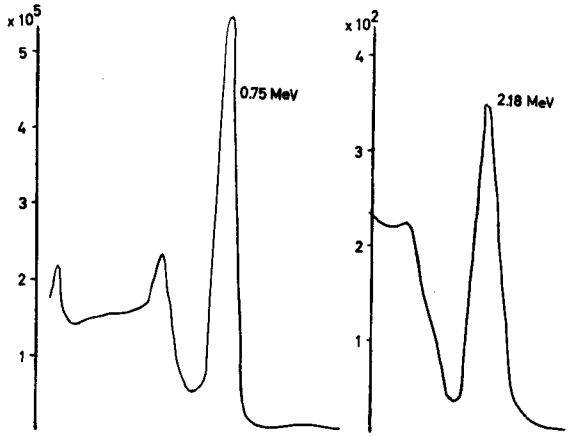

Fig. 2

Gamma spectrum of specimen 1.
(155-d cooling)

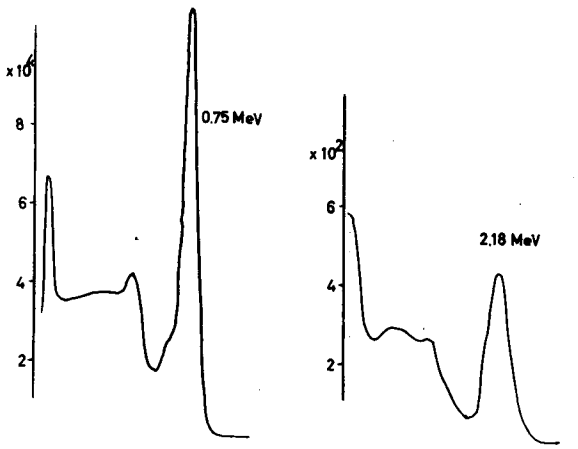

Fig. 3

Gamma spectrum of specimen 2.
(373-d cooling)

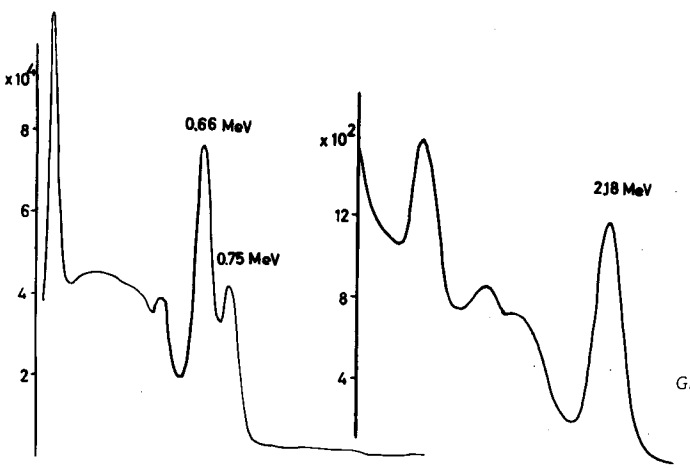

Fig. 4

Gamma spectrum of specimen 3.
(625-d cooling)

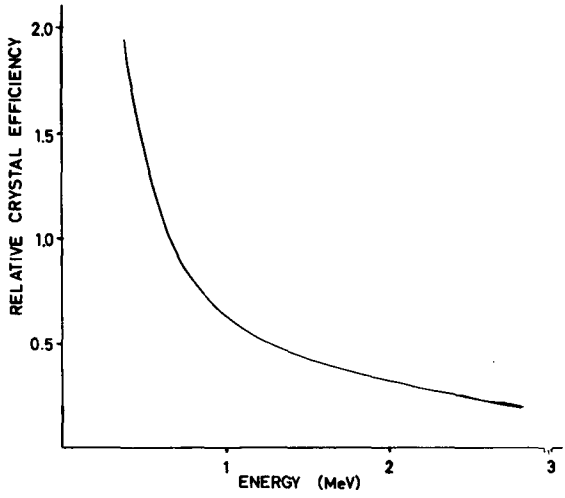

Fig. 5

Relative photo-peak efficiency curve of the $1\frac{3}{4}$ x 2-in sodium iodide crystal

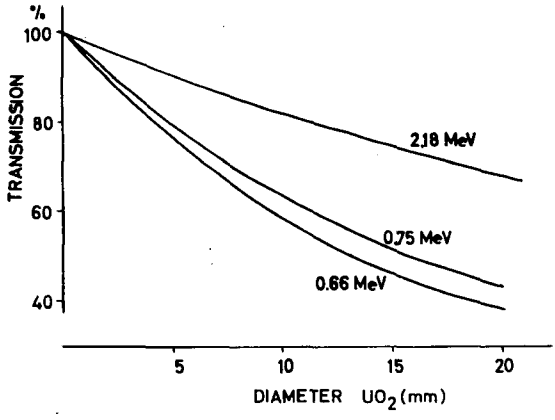

Fig. 6

Relative transmission curves of various gamma activities from UO_2 fuel

of UO_2, the mass absorption coefficients used being those given by BERRY [13]. It is not claimed that the curves are accurate, but it is considered that they give the relative values, and demonstrate how much less sensitive to self-absorption effects is the 2.18-MeV gamma-activity.

4.5. Fuel geometry

The final correction to the counting results is to calculate the observed activity per gram of fuel. As mentioned in 2.1, the volume of fuel scanned is considered to be a pencil of UO_2 of diam. 2 mm across the pellet diameter. The original density of the UO_2 is then used to calculate the weight.

4.6. Calculated activity

To determine the calibration factor F, the observed counting rates for Pr^{144}, and where possible Zr^{95}/Nb^{95} and Cs^{137}, corrected as described in 4.2 to 4.5, were compared with the total calculated activity per gram of fuel of the appropriate isotope for each of the three fuel specimens. To carry this out, samples of the pellets examined by spectrometry were dissolved and the burn-up determined accurately by the stable molybdenum method [1]. By use of the detailed irradiation history of each specimen,

TABLE I

DATA USED IN ACTIVITY CALCULATIONS

Isotope	Energy (MeV)	Half-life	Branching ratio (%)	Fission yield (%)
Pr^{144} (Ce^{144})	2.18	285 d	0.8	6.0
Zr^{95}	0.75	65 d	98	6.2
Nb^{95}	0.76	35 d	99	
Cs^{137}	0.66	30 yr	82	6.15

together with values of fission yield [14] and half-life and branching ratios [15], the activity of each gamma at the time of the gamma measurements could then be readily calculated. The constants used in the calculations are given in Table I. The calibration factor F represents the ratio of calculated activity to the corrected observed activity.

5. RESULTS

5.1. Element rotation

Some experiments were carried out to determine the degree of irradiation asymmetry of the elements due to their position in the reactor. The rod of specimen 2 was moved past the collimator until the selected pellet was being viewed by the collimator, and was then counted thirteen times, rotating the element through 90° after each count. The counting rates at 0.75 MeV and 2.18 MeV were then calculated, and the results demonstrated an apparent difference of about 9% between the 0.75-MeV activity viewing with the element at 0° and 180°, whereas the activities at 90° and 270° were the same and equal to the mean. A rather smaller asymmetry was noted with the 2.18-MeV activity. A similar effect was observed with specimen 3.

Hence, in all experiments, the elements were rotated axially while being counted to obtain a mean burn-up over the whole pellet cross-section.

Particularly with a hard gamma such as the Pr^{144} 2.18-MeV gamma, this would also help to even out possible migration effects.

5.2. Calibration results

Tables II, III and IV give the results of the calibration experiments on specimens 1, 2 and 3, respectively, and show the gamma counting-rates observed, the counting-rate per gram of fuel corrected as described in parts 4.2 - 4.5, the total activity of the particular gamma as calculated by the method described in part 4.6, and the calibration factor F.

TABLE II

SPECIMEN 1: RESULTS OF CALIBRATION EXPERIMENTS

Isotope	Cooling time (d)	γ/min (observed)	γ/min/g UO_2 (corrected)	γ/min/g UO_2 (calculated)	Calibration factor F ($\times 10^5$)
Zr/Nb^{95}	155	1.53×10^5	7.79×10^5	1.62×10^{11}	2.08
Pr^{144}	155	155	1.69×10^3	4.04×10^8	2.39
Zr/Nb^{95}	181	1.14×10^5	5.82×10^5	1.27×10^{11}	2.19
Pr^{144}	181	147	1.60×10^3	3.79×10^8	2.36

TABLE III

SPECIMEN 2: RESULTS OF CALIBRATION EXPERIMENTS

Isotope	Cooling time (d)	γ/min (observed)	γ/min/g UO_2 (corrected)	γ/min/g UO_2 (calculated)	Calibration factor F ($\times 10^5$)
Zr/Nb^{95}	373	2.42×10^4	1.12×10^5	2.48×10^{10}	2.21
Pr^{144}	373	156	1.47×10^3	3.50×10^8	2.37

The values for the 0.75 and 0.66-MeV peaks from specimen 3 are given only for the first two experiments. In the last two, the problem of allocation of counts in the partly resolved joint peak to Zr^{95}/Nb^{95} or to Cs^{137}, became too difficult. Even for the results quoted, the inaccuracy is high and they are included only to illustrate the method.

The calibration factors from all the experiments are collected in Table V, and it can be seen that the values calculated from the Pr^{144} activity results

TABLE VI

THE RELATIVE INTENSITIES OF THE HIGHER-ENERGY GAMMAS FROM Rh^{106}

Energy (MeV)			Relative intensity			
A	B	C	A	B	C	D
0.513	0.513	0.513	100	100	100	100
1.77	1.77	1.76	1.0	0.19	0.20	0.21
1.95	1.95	1.93	0.6	0.10	0.18	0.11
2.09	2.09	2.13	0.5	0.13	0.3	0.13
		2.30				
	2.36	2.37		0.17	0.6	0.21
2.41		2.44	1.0		0.03	
2.66	2.64	2.63	0.2	0.03	0.03	0.035

A. ALBURGER, J. et al., Phys. Rev. 100 (1955) 1357.
B. ROBINSON, R.L. et al., Phys. Rev. 119 (1960) 1962.
C. SEGAERT, O.J. et al., Nucl. Phys. 16 (1960) 138.
D. This paper

TABLE V

COMPARISON OF CALIBRATION FACTORS

Specimen	Pellet diam. (mm)	Cooling (d)	Calibration factor ($\times 10^5$)		
			Pr^{144}	Zr/Nb^{95}	Cs^{137}
1	12.6	155	2.39	2.08	
		181	2.36	2.19	
2	15.04	373	2.37	2.21	
3	14.8	508	2.28	2.40	2.18
		550	2.40	2.37	2.29
		625	2.40		
		646	2.25		

show very satisfactory agreement. (The results are given to three significant figures to aid comparison, but of course, the precision of the mean calibration factor is probably about 5%.)

The bias of only about 8% between the results from the Zr^{95}/Nb^{95} activity (specimens 1 and 2) and the Pr^{144} activity must also be regarded as satisfactory considering the difference in fuel diameter and the effect this may have on the assumptions made with respect to attenuation and geometry. It could also, of course, be readily explained by inaccurate fission yields and, more probably, the inaccuracy of the branching ratio of the 2.18-MeV gamma used (0.8%).

5.3. Rh^{106} gamma activity

Since there was a possibility of the 2.18-MeV peak being augmented by the 2.1-MeV peak from Rh^{106}, the 30-s daughter of Ru^{106}, thus causing errors, it was decided to examine this effect in detail. It was also obvious that if a clearly resolved peak from Rh^{106} at still higher energy, say that at 2.65 MeV, could be observed, this would offer the possibility of using the ratio between the counting rates at the two energies as a measure of the number of fissions in the specimen originating in U^{235} or in Pu^{239}, since the fission yields of Ru^{106} are widely different for these isotopes (0.38%, 4.57%). This, of course, was not applicable to the low-irradiated specimens described in the paper, but could be valid for many power-reactor elements.

The published values for the relative intensities of the higher-energy Ru^{106} gammas show wide divergence, and it was decided to check the values, fairly approximately, using the multichannel analyser and two different efficiency-calibrated sodium-iodide crystals (2 in × $1\frac{3}{4}$ in and 3 in × 3 in). The results obtained, together with the literature values, are presented in Table VI. Only the results for the higher-energy gammas are given, since the peaks at 1.13 MeV and 1.55 MeV were readily shown to be due to summation effects.

Using the determined relative intensity data and the branching ratio for the Rh^{106} 0.51-MeV gamma given in reference [15], calculation showed that for each of the specimens examined, interference from the Rh^{106} 2.1-MeV peak was negligible.

It was further shown that, even after long cooling times, specimens which had an appreciable percentage of fission events due to Pu^{239}, grown in situ, would not give a clearly resolved peak at 2.65 MeV because of Rh^{106}.

6. CONCLUSIONS

It has been shown possible to calibrate a gamma-scanning apparatus for quantitative burn-up determination by a simple procedure using the 2.18-MeV gamma-activity from Pr^{144}. The approximations made with respect to attenuation and fuel geometry and the inaccuracies of nuclear constants seem to cancel out, at least over the range of fuel diameters and cooling times described here. Continuing work should improve the precision of the calibration, at present believed to be about 5%, and check its validity

TABLE IV

SPECIMEN 3: RESULTS OF CALIBRATION EXPERIMENTS

Isotope	Cooling time (d)	γ/min (observed)	γ/min/g UO_2 (corrected)	γ/min/g UO_2 (calculated)	Calibration factor F ($\times 10^5$)
Cs^{137}	508	3.54×10^8	1.59×10^4	3.46×10^9	2.18
Zr/Nb^{95}	508	8.20×10^3	3.85×10^4	9.23×10^9	2.40
Pr^{144}	508	171	1.62×10^3	3.70×10^8	2.28
Cs^{137}	550	3.35×10^3	1.51×10^4	3.45×10^9	2.29
Zr/Nb^{95}	550	5.32×10^3	2.51×10^4	5.95×10^9	2.37
Pr^{144}	550	145	1.39×10^3	3.34×10^8	2.40
Pr^{144}	625	121	1.16×10^3	2.78×10^8	2.40
Pr^{144}	646	123	1.18×10^3	2.64×10^8	2.25

with fuel of different diameters. The absolute accuracy, of course, is still dependent on the accuracy of the nuclear data used, particularly the fission yield, and the irradiation history, but the 285-d half-life helps to reduce the importance of the latter.

REFERENCES

[1] FORSYTH, R.S. et al., TID-7629, 166-76.
[2] FUDGE, A.J. et al., TID-7629, 152-65.
[3] The Eighth Conference on Analytical Chemistry in Nuclear Technology, Gatlinburg, Tennessee, 6th-8th October (1964).
[4] BURIAN, R.J. and GATES, J.E., BMI-1319 (1959).
[5] BURIAN, R.J. et al., TID-7599, 382-90.
[6] WEST, D.B. et al., TID-7599, 391-98.
[7] DIGGLE, W.R. and BLACKADDER, W.H., TRG Report 603 (D) (1963).
[8] FORSYTH, R.S. and DIGGLE, W.R., U.K.A.E.A. Internal Document IG Memo 230 (D) (1959).
[9] Reactor Technology Report No. 14, KAPL-2000-11 (1960).
[10] CORNISH, F.W. et al., AWRE O-22/61 (1962).
[11] DJURLE, S. and WINQVIST, B., unpublished work, AB Atomenergi, Studsvik.
[12] USAEC Nuclear Data Tables, Part 3 (1960).
[13] BERRY, P.F., Nucleonics Data Sheet, Nucleonics 19 6 (1961).
[14] Reference Data Manual, Nucleonics 18 11 (1960).
[15] ALLEN, R.A. et al., AERE-R 2938, 2nd edition (1961).

FUEL LOCATION, HOMOGENEITY AND AMOUNT IN FLAT AND TUBULAR CONFIGURATIONS

P. de MEESTER
STUDIECENTRUM VOOR KERNENERGIE, MOL, BELGIUM

Abstract — Résumé — Аннотация — Resumen

FUEL LOCATION, HOMOGENEITY AND AMOUNT IN FLAT AND TUBULAR CONFIGURATIONS. The fuel elements for the materials testing reactor BR-2 can be assembled either with plates obtained by the picture-frame process, or with tubes obtained by co-extrusion. In the course of the fabrication and before reactor loading the fuel disposition, the homogeneity and the absolute amount have to be checked or measured.

The fuel disposition should be known for positioning of the core in plates and tubes and as a first quality evaluation of the product with regard to the geometrical specifications. Radiography at about 80-90 keV, autoradiography and gammagraphy with a thulium-170 source have been done. By radiographing the fuel tubes a lead mandrel with the X-ray film fixed to it was placed inside the tube and subsequent X-ray shots at different angles were taken. A radioactive source scanning the fuel tube along its centre line in combination with a film around the tube showed records with a high resolution.

The fuel homogeneity is to be controlled in view of a safe reactor operation, i. e. on the one hand to avoid exaggerated fuel concentrations that could give rise to vapour formation in the operating PWR, and on the other hand to guarantee a sufficient and evenly spread fuel load. Radiographs can be used for a visual check. However, if a quantitative analysis is needed, a better device is a scintillation gamma spectrometer measuring the proper radiation emitted by the U^{235}. An analysis of the results on some 400 fuel plates and on a first batch of fuel tubes is given. Forming characteristics and typical end-forms can be controlled. Absorption measurements with an activated source gave less good results. Digital results from static measurements and continuous recording are discussed.

The fuel amount as an absolute quantity should be known per zone for actual reactor-operation calculations and per complete element for reasons of fuel accounting and for comparison with post-irradiation burn-up evaluation. The fabrication and the use of the different standards are considered. Accuracy and elimination of errors are discussed.

Some possible future improvements in the tests are proposed.

RÉPARTITION, HOMOGÉNÉITE ET QUANTITÉ DU COMBUSTIBLE DANS LES ÉLÉMENTS A CONFIGURATION PLATE OU TUBULAIRE. Les éléments combustibles pour le réacteur d'essai de matériaux BR-2 peuvent être réalisés, soit avec des plaques obtenues par cadrages, soit avec des tubes obtenus par coextrusion. Au cours de la fabrication et avant le chargement dans le réacteur, il faut vérifier ou mesurer la répartition, l'homogénéité et la quantité du combustible.

Il faut connaître la répartition du combustible pour le positionnement de l'âme dans les plaques et tubes ainsi que pour une première évaluation qualitative du produit du point de vue des spécifications géométriques. On a procédé à des radiographies à 80-90 keV, ainsi qu'à des autoradiographies et gammagraphies avec une source au thulium-170. Pour l'examen radiographique des tubes de combustible, on a introduit dans le tube un mandrin en plomb auquel était fixé un film sensible aux rayons X, puis on a fait des radiographies sous divers angles. En utilisant une source radioactive se déplaçant le long de l'axe du tube et un film placé autour du tube, on a obtenu des enregistrements avec un très bon contraste.

Il faut contrôler l'homogénéité du combustible pour assurer la sécurité du fonctionnement du réacteur, c'est-à-dire pour éviter toute concentration excessive de combustible pouvant donner lieu à des formations de vapeur pendant le fonctionnement du réacteur et pour garantir que le chargement de combustible est suffisant et régulièrement réparti. On peut faire appel à des radiographies en vue d'une vérification visuelle. Cependant, s'il est nécessaire de faire une analyse quantitative, il est préférable d'utiliser un spectromètre gamma à scintillation permettant de mesurer le rayonnement propre émis par l'uranium-235. Le mémoire contient une analyse des résultats obtenus pour quelque 400 plaques de combustible et pour un premier lot de tubes de combustible. Il est possible de contrôler les caractéristiques de déformabilité et les formes finales. La mesure de l'absorption à l'aide d'une source activée donne des résultats moins satisfaisants. L'auteur discute les données numériques obtenues à partir de mesures statiques et d'enregistrements continus.

Il faut connaître la quantité absolue de combustible par zone pour le calcul des paramètres de fonctionnement du réacteur, et par élément pour la comptabilité du combustible ainsi qu'aux fins de comparaison des taux d'irradiation. Le mémoire traite de la fabrication et de l'utilisation des divers étalons. Il discute le degré de précision et l'élimination des erreurs.

L'auteur propose plusieurs améliorations des opérations de contrôle.

ПОЛОЖЕНИЕ, ГОМОГЕННОСТЬ И КОЛИЧЕСТВО ТОПЛИВА В ПЛОСКИХ И ТРУБЧАТЫХ КОНФИГУРАЦИЯХ. Тепловыделяющие элементы для материаловедческого реактора BR-2 можно монтировать либо с пластинками, полученными в результате процесса кадровой рамки, либо с трубками, полученными с помощью одновременного продавливания. В процессе изготовления и до загрузки реактора необходимо проверить или измерить расположение, гомогенность и абсолютное количество топлива.

Расположение топлива должно быть известно для помещения сердечника в пластинах и трубках и для первой оценки качества продукта в отношении геометрических спецификаций.

С помощью тулия-170 были произведены радиография приблизительно при 80-90 кэв, авторадиография и гаммаграфия. При радиографии топливных трубок свинцовую оправку с прикрепленной к ней рентгеновской пленкой помещают внутрь трубки. Затем под различными углами делают рентгеновские снимки. Радиоактивный источник, сканнирующий топливную трубку вдоль ее центральной линии, в сочетании с пленкой вокруг трубки показывает записи, имеющие большую разрешающую способность.

Гомогенность топлива необходимо контролировать для обеспечения безопасной работы реактора, т.е., с одной стороны, с целью избежать избыточных концентраций топлива, которые могут вызвать парообразование при работе реактора, охлаждаемого водой под давлением, а с другой - обеспечить достаточную и равномерно распределенную топливную загрузку. Радиографы можно использовать для визуальной проверки. Если необходимо сделать количественный анализ, то лучшим прибором является сцинтилляционный гамма-спектрометр, измеряющий собственное излучение, которое испускает уран-235. Приводится анализ результатов, связанных приблизительно с 400 топливными пластинками и первой партией топливных трубок. Можно контролировать характеристики формирования и типичные концевики. Результаты абсорбционных измерений с помощью активированного источника являются несколько худшими. Рассматриваются цифровые результаты статических измерений и непрерывной записи. Для расчетов фактической работы реактора должно быть известно количество топлива, как абсолютное количество, на каждую зону и на каждый полный элемент в целях учета топлива и сравнения с оценкой выгорания после облучения. Рассматриваются изготовление и использование различных стандартов, а также точность и устранение погрешностей.

Предлагаются некоторые улучшения при проведении испытаний в будущем.

DISPOSICION, HOMOGENEIDAD Y CANTIDAD DE COMBUSTIBLES EN CONFIGURACIONES PLANAS Y TUBULARES. Los elementos combustibles para el reactor de ensayo de materiales BR-2 pueden armarse con placas tipo cuadro, o bien con tubos preparados por coextrusión. En el curso de la elaboración y antes de cargar el reactor, es nesesario verificar o medir la disposición, homogeneidad y cantidad absoluta de combustible.

La disposición del combustible debe conocerse para fijar la ubicación del alma en placas y tubos, y también como primera evaluación de la calidad del producto en lo que atañe a las especificaciones sobre su forma geométrica. Se han efectuado inspecciones mediante radiografía a unos 80-90 keV, autorradiografía y gammagrafía con una fuente de ^{170}Tm. Para radiografiar los tubos de combustible, se colocó en su interior un mandril de plomo al cual se había fijado la película de rayos X y se tomaron luego varias exposiciones desde distintos ángulos. Una fuente radiactiva usada para explorar el tubo longitudinalmente, combinada con una película dispuesta alrededor del tubo, permitió obtener registros de elevada resolución.

La homogeneidad del combustible debe controlarse con miras a un foncionamiento seguro del reactor, es decir, se han de evitar por una parte concentraciones excesivas de combustible que podrían producir vapor en el reactor de agua a presión (PWR) en funcionamiento, y por otra parte, garantizar una carga de combustible suficiente y uniformemente distribuida. Como verificación visual, puede usarse la radiografía. En cambio, si se necesita un análisis cuantitativo conviene emplear un espectrómetro de centelleo gamma que mida la radiación emitida por el ^{235}U. Se analizan en la memoria los resultados obtenidos con unas 400 placas de combustible y con una primera partida de tubos. Este método permite controlar las características de conformación y los casquetes. Las mediciones de absorción con una fuente radiactiva no dieron resultados tan satisfactorios. Se analizan en la memoria resultados numéricos de mediciones estáticas y de registros continuos.

La cantidad absoluta de combustible en cada zona debe conocerse para poder realizar los cálculos relativos al funcionamiento del reactor y también debe conocerse la cantidad de combustible contenida en casa elemento

completo, para poder llevar el control de las existencias de combustible y poder comparar con la evaluación del grado de combustión realizada después de la irradiación. Se considera en la memoria la elaboración y el uso de distintos elementos patrones. Se analizan el grado de exactitud y la eliminación de errores.

Se proponen algunas mejoras que podrían introducirse en los ensayos.

1. INTRODUCTION

A description is given of several assay techniques for MTR-type elements, developed at S.C.K./C.E.N. Mol some of which are already in use on a routine basis in the Belgian nuclear industry.

The fuel elements considered are those of the Belgian engineering test reactor BR2 which can operate at a maximum thermal flux of 10^{15} n/cm^2· s (Fig. 1) [1]. The fuel elements are assemblies, about 78 mm outer diameter, of concentric tubes, each with a fuelled length of about 760 mm. They contain 90% enriched-uranium fuel in the form of aluminium-clad U 24%-Al alloy tubes or bent plates. A standard element has six tubes for a total load of 244 g U^{235}. The concentric tubular form of the fuel assemblies allows the irradiation of small samples in a central experiment hole at very high thermal and epithermal fluxes.

The fuel elements generate large amounts of heat which are removed by the cooling light water. A maximum heat flux of about 400 W/cm^2 is reached, which is based on a fuel-load figure of 38.7 mg U^{235} cm^2. This figure is characteristic for plates as well as for tubes designed to be assembled with BR2 fuel elements, and thus fuel-element specifications impose tolerances on that figure, actually being $\pm$ 12%/cm^2 [2].

Two ways of assembling the BR2 fuel elements are possible; an assembly consists of a concentric arrangement of either fuel tubes or plates held at their ends by fittings, which are positioned by a central support tube. The plates are produced by the picture-frame technique, sheared and bent over 120°. Sets of three plates form tubes which are assembled progressively from the inner diameter to the outer one by a deformation locking technique. The tubes are produced by a coextrusion and cold drawing technique [3]. Data concerning the geometry and dimensions of the fuel element are given in Table I.

In the assay of such fuel elements some of the major items to be carried out in the course of fabrication and before reactor loading are the position of the meat, its homogeneity and the absolute amount of fuel in a plate, a tube or a complete fuel element.

2. FUEL LOCATION

2.1. Principle

The rolled fuel plates and the coextruded fuel tubes are to be sheared to their appropriate dimensions so that the meat is well positioned relative to the edges. On the other hand, in the scope of fabrication process studies a very important factor to be controlled and measured is the geometrical end forms of the fuel in plates as well as well as in tubes.

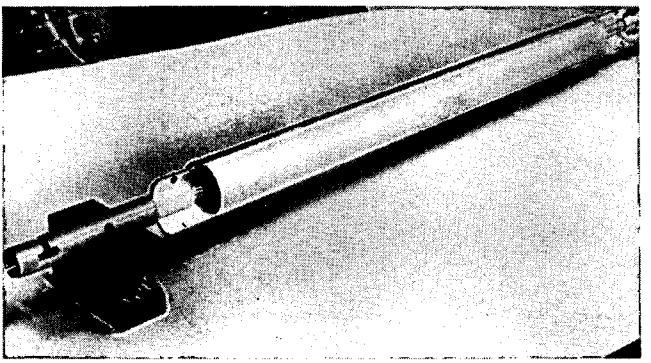

Fig. 1

BR2 fuel element

TABLE I

DATA FOR THE BR2 FUEL ELEMENT

Tube No.	Inner diam. (mm)	Minimum width of active core per plate (mm)	U^{235} amount per plate (g)
1	32.0	24.59	7.25
2	40.5	33.15	9.83
3	49.0	41.55	12.27
4	57.6	50.08	14.80
5	66.1	58.62	17.32
6	74.6	67.21	19.86

Wall thickness	: 1.27 mm
Cladding thickness	: 0.38 mm
Fuel alloy (meat) thickness	: 0.51 mm
Length of plate or tube	: 970 mm
Length of active core	: 762 ± 12.7 mm

Different techniques for fuel location have been used and compared. They should give information on the fuelled area, which can be easily interpreted and which should geometrically correspond as well as possible to the meat region. The fundamentals of these techniques are described [4, 5].

2.2. Radiography

The radiography of fuel plates is now merely a routine procedure. Two X-ray units, a Baltograph 200 and a Baltospot 300, were used with Gevaert

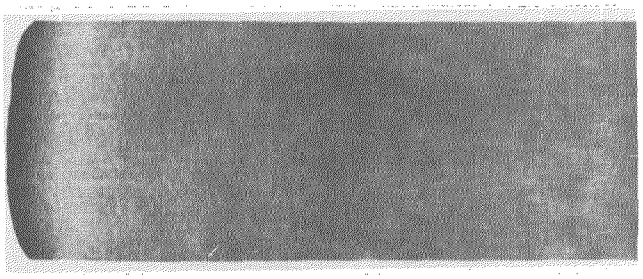

Fig. 2

Radiograph of extremity of fuel plate C.
Gevaert Litholine 081P, 100 kV, 3mA, 5 min, FF 70 cm, developer G 201

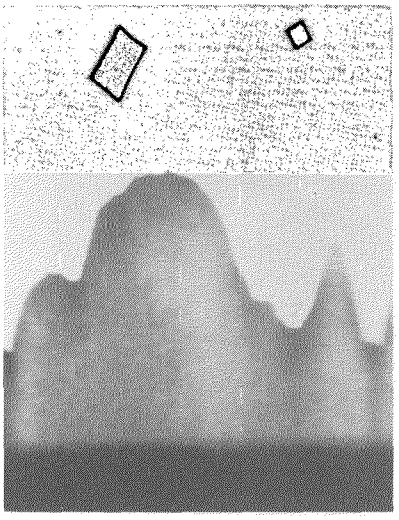

Fig. 3

Radiograph of fuel tube extremity.
Rotating while exposed.
Gevaert D7 film, 75 kV, 5 mA, 1.5 min,
FF 70 cm, developer G 201.

Scientia emulsions Structurix D7 and the shrinkage-free Litholine 081 p. As a basis for comparison for the different techniques a radiograph of a plate extremity is given with the appropriate data (Fig. 2). A marked dog-boning effect is visible, followed by a thinning of the alloy and a subsequent steady rise in fuel content.

The coextruded tubes can be radiographed by subsequent shots, the tube being turned over a given angle for each exposure. A more elegant technique, however, consists in radiographing the tube while continuously turning on two motor-driven cylinders. The X-ray unit stands above this rotation device, and over the tube is a lead collimator box with a 1-cm wide slit. In both cases the X-ray film is wound on a lead mandrel inside the

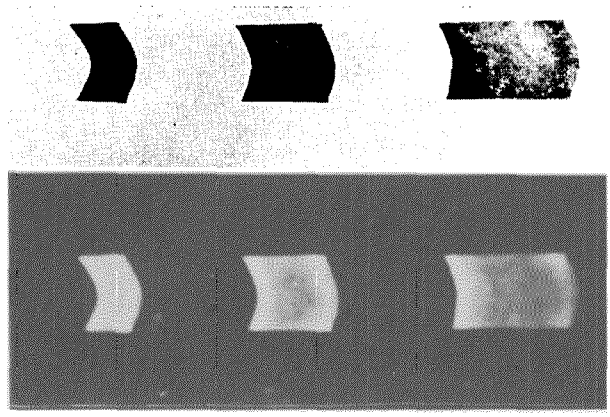

Fig. 4

Top: Radiograph of plate with separate fuelled areas. Gevaert Structurix D7, 75 kV, 3 mA, 1 min, FF 70 cm, developer G201.
Bottom: Autoradiograph of same plate area, Gevaert Structurix D10, 7 h.

tube so as to provide a close contact between the film and the inner wall of the tube. A tube end radiographed in this way is shown in Fig. 3.

2.3. Autoradiography

Autoradiographs have been obtained with the sensitive Gevaert Structurix D 10 emulsion. The contact method was used with about 5 – 15-h exposure time in a radiation-free space. Dense markers between fuel plate or tube and emulsion permit proper location. The edge resolution is only slightly lower than that with through radiography. Figures 4a and 4b show the difference between an X-ray graph and an autoradiograph of three small fuelled regions in a rolled plate. Figure 5 shows an inner and an outer autoradiograph of a coextruded tube end. The best results are obtained when the unwrapped film emulsion is placed on the plate or tube. In this way the closest contact is obtained and interfering effects such as paper texture and wrapping designs of the envelope can be avoided.

2.4. Gammagraphy

A device to check the fuel location and the distribution of the fuel over the total length of the tube has been built using a radioactive source (Fig. 6). Several sources have been tried; Tm^{170} turned out to be the most appropriate and most economic one. A source of 1 Ci encapsulated in a 3-mm-thick aluminium tube is mounted between two 10-mm-thick lead cylinders, so that only rays with relatively little parallax are emitted to the fuel tube which absorbs part of them (Fig. 7). A film emulsion is wound on the tube and covered by black paper to protect it from light. A 5-mm-thick lead tube surrounds the complete device as a shielding for the operator. The source hangs on a nylon wire wound on a motor-driven wheel; in this way the source

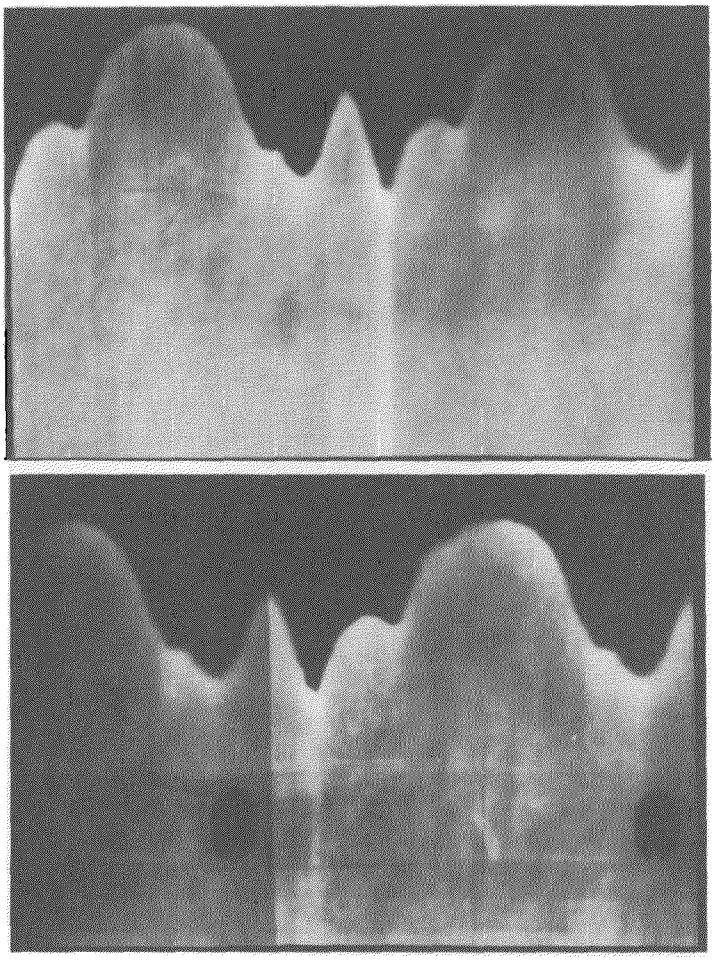

Fig. 5

Autoradiograph of fuel tube extremity. Gevaert Structurix D10, 15 h.

Top: Inner side.
Bottom: Outer side.

can scan the complete tube length while the fuel tube with lead shielding rotates on a turning table to smear out the geometrical asymmetry factor. Being lowered into the extreme position the source automatically rises again and will return into its own lead castle which rises further with it up to a preset micro-switch position.

Part of a gammagraph showing the extremity of a fuel tube is given in Fig. 8. The emulsion was Gevaert D 7 and the scanning speed of the source was about 1 cm/min. The complete tube was gammagraphed in one hour. Higher speeds (e.g. 10 min for a tube) can be obtained with D10 emulsion but then the resolution is reduced, which is partly because of an opposing autoradiography effect.

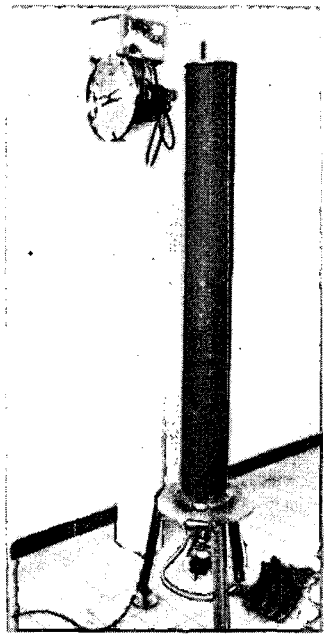

Fig. 6

Gammagraphy unit for BR2 tubes

3. FUEL HOMOGENEITY

3.1. Principle and equipment

As mentioned above, the fuel concentration is set at 38.7 mg/cm^2. The tolerance on this figure has been narrowed from ± 15% /in^2 to ± 12%/cm^2. A homogeneous distribution of the fuel is not only necessary to provide a smooth distribution of neutron flux and power in the operating reactor, but, moreover, the maximum permissible values are to be determined so as to avoid insufficient fuel loading as well as locally too high fluxes which may give rise to hot spots and reactor accidents. For these reasons a check for possible local variations in U^{235} concentration is highly desirable.

Several systems are used for checking the fuel homogeneity in elements. Radiography gives a clear picture, easy to interpret and to understand. Quantitative homogeneity results obtained by radiographic film technique, however, are less reliable on large surfaces and quite tedious to obtain. Most devices actually use a scintillation-counter system. The two principles adopted are either the absorption measurement of X-rays described by several authors [6, 7] or the measurement of the gamma-rays emitted by the fuel, which is the method used in several other institutes [8, 9, 10]; the latter procedure has also been adopted at S.C.K./C.E.N., Mol.

In our laboratory work is being done on an automatic scanning unit and on static manually operated equipment. Both devices are equipped with a

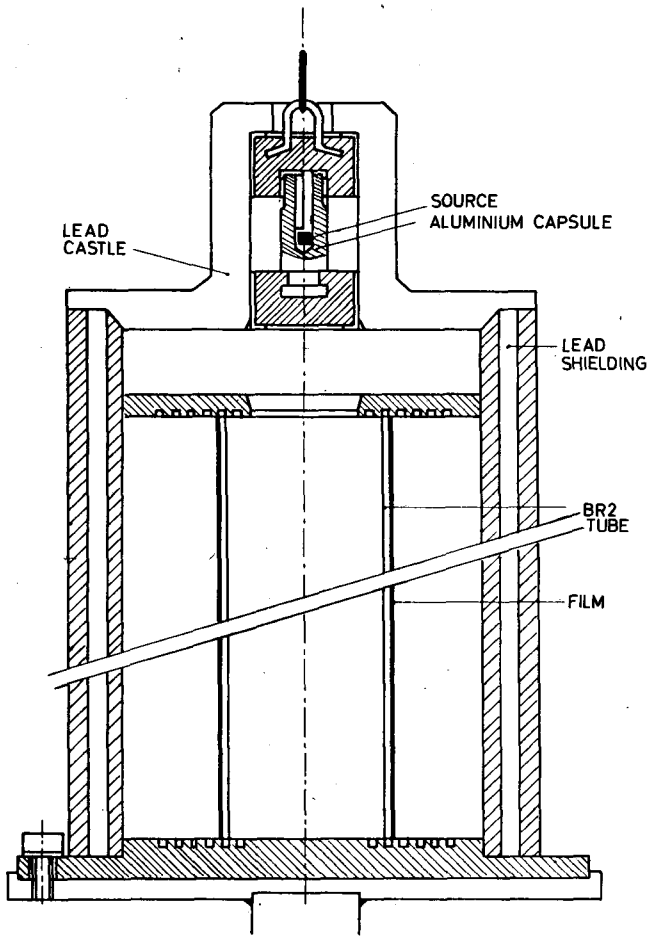

Fig. 7

Sketch of the mounting of the Tm^{170} source

NaI(Tl) scintillation crystal with preamplifier and high voltage, amplifier and single-channel pulse-height analyser. Scalers and a recording rate-meter provide digital readings and recorded curves. The static apparatus and static measurements on plates have already been described [11, 12, 13].

The automatic scanning device and a set of collimators are shown in Figs. 9 and 10. Plates or tubes of 1-m length can be scanned in lapses varying from 30 s to several hours. The scintillation crystal in its lead castle can make a transverse movement so that different lines parallel to the length direction can be measured subsequently; an electronically steered programme can provide different automatic scanning schemes. A radioactive source can be put on top of the lead castle to make absorption measurements. Several 10-mm-thick lead collimators are available, thus providing the possibility of measuring with different resolutions and speeds.

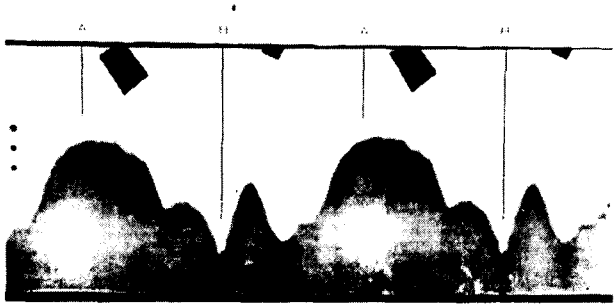

Fig. 8

Gammagraph of fuel tube extremity. Tm^{170} source 1 Ci. Gevaert Structurix D7, scanning speed: 1 cm/min.

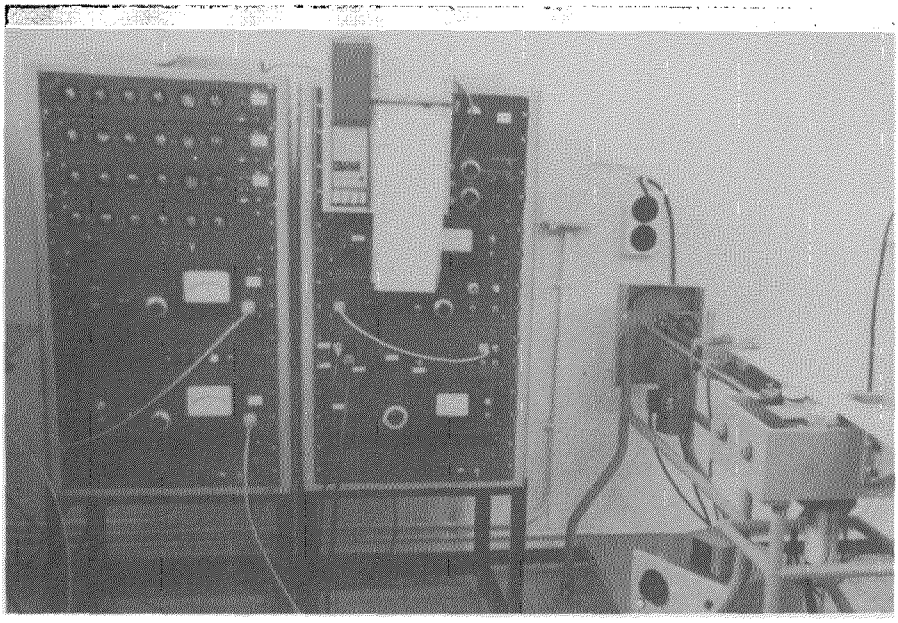

Fig. 9

Automatic gamma-scanning apparatus

The six different tube sizes for BR2 fuel elements can be measured either on the automatic scanning device or on the static apparatus where the emission of beta- and gamma-rays from a 1-cm^2 area is simultaneously recorded. An appropriate collimator for each tube exists; a central lead cylinder is attached to a fixed rod so as to shield the counter for radiation from the opposite tube wall (Fig. 11).

The beta radiation used is mainly the 2.32-MeV of U^{238}. The beta counting is done by a proportional counter in the gamma collimator opening of 1 cm^2. This cavity is penetrated in its centre and perpendicularly to its axis by nickel 0.05-mm wires held by Teflon insulators and forming anodes.

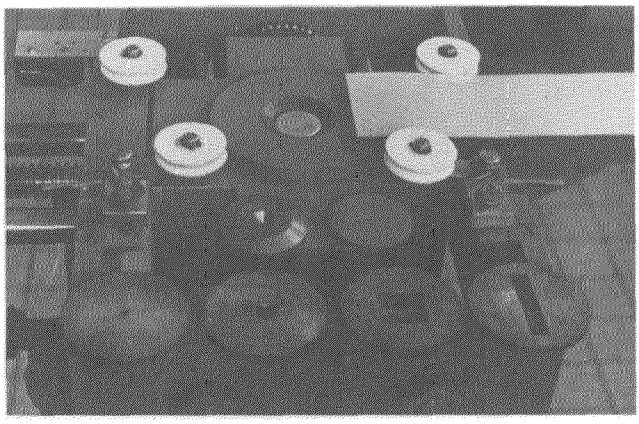

Fig. 10

Detail of gamma-scanning apparatus with set of collimators

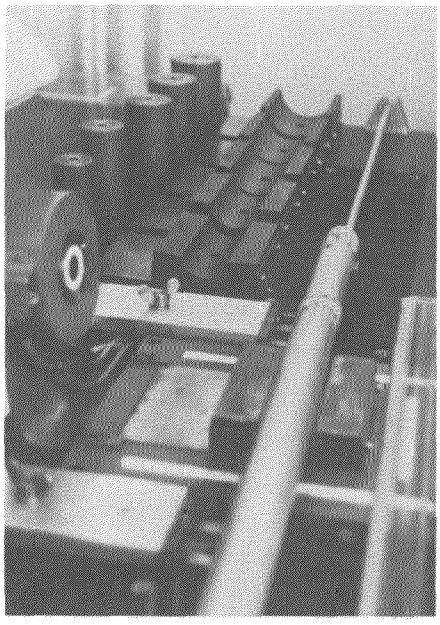

Fig. 11

Static apparatus with set of tube collimators

The counting gas, namely 90% argon with 10% methane, is circulated through the cavity. The counter is closed by a gold-plated 6-μm-thick Mylar window. A well-stabilized high-voltage source, a double discriminator with high sensitivity and a scaler-timer unit with low voltage supply form the electronic equipment.

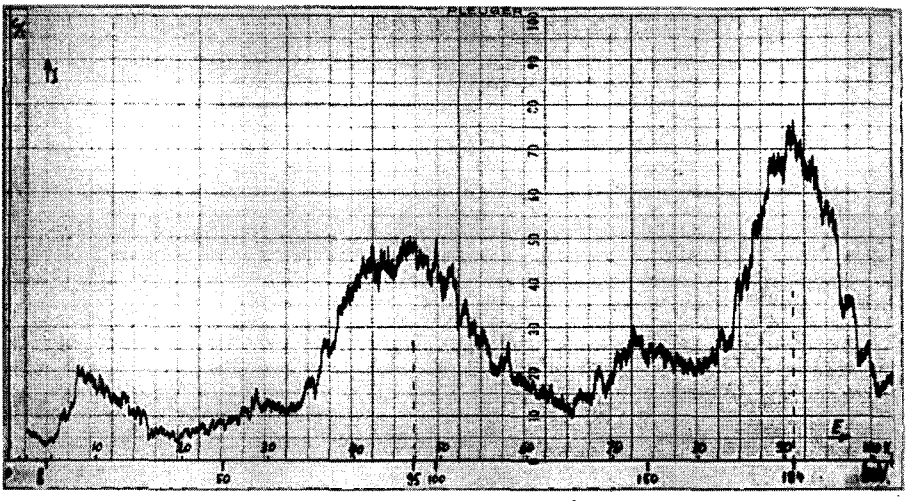

Fig. 12

Measured spectrum of the 90% enriched uranium alloy

The gamma counting is normally done by the scintillation crystal detection of the 184-keV gamma-ray from the excited state of Th^{231}, produced from the predominant alpha-decay mode of U^{235}. Reliable results, based on proportionality of the U^{235} amount and 184-keV gamma-ray intensity, can be obtained when equilibrium has been reached, i.e. some 10 d after chemical separation. The spectrum as measured on the 90% enriched U 24%-Al alloy is given in Fig. 12. These measurements, appropriately corrected for self-shielding, are proportional to the amount of U^{235} in the fuel element. However, if only one enrichment is used and if this is accurately known, it is advantageous to make integral measurements with a base-line set at 35 keV, being a minimum just below the 95-keV peak and surrounding peaks. The count rate is then about four times higher, resulting in an accuracy twice as good for the same counting time or scanning speed or a four-times faster counting or scanning for the same accuracy. The correction for self-shielding is much smaller, which is extremely interesting for the homogeneity measurements of fuel-plate stacks, or of complete fuel elements. The relative deviation of the measured count from the corrected value for a stack of five BR2 fuel plates has been measured for single-channel measurements on the 184-keV and on the 95-keV peaks with a 20-keV-wide window and also integrated above 35 keV. The results are given in Fig. 13. The self-absorption has been corrected according to the procedure of WHITE and PERRY [14]. The relative deviation was 22% for the 184-keV peak, 3.75% for the 95-keV peak and 9.5% for the integral measurement.

3.2. Measurements and results

The coextruded fuel tube, taken as an example in this report, has been beta-gamma measured along two diametrically opposed generatrices a and b

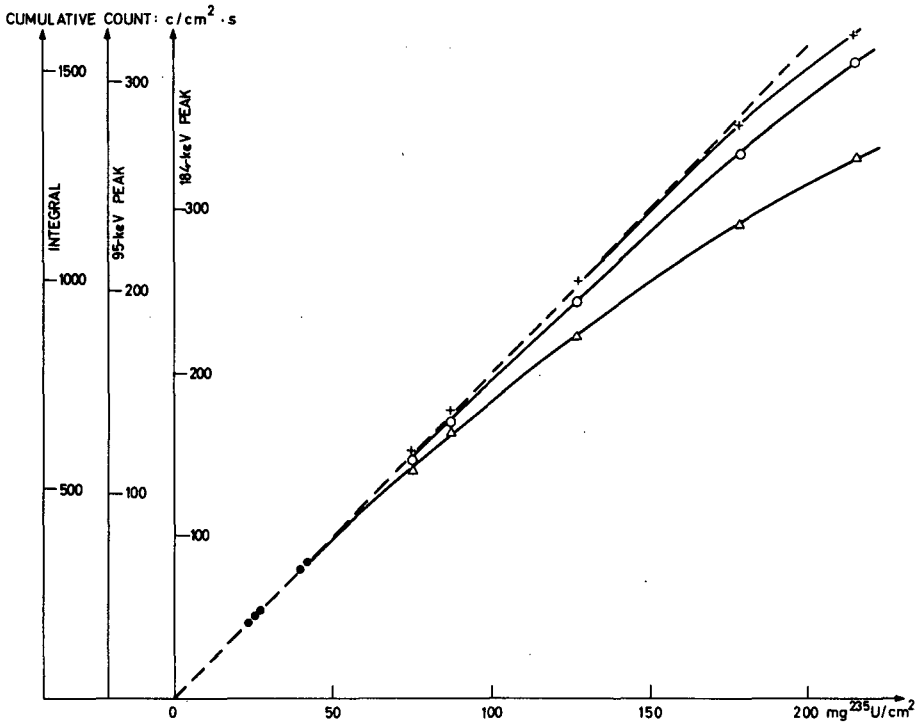

Fig. 13

Gamma-ray intensity measurements on fuel-plate stacks with 2, 3, 4 and 5 plates

Δ uncorrected measurement on the 184-keV peak of U^{235}

\+ uncorrected measurement on the 95-keV peak of uranium

O uncorrected integral measurement above 35 keV

— — — measurements corrected for self-absorption

(as indicated in Fig. 8). The readings were corrected for self-absorption and for cladding absorption, and the measuring points thus obtained are plotted in Fig. 14; the agreement with Fig. 8 is evident. Metallographic examination confirmed the absolute figures to better than 0.03-mm alloy thickness.

The automatic scanning device permits a fast quality control but can also be a valuable measuring tool in fabrication studies. Using gamma-ray recording as a precise laboratory tool one should examine the appropriate parameters to reach the precisions wanted. Measurement characteristics for obtaining a precision of better than 1% at 99% confidence level are given in Table II and compared with the characteristics to obtain but 3% accuracy at 96% confidence level. Count-reducing factors for different collimators are experimentally measured with the described apparatus while the calculated time-constants have been controlled experimentally.

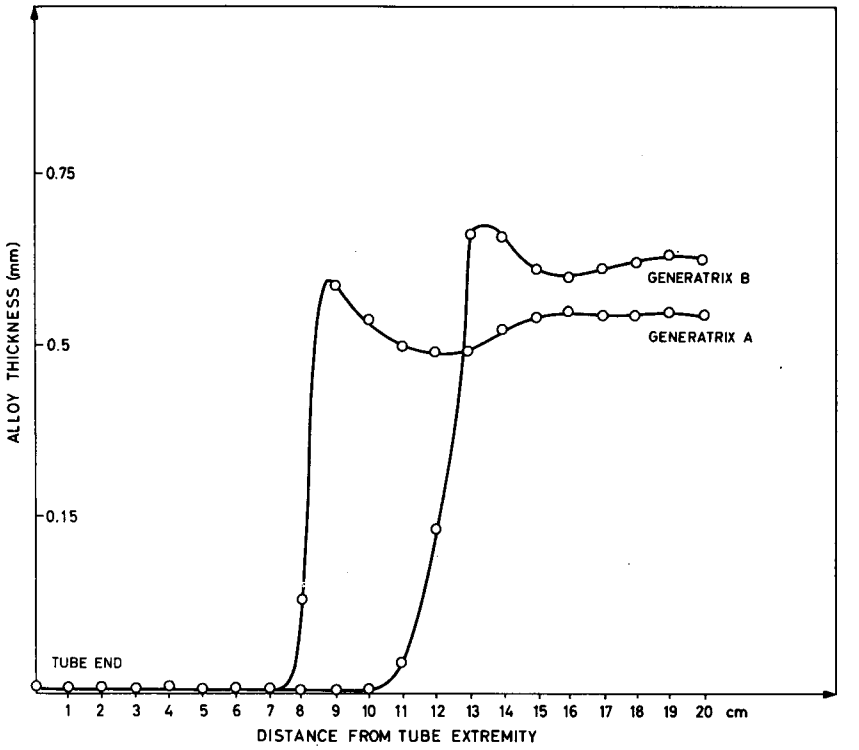

Fig. 14

Thickness of fuel alloy along two generatrices of a co-extruded tube as measured by the static beta-gamma unit, using a tube collimator

Measurements with different collimators and resolutions and at various speeds are given in Fig. 15 of the same area of plate C, corresponding to the area shown in Fig. 2. The increase in resolution on fuel homogeneity is clearly visible. It is, however, quite impractical to use collimators smaller than 10 mm^2. To investigate the homogeneity pattern on a smaller scale it is much more appropriate to use a microradiographic technique [15].

For the quality control of fuel components on a fabrication or a reception scale, one should choose the collimators and scanning speeds which are appropriate to detect the tolerances imposed by the specification. According to actual BR2 specifications the homogeneity is checked on the 1-cm^2 basis, the tolerance being a 12% deviation. Formerly, measurements on the square-inch scale have been made, with 15% and 10% tolerances. A quick check yielding an approximate fuel content of the complete plate and a rough homogeneity pattern can be obtained in one-minute scannings of the complete plates by simultaneous chart recording and scaler reading. The complete operation of recording, reading and replacing a fuel plate takes less than two minutes. A recorder graph of such "quick-check" measurements is given in Fig. 16. Plates A, B, C, D, E, F, G and H of different sizes are subsequently passed. The nominal value reading and the lower and higher

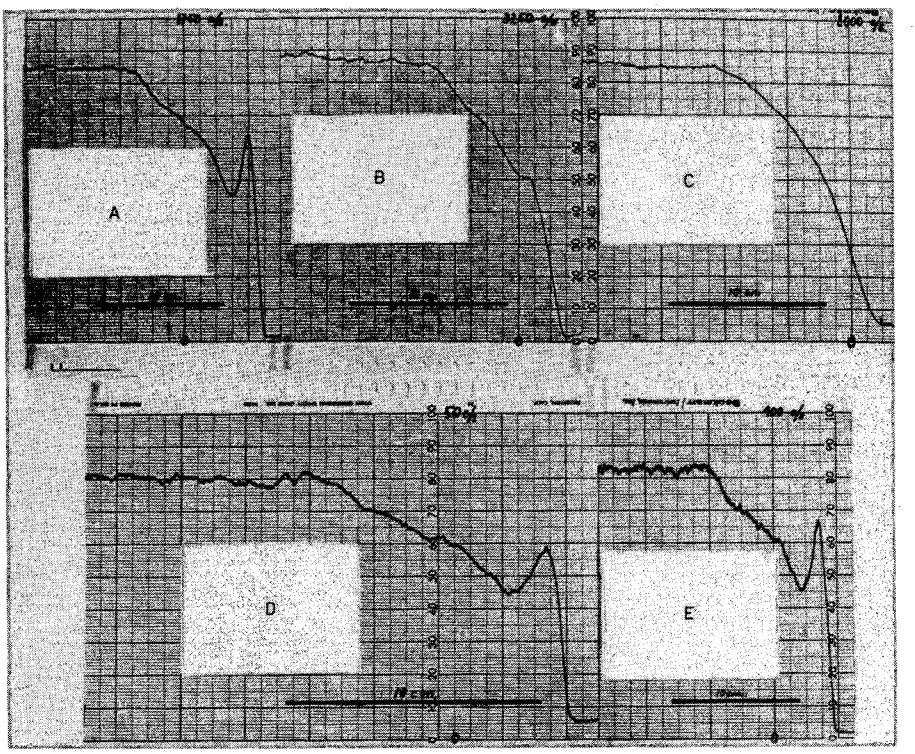

Fig. 15

Same area of plate C scanned with different collimators, speeds and time constants.

A
Collimator: 10 × 50 mm²
Time constant: 20 s
Full scale: 0 - 1750 cps
Scanning speed: 0.5 cm/min

B
Collimator: 1 in²
Time constant: 5 s
Full scale: 0 - 3250 cps
Scanning speed: 4 cm/min

C
Collimator: none
Time constant: 5 s
Full scale : 0 - 800 cps
Scanning speed: 4 cm/min

D
Collimator: 10 mm² conical
Time constant: 100 s
Full scale: 0 - 50 cps
Scanning speed: 0.25 cm/min

E
Collimator: 10 × 10 mm²
Time constant: 20 s
Full scale: 0 - 400 cps
Scanning speed: 0.5 cm/min

tolerance readings on appropriate standards are indicated on the graph; the collimator had a 1 × 1-in opening, the time constant was 1 s and full-scale range of the recorder was 0 to 3500 counts/s. The advantage of such quick checks is that a first selection can be made by an easy operation. Plates F, G and H look well between the tolerances, while plates C and D can immediately be rejected. Plate E will probably be rejected for an exaggerated

TABLE II

MEASUREMENT CHARACTERISTICS

Collimators	Count-reducing factor	Time constant for standard fuel plate to obtain an accuracy of better than ± 1% on a 99% confidence level (s)	Corresponding scanning speed	Total time for scanning of one fuel plate	Time constant for about ± 3% accuracy at 96% confidence level (s)	Corresponding scanning speed	Total time for scanning of one fuel plate
None	1	5	1 cm in 10 s	13-14 min	1	1 cm in 1.5 s	2 min
25.4 × 25.4 mm^2	0.416	5 (20)	1 cm in 10 s	13-14 min	1	1 cm in 1.5 s	2 min
10 × 50 mm^2	0.224	20	1 cm in 1 min 40 s	2 1/2 h	1	1 cm in 4 s	5 min
10 × 10 mm^2	0.0525	20	1 cm in 1 min 40 s	2 1/2 h	5	1 cm in 20 s	25 min
10 mm^2 conical	0.0063	100	1 cm in 27.5 min	22 h	10	1 cm in 4.5 min	~6 h
3 × 3 mm^2	0.00115	500	1 cm in 143 min	200 h	100-(500)	1 cm in 22.5 min	~30 h

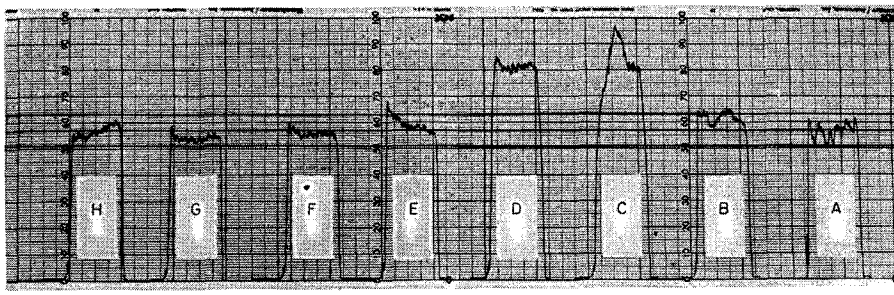

Fig. 16

1-min scannings of 8 fuel plates

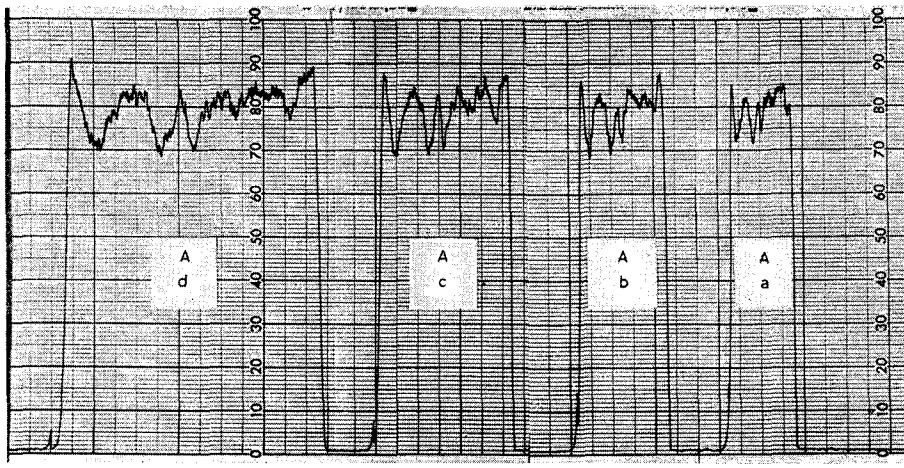

Fig. 17

Scanning of plate A at different speeds. Scanning times are resp. 44.6 s, 61.1 s, 93.7 s and 179.7 s. Collimator: 1 in × 1 in, time constant: 1 s, full scale : 0-2500 cps

dog-boning while plates A and B can be considered as doubtful and will thus be re-examined carefully. Out of a batch of several hundreds of fuel plates 1.5% had to be rejected for too high a fuel content, 1% stayed under the acceptance level, while 6% were border-line cases, mainly with slightly excessive dog-boning values. It should be noted, however, that by curing this widely-known defect one often gets fading which influences the fuel homogeneity along the plate axis much more and gives rise to strong flux distortions. It is clear that measurements on the end effects and on very localized heterogeneities are very inaccurate by such "quick checks". This effect is visualized in Fig. 17 where plate A has been scanned at different speeds varying from 45 s to 3 min for a complete scanning.

More detailed homogeneity measurements of plates A, C, D and E are given in Fig. 18. A collimator of 10×10 mm^2 was used while each scanning took about 50 min. These recordings can be compared with absorption

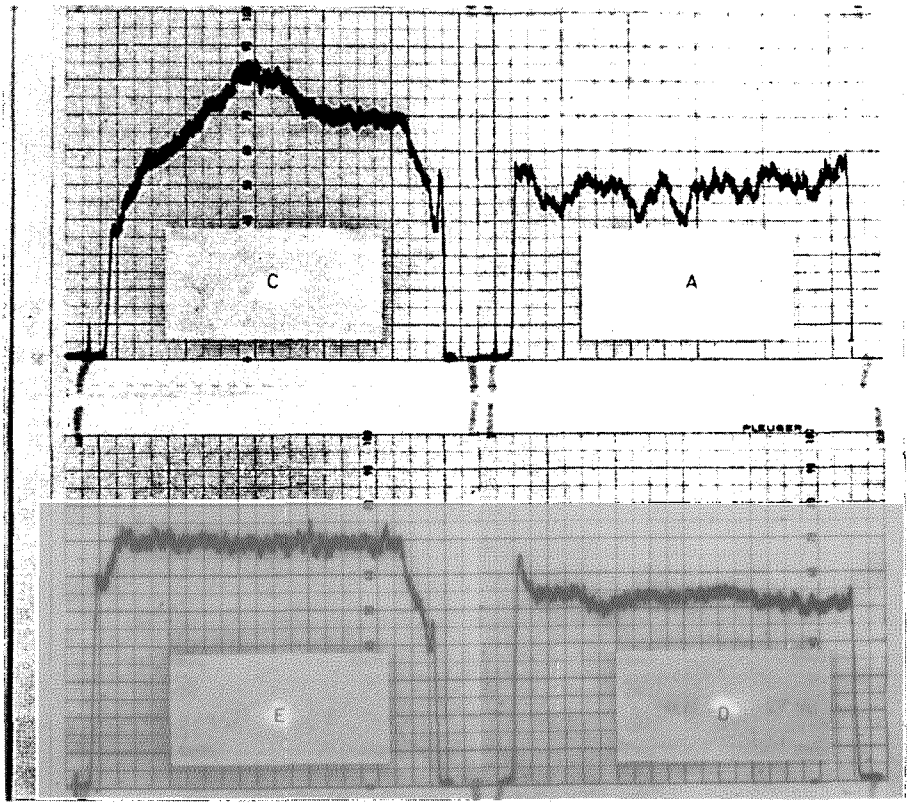

Fig. 18

Detailed scanning of plates A, C, D, E
Collimator: 10 × 10 mm², T.C.: 5 s; scanning time: 50 min; full scale: 0-500 cps

measurements with a 1-Ci Tm^{170} source using a 3 × 3-mm² collimator (Fig. 19). The general profile is the same but because of the smaller collimator it is possible to get a higher resolution for comparable scanning speeds.

Figure 20 shows a recording with the 10 × 10-mm² collimator of plate C along its central axis and along two parallel lines 2 cm apart on each side of it. Near the end of the plate, at the place indicated, a transverse scanning has been made which reveals a marked heterogeneity in the direction perpendicular to the rolling direction.

Scanning measurements have been carried out on finished fuel elements and on stacks of fuel plates to obtain a picture of the over-all homogeneity of an element. On this occasion the self-shielding effect has been checked. Figure 21 shows 3-min recordings for a stack of five fuel plates with the 1-in² collimator and with an integral measurement above 35 keV. In the first scanning the order of the plates was A, B, E, F and G, while in the second the stacking of fuel plates has been reversed; in the third scanning plate B, the fourth one, as seen by the counter, has been replaced by plate

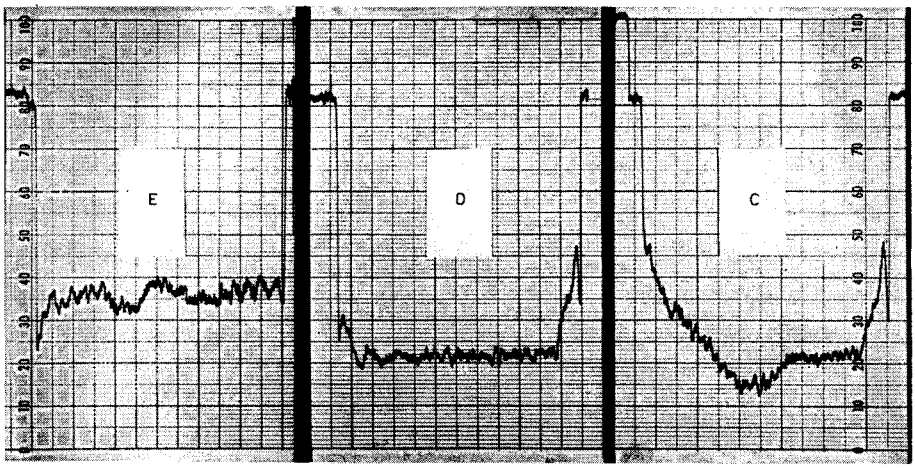

Fig. 19

Absorption measurements of plates C, D and E.
Tm^{170} source 1 Ci, collimator : 3 × 3 mm², T.C.: 5 s, full scale: 3000-7000 cps

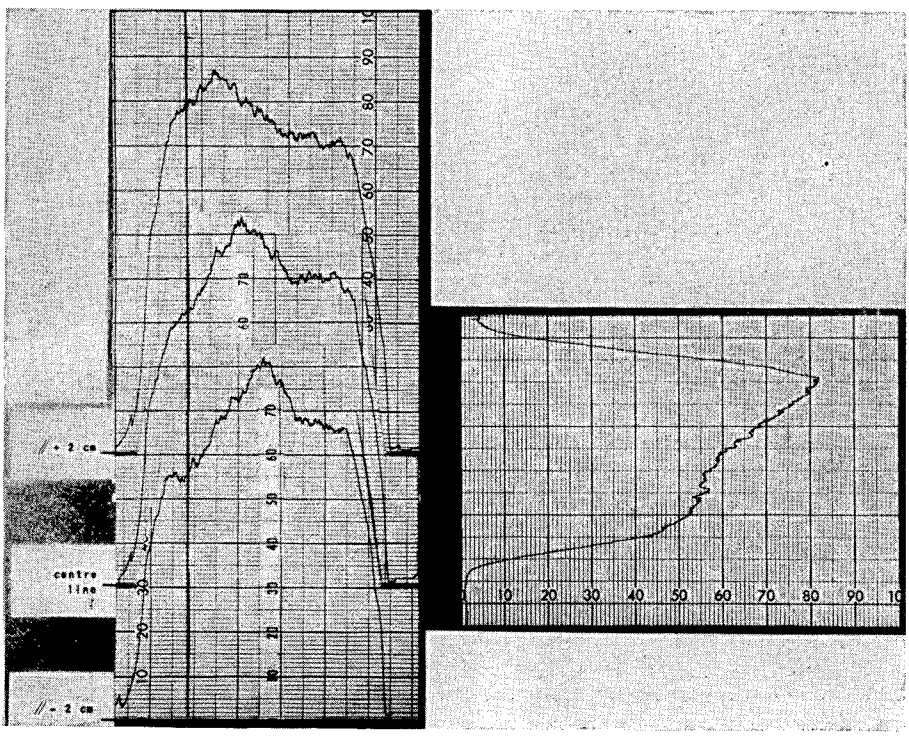

Fig. 20

Three parallel lengthwise scannings of plate C 2 cm apart from each other, and one transverse scanning near the end of the plate. Collimator: 10 × 10 mm².

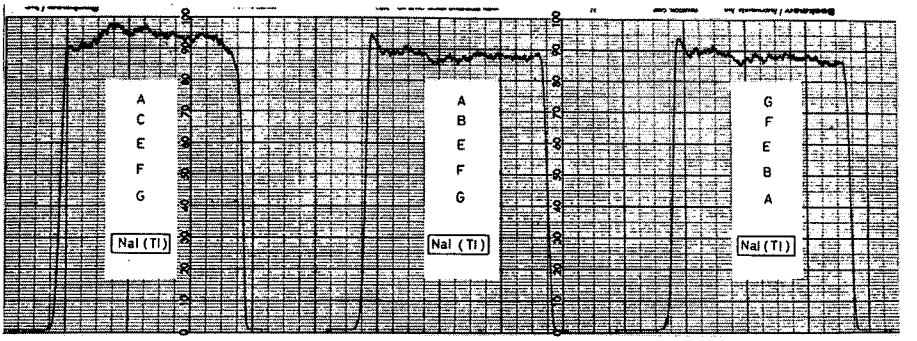

Fig. 21

Fuel-plate stack measurements with 1 × 1-in collimator

(a) Plates A, B, E, F and G piled in this sequence
(b) Plates G, F, E, B, A piled in this sequence
(c) Plates G, F, E, C, A piled in this sequence

C. The total count for the first two scannings differs only by 0.15% while the total deviation due to self-absorption was the same in the three cases, namely 8.6%.

An application of the gamma-scanning measuring procedure as a laboratory technique is for the investigation of end forms in sandwich rolling or coextrusion processes. Since such studies are normally performed with natural uranium it is advantageous to use the absorption technique which can yield a much higher counting rate than the proper emission of natural uranium. An experimental plate with several fuel regions of different sizes and end forms has been measured by proper gamma emission and by absorption of the gamma-rays emitted by a Tm^{170} source. The recordings are shown in Fig. 22. The high resolution and the clear indication of the end forms make this method quite attractive for such studies.

4. FUEL AMOUNT

Principle and results

Not only the homogeneous re-partition of the fuel in the element should be sufficiently known, but it is also of interest to obtain accurate measurements on the total fuel amount in an element. Fuel accountancy is a delicate item in fuel handling for which too often one has to rely on written certificates and, on the other hand, a precise fuel content is a most valuable point for subsequent post-irradiation tests on burn-up evaluation of given fuel assemblies and components.

A series of standards for fuel tubes as well as for fuel plates has been developed and determined by counting and chemical analysis. The standards thus obtained agreed within the experimental error with the calculated determination as given by WHITE and PERRY [14].

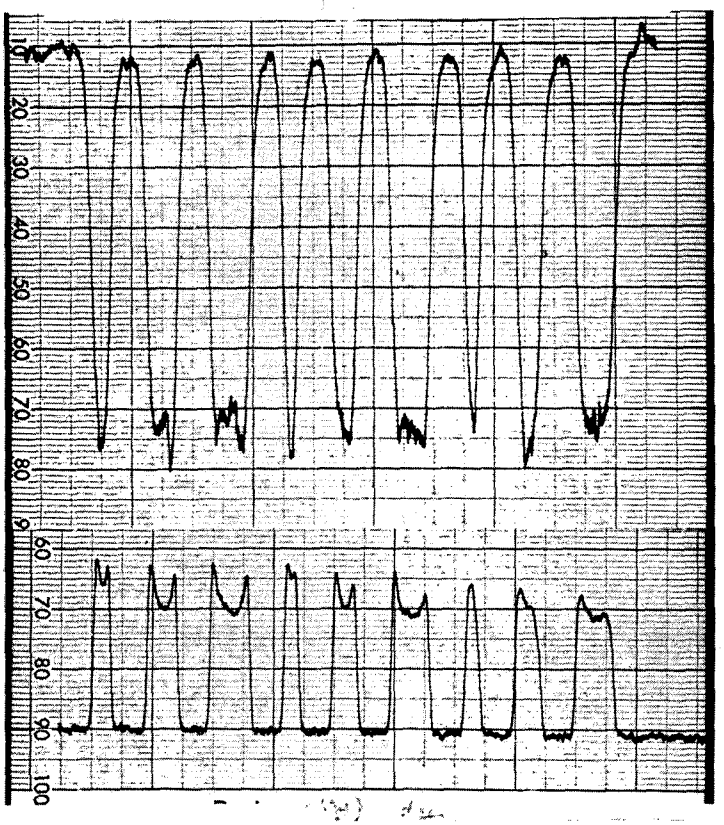

Fig. 22

Recordings of experimental fuel plate with natural uranium.
Lower chart: Gamma emission of the 95-keV peak.
Collimator: 10 × 50 mm, T.C.: 20 s, scanning speed: 1 m/h, full scale: 0-500 cps
Upper chart: Absorption measurement.
Tm^{170} source 1 Ci, collimator: 3 × 50 mm, T.C.: 5 s, full scale: 3000-13 000 cps.

By simultaneous digital reading and recording while measuring the fuel plates it was thus possible to measure the uranium amount per fuel plate within 0.1% standard error.

Rather large discrepancies in claimed fuel amount of BR2 plates have been encountered. The given fuel amounts were based on Archimedes density measurements. Nevertheless, this method should not be rejected since it has been shown that a more sophisticated measurement based on the same principle may yield a high accuracy [16], as supported by other statements in the literature. These measurements, however, are performed on fuel cores before rolling or extrusion. On formed fuel plates or tubes it is more appropriate to measure the fuel amount by the principle of gamma-ray recording. A comparison of fuel values claimed for the mentioned plates and of values measured in our laboratory is given in Table III.

TABLE III

A COMPARISON OF FUEL VALUES

Plate	Claimed U^{235} amount (g)	Measured U amount (g)
A	18.48	18.45 ± 0.20
B	17.48	17.55 ± 0.20
C	19.23	23.30 ± 0.20
D	18.66	22.70 ± 0.20
E	15.18	15.10 ± 0.15
F	11.64	11.65 ± 0.10
G	11.64	11.30 ± 0.10
H	11.74	11.80 ± 0.10

The bottle-neck in these problems always remains the fabrication of extremely homogeneous and appropriate standards whose fuel content is precisely known. An appealing technique is the fabrication of standards starting from a levitation molten alloy [17]. Nominal, high- and low-tolerance standards can so be obtained in forms similar to the fuel-element geometry, the absolute errors decreasing to a few hundreths of a per cent.

5. CONCLUSIONS

The methods for the control of fuel location, homogeneity and amount are satisfactory.

Autoradiography, an easy and relatively inexpensive tool for fuel location, is appealing for tubes, especially in the experimental fabrication phase since both an inside and an outside picture are obtainable. Inside pictures can be obtained by classical radiography; the results on outside pictures obtained by a central scanning Tm^{170} source have a higher quality than the former. Good qualitative information on fuel homogeneity results from these techniques.

Quantitative results on fuel homogeneity are given by beta- and gamma-scanning. Gamma measurements on the 184-keV peak are made, but if the enrichment is known, the integral measurements above 35 keV give faster or easier results especially for stacks of fuel plates or for completed elements. For elements with natural uranium, beta-scannings and especially absorption measurements with radioactive sources such as Tm^{170}, are the most appropriate of the methods described. It has been shown that the scanning devices can play an interesting role as a laboratory tool for fabrication studies, where a variety of collimators and scanning speeds can provide extremely useful information. This method can contribute to a better

understanding, not only in the field of extrusion and rolling techniques, but also in the field of fuel evaluation and the definition of specifications and tolerances.

The fabrication techniques of high-quality standards have been improved. The equipment with such standards has to be extended so as to yield measurement precisions up to 0.03%.

Effective X-ray absorption measurements of uranium and U-Al alloys from 120 to 200 keV, as well as self-absorption measurements on these materials in the complete range up to 200 keV, would assist in elucidating the problem of choosing the right gamma-energy range for the detection of fuel homogeneity and for the measurement of the fuel amount.

ACKNOWLEDGEMENTS

Thanks are due to S.C.K./C.E.N. for the interest and the encouragement, and for providing the necessary equipment. The technical assistance of Messrs. H. Inniger and M. Moulaert is gratefully acknowledged, as well as the assistance of the electronics section and of Mrs. P. Heylen and her metallographic team. Thanks are also due to the S.A. Métallurgie et Mécanique Nucléaires, Dessel, Belgium for providing fuel-element standards. Finally, the author is much indebted to Mr. R. Deknock and other colleagues of the non-destructive testing group.

REFERENCES

[1] RUSH, D. et al., Belgian Engineering Test Reactor BR2, Design and Safety Report BLG 59 (1961).
[2] BR2 Fuel Element Specification, Mol, November (1954).
[3] FLIPOT, J., DEPOITIER, J. and MASSAUX, H., S.C.K./C.E.N., R. 2341. (1965).
[4] COMPTON, A.H. and ALLISON, S.K., X-rays in Theory and Experiment, New York, Van Nostrand, (1957).
[5] NICKERSON, R.A., Nondestructive Testing, Jan.-Feb. (1958) 24-27, 41.
[6] COTTERELL, K., Applied Materials Research, April (1954) 102-112.
[7] FOSTER, B.E., SNYDER, S.D. and McCLUNG, R.W., Proc. 4th Int. Conf. on Nondestructive Testing, London (1963) 339-342.
[8] McGONNAGLE, W.J., TID-7560, USAEC, Jan. (1958) 197-208.
[9] McGONNAGLE, W.J., TID-19821 (1963).
[10] BEYER, N.S., Proc. 4th Int. Conf. on Nondestructive Testing, London (1963) 331-334.
[11] DE MEESTER, P. et al., TID-7642, 1 (1963) 182-196.
[12] PLANQUART, J. et al., 3rd UN Int. Conf. PUAE, A/CONF.28/P/716 (1964).
[13] DE MEESTER, P., BRABERS, M.J. and DEKNOCK, R., Brit. J. non-destr. Test. 6, 4 (1964) 123-129.
[14] WHITE, J.F.K. and PERRY, R.B., COO-272, November (1960).
[15] NEIDER, R. and DE MEESTER, P., See these Proceedings (SM 63/42).
[16] VAN HOVE, L., private communication (1964).
[17] VAN AUDENHOVE, J., (to be published) 1965.

DISCUSSION

R.S. SHARPE: I note that you use thulium as a transmission radiation for homogeneity measurement. Do you not consider that the energy of this radiation is too high for adequate contrast?

P. de MEESTER: The 80 keV of Tm^{170} is not the only one to consider; there is also the bremsstrahlung at 50 keV which is fairly important. For our fuel plates with a uranium concentration of about 45 mg/cm^2 this gave satisfactory results.

R.S. SHARPE: How long does it take to make a thickness measurement over the "dog-bone" region using your smallest collimator?

P. de MEESTER: The smallest collimator we normally use is 10 mm^2 with a conical opening. It takes 22 h to get a precision of 1% at 99% confidence level for a complete fuel plate.

J.E. LOVETT: I would like to comment that, in some preliminary work carried out in the United States of America "dog-boning" in U-Al alloy plates could be detected quite easily using a slit collimator $\frac{1}{2}$ in $\times$ $1\frac{1}{2}$ in and counting under static conditions the 184-keV gamma from U^{235}. Successive counting for periods of one minute, moving the plate 1/4 in each time, showed the "dog-bone" as a count rate perhaps 50% greater than that from the central portions of the plate. The work was not pursued to develop a continuous scan at that time, although several authors have since developed scanning techniques under circumstances where "dog-boning" was not a primary concern.

P. de MEESTER: Former work at Mol also included static measurements with a 1-cm^2 or 10-mm^2 collimator, and gave good results. To save time and obtain a complete homogeneity record, automatic scanning was adopted. I should make it clear to both Mr. Sharpe and Mr. Lovett that the smaller collimator is used only for laboratory work; for fuel evaluation, measurements of 1 cm^2 are quite sufficient.

J. GÉRARD: Have you made a qualitative or quantitative comparison of the precision of the different methods of scanning the plates?

P. de MEESTER: For experimental natural uranium plates we found the transmission method the best, while for tests on enriched uranium plates we prefer the radiation from the uranium itself.

J. GÉRARD: Are you not afraid that when you use gamma counting over a wide range of the spectrum, the latter may be affected by daughter products of uranium (its age) or of the isotopes which may be present as a result of recycling the enriched uranium?

P. de MEESTER: You are quite right to mention this. Nevertheless, we know the batch of fuel, and this effect can be corrected for a given batch. Since self-absorption is much less pronounced, the precision is still superior for complete elements provided the corrections I mentioned are made.

SYMPOSIUM ON NON-DESTRUCTIVE TESTING IN NUCLEAR TECHNOLOGY

HELD AT BUCHAREST, 17-21 MAY 1965

CHAIRMEN OF SESSIONS

Session I	H. HULUBEI	Romania
Session II	A. KISELEV	USSR
Session III	P. de MEESTER	Belgium
Session IV	P. THOMÉ	France
Session V	R. F. HANSTOCK	United Kingdom
Session VI	G. LECCIOSOTTI	Italy
Session VII	G. H. TENNEY	United States of America
Session VIII	R. FORSYTH	Sweden
Session IX	R. SEIFERT	Federal Republic of Germany

SECRETARIAT OF THE SYMPOSIUM

Scientific Secretaries:	J. C. DELANEY	Division of Nuclear Power Reactors, IAEA
	A. PUSHKOV	Division of Nuclear Power Reactors, IAEA
Administrative Secretary:	K. ZYBYLSKI	Division of Scientific and Technical Information
Editor:	MONICA KRIPPNER	Division of Scientific and Technical Information
Records Officer:	D. MITCHELL	Division of Languages

LIST OF PARTICIPANTS

Name	Institution	Nominating State or Organization
Alecu, M.	Institute of Atomic Physics, Bucharest	Romania
Allain, C.	Commissariat à l'énergie atomique, CEN de Saclay, Services de Technologie, Gif-sur-Yvette (S. et O.)	France
Andreescu, N.	Institute of Atomic Physics, Bucharest	Romania
Aoki, T.	Atomic Fuel Corporation, 2-7 Hirakaw-cho Chiyoda-ku, Tokyo	Japan
Baffigo, V.	Sorin, Società Ricerche Impinati Nucleari, Saluggia (Vercelli)	Italy
Ballard, D.	Sandia Laboratory. Sandia Base, Albuquerque, New Mex.	USA
Bally, D.	Institute of Atomic Physics, Bucharest	Romania
Bertoletti, S.	Centro Informazioni Studi Experienze, C. P. 3968, Milan	Italy
Blom, G.	Euroters, Place Rogier, Brussels	Netherlands
Brebant, C.	CEN de Cadarache, Département de métallurgie, St. Paul-les-Durance (B. du R.)	France
Bonnet, P.	Service de métallurgie, CCR Ispra Varese, Italy	EURATOM
Cizek, L.	National Research Institute for Materials and Technology, Opletalova 25, Prague	Czechoslovakia
Condé, J. F. G.	O. E. C. D. Dragon Project, Atomic Energy Establishment, Winfrith, Dorchester, Dorset, England	OECD/ENEA
Delaney, J. C.	Division of Nuclear Power and Reactors, IAEA, Kärntner Ring, Vienna	IAEA
Destribats, Marie-Thérèse	CEN de Saclay, B. P. 2, Gif-sur-Yvette, (S. et O.)	France

Name	Institution	Nominating State or Organization
Dory, J.	Société des realisations ultrasoniques, 9, rue Chaussée de Paris, Meaux, (S. et M.)	France
Engelmann, C.	Département de métallurgie – S. R. M. P. C., B. P. 2, Gif-sur-Yvette, (S. et O.)	France
Filip, R.	V. I. Lenin Works National Corp., Nuclear Power Stations Division, Pilsen	Czechoslovakia
Francis, W.	Phillips Petroleum Co. Atomic Energy Div. P. O. B. 2067, Idaho Falls, Idaho	USA
Forsyth, R.	AB Atomenergi, Studsvik, Nyköping	Sweden
Gérard, J.	Métallurgie et Mécanique Nucléaires, 12 Europalaan, Dessel	Belgium
Gerasimov, V. G.	Energetics Institute, Moscow	USSR
Gevantman, L. H.	Mission to the International Atomic Energy Agency, Schmidg. 14, Vienna VIII. Austria	USA
Glantz, G.	Institute of Atomic Physics Bucharest	Romania
Gorski, V.	State Committee on utilisation of Atomic Energy	USSR
Grignon, F.	CEA, 33 rue de la Fédération, Paris	France
Hanstock, R. F.	The Reactor Materials Laboratory, U. K. A. E. A., Colcheth, Warrington, Lancs., England	UK
Horvat, D.	Nuklearni Institut "Jozef Stefan", Jamova 39, Ljubljana, Slovenia	Yugoslavia
Hulubei, H.	Institute of Atomic Physics, Bucharest	Romania
Jansen, J. C.	CCR Ispra Varese, Italy	EURATOM
Kadlez, K.	Simmering Graz Pauker AG, Mariahilfe Strasse 32, Vienna	Austria

Name	Institution	Nominating State or Organization
Kiselev, A.	State Committee on Utilization of Atomic Energy	USSR
Knudsen, P.	Danish Atomic Energy Commission Research Establishment Risö, Roskilde	Denmark
Koinig, H.	Institute for Theoretical Physics, University of Innsbruck, Innsbruck	Austria
Koss, P.	Handelsministerium für Handel und Wiederaufbau, Vienna	Austria
Lăbuscă, Elena	Institute of Atomic Physics, Bucharest	Romania
Lafaurie, F.	CEA, Service de fabrications industrielles des combustibles, Centre de Saclay	France
Leccisotti, G.	Ministère de la Santé, Rome	Italy
Libotte, P.	Société Belge pour l'Industrie Nucléaire, S. A., 35, rue des Colonies, Brussels	Belgium
Listwan, W.	Instytut Baden Jadrowych Z-XX, Swietokrzyska 21, Warsaw	Poland
Lovett, J. E.	United States Atomic Energy Commission, Washington, D. C.	USA
Lucas, Monique	CEN de Saclay – DPC. IS-SSM, B. P. 2, Gif-sur-Yvette. (S. et O.)	France
Lund, S. A.	Danish Central Welding Institution, 47, Nygaardsvej, Copenhagen Ø	Denmark
Lungu, S.	Institute of Atomic Physics, Bucharest	Romania
Malinowski, W.	Institute of Nuclear Research, Swierk, Z-XIV, Warsaw	Poland
Mann, C. A.	Reactor Fuel Element Labs., The Reactor Group, U. K. A. E. A., Springfields Works, Salwick, Preston, Lancs., England	UK
Marchandise, H.	51 rue Belliard, Brussels, Belgium.	EURATOM

Name	Institution	Nominating State or Organization
Maurel, J.	CEN de Fontenay-au-Roses, DC – S. E. C. P. E. R., B. P. 6, Fontenay-aux-Roses (Seine)	France
McClung, R. W.	Oak Ridge National Laboratory, P. O. B. X. Oak Ridge, Tenn. 37831.	USA
McEachern, A. D.	Atomic Energy of Canada, Ltd., Development Engineering Div., Chalk River, Ontario	Canada
McKane, R.	E. I. du Pont de Nemours & Co., Bldg. 723 A., Savannah, River Plant, Aiken, S. C.	USA
Meester, P. de	S. C. K. /C. E. N., Boeretang, 200 Mol	Belgium
Mirion, I.	Institute of Atomic Physics, Bucharest	Romania
Nakičenović, S.	Division of Safeguards and Inspection, IAEA, Kärntner Ring, Vienna	IAEA
Neider, R.	Bundesanstalt für Materialprüfung, (Dahlem), Unter den Eichen 87, 1. Berlin 45	Federal Republic of Germany
Nyström, U.	AB Atomenergi, Studsvik, Nyköping	Sweden
Oquidam, B.	Centre de recherches, Les Bérauds, Romans s/Ysère, (Drôme)	France
Pawlowski, Z.	Institute for Basic Technical Problems of the Polsih Academy of Sciences, Swietokrzyska, 21, Warsaw	Poland
Pintelon, M.	Association des Industriels de Belgique, 29, Avenue André Drouart, Brussels 16	Belgium
Prot, A.	CEN de Saclay, B. P. 2, Gif-sur-Yvette (S. et O.)	France
Pugnetti, G.	Comitato Nazionale Energia Nucleare, C. S. N. Casaccia, Via Anguillarese, Rome	Italy
Purica, I.	Institute of Atomic Physics, Bucharest	Romania

Name	Institution	Nominating State or Organization
Pushkov, A.	Division of Nuclear Power and Reactors, IAEA, Kärntner Ring, Vienna	IAEA
Raad, J.A. de	Röntgen Technische Dienst N.V., Delftweg 144, Rotterdam - 8.	Netherlands
Rapin, M.	CEA, 33 rue de la Fédération, Paris	France
Roussel, E.	CEN de Saclay, Dép. de métallurgie - L.E.C.I., B.P. 2, Gif-sur-Yvette (S. et O.)	France
Sala, L.	C.N.E.N. - Casaccia, Rome	Italy
Salvi, P.	Ministero Industria e Comercio, D.G.E.E.I.B., Rome	Italy
Sanders, T.	Vereinigung der Technischen Überwachungs-Vereine, Rottstrasse, Essen	Federal Republic of Germany
Sasao, N.	Atomic Fuel Corporation, 2-7 Hirakaw-cho Chiyoda-ku, Tokyo	Japan
Seifert, R.	Laboratory of Richard Seifert & Co. Hamburg 13	Federal Republic of Germany
Sharpe, R.	Research Group, A.E.R.E. Harwell, Didcot, Berks., England	UK
Spagna, F.	Associazione EURATOM-CNEN Reacteurs à neutrons Rapides, Via Mazzini, 2, Bologna	Italy
Stoian, D.	Institute of Atomic Physics, Bucharest	Romania
Szivos, K.	Central Research Institute for Physics, Csillebérc, Budapest XII	Hungary
Tenney, G.	Los Alamos Scientific Laboratory, P.O.B. 1663, Los Alamos, N. Mex. 87544.	USA
Thomé, P.	CEN de Saclay, B.P. 2, Gif-sur-Yvette (S. et O.)	France
Tóth, M.	Central Research Institute for Physics, Csillebérc, Budapest XII	Hungary

Name	Institution	Nominating State or Organization
Van der Linde, A.	Reactor Centrum Nederland Petten	Netherlands
Vasseur, C.	Société des réalisations ultrasoniques, 9, Chaussée de Paris, Meaux (S. et M.)	France
Verstappen, G.	S. C. K. /C. E. N., Boeretang, 200, Mol	Belgium
Warlton, D.	Battelle Northwest Laboratory, Richland, Wash.	USA
Wells, F.	U. K. A. E. A., A. E. R. E., Harwell, Berks., England	UK

AUTHOR INDEX

Roman numerals refer to the volume number;
Arabic numerals indicate the first page of the paper by an author; and
underlined arabic numerals refer to participation in a Discussion.

TRANSLITERATION INDEX

Вяхорев, В.Г.	Vyakhorev, V.G.
Герасимов, В.Г.	Gerasimov, V.G.
Горский, В.В.	Gorsky, V.V.
Денискин, В.П.	Deniskin, V.P.
Захаров, В.М.	Zakharov, V.M.
Никитин, Г.А.	Nikitin, G.A.
Попов, В.К.	Popov, V.K.
Пронякин, В.Т.	Pronyakin, V.T.
Трахтенберг, Л.И.	Trakhtenberg, L.I.
Филипп, Р.	Filip, R.
Ходулев, Б.С.	Khodulev, B.S.
Шкарлет, Ю.М.	Shkarlet, Yu.M.

IAEA SALES AGENTS

Orders for Agency publications can be placed with your bookseller or any of our sales agents listed below:

ARGENTINA
Comisión Nacional de
Energía Atómica
Avenida del Libertador
General San Martin 8250
Buenos Aires - Suc. 29

AUSTRALIA
Hunter Publications,
23 McKillop Street
Melbourne, C.1

AUSTRIA
Georg Fromme & Co.
Spengergasse 39
Vienna V

BELGIUM
Office international de librairie
30, avenue Marnix
Brussels 5

BRAZIL
Livraria Kosmos Editora
Rua do Rosario, 135-137
Rio de Janeiro

Agencia Expoente Oscar M. Silva
Rua Xavier de Toledo, 140-1° Andar
(Caixa Postal No. 5.614)
São Paulo

BYELORUSSIAN SOVIET SOCIALIST REPUBLIC
See under USSR

CANADA
The Queen's Printer
Ottawa, Ontario

CHINA (Taiwan)
Books and Scientific Supplies
Service, Ltd.,
P.O. Box 83
Taipei

CZECHOSLOVAK SOCIALIST REPUBLIC
S.N.T.L.
Spolena 51
Nové Město
Prague 1

DENMARK
Ejnar Munksgaard Ltd.
6 Nörregade
Copenhagen K

FINLAND
Akateeminen Kirjakauppa
Keskuskatu 2
Helsinki

FRANCE
Office international de
documentation et librairie
48, rue Gay-Lussac
Paris 5e

GERMANY, Federal Republic of
R. Oldenbourg
Rosenheimer Strasse 145
8 Munich 8

HUNGARY
Kultura
Hungarian Trading Co. for Books
and Newspapers
P.O.B. 149
Budapest 62

ISRAEL
Heiliger and Co.
3 Nathan Strauss Street
Jerusalem

ITALY
Agenzia Editoriale Internazionale
Organizzazioni Universali (A.E.I.O.U.)
Via Meravigli 16
Milan

JAPAN
Maruzen Company Ltd.
6, Tori Nichome
Nihonbashi
(P.O. Box 605)
Tokyo Central

MEXICO
Librería Internacional
Av. Sonora 206
Mexico 11, D.F.

NETHERLANDS
N.V. Martinus Nijhoff
Lange Voorhout 9
The Hague

NEW ZEALAND
Whitcombe & Tombs, Ltd.
G.P.O. Box 1894
Wellington, C.1

NORWAY
Johan Grundt Tanum
Karl Johans gate 43
Oslo

PAKISTAN
Karachi Education Society
Haroon Chambers
South Napier Road
(P.O. Box No. 4866)
Karachi 2

POLAND
Ośrodek Rozpowszechniana
Wydawnictw Naukowych
Polska Akademia Nauk
Pałac Kultury i Nauki
Warsaw

ROMANIA
Cartimex
Rue A. Briand 14-18
Bucarest

SOUTH AFRICA
Van Schaik's Bookstore (Pty) Ltd.
Libri Building
Church Street
(P.O. Box 724)
Pretoria

SPAIN
Librería Bosch
Ronda de la Universidad 11
Barcelona

SWEDEN
C.E. Fritzes Kungl. Hovbokhandel
Fredsgatan 2
Stockholm 16

SWITZERLAND
Librairie Payot
Rue Grenus 6
1211 Geneva 11

TURKEY
Librairie Hachette
469, Istiklâl Caddesi
Beyoğlu, Istanbul

UKRAINIAN SOVIET SOCIALIST REPUBLIC
See under USSR

UNION OF SOVIET SOCIALIST REPUBLICS
Mezhdunarodnaya Kniga
Smolenskaya-Sennaya 32-34
Moscow G-200

UNITED KINGDOM OF GREAT BRITAIN AND NORTHERN IRELAND
Her Majesty's Stationery Office
P.O. Box 569
London, S.E.1

UNITED STATES OF AMERICA
National Agency for
International Publications, Inc.
317 East 34th Street
New York, N.Y. 10016

VENEZUELA
Sr. Braulio Gabriel Chacares
Gobernador a Candilito 37
Santa Rosalía
(Apartado Postal 8092)
Caracas D.F.

YUGOSLAVIA
Jugoslovenska Knjiga
Terazije 27
Belgrade

IAEA publications can also be purchased retail at the United Nations Bookshop at United Nations Headquarters, New York, at the news-stand at the Agency's Headquarters, Vienna, and at most conferences, symposia and seminars organized by the Agency.

In order to facilitate the distribution of its publications, the Agency is prepared to accept payment in UNESCO coupons or in local currencies.

Orders and inquiries from countries where sales agents have not yet been appointed may be sent to:

Distribution and Sales Group, International Atomic Energy Agency,
Kärntner Ring 11, Vienna I, Austria

INTERNATIONAL
ATOMIC ENERGY AGENCY
VIENNA, 1965

PRICE: USA and Canada: US $9.00
Austria and elsewhere: S 189,-
(£2.14.0; F.Fr. 36,-; DM 31,50)